National Library
of Canada

Acquisitions and
Bibliographic Services Branch

395 Wellington Street
Ottawa, Ontario
K1A 0N4

Bibliothèque nationale
du Canada

Direction des acquisitions et
des services bibliographiques

395, rue Wellington
Ottawa (Ontario)
K1A 0N4

Your file Votre référence

Our file Notre référence

NOTICE

The quality of this microform is heavily dependent upon the quality of the original thesis submitted for microfilming. Every effort has been made to ensure the highest quality of reproduction possible.

If pages are missing, contact the university which granted the degree.

Some pages may have indistinct print especially if the original pages were typed with a poor typewriter ribbon or if the university sent us an inferior photocopy.

Reproduction in full or in part of this microform is governed by the Canadian Copyright Act, R.S.C. 1970, c. C-30, and subsequent amendments.

AVIS

La qualité de cette microforme dépend grandement de la qualité de la thèse soumise au microfilmage. Nous avons tout fait pour assurer une qualité supérieure de reproduction.

S'il manque des pages, veuillez communiquer avec l'université qui a conféré le grade.

La qualité d'impression de certaines pages peut laisser à désirer, surtout si les pages originales ont été dactylographiées à l'aide d'un ruban usé ou si l'université nous a fait parvenir une photocopie de qualité inférieure.

La reproduction, même partielle, de cette microforme est soumise à la Loi canadienne sur le droit d'auteur, SRC 1970, c. C-30, et ses amendements subséquents.

Canada

University of Alberta

Synthesis and Properties of Alkyne Bridged Heterobimetallic Complexes

by

John Scott Washington ©

A thesis
submitted to the Faculty of Graduate Studies and Research
in partial fulfilment of the requirements
for the degree of Doctor of Philosophy

Department of Chemistry

Edmonton, Alberta
Fall, 1994

National Library
of Canada

Acquisitions and
Bibliographic Services Branch

395 Wellington Street
Ottawa, Ontario
K1A 0N4

Bibliothèque nationale
du Canada

Direction des acquisitions et
des services bibliographiques

395, rue Wellington
Ottawa (Ontario)
K1A 0N4

Your file Votre référence

Our file Notre référence

The author has granted an irrevocable non-exclusive licence allowing the National Library of Canada to reproduce, loan, distribute or sell copies of his/her thesis by any means and in any form or format, making this thesis available to interested persons.

The author retains ownership of the copyright in his/her thesis. Neither the thesis nor substantial extracts from it may be printed or otherwise reproduced without his/her permission.

L'auteur a accordé une licence irrévocable et non exclusive permettant à la Bibliothèque nationale du Canada de reproduire, prêter, distribuer ou vendre des copies de sa thèse de quelque manière et sous quelque forme que ce soit pour mettre des exemplaires de cette thèse à la disposition des personnes intéressées.

L'auteur conserve la propriété du droit d'auteur qui protège sa thèse. Ni la thèse ni des extraits substantiels de celle-ci ne doivent être imprimés ou autrement reproduits sans son autorisation.

ISBN 0-315-95282-2

Canada

University of Alberta

Release Form

Name of Author:	John Scott Washington
Title of Thesis:	Synthesis and Properties of Alkyne Bridged Heterobimetallic Complexes
Degree:	Doctor of Philosophy
Year this Degree Granted:	1994

Permission is hereby granted to the University of Alberta to reproduce single copies of this thesis and to lend or sell such copies for private, scholarly or scientific research purposes only.

The author reserves other publication rights, and neither the thesis nor extensive extracts from it may be printed or otherwise reproduced without the author's written permission.

(Signed) ______
John Washington

Permanent Address:
5804 - 94B Avenue
Edmonton, Alberta
T6B 0Z4

Date: May 11, 1994

University of Alberta

Faculty of Graduate Studies and Research

The undersigned certify that they have read, and recommended to the Faculty of Graduate Studies and Research for acceptance, a thesis entitled **Synthesis and Properties of Alkyne Bridged Heterobimetallic Complexes** submitted by John Scott Washington in partial fulfilment of the requirements for the degree of Doctor of Philosophy.

J. Takats (Supervisor)

Charles P. Casey

C.P. Casey

W.A.G. Graham

Robert B Jordan

R.B. Jordan

D. T. Lynch

D.T. Lynch

J. Stryker

Date: May 11, 1994

To my father

Abstract

The preparation and reactions of $Os(CO)_4(\eta^2\text{-alkyne})$ complexes were investigated.

$Os(CO)_4(\eta^2\text{-HCCH})$, **1**, reacts readily with $CpM(CO)_2$ (M = Co, Rh, Ir) to yield dimetallacyclopentenone compounds. For M = Co, Rh, $[\mu\text{-}\eta^3\text{:}\eta^1\text{-}C_2H_2C(O)]Os(CO)_4MCp$ (M = Co, **2a**; Rh, **2b**) species are generated while for M = Ir, the reaction occurs without ligand loss to yield $[\mu\text{-}\eta^1\text{:}\eta^1\text{-}C_2H_2C(O)]Os(CO)_4IrCp(CO)$, **3**. Low temperature NMR studies indicate that CO loss from **1** is the probable initial step in the reaction. The reaction of **2a** with PMe_3 or PMe_2Ph yields dimetallacyclopentenone complexes whereby the phosphine is attached to the Os centre. A similar reaction with **2b** produces a dinuclear Os-carbene complex resulting from phosphine attack at the alkyne bridge.

The reaction of **1** with $CpM(CO)(PR_3)$ (M = Co, Rh; PR_3 = PMe_3, PMe_2Ph, $PMePh_2$) shows remarkable phosphine and metal dependence. For M = Rh and PR_3 = PMe_2Ph, $PMePh_2$, the dimetallacyclopentenones $[\mu\text{-}\eta^3\text{:}\eta^1\text{-}C(O)C_2H_2]Os(CO)_3RhCp(PR_3)$ (PR_3 = PMe_2Ph, **5a**; $PMePh_2$, **5b**) are formed. However, by changing the metal and/or the phosphine, the hydrocarbyl-bridged zwitterionic species $[\mu\text{-}\eta^1\text{:}\eta^2\text{-}HCCH(PR_3)](\mu\text{-}CO)\text{-}Os(CO)_3MCp$ (M = Rh, PR_3 = PMe_3, **7**; M = Co, PR_3 = PMe_3, **6a**, PMe_2Ph, **6b**, $PMePh_2$, **6c**) are synthesized. A low temperature NMR study into the formation of **7** indicated a marked solvent dependence for the reaction as well.

The reactions of the asymmetric $Os(CO)_4(\eta^2\text{-alkyne})$ complexes with $(\eta^5\text{-}C_5H_5)M(CO)_2$ (R = H, Me) were also carried out. For $Os(CO)_4[\eta^2\text{-}HCC(CH_3)]$, the reaction with $CpM(CO)_2$ proceeded to yield $[\mu\text{-}\eta^1\text{:}\eta^1\text{-}$

$(CH_3)CCHC(O)]Os(CO)_4M(CO)Cp$, (M = Co, **17a**; Rh, **17b**; Ir, **17c**); the same, single regioisomer was produced in each case. The reaction of $Os(CO)_4[\eta^2$-$HCC(CF_3)]$ with $Cp^*Co(CO)_2$ resulted the formation of a dimetallacyclopentenone, **16**. However, for M = Rh, Ir, the formation of dimetallacyclobutene species $[\mu$-η^1:η^1-$(CF_3)CCH]Os(CO)_4MCp^*(CO)$ (M = Rh, **14b**; Ir, **15**) was seen. Again, the reaction proceeds in a regioselective manner as only one regioisomer was observed. The regioselectivity of the condensation reactions involving propyne and trifluoropropyne was also important in the formulation of reaction mechanisms that were consistent with the polarization of the alkyne. Attempts to generate another asymmetric Os-alkyne complex *via* low temperature photolysis of $Os(CO)_5$ in the presence of propargyl chloride resulted in an oxidative-addition reaction to produce *cis*-$Os(CO)_4(\eta^1$-$CH{=}C{=}CH_2)Cl$, **21**. Also, many of the bimetallic compounds synthesized display interesting fluxional behaviour, particularly with regard to the carbonyl ligands. Numerous low temperature NMR experiments were performed to elucidate the mechanisms of these fluxional processes and, in addition, activation parameters for these processes were determined.

$Os(CO)_4[\eta^2$-$C_2(CH_3)_2]$, **20**, was prepared *via* the low temperature photolysis of $Os(CO)_5$ in the presence of excess 2-butyne. Not unexpectedly, **20** reacts with $CpM(CO)_2$ to produce dimetallacyclopentenones, $[\mu$-η^1:η^1-$C_2(CH_3)_2C(O)]Os(CO)_4M(CO)Cp$, (M = Co, **18a**; Rh, **18b**; Ir,, **18c**). However, **20** also reacts with electron-rich alkynes such as 2-butyne, 3-hexyne and 4-octyne to yield the Os-cyclopentadienone species $Os(CO)_3(\eta^4$-$C_4Me_2R_2CO)$ (R = Me, **24a**; Et, **25a**; n-Pr, **25b**).

Acknowledgements

Although only one name appears on this Thesis, its completion could not have been achieved without the support and assistance of a number of people. I wish to express my gratitude to my co-workers and colleagues.

First and foremost, I would like to thank Prof. Josef Takats not only for his guidance and dedication, but for his sincere friendship as well. Joe's enthusiasm for chemistry is only matched by the concern he has for the well-being of his students; he truly stands apart. The hospitality of the Takats family, Mickey, Lisa and Michael, is also fondly remembered.

The Takat's research group provided a pleasant and stimulating environment in which to work. I thank my colleagues Gong-Yu Kiel, Steve Astley, Melinda Burn, Mark Sandercock, Wenyi Fu, Jürgen Jacke, Torsten Funk, Ken Hoffman, Xingwang Zhang, Yimin Sun and Jason Cooke for their friendship and, when needed, their sympathy.

I was fortunate to make numerous friends throughout my tenure. In particular Al Chilton, Bob McDonald, Shaun Duhaime and the members of the Chemistry hockey team made my stay enjoyable.

The assistance of the NMR staff, led by Dr. Tom Nakashima, was indispensable to my work. In particular, Glen Bigam kept an ornery 360 MHz NMR machine in good working order so I could complete my (endless) variable temperature NMR runs. Tom Brisbane and Lai Kong also performed numerous experiments for me; their enthusiasm and professionalism is appreciated. Gerdy Aarts went above the call of duty in carrying out several magnetization transfer experiments. Also, the patience of Prof. R.E.D. McClung, pertaining to the NMR simulation programs, is appreciated as were the X-ray structure determinations and helpful discussions provided by Bernie Santarsiero, Bob McDonald, Andrew Bond and Robin Rogers.

The prompt elemental analyses provided by Darlene Mahlow and Andrea Dunn, along with the mass spectra recorded by Andrew Jodhan are gratefully acknowledged. Numerous members of the machine (Hubert Hofmann, Randy Benson, Dieter Starke, Theo van Esch) and glassblowing (Gerald Streefkerk, John Toonen) shops kept needed equipment in top working order.

I would also like to thank NSERC and the University of Alberta for financial support.

The unwavering support of my family, especially my parents, in my academic pursuits will not be forgotten. I would also like to thank the Jensens for accepting me into the fold and making me feel like one of the family.

Finally, I would like to thank my wife, Andrea for her loyalty, patience and encouragement, all of which allowed my goals to come to fruition. Her unwavering love and understanding made me realize that she is the most important part of my life.

Table of Contents

Chapter 1

Introduction 1

1.1. Synergic Bonding in Transition Metal Complexes and the Eighteen Electron Rule

1.2. The Isolobal Analogy 5

1.3. Alkyne Bonding to Transition Metal Complexes 8

1.3.1. General Description of Bonding 8

1.3.2. Alkyne Bonding to $M(CO)_4$ (M = Fe, Ru, Os) Fragment 10

1.4. Comparison of $Os(CO)_4(\eta^2\text{-HCCH})$ to $Os(CO)_4(\eta^2\text{-}H_2CCH_2)$: Four Electron Destabilization 12

1.5. Survey ofAlkyne Bridged Dimetallic Complexes 19

1.5.1. Condensation Reactions Involving $M(CO)_4(\eta^2\text{-alkyne})$ (M = Ru, Os) 19

1.5.2. Synthesis of Dimetallacyclobutene Complexes 20

1.5.3. Bonding in Dimetallacyclobutene Complexes 24

1.5.4. Synthesis of Dimetallacyclopentenone Complexes 26

1.6. Scope of Present Work 30

1.7. References 32

Chapter 2

Reaction of $Os(CO)_4(\eta^2\text{-HCCH})$ with $CpM(CO)_2$ (M = Co, Rh, Ir) 38

2.1. Introduction 38

2.2. Synthesis and Characterization of Bimetallic Compounds 40

2.2.1. Synthetic Aspects 40

2.2.2. Characterization of $Os(CO)_4(C_2H_2)MCp(CO)$ (M = Co; **2a**, Rh; **2b**) 42

2.2.3. Characterization of $Os(CO)_4(C_2H_2)(CO)IrCp(CO)$, **3** 52

2.3. Molecular Structure of $[\mu\text{-}\eta^1{:}\eta^1\text{-}C_2H_2C(O)]Os(CO)_4IrCp(CO)$ 58

2.4. Fluxional Behaviour of Complexes **2a-b** and **3** 65

2.4.1. Variable Temperature ^{13}C NMR Behaviour of $[\mu\text{-}\eta^3{:}\eta^1\text{-}C_2H_2C(O)]Os(CO)_4MCp$ (M = Co; **2a**, Rh; **2b**) 65

2.4.2. Variable Temperature ^{13}C NMR Behaviour of $[\mu\text{-}\eta^1{:}\eta^1\text{-}C_2H_2C(O)]Os(CO)_4IrCp(CO)$, **3** 69

2.5. Proposed Mechanism for the Formation of Dimetallacyclopentenones 73

2.5.1. Formation of $[\mu\text{-}\eta^3{:}\eta^1\text{-}C_2H_2C(O)]Os(CO)_4RhCp$, **2b** 73

2.5.2. Formation of $[\mu\text{-}\eta^1{:}\eta^1\text{-}C_2H_2C(O)]Os(CO)_4IrCp(CO)$, **3** 78

2.6. Conclusions 80

2.7. Experimental Section 82

2.7.1. Solvents and General Techniques 82

2.7.2. Physical Measurements 83

2.7.3. Photochemical Techniques 83

2.7.4. Starting Materials and Reagents 86

2.7.5. Synthetic Procedures 86

2.7.6. X-ray Structure Determination of **3** 89

2.8. References 94

Chapter 3

Reaction of $Os(CO)_4(\eta^2\text{-}HCCH)$ with $CpM(CO)(PR_3)$ (M = Co, Rh; PR_3 = PMe_3, PMe_2Ph, $PMePh_2$) 100

3.1. Introduction 100

3.2. Reaction of $Os(CO)_4(\eta^2\text{-}HCCH)$ with $CpRh(CO)(PR_3)$ $(PR_3 = PMe_2Ph, PMePh_2)$ 102

  3.2.1. Characterization of $[\mu\text{-}\eta^3{:}\eta^1\text{-}C(O)C_2H_2]\text{-}Os(CO)_3RhCp(PR_3)$, ($PR_3 = PMe_2Ph$, **5a**; $PMePh_2$, **5b**)... 103

  3.2.2. Molecular Structure of $[\mu\text{-}\eta^3{:}\eta^1\text{-}C(O)C_2H_2]Os(CO)_3RhCp(PMe_2Ph)$, **5a** 106

3.4. Fluxional Behaviour of $[\mu\text{-}C(O)C_2H_2]Os(CO)_3RhCp(PR_3)$, ($PR_3 = PMe_2Ph$, **5a**; $PMePh_2$, **5b**) 112

  3.4.1. Variable Temperature ^{13}C NMR Behaviour 112

  3.4.2. Variable Temperature ^1H NMR Behaviour 115

3.5. Reaction of $Os(CO)_4(\eta^2\text{-}HCCH)$ with $CpM(CO)(PR_3)$ ($M = Co$; $PR_3 = PMe_3, PMe_2Ph, PMePh_2$; $M = Rh$; $PR_3 = PMe_3$): Unexpected Formation of Zwitterionic Compounds 118

  3.5.1. Characterization of $[\mu\text{–}\eta^1{:}\eta^2\text{-}HCCH(PR_3)](\mu\text{-}CO)\text{-}Os(CO)_3MCp$, ($M = Co$; $PR_3 = PMe_3$, **6a**; PMe_2Ph, **6b**; $PMePh_2$, **6c**; $M = Rh$, $PR_3 = PMe_3$, **7**) 119

  3.5.2. Molecular Structure of $[\mu\text{–}\eta^1{:}\eta^2\text{-}HCCH(PMe_3)](\mu\text{-}CO)Os(CO)_3RhCp$, **7** 124

3.6. Comparison of **6a-c** and **7** to Similar Hydrocarbyl Bridged Zwitterionic Species 129

3.7. Formation of Compounds **5a-b**, **6a-c** and **7**: Plausible Reaction Pathways 131

3.8. Conclusions 135

3.9. Experimental Section 137

  3.9.1. Starting Materials and Reagents 137

  3.9.2. Synthetic Procedures 137

  3.9.3. X-ray Structure Determination of **5a** 142

3.9.4. X-ray Structure Determination of 7 146

3.10. References 150

Chapter 4

Synthesis of [μ-$C_2H_2C(O)$](μ-$CO)_2Os(CO)_2(PMe_3)Rh(\eta^5$-$C_9H_7$) ($C_9H_7$ = Indenyl) and Reaction of [μ-η^3:η^1-$C_2H_2C(O)$]$Os(CO)_4MCp$ (M = Co, Rh) with Phosphines 156

- **4.1.** Introduction 156
- **4.2.** Reaction of $Os(CO)_4(\eta^2$-HCCH) with (η^5-$C_9H_7)Rh(CO)(PMe_3$) 158
  - **4.2.1.** Synthetic Aspects 158
  - **4.2.2.** Characterization of $OsRh(CO)_5(C_2H_2)(C_9H_7)(PMe_3)$, 9 158
  - **4.2.3.** Molecular Structure of [μ-η^1:η^1-$C_2H_2C(O)$]-(μ-$CO)_2Os(CO)_2(PMe_3)Rh(\eta^5$-$C_9H_7$), 9 163
- **4.3.** Reaction of [μ-η^3:η^1-$C_2H_2C(O)$]$Os(CO)_4MCp$ (M = Co, Rh) with Phosphines 170
  - **4.3.1** Synthetic Aspects 170
  - **4.3.2.** Characterization of $OsCo(CO)_5(C_2H_2)(PMe_3)Cp$ (PR_3 = PMe_3, **10a**; PMe_2Ph, **10b**) 171
  - **4.3.3.** Characterization of $OsRh(CO)_5(C_2H_2)(PMe_3)Cp$ (PR_3 = PMe_3, **11a**; PMe_2Ph, **11b**) 176
- **4.4.** Formation of Products 182
- **4.5.** Conclusions 187
- **4.6.** Experimental Section 189
  - **4.6.1.** Starting Materials and Reagents 189
  - **4.6.2.** Synthetic Procedures 189

4.6.3. X-ray Structure Determination of
$[\mu\text{-}C_2H_2C(O)](\mu\text{-}CO)_2Os(CO)_2(PMe_3)Rh(\eta^5\text{-}C_9H_7)$, **9**........ 194
4.7. References.. 198

Chapter 5

Reaction of $Os(CO)_4[\eta^2\text{-}HCC(CF_3)]$ with $(\eta^5\text{-}C_5R_5)M(CO)_2$ (R = Me, M = Co, Rh, Ir; R = H, M = Rh). Synthesis, Characterization and Fluxional Behaviour of Dimetallacyclobutenes and Dimetallacyclopentenones.. 203
5.1. Introduction.. 203
5.2. Synthesis and Characterization of Compounds........................ 206
5.2.1. Synthesis of $[\mu\text{-}(CF_3)CCH]Os(CO)_4M(\eta^5\text{-}C_5R_5)(CO)$,
(R = Me, Cp*: M = Rh, Ir; R = H, Cp: M = Rh).................. 206
5.2.2. Characterization of
$[\mu\text{-}(CF_3)CCH]Os(CO)_4M(\eta^5\text{-}C_5R_5)(CO)$
(R = Me, M = Rh, Ir; R = H, M = Rh)................................ 207
5.3. Molecular Structure of $[\mu\text{-}(CF_3)CCH]Os(CO)_4Ir(CO)Cp^*$, **15**...... 215
5.4. Formation of Heterodimetallacyclobutenes **14a-b**, **15**:
Plausible Pathway.. 221
5.5 Fluxional Behaviour of Heterodimetallacyclobutenes,
14a-b and **15**.. 227
5.5.1. Variable Temperature ^{13}C NMR Behavior.................... 227
5.5.2. Magnetization Transfer Experiment on **15**...................... 231
5.6. Synthesis and Characterization of
$[\mu\text{-}\eta^3:\eta^1\text{-}(CF_3)CCHC(O)]Os(CO)_4CoCp^*$, **16**................................. 235
5.7. Fluxional ^{13}C NMR Behaviour of
$[\mu\text{-}\eta^3:\eta^1\text{-}(CF_3)CCHC(O)]Os(CO)_4CoCp^*$.. 238

5.8. Conclusions 240
5.9. Experimental Section 242
  5.9.1. Starting Materials and Reagents 242
  5.9.2. Synthetic Procedures 242
  5.9.3. X-ray Structure Determination of **15** 245
5.10. References 249

Chapter 6

Reaction of $Os(CO)_4(\eta^2\text{-}(CH_3)CCR)$ (R = H, CH_3) with $CpM(CO)_2$ (M= Co, Rh, Ir): Generation of Dimetallacyclopentenones 254
6.1. Introduction 254
6.2. Reactions of $Os(CO)_4[\eta^2\text{-}(CH_3)CCH]$ 256
  6.2.1. Synthesis of $[\mu\text{-}(CH_3)C_2HC(O)]Os(CO_4MCp(CO)$ (M = Co, Rh, Ir) 256
  6.2.2. Characterization of $[\mu\text{-}(CH_3)C_2HC(O)]\text{-}Os(CO)_4MCp(CO)$, (M = Co, Rh, Ir) 256
6.3. Molecular Structure of $[\mu\text{-}\eta^1\text{:}\eta^1\text{-}(CH_3)CCHC(O)]\text{-}Os(CO)_4Rh(CO)Cp$, **17b** 264
6.4. Reactions of $Os(CO)_4[\eta^2\text{-}C_2(CH_3)_2]$ 271
6.5. Variable Temperature ^{13}C NMR Behavior of $[\mu\text{-}\eta^1\text{:}\eta^1\text{-}(CH_3)C_2RC(O)]Os(CO)_4M(CO)Cp$ (M = Co, Rh, Ir; R = H, CH_3) 276
6.6. Formation of Heterodimetallacyclopentenones: Plausible Pathway 282
6.7. Conclusions 286
6.8. Experimental Section 288
  6.8.1. Starting Materials and Reagents 288

6.8.2. Synthetic Procedures 288
6.8.3. X-ray Structure Determination of **17b** 292
6.9. References 297

Chapter 7

Photoreaction of $Os(CO)_5$ with Propargyl Chloride:
Preparation of $Os(CO)_4(\eta^1\text{-}HC{=}C{=}CH_2)Cl$ 300
7.1. Introduction 300
7.2. Synthesis and Characterization of
$Os(CO)_4(\eta^1\text{-}CH{=}C{=}CH_2)Cl$, **21** 303
7.2.1. Synthesis of $Os(CO)_4(\eta^1\text{-}CH{=}C{=}CH_2)Cl$ 303
7.2.2. Characterization of $Os(CO)_4(\eta^1\text{-}CH{=}C{=}CH_2)Cl$ 304
7.3. Mechanistic Pathway for Formation of
$Os(CO)_4(\eta^1\text{-}CH{=}C{=}CH_2)Cl$, **21** 312
7.4. Attempted Reactions of $Os(CO)_4(\eta^1\text{-}CH{=}C{=}CH_2)Cl$, **21** 316
7.5. Conclusions 318
7.6. Experimental Section 319
7.6.1. Starting Materials and Reagents 319
7.6.2. Synthetic Procedures 319
7.7. References 321

Chapter 8

Synthesis of $Os(CO)_4(\eta^2$-butyne) and Reactions with Alkynes 326
8.1. Introduction 326
8.2. Synthesis and Characterization of $Os(CO)_4(\eta^2\text{-}C_2Me_2)$, **20** 328
8.2.1. Synthesis of $Os(CO)_4(\eta^2\text{-}C_2Me_2)$, **20** 328
8.2.2. Characterization of $Os(CO)_4(\eta^2\text{-}C_2Me_2)$, **20** 329

8.3. Reaction of $Os(CO)_4(\eta^2\text{-}C_2Me_2)$ with 2-butyne 333
8.3.1. Characterization of $Os(CO)_4(2\text{-butyne})_2$, **24a** 334
8.3.2. Synthesis of $M(CO)_3(\eta^4\text{-}C_4R_4CO)$ (M = Ru, Os; R = Me, Et, n-Pr) 336
8.3.3. Characterization of $M(CO)_3(\eta^4\text{-}C_4R_4CO)$ (M = Ru, Os) 337
8.4. Reaction of $Os(CO)_4(\eta^2\text{-}C_2Me_2)$ with Alkynes 343
8.4.1. Synthesis of $Os(CO)_3(\eta^4\text{-}C_4Me_2R_2'CO)$ Complexes (R' = Et, n-Pr) 343
8.4.2. Characterization of $Os(CO)_3(\eta^4\text{-}C_4R_2R_2'CO)$ (R = Me, R' = Et, n-Pr) 344
8.5. Molecular Structure of $Os(CO)_3(C_4Me_2Et_2CO)$, **25a** 348
8.6. Proposed Mechanism for Formation of Metal-Cyclopentadienone Species 354
8.7. Scope of the Coupling Reactions 361
8.7.1. Extension of Alkyne Coupling Reactions 361
8.7.2. Use of $M(CO)_3(\eta^4\text{-}C_4R_4CO)$ in Catalysis 362
8.8. Conclusions 364
8.9. Experimental Section 365
8.9.1. Starting Materials and Reagents 365
8.9.2. Synthetic Procedures 365
8.9.3. X-ray Structure Determination of **25a** 372
8.10. References 377

Chapter 9

Conclusions 383
9.1. References 390

Appendix

Use of Eyring Equation to Calculate Activation Parameters 392

References 397

List of Tables

Chapter 2

Table 2.1 FT-IR Data for **2a** and **2b** 44

Table 2.2 FT-IR Data for **2a** and **2b** for the Acyl Carbonyl 45

Table 2.3 FT-IR Data for **2a**, **2b** and Cyclic Ketones 47

Table 2.4 ^{1}H NMR Data for **2a** and **2b** 49

Table 2.5 ^{13}C NMR Data for **2a** and **2b** and Related Compounds 50

Table 2.6 FT-IR Data for $[\mu\text{-}C_2H_2C(O)]Os(CO)_4IrCp(CO)$, **3** 53

Table 2.7 FT-IR Data for **3** and Related Compounds 54

Table 2.8 ^{1}H NMR Data for **3** and Related Compounds 56

Table 2.9 ^{13}C NMR Data for **3** and Related Compounds 57

Table 2.10 Selected Bond Lengths (Å) for **3** 61

Table 2.11 Selected Angles (deg) for **3** 62

Table 2.12 Activation Parameters for CO Exchange in $[\mu\text{-}\eta^3\text{:}\eta^1\text{-}C_2H_2C(O)]Os(CO)_4MCp$ (M = Co, Rh) 68

Table 2.13 Drying Agents for Solvents 82

Table 2.14 Summary of Crystallographic Data for **3** 90

Table 2.15 Fractional Coordinates and Isotropic Thermal Parameters for **3** 92

Table 2.16 Selected Weighted Least-Squares Planes 93

Chapter 3

Table 3.1 Cone Angles and pKa Values for Selected Phosphines 102

Table 3.2 ^{13}C NMR Data for Ring Carbons of Dimetallacyclopentenones.. 104

Table 3.3 ^{1} H NMR Data for Ring Protons of Dimetallacyclopentenones.. 105

Table 3.4 Selected Bond Lengths (Å) for **5a**...................................... 109

Table 3.5 Selected Angles (deg) for **5a**.. 109

Table 3.6 Activation Parameters for Carbonyl Exchange in [μ-C(O)C_2H_2]Os(CO)$_3$RhCp(PR$_3$) (PR$_3$ = PMe$_2$Ph, **5a**; PMePh$_2$, **5b**)... 115

Table 3.7 ^{1}H NMR Data for [μ–η^1:η^2-HCCH(PR$_3$)](μ-CO)Os(CO)$_3$MCp.......................... 120

Table 3.8 ^{13}C NMR Data for [μ–η^1:η^2-HCCH(PR$_3$)]-(μ-CO)Os(CO)$_3$MCp, (M = Rh, Co) (PR$_3$ = PMe$_3$, PMe$_3$, PMe$_2$Ph, PMePh$_2$)............................. 122

Table 3.9 ^{13}C NMR (Carbonyl Region) Data for [μ–η^1:η^2-HCCH(PR$_3$)](μ-CO)Os(CO)$_3$MCp (M = Rh, Co; PR$_3$ = PMe$_3$, PMe$_3$, PMe$_2$Ph, PMePh$_2$)....... 123

Table 3.10 Selected Bond Lengths (Å) for **7**.. 126

Table 3.11 Selected Angles (deg) for **7**... 126

Table 3.12 Summary of Crystallographic Data for **5a**......................... 143

Table 3.13 Atomic Coordinates and Equivalent Isotropic Displacement Parameters for **5a**.. 145

Table 3.14 Summary of Crystallographic Data for **7**........................... 147

Table 3.15 Atomic Coordinates and Equivalent Isotropic Displacement Parameters for **7**.. 149

Chapter 4

Table 4.1 ^{13}C NMR Data for **9** and Related Compounds................ 160

Table 4.2 Selected Bond Lengths (Å) for **9**.. 165

Table 4.3 Selected Angles (deg) for **9**.. 166

Table 4.4 Ring Slip Values for **9** and Related (η^5-C_9H_7)RhL_2 Compounds.. 169

Table 4.5 ^{1}H NMR Data for **9** and **10a-b**.. 172

Table 4.6 ^{13}C NMR Data for **9** and **10a-b**... 173

Table 4.7 ^{13}C NMR Data (Carbonyl Region) for **9** and **10a-b**........... 175

Table 4.8 ^{1}H NMR Data for **11a-b** and Related Compounds.......... 178

Table 4.9 ^{13}C NMR Data for **11a-b** and Related Compounds......... 179

Table 4.10 Summary of Crystallographic Data for **9**........................... 195

Table 4.11 Positional (x 10^4) and Isotropic Displacement (x 10^2) Parameters for **9**... 197

Chapter 5

Table 5.1 FT-IR Data for Heterodimetallacyclobutenes................... 208

Table 5.2 ^{1}H NMR Data for Heterodimetallacyclobutenes............. 210

Table 5.3 ^{13}C NMR Data for Ring Carbons in [μ-η^1:η^1-(CF_3)CCH]$Os(CO)_4M$(η^5-C_5R_5)(CO)..................... 212

Table 5.4 Selected Bond Lengths (Å) for **15**....................................... 217

Table 5.5 Selected Angles (deg) for **15**.. 217

Table 5.6 Activation Parameters for CO Exchange in (μ-TFP)$Os(CO)_4M$(η^5-C_5R_5)(CO) (R = Me, M = Rh, Ir; R = H, M = Rh)................................ 233

Table 5.7 Activation Parameters for CO Exchange in [μ–η^3:η^1-(CF_3)CCHC(O)]$Os(CO)_4CoCp^*$............................ 240

Table 5.8 Summary of Crystallographic Data for **15** 246

Table 5.9 Positional (x10^3) and Isotropic Thermal (x10^2) Parameters for **15** 248

Chapter 6

Table 6.1 FT-IR Data for $[(CH_3)CCH]Os(CO)_4M(CO)_2Cp$, (M = Co, Rh, Ir) 257

Table 6.2 ^1H NMR Data for $[(CH_3)CCH]Os(CO)_4M(CO)_2Cp$, (M = Co, Rh, Ir) 258

Table 6.3 ^{13}C NMR Data for $[\mu\text{-}\eta^1\text{:}\eta^1\text{-}(CH_3)CCHC(O)]\text{-}Os(CO)_4M(CO)Cp$, (M = Co, Rh, Ir) 260

Table 6.4 $C_\alpha\text{-}C_{acyl}$ Coupling Data for $[\mu\text{-}\eta^1\text{:}\eta^1\text{-}(CH_3)CCHC(O)]Os(CO)_4M(CO)Cp$, (M = Co, Rh, Ir) 263

Table 6.5 Selected Bond Lengths (Å) for **17b** 267

Table 6.6 Selected Angles (deg) for **17b** 267

Table 6.7 FT-IR Data for $[\mu\text{-}\eta^1\text{:}\eta^1\text{-}C_2(CH_3)_2C(O)]\text{-}Os(CO)_4M(CO)Cp$, (M = Co, Rh, Ir) 272

Table 6.8 ^1H NMR Data for $[\mu\text{-}\eta^1\text{:}\eta^1\text{-}C_2(CH_3)_2C(O)]\text{-}Os(CO)_4M(CO)Cp$, (M = Co, Rh, Ir) 273

Table 6.9 ^{13}C NMR Data for $[\mu\text{-}\eta^1\text{:}\eta^1\text{-}C_2(CH_3)_2C(O)]\text{-}Os(CO)_4M(CO)Cp$, (M = Co, Rh, Ir) 273

Table 6.10 Activation Parameters for CO Exchange in $[\mu\text{-}\eta^1\text{:}\eta^1\text{-}(CH_3)C_2RC(O)]Os(CO)_4Ir(CO)Cp$ 281

Table 6.11 Summary of Crystallographic Data for **17b** 293

Table 6.12 Fractional Coordinates and Isotropic Thermal Parameters for **17b** 295

Table 6.13 Selected Weighted Least-Squares Planes 296

Chapter 7

Table 7.1 Assignment of IR Bands in
cis-$Os(CO)_4(\eta^1\text{-}CH{=}C{=}CH_2)Cl$ 305
Table 7.2 IR Data for σ-Allenyl Complexes 306
Table 7.3 ^1H NMR Data for **21** and Related Compounds 308
Table 7.4 ^{13}C NMR Data for **21** and Related Compounds 311

Chapter 8

Table 8.1 ^{13}C NMR Data for $Os(CO)_4(\eta^2\text{-}RCC'R')$ Species 332
Table 8.2 FT-IR Bands for $M(CO)_3(\eta^4\text{-}C_4R_4CO)$
(M = Ru, Os; R = Me, Et, n-Pr) 338
Table 8.3 ^{13}C NMR Data for $M(CO)_3(\eta^4\text{-}C_4R_4CO)$
(M = Ru, Os; R = Me, Et, n-Pr) 342
Table 8.4 ^{13}C NMR Data for $Os(CO)_3(C_4R_2R_2'CO)$
(R' = Et, n-Pr) 345
Table 8.5 FT-IR Bands for $Os(CO)_3(C_4Me_2R'_2CO)$
(R' = Et, n-Pr) 347
Table 8.6 Selected Bond Lengths (Å) for **25a** 351
Table 8.7 Selected Angles (deg) for **25a** 351
Table 8.8 Summary of Crystallographic Data for **25a** 373
Table 8.9 Positional ($x10^3$) and Isotropic Thermal ($x10^2$)
Parameters for **25a** 375
Table 8.10 Selected Weighted Least-Squares Planes 376

Appendix

Table A.1 Rate and Temperature Data for Carbonyl Scrambling in **14a** 396

List of Figures

Chapter 2

Figure 2.1 FT-IR Spectra of **2a** in the Carbonyl Region.................... 43

Figure 2.2 ORTEP View of [μ-$C_2H_2C(O)$]$Os(CO)_4IrCp(CO)$, **3**........... 60

Figure 2.3 Variable Temperature ^{13}C NMR Spectra of **2b** (Carbonyl Region).. 66

Figure 2.4 Variable Temperature ^{13}C NMR Spectra of **3** (Carbonyl Region).. 70

Figure 2.5 Low Temperature Photolysis Apparatus......................... 84

Figure 2.6 Set-up for External Photolysis.. 85

Chapter 3

Figure 3.1 ORTEP View of [μ-$C(O)C_2H_2$]$Os(CO)_3RhCp(PMe_2Ph)$, **5a**.......................... 107

Figure 3.2 Alternate ORTEP View of [μ-$C(O)C_2H_2$]$Os(CO)_3RhCp(PMe_2Ph)$, **5a**.......................... 108

Figure 3.3 Variable Temperature ^{13}C NMR Spectra of [μ-$C(O)C_2H_2$]$Os(CO)_3RhCp(PMePh_2)$, **5b**.......................... 113

Figure 3.4 Variable Temperature ^{1}H NMR Spectra of **5a**................ 116

Figure 3.5 ORTEP View of [μ–η^1:η^2-$HCCH(PMe_3)$](μCO)$Os(CO)_3MCp$, **7**.................. 125

Chapter 4

Figure 4.1 ORTEP View of [μ-η^1:η^1-$C_2H_2C(O)$]-(μ-CO)$_2Os(CO)_2(PMe_3)Rh(\eta^5$-$C_9H_7)$, **9**.............................. 164

Figure 4.2 ^{13}C NMR of **10b** in the Carbonyl Region.......................... 174

Chapter 5

Figure 5.1 $^{1}H\{^{19}F\}$ NMR Experiment on Alkyne Proton of **14b**...... 211

Figure 5.2 ORTEP View of $(OC)_4Os(\mu\text{-}TFP)IrCp^*(CO)$, **15**................. 216

Figure 5.3 Variable Temperature ^{13}C NMR of **15**
in the Carbonyl Region.. 228

Figure 5.4 ^{13}C NMR Spectra of **14a** and **14b**
in the Carbonyl Region.. 231

Figure 5.5 Magnetization Transfer Experiment on **15** at -75 °C....... 232

Figure 5.6 Variable Temperature ^{13}C NMR of **16**
in the Carbonyl Region.. 238

Chapter 6

Figure 6.1 Selective $^{13}C\{^{1}H\}$ NMR Experiments on
Acyl Carbon of **17c**.. 261

Figure 6.2 ORTEP View of $[\mu\text{-}\eta^1{:}\eta^1\text{-}(CH_3)CCHC(O)]$-
$Os(CO)_4Rh(CO)Cp$, **17b**... 265

Figure 6.3 Alternate ORTEP View of $[\mu\text{-}\eta^1{:}\eta^1\text{-}(CH_3)CCHC(O)]$-
$Os(CO)_4Rh(CO)Cp$, **17b** Looking Down Ring Plane........ 266

Figure 6.4 Variable Temperature ^{13}C NMR of **18c**
in the Carbonyl Region.. 277

Figure 6.5 ^{13}C NMR of $[\mu\text{-}\eta^1{:}\eta^1\text{-}C_2(CH_3)_2C(O)]$-
$Os(CO)_4Co(CO)Cp$, **18a**, at Ambient Temperature.......... 280

Chapter 8

Figure 8.1 ^{13}C NMR of **24a**, **24b** and **25a** in the Ring Region........... 346

Figure 8.2 Perspective View of **25a**.. 349

Figure 8.3 'Ball-and-Stick Representation of
Cyclopentadienone Ring Skeleton of **25a**.......................... 350

Appendix

Figure A.1 Variable Temperature ^{13}C NMR Spectra for **14a**
in the Carbonyl Region.. 394
Figure A.2 Simulated ^{13}C NMR Spectra for **14a**
in the Carbonyl Region.. 395

List of Schemes

Chapter 1

Scheme 1.1 Molecular Orbital Diagram for Octahedral ML_6 Complex 2
Scheme 1.2 MO Diagram for Carbon Monoxide 3
Scheme 1.3 Pictorial Representation of CO 5σ Orbital 3
Scheme 1.4 M-CO Bonding 4
Scheme 1.5 Canonical Forms of M-CO Bonding 5
Scheme 1.6 Bonding Interactions in ML_5 Fragment (C_{4v} symmetry) 6
Scheme 1.7 Comparison of d^7-ML_5 to Methyl Radical 7
Scheme 1.8 Metal-Alkyne Bonding 8
Scheme 1.9 Four-Electron Metal-Alkyne Bonding 10
Scheme 1.10 Interaction Diagram for $M(CO)_4(\eta^2$-alkyne) 11
Scheme 1.11 Preparation of $Os(CO)_4(\eta^2-C_2H_4)$ 12
Scheme 1.12 Preparation of $Os(CO)_4(\eta^2$-alkyne) 13
Scheme 1.13 Reaction of $Os(CO)_4(\eta^2-C_2H_2)$ with PMe_3 14
Scheme 1.14 Labilization of CO in $Os(CO)_4(\eta^2$-alkyne) 14
Scheme 1.15 Interaction Between $\pi_\perp$ and d_{yz} Orbitals in $Os(CO)_4(\eta^2-C_2H_2)$ 15
Scheme 1.16 Structure of $Ir(PMe_2Ph)_3(C_2Me_2)^+$ 17
Scheme 1.17 Interaction Diagram for $Ir(PMe_2Ph)_3(C_2Me_2)^+$ 18
Scheme 1.18 Reaction of $M(CO)_4(\eta^2$-HFB) with $M(CO)_5$ (M = Ru, Os) 19
Scheme 1.19 Reaction of $Os(CO)_4(\eta^2-C_2H_2)$ with $M(CO)_5$ (M = Ru, Os) 20

Scheme 1.20 Synthesis of $Ir_2Cl_2(CO)_2(\mu\text{-}C_2R_2)(\mu\text{-dppm})_2$ ($R = CF_3, CO_2Me$)........ 21

Scheme 1.21 Synthesis of $Cp_2Ir_2(CO)_2(\mu\text{-}C_6H_4)$........ 22

Scheme 1.22 Synthesis of $(\mu\text{-HFB})Pt_2(COD)_2$........ 23

Scheme 1.23 Synthesis of $CpMo(CO)(\mu\text{-}CO)(PPh_3)\text{-}(\mu\text{-}C_2Ph_2)Re(CO)_3$........ 24

Scheme 1.24 Interaction Diagram for $Os_2(CO)_8(\mu\text{-}C_2H_2)$........ 25

Scheme 1.25 Synthesis of $[\mu\text{-}C_2(CF_3)_2C(O)]Cp_2Rh(CO)_2$........ 27

Scheme 1.26 Synthesis of $[\mu\text{-}\eta^3\text{:}\eta^1\text{-}C_2Ph_2C(O)](\mu\text{-}CO)M_2Cp_2(CO)$.... 29

Scheme 1.27 Synthesis of $[\mu\text{-}\eta^3\text{:}\eta^1\text{-}C_2H_2C(O)]Ru_2(CO)_6(\mu\text{-dppm})$... 29

Chapter 2

Scheme 2.1 Synthesis of Acetylene Bridged Os-M (M = Co, Rh, Ir) Complexes........ 41

Scheme 2.2 Representation of Stretching Bands for $Os(CO)_4$ Unit in **2a** and **2b**........ 44

Scheme 2.3 Turnstile Exchange in **2a** and **2b**........ 67

Scheme 2.4 Truncated Merry-Go-Round Exchange in **3**........ 71

Scheme 2.5 Proposed Mechanism for Formation of **2**........ 76

Scheme 2.6 ^{13}CO Equilibration in **2b**........ 78

Chapter 3

Scheme 3.1 Turnstile Exchange in $[\mu\text{-}C(O)C_2H_2]Os(CO)_3RhCp(PR_3)$ ($PR_3 = PMe_2Ph$, **5a**; $PMePh_2$, **5b**)........ 114

Scheme 3.2 Fluxional Behaviour of Alkyne Bridge in **5a** and **5b**........ 117

Scheme 3.3 Formation of $[\mu\text{-}\eta^1{:}\eta^2\text{-HCCH(PR}_3)](\mu\text{-CO})$-$\mathrm{Os(CO)_3MCp}$ (M = Rh, $\mathrm{PR_3 = PMe_3}$; M = Co, $\mathrm{PR_3 = PMe_3, PMe_2Ph, PMePh_2}$)........................ 119

Scheme 3.4 Synthesis of Zwitterionic Dimetallic Species Via Nucleophilic Attack of a Bridging Acetylide Unit...... 129

Chapter 4

Scheme 4.1 Proposed Pathway for Formation of **10a-b**.................... 183

Scheme 4.2 Alternate Mechanism for the Formation of **10a-b**...... 184

Scheme 4.3 Plausible Pathway for Formation of **11a-b**.................... 185

Scheme 4.4 Formation of **9**; Plausible Pathway................................. 187

Chapter 5

Scheme 5.1 Synthesis of $[\mu\text{-(CF}_3)\mathrm{CCH]Os(CO)_4M(\eta^5\text{-}C_5R_5)(CO)}$ (R = Me, M = Rh, Ir; R = H, M = Rh)............................ 207

Scheme 5.2 Alkyne Molecular Orbitals in $\mathrm{M_2}(\mu\text{-TFP})$ Complexes.. 220

Scheme 5.3 Mechanism for Formation of $[\mu\text{-(CF}_3)\mathrm{CCH}]$-$\mathrm{Os(CO)_4MCp'(CO)}$ (Cp*: M = Rh, Ir, Cp: M = Rh)........ 222

Scheme 5.4 Alternate Mechanism for Formation of $[\mu\text{-(CF}_3)\mathrm{CCH]Os(CO)_4MCp'(CO)}$ (Cp*: M = Rh, Ir, Cp: M = Rh).. 224

Scheme 5.5 Postulated Mechanism for ^{13}CO Exchange in $[\mu\text{-(CF}_3)\mathrm{CCH]Os(CO)_4MCp'(CO)}$ (Cp*: M = Rh, Ir, Cp: M = Rh).. 225

Scheme 5.6 Alternate Mechanism for ^{13}CO Exchange in $[\mu\text{-}(CF_3)CCH]Os(CO)_4MCp'(CO)$ (Cp^*: M = Rh, Ir, Cp: M = Rh) 226
Scheme 5.7 Truncated Merry-Go-Round Exchange in **15** 229
Scheme 5.8 Reaction of $Os(CO)_4(\eta^2\text{-}TFP)$ with $Cp^*Co(CO)_2$ 236
Scheme 5.9 Mechanism for Formation of $[\mu\text{-}\eta^3{:}\eta^1\text{-}(CF_3)CCHC(O)]Os(CO)_4CoCp^*$, **16** 237
Scheme 5.10 Turnstile Carbonyl Exchange Mechanism 239

Chapter 6

Scheme 6.1 Structure of $Os(CO)_4(\eta^2\text{-}C_2H_4)$ and **17b** 270
Scheme 6.2 Truncated-Merry-Go- Round Carbonyl Exchange for **18c** 279
Scheme 6.3 Proposed Mechanism for the Formation of **17a-c** 284

Chapter 7

Scheme 7.1 Preparation of $Os(CO)_4(\eta^1\text{-}CH{=}C{=}CH_2)Cl$, **21** 303
Scheme 7.2 Representation of CO Bands for *trans*-$Os(CO)_4(CHCCH_2)Cl$ 304
Scheme 7.3 Representation of CO Bands for *cis*-$Os(CO)_4(CHCCH_2)Cl$ 304
Scheme 7.4 Mechanism for Formation of $Os(CO)_4(\eta^1\text{-}CH{=}C{=}CH_2)Cl$ 312
Scheme 7.5 [1, 3] Pt Rearrangement in $Pt(Br)(PPh_3)_2(\eta^1\text{-}CH_2C_2Ph)$ 313
Scheme 7.6 Mechanism for Formation of **21** via Nucleophilic Attack 315

Scheme 7.7 Reaction of η^3-Allenyls with Nucleophiles................. 317

Chapter 8

Scheme 8.1 Representation of Vibrational Bands in $Os(CO)_4(\eta^2\text{-}C_2Me_2)$.. 330

Scheme 8.2 Representation of Vibrational Modes in $M(CO)_3(\eta^4\text{-}C_4R_4CO)$.. 337

Scheme 8.3 Orbital Interaction Between $Os(CO)_3$ Fragment and Butadiene... 353

Scheme 8.4 Possible Mechanisms for Formation of **25a-b**.............. 355

Scheme 8.5 Generation of a Ruthenacyclobutenone........................ 356

Scheme 8.6 Generation of an Osmacyclobutenone........................... 358

Scheme 8.7 Proposed Pathway for Formation of **25a-b**.................... 359

Scheme 8.8 $Ru(CO)_3(C_4Ph_4CO)$ as a Catalytic Precursor................. 362

Scheme 8.9 Proposed Mechanism for Catalytic Disproportionation of Aldehydes.................................. 363

List of Abbreviations and Symbols

Å	Angström(s)
anal.	analyses
APT	attached proton test
atm	atmosphere(s)
br	broad
b.p.	boiling point
BTMSA	bis(trimethylsilyl)acetylene, $C_2(Si(CH_3)_3)_2$
ca.	circa (approximately)
calcd	calculated
COE	cyclooctene
Cent	centroid
Cp	cyclopentadienyl, C_5H_5
Cp^*	pentamethylcyclopentadienyl, $C_5(CH_3)_5$
COD	1, 5-cyclooctadiene
Cy	cyclohexyl, C_6H_{11}-
δ	chemical shift (TMS, trimethylsilane, $Si(CH_3)_4$)
Δ	ring slippage parameter (reference to X-ray results)
Δ	chemical shift difference (reference to NMR results)
d	doublet
DANTE	Delays Alternating with Nutations for Tailored Excitation
dd	doublet of doublets
ddd	doublet of doublets of doublets
deg	degree(s)
DMAD	dimethyl acetylenedicarboxylate, $C_2(CO_2CH_3)_2$

dmpm	bis(dimethylphosphino)methane, $(CH_3)_2PCH_2P(CH_3)_2$
dppm	bis(diphenylphosphino)methane, $(C_6H_5)_2PCH_2P(C_6H_5)_2$
dq	doublet of quartets
E.I.	electron impact
esd	estimated standard deviation
Et	ethyl, CH_3CH_2-
eV	electron volt(s)
FAB	fast atom bombardment
FT-IR	Fourier Transform Infrared
GWV	Glaswerk Wertheim
h	hour(s)
H.A.	hinge angle
HFB	hexafluoro-2-butyne, $C_2(CF_3)_2$
HOMO	Highest Occupied Molecular Orbital
hv	radiation
Hz	Hertz
J	coupling constant
K	Kelvin
λ	wavelength
LUMO	Lowest Unoccupied Molecular Orbital
m	multiplet (reference to NMR spectra)
m	medium (reference to IR spectra)
Me	methyl, CH_3-
mg	milligrams
MHz	megahertz

mL	milliliters
mmol	millimoles
MS	mass spectrometry
nm	nanometers
NMR	nuclear magentic resonance
Nu	nucleophile
n-Pr	n-propyl, $CH_3CH_2CH_2$-
ν	stretching frequency
$\Delta\nu_{1/2}$	linewidth at half-height
Ph	phenyl, C_6H_5-
ppm	parts per million
q	quartet
qd	quartet of doublets
s	second(s)
s	singlet (with reference to NMR spectra)
s	strong (with reference to IR spectra)
t	triplet
τ	delay time (DANTE experiments)
T_1	relaxation time
^{t}Bu	tertiary-butyl, $C(CH_3)_3$-
tfac	1,1,1-trifluoro-2,4-cylopentedionate
TFP	trifluoropropyne, $HCC(CF_3)$
THF	tetrahydrofuran
w	weak
v	very

Chapter 1

Introduction

1.1. Synergic Bonding in Transition Metal Complexes and the Eighteen Electron Rule

Organometallic compounds, as defined by Yamamoto, are *organic compounds with direct metal-carbon bonds*.[1] The great majority of organometallic complexes obey what has become known as the eighteen electron rule. Put simply, the sum of the metal valence electrons and the electrons donated by the ligands should total eighteen.[2] In many ways, the eighteen electron rule is the organometallic equivalent of the familiar octet rule. For example, a carbon atom has four valence orbitals, one 2*s* and three 2*p* orbitals. Placing an electron pair in each of these orbitals, or an electron pair in each of the four sp^3 hybrid orbitals, will satisfy the octet rule for a total of eight electrons. In an organometallic complex, there are a total of nine valence orbitals; one n*s*, three n*p* and five (n-1)*d* orbitals. These will combine with the ligand orbitals to form molecular orbitals, nine of which are either bonding or non-bonding; the remainder are anti-bonding. Thus, the number of electrons required to completely fill the bonding and non-bonding orbitals is eighteen, forming the basis of the eighteen electron rule. This is shown in Scheme 1.1.

However, the diagram does not fully illustrate the subtleties of the eighteen electron rule. If the ligand field splitting energy, Δ_o, is small due to the presence of weak to moderate field ligands then complexes with more than eighteen electrons may result. This is the case with $Ni(H_2O)_6^{2+}$ which has twenty valence electrons. Since Δ_o is small, the placement of two electrons in the anti-bonding e_g^* orbitals has only a slight destabilizing effect, and this loss in energy is more than compensated by the sixth Ni-

OH_2 bond formation. If strong field ligands with little or no π bonding interactions are present then Δ_o is large and complexes with less than eighteen valence electrons are possible. The large Δ_o value prevents population of the e_g^* orbitals and, while the metal-ligand bonding orbitals are filled, the non-bonding t_{2g} orbitals do not necessarily have to be occupied. An example is $Mo(NCS)_6^{2-}$ which has only fourteen valence electrons. For organometallic complexes, the eighteen electron rule is most often obeyed for compounds in which the metal is in a relatively low oxidation state and complexed to the π-acidic type of ligands that are near the top of the spectrochemical series. This leads into the concept of synergic bonding.

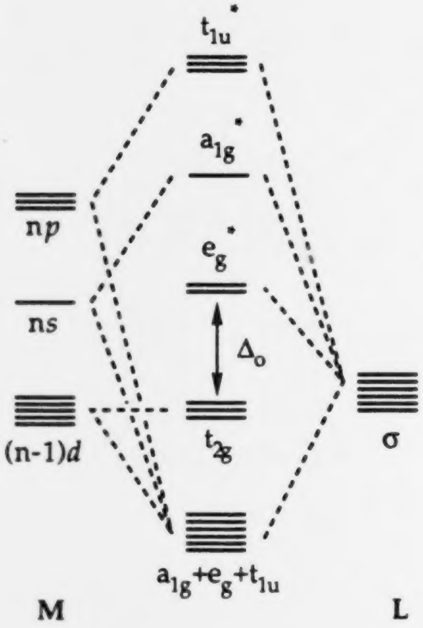

Scheme 1.1: Molecular Orbital Diagram for Octahedral ML_6 Complex

The development of Crystal Field Theory relied on a purely electrostatic approach dealing with the attraction between the positively charged metal nucleus and the lone pair of electrons on the incoming ligand.[3] Thus, the metal centre acts as a Lewis acid and the ligand as a Lewis base. However, this electrostatic approach failed to explain the strong bonding of carbon monoxide to metal centres as CO is only a weak donor ligand. To aid in the explanation of this phenomenon, a simplified Molecular Orbital Diagram of the CO ligand, showing the HOMO and LUMO orbitals, is shown in Scheme 1.2.[2b]

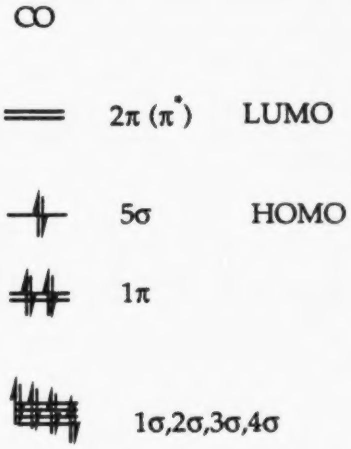

Scheme 1.2: MO Diagram for Carbon Monoxide

The 5σ orbital has a significant contribution from the carbon 2*s* orbital and only a small contribution from the oxygen 2*p* orbital. Thus, this orbital represents the lone pair on the carbon atom and since it is also the HOMO orbital of CO, it donates electron density to the metal centre. A valence bond representation of this orbital in shown in Scheme 1.3.

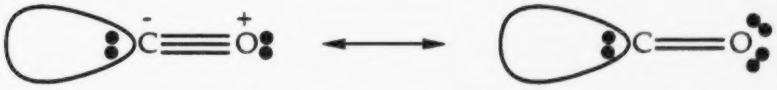

Scheme 1.3: Pictorial Representation of CO 5σ Orbital

The lowest unoccupied molecular orbitals (LUMO) of CO are the 2π orbitals that are simply the anti-bonding or π^* molecular orbitals.

In Scheme 1.1, the non-bonding t_{2g} set represents the triply degenerate metal d_{xy}, d_{xz} and d_{yz} orbitals. In low oxidation state metal complexes, some or all of these orbitals are filled. The metal-CO bonding consists of two separate components; one σ in nature, the other a π interaction. This bonding is shown in Scheme 1.4.

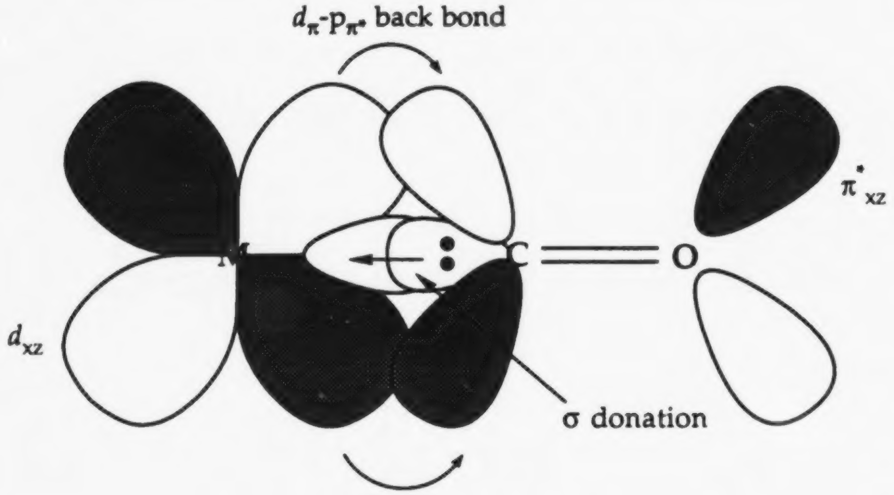

Scheme 1.4: M-CO Bonding

The above scheme shows the bonding in the xz plane; it is important to note that another $d_\pi \rightarrow p_{\pi^*}$ bonding interaction occurs in a perpendicular plane. The metal to carbonyl interaction is referred to as backbonding. Although the σ and π bonding systems were considered separately, they are reliant upon one another. As OC→M donation increases the electron density at the metal centre, it is relieved by the $d_\pi \rightarrow p_{\pi^*}$ backbonding. This is a synergic chemical bonding. This backbonding also increases the M-CO bond order and concomitantly decreases the C-O bond order, as seen in Scheme 1.5.

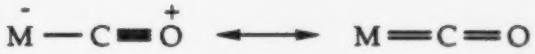

$$\overset{-}{M}-C\equiv\overset{+}{O} \longleftrightarrow M=C=O$$

Scheme 1.5: Canonical Forms of M-CO Bonding

The synergic M-CO bonding has important implications regarding the eighteen electron rule. Since the t_{2g} orbitals interact strongly with the CO 2π orbitals it is important that they are filled. This interaction also lowers the energy of the t_{2g} set, increasing Δ_o, and stabilizes the complex. Thus, it is not only important to have the maximum number of t_{2g} electrons to interact with the CO 2π orbitals but to ensure that the anti-bonding e_g^* orbitals remain empty. In the case of an octahedral d^6 complex, there are six d electrons in the t_{2g} set and twelve electrons donated by the ligands for a total of eighteen. In non-octahedral geometries, the d orbitals not involved in σ bonding will form π interactions. Thus, for eighteen electron complexes, coordination number and electron count are intimately related and dependent upon the presence of π-acidic ligands such as carbon monoxide and phosphines.

1.2. The Isolobal Analogy

The isolobal analogy, championed by Roald Hoffmann, is a way of providing a link between organic and organometallic chemistry.[4] Essentially, frontier orbitals of organometallic fragments are constructed and then compared to those of simple organic building blocks such as CH_3, CH_2 and CH. A library of inorganic fragments may then be built; a process called "isolobal mapping". The next question is, exactly how are these frontier orbitals constructed?

One can start using an octahedral complex with six bonding hybrid orbitals, six anti-bonding hybrid orbitals and the three metal orbitals of the t_{2g} set (Scheme 1.1). In the case of $W(CO)_6$, this results in a closed shell. However, if only five ligands interact with the metal centre but the parent octahedral symmetry is partially retained (C_{4v} symmetry), a different situation results (Scheme 1.6).[4c]

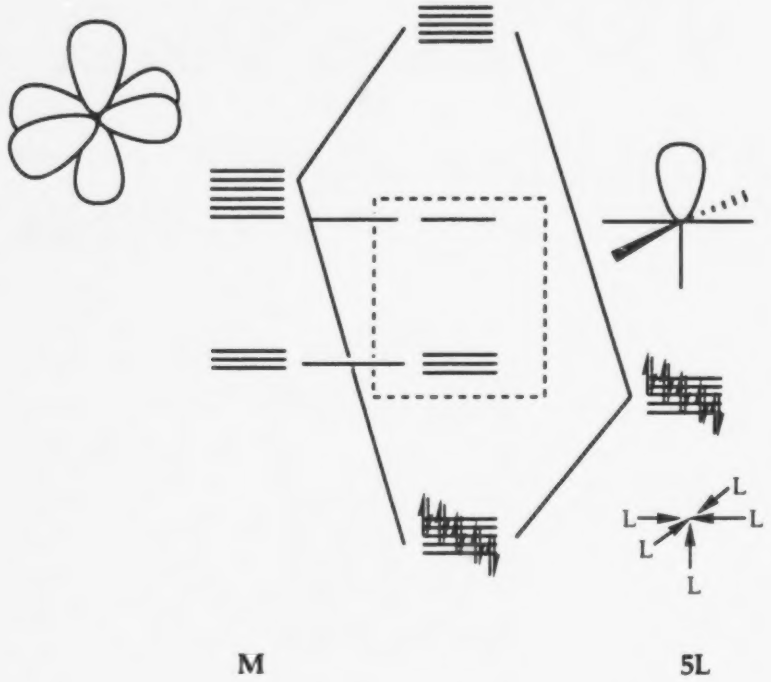

Scheme 1.6: Bonding Interactions in ML_5 Fragment (C_{4v} symmetry)

The metal *d* electrons occupy the frontier orbitals, namely the t_{2g} set and the remaining high energy hybrid orbital not involved in the M-L σ bonding. In the case of Mn^0, seven electrons are placed in these orbitals. Thus, a d^7-ML_5 fragment is similar to a methyl radical (Scheme 1.7).[4c] The term isolobal indicates that the frontier orbitals of two fragments are similar. In other words, the number, shape, symmetry and approximate energies of the frontier orbitals are comparable.

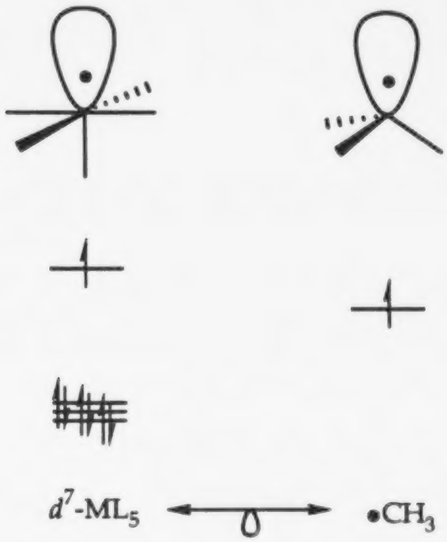

Scheme 1.7: Comparison of d^7-ML$_5$ to Methyl Radical

The two-headed arrow with a tear-drop indicates that the fragments are isolobal to one another. Since a d^8-ML$_5$ fragment has one more electron in its frontier orbital it would be isolobal to CH_3^- and to NH_3. Following this line of reasoning, a d^6-ML$_5$ fragment would be isolobal to CH_3^+ and to BH_3. As well, the mapping can be extended to include ligands such as PR_3 and η^5-C_5H_5. The phosphine is considered equivalent to a carbonyl while the cyclopentadienyl ligand is counted as an anionic six-electron donating ligand, equivalent to three carbonyls. It is important to note that the frontier orbitals of the organic and organometallic fragments will not be exactly the same. Therefore, although the isolobal analogy is useful in rationalizing organometallic structures and has synthetic predictive power, exceptions to the isolobal analogy are not uncommon.

1.3. Alkyne Bonding to Transition Metal Complexes

1.3.1. General Description of Bonding

The synergic bonding between a metal centre and a carbonyl has been explained previously; the bonding between a metal and an alkyne is also synergic. The Dewar-Chatt-Duncanson model, initially formulated to account for metal-olefin bonding, can be used to explain the interaction between a metal and an alkyne.[5] A qualitative picture of this bonding is shown is Scheme 1.8.

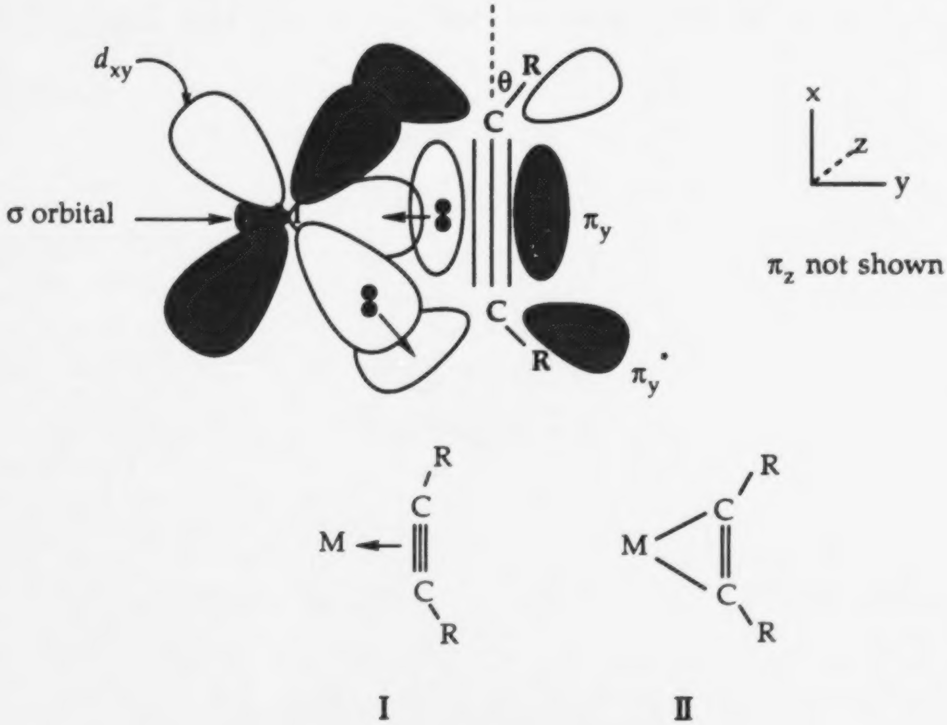

Scheme 1.8: Metal-Alkyne Bonding

The alkyne formally donates an electron pair from its filled π_y orbital to a hybrid orbital on the metal centre. This is the σ component of the bonding. The metal→alkyne backbonding is electron donation from the metal d_{xy} orbital to the π_y^* orbital of the alkyne. Forms I and II represent the limiting formulations of metal-alkyne bonding. In I, there is only limited backbonding and the alkyne should have short C-C bond distances and C-C-R angles approaching linear values. In II, extensive metal→alkyne backbonding will lengthen the C-C triple bond so that the structure can best be described as a metallacyclopropene. As the backbonding increases, the substituents on the carbon atoms will bend back by an angle θ. Structure II is favoured for alkynes with electron withdrawing substituents that lower the energy of the π^* orbitals, making them more accessible for backbonding interactions.[6]

The above description assumes that the alkyne is acting as a two electron donor. However, unlike alkenes, alkynes have two filled π molecular orbitals. Both of these π orbitals may interact with the metal centre, allowing the alkyne to act as a formal four electron donating ligand.[7] The additional metal-alkyne interaction is shown in Scheme 1.9, the full four electron picture is the sum of Schemes 1.8 and 1.9. For clarity, the interaction has been separated into the π and δ components. Due to the poor orbital overlap, the δ-bonding interaction is quite weak. A bonding interaction between the π_z orbital with the metal d_{xz} orbital is only possible if the metal orbital is empty; if the metal orbital is occupied, a repulsive interaction may occur. This possible scenario will be addressed in a later section. Finally, the valence bond representations of the four electron donation case are indicated by III and IV.

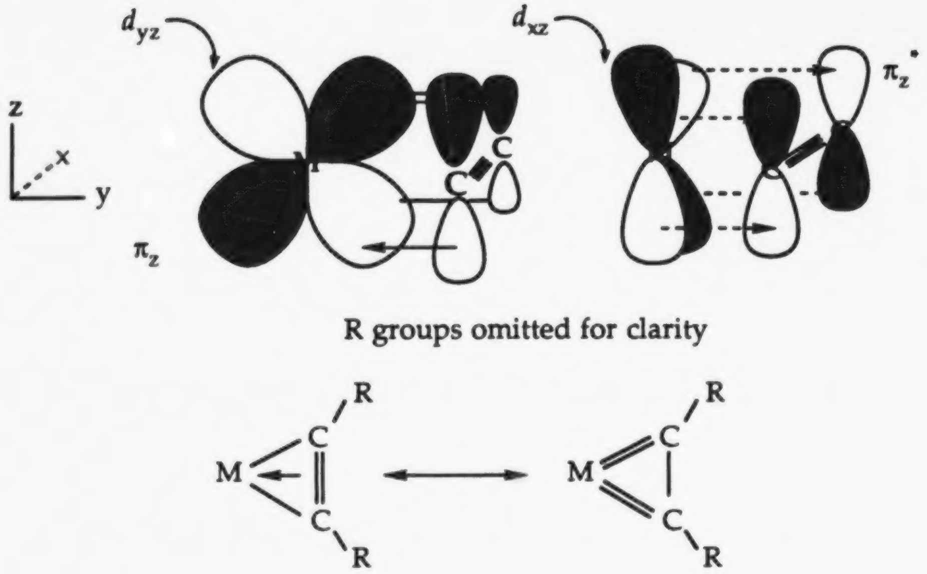

R groups omitted for clarity

III IV

Scheme 1.9: Four-Electron Metal-Alkyne Bonding

1.3.2. Alkyne Bonding to $M(CO)_4$ (M = Fe, Ru, Os) Fragment

The bulk of the work in this thesis is centred around reactions involving $Os(CO)_4(\eta^2\text{-alkyne})$ species, compounds where the alkyne acts as a two-electron donor. Thus, it is important to have at least a qualitative picture of the metal-alkyne bonding in these complexes. The binary carbonyls $M(CO)_5$ (M = Fe, Ru, Os) have trigonal bypyramidal structures. Thus, one would initially assume that $M(CO)_4(\eta^2\text{-alkyne})$ compounds would have the same geometry. X-ray crystallographic and spectroscopic studies have confirmed that the alkyne occupies an equatorial coordination site and is aligned parallel to the equatorial plane.[8,9,10] Calculations by Hoffmann have provided a qualitative picture of the $M(CO)_4$ frontier orbitals. The interaction of the $M(CO)_4$ frontier orbitals with the HOMO and LUMO orbitals of the alkyne ligand provides a rationale for the observed orientation of the alkyne.

Another way of describing the geometry of $M(CO)_4(\eta^2\text{-alkyne})$ compounds is as *cis*-$M(CO)_4L_2$ (C_{2v} symmetry) species whereby the alkyne occupies two coordination sites under octahedral geometry. The frontier orbitals of the d^8-$M(CO)_4$ fragment have been generated by Hoffmann; under C_{2v} symmetry the fragment is isolobal to methylene, CH_2. An interaction diagram is shown in Scheme 1.10 to give a qualitative picture of the metal-alkyne bonding in these complexes.[4d]

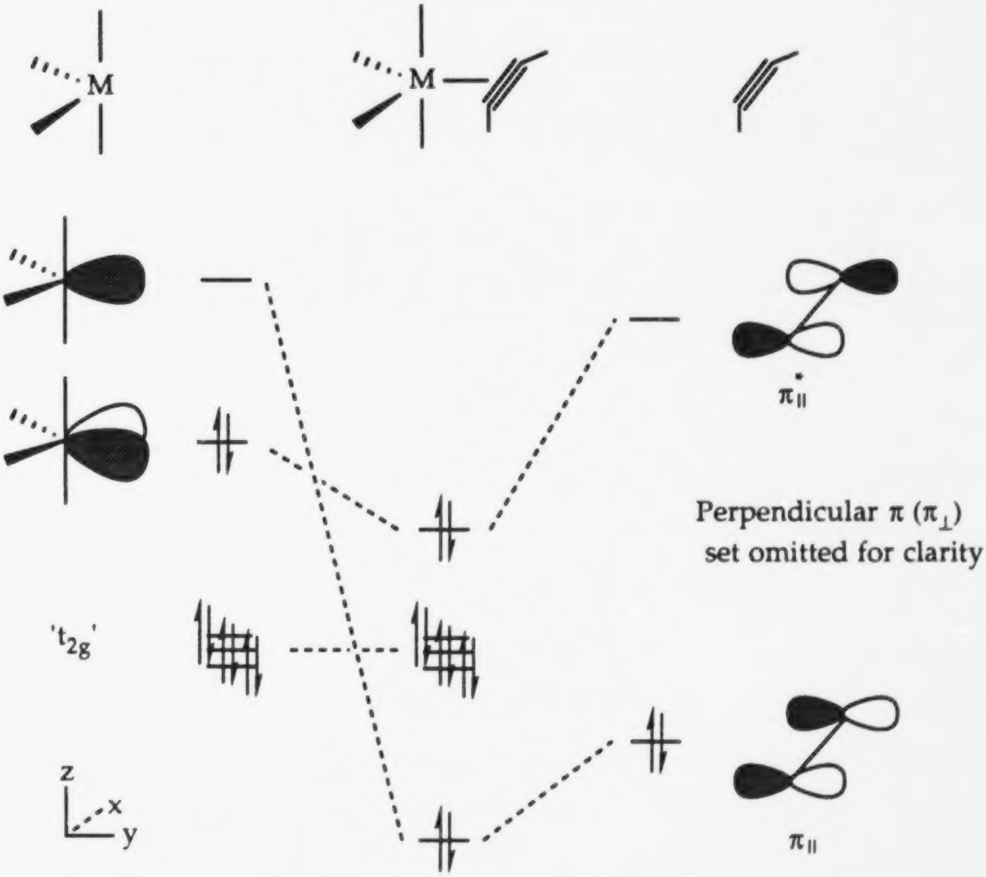
M
M
't_{2g}'
z
x
y
$\pi^*_{\parallel}$
$\pi_{\parallel}$
Perpendicular π ($\pi_{\perp}$) set omitted for clarity

Scheme 1.10: Interaction Diagram for $M(CO)_4(\eta^2\text{-alkyne})$

From the diagram it can readily be seen that the alkyne will occupy an equatorial site with an orientation parallel to the equatorial plane. This arrangement maximizes both the σ-bonding and backbonding interactions. For example, if the alkyne was orientated perpendicular to the equatorial plane, there would be a decrease in metal→alkyne backbonding as this would result in zero overlap between the occupied metal fragment frontier orbital and the $\pi_{||}^*$ orbital of the alkyne. Metal→alkyne backbonding would be possible from the metal d_{yz} orbital, but this orbital is already involved in metal→CO backbonding interactions with the two axial carbonyls.

1.4. Comparison of $Os(CO)_4(\eta^2\text{-}C_2H_2)$ to $Os(CO)_4(\eta^2\text{-}C_2H_4)$: Four Electron Destabilization

The Os-ethylene complex, $Os(CO)_4(\eta^2\text{-}C_2H_4)$, is obtained as a byproduct in the photochemical reaction of $Os_3(CO)_{12}$ with ethylene (Scheme 1.11).[11]

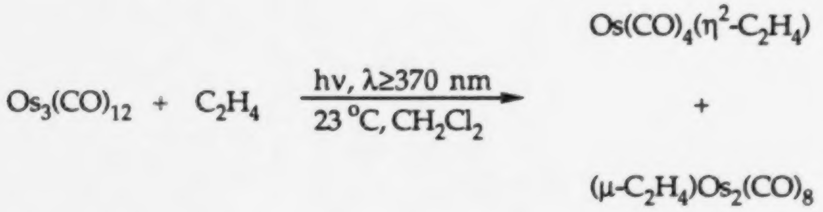

$$Os_3(CO)_{12} + C_2H_4 \xrightarrow[23\,^\circ C,\ CH_2Cl_2]{h\nu,\ \lambda \geq 370\ nm} \begin{array}{c} Os(CO)_4(\eta^2\text{-}C_2H_4) \\ + \\ (\mu\text{-}C_2H_4)Os_2(CO)_8 \end{array}$$

Scheme 1.11: Preparation of $Os(CO)_4(\eta^2\text{-}C_2H_4)$

The complex is stable in solution at room temperature for several hours, however a full investigation of its thermal stability has not been made.[12] Norton has noted that neat $Os(CO)_4(\eta^2\text{-}C_2H_4)$ yellows upon prolonged standing at room temperature.[11c]

Both $Os(CO)_4(\eta^2\text{-}C_2H_2)$ and $Os(CO)_4(\eta^2\text{-}C_2H_4)$ can be prepared *via* the photolysis of $Os(CO)_5$ in the presence of acetylene or ethylene. A general photochemical synthesis of $Os(CO)_4(\eta^2\text{-alkyne})$ species has been developed in our laboratories (Scheme 1.12); only a few representative examples are shown.[10]

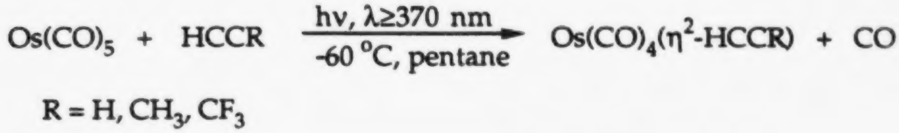

$$Os(CO)_5 + HCCR \xrightarrow[-60\ ^{o}C,\ pentane]{h\nu,\ \lambda\geq370\ nm} Os(CO)_4(\eta^2\text{-}HCCR) + CO$$

$$R = H, CH_3, CF_3$$

Scheme 1.12: Preparation of $Os(CO)_4(\eta^2\text{-alkyne})$

The resulting Os-alkyne complexes have varying degrees of thermal stability; the simple acetylene complex is only stable at temperatures below 0 °C, the propyne analogue is stable only below -15 °C. Using an activated alkyne such as trifluoropropyne enables the manipulation of the resulting complex at temperatures up to 15 °C. Thus, low temperature photochemistry offers the only rational route for the synthesis of these Os-alkyne complexes; they are too temperature sensitive for ordinary thermal methods.

For ease of discussion, only $Os(CO)_4(\eta^2\text{-}C_2H_2)$ and $Os(CO)_4(\eta^2\text{-}C_2H_4)$ will be compared. The Os-acetylene complex, $Os(CO)_4(\eta^2\text{-}C_2H_2)$, exhibits unusual reactivity. For instance, the carbonyls in $Os(CO)_4(\eta^2\text{-}C_2H_2)$ readily exchange with ^{13}CO when a solution of $Os(CO)_4(\eta^2\text{-}C_2H_2)$ is stirred under 1 atm of ^{13}CO at 0 °C.[10] In fact, a CO atmosphere suppresses the decomposition of $Os(CO)_4(\eta^2\text{-}C_2H_2)$. This is not the case for $Os(CO)_4(\eta^2\text{-}C_2H_4)$ or $Os(CO)_5$. Also, $Os(CO)_4(\eta^2\text{-}C_2H_2)$ reacts readily with PMe_3 at 0 °C resulting in the displacement of one molecule of carbon monoxide (Scheme 1.13).[12]

$$Os(CO)_4(\eta^2\text{-}C_2H_2) + PMe_3 \xrightarrow[0^{\circ}C]{\text{pentane,}} Os(CO)_3(PMe_3)(\eta^2\text{-}C_2H_2) + CO$$

Scheme 1.13: Reaction of $Os(CO)_4(\eta^2\text{-}C_2H_2)$ with PMe_3

Again, this labilization of a carbonyl ligand is not seen in the case of $Os(CO)_4(\eta^2\text{-}C_2H_4)$ which is unreactive towards phosphines at room temperature.

Thus, different reactivity patterns are seen for $Os(CO)_4(\eta^2\text{-}C_2H_2)$ and $Os(CO)_4(\eta^2\text{-}C_2H_4)$ with the major difference being the labilization of CO in the Os-acetylene complex (Scheme 1.14). The $Os(CO)_3(C_2H_2)$ intermediate can then be scavenged by two-electron donors.

$$Os(CO)_4(\eta^2\text{-alkyne}) \rightleftharpoons \text{'}Os(CO)_3(\text{alkyne})\text{'} + CO$$

Scheme 1.14: Labilization of CO in $Os(CO)_4(\eta^2\text{-alkyne})$

The difference in stability and reactivity between $Os(CO)_4(\eta^2\text{-}C_2H_2)$ and $Os(CO)_4(\eta^2\text{-}C_2H_4)$ is surprising as both are eighteen electron complexes and have an unsaturated organic molecule donating two electrons. In fact, the interaction diagram for $Os(CO)_4(\eta^2\text{-}C_2H_2)$ can also be used to describe the bonding in $Os(CO)_4(\eta^2\text{-}C_2H_4)$. The only difference is that $Os(CO)_4(\eta^2\text{-}C_2H_2)$ has an additional π orbital set perpendicular to the equatorial plane. Thus, investigations into the differing properties of $Os(CO)_4(\eta^2\text{-}C_2H_2)$ and $Os(CO)_4(\eta^2\text{-}C_2H_4)$ should centre on the role of this perpendicular π orbital set.

Odile Eisenstein partially addressed this question in a theoretical study of structural isomerism in alkyne complexes of d^8 metals.[9] In the interaction diagram (Scheme 1.10) for $Os(CO)_4(\eta^2\text{-}C_2H_2)$ the $\pi_{\perp}$ set was omitted. However, the filled d_{yz} orbital has the symmetry of the filled $\pi_{\perp}$ orbital of the acetylene and may interact (Scheme 1.15).

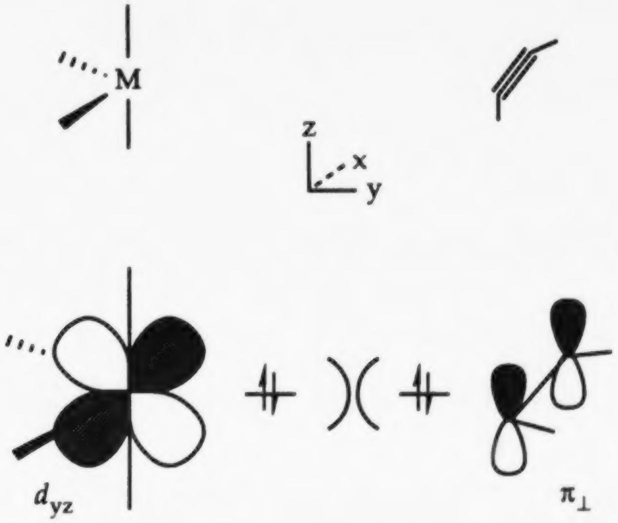

Scheme 1.15: Interaction Between $\pi_{\perp}$ and d_{yz} Orbitals in $Os(CO)_4(\eta^2\text{-}C_2H_2)$

Since both orbitals are occupied a repulsive interaction occurs; this was mentioned in Section 1.3.1. in describing four electron donation in alkynes. This interaction results in a decrease in the total bonding between the $Os(CO)_4$ fragment and the acetylene and is referred to as a four-electron destabilization. The four electron destabilization can manifest itself in the metal-alkyne bonding. Alkynes are better π acids than olefins as reflected in the higher carbonyl IR band frequencies in $Os(CO)_4(\eta^2\text{-}C_2H_2)$ as compared to $Os(CO)_4(\eta^2\text{-}C_2H_4)$.[10,11c] However, there is evidence for alkyne lability in $M(CO)_4(\eta^2\text{-alkyne})$ (M = Ru, Os) complexes, such as $Ru(CO)_4(\eta^2\text{-BTMSA})$ (BTMSA $C_2(SiMe_3)_2$) which decomposes to give $Ru_3(CO)_{12}$.[8] This decomposition can be slowed by the addition of free BTMSA. In the case of $Os(CO)_4(\eta^2\text{-}C_2H_4)$ this four electron destabilization does not exist due to the absence of a filled $\pi_{\perp}$ orbital, resulting in marked differences in reactivity.

The differences in stability between various $Os(CO)_4(\eta^2$-alkyne) complexes can also be partially explained using the four-electron destabilization model. Thermally stable compounds are formed only when acceptor ligands such as HFB (HFB: $C_2(CF_3)_2$) are used.[13] These electron withdrawing substituents delocalize the $\pi_{\perp}$ orbital, decreasing its interaction with the filled metal d_{yz} orbital.[9] The destabilization is decreased and the equilibrium in Scheme 1.14 is shifted to the left. Also, the presence of π-acidic CO ligands helps delocalize the filled metal orbitals, reducing the d_{yz}-$\pi_{\perp}$ overlap. An example of how changing the ligands and acceptor nature of the alkyne effects the equilibrium in Scheme 1.14 is available. The complex $Fe[P(OMe)_3]_3(C_2Ph_2)$ can be readily prepared and is stable at room temperature.[14] The replacement of the three carbonyls by phosphites and the presence of a only a moderately π-acidic alkyne increases the four-electron destabilization so that the equilibrium (Scheme 1.14) is shifted to the right. This compound is interesting because it gives insight into the related $Os(CO)_3$(alkyne) intermediate, thus further discussion of these d^8-ML_4 species is warranted.

Eisenstein and co-workers[9] have studied the orbital interactions for $Ir(PMe_2Ph)_3(C_2Me_2)^+$,[15] which is isoelectronic to $Fe[P(OMe)_3]_3(C_2Ph_2)$. The Ir-alkyne species has been characterized by X-ray crystallography and has approximate C_s symmetry. The phosphorus atom that lies along the mirror plane has an Ir-P bond distance significantly shorter than the other two Ir-P separations, thus it is incorrect to characterize this complex as having distorted tetrahedral geometry. However, if the alkyne carbons are considered separately, the geometry can be described as square pyramidal whereby the unique phosphorus atom occupies the axial position (Scheme 1.16).

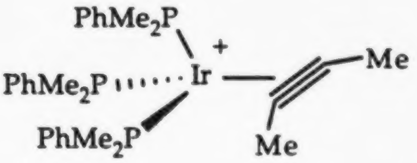

Scheme 1.16: Structure of $Ir(PMe_2Ph)_3(C_2Me_2)^+$

For the theoretical calculations, C_s symmetry was assumed as it most closely resembles the solid state structure.[9] The orbital interaction diagram for $Ir(PMe_2Ph)_3(C_2Me_2)^+$ is taken from Eisenstein's paper but is also applicable to the isoelectronic $Os(CO)_3$(alkyne) intermediate (Scheme 1.17).

The metal orbitals were taken from a d^8-ML_3 fragment of C_{3v} symmetry, although the symmetry labels are those of the C_s point group. The three low-lying orbitals are essentially non-bonding while the upper three orbitals are well suited for interaction with the incoming alkyne; the 2a" orbital is the metal fragment HOMO, 3a' the LUMO. The metal-acetylene σ bond is due to the strong overlap between the acetylene $\pi_{||}$ orbital and the metal 4a' orbital. The $\pi_{||}^*$-1a" and $\pi_{||}^*$-2a" is responsible for the metal-acetylene backbonding. There is a destabilizing interaction between the $\pi_{\perp}$ and metal 2a'. However, this is compensated by a $\pi_{\perp}$-3a' overlap that is stabilizing. Thus, the acetylene is bonded to the metal *via* three bonds, one σ, one metal→acetylene π back bond and one acetylene→metal π bond. This is referred to as four electron donation.

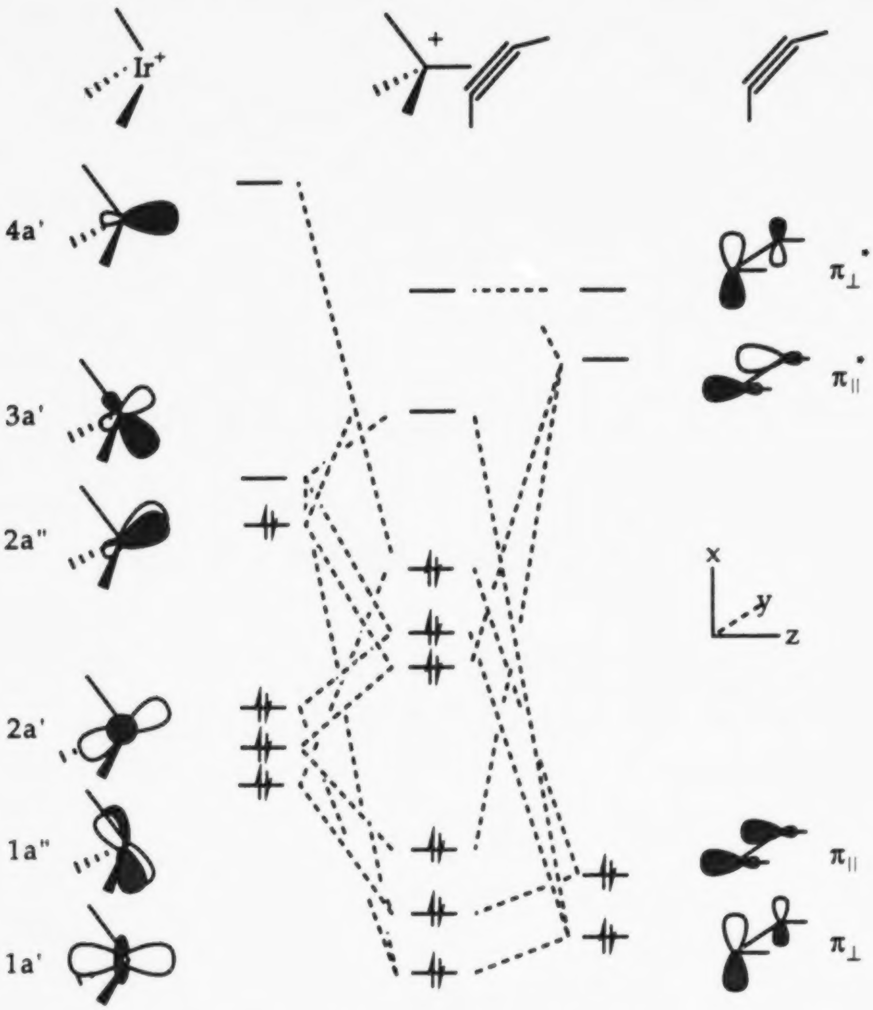

Scheme 1.17: Interaction Diagram for Ir(PMe$_2$Ph)$_3$(C$_2$Me$_2$)$^+$

For Os(CO)$_3$(alkyne), the metal 3a' orbital is significantly stabilized by donation from the acetylene $\pi_\perp$ orbital. Recall that, in Os(CO)$_4$(η^2-alkyne), this alkyne orbital was interacting with a filled metal orbital in a destabilizing manner. The rather facile CO labilization in Os(CO)$_4$(η^2-alkyne) to form the Os(CO)$_3$(alkyne) intermediate could be, in part, due to the donation of four electrons by the alkyne that relieves the four electron destabilization. Also, the metal 3a' orbital will readily add an additional ligand such as ^{13}CO, resulting in facile CO exchange. It should also be noted that $Ir(DMAD)_2(PMe_2Ph)_3^+$ is stable, rather than the mono-alkyne complexes seen with C_2Ph_2 and C_2Me_2.[9] This compound is isoelectronic to $Os(CO)_4(\eta^2\text{-}C_2H_2)$ and illustrates the importance of π-acidic ligands (and alkynes) in decreasing the four-electron destabilization.

1.5. Survey of Alkyne Bridged Dimetallic Complexes

1.5.1. Condensation Reactions Involving $M(CO)_4(\eta^2\text{-alkyne})$ (M = Ru, Os)

During the synthesis and characterization of $Ru(CO)_4(\eta^2\text{-HFB})$ a rather serendipitous discovery was made. The Ru-alkyne complex readily scavenged any $Ru(CO)_5$ in solution to form a dimetallic product of formula $(\mu\text{-HFB})Ru_2(CO)_8$. Thus, two eighteen electron species were undergoing a condensation reaction to form an alkyne bridged dimetallic species. This reactivity was displayed by the Os congener as well (Scheme 1.18).[13]

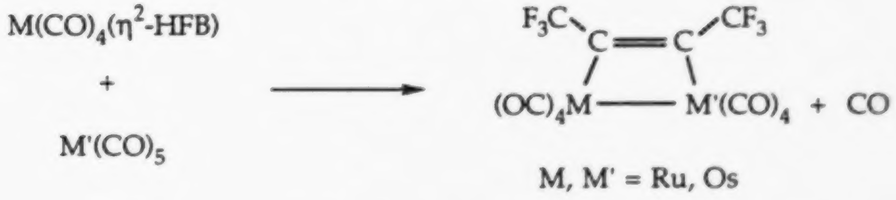

Scheme 1.18: Reaction of $M(CO)_4(\eta^2\text{-HFB})$ with $M(CO)_5$ (M = Ru, Os)

The synthesis of $Os(CO)_4(\eta^2\text{-}C_2H_2)$ led to the formation of alkyne bridged dimetallic compounds, however, additional discoveries were also made. The condensation reaction of $Os(CO)_4(\eta^2\text{-}C_2H_2)$ with $M(CO)_5$ (M = Ru, Os) displayed a rather surprising metal dependence and, in the case of $Ru(CO)_5$, two coordinatively saturated, eighteen electron species reacted to yield an eighteen electron dimetallic complex *without* ligand loss (Scheme 1.19).[10] As seen, the condensation reactions generate dimetallacyclobutenes and pentenones, both of which have been reported in the literature. However, the synthesis of alkyne bridged dimetallic compounds *via* this method is unprecedented; therefore, a brief survey of alkyne bridged dimetallic species will be given.

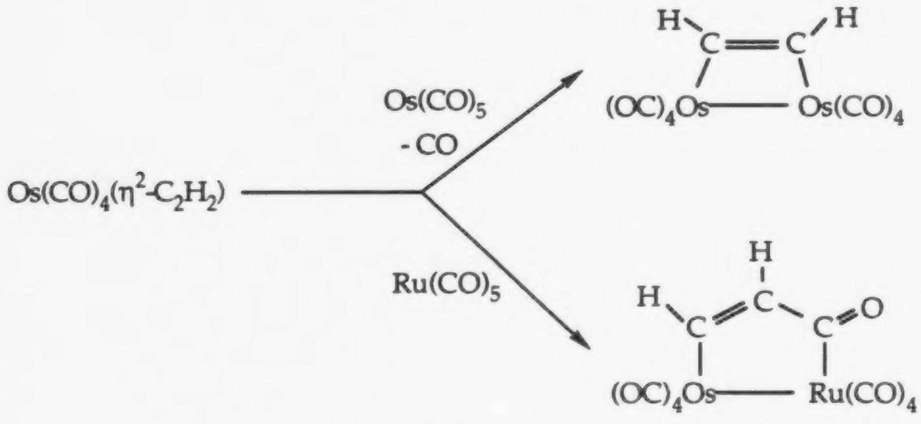

Scheme 1.19: Reaction of $Os(CO)_4(\eta^2-C_2H_2)$ with $M(CO)_5$ (M = Ru, Os)

1.5.2. Synthesis of Dimetallacyclobutene Complexes

An alkyne can bridge two metal centres in two ways; as a two electron donor (**A**) in a parallel bonding mode or as a four electron donor (**B**) such that the alkyne is orientated perpendicular to the metal-metal bond.[16]

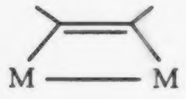

A

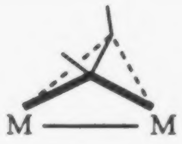

B

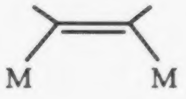

C

This discussion of alkyne-bridged dimetallic species will only centre on the alkyne as a two electron donor. Also, complexes without a metal-metal bond (**C**) which can be described as *cis*-dimetallated olefins, will not be discussed.

A number of alkyne bridged complexes (**A**) have been reported in the literature. The first report of a dimetallacyclobutene ring was made in 1970 for $Fe_2(CO)_8(\mu\text{-}C_6F_4)$.[17] Also, a theoretical molecular orbital study was made on parallel and perpendicular alkyne compounds in 1982 in which Hoffmann and co-workers published a list of complexes that had been characterized by X-ray crystallography.[16] Thus, even more than a decade ago, there was significant interest in alkyne bridged dimetallic complexes.

The synthesis of these complexes such as **A** usually involves the addition of an alkyne to a pre-formed dinuclear centre.[18] One of the most common methods is the addition of an alkyne to a M_2L_2 (L_2 = bidentate ligand) species, to generate parallel-bridged acetylene complexes.[19] For example, the reaction of $[IrCl(CO)(\mu\text{-dppm})_2]_2$ (dppm = $(Ph_2P)_2CH_2$) with DMAD or HFB (DMAD; $C_2(CO_2Me)_2$, HFB; $C_2(CF_3)_2$) generates the corresponding alkyne bridged dimetallic complexes (Scheme 1.20).[19d]

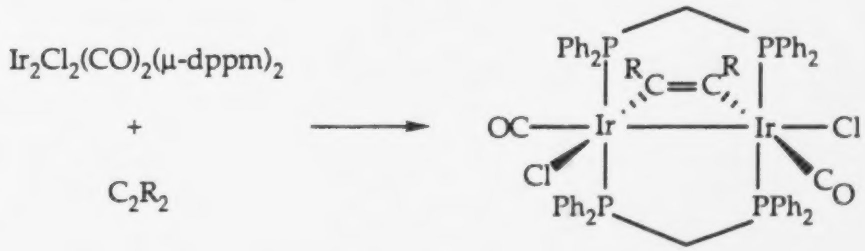

Scheme 1.20: Synthesis of $Ir_2Cl_2(CO)_2(\mu\text{-}C_2R_2)(\mu\text{-dppm})_2$ (R = CF_3, CO_2Me)

Reactions of this type have the benefit of the stabilizing bidentate ligand to preserve the binuclear structure and, in many cases, the alkyne initially attacks an electron deficient metal centre. Unfortunately, the range of heterodimetallic complexes is quite small, most of the complexes are homodimetallic. Also, while this method is applicable for activated alkynes such as DMAD and HFB, donor alkynes do not react readily thus limiting the range of potential compounds.

Alkynes can also react with dimetallic metal centres that are not linked by bidentate ligands to form complexes such as **A**, although this is a significantly less common method.[20] For example, the reaction of DMAD with $Cp_2M_2(CO)_4$ (M = Fe, Ru) yields an alkyne bridged dimetallic species.[20a] This method seems to suffer from the lack of readily available dimetallic compounds that will react with alkynes.

The final method utilizes the reaction of alkynes with monomeric organometallic compounds, initiated by thermal or photochemical means.[17,21] For example, mixing $Pt(PPh_3)_2(CO)_2$ and DMAD under a CO atmosphere at room temperature results in the formation of $Pt_2(CO)_2(PPh_3)_2(\mu\text{-DMAD})$[21a] while heating $CpRh(CO)_2$ and HFB results in a mixture of products, one of which is $Cp_2Rh_2(CO)_2(\mu\text{-HFB})$.[21b,c] The photochemically induced reaction of benzene with $CpIr(CO)_2$ also produces a dimetallacyclobutene species (Scheme 1.21).[21f]

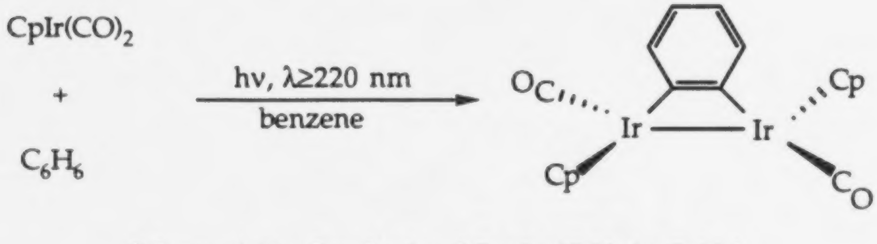

Scheme 1.21: Synthesis of $Cp_2Ir_2(CO)_2(\mu\text{-}C_6H_4)$

The major drawbacks are that only homodimetallic complexes can be synthesized and often there is relatively poor product control.

Thus, the discovery of the facile condensation reactions involving $Ru(CO)_4(\eta^2\text{-HFB})$ or $Os(CO)_4(\eta^2\text{-}C_2H_2)$ introduced a novel synthetic method for the synthesis of alkyne bridged dimetallic compounds.[10,13] Previously, Stone and co-workers had utilized the reaction of the $Pt(\eta^2\text{-HFB})(\eta^4\text{-COD})$ (COD = cyclo-octa-1,5-diene) with $Pt(COD)_2$ to yield $(\mu\text{-HFB})Pt_2(COD)_2$ (Scheme 1.22).[22]

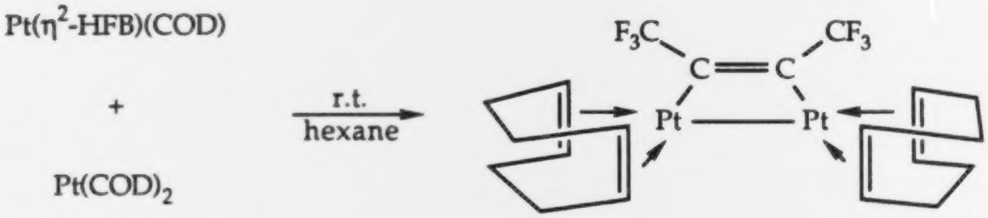

Scheme 1.22: Synthesis of $(\mu\text{-HFB})Pt_2(COD)_2$

A following paper reported the synthesis of the BTMSA-bridged diplatinum compounds and the Ni analogue, $(\mu\text{-BTMSA})Ni_2(COD)_2$, was also prepared.[23] It should be noted that Stone did not mention the synthesis of any alkyne-bridged species that incorporated two different metal centres. Also, Stone has used Pt-alkyne complexes to synthesize species related to **B**, with the exception that no Pt-Pt metal-metal bond is present.[23] Several other reports have been published that deal with the use of mononuclear metal-alkyne species in the generation of dimetallic species.[24] However, none of the reported compounds satisfies the criteria of having a structure similar to **A**.

In addition, Beck has developed a synthetic strategy whereby two monomeric transition metal species react to form the desired dimetallic product.[25] The method involves anionic organometallic nucleophiles such as $Re(CO)_5^-$ reacting with alkynes coordinated to a cationic metal centre. Beck and co-workers have succeeded in synthesizing complexes of form **B** shown in Scheme 1.23, where the alkyne is a four electron donor.[25]

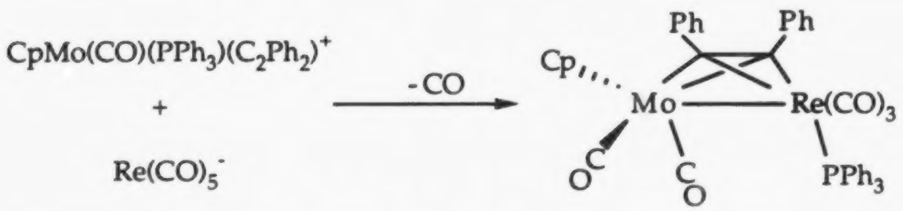

Scheme 1.23: Synthesis of $CpMo(CO)(\mu\text{-}CO)(PPh_3)(\mu\text{-}C_2Ph_2)Re(CO)_3$

Recent publications from the München group have reported a wide variety of hydrocarbyl-bridged dimetallic species, however, no reports of dimetallacyclobutene species have appeared.[26]

1.5.3. Bonding in Dimetallacyclobutene Complexes

As mentioned, Hoffmann has discussed the bonding in parallel alkyne bridged dimetallic species. The interaction diagram for $Os_2(CO)_8(\mu\text{-}C_2H_2)$ is shown in Scheme 1.24.[16]

The bonding diagram considers the parallel bridging acetylene as a dianion that contributes an electron pair to each metal centre. Thus, to preserve the neutrality of the complex, each Os centre is given a d^7 electron count. The $Os_2(CO)_8^{2+}$ fragment is derived from two d^7-ML_4 fragments using the isolobal analogy and only the valence orbitals are shown.

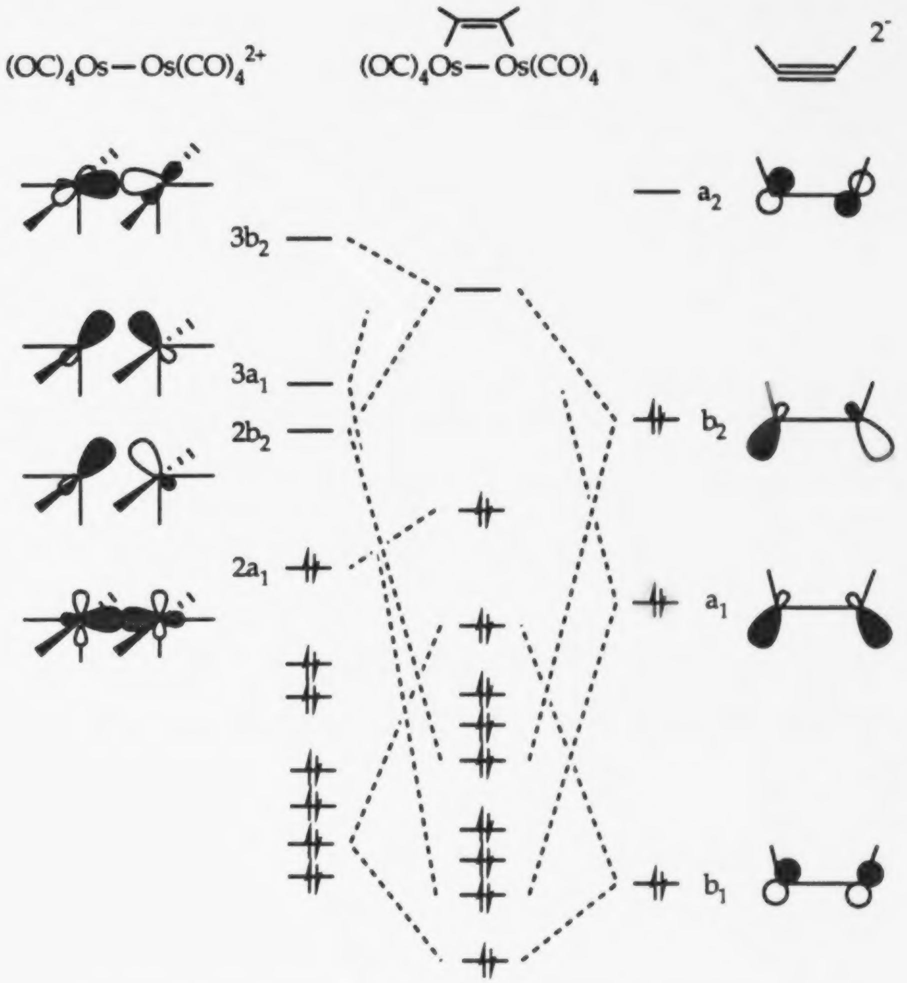

Scheme 1.24: Interaction Diagram for $Os_2(CO)_8(\mu\text{-}C_2H_2)$

The bonding in $Os_2(CO)_8(\mu\text{-}C_2H_2)$ is relatively simple. The filled a_1 orbital of the $C_2H_2^{2-}$ fragment interacts strongly with the empty $3a_1$ orbital of the $Os_2(CO)_8^{2+}$ fragment. There is also a significant acetylene b_2-dinuclear $2b_2$ overlap; these two interactions represent the Os-C(acetylene) bonds. The other π set of the acetylene fragment does not interact significantly with the dinuclear fragment orbitals. Also, the dinuclear HOMO, the $2a_1$ orbital, does not interact with the acetylene fragment; this orbital represents the metal-metal single bond. A theoretical calculation carried out on (μ-C_2H_4)$Os_2(CO)_8$ using a neutral $Os_2(CO)_8$ fragment resulted in similar metal-based frontier orbitals; the only exception was that the relative positions of the $2b_2$ and $3a_1$ orbitals were reversed.[27]

1.5.4. Synthesis of Dimetallacyclopentenone Complexes

A dimetallacyclobutene that has inserted a molecule of CO into the metal-C(acetylene) bond becomes a dimetallacyclopentenone. Just as there are several types of μ-alkyne bridges, there are different types of dimetallacyclopentenones.

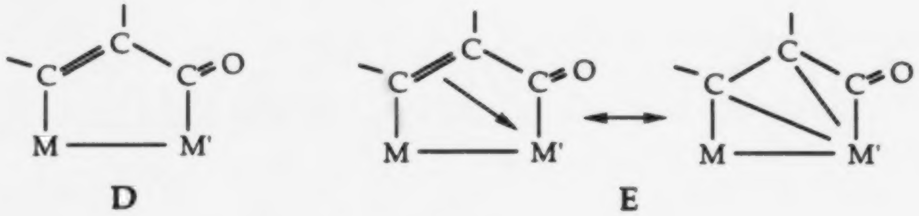

Both structural types, **D** and **E**, have been reported in the literature although they are much less common than **A**, **B** and **C**.

In complexes such as **D**, the C-C double bond remains non-coordinated. The structure can be thought of as an α,β-unsaturated ketone bridging two metal centres. There are relatively few examples of complexes such as **D** reported in the literature.[10,191,28] In fact, only three reports have been made regarding this type of dimetallacyclopentenone, one of which emanated from our laboratories. The synthesis of [μ-$C_2H_2C(O)$]$Os(CO)_4Ru(CO)_4$ from $Os(CO)_4(\eta^2$-HCCH) and $Ru(CO)_5$ was shown in Scheme 1.19 and will not be discussed further.[7]

The first example of a true dimetallacyclopentenone (**D**), one where the C=C double bond remains non-coordinated, appeared in 1981.[28] Dickson and co-workers isolated [μ-$C_2(CF_3)_2C(O)$]$Cp_2Rh(CO)_2$ as one of three major products in the reaction of [$Rh(CO)_2Cl$]$_2$ with HFB followed by addition of TlCp, the other two products are *cis* and *trans*-[μ-$C_2(CF_3)_2$]$Cp_2Rh(CO)_2$ (Scheme 1.25). This complex is decarbonylated by Me_3NO to yield *cis* and *trans*-[μ-$C_2(CF_3)_2$]$Cp_2Rh(CO)_2$, yet, bubbling CO at room temperature through a solution of the alkyne bridged species does not regenerate [μ-$C_2(CF_3)_2C(O)$]$Cp_2Rh(CO)_2$. However, considering the forcing conditions used in the original preparation, it is possible that the dimetallacyclopentenone is formed from a dimetallacyclobutene *via* CO insertion.

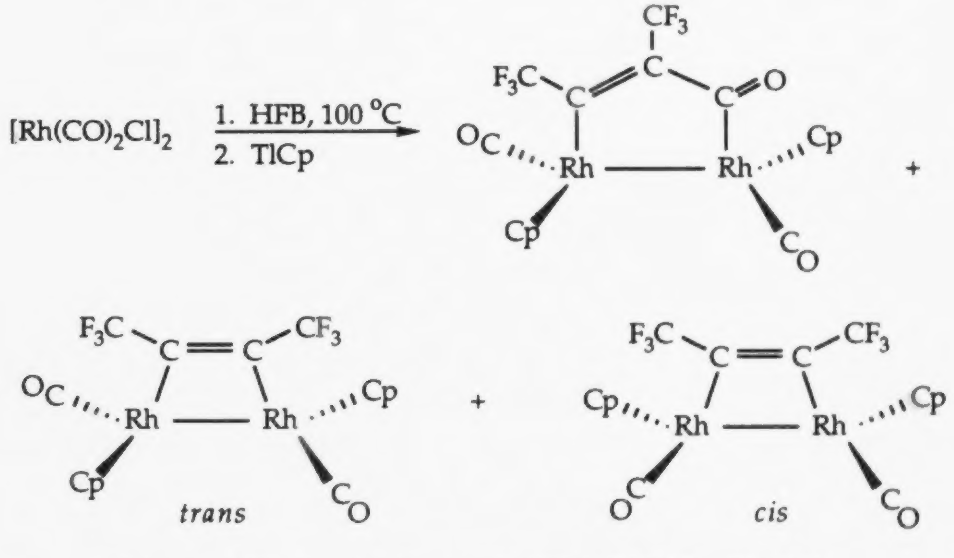

Scheme 1.25: Synthesis of [μ-$C_2(CF_3)_2C(O)$]$Cp_2Rh(CO)_2$

Gladfelter and co-workers were also able to synthesize a species with a dimetallacyclopentenone core.[191] The reaction of $Ru_2(CO)_5$(μ-dmpm)$_2$ (dmpm = $(CH_3)_2PCH_2P(CH_3)_2$) with DMAD results in the formation of [μ-

$C_2(CO_2Me)_2C(O)]Ru_2(CO)_4(\mu\text{-dmpm})_2$. The reaction is quite unusual in that it displays a marked dependence on the concentration of the reactants; the formation of $[\mu\text{-}C_2(CO_2Me)_2C(O)]Ru_2(CO)_4(\mu\text{-dmpm})_2$ is only observed when dilute solutions are used. Also, the carbonylation of $[\mu\text{-}C_2(CO_2Me)_2]$-$(\mu\text{-dmpm})_2Ru_2(CO)_4$ to produce $[\mu\text{-}C_2(CO_2Me)_2C(O)](\mu\text{-dmpm})_2Ru_2(CO)_4$ does not proceed even at 120 °C and 68 atm CO.

In both reported cases, the production of the dimetallacyclopentenone could not be effected by the simple carbonylation of an alkyne-bridged species. In fact, in the examples of parallel acetylenes complexes, no mention of carbonylation reactions to produce dimetallacyclopentenones was made. Thus, the routes to compounds such as **D**, are, at the present time, rather unclear and subject to spurious results. This most likely accounts for the distinct lack of reported non-coordinated dimetallacyclopentenones.

Contrary to the two examples above, a structure such as **E** , where the olefinic moiety is coordinated to a metal centre, is much more common in the literature.[20a,29] This is mostly due to the efforts of Knox and coworkers at the University of Bristol where a large body of work has been carried out on diruthenium and di-iron systems.[20a,29a-f] As with the synthesis of species such as **A**, the reaction of an alkyne with a pre-formed dinuclear centre was used to synthesize coordinated dimetallacyclopentenones. The first report of a coordinated dimetallacyclopentenone was made in 1980, using $Cp_2M_2(CO)_4$ (M = Fe, Ru) as the dinuclear starting material (Scheme 1.26).[29a]

The product is drawn to illustrate that the olefinic fragment is bound to the metal centre; however, the ring is not planar. The compound $[\mu\text{-}\eta^3\text{:}\eta^1\text{-}C_2Ph_2C(O)](\mu\text{-CO})Ru_2Cp_2(CO)$ has been utilized extensively by Knox and co-workers in the synthesis of various hydrocarbyl bridged diruthenium species and in C-C bond forming reactions.[30] In fact, Knox has referred to $[\mu\text{-}\eta^3\text{:}\eta^1\text{-}C_2Ph_2C(O)](\mu\text{-}CO)Ru_2Cp_2(CO)$ as "one of the pillars of the development of organoruthenium chemistry in my laboratory".[30a]

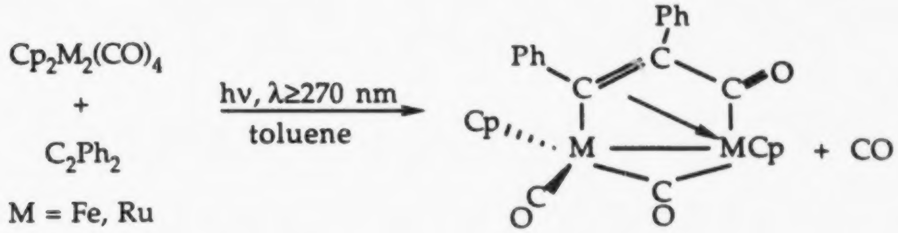
$Cp_2M_2(CO)_4$
+
C_2Ph_2
M = Fe, Ru
hν, λ≥270 nm
toluene
Ph
Ph
C
C
C
O
Cp
M
MCp
C
O
C
O
+ CO

Scheme 1.26: Synthesis of $[\mu\text{-}\eta^3\text{:}\eta^1\text{-}C_2Ph_2C(O)](\mu\text{-}CO)M_2Cp_2(CO)$

G.-Y. Kiel and M. Sandercock of our laboratory also synthesized a diruthenium complex containing a coordinated dimetallacyclopentenone. The synthetic strategy involved the reaction of acetylene with a dppm bridged diruthenium species (Scheme 1.27).[29i]

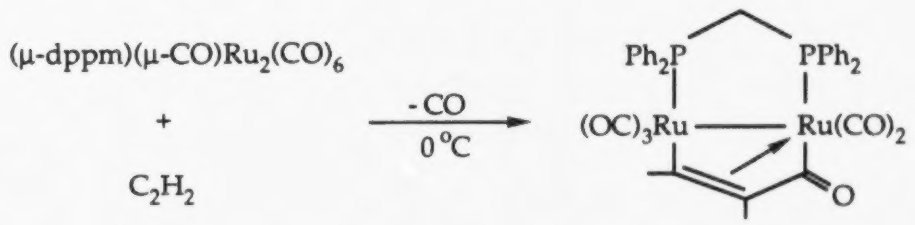
$(\mu\text{-dppm})(\mu\text{-CO})Ru_2(CO)_6$
+
C_2H_2
- CO
0 °C
Ph_2P
PPh_2
$(OC)_3Ru$
$Ru(CO)_2$
O

Scheme 1.27: Synthesis of $[\mu\text{-}\eta^3\text{:}\eta^1\text{-}C_2H_2C(O)]Ru_2(CO)_6(\mu\text{-dppm})$

The iron analogue, $[\mu\text{-}\eta^3\text{:}\eta^1\text{-}C_2H_2C(O)]Fe_2(CO)_6(\mu\text{-dppm})$, was reported by Knox some time ago; however the Os congener has not yet been prepared, due to the lack of the dinuclear starting material.

1.6. Scope of Present Work

Dimetallic compounds occupy a distinct position in organometallic chemistry between monomeric transition metal compounds and metal clusters and surfaces. Casey and Knox have shown that dinuclear systems can moderate a variety of C-C bond forming reactions.[30,31] These may have important applications in organic synthesis.[32] Also, the use of dimetallic compounds in catalysis has been reported.[33] It is hoped that dimetallic compounds can provide a smooth link between monomeric complexes, which are used in homogeneous catalysis, and metal clusters and surfaces used in heterogeneous catalysis.

Surprisingly, in light of the interest in dimetallic systems, the synthesis of hydrocarbyl, particularly alkyne, bridged dimetallic compounds has followed the same synthetic method for more than a decade. The reaction of an alkyne with a pre-formed dinuclear centre however, is limited by the range of suitable starting materials. This is most apparent in the synthesis of heterodimetallic species. The unprecedented reaction of $Os(CO)_4(\eta^2\text{-alkyne})$ with coordinatively saturated eighteen electron species allows a route to overcoming this synthetic hurdle. The aforementioned reaction is a unique method of synthesizing homo- and heterodimetallacyclo-butenes and pentenones. Thus, studies were carried out to investigate and to extend the limits of this novel reaction, specifically by varying the alkyne and the metal centres. Also, it was believed that further information could be obtained about the unusual properties of the $M(CO)_4(\eta^2\text{-alkyne})$ (M = Ru, Os) species in regards to the proposed four-electron destabilization. The results presented in this thesis are a continuation of the initial studies involving the reactions of $M(CO)_4(\eta^2\text{-alkyne})$ with coordinatively saturated eighteen- electron compounds.

1.7. References

1. Yamamoto, A. *Organotransition Metal Chemistry: Fundamental Concepts and Applications*, Wiley: New York, 1986, Chapter 1, pg. 7.

2. (a) Mitchell, P.R.; Parish, R.V. *J. Chem. Ed.* **1969,** *46,* 811. (b) Lukehart, C.M. *Fundamental Transition Metal Organometallic Chemistry*; Brooks/Cole: Monterey, CA, 1985; Chapters 1-2. (c) Tolman, C.P. *Chem. Soc. Rev.* **1972,** *1,* 337. (d) Porterfield, W.W. *Inorganic Chemistry: A Unified Approach*, Addison-Wesley: Menlo Park, CA., 1984, Chapter 10.

3. Huheey, J.E. *Inorganic Chemistry*, Harper & Row: New York: 1983, Chapters 8-10.

4. (a) Albright, T.A.; Burdett, J.K.; Whangbo, M.H. *Orbital Interactions in Chemistry*; Wiley: New York; 1985. (b) Elian, M.; Hoffmann, R. *Inorg. Chem.* **1975,** *14,* 1058. (c) Hoffmann, R. *Angew. Chem. Int. Ed. Engl.* **1982,** *21,* 711. (d) Hoffmann, R. *Science* **1981,** *211,* 11.

5. (a) Dewar, M.J.S. *Bull. Soc. Chim. Fr.* **1951** *18,* C79. (b) Chatt, J.; Duncanson, L.A. *J. Chem. Soc.* **1955,** *1955,* 2939.

6. Lukehart, C.M. *Fundamental Transition Metal Organometallic Chemistry*; Brooks/Cole: Monterey, CA, 1985; Chapter 5.

7. Templeton, J.L. *Adv. Organomet. Chem.* **1989,** *29,* 1.

8. Ball, R.G.; Burke, M.R.; Takats, J. *Organometallics* **1987**, *6*, 1918.

9. Marinelli, G.; Streib, W.E.; Huffman, J.C.; Caulton, K.G.; Gagné, M.R.; Takats, J.; Dartiguenave, M.; Chardon, C.; Jackson, S.A.; Eisenstein, O. *Polyhedron* **1990**, *9*, 1867.

10. Burn, M.J.; Kiel, G.-Y.; Seils, F.; Takats, J.; Washington, J. *J. Am. Chem. Soc.* **1989**, *111*, 6850.

11. (a) Burke, M.R.; Takats, J.; Grevels, F.-W.; Reuvers, J.G.A. *J. Am. Chem. Soc.* **1983**, *105*, 4092. (b) Takats, J. *Polyhedron* **1988**, *7*, 931. (c) Bender, B.R.; Norton, J.R.; Miller, M.M.; Anderson, O.P.; Rappé, A.K. *Organometallics* **1992**, *11*, 3427.

12. Kiel, G.-Y. personal communication.

13. Gagné, M.R.; Takats, J. *Organometallics* **1988**, *7*, 561.

14. Harris, T.V.; Rathke, J.W.; Muetterties, E.L. *J. Am. Chem. Soc.* **1978**, *100*, 6966.

15. (a) Rappoli, B.J.; Churchill, M.R.; Janik, T.S.; Rees, W.M.; Atwood, J.D. *J. Am. Chem. Soc.* **1987**, *109*, 5145 (b) Huffman, J.C.; Lewis, L.N.; Caulton, K.G. *Inorg. Chem.* **1980**, *19*, 2755. (c) The compound $Co(PMe_3)_3(C_2Ph_2)^+$ has also been reported: Capelle, B.; Dartiguenave, M.; Dartiguenave, Y.; Beauchamp, A.L. *J. Am. Chem. Soc.* **1983**, *105*, 4662.

16. Hoffman, D.M.; Hoffmann, R.; Fisel, C.R. *J. Am. Chem. Soc.* **1982**, *104*, 3858 and references therein.

17. (a) Roe, D.M.; Massey, A.G. *J. Organomet. Chem.* **1970**, *23*, 547. (b) Bennett, M.J.; Graham, W.A.G.; Stewart, R.P.; Tuggle, R.M. *Inorg. Chem.* **1973**, *12*, 2944.

18. (a) Winter, M.J. *Adv. Organomet. Chem.* **1989**, *29*, 101. (b) Sappa, E.; Tiripicchio, A.; Blaustein, P. *Chem. Rev.* **1983**, *83*, 203.

19. (a) Jenkins, J.A.; Cowie, M. *Organometallics* **1992**, *11*, 2774. (b) Jenkins, J.A.; Cowie, M. *Organometallics* **1992**, *11*, 2767. (c) Hilts, R.W.; Franchuk, R.A.; Cowie, M. *Organometallics* **1991**, *10*, 304. (d) Sutherland, B.R.; Cowie, M. *Organometallics* **1984**, *3*, 1869. (e) Cowie, M.; Dickson, R.S. *Inorg. Chem.* **1981**, *20*, 2682. (f) Cowie, M.; Dickson, R.S.; Hames, B.W. *Organometallics* **1984**, *3*, 1879. (g) Johnson, K.A.; Gladfelter, W.L. *Organometallics* **1989**, *8*, 2866. (h) Mague, J.T. *Polyhedron* **1990**, *9*, 2635. (i) Mague, J.T. *Organometallics* **1986**, *5*, 918. (j) Mague, J.T.; Klein, C.L.; Majeste, R.J.; Stevens, E.D. *Organometallics* **1984**, *3*, 1860. (k) Mague, J.T. *Inorg. Chem.* **1983**, *22*, 1158. (l) Johnson, K.A.; Gladfelter, W.L. *Organometallics* **1992**, *11*, 2534. (m) Field, J.S.; Haines, R.J.; Sundermeyer, J.; Woollam, S.F. *J. Chem. Soc., Dalton Trans.* **1993**, 3749.

20. (a) Dyke, A.F.; Knox, S.A.R.; Naish, P.J.; Taylor, G.E. *J. Chem. Soc. Dalton Trans.* **1982**, 1297. (b) Wong, Y.S.; Paik, H.N.; Chieh, P.C.; Carty, A.J. *J. Chem. Soc., Chem. Comm.* **1975**, 309. (c) Carty, A.J.; Mott, G.N.; Taylor, N.J. *J. Organomet. Chem.* **1981**, *212*, C54.

21. (a) Koie, Y.; Shinoda, S.; Saito, Y.; Fitzgerald, B.J.; Pierpont, C.G. *Inorg. Chem.* **1980**, *19*, 770. (b) Dickson, R.S.; Mok, C.; Pain, G. *J. Organomet. Chem.* **1979**, *166*, 385. (c) Dickson, R.S.; Kirsch, H.P.; Lloyd, D.J. *J. Organomet. Chem.* **1975**, *101*, C48. (d) Boag, N.M.; Green, M.; Howard, J.A.K.; Spencer, J.L.; Stone, F.G.A. *J. Chem. Soc., Chem. Commun.* **1977**, 930. (e) Smart, L.E.; Browning, J.; Green, M.; Laguna, A.; Spencer, J.L.; Stone, F.G.A. *J. Chem. Soc., Dalton Trans.* **1977**, 1777. (f) Rausch, M.D.; Galinger, R.G.; Gardner, S.A.; Brown, R.K.; Wood, J.S. *J. Am. Chem. Soc.* **1977**, *99*, 7870.

22. Boag, N.M.; Green, M.; Stone, F.G.A. J. *Chem. Soc., Chem. Commun.* **1980**, 1281.

23. Boag, N.M.; Green, M.; Howard, J.A.K.; Stone, F.G.A.; Wadepohl, H. *J. Chem. Soc., Dalton Trans.* **1981**, 862.

24. (a) Davidson, J.L. J. *Chem. Soc., Dalton Trans,* **1983**, 1667. (b) Jeffery, J.C.; Went, M.J. *J. Chem. Soc., Dalton Trans.* **1990**, 567. (c) Kraatz, H.-B.; Went, M.J.; Jeffery, J.C. *J. Organomet. Chem.* **1990**, *394*, 167.

25. (a) Beck, W.; Müller, H.-J.; Nagel, U. *Angew. Chem. Int. Ed. Engl.* **1986**, *25*, 734. (b) Müller, H.-J.; Polborn, K.; Steimann, M.; Beck, W. *Chem. Ber.* **1989**, *122*, 1901.

26. (a) Breimair, J.; Niemer, B.; Raab, K.; Beck, W. *Chem. Ber.* **1991**, *124*, 1059. (b) Steil, P.; Beck, W.; Stone, F.G.A. *J. Organomet. Chem.* **1989**, *368*, 77. (c) Beck, W.; Niemer, B.; Breimair, J.; Heidrich, J. *J. Organomet. Chem.*

1989, *372*, 79. (d) Müller, H.-J.; Nagel, U.; Steimann, M.; Polborn, K.; Beck, W. *Chem. Ber.* **1989**, *122*, 1387. (e) Appel, M.; Heidrich, J.; Beck, W. *Chem. Ber.* **1987**, *120*, 1087. (f) Fritz, P.M.; Polborn, K.; Steimann, M.; Beck, W. *Chem. Ber.* **1989**, *122*, 889. (g) Müller, H.-J.; Nagel, U.; Beck, W. *Organometallics* **1987**, *6*, 193. (h) Beck, W.; Niemer, B.; Wieser, M. *Angew. Chem. Int. Ed. Engl.* **1993**, *32*, 923.

27. Bender, B.R.; Bertoncello, R.; Burke, M.R.; Casarin, M.; Granozzi, G.; Norton, J.R.; Takats, J. *Organometallics* **1989**, *8*, 1777.

28. Dickson, R.S.; Gatehouse, B.M.; Nesbit, M.C.; Pain, G.N. *J. Organomet. Chem.* **1981**, *215*, 97.

29. (a) Dyke, A.F.; Knox, S.A.R.; Naish, P.J.; Taylor, G.E. *J. Chem. Soc., Chem. Commun.* **1980**, 409. (b) Hogarth, G.; Kayser, F.; Knox, S.A.R.; Morton, D.A.V. *J. Chem. Soc., Chem. Comm.* **1988**, 358. (c) Dyke, A.F.; Knox, S.A.R.; Taylor, G.E.; *J. Chem. Soc., Chem. Commun.* **1980**, 411. (d) Dyke, A.F.; Knox, S.A.R.; Naish, P.J.; Taylor, G.E. *J. Chem. Soc., Chem. Commun.* **1980**, 409. (e) Gracey, B.P.; Knox, S.A.R.; MacPherson, K.A.; Orpen, A.G. *J. Chem. Soc., Dalton Trans.* **1985**, 1935. (f) Hogarth, G.; Knox, S.A.R.; Lloyd, B.R.; MacPherson, K.A.; Morton, D.A.V.; Orpen, A.G.; Stobart, S.R. *J. Chem. Soc., Dalton Trans.* **1988**, 360. (g) Fontaine, X.L.R.; Jacobsen, G.B.; Shaw, B.L.; Thornton-Pett, M. *J. Chem. Soc., Dalton Trans,* **1988**, 741. (h) Boag, N.M.; Goodfellow, R.J.; Green, M.; Hessner, B.; Howard, J.A.K.; Stone, F.G.A. *J. Chem. Soc., Dalton Trans.* **1983**, 2585. (i) Kiel, G.-Y.; Takats, J. *Organometallics* **1989**, *8*, 839. (j) Wong, A.; Pawlick, R.V.; Thomas, C.G.; Leon, D.R.; Liu, L.-K. *Organometallics* **1991**, *10*, 530.

30. (a) Knox, S.A.R. *J. Organomet. Chem.* **1990**, *400*, 255. (b) Knox, S.A.R. *Pure. Appl. Chem.* **1984**, *56*, 81.

31. (a) Casey, C.P.; Meszaros, M.W.; Fagan, P.J.; Bly, R.K.; Marder, S.R.; Austin, E.A. *J. Am. Chem. Soc.* **1984**, *108*, 4043. (b) Casey, C.P.; Fagan, P.J. *J. Am. Chem. Soc.* **1982**, *104*, 4950. (d) Casey, C.P.; Audett, J.D. *Chem. Rev.* **1986**, *86*, 339 and references therein.

32. (a) Lewandos, G.S.; Doherty, N.M.; Knox, S.A.R.; MacPherson, K.A.; Orpen, A.G. *Polyhedron* **1988**, *7*, 837. (b) Casey, C.P.; Konings, M.S.; Marder, S.R. *Polyhedron* **1988**, *7*, 881. (c) Casey, C.P.; Konings, M.S.; Godhes, M.A.; Meszaros, M.W. *Organometallics* **1988**, *7*, 2103. (d) Mirkin, C.A.; Lu, K.L.; Geoffroy, G.L.; Rheingold, A.L.; Staley, D.L. *J. Am. Chem. Soc.* **1989**, *111*, 7279.

33. (a) Kubiak, C.P.; Eisenberg, R. *J. Am. Chem. Soc.* **1980**, *102*, 3637. (b) Kubiak, C.P.; Woodcock, C.; Eisenberg, R. *Inorg. Chem.* **1982**, *21*, 2119. (c) Cowie, M.; Southern, T.G. *Inorg. Chem.* **1982**, *21*, 246. (d) Ojima, I.; Okabe, M.; Kato, K.; Horvath, I.T.; *J. Am. Chem. Soc.* **1988**, *110*, 150.

Chapter 2

Reaction of $Os(CO)_4(\eta^2\text{-}HCCH)$ with $CpM(CO)_2$ (M = Co, Rh, Ir)

2.1. Introduction

Following the synthesis of $M(CO)_4(\eta^2\text{-HFB})$ (M = Ru, Os; $C_2(CF_3)_2$ = HFB) complexes, it was discovered that these compounds undergo facile metal condensation reactions with $M(CO)_5$ (M = Ru, Os) and $Cp^*M(CO)_2$ (M = Co, Rh, Ir; Cp^* = C_5Me_5) to produce hexafluorobutyne bridged bimetallic species.[1]

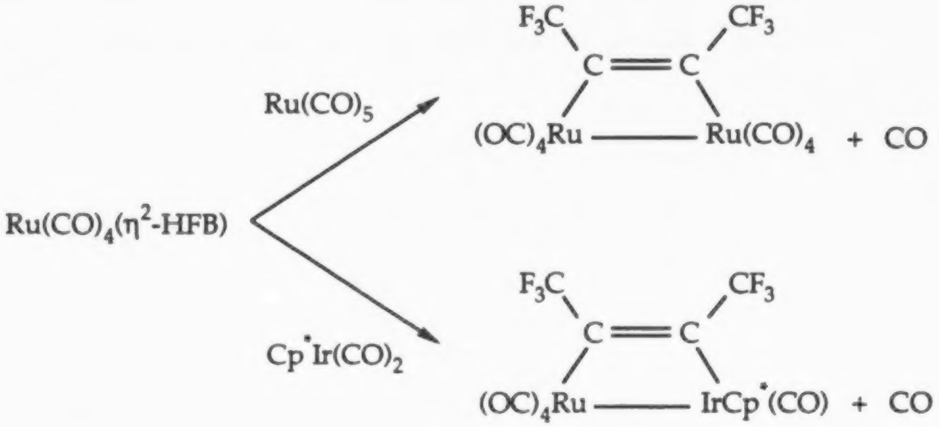

The synthesis of $Os(CO)_4(\eta^2\text{-}HCCH)$, **1**, afforded further opportunity to investigate these condensation reactions. There are several features that make compound **1** desirable in this regard. First, the use of a third row metal increases the possibility of synthesizing and isolating stable compounds, a feature well recognized in this field. Second, although acetylene is no longer a common feedstock of the chemical industry,[2a] the products of the condensation reaction can be viewed as good models for the surface adsorption and further transformations of acetylene.[2] The ready availability of large amounts of acetylene, and its low cost, are practical considerations. Compounds derived from **1** are amenable to analysis by common spectroscopic means. Thus, ^{1}H NMR and ^{13}C NMR spectroscopy also can be used to fully characterize the complexes.[3] The use of ^{13}C NMR spectroscopy to probe the alkyne carbons in the HFB bimetallic compounds was hampered by the C-F coupling and the long relaxation times[3] of the quaternary alkyne carbons.

The reaction of $Os(CO)_4(\eta^2\text{-}HCCH)$, **1**, with $M(CO)_5$ (M = Ru, Os) was investigated by G.-Y. Kiel of our laboratories;[4] the reaction is strongly metal dependent.

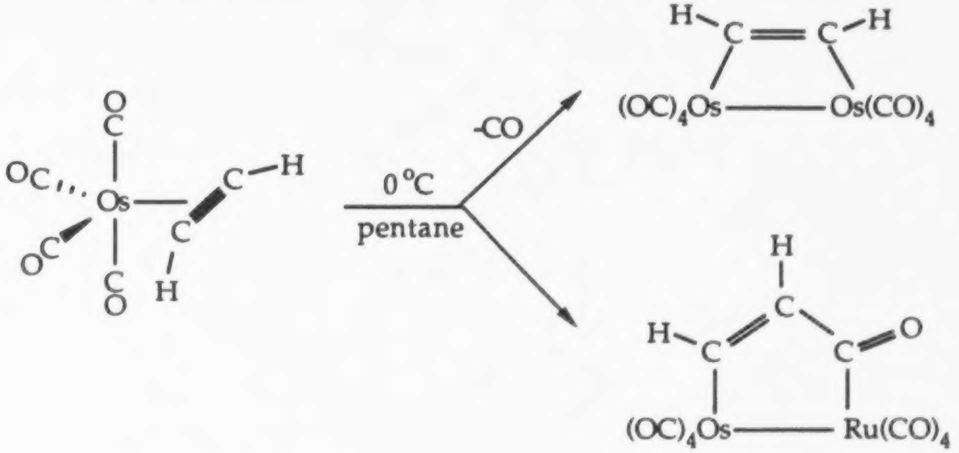

As shown above, the reaction generates different bimetallic complexes depending on which metal is used. The reaction with $Os(CO)_5$ gives a diosmacyclobutene while the reaction with $Ru(CO)_5$ results in the formation of a dimetallacyclopentenone. Remarkably, in the case of

$Ru(CO)_5$, two eighteen electron species react to generate another eighteen electron compound *without* ligand loss.

In light of the facility of the reaction and intriguing metal dependence seen above, the reaction of $Os(CO)_4(\eta^2\text{-}HCCH)$, **1**, with $CpM(CO)_2$ (M = Co, Rh, Ir; Cp = C_5H_5) was also investigated. A preliminary account of this investigation has been published.[4]

2.2. Synthesis and Characterization of Bimetallic Compounds

2.2.1. Synthetic Aspects

The reaction of $Os(CO)_4(\eta^2\text{-}C_2H_2)$, **1**, with $CpM(CO)_2$ (M = Co, Rh, Ir) was carried out using a procedure developed by G.-Y. Kiel for the reaction of **1** with $M(CO)_5$ (M = Os, Ru). A pentane solution of $Os(CO)_4(\eta^2\text{-}C_2H_2)$, **1**, and $CpM(CO)_2$ (M = Co, Rh, Ir) was slowly warmed from -78 °C to 10 °C using a dry ice/acetone bath. The reaction was monitored using FT-IR spectroscopy in the carbonyl region, 2200-1600 cm^{-1}. It was convenient to follow the decrease of the $Os(CO)_4(\eta^2\text{-}C_2H_2)$ band at 2122 cm^{-1} or the two CO stretching bands of $CpM(CO)_2$ (M = Co, Rh, Ir). Also, it was possible to observe a new band in the region near 2100 cm^{-1}, which is a characteristic high frequency band of a bimetallic complex. The region of 2040 cm^{-1} to 1990 cm^{-1} was often complex due to the overlap of the CO bands of **1** and the bimetallic product. The reactions proceed at temperatures near 0-5 °C as evidenced by a color change and, in the case of $CpIr(CO)_2$, the formation of a yellow precipitate. To ensure complete reaction, the solutions were maintained at 0-5 °C for *ca.* 1 h and then allowed to warm to room temperature. The Co and Rh complexes were isolated by removing the solvent *in vacuo* followed by a recrystallization from pentane; for

$CpIr(CO)_2$, the resulting precipitate was first isolated at low temperature and then purified by washing with pentane.

To reduce the formation of byproducts from the decomposition of $Os(CO)_4(\eta^2\text{-}C_2H_2)$, it is necessary to use an excess of $CpM(CO)_2$ (M = Co, Rh, Ir). The excess Group IX metal complexes can be removed easily by sublimation or by washing with pentane. The use of a hydrocarbon solvent in the case of $CpIr(CO)_2$ is important as the bimetallic product precipitates in nearly pure form; any excess starting materials can be washed away using pentane. All of the resulting bimetallic complexes can be handled in air at room temperature but are stored under an inert atmosphere at 5 °C.

As indicated in Scheme 2.1, the reaction of $Os(CO)_4(\eta^2\text{-}C_2H_2)$, **1**, with $CpM(CO)_2$ (M = Co, Rh, Ir) yields products of formula $Os(CO)_4(C_2H_2)$-$IrCp(CO)_2$ or $Os(CO)_4(C_2H_2)MCp(CO)$ (M = Co, Rh).

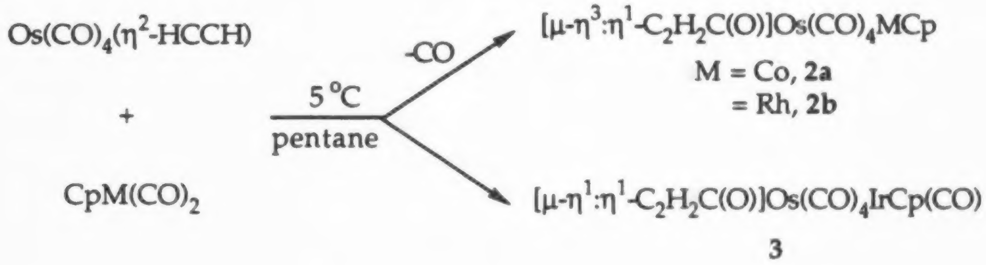
$Os(CO)_4(\eta^2\text{-}HCCH)$
+
$CpM(CO)_2$
5 °C
pentane
-CO
$[\mu\text{-}\eta^3\text{:}\eta^1\text{-}C_2H_2C(O)]Os(CO)_4MCp$
M = Co, **2a**
= Rh, **2b**
$[\mu\text{-}\eta^1\text{:}\eta^1\text{-}C_2H_2C(O)]Os(CO)_4IrCp(CO)$
3

Scheme 2.1: Synthesis of Acetylene Bridged Os-M Complexes

Since it is anticipated that the structures of **2a-b** and **3** will be markedly different, the characterization of these two structural types will be dealt with in separate sections.

2.2.2. Characterization of $Os(CO)_4(C_2H_2)MCp(CO)$ (M = Co, **2a**; Rh, **2b**)

The mass spectra and elemental analyses of **2a-b** indicated that dinuclear species of formula $Os(CO)_4(C_2H_2)MCp(CO)$ (M = Co, Rh) had been formed. On the basis of the previous condensation reactions and reports from Knox and co-workers,[5] the three most likely structures for such a molecular formulation are shown below.

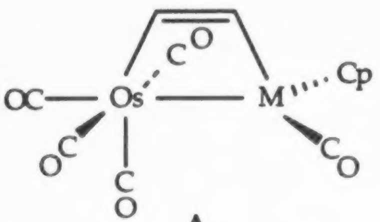

A

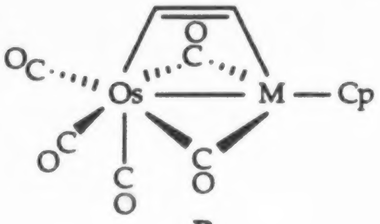

B

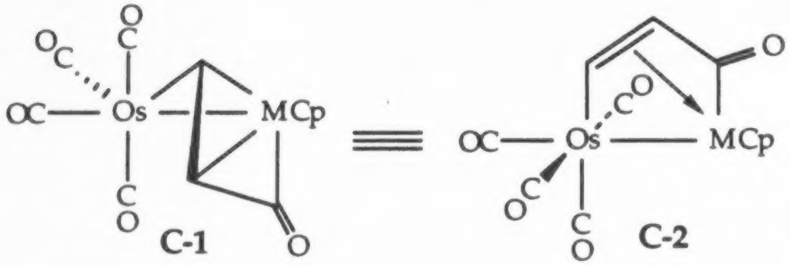

C-1 **C-2**

Designations **C-1** and **C-2** indicate different formalisms in describing the bonding in the dimetallacyclopentenone complex. The FT-IR spectra of **2a** and **2b** each consisted of four terminal CO bands in the range of 2110-1995 cm^{-1} plus an additional band near 1780 cm^{-1}. This low frequency band could be assigned to either a bridging carbonyl or to an acyl group resulting from the formation of a dimetallacyclopentenone ring, immediately ruling out the simple dimetallacyclobutene, **A**. Even though the low frequency band is in the range known for bridging carbonyls, the presence of four terminal bands eliminates structure **B** as only three terminal carbonyl bands would be expected. Thus, structure **C** seems to fit the IR data and the FT-IR spectrum of **2a** is shown in Figure 2.1.

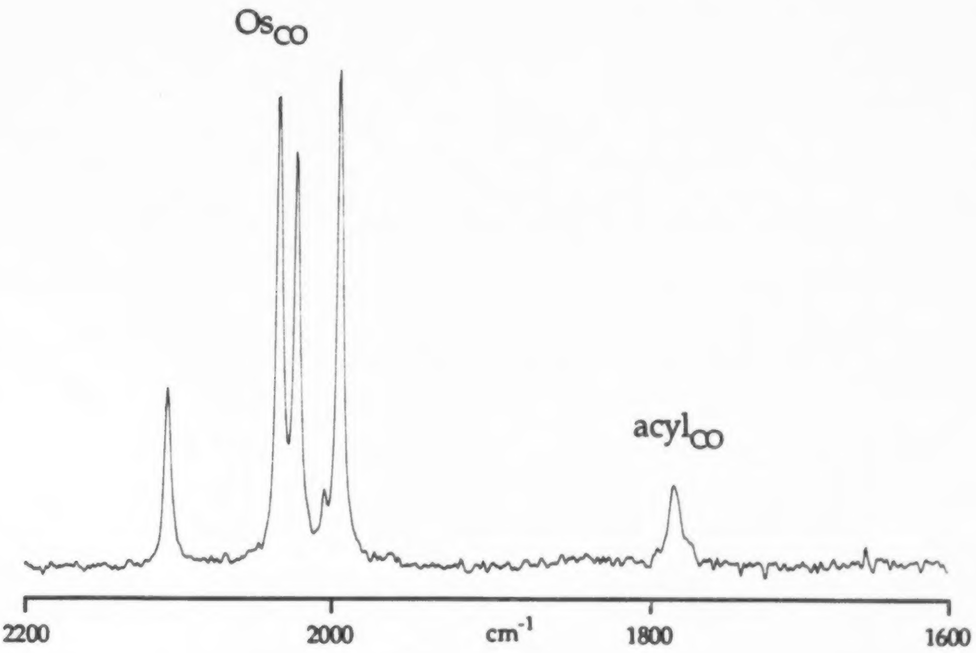

Figure 2.1: FT-IR Spectra of **2a** in the Carbonyl Region

The energies and intensities of the four terminal carbonyl bands of **2b** (and **2a**) are consistent with those seen in $Os(CO)_4(X)_2$ (X = Cl, Br; C_{2v} symmetry) or $Os(CO)_4(R)(X)$ (X = Cl, R= alkyl; C_s symmetry) compounds.[6] In structure **C**, the Os centre has approximate local C_s symmetry even though, as a whole, **2a** and **2b** have only C_1 symmetry. Thus, using the assignment of the carbonyl bands in $Os(CO)_4(Cl)_2$ by Hales and Irving as a reference, the terminal carbonyl bands in **2a** and **2b** can be readily assigned (Table 2.1).[6b] A pictorial representation of the carbonyl stretching modes is given in Scheme 2.2.

Table 2.1: FT-IR Data for **2a** and **2b**

	ν(CO) (pentane, cm^{-1})[a]			
	$Os(CO)_4$			
Compound	A'(1)	A"(2)	A'(2)	A"(1)
2a	2107(w)	2035(s)	2023(m)	1996(s)
2b	2107(w)	2033(s)	2027(m)	1997(s)
cis-$Os(CO)_4(Cl)_2$[b]	2187(w)	2120(s)	2094(m)	2054(s)
cis-$Os(CO)_4(CH_3)_2$[c]	2130(w)	2044(s)	2012(m)	1979(s)

[a] For compounds with symmetrical substituents (C_{2v} symmetry): A'(1) = $a_1(1)$, A"(1) = b_1, A'(2) = $a_1(2)$, A"(2) = b_2. [b] In cyclohexane. Hales, L.A.W.; Irving, R.J. *J. Chem. Soc.(A)* **1967**, 1389. [c] In methylcyclohexane. Carter, W.J.; Kelland, J.W.; Okrasinski, S.J.; Warner, K.E.; Norton, J.R.; *Inorg. Chem.* **1982**, *21*, 3955.

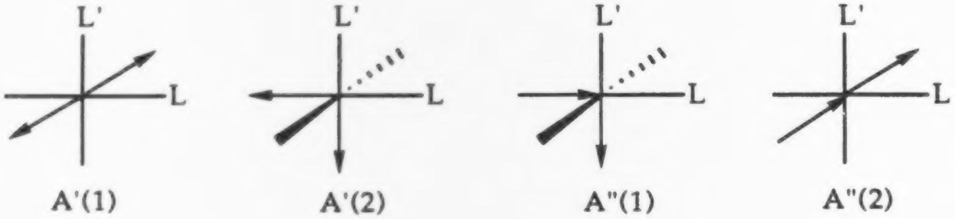

Scheme 2.2: Representation of Stretching Bands for $Os(CO)_4$ Unit

In $Os(CO)_4(L)(L')$ fragments of C_s symmetry, the symmetrical A'(1) band is readily identified *via* its high frequency and relatively low intensity. This band was very useful in the initial identification of bimetallic compounds derived from $Os(CO)_4(\eta^2\text{-HCCH})$ as it immediately suggests a *cis*-$Os(CO)_4(L)(L')$ geometry. The frequencies of the Os-CO IR bands for **2a** and **2b** are almost identical; the largest deviation is in the

A'(2) band where a difference of 4 cm^{-1} is observed. All of the other IR bands are within 2 cm^{-1}. This indicates that the electron density on the Os centre in **2a** and **2b** is essentially the same, surprising since Rh is a more basic metal centre than Co. Thus, the metal-metal bond may be acting as an electron sink, causing the electron density on the Os centre to be the same for **2a** and **2b**.

As mentioned, a fifth carbonyl IR band near 1780 cm^{-1} was observed for **2a** and **2b**. This band is characteristic of an acyl stretching band for a dimetallacyclopentenone ring where the unsaturated organic moiety is bound to a metal centre, such as found in structure **C**.[5] The acyl bands for **2a** and **2b** are listed in Table 2.2 along with some relevant examples from the literature.

Table 2.2: FT-IR Data for **2a** and **2b** for the Acyl Carbonyl

Compound	ν(acyl) (cm^{-1})
$[\mu\text{-}\eta^3:\eta^1\text{-}C_2H_2C(O)]Os(CO)_4CoCp$, **2a**	1734^a $(1778)^b$
$[\mu\text{-}\eta^3:\eta^1\text{-}C_2H_2C(O)]Os(CO)_4RhCp$, **2b**	1738^a $(1783)^b$
$[\mu\text{-}\eta^3:\eta^1\text{-}C_2H_2C(O)]Ru_2Cp_2(CO)_2{}^d$	1753^b
$[\mu\text{-}\eta^3:\eta^1\text{-}C_2H_2C(O)]Fe_2(CO)_5(\mu\text{-dppm})^e$	1747^b
$[\mu\text{-}\eta^3:\eta^1\text{-}C_2H_2C(O)]Ru_2(CO)_5(\mu\text{-dppm})^f$	1712^c

[a] In CH_2Cl_2. [b] In pentane. [c] In THF. [d] Dyke, A.F.; Knox, S.A.R.; Naish, P.J.; Taylor, G.E. *J. Chem. Soc. Dalton Trans.* **1982**, 1297. [e] Hogarth, G.; Kayser, F.; Knox, S.A.R.; Morton, D.A.V. *J. Chem. Soc., Chem. Comm.* **1988**, 358 (dppm = $(Ph_2P)_2CH_2$). [f] Kiel, G.-Y.; Takats, J. *Organometallics* **1989**, *8*, 839.

As can be seen from the above Table, the acyl band frequencies obtained for **2a** and **2b** in CH_2Cl_2 are in accord with values for similar compounds also obtained in polar solvents. Changing to a non-polar solvent such as pentane raises the frequency of the acyl stretching band by approximately 45 cm^{-1}. This is due to the polarization of the C=O bond which is more pronounced in polar solvents, causing increased contribution from II. This results in a lengthening of the C-O bond and causes a reduction in the C=O stretching band frequency, a phenomenom well recognized in organic and organometallic chemistry.[7]

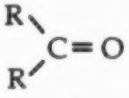

I

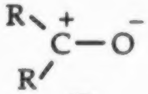

II

The acyl band frequencies obtained for **2a** and **2b** (in pentane) seem, at first, to be anomalously high. For comparison, a sample of acetone dissolved in pentane has the ketonic band at 1722 cm^{-1}. However, a more appropriate description of the acyl moiety would be as part of a metallacyclopropanone.

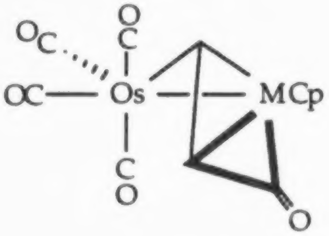

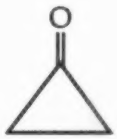

cyclopropanone

Thus, in **2a** and **2b**, even though a five membered dimetallacyclopentenone ring is present, the acyl unit has an IR stretching band characteristic of a smaller ring. For comparison, the stretching band frequencies of several cyclic ketones are listed in Table 2.3.

Table 2.3: FT-IR Data for **2a** ,**2b** and Cyclic Ketones

Compound	ν(acyl) (cm^{-1})
[μ-η^3:η^1-$C_2H_2C(O)$]$Os(CO)_4CoCp$, **2a**	1734[a] (1778)[b]
[μ-η^3:η^1-$C_2H_2C(O)$]$Os(CO)_4RhCp$, **2b**	1738[a] (1783)[b]
cyclopropanone[c]	1813
cyclobutanone[d]	1775
cyclopentanone[e]	1751

[a] In CH_2Cl_2. [b] In pentane. [c] In CH_2Cl_2, Turro, N.J.; Hammond, W.B. *J. Am. Chem. Soc.* **1966,** *88*, 3672. [d] Kaarsemaker, S.; Coops, *J. Rec. Trav. Chim.* **1951,** *70*, 1033. [e] Silverstein, R.M.; Bassler, G.C.; Morrill, T.C. *Spectrometric Identification of Organic Compounds,* Wiley: New York, 1981, pg. 119.

There are two reasons for the increase in CO stretching band frequency as ring size decreases. First, as the C-C(O)-C bond angle decreases there is increased interaction with the C-C bond stretching. Additional energy is required to overcome this interaction, manifesting itself as an increase in C=O bond stretching frequency.[8a] Also, as the ring size decreases, the amount of *s* orbital character of the carbon atoms rises, increasing the electronegativity of these carbon atoms.[8b] This creates an inductive effect which results in less polarization of the C=O bond and increases the energy of the acyl stretching band. Also of interest is that **2a** and **2b** can be thought of as having two fused three-membered rings that are stabilized on a bimetallic framework. Cyclopropanone, on the other hand, is unstable at room temperature and polymerizes rapidly *via* addition to the ketonic functionality.[9]

The ^{1}H NMR spectra of **2a** and **2b** are also characteristic of a dimetallacyclopentenone with a coordinated double bond.[5] The labelling shown below follows the convention used for α,β-unsaturated ketones.

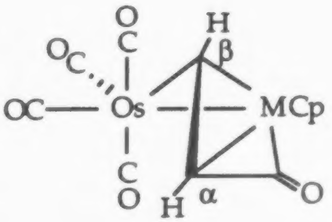

The β hydrogen is attached to a bridging carbene carbon and is expected to resonate in the lowfield region,[10] whereas the α-H is expected to show an upfield coordination shift. The ^{1}H NMR spectroscopic data for **2a** and **2b**, plus other related compounds, are given in Table 2.4.

There is a rather dramatic ^{1}H NMR chemical shift difference between the α and β protons. This is a characteristic feature of bimetallic compounds containing a μ-η^3:η^1-$C_2H_2C(O)$ unit and thus ^{1}H NMR spectroscopy can be used as a quick diagnostic test for the presence of these compounds. The presence of two widely separated ^{1}H NMR signals also rules out a dimetallacyclobutene structure as two relatively closely spaced ^{1}H NMR signals would be expected for structures **A** or **B**.[3] For **2b**, $^2J_{Rh\text{-}H}$ coupling is observed only for the α-hydrogen even though the β-hydrogen is also only separated from the Rh centre by two bonds. However, a similar observation was made by Shaw and co-workers for $[\mu\text{-}\eta^3\text{:}\eta^1\text{-}C_2H_2C(O)](\mu\text{-dppm})Pt(PPh_3)Fe(CO)_2$ where markedly different ^{195}Pt-^{1}H spin-spin coupling was observed for the two different ring protons.[5d] For the α-hydrogen, a value of $^2J_{Pt\text{-}H}$ = 203 Hz was reported while a value of $^2J_{Pt\text{-}H}$ = 37 Hz was recorded for the β-hydrogen. This trend is in accord with the results obtained for **2b** as, in both cases, the M-H_α (M = Rh, Pt) coupling is much larger than the M-H_β coupling.

Table 2.4: ^{1}H NMR Data for **2a** and **2b**

	δ (ppm, CD_2Cl_2)		
Compound	H_α	H_β	$^3J_{H\text{-}H}$[a]
[μ-$C_2H_2C(O)$]$Os(CO)_4CoCp$, **2a**	4.13	8.45	7.9
[μ-$C_2H_2C(O)$]$Os(CO)_4RhCp$, **2b**	5.00[b]	7.85	7.4
[μ-$C_2H_2C(O)$]$Ru_2Cp_2(CO)_2$[c]	3.42	10.94	7.0
[μ-$C_2H_2C(O)$]$Fe_2(CO)_5$(μ-dppm)[d]	3.63	8.63	7.0
[μ-$C_2H_2C(O)$]$Ru_2(CO)_5$(μ-dppm)[e]	4.59	8.19	8.5

[a] Couplings in Hertz. [b] $^2J_{Rh\text{-}H\alpha}$ = 3.0 Hz. [c] Dyke, A.F.; Knox, S.A.R.; Naish, P.J.; Taylor, G.E. *J. Chem. Soc. Dalton Trans.* **1982**, 1297. [d] Hogarth, G.; Kayser, F.; Knox, S.A.R.; Morton, D.A.V. *J. Chem. Soc., Chem. Comm.* **1988**, 358 (dppm = $(Ph_2)P_2CH_2$). [e] Kiel, G.-Y.; Takats, J. *Organometallics* **1989**, *8*, 839.

The chemical shift differences observed for **2a** and **2b** in the ^{1}H NMR spectra are mirrored in the ^{13}C NMR spectra as the bridging carbene character of the β carbon is readily apparent. The ^{13}C NMR results for **2a** and **2b** are collected in Table 2.5. The ^{13}C NMR data for **2a** and **2b** are in accord with previous results from Knox and co-workers and from within our own laboratories.[5] The β carbons are all shifted downfield, consistent with their formulation as μ-carbenes. In fact, all of the C_β ^{13}C NMR resonances fall within the range (100-210 ppm) proposed by Hermann for an alkylidene unit bridging two metal centres.[10] The fact that the C_β ^{13}C NMR shifts lie at the highfield end of this range may imply an electron rich Os-M (M = Co, Rh) core.[11] The C_α resonances are consistent with those of a coordinated olefinic moiety as first stated by Knox.

Table 2.5: ^{13}C NMR Data for **2a** and **2b** and Related Compounds

	δ (ppm, CD_2Cl_2)	
Compound	C_α	C_β
[μ-$C_2H_2C(O)$]$Os(CO)_4CoCp$, **2a**	35.8	120.2
[μ-$C_2H_2C(O)$]$Os(CO)_4RhCp$, **2b**	44.4	115.7[a]
[μ-$C_2H_2C(O)$]$Ru_2Cp_2(CO)_2$[b]	24.0	156.7
[μ-$C_2H_2C(O)$]$Fe_2(CO)_5$(μ-dppm)[c]	44.8	168.4
[μ-$C_2H_2C(O)$]$Ru_2(CO)_5$(μ-dppm)[d]	55.4	161.9

[a] $^1J_{Rh\text{-}C\beta}$ = 16.1 Hz. [b] Dyke, A.F.; Knox, S.A.R.; Naish, P.J.; Taylor, G.E. *J. Chem. Soc. Dalton Trans.* **1982**, 1297. [c] Hogarth, G.; Kayser, F.; Knox, S.A.R.; Morton, D.A.V. *J. Chem. Soc., Chem. Comm.* **1988**, 358 (dppm = $(Ph_2)P_2CH_2$). [d] Kiel, G.-Y.; Takats, J. *Organometallics* **1989**, *8*, 839.

A surprising feature is that while the C_β carbon shows characteristic $^1J_{Rh\text{-}C}$ coupling of 16.1 Hz,[12] no Rh-C coupling is observed to the C_α carbon. This may imply that the valence bond formalism (**C-1**) for the bonding in **2a** and **2b** is not completely descriptive of the bonding. In fact, a significant contribution from **C-2** may be present or perhaps even a contribution from the ketenic structure, **C-3**.[5g]

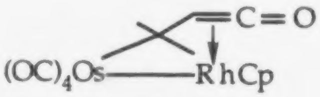

C-3

Still puzzling is that ${}^{2}J_{Rh\text{-}H}$ coupling can be observed in the case of the α proton, while no ${}^{1}J_{Rh\text{-}C\alpha}$ coupling is seen. One possibility is a coincidental cancellation of factors in the coupling constant expression whereby terms of similar magnitude but opposite sign are present.[13a] Alternatively, it has been suggested that the greater the π bonding character in the Rh-C bond, the smaller the Rh-C coupling constant. This has been suggested to explain the small Rh-C coupling observed with Rh-Cp (Cp = η^5-C_5H_5) as compared to other ${}^{1}J_{Rh\text{-}C}$ values.[13a] Finally, in (tfac)Rh(η^2-C_2H_4)$_2$ (tfac = 1,1,1-trifluoro-2,4-cylopentedionate), no Rh-C coupling to the ethylene carbons is observed. Vrieze and co-workers have suggested that the value of ${}^{1}J_{Rh\text{-}C}$ is smaller than the observed linewidth of $\Delta\nu_{1/2}$ = 20 Hz.[13b] A similar effect may be present for **2b** where the C_α ^{13}C NMR signal has a linewidth at half-height of 6 Hz. For comparison, the linewidth of the β carbon signal is 4 Hz, thus the Rh-C coupling to the α carbon would still have to be quite small. The best possible explanation for the spin-spin coupling results obtained for **2b** is it that a combination of the above factors are at work.

The structure of **2a-b** could be described as **C** on the basis of FT-IR, ^{1}H NMR, and ^{13}C NMR spectroscopies. However, to completely confirm the regioselectivity of the reaction, it is necessary to analyze the ^{13}C NMR spectra in the carbonyl region. Samples of ^{13}CO enriched **2a** and **2b** were readily synthesized from the ^{13}CO enriched starting materials. In the low temperature ^{13}C NMR spectrum of **2b** a doublet at 216.7 ppm with ${}^{1}J_{Rh\text{-}C}$ = 24.0 Hz was observed. This Rh-C coupling is consistent with Rh-C single bond coupling,[12] confirming that the acyl group was bound to the Rh centre. The level of enrichment was sufficient that, for the Os carbonyls, *trans* ^{13}C-^{13}C coupling could be seen for two of the osmium bound carbonyls. However, as expected, no ^{13}C-^{13}C coupling was seen for the acyl carbon, further indicating that the acyl was attached to the Rh metal. For **2a**, the acyl signal was present at 232.9 ppm. This lowfield position is characteristic of an acyl carbon bound to a Co centre; an Os bound acyl would have a ^{13}C NMR chemical shift of approximately 200 ppm.[12] Also, as in **2b**, the acyl signal for **2a** displayed no *trans* ^{13}C-^{13}C coupling indicating that the same regio-isomer was present in both cases. Further discussion of the ^{13}C NMR spectra of **2a-b** in the carbonyl region will be given in Section 2.3.

2.2.3. Characterization of $Os(CO)_4(C_2H_2)(CO)IrCp(CO)$, 3

The reaction between $Os(CO)_4(\eta^2\text{-}HCCH)$, **1**, and $CpIr(CO)_2$ proceeds to yield a yellow precipitate which is only sparingly soluble in hydrocarbon solvents such as pentane and hexane, but very soluble in CH_2Cl_2. The mass spectrum and elemental analysis are consistent with the formula $Os(CO)_4(C_2H_2)(CO)IrCp(CO)$, **3**, indicating that the reaction occurrs without ligand loss. This phenomenon, whereby two coordinatively saturated, eighteen electron species react to yield an eighteen electron bimetallic complex without ligand loss, has been observed previously in our laboratories in the reaction of $Os(CO)_4(\eta^2\text{-}HCCH)$ with $Ru(CO)_5$.[4] In that case, the reaction proceeded to yield a dimetallacyclopentenone (Scheme 2.2), and a similar structure is proposed for **3**. Thus, the condensation again yields a dimetallacyclopentenone, but unlike **2a** and **2b**, the olefinic moiety is not coordinated to the metal centre.

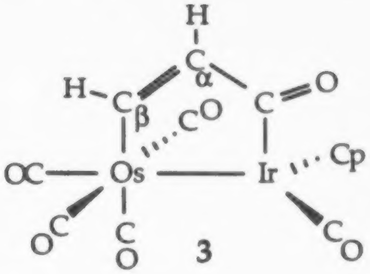

3

The FT-IR spectrum of **3** is in accord with the above structure. In the region 2115-1990 cm^{-1}, five terminal carbonyl bands were seen. Four of these were assigned to an $Os(CO)_4(L)(L')$ fragment with C_s local symmetry and the remaining signal was assigned to the Ir-CO stretching band (Table 2.6).

Table 2.6: FT-IR Data for $[\mu\text{-}\eta^1\text{:}\eta^1\text{-}C_2H_2C(O)]Os(CO)_4IrCp(CO)$, **3**

	ν(CO) (pentane, cm^{-1})[a]				
	$Os(CO)_4$				
Compound	A'(1)	A"(2)	A'(2)	A"(1)	Ir-CO
3	2112(w)	2039(s)	2035(m)	2004(s)	1992(w)

[a] Assigment based on Hales, L.A.W.; Irving, R.J. *J. Chem. Soc.(A)* **1967**, 1389.

In the FT-IR spectrum of **3**, a sixth band was observed in the acyl region at 1636 cm^{-1}. This indicated that the hydrocarbyl bridge between the two metal centres contained an α,β-unsaturated ketone whereby the carbon-carbon double bond remains non-coordinated. Surprisingly, there are relatively few examples of this structural type in the literature, but, in each case, the low frequency of the acyl stretching band is an important diagnostic tool (Table 2.7).[4,14]

Table 2.7: FT-IR Data for **3** and Related Compounds

Compound	ν(acyl) (cm^{-1})
$[\mu-\eta^1:\eta^1-C_2H_2C(O)]Os(CO)_4IrCp(CO)$, **3**	1636[a] (1598)[b]
$[\mu-\eta^1:\eta^1-C_2H_2C(O)]Os(CO)_4Ru(CO)_4$[c]	1635[a]
$[\mu-\eta^1:\eta^1-C_2(CF_3)_2C(O)]Rh_2Cp_2(CO)_2$[d]	1628[a]
2-cyclopenten-1-one[e]	1707
2-cyclohexen-1-one[e]	1686
acetone[f]	1722

[a] In pentane. [b] In CH_2Cl_2. [c] Burn, M.J.; Kiel, G.-Y.; Seils, F.; Takats, J.; Washington, J. *J. Am. Chem. Soc.* **1989**, *111*, 6850. [d] Dickson, R.S.; Gatehouse, B.M.; Nesbit, M.C.; Pain, G.N., *J. Organomet. Chem.* **1981**, *251*, 97. [e] Neat, Aldrich Library of FT-IR Spectra. [f] Personal observation.

As seen in the Table, the acyl band of **3** compares favourably to the other μ-$C_2R_2C(O)$ dimetallic compounds. For comparison, the FT-IR of acetone was included as an example of a saturated ketone. The presence of a carbon-carbon double bond next to the ketone results in a reduction in the frequency of the ketonic stretching band. This is attributed to the delocalization of the electron density in α,β-unsaturated ketones whereby the charge-separated structure, **IV**, makes a significant contribution.[15]

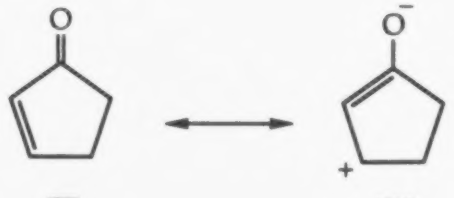

III **IV**

A contribution from **IV** will reduce the C-O bond order and thus reduce the C=O stretching band frequency. Compared to the organic analogue, 2-cyclopenten-1-one, the acyl band frequency is considerably lower. This is due to the electronic effect of the metal centres as it may allow stabilization of canonical form **IV**.

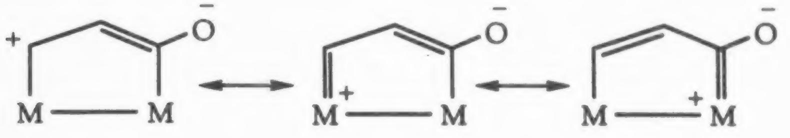

In **2a** and **2b**, canonical form **IV** is not possible due to the olefinic coordination. This, coupled with the aforementioned ring strain effects, causes an increase of almost 150 cm^{-1} in the acyl IR band frequency of **2a** and **2b** as compared to **3**. Thus, the frequency of the acyl band is very discriminating between the two types of dimetalla-cyclopentenones observed. As a final note, for **3**, there is a decrease of 38 cm^{-1} in the acyl stretching frequency when changing solvents from pentane to CH_2Cl_2. The increased polarity of CH_2Cl_2 allows stabilization of the charge separated canonical form, thus decreasing the C=O bond order.

The ^1H NMR spectrum of **3** also indicated the presence of a μ-$C_2R_2C(O)$ bridge. Generally, in the ^1H NMR spectra of α,β-unsaturated ketones the β hydrogen resonates downfield of the α proton.[16] This is a direct result of the delocalization of electron density which causes the β carbon to have a partial positive charge. This property allows for ready assignment of the ^1H NMR spectra of these complexes (Table 2.8).

Table 2.8: ^1H NMR Data for **3** and Related Compounds

Compound	δ (ppm, CD_2Cl_2) H_α	H_β	$^3J_{H\text{-}H}$[a]
$[\mu\text{-}C_2H_2C(O)]Os(CO)_4IrCp(CO)$, **3**	7.51	7.98	9.1
$[\mu\text{-}C_2H_2C(O)]Os(CO)_4Ru(CO)_4$[b]	7.46	8.17	9.0
2-cyclopenten-1-one[c]	6.10	7.71	5.7[d]
2-cyclohexen-1-one[c]	5.93	6.88	10.5[d]

[a] Coupling constants in Hertz. [b] Burn, M.J.; Kiel, G.-Y.; Seils, F.; Takats, J.; Washington, J. *J. Am. Chem. Soc.* **1989,** *111*, 6850. [c] In $CDCl_3$, Aldrich Library of NMR Spectra. [d] Schreurs, J.; van Noorden-Mudde, C.A.H.; van de Ven, L.J. M.; de Haan, J.W. *Org. Mag. Reson.* **1980,** *13*, 354.

The ^1H NMR chemical shift values for **3** match those of the only other unsubstituted dimetallacyclopentenone in the literature, $[\mu\text{-}C_2H_2C(O)]Os(CO)_4Ru(CO)_4$. Also, the chemical shift difference between the α and β protons is much smaller than observed in **2a-b**. Compared to 2-cyclopenten-1-one, the proton signals for **3** are shifted downfield and the shift difference between the α and β protons is smaller. This is most likely due to the substituent effect of having two metals σ-bound to the α,β-unsaturated ketone. In addition, the ring geometry (bond distances and angles) will differ between **3** and 2-cyclopenten-1-one; since the chemical shifts in cyclic α,β-unsaturated ketones are dependent on ring size, this may also play a significant role. Finally, the H-H spin-spin coupling value of 9.1 Hz is close to the typical values of 8-12 Hz found for olefinic protons in a Z configuration.[17] In **2a** and **2b**, the H-H couping is closer to 7 Hz, resulting from a distortion of the C-C double bond upon olefin coordination.

The ^{1}H NMR results for **3** are, as in **2a** and **2b**, mirrored in the ^{13}C NMR spectrum. In fact, the larger range of ^{13}C NMR resonances makes the shift differences between the α and β carbons quite apparent. The ^{13}C NMR data for the ring carbons of **3** is listed in Table 2.9. The ^{13}C NMR chemical shifts of cyclopentenone and the listed organometallic compounds are very similar. In all given cases, the α carbon is upfield of the β carbon by roughly 30 ppm, consistent with the predictions by Levin regarding the correlation between charge density and ^{13}C NMR chemical shifts in α,β-unsaturated ketones.[15]

Table 2.9: ^{13}C NMR Data for **3** and Related Compounds

	δ (ppm, CD_2Cl_2)	
Compound	C_α	C_β
$[\mu\text{-}C_2H_2C(O)]Os(CO)_4IrCp(CO)$, **3**	132.1	166.9
$[\mu\text{-}C_2H_2C(O)]Os(CO)_4Ru(CO)_4$[a]	131.4	166.5
2-cyclopenten-1-one[b]	134.6	164.9

[a] Burn, M.J.; Kiel, G.-Y.; Seils, F.; Takats, J.; Washington, J. *J. Am. Chem. Soc.* **1989**, *111*, 6850. [b] In $CDCl_3$, Loots, M.J.; Weingarten, L.R.; Levin, R.H. *J. Am. Chem. Soc.* **1976**, *98*, 4571.

The final task was the determination of the regioselectivity of the reaction; based on the available data both **3** and **3'** were possible. The acyl signal for **3** appeared in the ^{13}C NMR spectrum at 203.7 ppm. Unfortunately, the ^{13}C NMR chemical shift ranges for carbonyls bound to

Os or Ir are quite similar thus effectively negating the use simple chemical shift values to determine which regio-isomer was present.[12] However, no ^{13}C-^{13}C coupling was observed for the acyl signal even though *trans* ^{13}C-^{13}C coupling was observed between two terminal carbonyls, indicating that **3** was the regio-isomer formed. This result is also in accord with **2a** and **2b** since the reaction proceeds so that the acyl is bound to the Group IX metal centre.

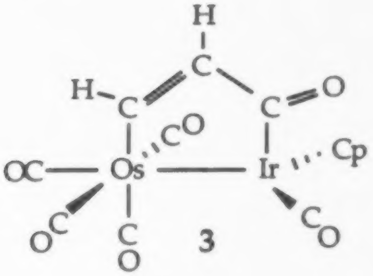

3

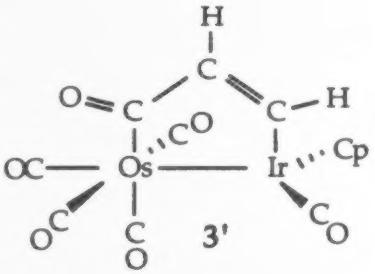

3'

2.3. Molecular Structure of $[\mu\text{-}\eta^1{:}\eta^1\text{-}C_2H_2C(O)]Os(CO)_4IrCp(CO)$, 3

As mentioned, the determination of the regioselectivity of the reaction to produce **3** was largely based on the lack of ^{13}C-^{13}C coupling in the ^{13}C NMR spectrum. Also, there is a lack of solid state structural data on μ-$C_2H_2C(O)$ species as only X-ray structures of bimetallic species bridged by substituted α,β-unsaturated ketones have been reported.[14,18] The X-ray structure of $[\mu\text{-}\eta^1{:}\eta^1\text{-}C_2H_2C(O)]Os(CO)_4Ru(CO)_4$ has been determined.[4,19] Thus, to confirm unambiguously the regioselectivity of the condensation and to provide additional X-ray structural data on this class of dimetallacyclopentenones, a single crystal X-ray structural determination was carried out on **3**. The result of this investigation is given in Figure 2.2.

The relevant bond distances and angles for **3** are listed in Tables 2.10 and 2.11, respectively. The X-ray crystallographic study confirms that the hydrocarbyl bridge is oriented such that the acyl is bound to the Ir centre. The Os centre is six-coordinate while the Ir centre has a three-legged piano stool geometry, and, overall, the molecule has C_1 symmetry.

Some problems arose during the X-ray crystal structure determination of **3**. First, high quality crystals were difficult to obtain and were flat, which caused difficulty in the application of the absorption correction. The metal atoms were readily located and, with just the metal atoms in place, most of the electron density was accounted for with R = 0.119. The cyclopentadienyl ring and the bridging ligand could be refined. The major problem was with the carbonyl ligands on the two metal centres. From the Fourier Difference maps, the C11 and C13 carbonyls on Os were disordered with each having two resolvable positions. These positions were then refined with each at 50% occupancy. There was also large thermal motion for the C10 and C9 carbonyls, however this disorder could not be resolved. In the final refinement a value of R = 0.059 was obtained. Although this appears to be a reasonable value, much of the electron density is accounted for by the Os and Ir centres. The large absorption effects coupled with the disorder result in a poorly defined structure with relatively high esd values for the bond lengths and angles. The overall structure and metal-metal separation is clear, however, only a prudent interpretation of the other metrical parameters can be made.

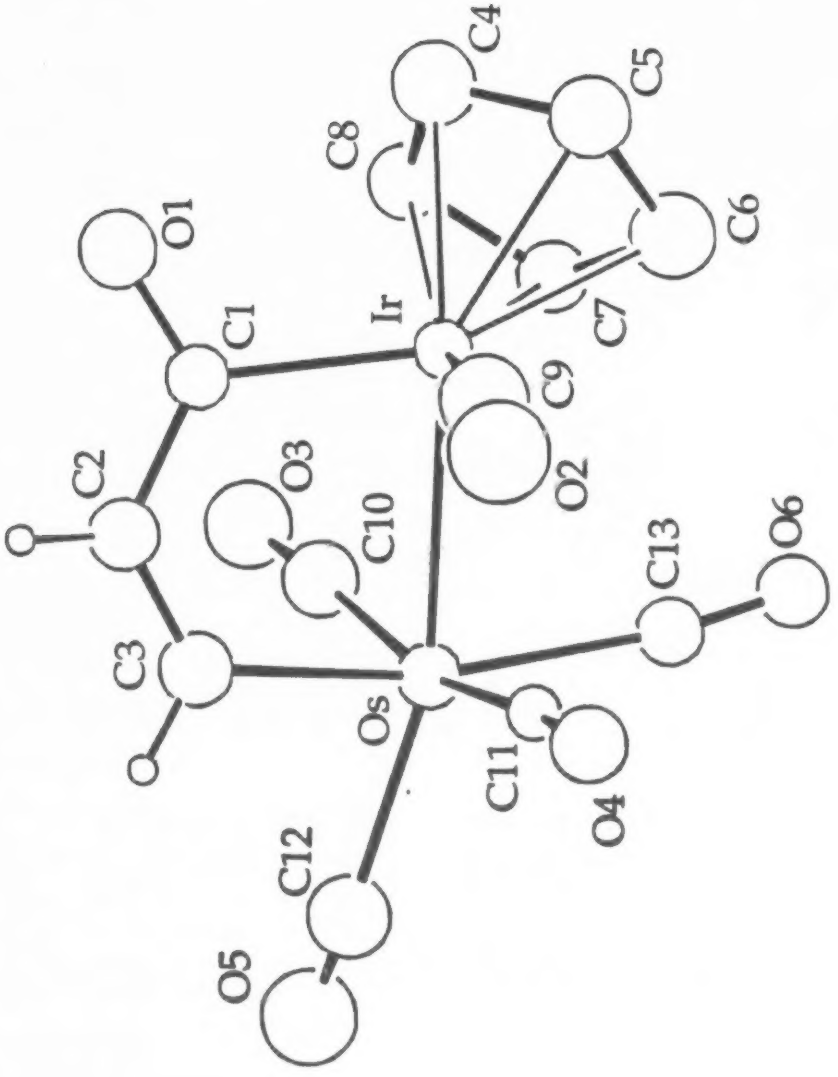
C4
C5
C8
O1
C6
C1
Ir
C7
C9
C2
O3
O2
C10
C13
O6
C3
Os
C11
O4
C12
O5

Figure 2.2: ORTEP View of [μ-$C_2H_2C(O)$]$Os(CO)_4IrCp(CO)$, 3

Table 2.10: Selected Bond Lengths (Å) for **3**

Ir-Os	2.785(2)	O2-C9	1.12(4)
Ir-C1	2.07(3)	O3-C10	1.13(3)
C1-C2	1.45(4)	O4-C11	1.18(4)
C2-C3	1.31(4)	O5-C12	1.07(8)
O1-C1	1.24(3)	O6-C13	1.15(7)
Ir-C9	1.80(3)	O4'-C11'	1.15(6)
Os-C3	2.15(3)	O5'-C12'	1.15(6)
Cent-Ir	1.95	O6'-C13'	1.25(8)
Os-C10	1.91(3)	Os-C11'	1.95(5)
Os-C11	1.95(3)	Os-C12'	1.87(5)
Os-C12	2.19(6)	Os-C13'	1.72(6)
Os-C13	2.12(5)		

Table 2.11: Selected Angles (deg) for 3

Os-Ir-C1	84.7(6)	C3-Os-C13'	172(2)
Os-Ir-C9	91(1)	C10-Os-C13'	87(2)
C1-Ir-C9	88(1)	C11-Os-C13'	99(2)
Ir-Os-C3	83.9(7)	C12-Os-C13'	93(3)
Ir-Os-C10	78.8(8)	C11'-Os-C13'	105(2)
C3-Os-C10	86(1)	C12'-Os-C13'	75(2)
Ir-Os-C11	85(1)	Ir-C1-O1	116(2)
C3-Os-C11	89(1)	Ir-C1-C2	122(2)
C10-Os-C11	163(1)	O1-C1-C2	122(2)
Ir-Os-C12	164(2)	C1-C1-C2	122(3)
C3-Os-C12	83(2)	Os-C3-C2	123(2)
C10-Os-C12	91(2)	Cent-Ir-Os	125.1
C11-Os-C12	104(2)	Cent-Ir-C1	123.7
Ir-Os-C13	83(1)	Cent-Ir-C9	130.8
C3-Os-C13	166(1)	Ir-Os-C13'	98(2)
C10-Os-C13	97(1)	Ir-Os-C12'	173(2)
C11-Os-C13	84(2)	Ir-C9-O2	170(3)
C12-Os-C13	111(2)	Os-C10-O3	176(3)
Ir-Os-C11'	105(2)	Os-C11-O4	174(4)
C3-Os-C11'	82(2)	Os-C12-O5	164(5)
C10-Os-C11'	166(2)	Os-C13-O6	172(4)
C12-Os-C11'	82(2)	Os-C11'-O4'	172(4)
C13-Os-C11'	96(2)	Os-C12'-O5'	172(5)
C3-Os-C12'	103(2)	Os-C13'-O6'	165(4)
C10-Os-C12'	103(1)	C13-Os-C12'	90(2)
C11'-Os-C12'	75(2)	C11-Os-C12'	94(2)

The dimetallacyclopentenone core in **3** is readily visible in the solid-state structure, and resembles a distorted 2-cyclopenten-1-one molecule. The Os-Ir bond distance is 2.785(2) Å, which indicates a metal-metal single bond. This can be compared to the results obtained by Pomeroy for $[Os(CO)_4]_2IrCp^*(CO)$, where the Os-Ir bond distances are 2.7902(5) Å and 2.8124 Å.[20] The average Os-Ir bond lengths found[21] in $Os_3H_3(CO)_{11}[Ir(PPh_3)]$ are 2.779(4) Å and the average, unbridged Os-Ir separation[22] in $Os_3Ir(\mu\text{-}H)_2(\mu\text{-}Cl)_2(CO)_{12}$ is 2.776(5) Å, thus the Os-Ir bond length in **3** is within expected values.

The Os-C3 distance is 2.15(3) Å while the Ir-C1 separation is 2.07(3) Å. Due to the disorder, comparison of these bond distance with each other will not be made; however, the M-C (M = Os, Ir) distances do suggest metal-carbon single bonds. For example, the Os-C bond distances[23a] in $[\mu\text{-}C_2(CO_2Me)_2]Os_2(CO)_8$ are 2.138(5) and 2.217(2) Å while the average Ir-C bond length[23b] in $(\mu\text{-}C_6F_4)Ir_2Cp_2(CO)_2$ is 2.035(3) Å. The C2-C3 distance is 1.31(4) Å and while the esd is rather large, this bond distance is close to the 1.340(13) Å expected for a conjugated C-C double bond.[24] The C2-C3 bond distance can be compared with C-C double bond distances in other dimetallacyclopentenones. In $[\mu\text{-}C_2(CO_2Me)_2C(O)](\mu\text{-dmpm})_2Ru_2(CO)_4$ (dmpm = $(Me_2P)_2CH_2$), the C-C double bond distance is 1.340(4) Å while in $[\mu\text{-}C_2(CF_3)_2C(O)]Rh_2Cp_2(CO)_2$, the C=C bond length is 1.336(5) Å.[14,18] The C-C double bond distance in **3** seems to be shorter than in the examples quoted, but the large esd makes a meaningful comparison difficult. The C1-C2 separation in **3** is 1.45(4) Å, which is in the range expected for a $C(sp^2)\text{-}C(sp^2)$ single bond length of 1.464(18) Å in a conjugated α, β-unsaturated ketone.[24] The C-C single bond lengths in $[\mu\text{-}C_2(CO_2Me)_2C(O)]\text{-}(\mu\text{-dmpm})_2Ru_2(CO)_4$ and $[\mu\text{-}C_2(CF_3)_2C(O)]Rh_2Cp_2(CO)_2$ are 1.496(4) and

1.499(8) Å, respectively.[14,18] This shortening of the C-C single bond in α,β-unsaturated ketones is expected due to the contribution from canonical form II. Finally, the C1-O1 distance of 1.24(3) distance is in accord with the formulation as an α,β-unsaturated ketone as the C=O distance in the diruthenium complex is 1.23(3) Å and 1.213(8) Å for the dirhodium species.[14,18]

Previously, it was stated that **3** resembles a distorted 2-cyclopenten-1-one. The C1-C2-C3 angle is 122(3)°; the organic analogue, 2-cyclopenten-1-one, is thought to be nearly planar,[25] and the comparable C-C-C angle is calculated to be 110°.[26] The Ir-C1-C2 and Os-C3-C2 angles are 122(2)° and 123(2)°, respectively, close to idealized sp^2 values. The bond angles centred on the metal atoms are compressed, the Os-Ir-C1 angle is 84.7(6)° and the Ir-Os-C3 angle is 83.9(7)°. This is a result of the *ca*. 2.8 Å metal separation, far from the equivalent separation of *ca*. 1.53 Å in 2-cyclopenten-1-one. This also causes the organic fragment to distort out of planarity as the angle between the C3-Os-Ir and C1-O1-C2-C3 planes is 15.5°.

The geometry around the metal centres, particularly Os, will be greatly affected by the disorder of the carbonyl ligands, thus only a cursory analysis will be given. The Os centre can be described as having distorted octahedral geometry with the $Os(CO)_4(L)(L')$ fragment having local C_s symmetry, as expected from the FT-IR spectrum. Although there is disorder of the carbonyl ligands in **3**, the upward bending is still apparent and present in a number of related compounds. The upward bending of the equatorial carbonyls will be discussed in Chapter 6 using a more reliable crystal structure. A interesting feature is that the carbonyl on Ir is nearly co-planar with the equatorial carbonyls (C(11)O(4), C(12)O(5), C(10)O(3)) on the Os centre; this has important implications concerning the fluxional behaviour of the compound (*vide infra*).

2.4. Fluxional Behaviour of Complexes 2a-b and 3

2.4.1. Variable Temperature ^{13}C NMR Behaviour of [μ-η^3:η^1-$C_2H_2C(O)$]$Os(CO)_4MCp$ (M = Co, 2a; Rh, 2b)

The variable temperature ^{13}C NMR spectra of **2b** in the carbonyl region are shown in Figure 2.3. Similar spectra are obtained for **2a**.

The low temperature limiting ^{13}C NMR spectra of **2a** and **2b** in the carbonyl region are as expected for the proposed structures. In each case, a lowfield signal due to the acyl carbonyl is present along with four ^{13}C NMR resonances in the region associated with terminal carbonyls bound to an Os centre.[12] The level of enrichment was sufficient to allow for the observation of ^{13}C-^{13}C spin-spin coupling (**2a**: $^2J_{C\text{-}C}$ = 36.1 Hz; **2b**: $^2J_{C\text{-}C}$ = 37.2 Hz) between the two *trans* equatorial carbonyls on the Os centre. The phenomena of spin-spin coupling between two *trans* carbonyls on an Os centre has been reported previously; Shapley reported a value of $^2J_{C\text{-}C}$ = 35 Hz for $Os_3(CO)_{10}(C_7H_8)$ (C_7H_8 = norbornadiene).[27] The *trans* ^{13}C-^{13}C coupling also aids in verifying the proposed octahedral geometry about the Os centre. It is also of note that the two *trans* carbonyls are shifted to lower field relative to the remaining two terminal carbonyls. This has been observed previously and is the usual trend in saturated bimetallic and cluster Os compounds.[12,20,28]

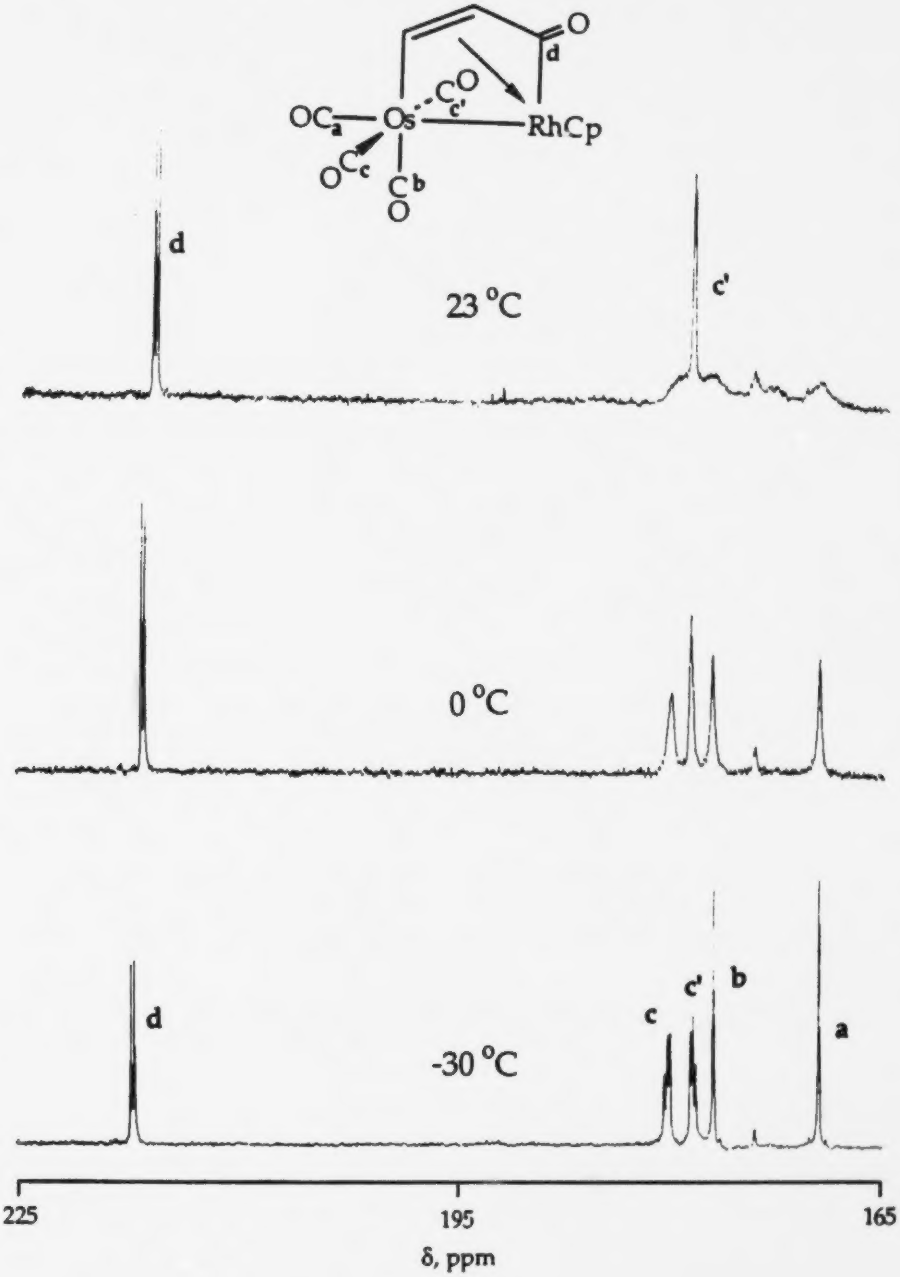

Figure 2.3: Variable Temperature ^{13}C NMR Spectra of **2b**

The two remaining carbonyl signals could not be positively assigned. However, in related compounds, the signal for the carbonyl *trans* to the metal-metal bond appears upfield of the carbonyl *trans* to the Os-C bond of the organic ring.[1,4] Thus, on this basis, the highest field terminal carbonyl signal will be assigned, in both **2a** and **2b**, to the carbonyl along the metal-metal vector; the remaining signal can then be assigned to the carbonyl *trans* to the cyclopentenone ring.

In referring to Figure 2.3, as the temperature is raised, three of the terminal carbonyl ^{13}C NMR resonances broaden; the acyl signal and the signal due to one of the *trans* equatorial carbonyls remain sharp. Further broadening is seen with increasing temperature; at 23 °C, there is coalescence of three terminal carbonyl signals, only the acyl and one equatorial carbonyl signal are unaffected. Therefore, a fluxional process is operating that exchanges three carbonyls on one of the trigonal faces of the Os centre. To account for the changes in the ^{13}C NMR spectra with temperature and taking into account the assignment of the carbonyl resonances, a 'turnstile' exchange mechanism is proposed (Scheme 2.3).[28a,29]

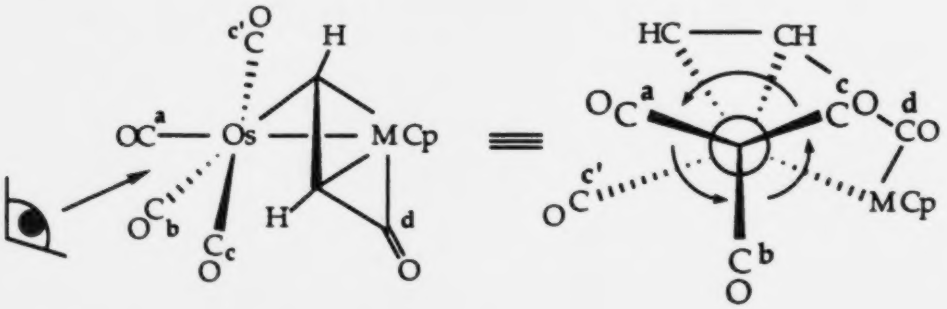

Scheme 2.3: Turnstile Exchange in **2a** and **2b**

On the Os centre, a single trigonal face may be composed of two equatorial carbonyls (one of these along the metal-metal vector) and the axial carbonyl. By undergoing a trigonal rotation these three carbonyls are interconverted, leaving the remaining terminal carbonyl unchanged, of course the acyl carbonyl is not affected.

The observed spectra may be simulated using a program developed by Prof. R.E.D. McClung of this Department.[30] This allows a rate constant to be obtained for each temperature and, using the Eyring equation, activation parameters may be calculated for the fluxional process (Appendix 1). The values of $\Delta H^{\ddagger}$ and $\Delta S^{\ddagger}$ for **2a** and **2b** are listed in Table 2.12.

Table 2.12: Activation Parameters for CO Exchange in $[\mu\text{–}\eta^3\text{:}\eta^1\text{-}C_2H_2C(O)]Os(CO)_4MCp$ (M = Co, Rh)

compound	$\Delta H^{\ddagger}$ (kJ/mol)	$\Delta S^{\ddagger}$ (J/mol·K)
2a	59.6 ± 3.0	27.4 ± 11.4
2b	61.0 ± 2.1	13.1 ± 7.6

The activation parameters obtained for **2a** and **2b** are, within experimental error, identical. This is not unexpected as, in each case, similar substituents are present on the Os centre. The only difference is the metal-metal bond, but, from the FT-IR data, the electron density on the Os centre is essentially the same between **2a** and **2b**. Pomeroy has noted that an increase in electron density on the metal centre reduces the activation barrier for a turnstile rotation.[28a] Since the electronic environment on Os is similar in **2a** and **2b**, similar values for $\Delta H^{\ddagger}$ and $\Delta S^{\ddagger}$ are obtained. The activation parameters for **2a** and **2b** can be compared the activation parameters obtained for trigonal rotation in $Os_3(CO)_{11}(P(OMe)_3)$ ($\Delta H^\ddagger$ = 30.2 ± 1.2 kJ/mol, $\Delta S^\ddagger$ = 2.3 ± 5.4 J/mol·K) where a more favourable exchange is seen possibly due to the presence of electron donating phosphite groups.[28a]

2.4.2. Variable Temperature ^{13}C NMR Behaviour of $[\mu\text{-}\eta^1\text{:}\eta^1\text{-}C_2H_2C(O)]Os(CO)_4IrCp(CO)$, 3

The variable temperature ^{13}C NMR spectra of $[\mu\text{-}\eta^1\text{:}\eta^1\text{-}C_2H_2C(O)]Os(CO)_4IrCp(CO)$, **3** in carbonyl region is shown in Figure 2.4. At the low temperature limit of -80 °C, six different carbonyl resonances are observed, consistent with the solid state structure. As in **2a** and **2b**, the lowest field ^{13}C NMR resonance of **3** can be immediately assigned to the acyl carbon attached to the Ir centre. Next, the two *trans* equatorial carbonyls signals are observed in their characteristic lowfield position and exhibit a ^{13}C-^{13}C spin-spin coupling of 36.0 Hz.[27] For **3**, the highest field signal is assigned to the CO bound to the Ir centre while the carbonyl *trans* to the Os-C sigma bond is assigned to the next highest field signal. The carbonyl along the Ir-Os vector is then assigned to the only remaining ^{13}C NMR resonance at 173.6 ppm. The rationale for this assignment will be deferred until the variable temperature behaviour has been discussed.

As the temperature of the NMR sample is raised, four of the terminal carbonyl signals broaden and coalesce. The acyl carbon signal and the carbonyl group *trans* to the Os-C sigma bond remain sharp. At room temperature, four ^{13}C NMR signals are observed. This indicates that although four carbonyls are involved in the fluxional process, they are only exchanging in a pairwise manner. Obviously, a different fluxional process is in operation for **3** then observed for **2a** and **2b**.

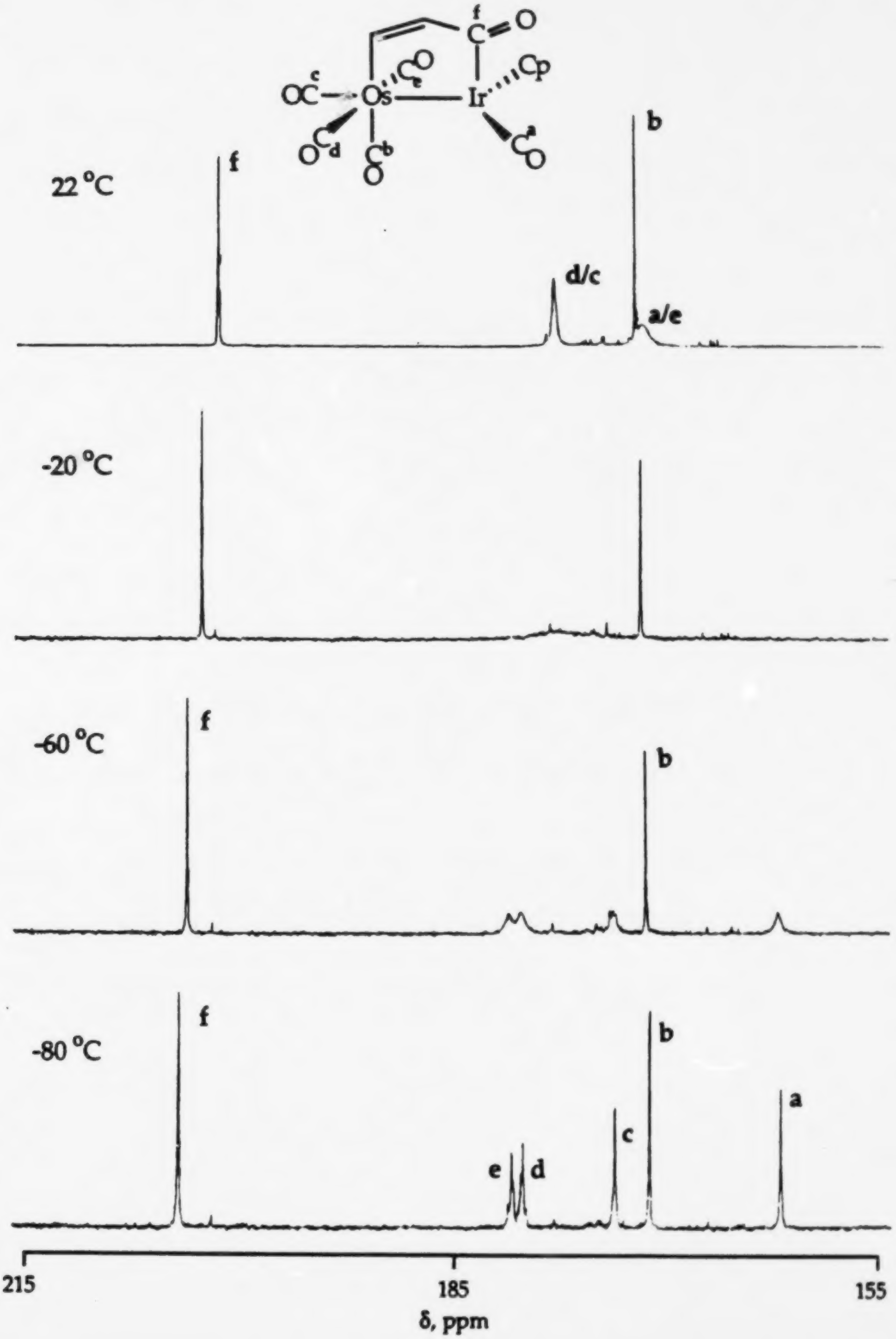

Figure 2.4: Variable Temperature ^{13}C NMR Spectra of 3 (Carbonyl Region)

To rationalize the changes in the ^{13}C NMR spectra seen with temperature for **3** a 'truncated-merry-go-round' exchange mechanism is postulated (Scheme 2.4).[20,31]

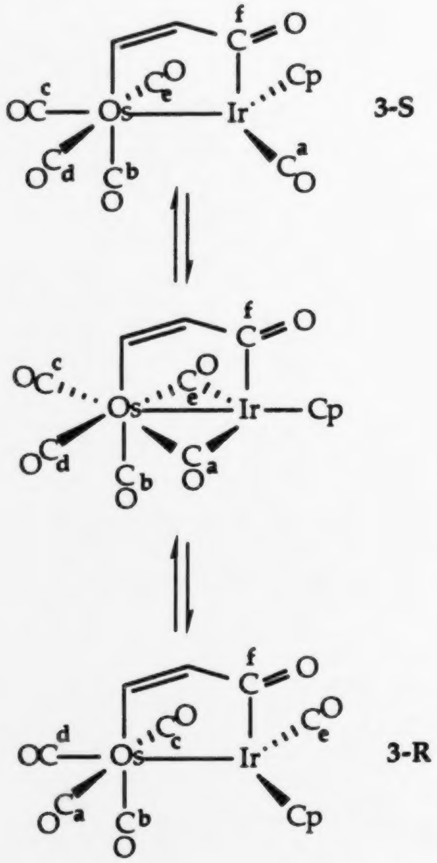

Scheme 2.4: Truncated Merry-Go-Round Exchange in **3**

The first step in the exchange process is the formation of a doubly carbonyl bridged intermediate. This intermediate is readily accessible as the Ir-CO is roughly in the same plane as the equatorial Os carbonyls. In the formation of this intermediate, CO_c and CO_d shift their positions slightly so that the intermediate has C_s symmetry as compared to C_1 symmetry in the unbridged form of **3**. The next step is the transfer of CO_e to the Ir centre and CO_a to the Os centre. Further exchange in this plane leading to a complete merry-go-round exchange is prevented by the Cp ligand. Thus, the process merely reverses itself and CO_a and CO_e are exchanged in a pairwise manner, as are CO_c and CO_d. The carbonyl *trans* to the Os-C σ bond, CO_b, and the acyl carbonyl, CO_f, are not involved in this fluxional process and their ^{13}C NMR signals remain sharp.

The labels **3-S** and **3-R** refer to the stereochemistry around the Ir centre, these structures are related by a mirror plane. The choice of **3-S** as the starting enantiomer was arbitrary since the truncated-merry-go-round process causes racemization due to the presence of an intermediate of C_s symmetry.

The exchange mechanism can also be used to fully assign the limiting ^{13}C NMR spectrum of **3**. The assignment of CO_b is confirmed as its signal remains sharp throughout the temperature range studied. The two *trans* equatorial carbonyls may be specifically assigned based on the average signals present at room temerature; the signal at ambient temperature limit is the average of the chemical shifts values for the two exchanging carbonyls. To further corroborate this, the solvent was changed from CD_2Cl_2 to toluene-d_8 in order to obtain a high temperature (+80 °C) spectrum. The chemical shift values for the terminal carbonyls were unaffected, however the acyl carbonyl resonance shifted upfield by 10 ppm. The reduction in the polarity of the solvent causes a significant decrease in the contribution of canonical form **IV**, thus altering the chemical environment and changing the chemical shift.

The ^{13}C NMR spectra of **3** can be simulated using the same method outlined for **2a** and **2b**. For **3**, activation parameters of $\Delta H^{\ddagger} = 40.9 \pm 1.2$ kJ/mol and $\Delta S^{\ddagger} = -18.8 \pm 4.7$ J/mol.K were calculated. The pairwise, in-plane exchange of metal-bound carbonyls is fairly prevalent in the literature. In $MM'(CO)_8(\mu\text{-HFB})$ the activation energies for a full merry-go-round exchange are trend RuRu (46.0 kJ/mol) < RuOs (60.2 kJ/mol) < OsOs (static at room temperature).[1] Pomeroy has reported a value of $\Delta G^{\ddagger}_{263K} = 59.4 \pm 1.3$ kJ/mol for truncated carbonyl exchange in $[Os(CO)_4]_2IrCp(CO)$ which is particularity relevant as it pertains to CO exchange between an $Os(CO)_4$ unit and a IrCp(CO) fragment.[20] A value of $\Delta G^{\ddagger}_{263K} = 45.8 \pm 1.3$ kJ/mol is found for **2c**, indicating that, in this case, the presence of an organic bridge lowers the activation barrier to CO exchange. For **3**, there is a large negative entropy of activation; a common feature of merry-go-round exchange mechanisms. The first step in the exchange process involves the synchronous formation of two carbonyl bridges, causing a change from C_1 to C_s symmetry. The formation of a more symmetrical intermediate would account for the unfavourable entropy of activation.[31a-b,32]

2.5. Proposed Mechanism for the Formation of Dimetallacyclopentenones

2.5.1. Formation of $[\mu\text{-}\eta^3\text{:}\eta^1\text{-}C_2H_2C(O)]Os(CO)_4RhCp$, 2b

The reaction of $Os(CO)_4(\eta^2\text{-HCCH})$ with $CpM(CO)_2$ (M = Co, Rh) proceeds with CO loss to yield dimetallacyclopentenones whereby the olefinic moiety is bound to the Rh or Co centre. In an attempt to elucidate the mechanistic features of the reaction, a low temperature ^{1}H NMR and ^{13}C NMR spectroscopic study was undertaken. The reaction was relatively simple as a NMR tube containing a CD_2Cl_2 solution of partially ^{13}CO enriched $Os(CO)_4(\eta^2\text{-}HCCH)$ and a slight excess of unenriched $CpRh(CO)_2$ was slowly warmed from -40 °C and monitored using NMR spectroscopy.

In the ^{13}C NMR spectrum at -40 °C, two intense peaks due to $Os(CO)_4(\eta^2\text{-}HCCH)$ were observed, plus a doublet (δ = 191.9 ppm, $^1J_{Rh\text{-}C}$ = 84.5 Hz) of very low intensity assigned to $CpRh(CO)_2$. The ^1H NMR spectrum showed only singlets a 6.18 ppm and 5.48 ppm, due to $Os(CO)_4(\eta^2\text{-}HCCH)$ and $CpRh(CO)_2$, respectively. The temperature was raised to -30 °C and no changes were observed in the ^1H NMR spectrum. However, the ^{13}C NMR spectrum showed a very slight increase in the intensity of the $CpRh(CO)_2$ signal. This indicated that $CpRh(^{13}CO)(CO)$ was forming; it should be noted that no free ^{13}CO or **2b** was detected. This phenomenon of ^{13}CO enrichment of the condensation partner prior to formation of the bimetallic product has been observed previously in the reaction of $Os(CO)_4(\eta^2\text{-}HCCH)$ with $Ru(CO)_5$.[33]

The temperature was raised to -20 °C. After 10 minutes at this temperature, the ^1H NMR spectrum was invariant. However, the ^{13}C NMR spectrum showed greatly increased concentrations of $CpRh(^{13}CO)(CO)$ along with the presence of a large amount of free ^{13}CO. After 35 minutes at this temperature, the presence of $[\mu\text{-}C_2H_2C(O)]Os(CO)_4RhCp$, **2b**, was also detected in the ^1H NMR and ^{13}C NMR spectra. This observation indicates that dissociation of CO appears to precede formation of the bimetallic species.

The temperature was then allowed to reach -10 °C. Increased amounts of **2b** and free ^{13}CO were seen, the level of $CpRh(^{13}CO)(CO)$ did not increase substantially. Also, a new bimetallic species was observed. Based on ^1H NMR (8.20: d, $^3J_{H\text{-}H}$ = 9.0 Hz, H_β; 7.33: d, $^3J_{H\text{-}H}$ = 9.0 Hz, H_α)

and ^{13}C NMR (219.8: d, $^1J_{Rh\text{-}C}$ = 25.2 Hz, acyl CO; 189.8: d, $^1J_{Rh\text{-}C}$ = 40.2 Hz, 2CO; 174.1: 2CO; 173.5: 1CO) spectroscopy, this compound is postulated to be [μ-η^1:η^1-$C_2H_2C(O)$]$Os(CO)_4RhCp(CO)$, the Rh congener of 3. Raising the temperature further to 0 °C and finally to 10 °C resulted in the increased formation of **2b** and [μ-η^1:η^1-$C_2H_2C(O)$]$Os(CO)_4RhCp(CO)$ so that, at the end of the reaction, only the two bimetallic compounds, free CpRh(^{13}CO)(CO) and free ^{13}CO were present. The NMR solution was purged with N_2 for 3 minutes. A subsequent ^{13}C NMR spectrum showed the disappearance of free ^{13}CO, but the relative concentrations of **2b** and [μ-η^1:η^1-$C_2H_2C(O)$]$Os(CO)_4RhCp(CO)$ remained unchanged. Also, leaving the resulting solution to stand for 20 h at ambient temperature gave no observable changes. Thus, **2b** is not formed *via* CO loss from [μ-η^1:η^1-$C_2H_2C(O)$]$Os(CO)_4RhCp(CO)$. Also, a bench-top experiment involving the reaction of $Os(CO)_4$(η^2-HCCH) and $CpRh(CO)_2$ under 1 atm. of CO in pentane solvent resulted in the exclusive production of **2b**. Thus, it may be postulated that the conditions required to form [μ-η^1:η^1-$C_2H_2C(O)$]$Os(CO)_4RhCp(CO)$ are solvent and concentration dependent.

In proposing a mechanism for the formation of **2b**, several features must be incorporated. The CO dissociation step must precede the formation of **2b** and also, **2b** is not formed from [μ-η^1:η^1-$C_2H_2C(O)$]$Os(CO)_4RhCp(CO)$. The ^{13}CO exchange with $CpRh(CO)_2$ should also be taken into account. A plausible mechanism is shown in Scheme 2.5.

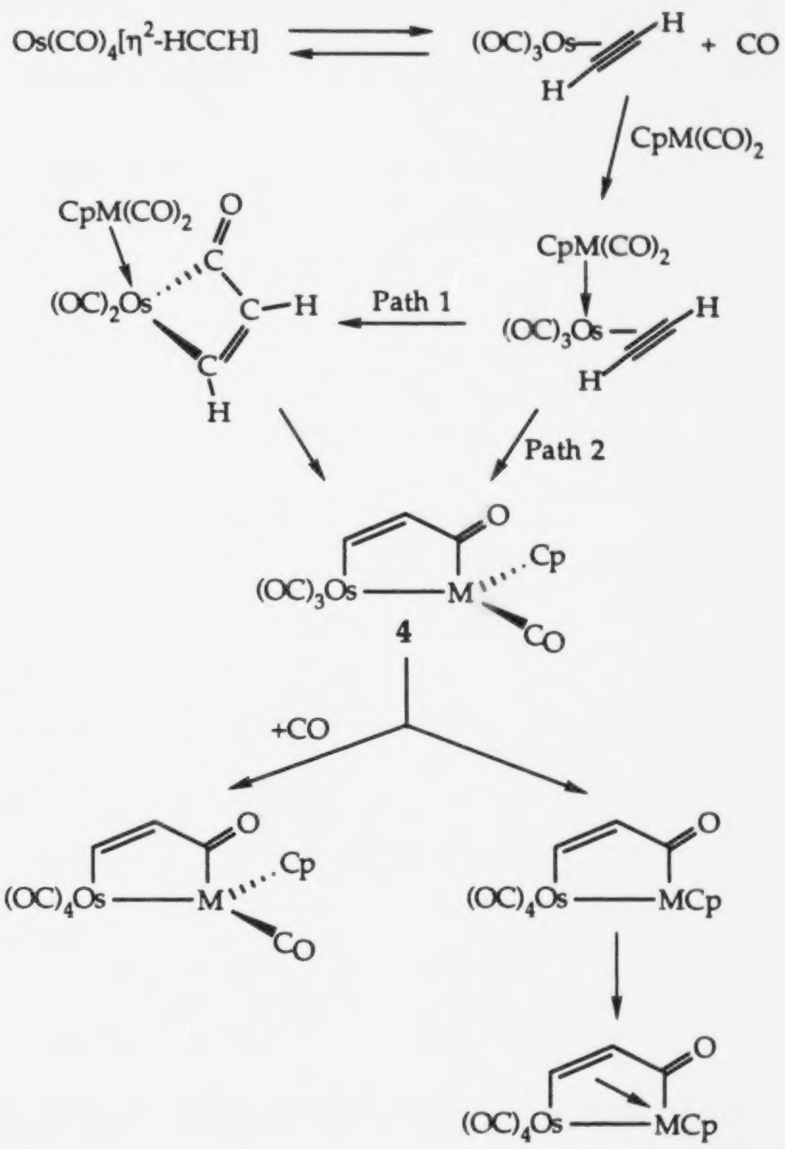
Os(CO)$_4$[η^2-HCCH]
(OC)$_3$Os
H
H
+ CO
CpM(CO)$_2$
CpM(CO)$_2$
(OC)$_3$Os
Path 1
Path 2
CpM(CO)$_2$
(OC)$_2$Os
C
O
C—H
C
H
(OC)$_3$Os
M
Cp
CO
O
4
+CO
(OC)$_4$Os
M
Cp
CO
O
(OC)$_4$Os
MCp
O
(OC)$_4$Os
MCp
O

Scheme 2.5: Proposed Mechanism for Formation of **2**

As stated, the initial step is dissociation of a CO ligand from $Os(CO)_4(\eta^2\text{-HCCH})$ followed by nucleophilic attack of $CpM(CO)_2$ at the vacant coordination site on the Os centre. The next step would be a CO insertion step, following either Path 1 or Path 2. There is evidence for a step similar to that seen on Path 1 as Tianfu Mao of our laboratories has synthesized the osmacyclobutenone compounds *cis*- and *trans*-(η^2-dppm)$Os(CO)_3[C_2H_2C(O)]$ (Scheme 8.6).[34a] Also, Green has observed CO insertion into a coordinated alkyne at a mononuclear Ru centre (Scheme 8.5).[34b] Path 2 would require a CO insertion involving a carbonyl on the Rh centre. This is plausible as the positively charged Rh centre would activate the carbonyl towards nucleophilic attack by one of the acetylenic carbons. For both pathways, intermediate **4** would be formed. The major difference in the two pathways is whether a mono- or di-nuclear CO insertion is taking place. Unfortunately, the low temperature studies did not provide sufficient information to discriminate between the two pathways.

Intermediate **4** could then undergo a CO transfer between the Rh and Os centres, followed by coordination of the olefinic moiety, resulting in the formation of **2b**. Also, it is possible that free CO could coordinate to **4** and form $[\mu\text{-}\eta^1\text{:}\eta^1\text{-}C_2H_2C(O)]Os(CO)_4RhCp(CO)$. This would account for the observation of this species in the NMR tube reaction.

The intermetallic CO exchange between $Os(CO)_4(\eta^2\text{-HCCH})$ and $CpRh(CO)_2$ must also be addressed. It is possible that another equilibrium occurs before the CO insertion step which equally distributes the ^{13}CO label (Scheme 2.6). The Scheme assumes CO dissociation from $Os(CO)_4(\eta^2\text{-HCCH})$. Initially, at -30 °C, no free ^{13}CO was observed even though the amount of $CpRh(^{13}CO)(CO)$ increased slightly; however the appearance of a substantial amount of $CpRh(^{13}CO)(CO)$ was accompanied by the observation of free ^{13}CO at -20 °C. Thus, it is likely that CO dissociation does occur concurrently with CpRh(^{13}CO)(CO) formation at -30 °C and the amount of free ^{13}CO was too small to be observed.

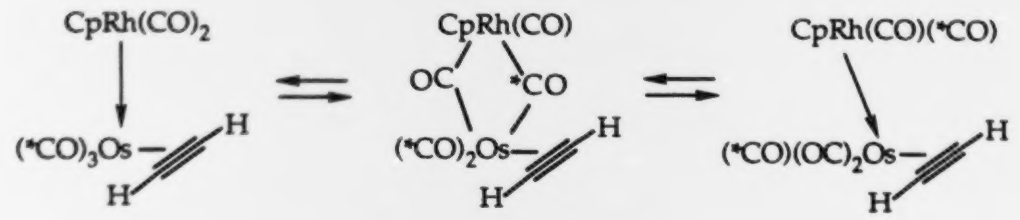

Scheme 2.6: ^{13}CO Equilibration in **2b**

2.5.2. Formation of [μ-η^1:η^1-$C_2H_2C(O)$]Os(CO)$_4$IrCp(CO), 3

A similar ^{1}H and ^{13}C NMR spectroscopic study in CD_2Cl_2 was undertaken between ^{13}CO enriched Os(CO)$_4$(η^2-HCCH) and unenriched CpIr(CO)$_2$. Observations parallel to the CpRh(CO)$_2$ reaction were made. At -40 °C, in the ^{1}H and ^{13}C NMR spectra, only signals due to Os(CO)$_4$(η^2-HCCH) were detected. As the temperature was warmed to -30 °C, small amounts of CpIr(^{13}CO)(CO) were observed. At -20 °C, increased levels of CpIr(^{13}CO)(CO) were present along with free ^{13}CO. This indicates that an intermetallic ^{13}CO exchange similar to that shown in Scheme 2.6 was taking place. Two singlets of low intensity (δ = 183.0 ppm and 178.2 ppm) due to an unidentified component were also present in the ^{13}C NMR spectrum. In the ^{1}H NMR spectrum, two additional singlets at 6.90 ppm and 5.76 ppm were also observed. Maintaining the temperature at -20 °C resulted in increased CpIr(CO)(^{13}CO) enrichment, increased free ^{13}CO levels and the appearance of signals, in both the ^{1}H and ^{13}C NMR spectra, due to [μ-η^1:η^1-$C_2H_2C(O)$]Os(CO)$_4$IrCp(CO), **3**.

The temperature was then raised to -10 °C, where similar observations to those at -20 °C were made. However, in the ^{13}C NMR spectrum, in addition to the signals observed at -20 °C, two new singlets at 198.8 ppm and 169.0 ppm were observed. The resonance at 198.8 ppm may indicate an acyl intermediate, although one cannot ascertain whether it is attached to an Os or an Ir centre. Raising the temperature to 0 °C saw a decrease in the intensities of the signals due to the unidentified intermediates but a large increase in the intensities of the signals due to **3**. There was also an initial increase in the concentration of free ^{13}CO, but after maintaining the temperature at 0 °C for 40 minutes, the amount of free ^{13}CO decreased while the amount of **3** increased. At +10 °C, only signals due to free ^{13}CO, **3** and CpIr(^{13}CO)(CO) were present. Raising and maintaining the temperature at +17 °C resulted in increased levels of **3** while the concentration of free ^{13}CO dropped dramatically, so that after 25 minutes at +17 °C, only a minute amount of free ^{13}CO was observed. In the final ^{1}H and ^{13}C NMR spectra, taken at 23 °C, only **3** and free CpIr(^{13}CO)(CO) were observed, no other species were present.

Several mechanistic features can be deduced from the low temperature ^{1}H and ^{13}C NMR spectroscopic studies. First, similar to the reaction of CpRh(CO)$_2$ with Os(CO)$_4$(η^2-HCCH), the reaction of CpIr(CO)$_2$ with Os(CO)$_4$(η^2-HCCH) appears to proceed *via* initial CO loss, most likely from the Os centre. Also, the re-coordination of the dissociated CO is indirectly observed as a decrease in the amount of free CO as the level of **3** increases. Thus, a mechanism similar to that shown in Scheme 2.5 is proposed. The major exception is that intermediate **4** is more likely to add an additional molecule of free CO to form the non-coordinated dimetallacyclopentenone. A possible explanation is that dimetallic compounds with two third row metals are less likely to have bridging carbonyl ligands, thus the transfer of an Ir bound CO to the Os centre would be less likely than in the case of **2b** (M = Rh).[1,20,31b-c,35] The net result would be that the pathway leading to the formation of a coordinated dimetallacyclopentenone would be unfavourable and **4** would simply react with free CO to form **3**. This is corroborated by the fact that **2b** forms more readily than **3**. The ^{13}C NMR evidence indicates that the reaction to form **2b** is over at +10 °C, while for **2c**, further heating to +17 °C is required to effect a full reaction in a comparable amount of time. Thus, the transfer of a CO molecule from the Rh to Os centre in **4** is competing with CO association while, for **3**, the association of free CO to **4** is much more favourable than intrametallic CO transfer.

2.6. Conclusions

The reaction of $Os(CO)_4(\eta^2\text{-}HCCH)$, **1**, with $CpM(CO)_2$ (M = Co, Rh, Ir) has been shown to be a useful and novel method of synthesizing dimetallacyclopentenones. The reactions proceed in a regioselective manner such that the acyl is attached to the Group IX metal centre. The metal dependence of the reaction is readily apparent as two different types of dimetallacyclopentenones are synthesized. The dimetallic complexes were characterized by a full range of spectroscopic techniques and, considering the dearth of data available, should provide useful models in the characterization of related compounds. The carbonyls ligands on **2a-b** and **3** were shown to be fluxional although the exchange mechanism is dependent on the structure of the dimetallic species. A mechanistic study provided some clues as to possible pathways leading to the formation of these dimetallic complexes. For both **2b** and **3**, the reaction proceeds *via* initial CO loss from $Os(CO)_4(\eta^2\text{-HCCH})$. However, for **2b**, it is thought that intrametallic CO transfer is more favourable than reaction with free CO, leading to the formation of a coordinated dimetallacyclopentenone. For **3**, the opposite is suggested as CO association preferentially occurs to form a non-coordinated dimetallacyclopentenone.

2.7. Experimental Section

2.7.1. Solvents and General Techniques

All solvents used were dried by distillation under N_2 from an appropriate drying agent (Table 2.13).

Table 2.13: Drying Agents for Solvents

Solvent	Drying Agent
Dichloromethane	Phosphorus Pentoxide
Pentane	Calcium hydride
Hexane	Sodium metal
Benzene	Potassium metal
Diethylether	Na-K alloy/benzophenone

Also, freeze-pump-thaw cycles were used to degas solvents for certain experiments. Pentane was stirred over concentrated H_2SO_4 for several cycles, then stirred over an aqueous solution of sodium bicarbonate, stirred over distilled water and finally dried over sodium sulphate before distillation from CaH_2. A similar procedure was used to precondition the hexane solvent before distillation from potassium. The deuterated solvents were stored over molecular sieves under a N_2 atmosphere.

All glassware were degreased with hexane before being soaked in a KOH-Ethanol (95%) solution. This was followed by a rinse with distilled water and soaking in a dilute (*ca.* 0.5 M) HCl solution. After a final rinse with distilled water, the glassware was dried at 120 °C before use. All synthetic procedures were carried out under purified nitrogen or argon atmospheres by using standard Schlenk techniques. The N_2 or Ar used in double manifold lines was purified by passing the gas through a heated (100 °C) column of BASF Cu catalyst (R3-11) to remove any trace oxygen and a column of Mallinkrodt Aquasorb to remove trace moisture. Unless otherwise stated, all other commercial gases were used as received.

2.7.2. Physical Measurements

Infrared spectra were obtained on a Bomem MB-100 Fourier transform spectrometer over the range 2200 - 1600 cm^{-1}. Solution samples were held between KBr (0.1 mm) plates. NMR samples were either septa sealed under inert atmosphere or flame sealed under vacuum. The ^{1}H, ^{13}C, ^{31}P and ^{19}F NMR spectra were collected on a Bruker WH-200, Bruker AM-300, Bruker WM-360, Bruker AM-400 or a Varian UNITY 500 spectrometer. Elemental analyses were carried out by the Microanalytical Laboratory of this Department. Mass spectra were recorded on an A.E.I. MS-12 Spectrometer operating at 16 or 70 eV.

2.7.3. Photochemical Techniques

The photochemical experiments were carried out using the immersion well shown in Figure 2.5. The immersion well was constructed by the Glass Service Laboratory of this Department and consisted of an outside cooling jacket, two ports for cooling solution, a gas inlet, two ports for solution sampling and a cooling insert into which the lamp is placed. The wavelength of the radiation was controlled using cut-off filters fashioned from Pyrex glass ($\lambda \geq 280$ nm) or GWV (Glaswerk Wertheim) glass ($\lambda \geq 370$ nm). The irradiation source was a Philips HPK 125 Watt Mercury Vapour lamp. The complete system, cooling well and insert, was used in the internal photolysis reactions. A methanol circulating/cooling solution, using a MGM Lauda Circulating Bath, maintained the reaction solution at a constant temperature and kept the lamp cool.

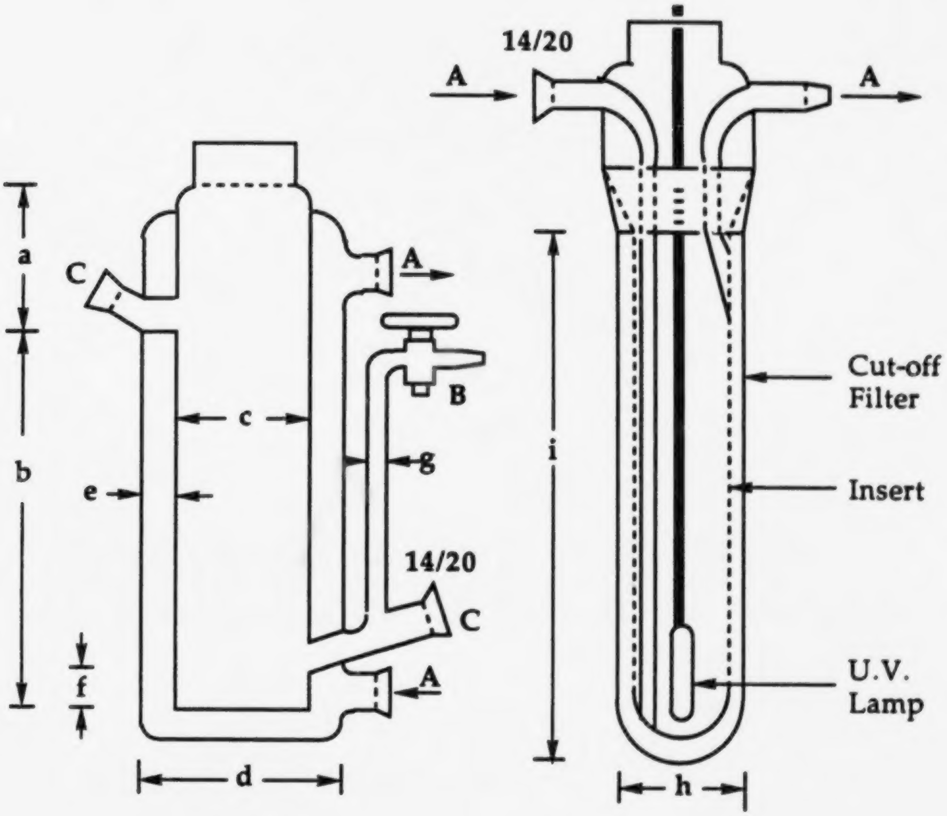
14/20
A
A
a
C
A
B
c
g
b
e
i
Cut-off Filter
Insert
14/20
C
f
A
U.V. Lamp
d
h

A: inlet/outlet cooling ports

B: gas inlet

C: sample ports

a: 3.0 cm
b: 12.0 cm
c: 4.5 cm
d: 7.0 cm
e: 1.25 cm
f: 1.0 cm
g: 0.5 cm (id)
h: 3.0 cm
i: 13.5 cm

Figure 2.5: Low Temperature Photolysis Apparatus

For external photolysis, the insert in Figure 2.6 was used alone with water as the cooling solvent. The appropriate cut-off filter was selected and a sample solution held in a Schlenk tube was positioned beside the insert.

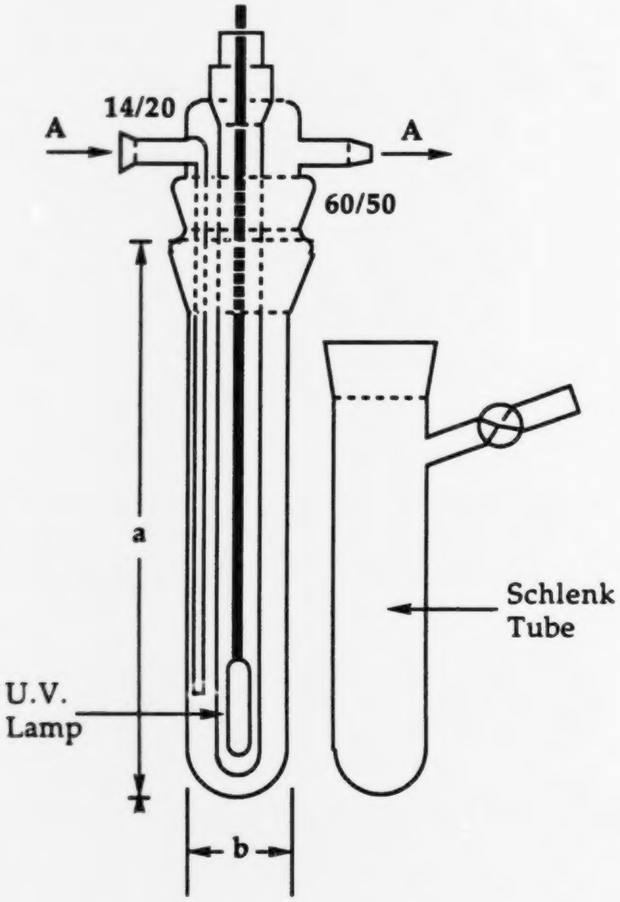
14/20
A
A
60/50
a
Schlenk Tube
U.V. Lamp
b

A: inlet/oulet cooling ports

a: 29.0 cm

b: 4.5 cm

Figure 2.6: Set-up for External Photolysis

2.7.4. Starting Materials and Reagents

Acetylene was purchased from Linde Gas Products and the acetone stabilizer removed by means of a dry ice/acetone trap. ^{13}CO (99.5 % ^{13}C) was purchased from Isotec, Inc. $CpCo(CO)_2$ was purchased from Strem Chemical Co. and used as received. A loan of OsO_4 was provided by Johnson-Mathey, Inc. $Os_3(CO)_{12}$[36] and $Os(CO)_5$[37], $Os(CO)_4(\eta^2\text{-}C_2H_2)$[4] were prepared by published procedures as were $CpRh(CO)_2$[38]and $CpIr(CO)_2$.[39]

2.7.5. Synthetic Procedures

Synthesis of $[\mu\text{-}\eta^3\text{:}\eta^1\text{-}C_2H_2C(O)]Os(CO)_4RhCp$, 2b

A pentane solution containing $Os(CO)_4(\eta^2\text{-}C_2H_2)$, **1**, (40.5 mg, 0.123 mmol) and $CpRh(CO)_2$ (35.8 mg, 0.160 mmol) was slowly warmed from -78 °C to 5 °C using a dry ice/acetone bath. At temperatures near 0 °C the light orange color of the solution began to darken. The solution was maintained at 5-10 °C and the reaction was monitored by IR spectroscopy. The reaction was complete in *ca.* 0.5 h after which time the solution was red-orange in color. The solvent was removed *in vacuo* and the red residue was extracted with pentane (2x10 mL). The combined extracts were filtered, reduced to half their volume and cooled to -80 °C overnight. The supernatant solution was filtered off and the red solid was washed with cold pentane (2x5 mL). The yield of **2b** was 51.0 mg (79%).

Formula Weight: 524.29

Mass Spectrum(140 °C, 70eV): M^+ (526, 24.2%), M^+-nCO (n = 0-5)

IR(pentane, cm^{-1}) ν(CO): 2107(w), 2033(s), 2027(m), 1997(s). ν(acyl): 1783(w).

^1H NMR(360 MHz, CD_2Cl_2) 7.85 (1H, d, $^2J_{H\text{-}H}$ = 7.4 Hz, H_β), 5.50 (5H, s, C_5H_5), 5.00 (1H, dd, $^2J_{H\text{-}H}$ = 9.1 Hz, $^2J_{Rh\text{-}H}$ = 3.0 Hz, H_α).

^{13}C NMR(90.5 MHz, CD_2Cl_2, 23 °C) 115.7 (d, $^{1}J_{Rh\text{-}C}$ = 16.1 Hz, C_β), 86.7 (d, $^{1}J_{Rh\text{-}C}$ = 5.0 Hz, C_5H_5), 44.4 (s, C_α).

^{13}C NMR(90.5 MHz, CD_2Cl_2, -30 °C) 216.9 (d, $^{1}J_{Rh\text{-}C}$ = 24.0 Hz, CO_d), 179.9 (CO_c), 178.0 ($CO_{c'}$), 176.7 (CO_b), 169.4 (CO_a).

Anal. Calcd. for $C_{12}H_7O_5OsRh$: C, 27.49; H, 1.35. Found: C, 27.79; H, 1.44.

Synthesis of $[\mu\text{–}\eta^3\text{:}\eta^1\text{-}C_2H_2C(O)]Os(CO)_4CoCp$, 2a

Using a similar procedure, **1** (40.5 mg, 0.123 mmol) and $CpCo(CO)_2$ (33.2 mg, 0.185 mmol) were used to obtain **2a** as a purple solid (32.1 mg, 55%).

Formula Weight: 480.32

Mass Spectrum(170 °C, 16eV): M^+ (482, 36.3%), M^+-nCO (n = 0-5)

IR(pentane, cm^{-1}) ν(CO): 2107(w), 2035(s), 2023(m), 1996(s). ν(acyl): 1778(w).

^{1}H NMR(360 MHz, CD_2Cl_2) 8.45 (1H, d, $^{2}J_{H\text{-}H}$ = 7.9 Hz, H_β), 5.07 (5H, s, C_5H_5), 4.13 (1H, d, $^{2}J_{H\text{-}H}$ = 7.9 Hz, H_α), .

^{13}C NMR(90.5 MHz, CD_2Cl_2, 23 °C) 120.2 (s, C_β), 83.6 (s, C_5H_5), 35.8 (s, C_α).

^{13}C NMR(90.5 MHz, CD_2Cl_2, -40 °C) 232.9 (CO_d), 179.7 (CO_c), 178.1 ($CO_{c'}$), 178.0 (CO_b), 169.6 (CO_a).

Anal. Calcd. for $C_{12}H_7CoO_5Os$: C, 30.00; H, 1.47. Found: C, 30.13; H, 1.41.

Synthesis of $[\mu\text{–}\eta^1\text{:}\eta^1\text{-}C_2H_2C(O)]Os(CO)_4IrCp(CO)$, 3

A pentane solution of **1** (17.0 mg, 0.052 mmol) and $CpIr(CO)_2$ (22.8 mg, 0.072 mmol) was slowly warmed from -78 °C to 10 °C. In the temperature range of 5-10 °C the light yellow color deepened and a fine, canary yellow precipitate formed. The reaction was maintained at 10 °C for *ca.* 2 h until the FT-IR showed no signals due to **1**. The solution was cooled to -78 °C to precipitate out all of the bimetallic complex. The solvent was removed by cannula filtration and the yellow solid was washed (3x10 mL) at -20 °C with pentane until the FT-IR spectra showed peaks only due to **3**. The resulting yellow powder was dried under vacuum overnight. The yield of **3** was 23.3 mg (69%).

Formula Weight: 641.59

Mass Spectrum(160 °C, 70eV): M^+ (642, 23.5%), M^+-nCO (n = 0-6)

IR(pentane, cm^{-1}) ν(CO): 2112(w), 2039(s), 2035(m), 2004(s), 1992(w). ν(acyl): 1636(w).

^1H NMR(360 MHz, CD_2Cl_2) 7.98 (1H, d, $^2J_{H\text{-}H}$ = 9.1 Hz, H_β), 7.51 (1H, d, $^2J_{H\text{-}H}$ = 9.1 Hz, H_α), 5.64 (5H, s, C_5H_5).

^{13}C NMR(90.5 MHz, CD_2Cl_2, 23 °C) 166.9 (s, Cβ), 132.1 (s, Cα), 84.9 (s, C_5H_5).

^{13}C NMR(90.5 MHz, CD_2Cl_2, -80 °C) 203.7 (CO_f), 180.9 (CO_e), 180.0 (CO_d), 173.6 (CO_c), 171.5 (CO_b), 162.6 (CO_a).

Anal. Calcd. for $C_{13}H_7IrO_6Os$: C, 24.34; H, 1.10. Found: C, 24.81; H, 1.22.

Synthesis of ^{13}CO Enriched 2a-b and **3**. A pentane solution of **1** was degassed by a freeze-pump-thaw cycle using liquid nitrogen. Approximately one atmosphere of ^{13}CO was admitted into the flask and the solution was stirred at 0 °C for 30 minutes. Solutions of **1-^{13}CO** were then subsequently used in reactions to generate the enriched dimetallic compounds. This resulted in approximately 30% ^{13}CO enrichment as determined from ^{13}C NMR integrations of the dimetallic compounds. Solutions of ^{13}CO enriched $CpM(CO)_2$ (M = Co, Rh, Ir) could be prepared by stirring pentane solutions of the aforementioned compounds under a ^{13}CO atmosphere at room temperature overnight. These could also be used in the generation of dimetallic compounds although adequate results were obtained using **1-^{13}CO** and unenriched $CpM(CO)_2$ (M = CO, Rh, Ir).

2.7.6. X-ray Structure Determination of 3

A yellow, X-ray quality crystals were grown by cooling a CH_2Cl_2/pentane solution of **3** to -5 °C. The X-ray data collection and structure refinement was carried out by Andrew Bond, a student with Prof. Robin Rogers at Northern Illinois University. The single crystal was mounted in a thin-walled glass capillary under an Argon atmosphere. Crystal data and general conditions of data collection and structure refinement are given in Table 2.14. The positions of the Ir and Os atoms were derived from a three dimensional Patterson map and the remaining non-hydrogen atoms were located in difference Fourier maps after least squares refinement. For **3**, three full data sets from different crystals were collected and only the best result is given. All H atoms were included at their idealized positions (calculated by assuming C-H = 0.95 Å and sp^3 or sp^2 geometry) and constrained to 'ride' with the attached C atom with B fixed at 5.5 $Å^2$.

The final atomic coordinates are given in Table 2.15 and selected bond distances, angles and weighted least-squares planes for **3** are given in Tables 2.10, 2.11 and 2.16, respectively.

Table 2.14: Summary of Crystallographic Data for **3**

Crystal Parameters	
formula	$C_{13}H_7O_6IrOs$
formula wt.	641.62
crystal size, mm	0.05 x 0.18 x 0.25
crystal system	triclinic
space group	$P\bar{1}$
a, Å	7.392(2)
b, Å	7.846(4)
c, Å	13.729(8)
α, deg	93.00(5)
β, deg	103.24(4)
γ, deg	106.35(3)
V, Å^3	737.9
Z	2
D_{calc}, g cm^{-3}	2.89
μ, cm^{-1}	187

Data Collection and Structure Refinement

diffractometer	Enraf-Nonius CAD4
radiation (λ [Å])	Mo K_α (0.71073)
monochromator	graphite
take-off angle, deg	2.0
temperature, °C	21
scan type	ω-2θ
scan width, deg in ω,	0.80 + $0.35\tan\theta$
2θ limit, deg	50.0
reflections measured	2589 ($\pm h$, $\pm k$, $\pm l$)
reflections used	1721 with $I > 3\sigma(I)$
variables	95
R^a	0.059
$R_w{}^b$	0.055
GOF[c]	2.12

[a] $R = \Sigma||F_o| - |F_c||/\Sigma|F_o|$

[b] $R_w = (\Sigma w(|F_o| - |F_c|)^2/\Sigma w F_o{}^2)^{1/2}$

[c] $\mathrm{GOF} = [\Sigma w(|F_o| - |F_c|)^2/(\mathrm{NO} - \mathrm{NV})]^{1/2}$

Table 2.15: Fractional Coordinates and Isotropic Thermal Parameters for 3

atom	*x*/*a*	*y*/*b*	*z*/*c*	*B*(equ), Å
Ir	0.3320(1)	0.6659(1)	0.34053(7)	4.45
Os	0.2777(1)	0.8352(2)	0.1675(1)	5.59
O1	0.423(2)	0.351(2)	0.286(1)	7.8(4)
O2	0.738(4)	0.888(4)	0.392(2)	13.0(8)
O3	-0.060(3)	0.492(3)	0.105(2)	10.0(6)
O4	0.675(5)	1.120(5)	0.274(2)	7.2(8)
O5	0.168(7)	0.907(6)	-0.065(4)	12(1)
O6	0.081(5)	1.046(4)	0.304(2)	6.7(7)
O4'	0.669(5)	1.136(4)	0.205(2)	6.5(7)
O5'	0.219(5)	1.042(5)	-0.009(3)	9(1)
O6'	0.036(6)	1.033(5)	0.236(2)	9(1)
C1	0.419(3)	0.495(3)	0.254(2)	5.2(4)
C2	0.481(3)	0.543(3)	0.164(2)	6.5(5)
C3	0.441(4)	0.675(4)	0.118(2)	7.0(6)
C4	0.049(4)	0.452(4)	0.352(2)	7.4(6)
C5	0.018(4)	0.629(3)	0.355(2)	6.5(5)
C6	0.148(5)	0.744(4)	0.444(2)	9.5(8)
C7	0.265(4)	0.634(4)	0.493(2)	8.5(7)
C8	0.207(5)	0.463(4)	0.440(2)	9.2(8)
C9	0.584(5)	0.802(5)	0.381(3)	10.2(9)
C10	0.061(4)	0.622(4)	0.130(2)	7.5(6)
C11	0.522(5)	1.014(5)	0.238(3)	3.7(7)
C12	0.231(9)	0.898(8)	0.012(5)	9(2)
C13	0.154(6)	0.983(6)	0.253(3)	6(1)
C11'	0.523(8)	1.025(7)	0.183(4)	7(1)
C12'	0.231(6)	0.967(6)	0.060(3)	6(1)
C13'	0.119(8)	0.943(7)	0.195(4)	7(1)

Table 2.16: Selected Weighted[a] Least-Squares Planes

Plane	Coefficients[b]				Defining Atoms with Deviations[c]			
1	0.7537	0.3862	-0.5317	2.7032	C4	-0.00960	C5	0.01305
					C6	-0.01141	C7	0.00553
					C8	0.00244	Ir	1.95292
2	-0.7091	-0.5193	-0.4770	4.1834	C1	0.00515	O1	0.2165
					C2	-0.14315	C3	-0.0913
					Os	0.22952	Ir	-0.2167
3	-0.6701	-0.4801	-0.5661	4.2333	C1	-0.06900	O1	0.06942
					C2	-0.06596	C3	0.06555
					Os	0.30475	Ir	-0.39823

Dihedral Angles[d]

Planes	Angle
1 - 2	118.78
1 - 3	112.92
2 - 3	6.01

---

[a] Weights are derived from the atomic and positional esd's using the method of Hamilton(Hamilton, W.C. *Acta. Crystallogr.* **1961,** *14,* 185.).

[b] Coefficients are for the form ax+by+cz-d=0 where x, y, and z are crystallographic coordinates.

[c] Deviations are in angstroms. Underlined atoms were not included in the definition of the plane.

[d] In degrees

2.8. References

1. Gagné, M.R.; Takats, J. *Organometallics* **1988**, *7*, 561.

2. (a) Parshall, G.W.; Ittel, S.D. *Homogenous Catalysis, 2nd Edition*, Wiley: New York; 1992, Chapter 8. (b) Gomez-Sal, M.P.; Johnson, B.F.G.; Kamarudin, R.E.; Lewis, J.; Raithby, P.R. *J. Chem. Soc., Chem. Commun.* **1985**, 1622. (c) Knox, S.A.R. *Pure. Appl. Chem.* **1984**, *56*, 81. (d) Rashidi, M.; Puddephatt, R.J. *J. Am. Chem. Soc.* **1986**, *108*, 7111.

3. (a) Wrackenridge, B.; Horchler, K. *Prog. Nucl. Magn. Reson. Spect.* **1990**, *22*, 209. (b) Silverstein, R.M.; Bassler, G.C.; Morrill, T.C. *Spectrometric Identification of Organic Compounds*, Wiley: New York, 1981, Ch. 5., pg. 253.

4. Burn, M.J.; Kiel, G.-Y.; Seils, F.; Takats, J.; Washington, J. *J. Am. Chem. Soc.* **1989**, *111*, 6850.

5. (a) Dyke, A.F.; Knox, S.A.R.; Naish, P.J.; Taylor, G.E. *J. Chem. Soc. Dalton Trans.* **1982**, 1297. (b) Hogarth, G.; Kayser, F.; Knox, S.A.R.; Morton, D.A.V. *J. Chem. Soc., Chem. Comm.* **1988**, 358. (c) Kiel, G.-Y.; Takats, J. *Organometallics* **1989**, *8*, 839. (d) Fontaine, X.L.R.; Jacobsen, G.B.; Shaw, B.L.; Thornton-Pett, M. *J. Chem. Soc., Dalton Trans.* **1988**, 741. (e) Gracey, B.P.; Knox, S.A.R.; MacPherson, K.A.; Orpen, A.G. *J. Chem. Soc., Dalton Trans.* **1985**, 1935. (f) Hogarth, G.; Knox, S.A.R.; Lloyd, B.R.; MacPherson, K.A.; Morton, D.A.V.; Orpen, A.G.; Stobart, S.R. *J. Chem. Soc., Dalton*

Trans. **1988**, 360. (g) Dyke, A.F.; Knox, S.A.R.; Naish, P.J.; Taylor, G.E. *J. Chem. Soc., Chem. Commun.* **1980**, 409.

6. (a) Tyler, D.R.; Altobelli, M.; Gray, H.B. *J. Am. Chem. Soc.* **1980,** *102*, 3022. (b) Hales, L.A.W.; Irving, R.J. *J. Chem. Soc.(A)* **1967**, 1389. (c) Carter, W.J.; Kelland, J.W.; Okrasinski, S.J.; Warner, K.E.; Norton, J.R. *Inorg. Chem.* **1982,** *21*, 3955.

7. Hallam, H.E. in *Infra-red Spectroscopy and Molecular Structure*; Davies, M., Ed.; Elsevier: New York, 1963; pg 405.

8. (a) Silverstein, R.M.; Bassler, G.C.; Morrill, T.C. *Spectrometric Identification of Organic Compounds*, Wiley: New York, 1981, Ch. 2., pg. 118-20. (b) Lowry, T.H.; Richardson, K.S. *Mechanism and Theory in Organic Chemistry, Third Edition*; Harper & Row: New York; 1987; Chapter 1, pg. 28-9.

9. Turro, N.J.; Hammond, W.B. *J. Am. Chem. Soc.* **1966,** *88*, 3672.

10. Herrmann, W.A. *Adv. Organomet. Chem.* **1982,** *20*, 159.

11. Cherkas, A. A.; Breckenridge, S. M.; Carty, A. J. *Polyhedron* **1992,** *11*, 1075.

12. Mann, B.E.; Taylor, B.F. *^{13}C NMR Data for Organometallic Compounds*; Academic: New York, 1981.

13. (a) Bodner, G.M.; Starhoff, B.N.; Doddrell, D.; Todd, L.J. *J. Chem. Soc., Chem. Commun.* **1970**, 1530. (b) Jesse, A.C.; Gijben, H.P.; Stufkens, D.J.S.; Vrieze, K. *Inorg. Chim. Acta.* **1978**, *31*, 203.

14. Dickson, R.S.; Gatehouse, B.M.; Nesbit, M.C.; Pain, G.N., *J. Organomet. Chem.* **1981**, *251*, 97.

15. Loots, M.J.; Weingarten, L.R.; Levin, R.H. *J. Am. Chem. Soc.* **1976**, *98*, 4571.

16. Lambert, J.B.; Shurvell, H.F.; Lightner, D.; Cooks, R.G. *Introduction to Organic Spectroscopy*, MacMillan: New York, 1987, Ch. 3., pg. 51.

17. Friebolin, H. *Basic One- and Two-Dimensional NMR Spectroscopy*, VCH: New York, 1991, pg. 77-84.

18. Johnson, K.A.; Gladfelter, W.L. *Organometallics* **1992**, *11*, 2534.

19. Kiel, G.-Y.; Takats, J. Manuscript in preparation.

20. Riesen, A.; Einstein, F.W.B.; Ma, A.K.; Pomeroy, R.K.; Shipley, J.A. *Organometallics* **1991**, *10*, 3629.

21. Johnson, B.F.G.; Lewis, J.; Raithby, P.R.; Azman, S.N.; Syed-Mustaffa, B.; Taylor, M.J.; Whitmire, K.H.; Clegg, W.J. *J. Chem. Soc., Dalton Trans.* **1984**, 2111.

22. Farrugia, L.J.; Orpen, A.G.; Stone, F.G.A. *Polyhedron* **1983**, *2*, 171.

23. (a) Burke, M.; Takats, J. *J. Organomet. Chem.* **1986**, *302*, C25. (b) Rausch, M.D.; Gastinger, R.G.; Gardner, S.A.; Brown, R.K.; Wood, J.S. *J. Am. Chem. Soc.* **1977**, *99*, 7870.

24. Allen, F.H.; Kennard, O.; Watson, D.G.; Brammer, L.; Orpen, A.G.; Taylor, R. *J. Chem. Soc., Perkin Trans. II* **1987**, S1.

25. Chadwick, D.; Legon, A.C.; Millen, D.J. *J. Chem. Soc., Chem. Commun.* **1969**, 1130.

26. Schreurs, J.; van Noorden-Mudde, C.A.H.; van de Ven, L.J. M.; de Haan, J.W. *Org. Mag. Reson.* **1980**, *13*, 354.

27. (a) Tachikawa, M.; Richter, S.I.; Shapley, J.R. *J. Organomet. Chem.* **1977**, *128*, C9. (b) Aime, S.; Osella, D. *J. Chem. Soc., Chem. Commun.* **1981**, 300.

28. (a) Alex, R.F.; Pomeroy, R.K. *Organometallics* **1987**, *6*, 2437. (b) Aime, S.; Osella, D.; Milone, L.; Rosenberg, E. *J. Organomet. Chem.* **1981**, *213*, 207.

29. (a) Adams, H.; Bailey, N.A.; Bentley, G.W.; Mann, B.E. *J. Chem. Soc., Dalton Trans.* **1989**, 1831. (b) Alex, R,F.; Pomeroy, R.K. *J. Organomet. Chem.* **1985**, *284*, 379. (c) Deeming, A.J.; Donovan-Mtunzi, S.; Kabir, S.E. *J. Organomet. Chem.* **1985**, *281*, C43. (d) Deeming, A.J.; Donovan-Mtunzi, S.; Kabir, S.E.; Manning, P.J. *J. Chem. Soc., Dalton Trans.* **1985**, 1037. (e) Deeming, A.J. *Adv. Organomet. Chem.* **1986**, *26*, 1. (f) Beringhelli, T.;

D'Alfonso, G.; Molinari, H.; Mann, B.E.; Pickup, B.T.; Spencer, C.M. *J. Chem. Soc., Chem. Commun.* **1986**, 796. (g) Rosenberg, E.; Thorsen, C.B.; Milone, L.; Aime, S. *Inorg. Chem.* **1985**, *24*, 231. (h) Gavins, P.D.; Mays, M.J. *J. Organomet. Chem.* **1976**, *162*, 389. (i) Bryan, E.G.; Forster, A.; Johnson, B.F.G.; Lewis, L.; Matheson, T.W. *J. Chem. Soc., Dalton Trans.* **1978**, 196. (j) Bryan, E.G.; Johnson, B.F.G.; Lewis, L. *J. Chem. Soc., Dalton Trans.* **1977**, 144.

30. McClung, R.E.D. *EXCHANGE: Program for the Simulation of NMR Spectra of Weakly-Coupled Exchanging Systems*, University of Alberta.

31. (a) Bond, E.; Muetterties, E.L. *Chem. Rev.* **1978**, *78*, 639. (b) Mann, B.E. in *Comprehensive Organometallic Chemistry*; Wilkinson, G.; Stone, F.G.A.; Abel, E.W., Eds.; Pergamon: New York, 1982; Vol. 3, pg 89. (c) Washington, J.; Takats, J. *Organometallics* **1990**, *9*, 925.

32. Schmidt, S.P.; Basolo, F.; Jensen, C.M.; Trogler, W.C. *J. Am. Chem. Soc.* **1986**, *108*, 1894.

33. Kiel, G.-Y.; personal communication.

34 (a). Mao, Tianfu; personal communication. (b). Burt, R.; Cooke, M.; Green, M. *J. Chem. Soc. (A)* **1970**, 2981.

35. Geoffroy, G.L. *Acc. Chem. Res.* **1980**, *13*, 469.

36. Johnson, B.F.G.; Lewis, J.; Kilty, P.A. *J. Chem. Soc. A* **1968**, 2859.

37. Rushman, P.; van Buuren, G.N.; Shiralian, M.; Pomeroy, R.K. *Organometallics* **1983**, *2*, 693.

38. Dickson, R.S.; Tailby, G.R. *Aust. J. Chem.* **1970**, *23*, 1531.

39. Warner, S.A.; Andrews, P.S.; Rausch, M.D. *Inorg. Chem.* **1973**, *12*, 2396.

Chapter 3

Reaction of $Os(CO)_4(\eta^2\text{-}HCCH)$ with $CpM(CO)(PR_3)$ ($M = Co, Rh$; $PR_3 = PMe_3, PMe_2Ph, PMePh_2$)

3.1. Introduction

In the previous Chapter, the unexpected reactivity of $Os(CO)_4(\eta^2\text{-}HCCH)$, **1**, towards coordinatively saturated organometallic species was reported. This reactivity is an important tool in the synthesis of alkyne bridged dimetallic compounds. Specifically, the condensation of **1** with $CpM(CO)_2$ ($M = Co, Rh$) results in the formation of heterodimetallic complexes containing a dimetallacyclopentenone ring.[1a]

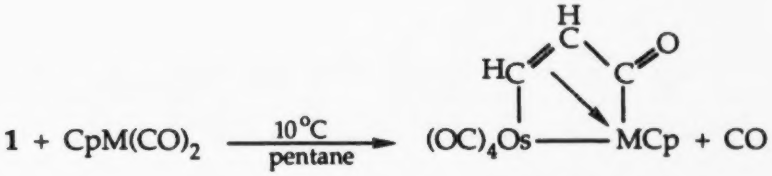

M = Co, **2a**
= Rh, **2b**

In order to determine the role of ancillary ligands in the condensation, the reaction of **1** with $CpM(CO)(PR_3)$ ($M = Co, Rh$; $PR_3 = PMe_3, PMe_2Ph, PMePh_2$) was investigated. There were several reasons for the use of phosphine ligands. First, compounds of the type $CpM(CO)(PR_3)$ ($M = Co, Rh$; $PR_3 = PMe_3, PMe_2Ph, PMePh_2$) may be readily synthesized and are thermally stable, although they are air sensitive. Second, the presence of a phosphorus nucleus allows the use of ^{31}P NMR spectroscopy, an invaluable spectroscopic aid. The compounds are also soluble in hydrocarbon solvents, an important consideration when monitoring reactions by FT-IR spectroscopy. Finally, the use of various substituted phosphines allows one to change the steric and electronic properties of the CpM(CO)(PR$_3$) complexes.

As stated, the main advantage of using phosphine ligands is the variety of electronic and steric properties available. The bonding between a phosphine and a transition metal centre is synergic, similar to M-CO bonding. The phosphine donates an electron pair to the metal centre in a σ bond, while accepting electron density into its empty *d* orbitals.[2]

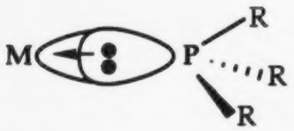

σ bond

M(hybrid) - Psp^3

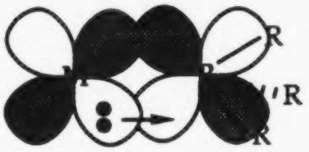

π bond

Md_π - Pd_π

Electron withdrawing substituents on the phosphine will lower the energy the phosphorus *d* orbitals and better metal-to-phosphine backbonding will result. Concomitant with this, electron withdrawing substituents weaken the electron donating ability of the phosphine. The basicity of a phosphine may be estimated by the pKa value of its conjugate phosphonium ion, the higher the pKa, the more basic the phosphine.[3a] The cone angle of a phosphine, first championed by Tolman, is a description of its steric requirements.[3b] The cone angles and pKa values for selected phosphines are listed in Table 3.1.[3a]

Table 3.1: Cone Angles and pKa Values (Conjugate Acid) for Selected Phosphines

Phosphine	Cone Angle (deg)	pKa
PMe_3	118	8.65
PMe_2Ph	122	6.50
$PMePh_2$	136	4.57
PPh_3	145	2.73

As can be seen, trimethylphosphine has the smallest cone angle and the highest pKa, therefore it should be an excellent ligand. As expected, the cone angles of PMe_2Ph and $PMePh_2$ are larger than PMe_3, and they are also less basic than PMe_3 due to the presence of electron withdrawing phenyl groups. Finally, PPh_3 is the most sterically hindered, and the presence of three phenyl groups make it the most π acidic of the series. In the series PMe_3, PMe_2Ph and $PMePh_2$, there is a relatively consistent change to increased steric bulk and in increased π acidity. Therefore, it was hoped that this variety of ligand properties would enable insights to be made into the role of the ligands in these condensation reactions.

3.2. Reaction of $Os(CO)_4(\eta^2\text{-}HCCH)$ with $CpRh(CO)(PR_3)$ (PR_3 = PMe_2Ph, $PMePh_2$)

The reaction between $Os(CO)_4(\eta^2\text{-}HCCH)$ and $CpRh(PR_3)(CO)$ (PR_3 = PMe_2Ph, $PMePh_2$) requires only mild thermal activation. A pentane solution containing **1** and a slight excess of $CpRh(PR_3)(CO)$ (PR_3 = PMe_2Ph, $PMePh_2$) is slowly warmed from -78 °C to 10 °C using a dry ice/acetone bath. Reaction occurs at 0 °C as evidenced by a darkening of the initial orange solution accompanied by the formation of an orange precipitate.

The reaction may be followed by the disappearance of the 2122 cm^{-1} peak of the $Os(CO)_4(\eta^2\text{-}HCCH)$ or the single carbonyl band due to the $CpRh(PR_3)(CO)$ (PR_3 = PMe_2Ph, $PMePh_2$) reagent. The reaction is deemed complete after consumption of all the $Os(CO)_4(\eta^2\text{-}HCCH)$ in solution; this is accompanied by the generation of a large amount of orange precipitate. The compounds are then isolated and washed with hydrocarbon to remove any excess $CpRh(PR_3)(CO)$ (PR_3 = PMe_2Ph, $PMePh_2$). The resulting dimetallic species are thermally stable and may be handled in air for short periods of time.

3.2.1. Characterization of $[\mu\text{-}\eta^3\text{:}\eta^1\text{-}C(O)C_2H_2]Os(CO)_3RhCp(PR_3)$ (PR_3 = PMe_2Ph, 5a; $PMePh_2$, 5b)

The elemental analyses and mass spectral data for **5a** and **5b** indicated that dimetallic species of formula $Os(CO_4(C_2H_2)(PR_3)RhCp$ had been formed.

$$\mathbf{1} + CpRh(CO)(PR_3) \xrightarrow[\text{pentane, -CO}]{10^\circ C} [\mu\text{-}C(O)C_2H_2]Os(CO)_3RhCpPR_3$$

PMe_2Ph, **5a**
PPh_2Me, **5b**

The ^1H NMR, ^{13}C NMR and FT-IR spectra of **5a** and **5b** are consistent with the formulation of a dimetallacyclopentenone ring.[4] The two most likely structures, conforming to the molecular composition and satisfying the eighteen-electron count for both metals, are shown below. In structure **A**, the acyl is attached to the Os centre, opposite to the results obtained for **2a** and **2b**. In **B**, the phosphine has migrated from Rh to the Os centre and the acyl is bound to the Group IX metal.

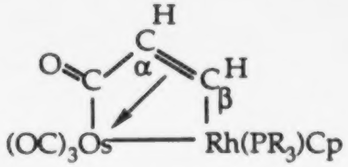

A

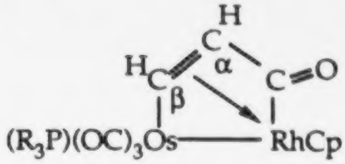

B

The ^{31}P NMR spectra for **5a-b** showed doublets with large ^{103}Rh-^{31}P coupling of 188-189 Hz; this is consistent with having the phosphine ligand directly attached to the Rh centre[5] and strongly suggestive of structure **A**.

A large ^{13}C NMR chemical shift difference between the α and β carbons is a characteristic of coordinated dimetallacyclopentenones.[4] Compounds **5a** and **5b** are no exception and the relevant ^{13}C NMR data are listed in Table 3.2.

Table 3.2: ^{13}C NMR Data for Ring Carbons of Dimetallacyclopentenones

	^{13}C NMR Data δ(ppm)	
Compound	C_α	C_β
$[\mu\text{-C(O)C}_2\text{H}_2]\text{Os(CO)}_3\text{RhCp(PMe}_2\text{Ph)}$, **5a**	52.8	156.0
$[\mu\text{-C(O)C}_2\text{H}_2]\text{Os(CO)}_3\text{RhCp(PMePh}_2\text{)}$, **5b**	53.0	156.2
$[\mu\text{-C}_2\text{H}_2\text{C(O)}]\text{Ru}_2\text{Cp}_2\text{(CO)}_2$[a]	24.0	156.7
$[\mu\text{-C}_2\text{H}_2\text{C(O)}]\text{Ru}_2\text{(CO)}_5(\mu\text{-dppm})$[b]	55.4	161.8
$[\mu\text{-C}_2\text{H}_2\text{C(O)}]\text{Os(CO)}_4\text{RhCp}$, **2b**	44.4	115.7

---

[a] Dyke, A.F.; Knox, S.A.R.; Naish, P.J.; Taylor, G.E. *J. Chem. Soc. Dalton Trans.* **1982**, 1297. [b] Kiel, G.-Y.; Takats, J. *Organometallics* **1989**, *8*, 839.

As seen in Chapter 2, the lowfield shift of the β carbon is characteristic of a μ-alkylidene moiety[6] and the highfield C_α signal is characteristic of a sp^3 hybridized carbon.[7] The β carbon also shows large Rh-C coupling (**5a**: $^1J_{Rh\text{-}C}$ = 35.2 Hz; **5b**: $^1J_{Rh\text{-}C}$ = 35.4 Hz) while the α carbon appears as a singlet, giving further support for structure **A**.

The large chemical shift differences seen in the ^{13}C NMR spectra are also mirrored in the ^1H NMR spectra, as seen in Table 3.3.

Table 3.3: ^{1} H NMR Data for Ring Protons of Dimetallacyclopentenones

	^{1} H NMR Data	δ (ppm)	
Compound	H_α	H_β	$^3J_{H\text{-}H}$[a]
$[\mu\text{-}C(O)C_2H_2]Os(CO)_3RhCp(PMe_2Ph)$, **5a**	4.72	8.82	6.4
$[\mu\text{-}C(O)C_2H_2]Os(CO)_3RhCp(PMePh_2)$, **5b**	4.77	9.03	6.4
$[\mu\text{-}C_2H_2C(O)]Ru_2Cp_2(CO)_2$[b]	3.42	10.94	7.0
$[\mu\text{-}C_2H_2C(O)]Ru_2(CO)_5(\mu\text{-dppm})$[c]	4.61	8.22	8.5
$[\mu\text{-}C_2H_2C(O)]Os(CO)_4RhCp$, **2b**	5.00	7.85	7.9

[a]Couplings in Hz. [b]Dyke, A.F.; Knox, S.A.R.; Naish, P.J.; Taylor, G.E. *J. Chem. Soc. Dalton Trans.* **1982**, 1297. [c]Kiel, G.-Y.; Takats, J. *Organometallics* **1989**, *8*, 839.

The H_β NMR signal is shifted well downfield, as expected for a μ-CH carbene unit.[6] The β protons also show large $^{103}Rh\text{-}^1H$ coupling (**5a**: $^2J_{Rh\text{-}H}$ = 18.9 Hz; **5b**: $^2J_{Rh\text{-}H}$ = 18.5 Hz) while the coupling to the α proton is significantly less (**5a**: $^3J_{Rh\text{-}H}$ = 6.3 Hz; **5b**: $^3J_{Rh\text{-}H}$ = 6.4 Hz). The relatively high frequency of the acyl stretching band in the FT-IR (**5a**: ν(acyl): 1696 cm^{-1}; **5b**: ν(acyl): 1698 cm^{-1}) also provides evidence for ring coordination.

This observation has been corroborated by workers in our laboratory where the acyl stretch for $[\mu\text{-}C_2H_2C(O)]Ru_2(CO)_5(\mu\text{-dppm})$ appears at 1712 cm^{-1}.[4c]

Finally, for compounds **5a** and **5b**, the low field acyl signals in the ^{13}C NMR spectra lacked ^{103}Rh - ^{13}C coupling, thus revealing that the acyl fragment of the ring was bound to the osmium centre. This is in contrast to the reaction of **1** with $CpRh(CO)_2$ (*vide supra*) where the acyl moiety is attached to the Group IX metal. Therefore, the replacement of one carbonyl ligand by a phosphine ($PR_3 = PMe_2Ph$, $PMePh_2$) in $CpRh(CO)_2$ results in opposite regiochemistry for the dimetallacyclopentenone ring.

3.2.2. Molecular Structure of $[\mu\text{-}\eta^3\text{:}\eta^1\text{-}C(O)C_2H_2]Os(CO)_3RhCp(PMe_2Ph)$, 5a

In light of the reaction of **1** with $CpRh(CO)_2$, the reversal of regioselectivity seen for **5a** and **5b** was unexpected. Even though the spectroscopic data were consistent with **A** as the correct formulation, an X-ray single crystal study on **5a** was undertaken to unequivocally confirm the nature of the product. Two ORTEP views of **5a** are shown in Figure 3.1 and Figure 3.2. The relevant bond distances and angles for **5a** are listed in Tables 3.4 and 3.5, respectively.

The X-ray structure clearly reveals the unexpected orientation of the cyclopentenone ring whereby the acyl moiety is attached to the Os centre. The severe twisting of the cyclopentenone ring to accommodate the alkene coordination is also readily apparent in Figure 3.2. The PMe_2Ph ligand remains bonded to Rh.

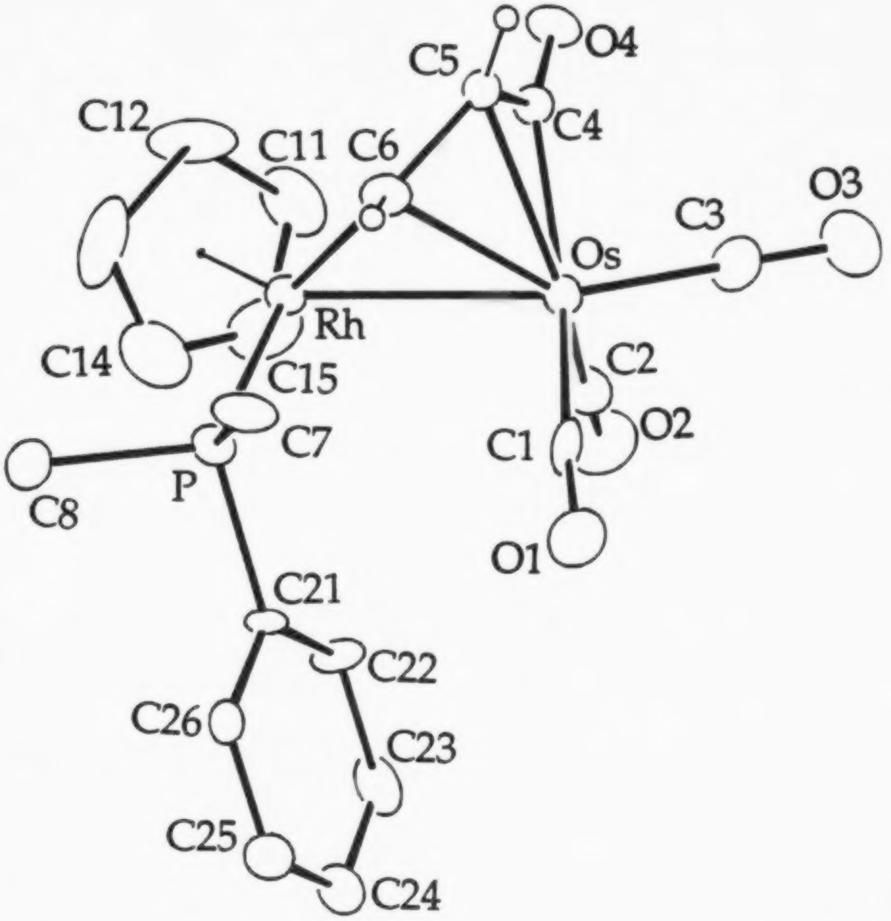
O4
C5
C4
C12
C11
C6
O3
C3
Os
Rh
C14
C2
C15
C7
O2
C1
C8
P
O1
C21
C22
C26
C23
C25
C24

Figure 3.1: ORTEP View of [μ-C(O)C_2H_2]Os$(CO)_3$RhCp(PMe_2Ph), **5a**

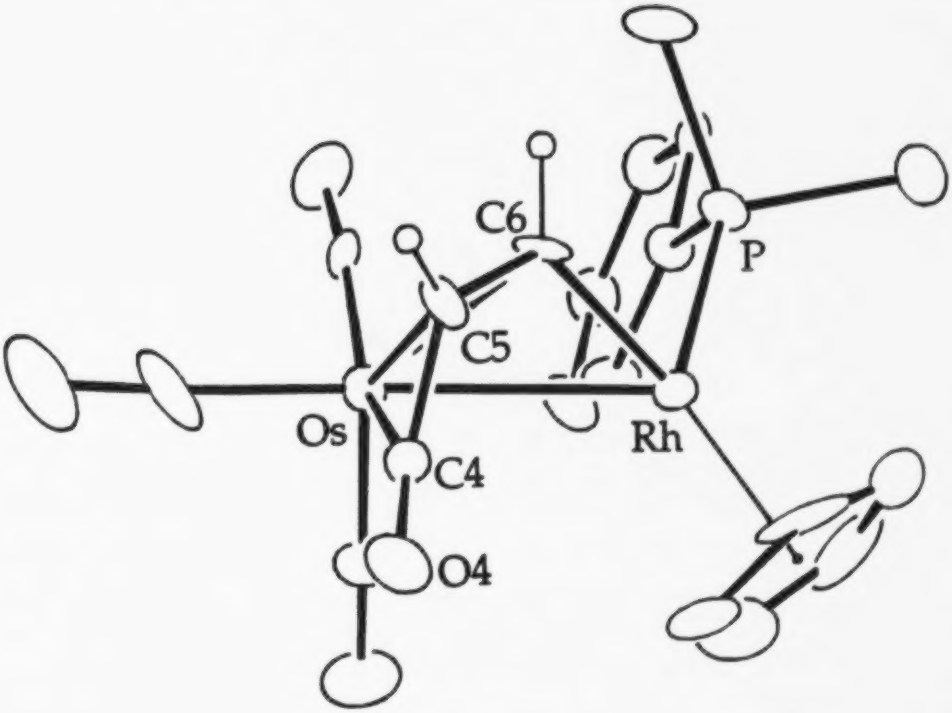
C6
P
C5
Os
Rh
C4
O4

Figure 3.2: Alternate ORTEP View of **5a**

Table 3.4: Selected Bond Lengths (Å) for **5a**

Os-Rh	2.780(2)	O1-C1	1.16(2)
Os-C1	1.93(2)	O2-C2	1.16(2)
Os-C2	1.84(2)	O3-C3	1.17(2)
Os-C3	1.78(2)	O4-C4	1.21(2)
Os-C4	2.05(1)	C4-C5	1.45(2)
Os-C5	2.29(1)	C5-C6	1.46(2)
Os-C6	2.24(1)	Rh-P	2.254(4)
Rh-C6	1.98(1)		

Table 3.5: Selected Angles (deg) for **5a**

Rh-Os-C1	95.9(4)	Os-Rh-C6	53.0(4)
Rh-Os-C2	90.6(5)	P-Rh-C6	89.9(4)
Rh-Os-C3	169.9(6)	Os-Rh-P	102.0(1)
Rh-Os-C4	79.2(4)	Rh-C6-C5	121(1)
Rh-Os-C5	72.0(4)	Rh-P-C7	118.9(4)
Rh-Os-C6	45.0(4)	Rh-P-C8	113.9(5)
C1-Os-C2	97.7(7)	Rh-P-C21	116.4(5)
C1-Os-C3	92.3(7)	C7-P-C8	99.3(7)
C1-Os-C4	159.3(6)	C8-P-C21	100.5(6)
C1-Os-C5	120.9(6)	Os-C1-O1	176(1)
C1-Os-C6	93.7(5)	Os-C2-O2	176(2)
C2-Os-C3	94.0(8)	Os-C3-O3	177(2)
C2-Os-C3	94.0(8)	Os-C4-O4	147(1)
C2-Os-C4	102.4(7)	Os-C4-C5	79.8(9)
C2-Os-C5	138.5(6)	O4-C4-C5	132(1)
C2-Os-C6	135.1(6)	Os-C5-C4	61.7(7)
C3-Os-C4	91.0(7)	Os-C5-C6	69.6(7)
C3-Os-C5	98.8(7)	C4-C5-C6	113(1)
C3-Os-C6	128.8(7)	Os-C6-Rh	82.0(5)
C4-Os-C5	38.5(5)	Os-C6-C5	72.9(7)
C4-Os-C6	68.6(5)	C5-Os-C6	37.6(4)

The Os-Rh bond distance is 2.780(2) Å. For comparison, the average Os-Rh separation in $[Os(CO)_4]_2RhCp(CO)$ is 2.833(9) Å.[8] The short Os-C5 and Os-C6 distances of 2.29(1) Å and 2.24(1) Å, respectively, confirm that the unsaturated moiety of the ring is bound to the osmium centre. A representative Os-C(sp^3) bond distance of 2.220(2) Å is seen in $(\mu\text{-}C_2H_4)Os_2(CO)_8$[9a] and the average Os-C distance for the bound ethylene in $Os(CO)_4(\eta^2\text{-}C_2H_4)$ is 2.22(1) Å.[9b] The Os-C4 bond distance is 2.05(1) Å, which is shorter than the value of 2.138(5) Å obtained for the Os-C(sp^2) bond length in $(\mu\text{-DMAD})Os_2(CO)_8$.[10]

The Rh-C6 bond distance of 1.98(1) Å is slightly shorter than the 2.021(6) Å found in $[\mu\text{-}C_2(CF_3)_2C(O)]Rh_2Cp_2(CO)_2$[11a] and the 2.06(5) Å found for $(\mu\text{-HFB})_2Rh_2(CO)_2(\mu\text{-dmpm})_2$ (dmpm = $(Me_2P)_2CH_2$),[11b] indicating a shorter than average Rh-C bond for **5a**. In $(\mu\text{-}CH_2)Rh_2Cp_2(CO)_2$, the Rh-C(methylene) bond distances are 2.029(4) Å and 2.055(4) Å.[11c-d] Also, the Rh-C bond distance in $(\mu\text{-DMAD})Rh_2Cl_2(\mu\text{-}CO)(\mu\text{-dppm})$ (dppm = $(Ph_2P)_2CH_2$) is 2.004(6) Å, a complex with no metal-metal bond.[12] Thus, the Rh-C6 bond distance is closer to that found in a *cis*-dimetallated olefin rather than the range of 2.023(5) to 2.128(5) Å expected for an alkyne bridging two metals connected by a metal-metal bond.[12]

The C5-C6 bond length is 1.46(2) Å, thus the formal C-C double bond between C5 and C6 lengthens considerably upon coordination to the Os centre as the average C=C bond distance is 1.316(15) Å while a C-C single bond is 1.530(15) Å.[13] The C-C bond distance in $Os(CO)_4(\eta^2\text{-}C_2H_4)$ is 1.48(2) Å, which Norton described as being closer to an osmacylopropane than an ethylene coordinated to an Os centre.[9b] In a related complex, $[\mu\text{-}C_2Ph_2C(O)]Ru_2Cp_2(CO)_2$, the comparable C-C bond distance is 1.423(6) Å.[4a]

This bond distance is significantly shorter than in **5a**, indicating a weaker olefin-metal interaction. Based on this, the Os-C5 and Os-C6 interaction can be described as having significant Os-C σ bond character and the fragment more closely resembles a localized osmacylopropane. In [μ-$C_2Ph_2C(O)$]$Ru_2Cp_2(CO)_2$ the C_α-C(acyl) bond distance is 1.461(5) Å[4a] which is similar to the C4-C5 length of 1.45(2) Å. This separation is shorter than the expected value of 1.514(16) Å for cylopentanones and more closely resembles the C_α-C(O) distance of 1.465(18) Å found for α,β-unsaturated ketones.[13] Knox rationalized these trends in C-C bond distance as arising from the contribution of several different resonance forms to the bonding.[4a] Contribution from III and IV would result in the shortening of the C4-C5 bond distance. However, since the C5-C6 distance has lengthened, form II must also make a substantive contribution, and is the dominant form.

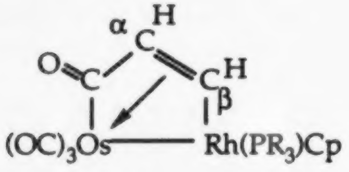

I

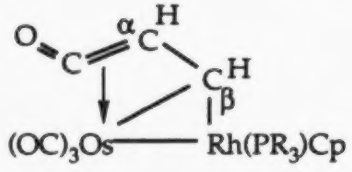

III

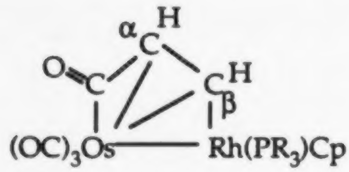

II

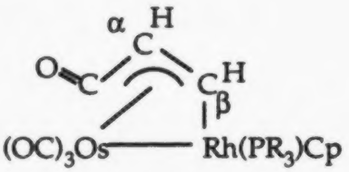

IV

The geometry about the Rh centre resembles a three-legged piano stool. The coordination geometry of the Os is more difficult to describe.

One description is that the Os has distorted octahedral geometry where CO(3) and Rh occupy axial positions. The remaining two carbonyl ligands, CO(1) and CO(2) occupy equatorial coordination sites. The C4-C5-C6 unit can be thought of as an allyl moiety that takes up the remaining two equatorial coordination sites. Alternatively, C4 can be envisaged as being *trans* to CO(1) while the mid-point between C5-C6 is *trans* to CO(2). Obviously, the resulting octahedral geometry is highly distorted. An interesting feature is that the Os-C3 bond distance is 1.78(2) Å, shorter than the other two Os-carbonyl bond lengths. The Os-C3 bond lies along the metal-metal vector ($\angle$ Rh-Os-C3 = 169.9(6)°) thus, the electron donation from the Rh centre enhances backbonding to this carbonyl, shortening the Os-C3 bond.

3.4. Fluxional Behaviour of [μ-η^3:η^1-C(O)C_2H_2]Os(CO)$_3$RhCp(PR$_3$) (PR$_3$ = PMe$_2$Ph, 5a; PMePh$_2$, 5b)

3.4.1. Variable Temperature ^{13}C NMR Behaviour

The variable temperature ^{13}C NMR spectra for **5a** and **5b** are similar. At the low temperature limit, four carbonyl signals are seen. One of the signals is downfield near 220 ppm, this corresponds to an acyl attached to the Os centre.[7] Three signals are also observed in the region expected for terminal carbonyls bound to an Os centre.[7] Thus, the limiting ^{13}C NMR spectra of **5a** and **5b** are in accord with the solid state structure. As the temperature is raised, the three terminal carbonyl signals broaden and eventually coalesce; the acyl signal remains unaffected. The changes in the ^{13}C NMR spectra of **5b** with temperature are shown in Figure 3.3.

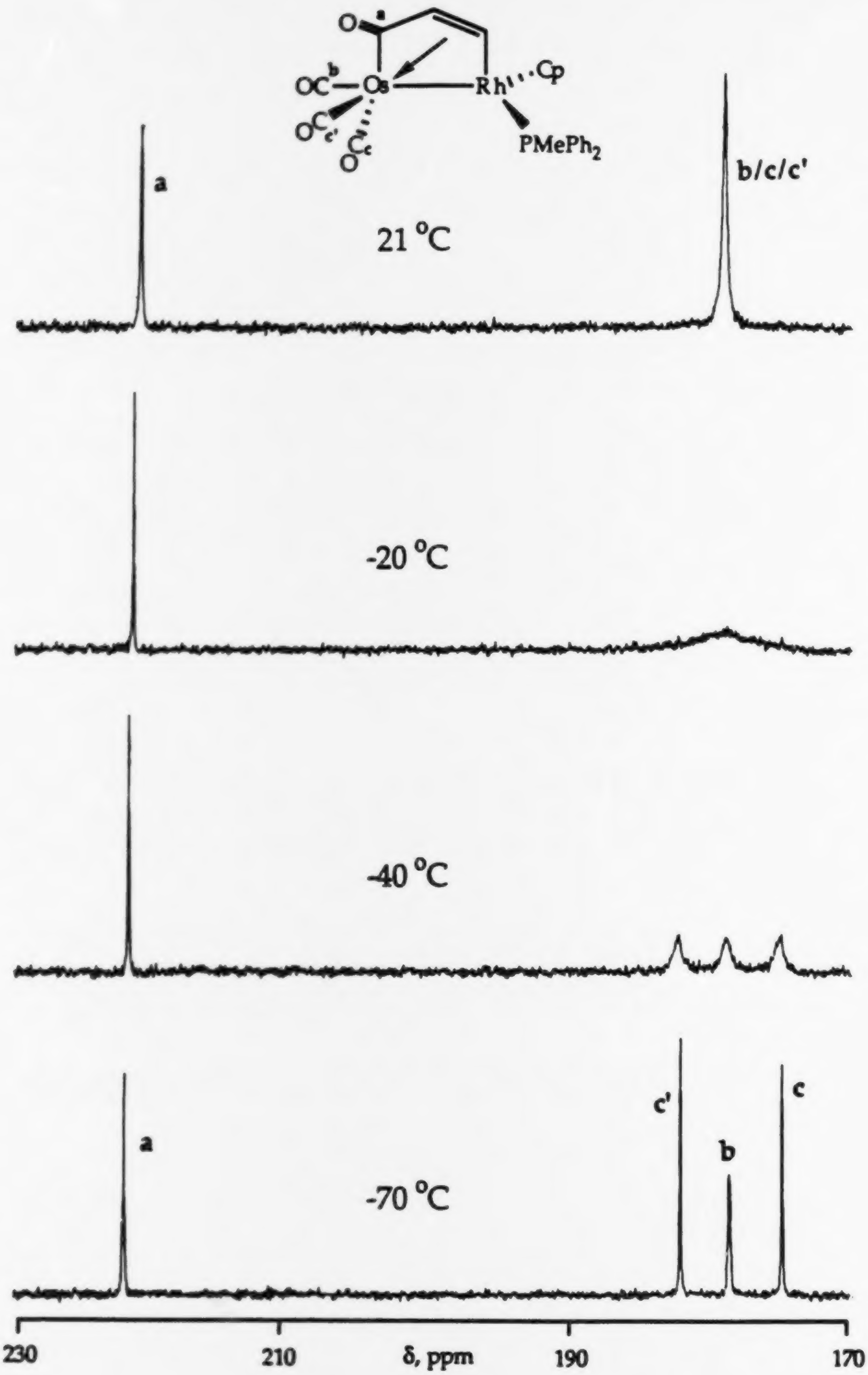

Figure 3.3: Variable Temperature ^{13}C NMR Spectra of **5b**

The three terminal carbonyls of **5a** and **5b** are rapidly exchanging at room temperature. A plausible mechanism for carbonyl scrambling is the "turnstile" process[15] described in Chapter 2 and illustrated in Scheme 3.1.

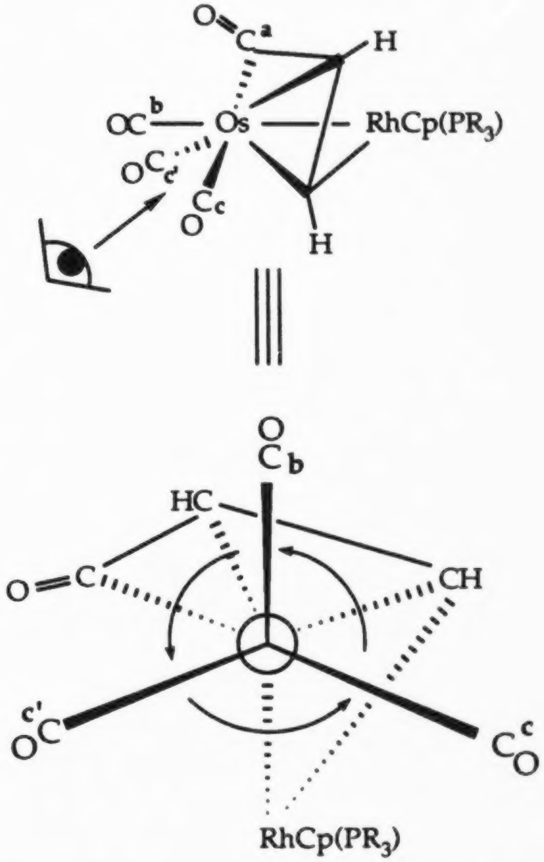

Scheme 3.1: Turnstile Exchange in [μ-C(O)C_2H_2]Os$(CO)_3$RhCp(PR_3)

(PR_3 = PMe_2Ph, **5a**; $PMePh_2$, **5b**)

In addition, only one of the terminal carbonyls (CO_b) appears as a doublet (**5a**: $^2J_{Rh\text{-}C}$ = 4.5 Hz; **5b**: $^2J_{Rh\text{-}C}$ = 4.2 Hz) and can be assigned to the carbonyl along the metal-metal vector. This carbonyl corresponds to

C(3)O(3) in the X-ray structure of **5a**. Similar long-range ^{103}Rh-^{13}C(carbonyl) coupling through a metal-metal bond has been observed by Cowie and co-workers for $(\mu\text{-dmpm})_2(\mu\text{-CO})_2Rh_2(CO)_2$ ($^2J_{Rh\text{-}C}$ = 3.0 Hz).[14] The other two terminal carbonyls cannot be definitively assigned.

The experimental ^{13}C NMR spectra of **5a** and **5b** can be readily simulated and the activation parameters are listed in Table 3.6. The activation parameters for the exchange process are similar for **5a** and **5b**, reflecting the related properties of the two phosphines. The slighter lower enthalpy of activation for **5a** can be attributed to the basicity difference between PMe_2Ph and $PMePh_2$, with the net effect being increased electron donation in the case of **5a**.[15a]

Table 3.6: Activation Parameters for Carbonyl Exchange in $[\mu\text{-C(O)}C_2H_2]Os(CO)_3RhCp(PR_3)$ ($PR_3 = PMe_2Ph$, **5a**; $PMePh_2$, **5b**)

Compound	ΔH‡ (kJ/mol)	ΔS‡ (J/mol·K)
5a	43.6 ± 1.4	-0.2 ± 5.9
5b	47.4 ± 2.0	4.8 ± 8.4

3.4.2. Variable Temperature ^{1}H NMR Behaviour

Unexpectedly, the ^{1}H NMR spectra of **5a** and **5b** also change with temperature. The ^{1}H NMR spectra at room temperature and at -20 °C for **5a** are shown in Figure 3.4.

As can be seen, the ^{1}H NMR signals for H_α, H_β and the methyl groups are quite broad at room temperature, at -20 °C these signals sharpen and the fine structure of the acetylenic ring proton signals may be observed. A reasonable explanation for the reversible lineshape changes is some fluxional process that would interconvert the H_α-H_β protons and the diastereotopic methyl groups.

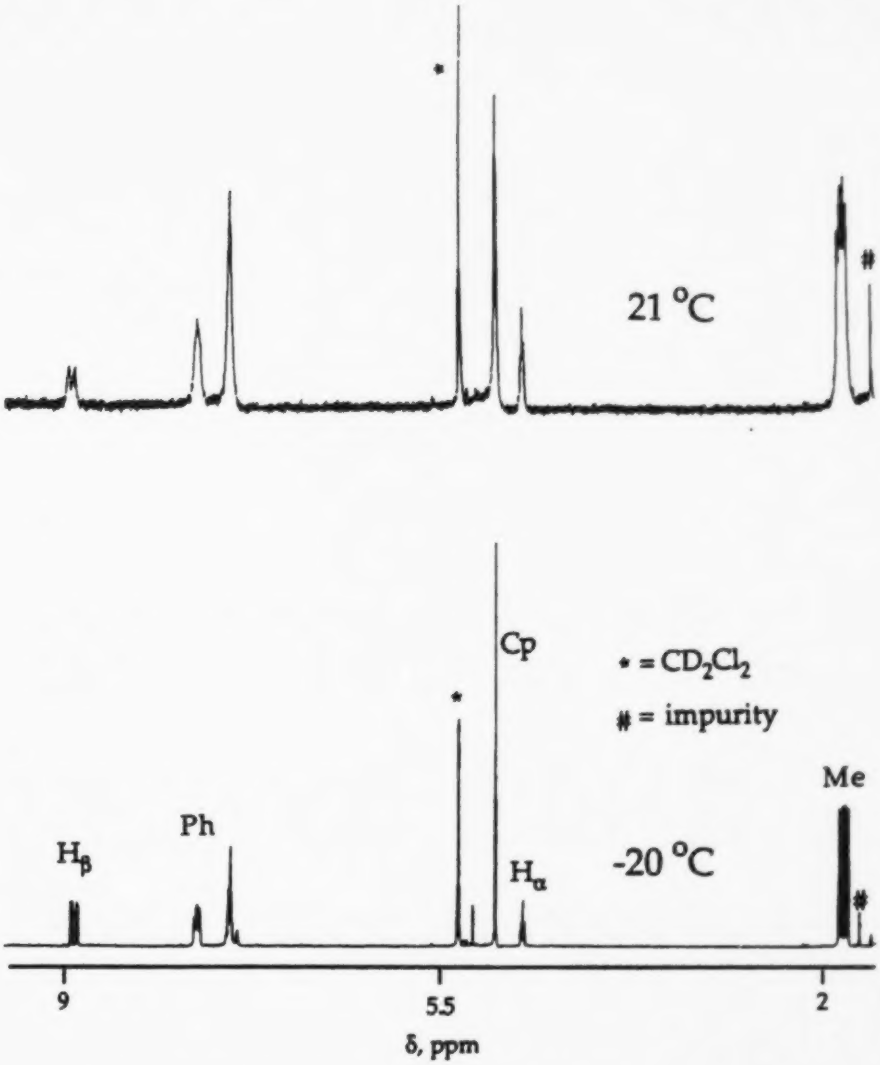

Figure 3.4: Variable Temperature ^{1}H NMR Spectra of **5a**

Knox and co-workers observed an interesting fluxional process in $[\mu\text{-}C_2Ph_2C(O)]Ru_2Cp_2(CO)_2$ whereby the Cp ligands, the terminal and acyl carbonyl groups, and the two ends of the bonded olefinic unit become equivalent on the NMR time scale. Knox has shown that this occurs *via* the process shown below.[4a]

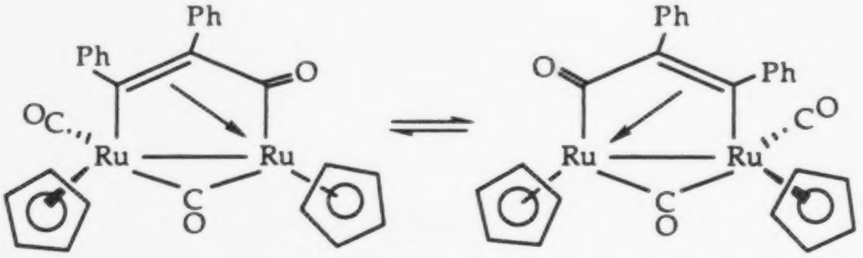
Ph
Ph
O
OC
Ru
Ru
C
O
Ph
Ph
O
CO
Ru
Ru
C
O

The process involves concerted insertion-deinsertion of CO into the ruthenium-alkyne bond, while the C=C bond remains bonded to the metal centres. A similar process was observed for [μ-$C_2H_2C(O)$]$Ru_2(CO)_5$(μ-dppm) whereby breaking of one alkyne-CO bond occurs synchronously with the formation of a new alkyne-CO bond.[4c,h]

A related process but occuring at the single Os centre would exchange H_α-H_β and, since it causes enantiomerization of the molecule, would also exchange the diastereotopic methyl groups (Scheme 3.2).

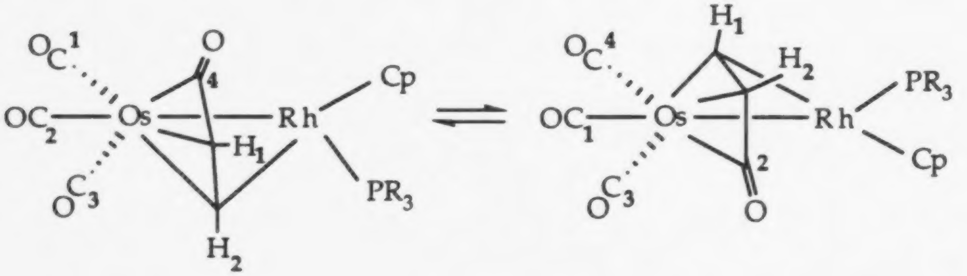
OC1
O
4
Cp
OC2
Os
Rh
H1
OC3
PR3
H2
H1
OC4
H2
PR3
OC1
Os
Rh
2
Cp
OC3
O

Scheme 3.2: Fluxional Behaviour of Alkyne Bridge in **5a-b**

However, this process would involve the acyl carbonyl as well which remains unchanged from -80 °C to room temperature. Consequently, we have no clear explanation as to the temperature dependent ^{1}H NMR behaviour of **5a-b**. It is possible that the line broadening observed in the ^{1}H NMR spectra is caused by the presence of a paramagnetic impurity. Alternatively, an isomerization reaction may be occuring with the second undetected isomer having a concentration below the detection limits of the spectrometer.

3.5. Reaction of $Os(CO)_4(\eta^2\text{-}HCCH)$ with $CpM(CO)(PR_3)$ (M = Co; PR_3 = PMe_3, PMe_2Ph, $PMePh_2$; M = Rh; PR_3 = PMe_3): Unexpected Formation of Zwitterionic Compounds

The reaction between $Os(CO)_4(\eta^2\text{-}HCCH)$, **1**, and $CpRh(PMe_3)(CO)$ or $CpCo(PR_3)(CO)$ (PR_3 = PMe_3, PMe_2Ph, $PMePh_2$) was carried out in similar manner as used in the synthesis of **5a** and **5b**. For example, a pentane solution containing **1** and a slight excess of $CpRh(PMe_3)(CO)$ was slowly warmed from -78 °C to 10 °C using a dry ice/acetone bath. Reaction occurs at 0 °C as evidenced by a color change from light orange to red and a fine, ruby red precipitate forms. The solution is maintained at 10 °C for 1 hour over which time the amount of precipitate increases and the color of the solution lightens to a light orange hue. At this time, no peaks due to **1** are present in the FT-IR spectrum, signalling that the reaction is complete. The resulting product, **7**, is almost completely insoluble in hydrocarbon, thus the precipitate is washed until the washings are colorless. This also ensures that all $CpRh(CO)(PR_3)$ is removed from the product. Similar observations are made for $CpCo(PR_3)(CO)$ (PR_3 = PMe_3, PMe_2Ph, $PMePh_2$). The only difference is that the precipitate is dark emerald green in color.

In all cases, the products precipitate from solution in analytically pure form. The resulting dimetallic species are thermally stable and may be handled in air for short periods of time, although they are best stored under an inert atmosphere at 5 °C.

3.5.1. Characterization of $[\mu\text{-}\eta^1\text{:}\eta^2\text{-HCCH(PR}_3)](\mu\text{-CO})\mathrm{Os(CO)_3MCp}$, (M= Co; $\mathrm{PR_3} = \mathrm{PMe_3}$, 6a; $\mathrm{PMe_2Ph}$, 6b; $\mathrm{PMePh_2}$, 6c; M = Rh, $\mathrm{PR_3} = \mathrm{PMe_3}$, 7)

The reaction of **1** with $\mathrm{CpRh(CO)(PMe_3)}$ in pentane solution under mild conditions leads to the formation of the ruby red solid **7**, while the reaction with $\mathrm{CpCo(PR_3)(CO)}$ ($\mathrm{PR_3} = \mathrm{PMe_3}$, $\mathrm{PMe_2Ph}$, $\mathrm{PMePh_2}$) gives emerald or olive green products (Scheme 3.3).

$$\begin{array}{c}\mathrm{Os(CO)_4(\eta^2\text{-}HCCH)}\\ + \\ \mathrm{CpM(PR_3)(CO)}\end{array} \xrightarrow[\text{-CO, }5\,^{\circ}\mathrm{C}]{\text{pentane}} [\mu\text{-}\eta^1\text{:}\eta^2\text{-HCCH(PR}_3)](\mu\text{-CO})\mathrm{Os(CO)_3MCp}$$

M = Co	M = Rh
$\mathrm{PR_3} = \mathrm{PMe_3}$, **6a**	$\mathrm{PR_3} = \mathrm{PMe_3}$, **7**
$= \mathrm{PMe_2Ph}$, **6b**	
$= \mathrm{PMePh_2}$, **6c**	

Scheme 3.3: Formation of $[\mu\text{-}\eta^1\text{:}\eta^2\text{-HCCH(PR}_3)](\mu\text{-CO})\mathrm{Os(CO)_3MCp}$ (M = Rh, $\mathrm{PR_3} = \mathrm{PMe_3}$; M= Co, $\mathrm{PR_3} = \mathrm{PMe_3}$, $\mathrm{PMe_2Ph}$, $\mathrm{PMePh_2}$)

Although **6a-c** and **7** have molecular formulations similar to **5a** and **5b**, the spectroscopic and physical properties of the compounds are substantially different. As mentioned **5a** and **5b** are orange in color; they are also slightly soluble in hydrocarbon solvents. In contrast, **7** is dark ruby red in color and completely insoluble in pentane. This dramatic change would not be expected in simply changing from a $\mathrm{PMe_2Ph}$ ligand in **5a** to PMe_3 in **7**. Thus, it was immediately apparent that a significant structural change had occurred indicating that the reaction of **1** with $CpM(PR_3)(CO)$ exhibits both marked metal and phosphine dependence.

The FT-IR and NMR data for **6a-c** and **7** did not allow for unambiguous determination of the structural formulation, but several basic structural features could be inferred from the spectroscopic data. The FT-IR spectrum of **7** gave rise to three terminal carbonyl bands plus a stretching band at 1714 cm^{-1}. This indicated the presence of a bridging carbonyl or the acyl group of a coordinated dimetallacyclopentenone ring. The ^{31}P NMR spectrum of **7** consisted of a doublet, however the ^{103}Rh-^{31}P spin-spin coupling was only 10.8 Hz. The one-bond ^{103}Rh-^{31}P coupling in $CpRh(PMe_3)(CO)$ is 186.0 Hz and 188.4 Hz for **5a**, thus, it appeared that in **7** the trimethylphosphine was no longer directly bound to the Rh centre.

The ^1H NMR data also provided structural clues. The ^1H NMR data for **6a-c** and **7** are listed in Table 3.7, the labelling of the α and β protons follows the convention of Carty.[16]

Table 3.7: ^1H NMR Data for $[\mu-\eta^1:\eta^2-HCCH(PR_3)](\mu-CO)Os(CO)_3MCp$

δ (ppm, CD_2Cl_2)[a]

Compound	H_α	$^3J_{P-H\alpha}$	H_β	$^2J_{P-H\beta}$	$^3J_{H-H}$
6a	9.20	31.6	3.62	20.8	9.2
6b	9.35	32.1	3.82	15.8	9.0
6c	9.60	30.6	4.06	15.6	9.5
7	8.27[b]	31.0	4.00[c]	20.2	9.3

[a] Couplings in Hertz. [b] Additional coupling of $^2J_{Rh-H\alpha} = 0.6$ Hz. [c] Additional coupling of $^2J_{Rh-H\beta} = 2.9$ Hz.

Two trends are immediately apparent. First, there is a large chemical shift difference between the α and β protons. As seen before, this is usually indicative of a structure in which one acetylenic carbon bridges two metal centres while the other acetylenic carbon is only bound to one metal.[4] Second, a large ^{31}P - ^{1}H coupling to both acetylenic hydrogens is seen which is best accommodated by assuming that the PMe_3 ligand is now bonded to the acetylene moiety. Alt and co-workers have prepared the mononuclear zwitterionic complex shown below and reported large ^{31}P-^{1}H couplings.[17a-b] . These values are in accord with those obtained for **6a-c** and **7**.

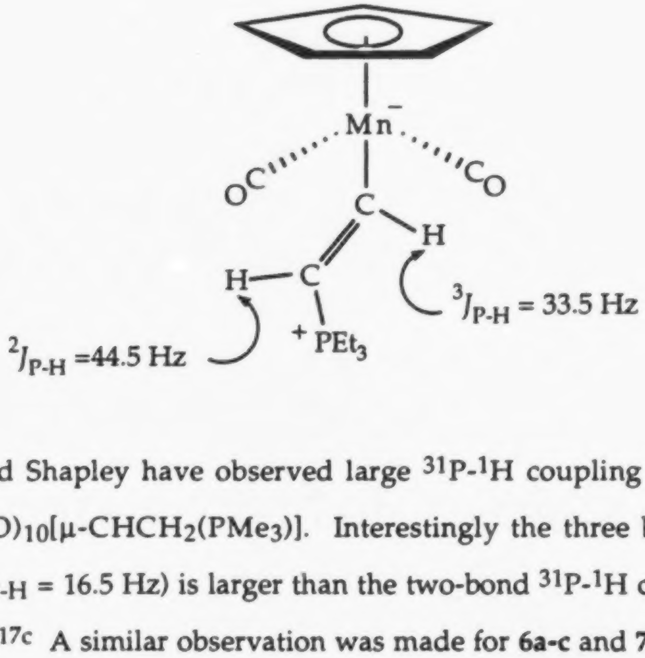

Churchill and Shapley have observed large ^{31}P-^{1}H coupling constants in $(\mu\text{-H})Os_3(CO)_{10}[\mu\text{-}CHCH_2(PMe_3)]$. Interestingly the three bond ^{31}P-^{1}H coupling ($^{3}J_{P\text{-}H}$ = 16.5 Hz) is larger than the two-bond ^{31}P-^{1}H coupling ($^{2}J_{P\text{-}H}$ = 11.0 Hz).[17c] A similar observation was made for **6a-c** and **7**.

The large chemical shift difference between the two acetylenic protons observed in the ^{1}H NMR spectra was also mirrored in the ^{13}C NMR data of compounds **6a-c** and **7**. The ^{13}C NMR data for the α and β carbons is given in Table 3.8.

For compounds **6a-c** and **7**, there is approximately a 60-65 ppm chemical shift difference between the α and β carbons. Also, for the β carbon, one observes large ^{31}P-^{13}C spin-spin coupling. The coupling of 82.3-76.1 Hz is in accord with that expected for one-bond phosphorus-carbon coupling.[5b] A smaller coupling of 7.3 Hz to the α carbon is observed for **7**. This coupling was not observed for **6a-c**, indicating that the α carbon was attached to the Co centre, where the effects of the quadropolar nucleus could make observation of the ^{31}P-^{13}C coupling difficult.[18] Also of note is that for **7**, both the α and β carbons show ^{103}Rh-^{13}C coupling that is consistent with having these carbon atoms directly attached to the Rh centre *via* σ bonds.[7] The chemical shift values indicate that the α acetylenic carbon may be bridging two metal centres, while the β carbon is attached only to the Rh/Co centre.[4] This is similar to that observed for **5a-b**, however, in **6a-c** and **7**, the PR_3 ligand is also bonded to the β carbon.

Table 3.8: ^{13}C NMR Data for $[\mu-\eta^1:\eta^2\text{-HCCH(PR}_3)](\mu\text{-CO})Os(CO)_3MCp$,
(M = Rh, Co; PR_3 = PMe_3, PMe_3, PMe_2Ph, $PMePh_2$)

δ (ppm, CD_2Cl_2)[a]

Compound	C_α	$^2J_{P\text{-}C\alpha}$	C_β	$^1J_{P\text{-}C\beta}$
6a	113.0	----	47.5	81.4
6b	111.7	----	47.5	77.9
6c	112.9	----	48.2	76.1
7	104.8	7.3[b]	44.2	82.3[c]

[a]Couplings in Hertz. [b]Additional coupling of $^1J_{Rh\text{-}C\alpha}$ =10.1 Hz. [c]Additional coupling of $^1J_{Rh\text{-}C\beta}$ = 20.4 Hz.

For further structural information, ^{13}CO enriched samples of **6a-c** and **7** were prepared and the results are listed in Table 3.9.

Table 3.9: ^{13}C NMR (Carbonyl Region) Data
for $[\mu-\eta^1:\eta^2\text{-HCCH(PR}_3)](\mu\text{-CO})\text{Os(CO)}_3\text{MCp}$
(M = Rh, Co; PR_3 = PMe_3, PMe_3, PMe_2Ph, $PMePh_2$)

	δ (ppm, CD_2Cl_2)			
Compound		CO		μ-CO
6a	193.1	186.1	185.2	282.1
6b	193.2	186.2	185.1	282.0
6c	193.5	186.6	185.2	279.4
7	192.8	185.5	184.2	262.2[a]

[a] Additional coupling of $^1J_{Rh\text{-}C}$ = 51.0 Hz.

The presence of three terminal carbonyls is immediately apparent. However, the chemical shifts of the terminal carbonyls of **6a-c** and **7** are very similar. In fact, there is less than a 1 ppm difference in the chemical shift. This indicates that these carbonyls must be attached to the Os centre since from **7** to **6a-c** there is a change in metal centres from Rh to Co; only the Os centre remains constant. Furthermore, changing the phosphine has little effect on the chemical shifts of the terminal carbonyls, indicating that the PR_3 ligand must be far removed from the Os centre. Finally, there is the appearance of a ^{13}C NMR signal in the lowfield region. Compared to the range of ^{13}C NMR chemical shifts seen for acyl moieties for compounds **2a-b** and **3** (Chapter 2) and **5a-b**, the chemical shifts observed for **6a-c** and **7** are substantially further downfield. Thus, one could conclude that the lowfield signal is not due to an acyl moiety, but, in fact, can be assigned to a bridging carbonyl.[7] For **7**, there is ^{103}Rh-^{13}C coupling of 51.0 Hz, which is significantly larger than the typical ^{103}Rh-^{13}C(acyl) coupling of 24.0 Hz observed in our laboratories.

3.5.2. Molecular Structure of [μ–η^1:η^2-HCCH(PMe$_3$)](μ-CO)Os(CO)$_3$RhCp, 7

The aforementioned spectroscopic data allowed for some basic inferences to be made concerning the structures of **6a-c** and **7**. However, the probability that trimethylphosphine had migrated to one of the acetylenic carbons needed complete confirmation, thus an X-ray crystallographic analysis was undertaken on a single crystal of **7**. The results of this study are shown in Figure 3.5. The relevant bond distances and angles for **7** are listed in Tables 3.10 and 3.11, respectively.

As seen, the PMe$_3$ ligand has migrated from Rh and is now part of a bridging zwitterionic hydrocarbyl moiety with a newly developed phosphonium center and the negative charge on the osmium atom. The bridging hydrocarbyl ligand is bonded in a μ-η^1,η^2 fashion. The Os-Rh metal-metal single bond and a bridging carbonyl completes the electronic requirements of both metal centers (V). Alternatively, a Rh→Os donor-acceptor bond may be postulated with the α carbon bearing a full negative charge and donating two electrons to the Rh centre (VI).

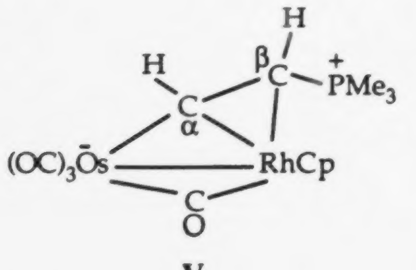

V

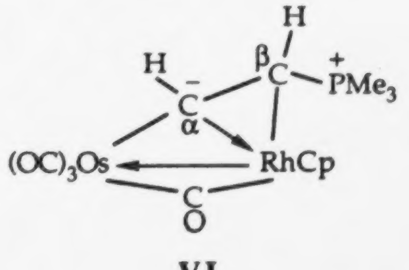

VI

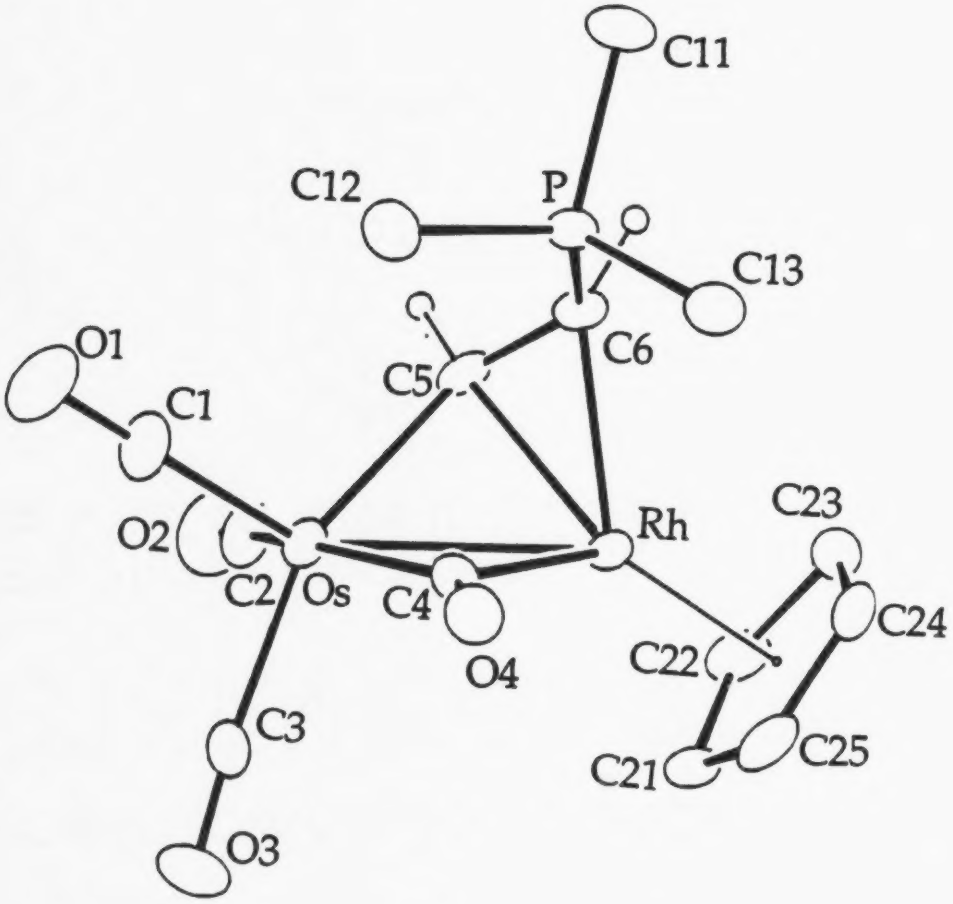
C11
C12
P
C13
C6
C5
O1
C1
O2
C2
Os
C4
Rh
C23
C24
C22
O4
C3
C21
C25
O3

Figure 3.5: ORTEP View of $[\mu-\eta^1:\eta^2\text{-HCCH(PMe}_3)](\mu\text{-CO})\text{Os(OC)}_3\text{RhCp}$, **7**

Table 3.10: Selected Bond Lengths (Å) for 7

Os-Rh	2.695(1)	P-C6	1.75(1)
Os-C1	1.86(2)	P-C11	1.81(1)
Os-C2	1.95(2)	P-C12	1.77(1)
Os-C3	1.95(2)	P-C13	1.79(1)
Os-C4	2.06(1)	O1-C1	1.18(2)
Os-C5	2.13(1)	O2-C2	1.14(2)
Rh-C4	2.04(1)	C3-O3	1.13(2)
Rh-C5	2.10(1)	O4-C4	1.16(2)
Rh-C6	2.15(1)	C5-C6	1.45(2)

Table 3.11: Selected Angles (deg) for 7

Rh-Os-C1	139.5(5)	Os-C4-Rh	82.3(4)
Rh-Os-C2	107.1(5)	Os-C4-O4	147.2(9)
Rh-Os-C3	108.4(4)	Rh-C4-O4	129.9(9)
Rh-Os-C4	48.5(4)	Os-C5-Rh	79.2(4)
Rh-Os-C5	50.0(4)	Os-C5-C6	125(1)
C1-Os-C2	102.9(7)	C4-Rh-C5	83.5(5)
C1-Os-C3	94.4(8)	C4-Rh-C6	86.4(4)
C1-Os-C4	101.8(6)	C5-Rh-C6	40.0(5)
C1-Os-C5	107.8(7)	P-C6-C5	131.8(9)
C2-Os-C3	96.4(8)	C6-P-C11	105.3(6)
C2-Os-C4	154.6(6)	C6-P-C12	117.4(7)
C2-Os-C5	84.8(7)	C6-P-C13	111.8(6)
C3-Os-C4	87.4(6)	Rh-C6-C5	68.3(6)
C3-Os-C5	157.0(6)	Rh-C6-P	120.7(5)
C4-Os-C5	82.2(6)	Rh-C5-C6	71.6(6)
Os-Rh-C4	92.5(4)	Os-C1-O1	179(1)
Os-Rh-C5	50.8(4)	Os-C2-O2	178(1)
Os-Rh-C6	81.8(3)	Os-C3-O3	176(1)

The Os-Rh separation of 2.695(1) Å is indicative of a metal-metal single bond, although it is significantly shorter than the Os-Rh separation of 2.780 Å seen in **5a**. The short Os-Rh bond length would favor **V** as Rh→Os donor-acceptor bonds are normally significantly longer. For example, the Rh→Os metal-metal bond length in $[\mu\text{-}C_2(CO_2Me)_2](\mu\text{-dppm})_2RhOs(CO)_3^+$ is 2.8744(3) Å.[19] The Os-C5 separation of 2.13(2) Å, and the Rh-C5 and Rh-C6 distances of 2.10(1) and 2.15(1) Å respectively, are in accord with their formulation as metal-carbon single bonds. The Os-C5 distance is comparable to the Os-C distance of 2.138(5) Å found in $[\mu\text{-}C_2(CO_2Me)_2]Os_2(CO)_8$.[10] The Rh-C distances are similar to those expected (2.023(5)-2.128(5) Å) for an alkyne bridging two metals connected by a metal-metal bond.[12] The Os-C5 and Rh-C5 distances are equivalent within one esd, even though Os(0) and Rh(I) have different bonding radii. This provides evidence that the methylene bridge interacts strongly with both metal centres. The Os-C4 (2.06(1) Å) and Rh-C4 (2.04(1) Å) bond distances are essentially equivalent. However, the Os-C4-O4 angle of 147.2(9)^o is larger than the Rh-C4-O4 angle of 129.9(9)^o, indicating that the bridging carbonyl is slightly skewed towards the Rh centre. The Os-C1 distance of 1.86(1) Å is shorter than the other two Os-carbonyl bond distances, which are, on average, 1.95(2) Å. The C1-O1 ligand is the carbonyl most in line with the Os-Rh vector, thus an increased Os→C1 backbonding interaction would be expected. A similar observation was made in the case of **5a**.

The C5-C6 bond distance is 1.45(2) Å, which is shorter than the 1.530(15) Å expected for a C-C single bond.[13] This indicates that the C5-C6 interaction has some double bond character; the coordinated olefinic C-C distance in **5a** is 1.46(2) Å. This shortening of the formal C-C single bond distance suggests another structural form of **7** may be drawn (**VII**).

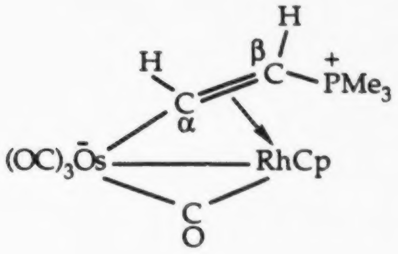

VII

In this structure, there is a formal double bond between C5 and C6 that is coordinated to the Rh centre. The actual structure of **7** can be thought of as a hybrid of **V** and **VII**, with negligible contribution from **VI**. Carty also noticed a shortening of the C-C bond in a series of zwitterionic μ-alkylidene compounds.[20]

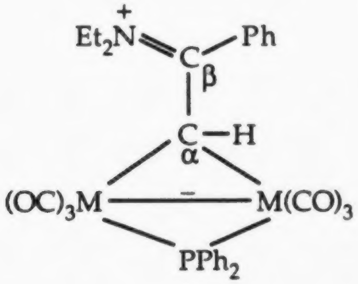

M	$d(C_\alpha\text{-}C_\beta)$, Å
Fe	1.427(5)
Ru	1.417(7)
Os	1.44(2)

Carty attributed this shortening to delocalization of the electron density over the hydrocarbyl's four-atom skeleton even though the α carbon has approximately tetrahedral geometry. Finally, the P-C6 bond length of 1.75(1) Å is close to the expected value of 1.800(15) Å.[13] In a related compound, $Fe_2(CO)_6[\mu\text{-}C{=}C(PCy_2H)Ph](\mu\text{-}PPh_2)$, the P-C bond distance is 1.787(7) Å.[21]

3.6. Comparison of 6a-c and 7 to Similar Hydrocarbyl Bridged Zwitterionic Species

The synthesis of a zwitterionic species is not novel as several groups, most notably those of Carty and Deeming, have reported[17,20,21,22] numerous di- and tri-metallic zwitterionic species. Normally the synthesis of complexes containing two-carbon bridging units involves nucleophilic attack on bridging acetylide ligands. An example is given is Scheme 3.4.[22b]

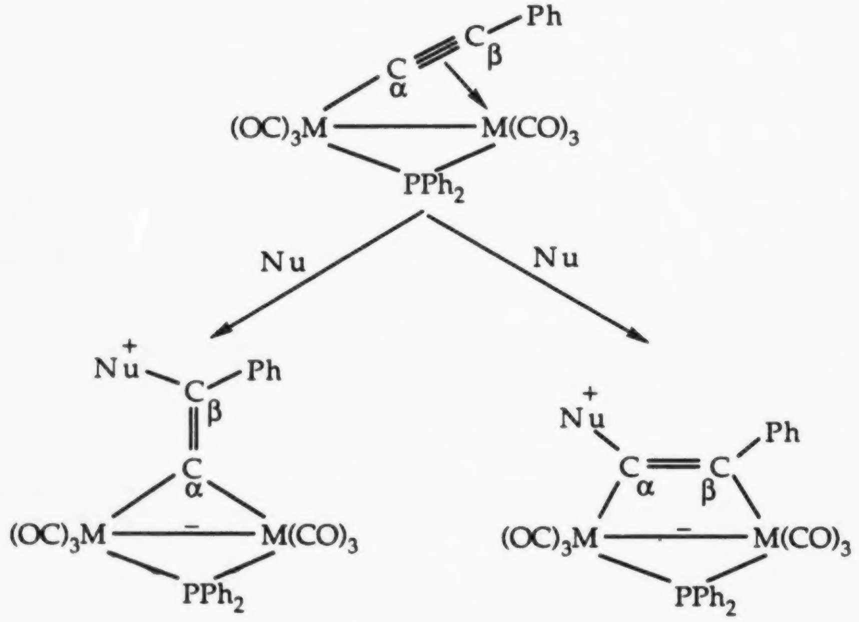
Ph
C
β
C
α
(OC)3M
M(CO)3
PPh2
Nu
Nu
Nu
+
Ph
C
β
C
α
−
(OC)3M
M(CO)3
PPh2
Nu
+
Ph
C
α
C
β
−
(OC)3M
M(CO)3
PPh2

M = Fe, Ru, Os
Nu = NR_3, NHR_2, PR_3

Scheme 3.4: Synthesis of Zwitterionic Dimetallic Species *Via* Nucleophilic Attack of a Bridging Acetylide Unit

In some cases, the initial nucleophilic attack may be followed by a proton transfer. The formation of **6a-c** and **7** is unusual since it appears to involve migration of the nucleophile, PR_3, from a metal center to a bridging acetylene moiety. The structures of **6a-c** and **7** are also rare in that the α carbon bridges both metals and the β carbon is only attached to one metal center. In previous work, C_α bridged species were limited to μ-alkylidene type complexes (**C**), whereas attachment of C_β resulted in rupture of the C_α bridge and formation of metallophenethylidenes (**D**).

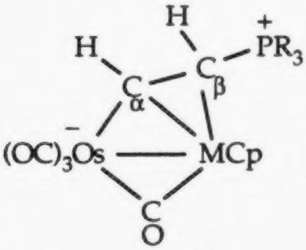

6a-c and **7**

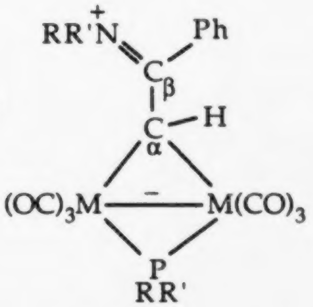

M = Fe, Ru, Os

C

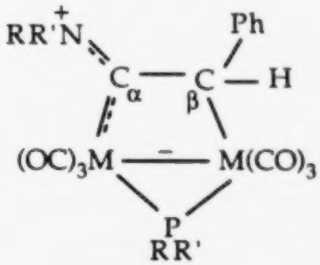

M = Fe, Ru, Os

D

Carty has summarized the ^{13}C NMR chemical shift data for several classes of zwitterionic hydrocarbyl bridged dimetallic compounds and used the data to ascertain the amount of carbene character in various types of two-carbon bridges.[16] Most closely related to **6a-c** and **7** are a series of metallophenethylidenes (**D**) prepared by Carty and co-workers.[22b] In complexes such as these, the range of carbon resonances for the α carbon is from 202.1 to 249.7 ppm, indicating significant carbene character. The β carbons resonate between 31.0 and 44.9 ppm. This can be compared to the ^{13}C NMR chemical shift values for **7**, which are 104.8 and 44.2 ppm for the α and β carbons, respectively. The upfield shift of the C_α resonance in **7** compared to **D** is due to its attachment to two metal centers as it resembles a bridging carbene. According to the data collected by Herrmann,[6] the ^{13}C NMR chemical shift range for alkylidene units bridging two metal centers is between 210-100 ppm. The C_α resonance for **7** lies inside this range, albeit at the highfield limit. In zwitterionic complexes such as **C**, the range of C_α resonances is from 28.8-75.0 ppm, which Carty has attributed to an electron rich M-M core. Therefore, in reference to Herrmann's parameters, the highfield position of the α carbon in **7** may then be due to the negative charge on the Os atom.

3.7. Formation of Compounds 5a-b, 6a-c and 7: Plausible Reaction Pathways

In view of the unexpected structures, attempts were made to follow the evolution of product formation, and thereby elucidate the reaction pathway, *via* low temperature NMR spectroscopic studies. The formation of **5a** was studied by low temperature ^1H NMR spectroscopy. A CD_2Cl_2 solution of $Os(CO)_4(\eta^2\text{-HCCH})$, **1**, and $CpRh(CO)(PMe_2Ph)$ was warmed from -60 °C to ambient temperature and the reaction was monitored using proton NMR spectroscopy. The results obtained did not provide much illumination. At -10 °C, only starting materials and a small amount of **5a** were seen. As the solution was warmed to 10 °C, a mixture of products was obtained, one of which could be identified as **5a**. Unfortunately, other intermediates could not be identified.

The formation of **7** was followed by a combination of ^1H, ^{13}C and ^{31}P NMR spectroscopies using ^{13}CO enriched $Os(CO)_4(\eta^2\text{-HCCH})$, **1**, and unenriched $CpRh(CO)(PMe_3)$ in CD_2Cl_2 solution. The use of CD_2Cl_2 was necessitated by the insolubility of **7** in aliphatic and aromatic solvents. As the solution was slowly warmed from -60 °C the reaction proceeded through several, unfortunately unidentifiable, intermediates, but at +10 °C only a single product was present. Surprisingly, this product was not **7** as it had quite different spectroscopic features. This product will be referred to as **8**.

The ^{1}H NMR spectrum at -40 °C showed only $Os(^{13}CO)_4(\eta^2\text{-}HCCH)$ and $CpRh(CO)(PMe_3)$ were present. Peaks due to **8** appeared at -20 °C. Warming the NMR sample to -10 °C resulted in increased formation of **8** but several other unidentified products also appeared. Finally, equilibration at 15 °C gave only **8**.

In the ^{13}C NMR spectrum at -40 °C, only peaks due to $Os(^{13}CO)_4(\eta^2\text{-}HCCH)$ were observed. Initially, at -20 °C, a signal due to $CpRh(^{13}CO)(PMe_3)$ also began to appear. This was unusual in that no free ^{13}CO was detected. However, upon maintaining the sample at -20 °C, a signal due to free ^{13}CO was detected, along with increased levels of $CpRh(^{13}CO)(PMe_3)$. This phenomenon of intermetallic CO exchange prior to formation of the bimetallic product has been observed previously in the reaction of $Os(^{13}CO)_4(\eta^2\text{-}HCCH)$ with $Ru(CO)_5$.[23] At 0 °C there was the observation of free ^{13}CO along with peaks due to **8** and a species postulated as having an acyl attached to an Os centre. At 10 °C, the peaks due to the Os-acyl species and $Os(^{13}CO)_4(\eta^2\text{-}HCCH)$ had all but disappeared and only peaks due to **8** and excess $CpRh(CO)(PMe_3)$ were seen. This was also accompanied by a significant decrease in the amount of free ^{13}CO.

The changes in the ^{31}P NMR spectra with temperature reflected changes similar to those observed in the ^{1}H and ^{13}C NMR spectra. At -40 °C, only a doublet due to $CpRh(CO)(PMe_3)$ was observed. At -20 °C, small satellite peaks centred on this doublet appeared due to the presence of CpRh(^{13}CO)(PMe$_3$). Between the temperatures of -20 °C and 0 °C, a number of ^{31}P NMR signals were present, one of which could be assigned to **8**. No free PMe$_3$ was detected. Finally, after allowing the solution to warm to 10 °C, only signals due to **8** and excess CpRh(CO)(PMe$_3$) were observed.

The ^{1}H NMR spectrum of **8** consisted of the expected signals due to the Cp and PMe$_3$ ligands plus two distinct downfield signals. The chemical shifts of the acetylenic protons were 8.53 and 7.64 ppm; the proton-proton coupling was 9.3 Hz. The similarity in chemical shift between the two ring protons rules out a structure similar to **5a-b** or **6a-c** and **7**. In the ^{13}C NMR spectrum, the acetylenic carbons resonate at 164.2 and 148.8 ppm, mirroring the results of the proton NMR spectrum. The ^{31}P NMR spectrum only showed a singlet at -56.0 ppm, indicating that the PMe$_3$ ligand was no longer directly attached to the Rh centre.[5] The ^{13}C NMR spectrum of the ^{13}CO enriched sample was extremely important in the assignment of the structure. The ^{13}C NMR spectrum consisted of four terminal carbonyl resonances. One of these, at 195.2 ppm, was a doublet with characteristic ^{103}Rh-^{13}C coupling of 84.4 Hz. Also, it appears in the chemical shift range for terminal carbonyls attached to a Rh centre, further corroborating its assignment. One of the terminal osmium-carbonyls at 181.9 ppm was a doublet with ^{31}P-^{13}C coupling of 96.7 Hz. This is consistent with a carbonyl *trans* to a phosphine and enabled the placement of the PMe$_3$ ligand onto the Os centre, *trans* to one of the equatorial carbonyls.[7] The other terminal carbonyl resonances at 181.7 and 169.4 ppm displayed *cis* ^{31}P-^{13}C couplings of 8.9 and 8.7 Hz, respectively. Finally, a doublet was observed at 225.7 Hz. Based on the similarity of the magnitude of the coupling ($^1J_{Rh\text{-}C}$ = 25.2 Hz) and its chemical shift, this signal was assigned to an acyl moiety attached to the Rh centre. Thus, the structure shown below is proposed for **8**.

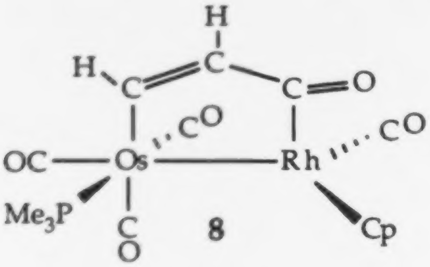

8

In the structure, the carbonyl on the Rh centre is placed on the opposite side of the metal-metal bond in relation to the PMe_3 ligand. The spectroscopic data does not require this; however, since no truncated merry-go-round exchange was observed at room temperature such a position is chemically more reasonable than the alternative arrangement. For compound **3**, it was observed that this is a very facile process and would be even more favoured for a Rh rather than an Ir centre.[1a,24] By placing the phosphine opposite the Rh carbonyl the first step in the exchange is effectively blocked and a static structure would be obtained. Attempts to isolate **8** were met with failure. Addition of non-polar solvents such as ether and hexane resulted in its conversion to **7**. The extreme insolubility of **7** no doubt plays an important role in this regard.

Although the reaction of $Os(CO)_4(\eta^2\text{-}HCCH)$ with $CpRh(CO)(PMe_3)$ in CD_2Cl_2 did not give **7** and the relevance of the NMR study on the mechanism of its formation may be questioned, the fact that **8** converts to **7** upon addition of hexane to CD_2Cl_2 indicates that it is, nevertheless, a possible intermediate. Admitting this to be the case, the question that still remains is the nature of the PMe_3 movement from Rh to Os and then onto the bridging organic ligands. The lability of the M-PR_3 bond is highly variable. Although observed in $CpCo(PPh_3)_2$[25] and $CpCo(PMe_3)_2$,[26] to our knowledge, no report of PR_3 dissociation from $CpM(CO)(PR_3)$ (M = Co, Rh) has been reported. In fact, Werner has evidence to indicate it is the carbonyl that is labile as the reaction of $CpCo(CE)(PMe_3)$ (E = O, S) with $CpMn(CO)_2(THF)$ yields the complex $Cp(PMe_3)Co(\mu\text{-}CO)(\mu\text{-}CE)MnCp(CO)$.[27,28] However, although Werner makes no mention of the reaction mechanism, $CpCo(CO)(PMe_3)$ does react with $P(OMe)_3$ to yield $CpCo(CO)[P(OMe)_3]$.[27] Thus, although unreported in the literature, it is possible that there could be a initial, yet undetected, phosphine dissociation from $CpRh(CO)(PMe_3)$ to result in the formation of **7-8**. However, no free PMe_3 was detected, and the reaction to form **7-8** occurs readily at low temperatures. We also note that the reaction of $Os(CO)_3(PMe_3)(\eta^2\text{-}C_2H_2)$ with $CpM(CO)_2$ (M = Co, Rh) in pentane gives, in both cases, a mixture of products, none of which are the zwitterionic species **6a** or **7**. Thus, we favour metal-assisted PR_3 migration in the initially formed Os-Rh species. Although no μ-PR_3 complexes are known, very recently Werner and co-workers reported the synthesis and X-ray crystal structure of a dirhodium complex, $[Rh_2Cl_2(\mu\text{-}Sb^iPr_3)(\mu\text{-}CPh_2)]$ which possesses a bridging trialkylstibane unit.[29] This then raises the possibility of an Os-Rh intermediate with a bridging PMe_3 ligand and lends support to our postulate of a metal-assisted PMe_3 migration.

3.8. Conclusions

The reaction of $Os(CO)_4(\eta^2\text{-}HCCH)$ with $CpM(CO)(PR_3)$ (M = Co, Rh; PR_3 = PMe_3, PMe_2Ph, $PMePh_2$) shows surprising metal and phosphine dependency. First, two different types of complexes, **5a-b** and **6a-c**, **7**, are synthesized depending on the metal and the substituents on the phosphine. For **5a-b**, the opposite regioselectivity to that in Chapter 2 is observed; the acyl carbon is attached to the Os centre. Also, both the alkyne protons/carbons and the carbonyls are fluxional, however, limiting spectra may be observed. The synthesis of the zwitterionic complexes **6a-c** and **7** was wholly unexpected, the use of X-ray crystallography was required to fully confirm the structure. These compounds were unusual in that the phosphine had migrated to the alkyne bridge from an eighteen electron centre; most phosphonium containing zwitterionic species are formed from the nucleophilic attack of a phosphine on a pre-formed hydrocarbyl bridge. Finally, the reaction to form **7** shows remarkable solvent dependence with non-polar solvents favouring the formation of the zwitterionic species. This is due to the extreme insolubility of **7** which shifts the equilibrium towards the charge-separated species.

3.9. Experimental Section

3.9.1. Starting Materials and Reagents

PMe_3, PMe_2Ph and $PMePh_2$ were purchased from Aldrich Chemical Company and used as received. $CpM(CO)(PR_3)$ (PR_3 = PMe_3, PMe_2Ph, $PMePh_2$) (M = Co,[30] Rh[5a,31]) were prepared by published procedures.

3.9.2. Synthetic Procedures

Synthesis of $[\mu\text{-}\eta^3\text{:}\eta^1\text{-}C(O)C_2H_2]Os(CO)_3RhCp(PMe_2Ph)$, 5a

A pentane solution containing 26.2 mg (0.080 mmol) of **1** and 30.4 mg (0.091 mmol) of $CpRh(CO)(PMe_2Ph)$ was slowly warmed from -78 °C to 10 °C using a dry ice/acetone bath. As the temperature neared 0 °C the original orange color darkened and an orange precipitate began to form. Continued stirring at 10 °C for 1 hour resulted in complete reaction, as judged by FT-IR. The volume of solvent was reduced to *ca.* 10 mL and the solution cooled to -78 °C to effect complete precipitation. The precipitate was isolated and washed with cold pentane (3×5mL). The yield was 32.4 mg (64%), **5a** may be recrystallized from CH_2Cl_2/pentane at -80 °C.

Formula Weight: 634.43

Mass Spectrum(200 °C, 16eV): M^+ (636, 6.4%), M^+-nCO (n = 0-4)

IR(CH_2Cl_2, cm^{-1}); ν(CO): 2043(m), 1968(s); ν(acyl): 1696(m).

^1H NMR(360 MHz, CD_2Cl_2, -20 °C) 8.82 (1H, dd, $^2J_{Rh\text{-}H}$ = 18.9 Hz, $^3J_{H\text{-}H}$ = 6.3 Hz, H_β), 7.73 (5H, m, Ph), 4.98 (5H, s, Cp), 4.72 (1H, dd, $^3J_{H\text{-}H}$ = 6.3 Hz, $^3J_{Rh\text{-}H}$ = 6.3 Hz, H_α), 1.84 (3H, d, $^2J_{P\text{-}H}$ = 9.2 Hz, CH_3), 1.79 (3H, d, $^2J_{P\text{-}H}$ = 9.5 Hz, CH_3).

^{13}C NMR(90.5 MHz, CD_2Cl_2, 23 °C) 156.0 (dd, $^1J_{Rh\text{-}C}$ = 35.2 Hz, $^2J_{P\text{-}C}$ = 14.8 Hz, C_β), 138.9 (d, $^1J_{P\text{-}C}$ = 48.0 Hz, C_{ipso}), 131.3 (d, $^2J_{P\text{-}C}$ = 11.6 Hz, C_{ortho}), 129.9 (s, C_{para}), 128.2 (d, $^3J_{P\text{-}C}$ = 9.6 Hz, C_{meta}), 88.5 (s, Cp), 52.8 (s, C_α), 21.3 (d, $^1J_{P\text{-}C}$ = 31.0 Hz, CH_3), 15.9 (d, $^1J_{P\text{-}C}$ = 31.3 Hz, CH_3).

^{13}C NMR(90.5 MHz, CD_2Cl_2, -80 °C) 222.4 (acyl), 181.9 (CO), 179.4 (d, $^2J_{Rh\text{-}C}$ = 4.5 Hz, CO), 175.2 (CO).

^{31}P NMR(81.0 MHz, CD_2Cl_2, 23 °C) 15.5 (d, $^1J_{Rh\text{-}P}$ = 188.4 Hz).

Anal. Calcd. for $C_{19}H_{18}O_4OsPRh$: C, 35.97; H, 2.86 Found: C, 35.84; H, 2.71.

Synthesis of [μ-η^3:η^1-$C(O)C_2H_2$]$Os(CO)_3RhCp(PMePh_2)$, 5b

Using a similar procedure, **1** (36.0 mg, 0.110 mmol) and $CpRh(CO)(PMePh_2)$ (48.2 mg, 0.122 mmol) were used to obtain **5b** as an orange solid (47.5 mg, 62%).

Formula Weight: 696.50

Mass Spectrum(200 °C, 16eV): M^+ (698, 0.3%), M^+-nCO (n = 0-4)

IR(CH_2Cl_2, cm^{-1}); ν(CO): 2045(m), 1970(s), 1698(m).

^1H NMR(360 MHz, CD_2Cl_2, -20 °C) 9.02 (1H, dd, $^2J_{Rh\text{-}H}$ = 18.5 Hz, $^3J_{H\text{-}H}$ = 6.4 Hz, H_α), 7.9-7.1 (10H, m, Ph), 4.77 (1H, m, H_β), 4.73 (5H, s, Cp), 2.05 (3H, d, $^2J_{P\text{-}H}$ = 9.1 Hz, CH_3).

^{13}C NMR(90.5 MHz, CD_2Cl_2, -20 °C) 156.0 (dd, $^1J_{Rh\text{-}C}$ = 35.4 Hz, $^2J_{P\text{-}C}$ = 14.4 Hz, C_β), 142.4 (d, $^1J_{P\text{-}C}$ = 46.5 Hz, C_{ipso}), 134.6 (d, $^2J_{P\text{-}C}$ = 12.5 Hz, C_{ortho}), 133.6 (d, $^1J_{P\text{-}C}$ = 46.4 Hz, C_{ipso}), 130.7 (s, C_{para}), 130.1 (d, $^2J_{P\text{-}C}$ = 10.8 Hz, C_{ortho}), 129.7 (s, C_{para}), 128.3 (d, $^3J_{P\text{-}C}$ = 10.3 Hz, C_{meta}), 128.1 (d, $^3J_{P\text{-}C}$ = 10.5 Hz, C_{meta}), 89.2 (s, Cp), 53.4 (s, C_α), 12.2 (d, $^1J_{P\text{-}C}$ = 30.4 Hz, CH_3).

^{13}C NMR(90.5 MHz, CD_2Cl_2, -70 °C) 222.0 (acyl), 181.1 (CO), 178.7 (d, $^2J_{Rh\text{-}C}$ = 4.2 Hz, CO), 174.9 (CO).

^{31}P NMR(81.0 MHz, CD_2Cl_2, 23 °C) 31.6 (d, $^1J_{Rh\text{-}P}$ = 189.7 Hz).

Anal. Calcd. for $C_{24}H_{20}O_4OsPRh$: C, 41.39; H, 2.89 Found: C, 41.25; H, 2.78.

Synthesis of $[\mu-\eta^1:\eta^2\text{-HCCH(PMe}_3)](\mu\text{-CO})Os(CO)_3RhCp$, 7

A pentane solution containing 27.4 mg (0.084 mmol) of **1** and 25.1 mg (0.092 mmol) of $CpRh(CO)(PMe_3)$ was slowly warmed from -78 °C to 10 °C using a dry ice/acetone bath. A ruby red precipitate began to form at 0 °C and continued stirring at 10 °C for 2 hours resulted in complete reaction as the supernatant lightened and no presence of **1** was detected by FT-IR. The red precipitate was isolated and washed with 5 mL portions of pentane until the washings were clear. The resulting solid was redissolved in CH_2Cl_2 (1 mL) and 10 mL of pentane was added to re-precipitate the red product. The pentane washing step was then repeated. The yield was 32.2 mg (67%). A suitable mass spectrum could not be obtained for **7** using E.I. and F.A.B. methods.

Formula Weight: 572.35

IR(CH_2Cl_2, cm^{-1}); ν(CO): 2022(s), 1948(s), 1928(s), 1714(m).

^1H NMR(360 MHz, CD_2Cl_2, 23 °C) 8.27 (1H, ddd, $^3J_{P\text{-}H}$ = 31.0 Hz, $^3J_{H\text{-}H}$ = 9.3 Hz, $^2J_{Rh\text{-}H}$ = 0.6 Hz, H_α), 5.29 (5H, d, $^2J_{Rh\text{-}H}$ = 0.7 Hz, Cp), 4.00 (1H, ddd, $^2J_{P\text{-}H}$ = 20.2 Hz, $^3J_{H\text{-}H}$ = 9.3 Hz, $^2J_{Rh\text{-}H}$ = 2.9 Hz, H_β), 1.65 (9H, d, $^2J_{P\text{-}H}$ = 13.0 Hz, CH_3).

^{13}C NMR(90.5 MHz, CD_2Cl_2, 23 °C) 262.2 (d, $^1J_{Rh\text{-}C}$ = 51.0 Hz, bridging CO), 192.8 (CO), 185.5 (CO), 184.2 (CO), 104.8 (dd, $^1J_{Rh\text{-}C}$ = 10.1 Hz, $^2J_{P\text{-}C}$ = 7.3 Hz, C_α), 87.4 (d, $^1J_{Rh\text{-}C}$ = 3.8 Hz, Cp), 44.2 (dd, $^1J_{P\text{-}C}$ = 82.3 Hz, $^1J_{Rh\text{-}C}$ = 20.4 Hz, C_β), 13.9 (d, $^1J_{P\text{-}C}$ = 56.6 Hz, CH_3).

^{31}P NMR(162.0 MHz, CD_2Cl_2, 23 °C) 23.8 (d, $^2J_{Rh\text{-}P}$ = 10.8 Hz).

Anal. Calcd. for $C_{14}H_{16}O_4OsPRh$: C, 29.38; H, 2.82. Found: C, 29.02; H, 2.62.

Synthesis of [μ–η^1:η^2-HCCH(PMe$_3$)](μ-CO)Os(CO)$_3$CoCp, 6a

Using a similar procedure, **1** (25.2 mg, 0.077 mmol) and CpCo(CO)(PMe$_3$) (24.1 mg, 0.106 mmol) were used to obtain **6a** as an emerald green solid (33.2 mg, 82%).

Formula Weight: 528.39

IR(CH_2Cl_2, cm^{-1}); ν(CO): 2022(s), 1946(s), 1921(s), 1699(m).

^{1}H NMR(360 MHz, CD_2Cl_2, 23 °C) 9.20 (1H, dd, $^3J_{P\text{-}H}$ = 31.6 Hz, $^3J_{H\text{-}H}$ = 9.2 Hz, H_α), 4.78 (5H, s, C_5H_5), 3.62 (1H, dd, $^2J_{P\text{-}H}$ = 20.8 Hz, $^3J_{H\text{-}H}$ = 9.2 Hz, H_β), 1.58 (9H, d, $^2J_{P\text{-}H}$ = 13.0 Hz, CH_3).

^{13}C NMR(90.5 MHz, CD_2Cl_2, 23 °C) 282.1 (bridging CO), 193.1 (CO), 186.1 (CO), 185.2 (CO), 113.0 (C_α), 84.6 (s, C_5H_5), 47.5 (d, $^1J_{P\text{-}C}$ = 81.4 Hz, C_β), 13.5 (d, $^1J_{P\text{-}C}$ = 55.9 Hz, CH_3).

^{31}P NMR(81.0 MHz, CD_2Cl_2) 24.3.

Anal. Calcd. for $C_{14}H_{16}CoO_4OsP$: C, 31.82; H, 3.05. Found: C, 31.57; H, 2.74.

Synthesis of [μ–η^1:η^2-HCCH(PMe$_2$Ph)](μ-CO)Os(CO)$_3$CoCp, 6b

Using a similar procedure, **1** (28.8 mg, 0.088 mmol) and CpCo(CO)(PMe$_2$Ph) (34.7 mg, 0.120 mmol) were used to obtain **6b** as an olive green solid (39.5 mg, 76%).

Formula Weight: 590.46

IR(CH_2Cl_2, cm^{-1}); ν(CO): 2021(s), 1946(s), 1921(s), 1699(m).

^{1}H NMR(360 MHz, CD_2Cl_2, 23 °C) 9.35 (1H, dd, $^3J_{P\text{-}H}$ = 32.1 Hz, $^3J_{H\text{-}H}$ = 9.0 Hz, H_α), 7.7-7.6 (5H, m, Ph), 4.77 (5H, s, C_5H_5), 3.82 (1H, dd, $^2J_{P\text{-}H}$ = 15.8 Hz, $^3J_{H\text{-}H}$ = 9.0 Hz, H_β), 2.14 (3H, d, $^2J_{P\text{-}H}$ = 13.3 Hz, CH_3), 1.52 (3H, d, $^2J_{P\text{-}H}$ = 13.4 Hz, CH_3).

^{13}C NMR(90.5 MHz, CD_2Cl_2, 23 °C) 132.1 (s, C_{para}), 129.4 (d, $^3J_{P\text{-}C}$ = 8.7 Hz, C_{meta}), 128.9 (d, $^2J_{P\text{-}C}$ = 10.8 Hz, C_{ortho}), 127.7 (d, $^1J_{P\text{-}C}$ = 75.7 Hz, C_{ipso}), 111.7

(s,C_α), 83.8 (s, C_5H_5), 47.5 (d, $^1J_{P\text{-}C}$ = 77.9 Hz, C_β), 11.0 (d, $^1J_{P\text{-}C}$ = 62.5 Hz, CH_3), 10.7 (d, $^1J_{P\text{-}C}$ = 54.5 Hz, CH_3).

^{13}C NMR(90.5 MHz, CD_2Cl_2, -20 °C) 282.0 (bridging CO), 193.2 (CO), 186.2 (CO), 185.1 (CO).

^{31}P NMR(81.0 MHz, CD_2Cl_2) 25.0.

Anal. Calcd. for $C_{19}H_{18}CoO_4OsP$: C, 38.65; H, 3.07. Found: C, 38.61; H, 2.82.

Synthesis of [μ–η^1:η^2-HCCH($PMePh_2$)](μ-CO)Os$(CO)_3$CoCp, 6c

Using a similar procedure, **1** (21.6 mg, 0.065 mmol) and CpCo(CO)($PMePh_2$) (35.9 mg, 0.102 mmol) were used to obtain **6c** as an olive green solid (22.7 mg, 53%). The relatively low yield of **6c** is likely due to the difficulty in preparing pure CpCo(CO)($PMePh_2$) as this compound was contaminated with small amounts of free $PMePh_2$.

Formula Weight: 652.53

IR(CH_2Cl_2, cm^{-1}); ν(CO): 2021(s), 1944(s), 1921(s), 1703(m).

^1H NMR(360 MHz, CD_2Cl_2, 23 °C) 9.60 (1H, dd, $^3J_{P\text{-}H}$ = 30.6 Hz, $^3J_{H\text{-}H}$ = 9.5 Hz, H_α), 7.8-7.5 (10H, m, Ph), 4.52 (5H, s, C_5H_5), 4.06 (1H, dd, $^2J_{P\text{-}H}$ = 15.6 Hz, $^3J_{H\text{-}H}$ = 9.5 Hz, H_β), 1.83 (3H, d, $^2J_{P\text{-}H}$ = 13.6 Hz, CH_3).

^{13}C NMR(90.5 MHz, CD_2Cl_2, 23 °C) 279.4 (bridging CO), 193.5 (CO), 186.6 (CO), 185.2 (CO), 133.5 (d, $^4J_{P\text{-}C}$ = 2.2 Hz, C_{para}), 133.13 (d, $^4J_{P\text{-}C}$ = 2.0 Hz, C_{para}), 132.2 (d, $^3J_{P\text{-}C}$ = 8.8 Hz, C_{meta}), 132.2 (d, $^3J_{P\text{-}C}$ = 8.5 Hz, C_{meta}), 129.6 (d, $^2J_{P\text{-}C}$ = 11.0 Hz, C_{ortho}), 129.5 (d, $^2J_{P\text{-}C}$ = 11.2 Hz, C_{ortho}), 127.9 (d, $^1J_{P\text{-}C}$ = 75.5 Hz, C_{ipso}), 126.9 (d, $^1J_{P\text{-}C}$ = 81.5 Hz, C_{ipso}), 112.9 (s,C_α), 85.1 (s, C_5H_5), 48.2 (d, $^1J_{P\text{-}C}$ = 76.1 Hz, C_β), 9.8 (d, $^1J_{P\text{-}C}$ = 57.7 Hz, CH_3).

^{31}P NMR(81.0 MHz, CD_2Cl_2) 27.6.

Anal. Calcd. for $C_{24}H_{20}CoO_4OsP$: C, 44.18; H, 3.09. Found: C, 44.11; H, 2.83.

Synthesis of ^{13}CO Enriched 5a-b, 6a-c and 7. A pentane solution of **1** was degassed by a freeze-pump-thaw cycle using liquid nitrogen. Approximately one atmosphere of ^{13}CO was admitted into the flask and the solution was stirred at 0 °C for 30 minutes. Solutions of **1-^{13}CO** were then subsequently used in reactions to generate the enriched dimetallic compounds.

3.9.3. X-ray Structure Determination of 5a

Red-brown, X-ray quality crystals were grown by cooling a CH_2Cl_2/hexane solution of **5a** to -5 °C. The X-ray data collection and structure refinement was carried out by Dr. B.D. Santarsiero at the Structure Determination Laboratory, Department of Chemistry, University of Alberta. Crystal data and general conditions of data collection and structure refinement are given in Table 3.12. Three intensity and orientation standards were checked after every 120 minutes of exposure time and showed no appreciable decay. The positions of the Rh and Os atoms were derived from a three dimensional Patterson map and the remaining non-hydrogen atoms were located in difference Fourier maps after least squares refinement. Reflection data were corrected for absorption by using the method of Walker and Stuart;[32] the minimum and maximum correction coefficients applied to F_o were 0.8224 and 1.3030. All H atoms were included at their idealized positions (calculated by assuming C-H = 0.95 Å and sp^3 or sp^2 geometry) and constrained to 'ride' with the attached C atom. The H atoms were assigned fixed, isotropic thermal parameters 1.2 times those of the parent C atom.

The final atomic coordinates are given in Table 3.13 and selected bond distances and angles for **5a** are given in Tables 3.4 and 3.5, respectively.

Table 3.12: Summary of Crystallographic Data for **5a**

Crystal Parameters

formula	$C_{19}H_{18}O_4OsPRh$
formula wt.	634.43
crystal size, mm	0.19 x 0.17 x 0.07
crystal system	monoclinic
space group	$P2_1/n$ (a non-standard setting of $P2_1/c$)
a, Å	13.112(4)
b, Å	10.072(3)
c, Å	15.184(2)
β, deg	101.32(3)
V, Å^3	1966(4)
Z	4
D_{calc}, g cm^{-3}	2.143
μ, cm^{-1}	73.92

Data Collection and Structure Refinement

diffractometer	Enraf-Nonius CAD4
radiation (λ [Å])	Mo K_α (0.71073)
monochromator	graphite crystal, incident beam
take-off angle, deg	3.0
temperature, ^oC	23
scan type	θ-2θ
scan rate, deg min^{-1}	1.4 - 6.7
scan width, deg in ω,	0.60 + 0.347tanθ
2θ limit, deg	50.0
reflections measured	4096 ($\pm h$, $\pm k$, $\pm l$)
reflections used	1490 with $I > 3\sigma(I)$
variables	230
R^a	0.048
$R_w{}^b$	0.046
GOF^c	1.414

$^aR = \Sigma||F_o| - |F_c||/\Sigma|F_o|$

$^bR_w = (\Sigma w(|F_o| - |F_c|)^2/\Sigma w F_o{}^2)^{1/2}$

$^c GOF = [\Sigma w(|F_o| - |F_c|)^2/(NO - NV)]^{1/2}$

Table 3.13: Atomic Coordinates and Equivalent Isotropic Displacement Parameters for **5a**

atom	*x*	*y*	*z*	*U*, Å^2
Os	0.00486(5)	0.022245(6)	0.61059(4)	3.06(2)
Rh	-0.02947(9)	0.2730(1)	0.78240(7)	2.73(3)
P	0.0986(3)	0.1548(4)	0.8684(3)	3.2(1)
O1	0.1716(9)	0.004(1)	0.6620(8)	6.1(4)
O2	-0.185(1)	0.050(1)	0.571(1)	7.4(5)
O3	0.040(2)	-0.220(1)	0.4249(9)	9.9(6)
O4	-0.1336(9)	0.475(1)	0.5569(7)	4.8(3)
C1	0.109(1)	0.087(2)	0.646(1)	3.7(5)
C2	-0.110(1)	0.113(2)	0.588(1)	4.1(5)
C3	0.023(2)	0.220(2)	0.498(1)	7.0(6)
C4	-0.061(1)	0.407(1)	0.5932(9)	3.0(3)
C5	0.042(1)	0.441(1)	0.6425(9)	3.5(5)
C6	0.075(1)	0.360(1)	0.723(1)	3.1(4)
C7	0.232(1)	0.195(1)	0.865(1)	4.2(5)
C8	0.103(1)	0.172(2)	0.990(1)	4.7(5)
C11	-0.194(1)	0.347(2)	0.739(1)	6.5(6)
C12	-0.140(1)	0.432(2)	0.804(2)	6.9(7)
C13	-0.117(1)	0.352(2)	0.879(1)	8.6(7)
C14	-0.154(2)	0.228(2)	0.855(1)	8.6(7)
C15	-0.198(2)	0.227(2)	0.774(2)	8.0(8)
C21	0.090(1)	-0.027(1)	0.8567(9)	2.6(4)
C22	0.008(1)	-0.084(1)	0.802(1)	3.4(5)
C23	0.003(1)	-0.218(2)	0.793(1)	5.3(5)
C24	0.081(1)	-0.310(2)	0.842(1)	4.5(5)
C25	0.166(1)	-0.243(2)	0.897(1)	4.5(5)
C26	0.171(1)	-0.106(1)	0.9074(9)	3.2(4)

3.9.4. X-ray Structure Determination of 7

A red, X-ray quality crystal of 7 was grown by cooling a CH_2Cl_2/hexane solution of 7 to -5 °C. The X-ray data collection and structure refinement was carried out by Dr. B.D. Santarsiero at the Structure Determination Laboratory, Department of Chemistry, University of Alberta. Crystal data and general conditions of data collection and structure refinement are given in Table 3.14. Three intensity and orientation standards were checked after every 120 minutes of exposure time and showed no appreciable decay. The positions of the Rh and Os atoms were derived from a three dimensional Patterson map and the remaining non-hydrogen atoms were located in difference Fourier maps after least squares refinement. Reflection data were corrected for absorption by using the method of Walker and Stuart;[32] the minimum and maximum correction coefficients applied to F_o were 0.6901 and 1.4825. All H atoms were included at their idealized positions (calculated by assuming C-H = 0.95 Å and sp^3 or sp^2 geometry) and constrained to 'ride' with the attached C atom. The H atoms were assigned fixed, isotropic thermal parameters 1.2 times those of the parent C atom.

The final atomic coordinates are given in Table 3.15 and selected bond distances and angles for 7 are given in Tables 3.10 and 3.11, respectively.

Table 3.14: Summary of Crystallographic Data for **7**

Crystal Parameters	
formula	$C_{15}H_{16}O_4OsPRh$
formula wt.	584.37
crystal size, mm	0.61 x 0.25 x 0.10
crystal system	orthorhombic
space group	$P2_12_12_1$
a, Å	8.093(2)
b, Å	16.116(3)
c, Å	12.959(2)
V, $Å^3$	1690(1)
Z	4
D_{calc}, g cm^{-3}	2.296
μ, cm^{-1}	85.89

Data Collection and Structure Refinement

diffractometer	Enraf-Nonius CAD4
radiation (λ [Å])	Mo K_α (0.71073)
monochromator	graphite crystal, incident beam
take-off angle, deg	3.0
temperature, °C	23
scan type	θ-2θ
scan rate, deg min^{-1}	1.6 - 6.7
scan width, deg in ω,	0.75 + 0.347tanθ
2θ limit, deg	50.0
reflections measured	4096 ($+h$, $+k$, $\pm l$)
reflections used	3028 with $I > 3\sigma(I)$
variables	190
R^a	0.050
$R_w{}^b$	0.060
GOF^c	1.838

$^aR = \Sigma||F_o| - |F_c||/\Sigma|F_o|$

$^bR_w = (\Sigma w(|F_o| - |F_c|)^2/\Sigma wF_o{}^2)^{1/2}$

$^c\mathrm{GOF} = [\Sigma w(|F_o| - |F_c|)^2/(\mathrm{NO} - \mathrm{NV})]^{1/2}$

Table 3.15: Atomic Coordinates and Equivalent Isotropic Displacement Parameters for 7

atom	x	y	z	U, Å^2
Os	0.10564(7)	-0.08393(3)	0.39836(4)	3.28(1)
Rh	0.1691(1)	0.8013(6)	0.40612(8)	2.69(2)
P	-0.1208(5)	0.0901(2)	0.2173(2)	3.23(7)
O1	-0.147(2)	-0.2028(8)	0.308(1)	7.3(4)
O2	0.440(2)	-0.1700(9)	0.352(1)	8.5(5)
O3	0.069(2)	-0.1442(9)	0.6225(9)	6.5(4)
O4	-0.161(1)	0.0377(7)	0.4801(8)	4.1(3)
C1	-0.051(2)	-0.1564(9)	0.344(1)	4.6(4)
C2	0.314(2)	-0.140(1)	0.368(1)	5.3(5)
C3	0.083(3)	-0.1251(9)	0.539(1)	5.4(5)
C4	-0.039(2)	0.0153(8)	0.442(1)	3.0(3)
C5	0.177(2)	-0.0007(9)	0.279(1)	5.0(5)
C6	0.087(2)	0.0736(8)	0.2488(9)	3.2(3)
C11	-0.121(2)	0.118(1)	0.82(1)	4.8(4)
C12	-0.257(2)	0.004(1)	0.229(1)	4.9(5)
C13	-0.206(2)	0.176(1)	0.286(1)	4.3(4)
C21	0.328(2)	0.109(1)	0.542(1)	4.8(4)
C22	0.427(2)	0.126(1)	0.456(1)	4.5(4)
C23	0.343(2)	0.1896(9)	0.3974(1)	4.8(4)
C24	0.195(2)	0.2122(9)	0.453(1)	5.5(5)
C25	0.193(2)	0.164(1)	0.540(1)	5.8(5)

3.10. References

1. (a) Burn, M.J.; Kiel, G.-Y.; Seils, F.; Takats, J.; Washington, J. *J. Am. Chem. Soc.* **1989**, *111*, 6850. (b) Gagné, M.R.; Takats, J. *Organometallics* **1988**, *7*, 561.

2. Lukehart, C.M. *Fundamental Transition Metal Organometallic Chemistry*; Brooks/Cole: Monterey, CA, 1985; Chapter 3.

3. (a) Rahman, M.M.; Lui, H.Y.; Prock, A.; Giering, W.P. *Organometallics* **1987**, *6*, 650. (b) Tolman, C.A. *Chem Rev.* **1977**, *77*, 313.

4. (a) Dyke, A.F.; Knox, S.A.R.; Naish, P.J.; Taylor, G.E. *J. Chem. Soc. Dalton Trans.* **1982**, 1297. (b) Hogarth, G.; Kayser, F.; Knox, S.A.R.; Morton, D.A.V. *J. Chem. Soc., Chem. Comm.* **1988**, 358. (c) Kiel, G.-Y.; Takats, J. *Organometallics* **1989**, *8*, 839. (d) Fontaine, X.L.R.; Jacobsen, G.B.; Shaw, B.L.; Thornton-Pett, M. *J. Chem. Soc., Dalton Trans.* **1988**, 741. (e) Gracey, B.P.; Knox, S.A.R.; MacPherson, K.A.; Orpen, A.G. *J. Chem. Soc., Dalton Trans.* **1985**, 1935. (f) Hogarth, G.; Knox, S.A.R.; Lloyd, B.R.; MacPherson, K.A.; Morton, D.A.V.; Orpen, A.G.; Stobart, S.R. *J. Chem. Soc., Dalton Trans.* **1988**, 360. (g) Dyke, A.F.; Knox, S.A.R.; Naish, P.J.; Taylor, G.E. *J. Chem. Soc., Chem. Commun.* **1980**, 409. (h) Sandercock, P.M.L. M.Sc. Thesis, University of Alberta, **1990**.

5. (a) Bitterwolf, T. *Inorg. Chim. Acta.* **1986**, *122*, 175. (b) Verkade, J.G.; Quin, L.D. *^{31}P NMR in Stereochemical Analysis* ; VCH: Deerfield Beach, FL., 1987; Chapters 13,14.

6. Herrmann, W.A. *Adv. Organomet. Chem.* **1982**, *20*, 159.

7. Mann, B.E.; Taylor, B.F. *^{13}C NMR Data for Organometallic Compounds*; Academic: New York, 1981.

8. Hsu, L.-Y.; Hsu, W.-L.; Jan, D.-Y.; Marshall, A.G.; Shore, S.G. *Organometallics* **1984**, *3*, 591.

9. (a) Anderson, O.P.; Bender, B.R.; Norton, J.R.; Larson, A.P.; Vergamini, P.J. *Organometallics* **1991**, *10*, 3145. (b) Bender, B.R.; Norton, J.R.; Miller, M.M.; Anderson, O.P.; Rappé, A.K. *Organometallics* **1992**, *11*, 3437.

10. (a) Burke, M. Ph.D. Thesis, University of Alberta, **1987**. (b) Burke, M.R.; Takats, J. *J. Organomet. Chem.* **1986**, *302*, C25.

11. (a) Dickson, R.S.; Gatehouse, B.M.; Nesbit, M.C.; Pain, G.N., *J. Organomet. Chem.* **1981**, *251*, 97. (b) Jenkins, J.A.; Cowie, M. *Organometallics* **1992**, *11*, 2774. (c) Herrmann, W.A.; Krüger, C.; Goddard, R.; Bernal, I. *Angew. Chem. Int. Ed. Engl.* **1977**, *89*, 342. (d) Herrmann, W.A.; Krüger, C.; Goddard, R.; Bernal, I. *J. Organomet. Chem.* **1977**, *140*, 73.

12. Cowie, M.; Southern, T.G. *Inorg. Chem.* **1982**, *21*, 246.

13. Allen, F.H.; Kennard, O.; Watson, D.G.; Brammer, L.; Orpen, A.G.; Taylor, R. *J. Chem. Soc., Perkin Trans. II* **1987**, S1.

14. Jenkins, J.; Cowie, M. *Organometallics* **1992**, *11*, 2767.

15. (a) Alex, R.F.; Pomeroy, R.K. *Organometallics* **1987**, *6*, 2437. (b) Adams, H.; Bailey, N.A.; Bentley, G.W.; Mann, B.E. *J. Chem. Soc., Dalton Trans.* **1989**, 1831. (c) Alex, R,F.; Pomeroy, R.K. *J. Organomet. Chem.* **1985**, *284*, 379. (d) Deeming, A.J.; Donovan-Mtunzi, S.; Kabir, S.E. *J. Organomet. Chem.* **1985**, *281*, C43. (e) Deeming, A.J.; Donovan-Mtunzi, S.; Kabir, S.E.; Manning, P.J. *J. Chem. Soc., Dalton Trans.* **1985**, 1037. (f) Deeming, A.J. *Adv. Organomet. Chem.* **1986**, *26*, 1. (g) Beringhelli, T.; D'Alfonso, G.; Molinari, H.; Mann, B.E.; Pickup, B.T.; Spencer, C.M. *J. Chem. Soc., Chem. Commun.* **1986**, 796. (h) Rosenberg, E.; Thorsen, C.B.; Milone, L.; Aime, S. *Inorg. Chem.* **1985**, *24*, 231. (i) Gavins, P.D.; Mays, M.J. *J. Organomet. Chem.* **1976**, *162*, 389. (j) Bryan, E.G.; Forster, A.; Johnson, B.F.G.; Lewis, L.; Matheson, T.W. *J. Chem. Soc., Dalton Trans.* **1978**, 196. (k) Bryan, E.G.; Johnson, B.F.G.; Lewis, L. *J. Chem. Soc., Dalton Trans.* **1977**, 144.

16. Cherkas, A. A.; Breckenridge, S. M.; Carty, A. J. *Polyhedron* **1992**, *11*, 1075.

17. (a) Alt, H.; Engelhart, H.E.; Steinlein, E. J. *Organomet. Chem.* **1988**, *344*, 227. (b) Alt, H.; Engelhart, H.E.; Steinlein, E. J. *Organomet. Chem.* **1989**, *362*, 117. (c) Churchill, M.R.; DeBoer, B.G.; Shapley, J.R.; Keister, J.B. *J. Am. Chem. Soc.* **1976**, *98*, 2357.

18. Harris, R.K. *Nuclear Magnetic Resonance Spectroscopy*, Wiley: New York, 1986, Chapter 5.

19. Hilts, R.W., Franchuk, R.A.; Cowie, M. *Organometallics* **1991**, *10*, 304.

20. Cherkas, A.A.; Mott, G.N.; Granby, R.; MacLaughlin, S.A.; Yule, J.E.; Taylor, N.J.; Carty, A.J. *Organometallics* **1988**, *7*, 1115.

21. Carty, A.J.; Mott, G.N.; Taylor, N.J.; Ferguson, G.; Khan, M.A.; Roberts, P.J. *J. Organomet. Chem.* **1978**, *149*, 345.

22. (a) Cherkas, A.A.; Hadj-Bagheri, N.; Carty, A.J.; Sappa, E.; Pellinghelli, M.A.; Tiripicchio, A. *Organometallics* **1990**, *9*, 1887. (b) Cherkas, A.A.; Randall, L.H.; Taylor, N.J.; Mott, G.N.; Yule, J.E.; Guinamant, J.L.; Carty, A.J. *Organometallics* **1990**, *9*, 1677. (c) Henrick, K.; McPartlin, M.; Deeming, A.J.; Hasso, S.; Manning, P. *J. Chem. Soc., Dalton. Trans.* **1982**, 899. (d) Wong, Y.S.; Paik, H.N.; Chieh, P.C.; Carty, A.J. *J. Chem. Soc., Chem. Comm.* **1975**, 309. (e) Carty, A.J.; Mott, G.N.; Taylor, N.J.; Yule, J.E. *J. Am. Chem. Soc.* **1978**, *100*, 3051. (f) Boyar, E.R.; Deeming, A.J.; Kabir, S.E. *J. Chem. Soc., Chem. Comm.* **1986**, 577 (g) Deeming, A.J.; Kabir, S.E.; Nuel, D.; Powell, N.I. *Organometallics* **1989**, *8*, 717. (h) Cherkas, A.A.; Carty, A.J.; Sappa, E.; Pellinghelli, M.A.; Tiripicchio, A. *Inorg. Chem.* **1987**, *26*, 3201. (i) MacLaughlin, S.A.; Johnson, J.P.; Taylor, N.J.; Carty, A.J.; Sappa, E. *Organometallics* **1983**, *2*, 352. (j) Carty, A.J.; Taylor, N.J.; Smith, W.F.; Lappert, M.F.; Pye, P.L. *J. Chem. Soc., Chem. Comm.* **1978**, 1017. (k) Carty, A.J.; Mott, G.N.; Taylor, N.J. *J. Organomet. Chem.* **1981**, *212*, C54. (l) Seyferth, D.; Hoke, J.B.; Wheeler, D.R. *J. Organomet. Chem.* **1988**, *341*, 421. (m) Carty, A.J.; Taylor, N.J.; Paik, H.N.; Smith, W.; Yule, J.G. *J. Chem. Soc., Chem. Comm.* **1976**, 41. (n) Carty, A.J.; Mott, G.N.; Taylor, N.J. *J. Organomet. Chem.* **1979**, *182*, C69. (o) Deeming, A.J.; Hasso, S. *J. Organomet. Chem.* **1976**, *112*, C39. (p) Cherkas, A.A.; Doherty, S.; Cleroux, M.; Hogarth, G.; Randall, L.H.; Breckenridge, S.M.; Taylor, N.J.; Carty, A.J.

Organometallics **1992,** *11,* 1701. (q) Breckenridge, S.M.; Taylor, N.J.; Carty, A.J. *Organometallics* **1991,** *10,* 837.

23. Kiel, G.-Y. personal communication.

24. (a) Mann, B.E. in *Comprehensive Organometallic Chemistry;* Wilkinson, G.; Stone, F.G.A.; Abel, E.W., Eds.; Pergamon: New York, 1982; Vol. 3, pg 89. (b) Washington, J.; Takats, J. *Organometallics* **1990,** *9,* 925. (c) Geoffroy, G.L. *Acc. Chem. Res.* **1980,** *13,* 469. (d) Riesen, A.; Einstein, F.W.B.; Ma, A.K.; Pomeroy, R.K.; Shipley, J.A. *Organometallics* **1991,** *10,* 3629.

25. Janowicz, A.H.; Bryndza, H.E.; Bergman, R.G. *J. Am. Chem. Soc.* **1981,** *103,* 1516.

26. Leonhard, K.; Werner, H. *Angew. Chem., Int. Ed. Engl.* **1977,** *16,* 649.

27. Werner, H.; Juthani, B. *J. Organomet. Chem.* **1981,** *209,* 211.

28. Werner, H.; Kolb, O.; Thometzek, P. *J. Organomet. Chem.* **1988,** *347,* 137.

29.. Schlab, P.; Mahr, N.; Wolf, J.; Werner, H. *Angew. Chem. Int. Ed. Engl.* **1994,** *33,* 97.

30. (a) Spencer, A.; Werner, H. *J. Organomet. Chem.* **1979,** *171,* 219. (b) Oliver, A.J.; Graham, W.A.G. *Inorg. Chem.* **1971,** *10,* 1165.

31. (a) Oliver, A.J.; Graham, W.A.G. *Inorg. Chem.* **1970**, *9*, 243. (b) Schuster-Woldan, H.G.; Basolo, F. *J. Am. Chem. Soc.* **1966**, *88*, 1657.

32. Walker, N.; Stuart, D. *Acta. Crystallogr., Sect. A: Found Crystallogr.* **1983**, *A39*, 158.

Chapter 4

Synthesis of $[\mu\text{-}C_2H_2C(O)](\mu\text{-}CO)_2Os(CO)_2(PMe_3)Rh(\eta^5\text{-}C_9H_7)$ (C_9H_7 = Indenyl) and Reaction of $[\mu\text{-}\eta^3\text{:}\eta^1\text{-}C_2H_2C(O)]Os(CO)_4MCp$ (M = Co, Rh) with Phosphines

4.1. Introduction

In the previous Chapter, it was shown than the reaction of $Os(CO)_4(\eta^2\text{-}HCCH)$ with $CpM(CO)(PR_3)$ (M = Co, Rh; PR_3 = PMe_3, PMe_2Ph, $PMePh_2$) gave dimetallacyclopentenones or dimetallic zwitterionic species. Thus, the ancillary ligands bound to Co or Rh have an effect on the observed product. However, as initially reported by Basolo,[1] the nature of the η^5-coordinated ligand can also affect the reactivity of the Group IX organometallic species. Specifically, Basolo found that $(\eta^5\text{-}C_9H_7)Rh(CO)_2$ (C_9H_7 = indenyl) reacts 3.8 x 10^8 times faster with PPh_3 than $CpRh(CO)_2$; both reactions produce the mono-phosphine substituted compound.[2] The reaction was shown to proceed *via* an associative mechanism whereby the η^5-coordinated ring "slips" to η^3-coordination upon coordination of the phosphine.

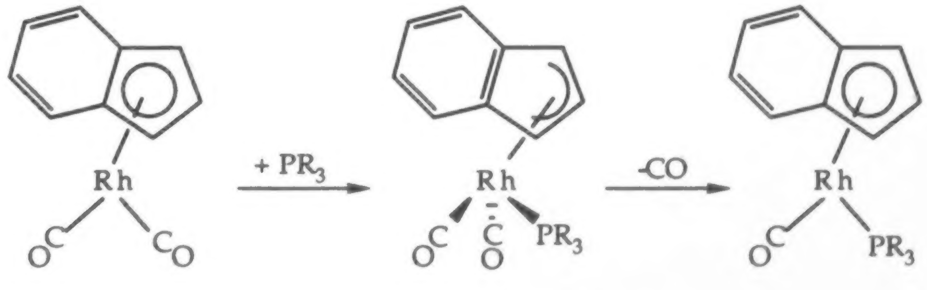

Ejection of CO is accompanied by the return of the indenyl ring to η^5-coordination. In the case of the indenyl complex it is the presence of the benzene ring, and the attendant aromatic stabilization in the η^3-coordinated intermediate, which is believed to be responsible for the rate acceleration towards associative substitution reactions as compared to the Cp analogue.[3] In light of this, the effects of the variability in the coordination mode of the indenyl ring regarding product formation were investigated. Specifically, the reaction of $(\eta^5\text{-}C_9H_7)Rh(CO)(PMe_3)$ with $Os(CO)_4(\eta^2\text{-HCCH})$ was carried out. Another reason for this particular reaction was that it was hoped that, perhaps, this reaction would shed some light on the unusual formation of $[\mu\text{-}\eta^1,\eta^2\text{-HCCH}(PMe_3)](\mu\text{-}CO)Os(CO)_3RhCp$, **7**.

A question that was not answered in forming **7** was the specific way the PMe_3 ligand was transferred from Rh to the bridging acetylenic fragment; in order to probe this the reaction of PR_3 with the dimetallacyclopentenone complexes **2a-b** was also investigated. The ligands chosen for the substitution reactions were the same phosphines used in Chapter 3. The reasons were twofold. First, a direct comparison between the substitution products obtained and complexes **5a-b, 6a-c** and **7** was desirable. Second, as outlined in the previous Chapter, phosphines are extremely versatile ligands. It is relatively simple to vary the electronic and steric properties of the phosphines[4] and they lend themselves to study by ^{31}P NMR spectroscopy .[5] This is especially useful in the reaction of PR_3 with **2b** where $^{103}Rh\text{-}^{31}P$ coupling would be valuable in determining the location of the phosphine ligand.[5,6]

4.2. Reaction of $Os(CO)_4(\eta^2\text{-}HCCH)$ with $(\eta^5\text{-}C_9H_7)Rh(CO)(PMe_3)$

4.2.1. Synthetic Aspects

The reaction of $Os(CO)_4(\eta^2\text{-}HCCH)$, **1**, with $(\eta^5\text{-}C_9H_7)Rh(CO)(PMe_3)$ was carried out in much the same fashion as described in Chapter 3. A pentane solution of $Os(CO)_4(\eta^2\text{-}HCCH)$ and a slight excess of $(\eta^5\text{-}C_9H_7)Rh(CO)(PMe_3)$ were slowly warmed from -78 °C to 0 °C. The reaction occurred at temperatures near 0 °C as evidenced by a darkening of the light orange solution and the appearance of a small amount of a dark orange precipitate. The reaction mixture was warmed to 10 °C to ensure complete reaction. After 2 h at this temperature, there was the presence of a dark orange precipitate and a dark orange solution. No peaks due to **1** were observed in the FT-IR. The solvent was removed *in vacuo* and the residue washed with a small amount of pentane to remove excess $(\eta^5\text{-}C_9H_7)Rh(CO)(PMe_3)$. The resulting residue was crystallized from a CH_2Cl_2/hexane solution at -20 °C to yield dark orange crystals.

4.2.2. Characterization of $OsRh(CO)_5(C_2H_2)(C_9H_7)(PMe_3)$, 9

The mass spectrum and elemental analysis indicated that a dinuclear species of composition $OsRh(CO)_5(C_2H_2)(C_9H_7)(PMe_3)$, **9**, had been formed.

$$\begin{array}{c} Os(CO)_4(\eta^2\text{-}HCCH) \\ + \\ (\eta^5\text{-}C_9H_7)Rh(CO)(PMe_3) \end{array} \xrightarrow{0\,^{\circ}C} \begin{array}{c} OsRh(CO)_5(C_2H_2)(C_9H_7)(PMe_3) \\ \mathbf{9} \end{array}$$

Thus, contrary to the formation of **5a-b** and **7**, the condensation reaction to produce **9** had proceeded without ligand loss. In addition, the immediately observable properties of **9**, such as solubility and color, also indicated that it had a structure different from **7**. A total of four bands were observed in the CO region in the FT-IR spectrum of **9**. However, only two of these (2053 cm^{-1}, 1991 cm^{-1}) were in the range normally associated with terminal carbonyls. The band at 1626 cm^{-1} was assigned to the acyl carbonyl of a non-coordinated dimetallacyclopentenone;[7] the remaining signal at 1805 cm^{-1} was assigned to a bridging carbonyl.

The ^1H NMR spectrum of **9** confirmed the presence of a non-coordinated dimetallacyclopentenone ring.[7a] Two acetylenic proton signals were present at 7.81 ppm (H_β) and 6.53 ppm (H_α) with the assignment of α and β-hydrogen signals based upon an α, β-unsaturated ketone. Also, ^1H-^1H spin-spin coupling of 9.4 Hz was observed, comparable to the value of 9.1 Hz recorded for $[\mu\text{-}C_2H_2C(O)]\text{-}Os(CO)_4IrCp(CO)$, **3**. The ^1H NMR spectrum also showed signals due to the indenyl ring and the PMe_3 ligand.

The correlation of ^{13}C NMR chemical shifts to the hapticity (η^5 or η^3) of a bound indenyl ring was first reported by Köhler in 1974.[8] Since that time, Baker and Marder have further investigated this relationship.[9] For ease of discussion, the labelling scheme shown below will be used when discussing the indenyl ring carbons. Upon ring slippage from η^5 to η^3 bonding, the ring junction carbons (C_4, C_9) will shift to lower field due to the anisotropic effect from the aromatic benzene ring. This was conclusively demonstrated by Merola and co-workers using two Ir-indenyl complexes which were characterized by X-ray crystallography.[10] For $(\eta^5\text{-}C_9H_7)Ir(COE)_2$ (COE = cyclo-octene) the C_4 and C_9 carbons resonate at 121.2 ppm. However, for $(\eta^3\text{-}C_9H_7)Ir(PMe_2Ph)_3$, the ring junction carbons appear at 156.7 ppm; representing a downfield shift of 25.5 ppm upon

$\eta^5 \rightarrow \eta^3$ ring slippage. Thus, ^{13}C NMR spectroscopy is an important diagnostic tool in determining the coordination mode of an indenyl ring.

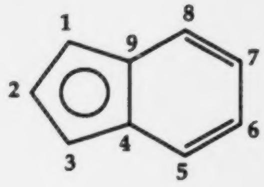

The ^{13}C NMR spectrum of **9** at room temperature showed a total of nine indenyl signals, implying a static indenyl ring in an asymmetric chemical environment. The indenyl carbon signals were assigned based on analogy with results obtained by previous workers, the numbering scheme shown above is retained (Table 4.1). The indenyl signals for **9** could not be assigned to individual carbon atoms within the pairs $C_{1,3}$, $C_{4,9}$, $C_{5,8}$ and $C_{6,7}$. As shown, the indenyl signals observed for **9** are in accord with those reported previously for an η^5-indenyl attached to a Rh centre. Particularly, the ring junction carbons, C_4 and C_9, have chemical shift values which are consistent with coordination to the Rh centre.

Table 4.1: ^{13}C NMR Data for **9** and Related Compounds

η^5 Carbons

	δ (ppm, CD_2Cl_2)				
Compound	$C_{1,3}$		C_2	$C_{4,9}$	
9	85.4[a]	86.4[b]	106.5[c]	117.7	118.1
(η^5-1,2,3-$C_9Me_3H_4$)$Rh(C_2H_4)_2$[g]	86.5	86.5	106.9	110.8	110.8
(η^5-C_9H_7)$Rh(C_2H_4)_2$[h]	78.7[d]	78.7[d]	92.1[e]	112.3[f]	112.3[f]

[a] $^1J_{Rh\text{-}C}$ = 3.8 Hz, [b] $^1J_{Rh\text{-}C}$ = 4.5 Hz, [c] $^1J_{Rh\text{-}C}$ = 3.4 Hz

[d] $^1J_{Rh\text{-}C}$ = 3.6 Hz, [e] $^1J_{Rh\text{-}C}$ = 4.8 Hz, [f] $^1J_{Rh\text{-}C}$ = 2.4 Hz

Benzene Carbons

Compound	δ (ppm, CD_2Cl_2) $C_{5,8}$		$C_{6,7}$	
9	121.3	121.4	125.4	125.5
$(\eta^5\text{-}1,2,3\text{-}C_9Me_3H_4)Rh(C_2H_4)_2$	117.3	117.3	123.0	123.0
$(\eta^5\text{-}C_9H_7)Rh(C_2H_4)_2$	119.5	119.5	123.8	123.8

---

[g] Kakkar, A.K.; Taylor, N.J.; Calabrese, J.C.; Nugent, W.A.; Roe, D.C.; Connaway, E.A.; Marder, T.B. *J. Chem. Soc., Chem. Commun.* **1989**, 990.

[h] Eshtiagh-Hosseini, M.; Nixon, J.F. *J. Less-Common Met.* **1978**, *61*, 107.

The two acetylenic carbons were also observed in the ^{13}C NMR spectrum. The signal at 153.6 ppm showed a ^{31}P-^{13}C coupling of 8.2 Hz, the other signal at 152.2 ppm was a singlet. In the ^{31}P NMR spectrum of **9** a singlet at -45.9 ppm was observed. Both the position and lack of coupling to Rh indicated that the PMe_3 ligand was now bonded to the Os centre and had migrated from the $(\eta^5\text{-}C_9H_7)Rh(CO)$ unit. Having secured the location of PMe_3, the lower field alkyne carbon signal can then be assigned to C_β. The chemical shift difference between the α and β-carbons was very small compared to the simple organic models and compound **3** in Chapter 2. This unusual result will be discussed more thoroughly in Chapter 6. Thus, the spectroscopic evidence indicated that a non-coordinated dimetallacyclopentenone ring was present with the PMe_3 ligand attached to the Os metal. To completely elucidate the structure, the ^{13}CO enriched material was prepared in order to ascertain the geometry around the metal centres.

The ^{13}C NMR spectrum of **9** was obtained at room temperature and a total of five carbonyl signals were seen. Also, a $^{13}C\{^{31}P\}$ decoupling experiment was carried out in order to decipher the ^{31}P-^{13}C coupling from any ^{103}Rh-^{13}C coupling. A doublet of doublets was observed at 213.6 ppm with $^{1}J_{Rh\text{-}C} = 56.0$ Hz and $^{2}J_{P\text{-}C} = 35.6$ Hz. The presence of both ^{103}Rh-^{13}C and ^{31}P-^{13}C coupling along with the relatively lowfield position allowed this signal to be assigned to bridging carbonyl *trans* to the Os-bound PMe_3 ligand.[5,11] The doublet at 222.1 ($^{1}J_{Rh\text{-}C} = 21.0$ Hz) was assigned to a second bridging carbonyl while the Rh bound acyl signal at 229.7 ppm appeared as a doublet with ^{103}Rh-^{13}C coupling of 29.3 Hz.[11] This assignment was based on the broadening of the bridging carbonyl signal, presumably due to unresolved *trans* ^{13}C-^{13}C coupling.[12] The Rh-acyl coupling allowed the regiochemistry of the dimetallacyclopentenone ring to be readily assigned. Finally, no terminal Rh-carbonyl signals were seen but two terminal Os-carbonyl signals were observed at 182.8 and 173.2 ppm. The signal at 182.8 ppm was assigned, based on its relative lowfield position, to a carbonyl *trans* to a bridging carbonyl.[13] The remaining signal was then assigned to a carbonyl *trans* to the organic bridge.[7a,14] Thus, the reaction of $Os(CO)_4(\eta^2\text{-}HCCH)$ with $(\eta^5\text{-}C_9H_7)Rh(CO)(PMe_3)$ gave a product formulated as $[\mu\text{-}\eta^1{:}\eta^1\text{-}C_2H_2C(O)](\mu\text{-}CO)_2Os(CO)_2(PMe_3)Rh(\eta^5\text{-}C_9H_7)$, **9**.

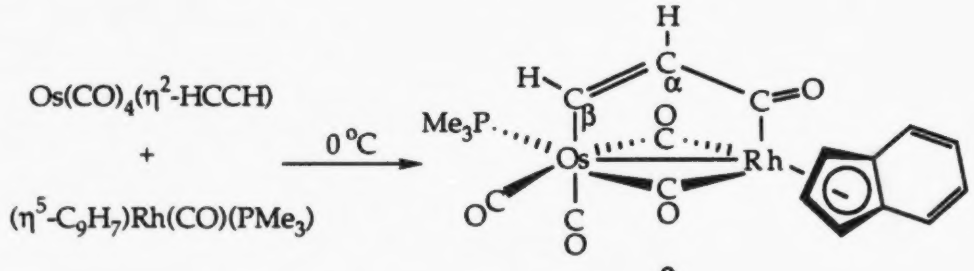
Os(CO)$_4$(η^2-HCCH)
+
(η^5-C$_9$H$_7$)Rh(CO)(PMe$_3$)
0 °C
H
C
α
H
C
β
C=O
Me$_3$P
O
C
Os
Rh
C
O
OC
C
O

9

4.2.3. Molecular Structure of $[\mu\text{-}\eta^1{:}\eta^1\text{-}C_2H_2C(O)](\mu\text{-}CO)_2\text{-}Os(CO)_2(PMe_3)Rh(\eta^5\text{-}C_9H_7)$, 9

As shown, the structure of **9** is significantly different from that of **5a** or **7**. In light of this difference, and to provide metrical parameters for dimetallacyclopentenone Os-Rh compounds, an X-ray crystallographic study was carried out on a single crystal of **9**. An ORTEP view of $[\mu\text{-}\eta^1{:}\eta^1\text{-}C_2H_2C(O)](\mu\text{-}CO)_2Os(CO)_2(PMe_3)Rh(\eta^5\text{-}C_9H_7)$, **9**, is given in Figure 4.1. The relevant bond distances and angles for **9** are listed in Tables 4.2 and 4.3, respectively.

The dimetallacyclopentenone ring is clearly present along with the PMe_3 ligand attached to the Os centre. The Os is formally seven coordinate, but, excluding the metal-metal bond, the geometry can be described as a distorted octahedron. The η^5-coordinated indenyl ligand attached to the Rh is nearly planar and excluding the metal-metal bond, the Rh geometry is best described as a three-legged piano stool.

The Os-Rh bond distance is 2.713(1) Å. This is shorter than the average Os-Rh bond distance of 2.833(9) Å for $[Os(CO)_4]_2RhCp(CO)$.[15] However, the metal-metal separation is similar to the Os-Rh bond distances for the two hydrocarbyl-bridged Os-Rh species, **5a** and **7**. Specifically, a bond distance of 2.780(2) Å was found for $[\mu\text{-}\eta^3{:}\eta^1\text{-}C(O)C_2H_2]Os(CO)_3RhCp(PMe_2Ph)$, **5a**, and a Os-Rh separation of 2.695(1) Å was observed for $[\mu\text{-}\eta^1{:}\eta^2\text{-}HCCH(PMe_3)](\mu\text{-}CO)Os(CO)_3RhCp$, **7**.

The Os-C5 bond distance is 2.136(9) Å which is comparable to the Os-C bond length of 2.15(3) Å for $[\mu\text{-}C_2H_2C(O)]Os(CO)_4IrCp(CO)$, **2c**. The Rh-C7 bond distance is 2.04(1) Å and indicates a Rh-C single bond. The Rh-acyl bond length in **5a** is 1.98(1) Å while in $[\mu\text{-}C_2(CF_3)_2C(O)]Rh_2Cp_2(CO)_2$ it is 2.021(6) Å.[7b]

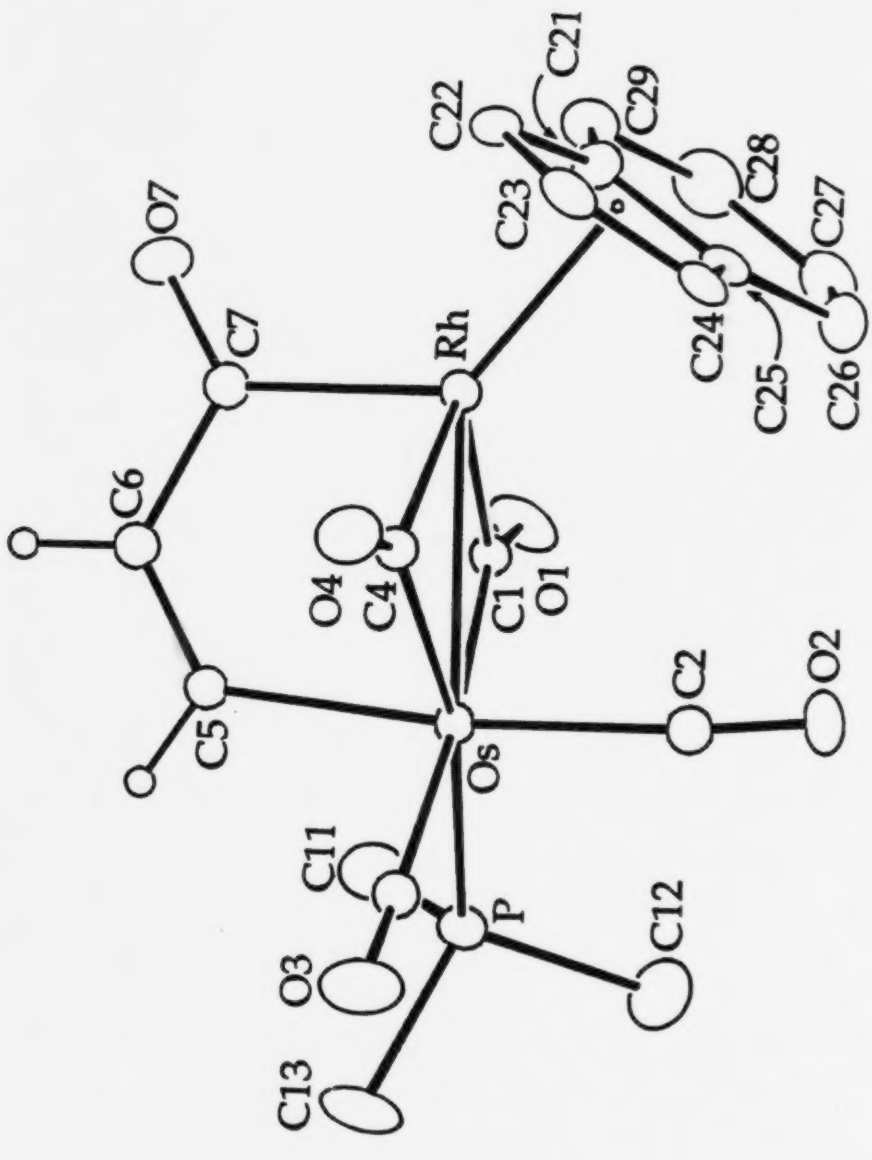
C21
C22
C29
C28
C23
C27
C24
C25
C26
O7
C7
Rh
C6
O4
C4
C1
O1
C2
O2
C5
Os
C11
P
C12
O3
C13

Figure 4.1: ORTEP View of

$[\mu\text{-}\eta^1\text{:}\eta^1\text{-}C_2H_2C(O)](\mu\text{-}CO)_2Os(CO)_2(PMe_3)Rh(\eta^5\text{-}C_9H_7)$, 9

Table 4.2: Selected Bond Lengths (Å) for **9**

Os-Rh	2.713(1)	O1-C1	1.18(1)
Os-C1	2.044(9)	O2-C2	1.10(1)
Os-C2	1.97(1)	O3-C3	1.10(1)
Os-C3	1.97(1)	O4-C4	1.19(1)
Os-C4	2.095(9)	O7-C7	1.19(1)
Os-C5	2.136(9)	C5-C6	1.32(1)
Os-C6	2.24(1)	C6-C7	1.51(1)
Rh-C1	2.057(9)	Os-P1	2.369(3)
Rh-C4	1.971(9)	Rh-C21	2.35(1)
Rh-C7	2.04(1)	Rh-C22	2.197(9)
Rh-C23	2.30(1)	Rh-C24	2.338(9)
Rh-C25	2.46(1)		

Table 4.3: Selected Angles (deg) for **9**

Rh-Os-P1	137.27(7)	Os-Rh-C4	50.1(3)
Rh-Os-C1	48.8(3)	Os-C1-O1	150.4(8)
Rh-Os-C2	90.2(3)	Os-C2-O2	174(1)
Rh-Os-C3	133.2(3)	Os-C3-O3	177.3(9)
Rh-Os-C4	46.2(3)	Os-C4-O4	142.3(7)
Rh-Os-C5	83.6(2)	Os-C1-Rh	82.8(3)
C1-Os-C2	90.3(4)	Os-C4-Rh	83.6(3)
C1-Os-C3	173.6(4)	Rh-C1-O1	126.5(7)
C1-Os-C4	94.6(4)	Rh-C4-O4	134.0(7)
C1-Os-C5	83.0(3)	C4-Rh-C7	89.5(4)
C2-Os-C3	95.7(4)	Os-C5-C6	125.1(7)
C2-Os-C4	96.6(4)	C5-C6-C7	122.9(9)
C3-Os-C4	86.9(4)	Rh-C7-O7	121.4(8)
C3-Os-C5	91.1(4)	Rh-C7-C6	117.9(6)
C4-Os-C5	81.7(3)	O7-C7-C6	120.7(9)
P1-Os-C1	88.7(3)	Os-Rh-C7	90.1(3)
P1-Os-C2	94.7(3)	C1-Rh-C4	98.1(4)
P1-Os-C3	88.6(3)	C1-Rh-C7	83.8(4)
P1-Os-C4	168.2(3)	Os-Rh-C1	48.4(2)
P1-Os-C5	87.5(3)		

The bond distances concerning the organic ring are also of interest. The C5-C6 separation is 1.32(1) Å which is close the the value of 1.340(13) Å expected for a conjugated C-C double bond.[16] In addition, the C=C bond distance in **3** is 1.31(4) Å, although the large esd values make a meaningful comparison difficult. The C6-C7 (1.51(1) Å) and the C7-O7 (1.19(1) Å) distances are also close to values expected for α,β-unsaturated ketones.[16] A more thorough discussion was given in Chapter Two.

The geometry around the Os centre is formally seven-coordinate but, as mentioned, the metal-metal bond may be neglected to give distorted octahedral geometry. The P1-Os-C4 bond angle is 168.2(3)°, a moderate deviation from the idealized value of 180° expected for an octahedral coordination geometry. A similar value of 173.6(4)° is seen for the C1-Os-C3 bond angle. This distortion is also reflected in the C1-Os-C4 bond angle of 94.6(4)°. The P1-Os-C1, P1-Os-C3 and P1-Os-C2 bond angles are 88.7(3)°, 94.7(3)° and 88.6(3)°, respectively. The near orthogonality of these bond angles explains why no ^{31}P-^{13}C coupling is observed for these carbonyls.[5] The Rh-C1 and Os-C1 bond distances are 2.057(9) Å and 2.044(9) Å, respectively. For comparison, the Rh-C4 and Os-C4 bond distances are 1.971(9) Å and 2.095(9) Å. Thus, the two carbonyls do not bridge the Os-Rh metal-metal bond in a symmetric fashion. The shorter Rh-C(bridge) bond length is to the carbonyl *trans* to the phosphine ligand. This difference in bond lengths manifests itself as a difference in the ^{103}Rh-^{13}C coupling constants in the ^{13}C NMR spectrum. For C4, the ^{103}Rh-^{13}C coupling constant is 56.0 Hz, while for C1 it is only 21.0 Hz. Therefore, from these coupling constants, it can be assumed that the asymmetries observed for the bridging carbonyls in the solid state are also present in solution.

Finally, the indenyl ring was confirmed to be η^5-coordinated to the metal centre, corroborating the ^{13}C NMR results. However, all of the metal-bonded carbon atoms are not equidistant to the Rh centre. As noted, an indenyl ring may also adopt a η^3-coordination mode. In addition to $(\eta^3\text{-}C_9H_7)Ir(PMe_2Ph)_3$,[10] other η^3-indenyl complexes characterized by X-ray crystallography are $(\eta^5\text{-}C_9H_7)(\eta^3\text{-}C_9H_7)W(CO)_2$[17a] and $(\eta^3\text{-}C_9H_7)Fe(CO)_3^-$.[17b] Marder and co-workers at the University of Waterloo have extensively investigated the phenomenon of slip-fold distortion in a number of $(\eta^5\text{-}C_9H_7)RhL_2$ complexes.

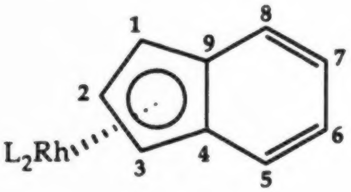

The ring slippage may be quantified using the parameter Δ, defined as the difference, in Å, between the average Rh-C(1,3) bond distances and the average Rh-C(4,9) bond distances.[9b-d,18] An ideal η^5-indenyl complex should have a value for Δ of *ca.* 0 Å, while values of 0.69-0.79 Å are observed for η^3-indenyl complexes.[9d,10,17] In addition, the slip-fold distortion of the indenyl ring may be described by the hinge angle (H.A.), defined in Table 4.4. This parameter describes the distortion of the indenyl ring away from planarity. The ring slippage parameter, Δ, is linked to the hinge angle; as the magnitude of Δ increases so does the hinge angle. Thus, large values of Δ are usually accompanied by large hinge angles. The results obtained for **9** and some representative compounds are given below (Table 4.4).

Table 4.4: Ring Slip Values for **9** and Related $(\eta^5\text{-}C_9H_7)RhL_2$ Compounds

Compound	Δ (Å)[a]	H.A.(deg)[b]
$[\mu\text{-}C_2H_2C(O)](\mu\text{-}CO)_2Os(CO)_2(PMe_3)Rh(\eta^5\text{-}C_9H_7)$, **9**	0.11	1.5
$(\eta^5\text{-}C_9H_7)Rh(CO)_2$[c]	0.20	9.2
$(\eta^5\text{-}C_9H_7)Rh(\eta^2\text{-}C_2H_4)_2$[d]	0.16	8.3
$(\eta^5\text{-}C_9H_7)Rh(PMe_3)_2$[d]	0.20	8.4
$(\eta^3\text{-}C_9H_7)Ir(PMe_2Ph)_3$[e]	0.79	----

[a] $\Delta = d_{ave}(Rh\text{-}C_{1,3}) - d_{ave}(Rh\text{-}C_{4,9})$. [b] H.A. (hinge angle) = angle between normals to the least squares planes defined by C_1, C_2, C_3 and C_1, C_3, C_4, C_9. [c] Kakkar, A.K.; Taylor, N.J.; Calabrese, J.C.; Nugent, W.A.; Roe, C.; Connaway, E.A.; Marder, T.B. *J. Chem. Soc., Chem. Commun.* **1989**, 990. [d] Marder, T.B.; Calabrese, J.C.; Roe, D.C.; Tulip, T.H. *Organometallics*, **1987**, *6*, 2012. [e] Merola, J.S.; Kacmarcil, R.T., Van Engen, D. *J. Am. Chem. Soc.* **1986**, *108*, 329.

The value of Δ = 0.11 Å obtained for **9** indicates there is a distortion from η^5 towards η^3 coordination in the ground state. However, the distortion seen for **9** is not the same as in related $(\eta^5\text{-}C_9H_7)RhL_2$ compounds. For the complexes investigated by Marder, the ring junction carbons (C_4 and C_9) are further away from the Rh centre than the C_1 and C_3 carbons. For **9**, one of the ring junction carbons (C21) is actually closer to the Rh centre than one of the $C_{1,3}$ carbons, namely C24. The value of Δ = 0.11 Å arises mainly from the large Rh-C25 bond distance of 2.46(1) Å. This would seem to indicate, in the case of **9**, the $\eta^5 \rightarrow \eta^3$ distortion is rather small and that the value of Δ alone does not accurately describe the slip-fold distortion. Further corroboration is provided by the almost negligible hinge angle of 1.5° observed for **9**, compared to values of *ca.* 8-9° reported by Marder. Therefore, although there is a slip-fold distortion of the indenyl ring in **9**, not unexpected considering the work Marder, the ring slippage is not the same as usually seen in (η^5-C_9H_7)RhL$_2$ compounds. This makes it difficult to quantify the amount of slip-fold distortion observed for **9**.

4.3. Reaction of [μ-η^3:η^1-$C_2H_2C(O)$]Os(CO)$_4$MCp (M = Co, Rh) with Phosphines

4.3.1. Synthetic Aspects

A filtered pentane solution containing [μ-η^3:η^1-$C_2H_2C(O)$]-Os(CO)$_4$MCp (M = Co, Rh) was cooled to 0 °C. To this was added an excess of PR$_3$ (PR$_3$ = PMe$_3$, PMe$_2$Ph) and the reaction mixture was warmed to room temperature. For both M = Co, Rh there was immediate reaction. In the case of M = Co, a light red precipitate and a red solution were formed while, for M = Rh, there was the formation of an orange precipitate. To ensure complete reaction, both the Co and Rh complexes were subsequently stirred at room temperature for 1 h. To isolate the Rh-phosphine complexes, only a simple filtration *via* cannula was required. For M = Co, the solutions were cooled prior to filtration to precipitate out any product still in solution. The resulting solids were washed with pentane to remove the excess phosphine and any unreacted dimetallic starting material. For M = Rh, the PR$_3$ containing products can be isolated in pure form without the need for recrystallization. In the case of the Co-PR$_3$ complexes, a recrystallization from diethyl ether was required to obtain analytically pure samples. Thus, it is important that the pentane solutions of the dimetallic complexes **2a-b** be filtered before use to prevent any hydrocarbon-insoluble matter from contaminating the final product. The yields of both the Co-PR_3 complexes (**10a**, 77%, **10b**, 69%) and the Rh-PR_3 compounds (**11a**, 80%, **11b**, 67%) were fairly good, indicating that, in each case, the amount of by-product formation is minimal. Finally, **2b** does not react with PPh_3 in CH_2Cl_2/hexane solution at 50 °C.

4.3.2. Characterization of $OsCo(CO)_5(C_2H_2)(PMe_3)Cp$ (PR_3 = PMe_3, 10a; PMe_2Ph, 10b)

The red coloration of the nearly pentane insoluble products immediately discounted the possibility that the reaction had proceeded to yield complexes similar to **6a-b**. The zwitterionic products observed in Chapter 3 were green in color. The elemental analyses and mass spectral data for **10a-b** indicated a molecular formula consistent with a product whereby the phosphine had simply added to the dimetallic starting material with no ligand loss.

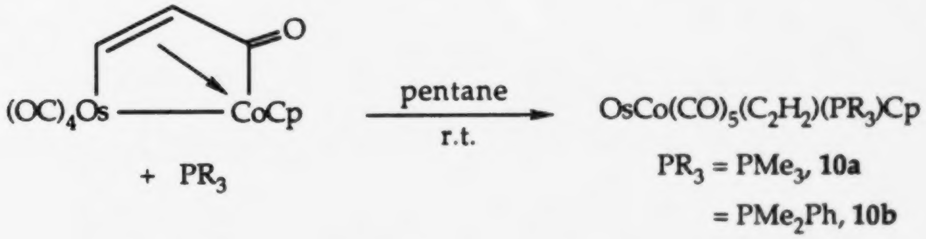

$OsCo(CO)_5(C_2H_2)(PR_3)Cp$
PR_3 = PMe_3, **10a**
= PMe_2Ph, **10b**

Thus, it was possible that the phosphine had simply coordinated to the Co centre and displaced the C=C double bond of the dimetallacyclopentenone ring.

In the IR spectrum of **10a**, a total of four bands were observed in the region between 2200 cm^{-1} and 1600 cm^{-1}. Of these, only two (2044 cm^{-1}, 1984 cm^{-1}) were characteristic of terminal carbonyls. The presence of only two terminal carbonyl bands of relatively low energy rules out simple phosphine coordination to the Co centre as four terminal carbonyl bands would be expected to arise from the $Os(CO)_4$ unit. One of the remaining carbonyl bands (1793 cm^{-1}) is in the range characteristic for bridging carbonyls, the other band at 1614 cm^{-1} is assigned to the acyl moiety of a non-coordinated dimetallacyclopentenone.[7] Similar observations were made for **10b**. Of note, is that the frequencies and intensities of the carbonyl bands observed for **10a-b** are very similar to those recorded for $[\mu\text{-}C_2H_2C(O)](\mu\text{-}CO)_2Os(CO)_2(PMe_3)Rh(\eta^5\text{-}C_9H_7)$, **9**.

The ^1H NMR spectra of **10a-b** indicated the presence of a non-coordinated dimetallacyclopentenone ring (Table 4.5).[7a] For comparison, the ^1H NMR data for **9** are also listed and indicate that it is likely that **10a-b** have the same structure as **9**.

Table 4.5: ^1H NMR Data for **9** and **10a-b**

δ (ppm, CD_2Cl_2)

Compound	H_α	$^4J_{P\text{-}H\alpha}$[a]	H_β	$^3J_{P\text{-}H\beta}$[a]	$^3J_{H\text{-}H}$[a]
9	6.53	1.6	7.81	9.4	9.4
10a	5.98	2.3	7.84	8.3	9.2
10b	6.02	2.0	7.72	8.0	9.1

[a] Couplings in Hertz.

The ^{1}H NMR results are mirrored in the ^{13}C NMR spectra of **9** and **10a-b** (Table 4.6). The assignments of H_α/C_α and H_β/C_β were made by comparison to previous results in Chapter 2.

Table 4.6: ^{13}C NMR Data for **9** and **10a-b**

	δ (ppm, CD_2Cl_2)		
Compound	C_α	C_β	$^2J_{P\text{-}C\beta}$ (Hz)
9	152.2	153.6	8.2
10a	144.3	154.0	6.9
10b	145.3	154.6	7.6

The ^{13}C NMR signals for the β-carbons, for **9** and **10a-b**, are all within 1 ppm, indicating that they are attached to the Os centre. The α-carbon resonances for **10a-b** are *ca.* 8 ppm upfield of those for **9**, due to the difference between the Co and Rh centres. The ^{31}P NMR chemical shifts of the bound phosphines (**10a**, δ = -43.3 ppm; **10b**, δ = -34.7 ppm) were similar to **9** (δ = -45.9 ppm) and implied coordination to the Os centre. Final confirmation that **10a-b** had the same structure as **9** came from the ^{13}C NMR spectra in the carbonyl region; the ^{13}C NMR spectrum of **10b** in the carbonyl region is shown in Figure 4.2.

For **10b**, five carbonyl signals were observed. Two of the signals were in the region expected for a terminal carbonyl bound to an Os centre.[11] The chemical shifts of these two signals were also very close to those recorded for **9** (Table 4.7). The remaining three signals were all at lower field, indicative of bridging carbonyls or an acyl carbonyl attached to Co.[11] The observation a bridging carbonyl, with ^{31}P-^{13}C coupling similar to that seen for **9**, allowed for the placement of the phosphine onto the Os centre.

This also enabled confirmation that **9** and **10a-b** had the same structure. One of the remaining lowfield carbonyl signals was then assigned to a bridging carbonyl, the other to an acyl carbonyl bound to the Co centre (Table 4.7).

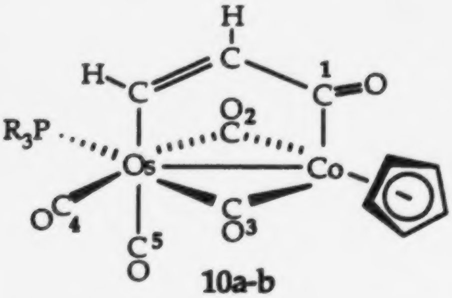

10a-b

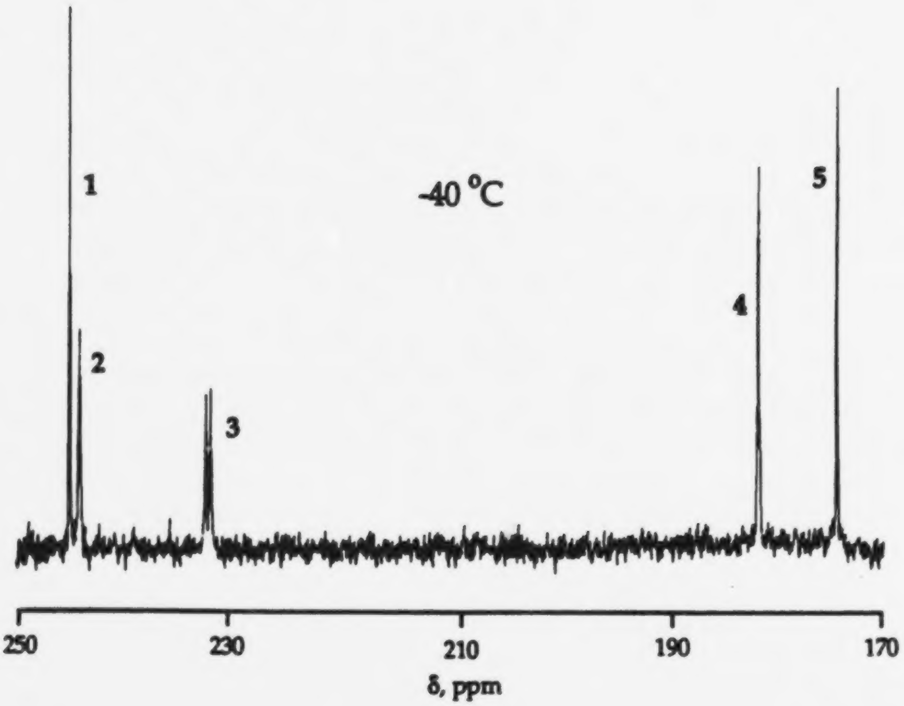

Figure 4.2: ^{13}C NMR of **10b** in the Carbonyl Region

Table 4.7: ^{13}C NMR Data (Carbonyl Region) for **9** and **10a-b**

Compound	δ (ppm, CD_2Cl_2) C_1	C_2	C_3	C_4	C_5	$^2J_{P\text{-}C3}$[a]
9	229.7[b]	222.1[c]	213.6[d]	182.8	173.2	35.6
10a	245.4	245.3	233.5	181.5	174.0[e]	42.7
10b	245.1	244.2	232.2	181.5[f]	174.4[g]	39.5

[a]Couplings in Hertz, [b]$^1J_{Rh\text{-}C}$ = 29.3 Hz, [c]$^1J_{Rh\text{-}C}$ = 21.0 Hz, [d]$^1J_{Rh\text{-}C}$ = 56.0 Hz, [e]$^2J_{P\text{-}C5}$ = 5.6 Hz, [f]$^2J_{P\text{-}C4}$ = 2.3 Hz, [g]$^2J_{P\text{-}C5}$ = 4.9 Hz.

For **10a-b**, the C1 and C2 signals have very similar chemical shifts. These signals were assigned based on their relative linewidths and intensities. For **10b**, the C3 signal can be immediately assigned as a bridging carbonyl due to the $^{31}P\text{-}^{13}C$ coupling of 39.5 Hz. This bridging carbonyl signal is quite broad (C3: $\Delta\nu_{1/2}$ = 14 Hz) and of low intensity. The C2 signal is also broad (C2: $\Delta\nu_{1/2}$ = 20 Hz) and of low intensity, thus it is assigned to the other bridging carbonyl. The C1 signal is sharper (C1: $\Delta\nu_{1/2}$ = 9 Hz) and of greater intensity, therefore it is assigned to the acyl carbonyl. The broadness of the C2 and C3 signals may be due to the quadropolar Co centre or the presence of *trans* C2-C4 coupling, regardless, the large differences in intensities and linewidths make the assignments fairly certain. In order to observe the fine structure of the carbonyl peaks for **10a-b**, it was necessary to cool the samples to *ca*. -40 °C. The compounds are not fluxional, as the temperature is lowered the signals for the Co bound carbonyls sharpen as a result of decoupling from the quadropolar metal centre.[19]

The reaction of $[\mu\text{-}\eta^3\text{:}\eta^1\text{-}C_2H_2C(O)]Os(CO)_4CoCp$ with phosphines does result in the formation of substituted dimetallic compounds. However, contrary to expectation, the product is not a Co-bound phosphine complex formed *via* the simple displacement of the dimetallacyclopentenone ring C=C double bond. A more complex reaction occurs whereby the phosphine is bonded to the Os centre, resulting in the formation of a dimetallacyclopentenone with two bridging carbonyls.

4.3.3. Characterization of $OsRh(CO)_5(C_2H_2)(PMe_3)Cp$ ($PR_3 = PMe_3$, 11a; PMe_2Ph, 11b)

The reaction of electron-rich phosphines ($PR_3 = PMe_3$, PMe_2Ph) with $[\mu\text{-}\eta^3\text{:}\eta^1\text{-}C_2H_2C(O)]Os(CO)_4RhCp$ resulted in the formation of insoluble orange complexes. For the case of PMe_3, the orange color of the product immediately ruled out the possibility that $[\mu\text{-}\eta^1\text{:}\eta^2\text{-}HCCH(PMe_3)](\mu\text{-}CO)Os(CO)_3RhCp$, **7**, had been formed. The elemental analyses for **11a-b** indicated that the reactions had proceeded to yield products whereby the phosphines had simply added to the dimetallic compounds, analogous to the formation of **10a-b**.

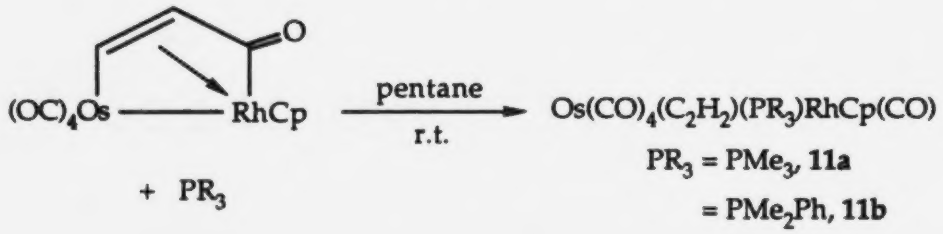

This also eliminated the possibility that species similar to $[\mu\text{-}\eta^3\text{:}\eta^1\text{-}C(O)C_2H_2]Os(CO)_3RhCp(PR_3)$ ($PR_3 = PMe_2Ph$, $PMePh_2$), **5a-b,** had been formed.

The FT-IR data for **11a-b** immediately ruled out any structural similarity between **11a-b** and **10a-b**. For **11a**, three terminal carbonyl signals were observed plus a band at 1752 cm^{-1}. This low energy band could be assigned either to a bridging carbonyl or to an acyl group of a η^3:η^1-coordinated dimetallacyclopentenone ring.[20] In the ^{31}P NMR spectrum of **11a**, a singlet at 7.8 ppm was observed. The lack of ^{103}Rh-^{31}P coupling indicated that the PMe$_3$ ligand was not bound to the Rh centre. Also, the lowfield position of this signal, as compared to **10a**, indicated that the PMe$_3$ ligand was not attached to the Os centre either. For comparison, the ^{31}P NMR signal for $[\mu-\eta^2:\eta^1\text{-HCCH(PMe}_3)](\mu\text{-CO})\text{Os(CO)}_3\text{RhCp}$, **7**, appears at 23.8 ppm.

The ^{1}H NMR spectra of **11a-b** provided some important structural clues. First, both the acetylenic protons resonated in the lowfield region of the ^{1}H NMR spectrum (*ca*. 6-10 ppm). Also, large ^{31}P-^{1}H spin-spin coupling was observed, reminiscent to that seen for **6a-c** and **7**. Large ^{31}P-^{1}H coupling has also been observed by Alt and co-workers in CpMn(CO)$_2$(HCCHPEt$_3$), **12**.[21a]

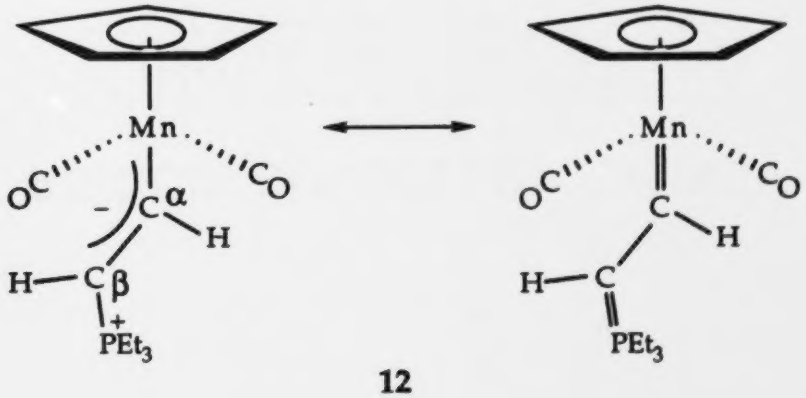

12

The ^{1}H NMR results for **11a-b** are collected in Table 4.8, and those for [μ–η^1:η^2-HCCH(PMe$_3$)](μ-CO)Os(CO)$_3$RhCp, **7**, and CpMn(CO)$_2$(HCCHPEt$_3$), **12**. The designation of the α and β protons follows Alt's labelling scheme and the assignment of the acetylenic protons is based on comparison to **12**. For all listed compounds, there is a fairly large chemical shift difference between the α and β protons. In compounds **11a**, **11b** and **12**, both acetylenic protons are in the lowfield region (*ca.* >6 ppm) while, for **7**, the β-proton signal is at 4.00 ppm. Thus, there appears to be fairly significant differences between the structures of **11a-b** and **7**.

Table 4.8: ^{1}H NMR Data for **11a-b** and Related Compounds

δ (ppm, CD_2Cl_2)^a

Compound	H_α	$^3J_{P\text{-}H\alpha}$	H_β	$^2J_{P\text{-}H\beta}$	$^3J_{H\text{-}H}$
11a	9.27	35.4	6.26	40.8	19.3
11b	9.41	34.9	6.41	39.3	19.2
12^e	11.15	28.9	5.70	38.1	18.7
7	8.27^b	31.0^d	4.00^c	20.2^d	9.3

^{a}Couplings in Hertz. ^{b}Additional coupling of $^2J_{Rh\text{-}H\alpha}$ = 0.6 Hz. ^{c}Additional coupling of $^2J_{Rh\text{-}H\beta}$ = 2.9 Hz. ^{d}For **3c**: $^2J_{P\text{-}H\alpha}$ = 31.0 Hz and $^3J_{P\text{-}H\beta}$ = 20.2 Hz. ^{e}Alt, H.; Engelhart, H.E.; Steinlein, E. *J. Organomet. Chem.* **1988**, *344*, 227.

For **11a** and **11b**, both protons show very large ^{31}P-^{1}H coupling; similar to that observed by Alt.[21a] This is consistent with having the PR$_3$ group directly attached one of the acetylenic carbons.[21] In addition, compared to **6a-c** and **7**, the ^{1}H-^{1}H coupling is very large. The large ^{1}H-^{1}H coupling indicates that the vicinal acetylenic protons are in a *trans* configuration. Values of *trans*-$^3J_{H\text{-}H}$ of 14-20 Hz are expected for *trans* proton pairs in ethylene derivatives, the *trans*-$^3J_{H\text{-}H}$ in ethylene is 19.1 Hz.[22] The value of 18.7 Hz reported by Alt and co-workers[21a] for **12** is very close to the values observed for **11a-b**. The ^1H-^1H coupling for **6a-c** and **7** is significantly smaller than that observed for **11a-b**. Finally, for **11b**, the PMe_2Ph analogue, only a doublet was seen in the ^1H NMR spectrum for the two diastereotopic methyl groups, implying that the molecule must possess a mirror plane or undergo a rearrangement such that a mirror plane is generated.

The ^{13}C NMR data of **11a-b** were invaluable in deducing the structure. Mirroring the ^1H NMR spectrum, only a single CH_3 resonance was seen for the PMe_2Ph ligand of **11b**. The acetylenic carbon signals for **11a-b** and **12** are listed in Table 4.9.

Table 4.9: ^{13}C NMR Data for **11a-b** and Related Compounds

	δ (ppm, CD_2Cl_2)[a]			
Compound	C_α	$^2J_{P\text{-}C\alpha}$	C_β	$^1J_{P\text{-}C\beta}$
11a	172.4	12.3	114.3	69.7
11b	175.9	12.2	112.3	70.2
12[b]	241.4	12.7	97.0	69.8

[a]Couplings in Hertz. [b]Alt, H.; Engelhart, H.E.; Steinlein, E. *J. Organomet. Chem.* **1988**, *344*, 227.

An important note is that no ^{103}Rh-^{13}C coupling was observed, the ^{31}P-^{13}C coupling was verified *via* a $^{13}C\{^{31}P\}$ NMR experiment on **11a**. Also, the chemical shift values observed for the α and β carbons of **11a-b** were not similar to any of those reported by Carty in his review of a variety of zwitterionic hydrocarbyl bridged species.[23] Therefore, this ruled out the possibility that a bimetallic species with a hydrocarbyl bridge had been formed.

All three species in Table 4.9 show large one bond phosphorus-carbon coupling of *ca*. 70 Hz and smaller two-bond coupling of *ca*. 12 Hz.[5,21a-b] In addition, all three species have a lowfield C_α signal, which, for **11a-b**, can be assigned to an Os-bound carbene.[11,24] The carbene carbon, C_α, resonates at a lower frequency in **11a-b** than in **12**. This would mainly be due to a metal effect as Mn is a second row metal and would cause a downfield shift for the carbene relative to a third row metal.[11,24b] Finally, the β-carbon signals for **11a-b** and **12** are similar. Thus, based on the spectroscopic similarities to **12**, a structure with an Os carbene is proposed for **11a-b**. The organic fragment is planar, thus the possibility of two equivalent methyl groups in PMe_2Ph is present; consistent with the NMR results.

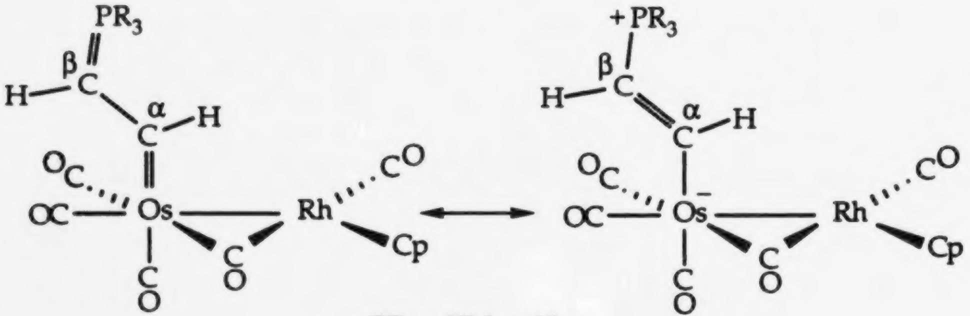

$PR_3 = PMe_3$, **11a**
$= PMe_2Ph$, **11b**

Unfortunately, the ^{13}C NMR spectra of the ^{13}CO enriched materials were not very enlightening. For **11b** at room temperature, only a broad signal centered at 203.8 ppm corresponding to four carbonyls was observed along with a peak at 180.3 ppm (1 CO). As the temperature was lowered to -60 °C, the broad signal became even broader while the signal at 180.3 ppm sharpened. A limiting ^{13}C NMR spectrum in the carbonyl region could not be obtained. However, the fluxionality of the carbonyls is in accord with the observation of only one methyl ^{1}H and ^{13}C signal for **11b**. Although the structure proposed for **11a-b** has a planar organic fragment, the molecule as a whole does not possess mirror symmetry. A rapid fluxional process interconverting the carbonyls which results in mirror symmetry, is required to render the methyl groups in the PMe$_2$Ph ligand equivalent. A possible fluxional process is shown below.

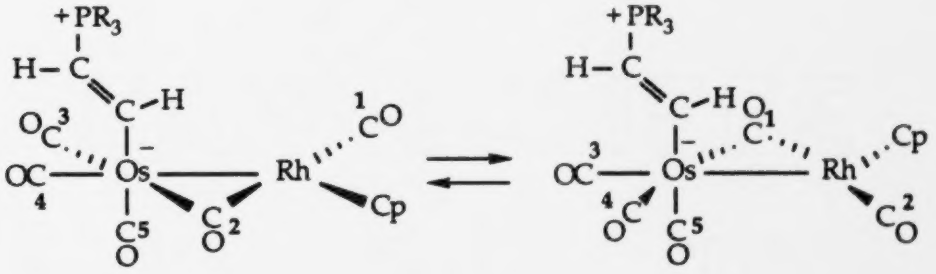

The process shown is very similar to the truncated merry-go-round process described in Chapter 2.[25,26] That is, CO$_1$ and CO$_2$ are exchanged in a pairwise fashion, as are CO$_3$ and CO$_4$; CO$_5$ is not involved in the fluxional process. However, the broad signal observed corresponds to four carbonyls, thus an additional process which involves rotation about the metal-metal bond must be taking place.[27]

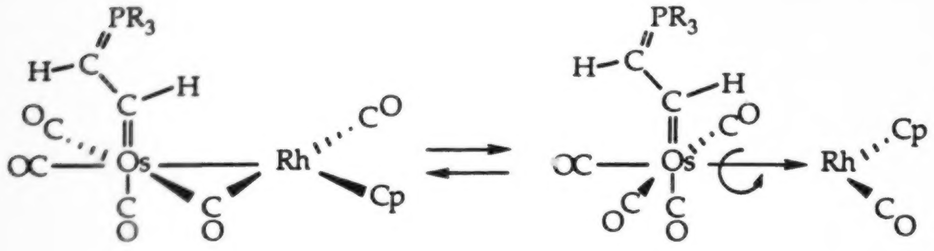

This would allow for the interconversion of four carbonyl ligands. It should also be noted that, assuming rapid rotation, the bimetallic structure with the Os→Rh donor-acceptor bond has C_s symmetry, thus the two methyl groups of the PMe_2Ph ligand in **11b** will be equivalent.

4.4. Formation of Products

As seen previously, the reactions investigated in this Chapter also gave rise to diverse products, subtly dependent on the metal and ancillary ligands. Thus, the proposed pathways for their formation will be more rationalization of the products than mechanisms that have predictive value for future reactions. Nevertheless, some common structural types have emerged which indicate that perhaps a general mechanism, with predictable variations, may be postulated to account for the condensation reactions and the reaction of dimetallacyclopentenones with PR_3 ligands. It was shown that the structure of complex **9**, $[\mu\text{-}C_2H_2C(O)](\mu\text{-}CO)_2Os(CO)_2(PMe_3)Rh(\eta^5\text{-}C_9H_7)$, was the same as **10a-b**, $[\mu\text{-}C_2H_2C(O)](\mu\text{-}CO)_2Os(CO)_2(PR_3)CoCp$ ($PR_3 = PMe_3$, **10a**; PMe_2Ph, **10b**), and that these structures are related to $[\mu\text{-}C_2H_2C(O)]Os(CO)_3(PMe_3)RhCp(CO$, **8**. In fact, **8** and **9, 10a-b** only differ by the presence of two terminal carbonyl ligands as opposed to two bridging carbonyl ligands. However, the conversion of **8** to the zwitterionic **7** is not mirrored by **9**.

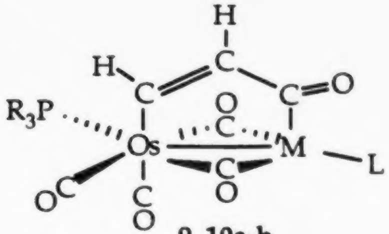

9, 10a-b

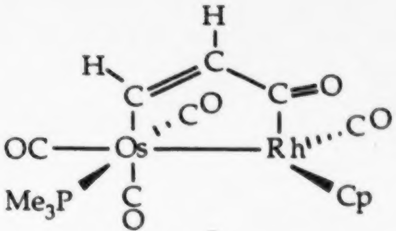

8

The reaction of **2a-b** with PR_3 was carried out with the hope of shedding some light onto the formation of zwitterionic **7**. However, for **2a**, simple addition onto the metallic frame was observed. An attractive initiating step would be attack by the phosphine at the Co centre, displacing the C=C double bond. However, as shown in Scheme 4.1, the metal assisted transfer of PR_3 would generate an intermediate which is the Co analogue of **8**. As seen in Chapter 3, the carbonyl ligands of **8** around the Os centre are static at room temperature, thus the last step to form **10a-b** would be unlikely. Therefore, a mechanism which incorporates initial attack at the Co centre appears disfavoured.

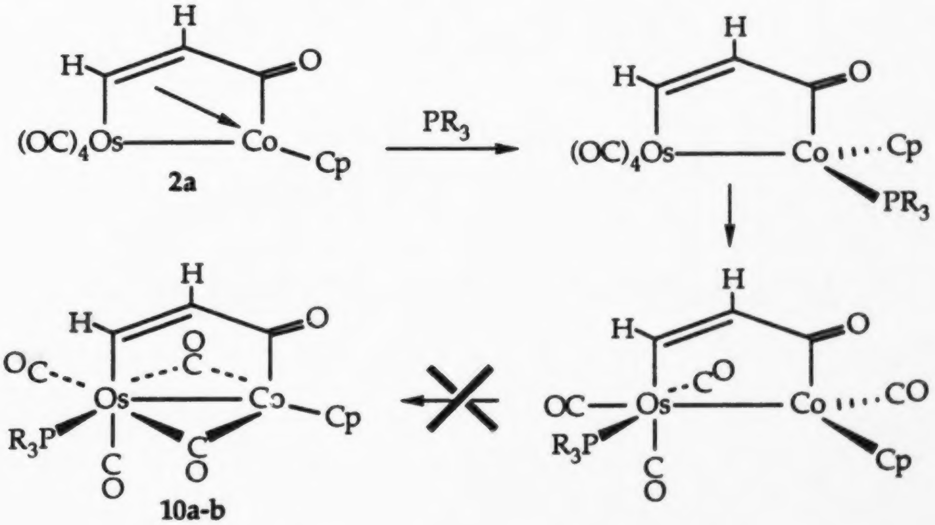

Scheme 4.1: Proposed Pathway for Formation of **10a-b**

An alternate mechanism to account for the formation of **10a-b** is nucleophilic attack at the Os centre which causes the formation of the doubly CO-bridged species; this is shown in Scheme 4.2.

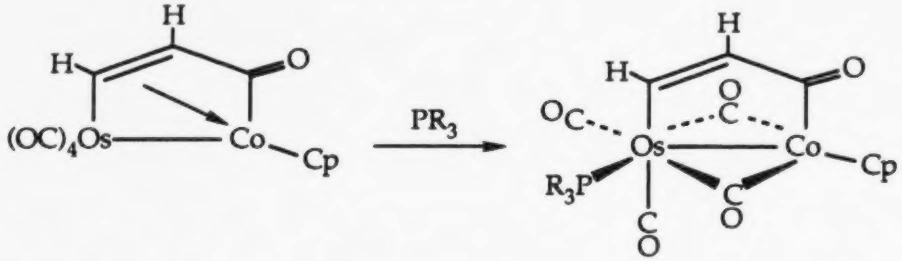

Scheme 4.2: Alternate Mechanism for the Formation of **10a-b**

This mechanism would account for the geometry at the Os centre, however, the intimate steps in this mechanism are not clear at this time.

Interestingly, reaction of PR$_3$ with the Rh complex, **2b**, did not involve addition to the metal but instead, nucleophilic attack on the organic ring. It appears that the stronger Rh-C(ring) bonding activates the ring towards nucleophilic attack.

If **2b** is assumed to more strongly resemble a coordinated dimetallacyclopentenone (**C-1**, Chapter 2) then nucleophilic attack at the β-carbon would be expected.^{28}

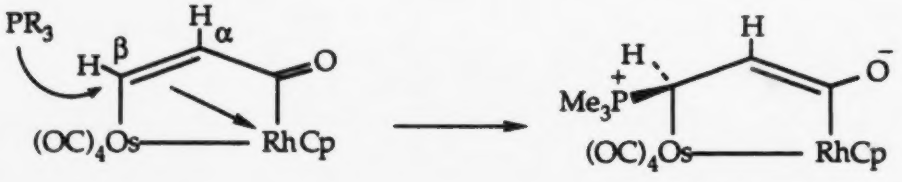

Initial phosphine attack at the β-carbon would result in the formation of a sixteen electron Rh centre. However, in order to account for the formation of **11a-b**, a significant rearrangement of the hydrocarbyl bridge would have to be proposed. A mechanism whereby there is initial attack at the α-carbon is also possible (Scheme 4.3).

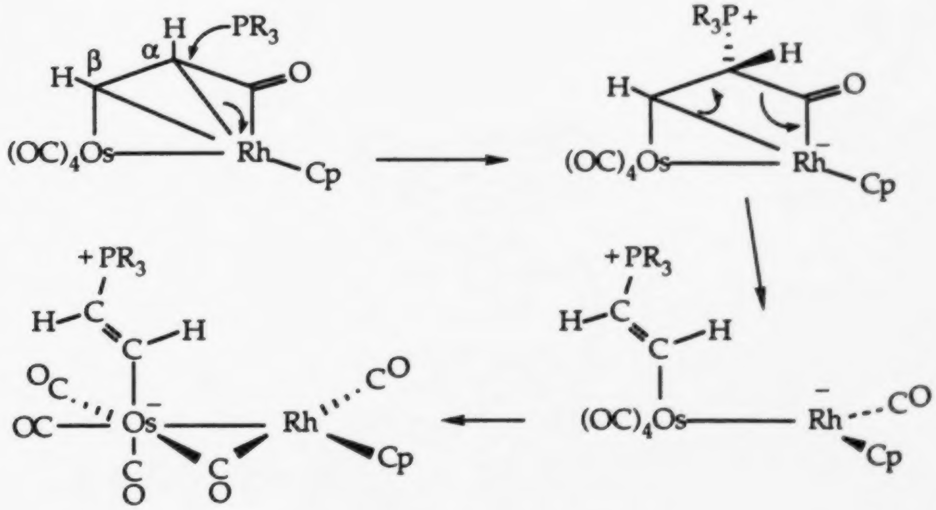

Scheme 4.3: Plausible Pathway for Formation of **11a-b**

Attack at the α-carbon would result in the formation of **11a-b** with minimal skeletal rearrangement, although the viability of the initial intermediate may be called into question. If **2b** is considered as a bimetallic system with a strained, fused cyclopropanone ring then the attack of PR_3 at the α-carbon would relieve the considerable ring strain. There is precedent in the literature for ring cleavage of cyclopropanones, however, the reaction with nucleophiles usually occurs at the carbonyl carbon.[29] Thus, the attack at the α-carbon more closely resembles nucleophilic attack on a cyclopropane resulting in a ring opening reaction.[30] For substituted cyclopropanes, nucleophilic ring cleavage reactions occur when two electron withdrawing substituents are present on the cyclopropane ring.[30b] Cyclopropane rings with only a single electron withdrawing group require a strong nucleophile or a very strained system in order to be cleaved *via* nucleophilic attack.[30e-g] Also, the activation of a fused cyclopropane ring towards ring cleavage by a carbonyl functionality has been observed. Tardella and co-workers have noted that ring cleavage of bicyclo[4.1.0]heptan-2-one is effected by pyridine hydrochloride while bicyclo[4.1.0]heptane was unreactive under the same conditions.[30c] Compound **2b** can be considered to consist of two fused metallacyclopropane rings attached to a metallacyclopropanone ring. Thus, substantial ring strain should be present along with additional activation from the carbonyl group.

The possibility of an initial CO deinsertion reaction to produce a dimetallacyclobutene intermediate followed by nucleophilic attack cannot, at this time, be ruled out. Nucleophilic attack at the acyl carbon is also possible, however, this process would be reversible and just regenerate **2b** and the phosphine. In fact, a satisfactory unified mechanism to account for the formation of **10a-b** and **11a-b** cannot be postulated at this time.

It is a legitimate question to ask why, contrary to the above, the rearrangement of the putative intermediate **8** to the zwitterionic compound **7** is accompanied by CO loss. At this stage, no rational explanation can be given.

Finally, we wish to comment on the formation of compound **9**. Since the geometry about Os is different from that in **8** the mechanism of its formation must also be different. Thus, the presence of an indenyl ring and its ready $\eta^5 \rightarrow \eta^3$ conversion apparently plays a substantive role. The mechanism in Scheme 4.4 is a plausible pathway for the formation of **9**. The presence of the η^3-coordination mode of the indenyl ring could result in PMe_3 transfer occurring to the electron deficient Os centre before CO association. The PMe_3 transfer to the Os metal would be accompanied by a return to η^5-coordination of the indenyl ligand. Coordination of free CO would then result in the formation of **9**. It is possible that the indenyl also exerts a steric effect, causing the PMe_3 transfer such that the phosphine is *trans* to the indenyl ring.

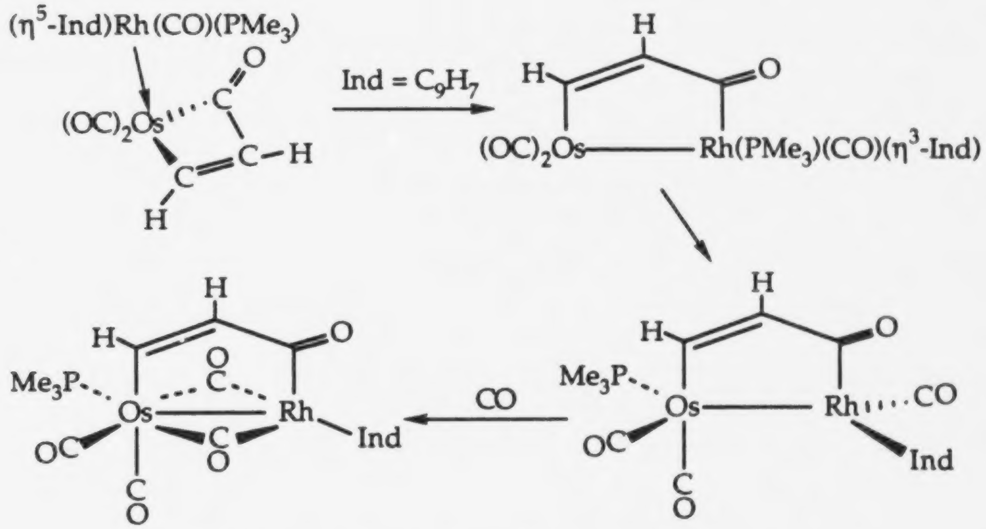

Scheme 4.4: Formation of **9**; Plausible Pathway

4.5. Conclusions

The reaction of $Os(CO)_4(\eta^2\text{-}HCCH)$, **1**, with $(\eta^5\text{-}C_9H_7)Rh(CO)(PMe_3)$ resulted in a product, $[\mu\text{-}\eta^1\text{:}\eta^1\text{-}C_2H_2C(O)](\mu\text{-}CO)_2Os(CO)_2(PMe_3)Rh(\eta^5\text{-}C_9H_7)$, **9**, which was similar to the previously described **8**. The major difference was the geometry about the Os centre; this was attributed to the difference between cyclopentadienyl and indenyl rings. The reactivity of

[μ-η^3:η^1-$C_2H_2C(O)$]Os(CO)$_4$MCp (M = Co, **2a**; Rh, **2b**) with phosphines (PR_3 = PMe_2Ph, $PMePh_2$) was also investigated. For M = Co, compounds similar to **9** were observed. Thus, initial phosphine attack at the Os centre was proposed. Surprisingly, the reaction of PR_3 with [μ-η^3:η^1-$C_2H_2C(O)$]Os(CO)$_4$RhCp did not yield the Rh analogues of **10a-b**. Instead, nucleophilic attack occurred at the α-carbon of the dimetallacyclopentenone ring to result in the formation of Os-carbene complexes, **11a-b**. Therefore, the reaction of [μ-η^3:η^1-$C_2H_2C(O)$]Os(CO)$_4$MCp (M = Co, **2a**; Rh, **2b**) with phosphines also displays marked metal dependence.

4.6. Experimental Section

4.6.1. Starting Materials and Reagents

(η^5-C_9H_7)Rh(CO)$_2$ was prepared from (η^5-C_9H_7)Rh(C_2H_4)$_2$ using the method of Eshtiagh-Hosseini and Nixon.[31] (η^5-C_9H_7)Rh(CO)(PMe$_3$) was prepared using the procedure of Bitterwolf.[6] The dimetallic compounds [μ-η^3:η^1-C_2H_2C(O)]Os(CO)$_4$MCp (M = Co, **2a**; Rh, **2b**) were synthesized as outlined in Chapter 2.

4.6.2. Synthetic Procedures

Synthesis of [μ-C_2H_2C(O)](μ-CO)$_2$Os(CO)$_2$(PMe$_3$)Rh(η^5-C_9H_7), 9

A pentane solution containing 24.5 mg (0.075 mmol) of **1** and 27.4 mg (0.085 mmol) of (η^5-C_9H_7)Rh(CO)(PMe$_3$) was slowly warmed from -78 °C to 10 °C using a dry ice/acetone bath. An orange precipitate began to form at 0 °C along with darkening of the original light orange solution. Continued stirring at 10 °C for 2 hours resulted in complete reaction as the amount of precipitate increased and the supernatant darkened further. No presence of **1** was detected by FT-IR. The solvent was removed *in vacuo* and the residue was washed with pentane (5 mL). The resulting solid was redissolved in CH_2Cl_2 (0.5 mL) and 5 mL of hexane was added. The solution was then kept at -20 °C overnight. The resulting orange crystals were isolated by inverse filtration and washed (2x5 mL) with pentane. The yield of **9** was 25.1 mg (52%).

Formula Weight: 650.43

Mass Spectrum(200 °C, 70 eV): M^+ (652, 0.2%), M^+-nCO (n = 0-4)

IR(pentane, cm^{-1}); ν(CO): 2053(m), 1991(s), 1805(m). ν(acyl): 1626(w).

^{1}H NMR(360 MHz, CD_2Cl_2, -20 °C) 7.81 (1H, dd, $^3J_{P\text{-}H}$ = 9.4 Hz, $^3J_{H\text{-}H}$ = 9.4 Hz, H_β), 7.35 (2H, m, $H_{6,7}$), 7.08 (2H, m, $H_{5,8}$), 6.53 (1H, dd, $^3J_{P\text{-}H}$ = 1.6 Hz, $^3J_{H\text{-}H}$ = 9.4 Hz, H_α), 6.22 (1H, m, H_2), 5.86 (2H, m, $H_{1,3}$), 1.80 (9H, d, $^2J_{P\text{-}H}$ = 10.3 Hz, CH_3).

^{13}C NMR(90.5 MHz, CD_2Cl_2, 23 °C) 153.6 (d, $^2J_{P\text{-}C}$ = 8.2 Hz, C_β), 152.2 (s, C_α), 125.5 (s, $C_{6,7}$), 125.4 (s, $C_{6,7}$), 121.4 (s, $C_{5,8}$), 121.3 (s, $C_{5,8}$), 118.1 (s, $C_{4,9}$), 117.7 (s, $C_{4,9}$), 106.5 (d, $^2J_{Rh\text{-}C}$ = 3.4 Hz, C_2), 86.4 (d, $^2J_{Rh\text{-}C}$ = 4.5 Hz, $C_{1,3}$), 85.4 (d, $^2J_{Rh\text{-}C}$ = 3.8 Hz, $C_{1,3}$), 18.2 (d, $^1J_{P\text{-}C}$ = 37.9 Hz, CH_3).

^{13}C NMR(90.5 MHz, CD_2Cl_2, 23 °C) 229.7 (d, $^1J_{Rh\text{-}C}$ = 29.3 Hz, acyl CO), 222.1 (d, $^1J_{Rh\text{-}C}$ = 21.0 Hz, bridge CO), 213.6 (dd, $^1J_{Rh\text{-}C}$ = 56.0 Hz, $^2J_{P\text{-}C}$ = 35.6 Hz, bridge CO), 182.8 (CO), 173.2 (CO).

^{31}P NMR(81.0 MHz, CD_2Cl_2, 23 °C) -45.9.

Anal. Calcd. for $C_{19}H_{18}O_5OsPRh$: C, 35.08; H, 2.79 Found: C, 35.01; H, 2.80.

Synthesis of [μ-$C_2H_2C(O)$](μ-CO)$_2$Os(CO)$_2$(PMe$_3$)CoCp, 10a

A small Schlenk flask charged with 18.5 mg (0.039 mmol) of [$\mu-\eta^3{:}\eta^1$-$C_2H_2C(O)$]Os(CO)$_4$CoCp, **2a** and 15 mL of pentane was added to dissolve the solid. The solution was filtered *via* cannula to a Ar-filled round bottomed flask and cooled to 0 °C. Excess PMe_3 (0.1 mL) was added resulting in the immediate formation of a red precipitate. The solution was stirred at room temperature for 1 hr after which time a large amount of red solid was present and the solution was light yellow in color. The reaction mixture was cooled to -20 °C and the supernatant removed *via* cannula. The solid was then washed with pentane (3x5 mL) at 0 °C. The yield of the red solid, [μ-$C_2H_2C(O)$](μ-CO)$_2$Os(CO)$_2$(PMe$_3$)CoCp, **10a**, was 16.6 mg (77%). This compound, **10a**, may further purified by recrystallization from Et_2O at -20 °C.

Formula Weight: 556.40.

Mass Spectrum(220 °C, 70 eV): M^+ (558, 5.2%), M^+-nCO (n = 0-5)

IR(CH_2Cl_2, cm^{-1}); ν(CO): 2044(m), 1984(s), 1793(m). ν(acyl): 1614(w).

^1H NMR(360 MHz, CD_2Cl_2, -20 °C) 7.84 (1H, dd, $^3J_{P-H}$ = 8.3 Hz, $^3J_{H-H}$ = 9.2 Hz, H_β), 5.98 (1H, dd, $^3J_{P-H}$ = 2.3 Hz, $^3J_{H-H}$ = 9.2 Hz, H_α), 5.05 (5H, s, Cp), 1.79 (9H, d, $^2J_{P-H}$ = 10.5 Hz, CH_3).

^{13}C NMR(90.5 MHz, CD_2Cl_2, 23 °C) 154.0 (d, $^2J_{P-C}$ = 6.9 Hz, C_β), 144.3 (s, C_α), 96.8 (s, Cp), 17.3 (d, $^1J_{P-C}$ = 38.2 Hz, CH_3).

^{13}C NMR(90.5 MHz, CD_2Cl_2, -35 °C) 245.4 (acyl), 245.3 (bridge CO), 233.5 (d, $^2J_{P-C}$ = 42.7 Hz, bridge CO), 181.5 (CO), 174.0 (CO).

^{31}P NMR(81.0 MHz, CD_2Cl_2, 23 °C) -43.3.

Anal. Calcd. for $C_{15}H_{16}CoO_5OsP$: C, 32.38; H, 2.90 Found: C, 32.58; H, 3.09.

Synthesis of [μ-$C_2H_2C(O)$](μ-CO)$_2$Os(CO)$_2$(PMe$_2$Ph)CoCp, 10b

Using a similar procedure, excess PMe_2Ph (0.2 mL) and [μ−η^3:η^1-$C_2H_2C(O)$]Os(CO)$_4$CoCp, **2a**, (24.2 mg, 0.050 mmol) were used to obtain **10b** as a red solid (21.5 mg, 69%).

Formula Weight: 618.49.

Mass Spectrum(220 °C, 70 eV): M^+ (620, 1.5%), M^+-nCO (n = 0-5)

IR(CH_2Cl_2, cm^{-1}); ν(CO): 2047(m), 1986(s), 1793(m). ν(acyl): 1614(w).

^1H NMR(360 MHz, CD_2Cl_2, -20 °C) 7.72 (1H, dd, $^3J_{P-H}$ = 8.0 Hz, $^3J_{H-H}$ = 9.1 Hz, H_β), 7.55 (5H, m, Ph), 6.02 (1H, dd, $^3J_{P-H}$ = 2.0 Hz, $^3J_{H-H}$ = 9.1 Hz, H_α), 5.05 (5H, s, Cp), 2.10 (3H, d, $^2J_{P-H}$ = 10.2 Hz, CH_3), 2.02 (3H, d, $^2J_{P-H}$ = 10.2 Hz, CH_3).

^{13}C NMR(90.5 MHz, CD_2Cl_2, 23 °C) 154.6 (d, $^2J_{P-C}$ = 7.6 Hz, C_β), 145.3 (s, C_α), 135.9 (d, $^1J_{P-C}$ = 55.3 Hz, C_{ipso}), 131.0 (s, C_{para}), 129.3 (d, $^2J_{P-C}$ = 10.7 Hz,

C_{ortho}), 129.0 (d, $^3J_{P\text{-}C}$ = 6.6 Hz, C_{meta}), 96.4 (s, Cp), 16.3 (d, $^1J_{P\text{-}C}$ = 38.1 Hz, CH_3), 14.6 (d, $^1J_{P\text{-}C}$ = 38.1 Hz, CH_3).

^{13}C NMR(90.5 MHz, CD_2Cl_2, -40 °C) 245.1 (acyl), 244.2 (bridge CO), 232.2 (d, $^2J_{P\text{-}C}$ = 39.5 Hz, bridge CO), 181.5 (CO), 174.4 (CO).

^{31}P NMR(81.0 MHz, CD_2Cl_2, 23 °C) -34.7.

Anal. Calcd. for $C_{20}H_{18}CoO_5OsP$: C, 38.84; H, 2.93 Found: C, 38.79; H, 2.72.

Synthesis of [η^1-HCCH(PMe$_3$)](μ-CO)Os(CO)$_3$RhCp(CO), 11a

A procedure similar to that used in the synthesis of **10a-b** was utilized. A pentane solution of [μ–η^3:η^1-$C_2H_2C(O)$]Os(CO)$_4$RhCp, **2b**, (30.7 mg, 0.059 mmol) was filtered into a Ar-filled round bottomed flask and cooled to 0 °C. Excess PMe$_3$ (0.1 mL) was added resulting in the immediate formation of a flocculent orange precipitate. The solution was stirred at room temperature for 0.5 hr after which time a large amount of orange solid was present and the solution was nearly colorless. The reaction mixture was filtered *via* cannula at room temperature. The solid was then washed with pentane (4x5 mL) at ambient temperature until the hydrocarbon solution was colorless. The yield of the orange solid, [η^1-HCCH(PMe$_3$)](μ-CO)Os(CO)$_3$RhCp(CO), **11a**, was 28.1 mg (80%). A suitable mass spectrum could not be obtained.

Formula Weight: 600.37.

IR(CH_2Cl_2, cm^{-1}); ν(CO): 2035(m), 1963(s), 1936(m), 1752(m).

^{1}H NMR(360 MHz, CD_2Cl_2, -20 °C) 9.27 (1H, dd, $^3J_{P\text{-}H}$ = 35.4 Hz, $^3J_{H\text{-}H}$ = 19.3 Hz, H_α), 6.26 (1H, dd, $^3J_{P\text{-}H}$ = 40.8 Hz, $^3J_{H\text{-}H}$ = 19.3 Hz, H_β), 5.37 (5H, s, Cp), 1.60 (9H, d, $^2J_{P\text{-}H}$ = 13.3 Hz, CH_3).

^{13}C NMR(90.5 MHz, CD_2Cl_2, 23 °C) 172.4 (d, $^2J_{P\text{-}C}$ = 12.3 Hz, C_α), 114.3 (d, $^1J_{P\text{-}C}$ = 69.7 Hz, C_β), 90.1 (s, Cp), 10.8 (d, $^1J_{P\text{-}C}$ = 57.3 Hz, CH_3).

^{13}C NMR(90.5 MHz, CD_2Cl_2, 0 ^{o}C) 204.0 (d, $J_{Rh\text{-}C}$ = 26.5 Hz, 4CO), 180.0 (1CO).

^{31}P NMR(81.0 MHz, CD_2Cl_2, 23 ^{o}C) 7.8.

Anal. Calcd. for $C_{15}H_{16}O_5OsPRh$: C, 30.01; H, 2.69 Found: C, 29.96; H, 3.15.

Synthesis of [η^1-HCCH(PMe_2Ph)](μ-CO)Os$(CO)_3$RhCp(CO), 11b

Using a similar procedure, excess PMe_2Ph (0.2 mL) and [$\mu-\eta^3:\eta^1$-$C_2H_2C(O)$]Os$(CO)_4$RhCp, **2b**, (18.2 mg, 0.035 mmol) were used to obtain **11b** as an orange solid (15.5 mg, 67%).

Formula Weight: 662.44.

IR(CH_2Cl_2, cm^{-1}); ν(CO): 2035(m), 1964(s), 1937(m), 1753(m).

^{1}H NMR(360 MHz, CD_2Cl_2, -20 ^{o}C) 9.41 (1H, dd, $^3J_{P\text{-}H}$ = 34.9 Hz, $^3J_{H\text{-}H}$ = 19.2 Hz, H_α), 7.59 (5H, m, Ph), 6.41 (1H, dd, $^3J_{P\text{-}H}$ = 39.3 Hz, $^3J_{H\text{-}H}$ = 19.2 Hz, H_β), 5.36 (5H, s, Cp), 1.83 (6H, d, $^2J_{P\text{-}H}$ = 13.2 Hz, CH_3).

^{13}C NMR(90.5 MHz, CD_2Cl_2, 23 ^{o}C) 175.9 (d, $^2J_{P\text{-}C}$ = 12.2 Hz, C_α), 134.2 (d, $^4J_{P\text{-}C}$ = 2.5 Hz, C_{para}), 131.2 (d, $^3J_{P\text{-}C}$ = 10.7 Hz, C_{meta}), 130.2 (d, $^2J_{P\text{-}C}$ = 12.2 Hz, C_{ortho}), 124.6 (d, $^1J_{P\text{-}C}$ = 70.2 Hz, C_{ipso}), 112.3 (d, $^1J_{P\text{-}C}$ = 70.2 Hz, C_β), 90.1 (s, Cp), 10.4 (d, $^1J_{P\text{-}C}$ = 58.8 Hz, CH_3).

^{13}C NMR(90.5 MHz, CD_2Cl_2, 23 ^{o}C) 203.8 (br, 4CO), 180.3 (1CO).

^{31}P NMR(81.0 MHz, CD_2Cl_2, 23 ^{o}C) 7.3.

Anal. Calcd. for $C_{20}H_{18}O_5OsPRh$: C, 36.26; H, 2.74 Found: C, 36.59; H, 2.94.

Synthesis of ^{13}CO Enriched 9. A pentane solution of **1** was degassed by a freeze-pump-thaw cycle using liquid nitrogen. Approximately one atmosphere of ^{13}CO was admitted into the flask and the solution was stirred at 0 ^{o}C for 30 minutes. The solution of **1-^{13}CO** was then subsequently reacted with (η^5-C_9H_7)Rh(CO)(PMe_3) to generate the enriched dimetallic compound, **9-^{13}CO**.

Synthesis of ^{13}CO Enriched 10a-b and 11a-b. The ^{13}CO enriched dimetallic compounds [μ-η^3:η^1-$C_2H_2C(O)$]Os$(CO)_4$MCp (M = Co, **2a**; Rh, **2b**) were synthesized as outlined in Chapter 2. These compounds were then reacted with the appropriate phosphine as detailed above.

4.6.3. X-ray Structure Determination of [μ-$C_2H_2C(O)$](μ-$CO)_2$Os$(CO)_2$(PMe_3)Rh(η^5-C_9H_7), 9

Yellow-orange, X-ray quality crystals were grown by cooling a CH_2Cl_2/hexane solution of [μ-$C_2H_2C(O)$](μ-$CO)_2$Os$(CO)_2$(PMe_3)Rh(η^5-C_9H_7), **9**, to -5 °C. The X-ray data collection and structure refinement was carried out by Dr. B.D. Santarsiero and Dr. R. McDonald at the Structure Determination Laboratory, Department of Chemistry, University of Alberta. Crystal data and general conditions of data collection and structure refinement are given in Table 4.10. Three intensity and orientation standards were checked after every 120 minutes of exposure time and showed no appreciable decay. The positions of the Rh and Os atoms were derived from a three dimensional Patterson map and the remaining non-hydrogen atoms were located in difference Fourier maps after least squares refinement. Reflection data were corrected for absorption by using the method of Walker and Stuart;[32] the minimum and maximum correction coefficients applied to F_o were 0.7398 and 1.1615. All H atoms were included at their idealized positions (calculated by assuming C-H = 0.95 Å and sp^3 or sp^2 geometry) and constrained to 'ride' with the attached C atom. The H atoms were assigned fixed, isotropic thermal parameters 1.2 times those of the parent C atom.

The final atomic coordinates are given in Table 4.11 and selected bond distances and angles for [μ-$C_2H_2C(O)$](μ-$CO)_2Os(CO)_2(PMe_3)Rh(\eta^5$-$C_9H_7$), **9**, are given in Tables 4.2 and 4.3, respectively.

Table 4.10: Summary of Crystallographic Data for **9**

Crystal Parameters	
formula	$C_{19}H_{18}O_5OsPRh$
formula wt.	650.43
crystal size, mm	0.29 x 0.14 x 0.13
crystal system	monoclinic
space group	$P2_1/n$ (a non-standard setting of $P2_1/c$)
a, Å	[illegible]8(3)
b, Å	[illegible].914(3)
c, Å	13.354(2)
β, deg	97.30(2)
V, Å^3	2030
Z	4
D_{calc}, g cm^{-3}	2.125
μ, cm^{-1}	71.64

Data Collection and Structure Refinement

diffractometer	Enraf-Nonius CAD4
radiation (λ [Å])	Mo K_α (0.71073)
monochromator	graphite crystal, incident beam
take-off angle, deg	2.0
temperature, °C	23
scan type	θ-2θ
scan rate, deg $\min^{-1}$	2.0 - 6.7
scan width, deg in ω,	0.80 + 0.347tanθ
2θ limit, deg	52.0
reflections measured	4133 (*h*, *k*, ±*l*)
reflections used	2858 with $I > 3\sigma(I)$
variables	209
R^a	0.050
$R_w{}^b$	0.062
GOF[c]	1.90

[a] $R = \Sigma||F_o| - |F_c||/\Sigma|F_o|$

[b] $R_w = (\Sigma w(|F_o| - |F_c|)^2/\Sigma w F_o{}^2)^{1/2}$

[c] $GOF = [\Sigma w(|F_o| - |F_c|)^2/(NO - NV)]^{1/2}$

Table 4.11: Positional (x 10^4) and Isotropic Displacement (x 10^2) Parameters for 9

atom	*x*	*y*	*z*	*U*, Å^2
Os	22.4(6)	1549.6(3)	3304.2(4)	2.55(1)
Rh	2499(1)	599.3(5)	3354.7(7)	2.56(3)
P1	-1361(4)	2382(2)	2130(3)	3.4(1)
O1	1527(13)	1203(6)	1340(6)	5.0(3)
O2	-2181(13)	223(6)	2748(10)	6.6(4)
O3	-1706(13)	2216(7)	4947(7)	6.6(4)
O4	1671(12)	942(6)	5363(6)	4.7(3)
O7	5389(11)	1400(6)	3458(8)	4.9(3)
C1	1312(14)	1214(7)	2198(9)	2.6(3)
C2	-1446(15)	714(7)	2978(10)	3.4(3)
C3	-1113(15)	1984(7)	4362(10)	3.2(3)
C4	1468(14)	1013(7)	4471(9)	2.8(3)
C5	1820(14)	2380(7)	3562(9)	2.7(3)
C6	3344(15)	2252(7)	3606(9)	3.2(3)
C7	4017(15)	1484(7)	3475(9)	3.2(3)
C11	-175(18)	2812(8)	1272(11)	5.0(5)
C12	-2988(20)	1974(10)	1315(12)	6.3(6)
C13	-2219(21)	3155(9)	2702(12)	6.4(5)
C21	3570(16)	-354(8)	2444(10)	3.6(4)
C22	4271(15)	-295(7)	3471(10)	3.5(4)
C23	3144(18)	-539(7)	4084(11)	4.3(4)
C24	1754(17)	-679(7)	3475(11)	4.2(4)
C25	1977(15)	-587(7)	2453(10)	3.4(4)
C26	995(18)	-684(8)	1522(11)	4.9(5)
C27	1590(22)	-550(9)	669(12)	6.1(6)
C28	3137(22)	-333(10)	636(12)	6.4(6)
C29	4149(18)	-224(9)	1507(10)	4.7(5)

4.7. References

1. Shuster-Wolden, H.G.; Basolo, F. *J. Am. Chem. Soc.* **1966,** *88,* 1657.

2. (a) M. Rerek, M.; Ji, L.N.; Basolo, F. *J. Chem. Soc., Chem. Commun.* **1983**, 1208. (b) Rerek, M.; Basolo; F. *J. Am. Chem. Soc.* **1984,** *106,* 5908.

3. For relevant articles on ring slip reactions see (a) O'Connor, J.M.; Casey, C.P. *Chem. Rev.* **1987,** *87,* 307. (b) Basolo, F. *Israel J. Chem.* **1986,** *27,* 233. (c) Basolo, F. *Inorg. Chim. Acta.* **1985,** *100,* 33. (d) Ji, L.N.; Rerek, M.E.; Basolo, F. *Organometallics* **1984,** *3,* 740.

4. (a) Rahman, M.M.; Lui, H.Y.; Prock, A.; Giering, W.P. *Organometallics* **1987,** *6,* 650. (b) Tolman, C.A. *Chem Rev.* **1977,** *77,* 313.

5. Verkade, J.G.; Quin, L.D. *^{31}P NMR in Stereochemical Analysis* ; VCH: Deerfield Beach, FL., 1987.

6. Bitterwolf, T. *Inorg. Chim. Acta.* **1986,** *122,* 175.

7. (a) Burn, M.J.; Kiel, G.-Y.; Seils, F.; Takats, J.; Washington, J. *J. Am. Chem. Soc.* **1989,** *111,* 6850. (b) Dickson, R.S.; Gatehouse, B.M.; Nesbit, M.C.; Pain, G.N., *J. Organomet. Chem.* **1981,** *251,* 97. (c) Johnson, K.A.; Gladfelter, W.L. *Organometallics,* **1992,** *11,* 2534.

8. Kölher, F.H. *Chem. Ber.* **1974,** *107,* 570.

9. (a) Baker, R.T,; Tulip, T,H. *Organometallics* **1986**, *5*, 839. (b) Marder, T.B.; Calabrese, J.C.; Roe, D.C.; Tulip, T.H. *Organometallics* **1987**, *6*, 2012. (c) Kakkar, A.K.; Taylor, N.J.; Calabrese, J.C.; Nugent, W.A.; Roe, D.C.; Connnaway, E.A.; Marder, T.B. *J. Chem. Soc., Chem. Commun.* **1989**, 990. (d) Kakkar, A.K.; Jones, S.F.; Taylor, N.J.; Collins, S.; Marder, T.B. *J. Chem. Soc., Chem. Commun.* **1989**, 1454.

10. Merola, J.S.; Kacmarcil, R.T., Van Engen, D. *J. Am. Chem. Soc.* **1986**, *108*, 329.

11. Mann, B.E.; Taylor, B.F. *^{13}C NMR Data for Organometallic Compounds*; Academic: New York, 1981.

12. Tachikawa, M.; Richter, S.I.; Shapley, J.R. *J. Organomet. Chem.* **1977**, *128*, C9.

13. (a) Riesen, A.; Einstein, F.W.B.; Ma, A.K.; Pomeroy, R.K.; Shipley, J.A. *Organometallics* **1991**, *10*, 3629. (a) Alex, R.F.; Pomeroy, R.K. *Organometallics* **1987**, *6*, 2437. (c) Aime, S.; Osella, D.; Milone, L.; Rosenberg, E. *J. Organomet. Chem.* **1981**, *213*, 207.

14. Gagné, M.R.; Takats, J. *Organometallics* **1988**, *7*, 561.

15. Hsu, L.-Y.; Hsu, W.-L.; Jan, D.-Y.; Marshall, A.G.; Shore, S.G. *Organometallics* **1984**, *3*, 591.

16. Allen, F.H.; Kennard, O.; Watson, D.G.; Brammer, L.; Orpen, A.G.; Taylor, R. *J. Chem. Soc., Perkin Trans. II* **1987**, S1.

17. (a) Nesmeyanov, A.W.; Ustynyuk, N.A.; Makarova, L.G.; Andrianov, U.G.; Sruchkov, Y.; Andrae, S.; Ustynyuk, A. *J. Organomet. Chem.* **1978**, *159*, 189. (b) Forschner, T.C.; Cutler, A.R.; Kullnig, R.K. *Organometallics* **1987**, *6*, 889.

18. Westcott, S.A.; Kakkar, A.K.; Stringer, G.; Taylor, N.J.; Marder, T.B. *J. Organomet. Chem.* **1990**, *394*, 777.

19. Harris, R.K. *Nuclear Magnetic Resonance Spectroscopy*, Wiley: New York, 1986, Chapter 5.

20. (a) Dyke, A.F.; Knox, S.A.R.; Naish, P.J.; Taylor, G.E. *J. Chem. Soc. Dalton Trans.* **1982**, 1297. (b) Kiel, G.-Y.; Takats, J. *Organometallics* **1989**, *8*, 839.

21. (a) Alt, H.; Engelhart, H.E.; Steinlein, E. J. *Organomet. Chem.* **1988**, *344*, 227. (b) Alt, H.; Engelhart, H.E.; Steinlein, E. *J. Organomet. Chem.* **1989**, *362*, 117. (c) Churchill, M.R.; DeBoer, B.G.; Shapley, J.R.; Keister, J.B. *J. Am. Chem. Soc.* **1976**, *98*, 2357.

22. Friebolin, H. *Basic One- and Two-Dimensional NMR Spectroscopy*, VCH: New York, 1991, pg. 77-84.

23. Cherkas, A. A.; Breckenridge, S. M.; Carty, A. J. *Polyhedron* **1992,** *11,* 1075.

24. (a) Gallop, M.A.; Roper, W.A. *Adv. Organomet. Chem.* **1986,** *25,* 121. (b) Brother, P.J.; Roper, W.A. *Chem. Rev.* **1988,** *88,* 1293.

25. Mann, B.E. in *Comprehensive Orgaonmetallic Chemistry*; Wilkinson, G.; Stone, F.G.A.; Abel, E.W., Eds.; Pergamon: New York, 1982; Vol. 3, pg 89.

26. (a) Bond, E.; Muetterties, E.L. *Chem. Rev.* **1978,** *78,* 639. (b) Washington, J.; Takats, J. *Organometallics* **1990,** *9,* 925.

27. Einstein, F.W.B.; Jones, T.; Pomeroy, R.K.; Rushman, P. *J. Am. Chem. Soc.* **1984,** *106,* 2707.

28. March, J. *Advanced Organic Chemistry, 3rd Edition,* Wiley: New York, 1985, pg. 664.

29. (a) Wasserman, H.H.; Clark, G.M.; Turley, P.C. *Topics Curr. Chem.* **1974,** *47,* 73. (b) Turro, N.J. *Acc. Chem. Res.* **1969,** *2,* 25.

30. (a) Blomberg, M.R.A.; Siegbahn, P.E.M.; Bäckvall, J.E. *J. Am. Chem. Soc.* **1987,** *109,* 4451. (b) Daishefsky, S.; Singh, R.K. *J. Am. Chem. Soc.* **1975,** *97,* 3239. (c) Pellacani, L.; Tardella, P.A.; Lareto, M.A. *J. Org. Chem.* **1976,** *41,* 1282. (d) Truce, W.E.; Lindy, L.B. *J. Org. Chem.* **1961,** *26,* 1463. (e) Cook, A,G.; Meyer, W.C.; Ungradt, K.E.; Mueller, R.H. *J. Org. Chem.* **1966,** *31,* 14.

(f) Meinwald, J.; Crandall, J.K. *J. Am. Chem. Soc.* **1966,** *88,* 1292. (g) Cristol, S.J.; Jarvis, B.B. *J. Am. Chem. Soc.* **1967,** *89,* 5885.

31. Eshtiagh-Hosseini, Nixon, J.F. *J. Less-Common Met.* **1978,** *61,* 107.

32. Walker, N.; Stuart, D. *Acta. Crystallogr., Sect. A: Found Crystallogr.* **1983,** *A39,* 158.

Chapter 5

Reaction of $Os(CO)_4[\eta^2\text{-}HCC(CF_3)]$ with $(\eta^5\text{-}C_5R_5)M(CO)_2$
(R = Me, M = Co, Rh, Ir; R = H, M = Rh)
Synthesis, Characterization and Fluxional Behaviour of Dimetallacyclobutenes and Dimetallacyclopentenones

5.1. Introduction

The reaction between $Os(CO)_4(\eta^2\text{-}HCCH)$, **1**, and $CpM(CO)_2$ (M = Co, Rh, Ir; Cp = C_5H_5) was described earlier in Chapter 2. The condensation proceeds to yield dimetallacyclopentenones and the product formation is strongly metal dependent.[1a] The reaction of $Os(CO)_4[\eta^2\text{-}C_2(CF_3)_2]$ with $Cp^*M(CO)_2$ (M = Co, Rh, Ir; Cp^* = C_5Me_5) also occurs readily and dimetallacyclobutenes are obtained.[1b] These condensation reactions have proven to be valuable tools in the synthesis of alkyne bridged heterobimetallic compounds.

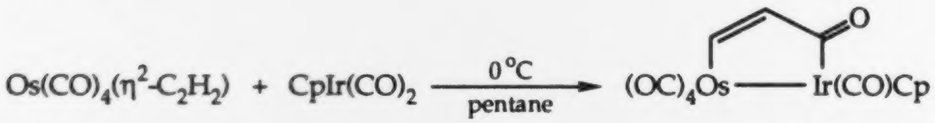
$Os(CO)_4(\eta^2\text{-}C_2H_2)$ + $CpIr(CO)_2$
0 °C
pentane
O
$(OC)_4Os$
Ir(CO)Cp

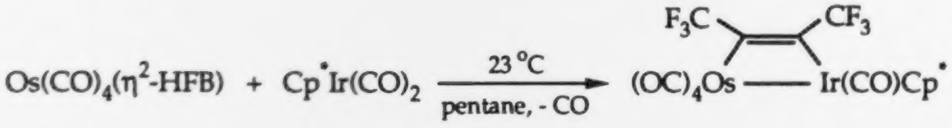
$Os(CO)_4(\eta^2\text{-}HFB)$ + $Cp^*Ir(CO)_2$
23 °C
pentane, - CO
F_3C
CF_3
$(OC)_4Os$
$Ir(CO)Cp^*$

However, owing to the symmetric nature of acetylene and hexafluorobutyne (HFB: $C_2(CF_3)_2$), the regioselectivity of the condensations could not be investigated. By investigating the regio–

selectivity of these condensations new insight might be obtained concerning the mechanism of these reactions. Thus, attention was turned to an unsymmetric alkyne, trifluoropropyne, (TFP: HC_2CF_3), in order to resolve this hitherto undetermined aspect of the reaction.

Trifluorpropyne has not been used[2] widely in organometallic chemistry and yet it is a versatile ligand. In fact, the most recent use of TFP in the synthesis of an organometallic compound was 1991[2a] while a TFP bridged bimetallic compound, $Pt_2(\eta^1\text{-}C_2CF_3)_2(\mu\text{-dppm})(\mu\text{-}CF_3CCH)$ (dppm = $(Ph_2P)_2CH_2$), was reported by Puddephatt in 1982.[2c] The TFP ligand combines the desirable properties of C_2H_2 and HFB. First, the alkyne proton is a useful spectroscopic aid. This proton can be observed readily using ^1H NMR spectroscopy, the chemical shift and any coupling patterns serve to deduce regioselectivity. The CF_3 group may be observed using ^{19}F NMR spectroscopy and this too may be used to determine the number and nature of any regioisomers. The major drawback of the TFP ligand is that the alkyne carbons exhibit F-C coupling. This coupling, plus the long quaternary carbon relaxation times (T_1), render observation of the alkyne carbon ^{13}C NMR signals extremely difficult.[3] However, this handicap may be overcome by using concentrated samples and long accumulation times. Also, the electron withdrawing nature of the CF_3 group lowers the energy of the alkyne π^* orbital, making it more accessible for M-alkyne backbonding. This gives metal-TFP complexes increased stability over their simple acetylene congeners.[4]

As mentioned, the CF_3 substituent is strongly electron withdrawing, and should result in the polarized structure shown. This is in agreement with the ^{13}C NMR data for the free alkyne (δ: C-H, 75.9 ppm; C-CF_3, 69.2

ppm). This unequal charge density on the *sp* carbons may help in the formation of single regioisomers.

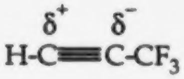

$$\overset{\delta^+}{\text{H-C}}\equiv\overset{\delta^-}{\text{C}}\text{-CF}_3$$

trifluoropropyne

However, a Mulliken population analysis has shown that the charge on the terminal *sp* carbon is -0.24 electrons while the central acetylenic carbon is almost neutral with a charge of only -0.01 electrons.[5a] The carbon atom of the strongly electron withdrawing trifluoromethyl substituent bears a charge of +0.81 electrons. These results were unexpected and thus the calculations were confirmed by Prof. M. Koblukowski of this Department.[5b] However, the ^{13}C NMR data for free trifluoropropyne contradict the theoretical calculations as the C-H carbon resonates downfield of the C-CF_3 carbon by approximately 7 ppm, indicating it is the terminal acetylenic carbon that bears the positive charge.[3] There are several possible explanations for these contradictory results. First, the Mulliken population analysis is dependent upon the basis set and the electron correlation scheme used.[5b] Varying results were obtained by Prof. M. Koblukowski depending on the basis set used. Also, the calculations are performed assuming idealized geometries in the gas phase.[5b] The interaction of solvent molecules with TFP could change the electronic charge distribution.

5.2. Synthesis and Characterization of Compounds

5.2.1. Synthesis of [μ-η^1:η^1-(CF_3)CCH]$Os(CO)_4M$(η^5-C_5R_5)(CO), (R = Me, Cp*: M = Rh, Ir; R = H, Cp: M = Rh)

The reaction of $Os(CO)_4$(η^2-TFP), **13**, with Cp*$M(CO)_2$ (M = Rh, Ir) or $CpRh(CO)_2$ proceeds readily. Slowly warming a solution of **13** from -40 °C to 15 °C in the presence of the appropriate Group IX metal complex results in the clean conversion to the corresponding heterodimetallic compound. The reactions were carried out using an excess of (η^5-C_5R_5)$M(CO)_2$ (R = H, Me). This is an important consideration as $Os(CO)_4$(η^2-TFP) will decompose to give several compounds, one of which is (μ-TFP)$Os_2(CO)_8$. This latter compound has solubility properties similar to the desired heterodimetallic compounds making purification difficult. However, using an excess of (η^5-C_5R_5)$M(CO)_2$ (R = H, Me) suppresses this decomposition route and most of the excess reagent may be removed using sublimation. Any remaining (η^5-C_5R_5)$M(CO)_2$ (R = H, Me), which is very soluble in hydrocarbons, can then be washed from the product using pentane.

The reaction may be conveniently monitored using FT-IR spectroscopy. During the course of the reaction one observes the decrease of the 2054 cm^{-1} signal of the $Os(CO)_4$(η^2-TFP) concomitant with the growth of a new signal in the range of 2117 to 2100 cm^{-1} that is the characteristic high frequency terminal CO stretch, a signature of the heterobimetallic complexes containing parallel alkyne bridges. It is also possible to monitor the decrease in the intensities of the signals for the Cp*$M(CO)_2$ complexes. It is noteworthy that the reaction with the simple cyclopentadienyl analogues proceeds only in the case of $CpRh(CO)_2$; with

Co or Ir, no conversion to heterodimetallic compounds is observed. Upon mild heating, only decomposition of $Os(CO)_4(\eta^2\text{-TFP})$ is seen. Thus, it seems that the increased electron density of the $Cp^*M(CO)_2$ compounds as compared to their $CpM(CO)_2$ analogues may play a role in the condensation reaction. The observation that, for $CpM(CO)_2$, only the Rh complex reacted is interesting. However, it is often observed that second row metal compounds display the highest reactivity. This "second row anomaly" is prevalent in the literature and is the subject of considerable discussion.[6] One aspect has recently been addressed as Ziegler has given an explanation for M-L bond strength differences down a triad based upon the relativistic effects of the metal *d* orbitals.[6b] All of the TFP bridged compounds are stable at room temperature and may be handled in air; although for long term storage the use of an inert atmosphere is recommended.

5.2.2. Characterization of $[\mu\text{-}\eta^1\text{:}\eta^1\text{-}(CF_3)CCH]Os(CO)_4M(\eta^5\text{-}C_5R_5)(CO)$ (R = Me, M = Rh, Ir; R = H, M = Rh)

The reactions of $Os(CO)_4(\eta^2\text{-}HC_2CF_3)$, **13**, with $(\eta^5\text{-}C_5R_5)M(CO)_2$ (R = Me: M = Rh, Ir; R = H: M = Rh) were complete within 2 h and similar compounds are formed (Scheme 5.1).

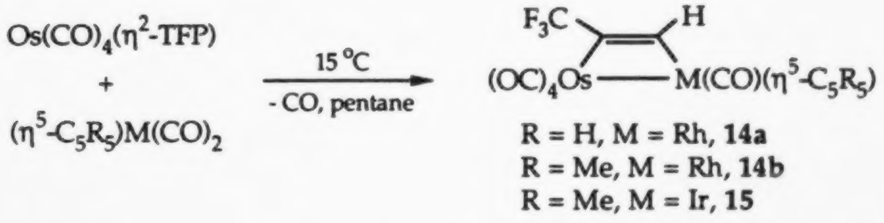

R = H, M = Rh, **14a**
R = Me, M = Rh, **14b**
R = Me, M = Ir, **15**

Scheme 5.1: Synthesis of $[\mu\text{-}\eta^1\text{:}\eta^1\text{-}(CF_3)CCH]Os(CO)_4M(\eta^5\text{-}C_5R_5)(CO)$ (R = Me, M = Rh, Ir; R = H, M = Rh)

The elemental analyses and mass spectra indicated that dinuclear species had been formed. The spectroscopic data obtained were consistent with the formulation as a dimetallacyclobutene species.[1] For all three compounds, the IR spectra showed only terminal carbonyl signals with no acyl carbonyl stretches visible. The carbonyl bands are listed in Table 5.1.

Table 5.1: FT-IR Data for Heterodimetallacyclobutenes

			ν(CO) (pentane, cm^{-1})		
	$Os(CO)_4$				Rh/Ir
Compound	A'(1)	A"(2)	A'(2)	A"(1)	M-CO
14a	2118(m)	2045(s)	2038(m)	2012(s)	2001(w)
14b	2107(m)	2034(s)	2028(m)	2001(s)	1984(w)
15	2109(m)	2037(s)	2027(m)	2001(s)	1971(w)

There are several interesting features present in the infrared spectrum of these compounds. As expected for compounds of C_1 symmetry, five carbonyl stretching bands are observed. In comparing the IR spectra of **14b** and **15**, the four carbonyl bands above 2000 cm^{-1} have almost exactly the same frequency. These can be assigned to the two A' and two A" bands of the $Os(CO)_4$ moiety, which has local C_s symmetry. A diagram of the stretching patterns of the carbonyl groups was seen previously in Scheme 2.2.

The highest energy band can be assigned to the symmetrical A'(1) stretch due to its relatively low intensity and high frequency. The remaining symmetrical stretch, A'(2), is assigned to the other signal of low intensity. The A"(1) and A"(2) stretches were assigned based upon a comparison with $Os(CO)_4(X)_2$ where a detailed vibrational analysis has been carried out by Hales and Irving.[7] The A"(2) band is assigned to the second highest energy band and the remaining A"(1) band is assigned to the lowest frequency Os-CO band. As stated, these assignments are based upon comparison with related systems, a confirmation of the assignment would require a full vibrational analysis using partially ^{13}CO enriched material.

The remaining low energy band, which varies depending upon the Group IX metal, can then be assigned to the Cp'M-CO stretch. The lower energy of this band in the case of **15** reflects the greater electron density of the Ir centre as compared to Rh, causing increased backbonding to the CO π^* orbitals, thus lowering the stretching frequency. However, the difference in electronic properties between Ir and Rh does not seem to be transferred to the Os centre as the frequencies of the Os-CO stretches remain essentially constant. It is interesting to note that the enhanced electron density seems to be only transmitted to the Ir-CO ligand and not transferred through the metal-metal bond. Thus, the Ir bound carbonyl is, in effect, acting as a type of electron sink.

The differences in the electronic properties between the Cp and Cp* ligands are reflected in the IR spectra of **14a** and **14b**. The Cp ligand is less electron donating than its pentamethyl analogue. This makes the Rh centre in **14a** less electron rich as evidenced by the 17 cm^{-1} increase in Rh-CO stretching frequency as one changes from Cp* to Cp. The decreased electron density on the Rh centre is also reflected in the Os-CO stretching frequencies which, on average, are 10 cm^{-1} higher in energy for (μ-TFP)Os$(CO)_4$RhCp(CO) than for the Cp* derivative. Thus, in this case, the Os-Rh bond has reacted to the change in electron density at the Rh centre.

Further comparison to other Cp derivatives could not be made as $CpM(CO)_2$ (M = Co, Ir) are unreactive towards $Os(CO)_4(\eta^2\text{-TFP})$.

The ^1H NMR spectra of the heterodimetallacyclobutenes consist of two resonances. One of these signals is assigned to the Cp or Cp* ligand while the other the alkyne proton resonance. The ^1H NMR resonances for the alkyne protons of **14a-b** and **15** are listed in Table 5.2.

Table 5.2: ^1H NMR Data for Heterodimetallacyclobutenes

	δ (ppm, CD_2Cl_2)[a]		
Compound	C-*H*	$^2J_{Rh\text{-}H}$	$^4J_{F\text{-}H}$
$(\mu\text{-TFP})Os(CO)_4Rh(CO)Cp$, **14a**	7.93	4.1	2.0
$(\mu\text{-TFP})Os(CO)_4Rh(CO)Cp^*$, **14b**	7.41	3.8	2.2
$(\mu\text{-TFP})Os(CO)_4Ir(CO)Cp^*$, **15**	7.97	–	2.2

[a]Couplings in Hz.

For all three compounds, the ^1H NMR signal for the alkyne proton is observed in the downfield region of the spectrum. This downfield position of the alkyne proton is consistent with previous work. Specifically, for $(\mu\text{-}\eta^1\text{:}\eta^1\text{-}C_2H_2)Os_2(CO)_8$, the ring protons appear at 6.96 ppm.[1a] Therefore, the observation of a downfield ^1H NMR proton resonance coupled with the elemental analysis and IR data allows the prediction of a dimetallacyclobutene structure.

As a consequence of the unsymmetrical nature of the TFP ligand, the reaction shown in Scheme 5.1 could produce two regioisomers, **A** and **B**.

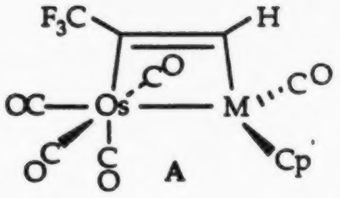
A

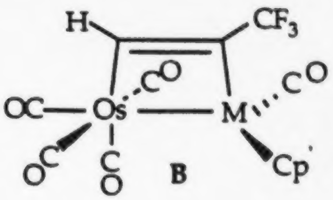
B

The ^1H and ^{19}F NMR spectra indicated that only a single regioisomer was formed but further spectroscopic work was required in order to confirm the actual structure. Despite the appearance of only one alkyne signal, the ^1H NMR spectra of **14a** and **14b** proved invaluable in determining the regioselectivity of the reaction. Specifically, for **14b**, a $^1H\{^{19}F\}$ experiment was carried out in order to reveal the orientation of the alkyne bridge (Figure 5.1).

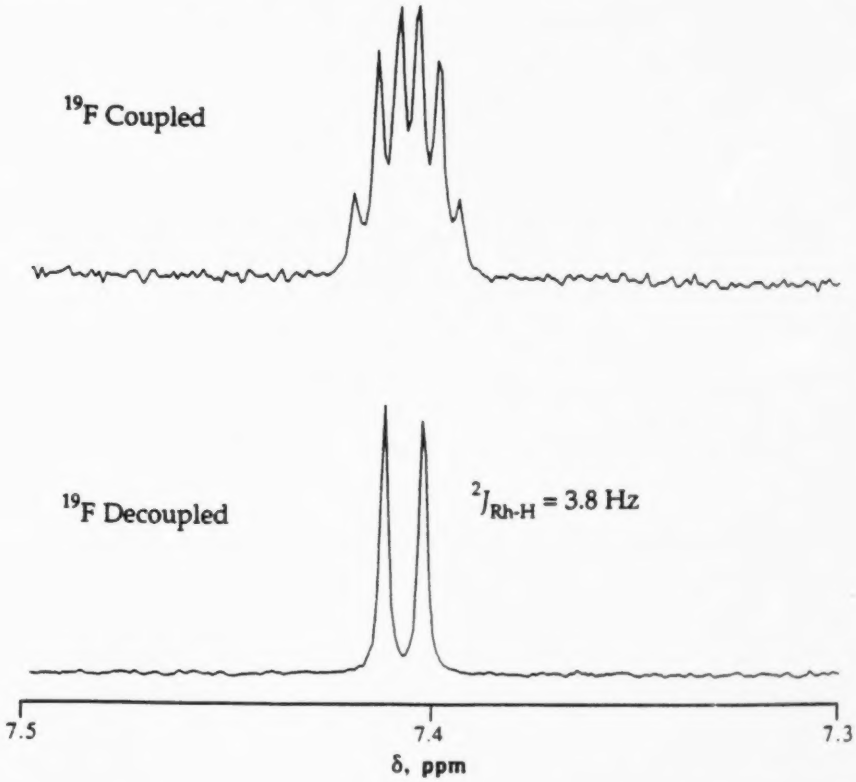

Figure 5.1: $^1H\{^{19}F\}$ NMR Experiment on Alkyne Proton of **14b**

A selective $^{1}H\{^{19}F\}$ NMR decoupling experiment showed the collapse of the apparent sextet of the acetylenic proton to a doublet with $^{2}J_{Rh\text{-}H}$ = 3.8 Hz. This is consistent with a regioisomer whereby the C-H is bound to the Rh centre (**A**) indicating that the alkyne bridge is formed in a regioselective manner. The fact that the rhodium-hydrogen coupling ($^{2}J_{Rh\text{-}H}$ = 3.8 Hz) is almost twice as large as the fluorine-hydrogen coupling ($^{4}J_{F\text{-}H}$ = 2.2 Hz) causes the alkyne proton signal to appear as a sextet and not a doublet of quartets as one would initially assume. A similar experiment was carried out on **14a** and gave analogous results with $^{2}J_{Rh\text{-}H}$ = 4.1 Hz and $^{4}J_{F\text{-}H}$ = 2.0 Hz.

In order to further corroborate the ^{1}H NMR results, the ^{13}C NMR spectra of **14a-b** and **15** were recorded. The quaternary TFP carbons were only observed after long accumulation times and the results are listed in Table 5.3.

Table 5.3: ^{13}C NMR Data for Ring Carbons in
$[\mu\text{-}\eta^1\text{:}\eta^1\text{-}(CF_3)CCH]Os(CO)_4M(\eta^5\text{-}C_5R_5)(CO)$

	δ (ppm, CD_2Cl_2)			Δ(ppm)[a]	
Compound	C-H	C-CF_3	$\delta_{C\text{-}H} - \delta_{C\text{-}CF_3}$[b]	$\Delta_{C\text{-}H}$	$\Delta_{C\text{-}CF_3}$
14a	118.7	96.9	21.8	42.8	27.7
14b	130.8	97.4	33.4	54.9	28.2
15	110.9	96.4	14.5	35.0	27.2
free TFP	75.9	69.2	6.7	--	--

[a] $\Delta = \delta_{C\text{-}R(complex)} - \delta_{C\text{-}R(free)}$ for R = H, CF_3. [b] In ppm.

For **14a** and **14b**, Rh-C coupling was used to corroborate the assignment of the regioisomer. In **14b**, the C-H carbon exhibits Rh-C coupling of 24.8 Hz, consistent with coupling over a Rh-C sigma bond.[8a] For the C-CF_3 carbon, a much reduced two-bond coupling of $^2J_{Rh\text{-}C}$ = 5.9 Hz is observed. This indicates that the C-H is indeed bonded to the Rh centre. Analogous results are seen for **14a**. Also, the range of C-CF_3 ^{13}C NMR shifts for **14a-b** and **15** is very small, 97.4-96.4 ppm. This indicates that the C-CF_3 carbon is attached to the same metal centre in each case. For comparison, in (μ-η^1:η^1-TFP)$Os_2(CO)_8$ the alkyne C-CF_3 signal appears in the ^{13}C NMR spectrum at 101.0 ppm,[8b] close to the observed values for **14a-b** and **15**. For **14a-b**, the alkyne C-H carbons show an expected shift to lower field compared to the C-CF_3 carbons, as they are attached to a second row metal.[8a] Unfortunately, there is a lack of ^{13}C NMR data available for (μ-C_2H_2)M_2L_n (L = ligand) species with second row metals. Therefore, a comparison will be made to (μ-HFB)Ru(CO)$_4$Rh(CO)Cp*, where the alkyne carbons attached to second row metals resonate at 123.0(C_{Ru}) and 129.0(C_{Rh}) ppm.[8c] Thus, the signals for the trifluoropropyne-bridged species appear with chemical shifts consistent with the acetylene and HFB bridged complexes.

The ^{13}C NMR signals for trifluoropropyne shift dramatically upon coordination. For free TFP, the C-H carbon resonates at 75.9 ppm while the C-CF_3 signal appears at 69.2 ppm. Upon formation of the dimetallacyclobutenes **14a-b** and **15**, the C-H and C-CF_3 signals shift downfield. The shift to lower field is not unexpected as the hybridization has changed from *sp* to *sp*^{2} with a concomitant change in anisotropic effects. For complex **14b**, the C-CF_3 signal shifts downfield by 28.2 ppm which is in agreement with the value obtained for **15**. This is reasonable because in both cases, the C-CF_3 carbon is attached to an osmium centre. However, the C-H signal of **14b** shifts downfield by 54.9 ppm, a significantly larger change than in **15** as the C-H carbon is now bound to a second row metal, causing the shift to lower field. There is also a 12.1 ppm upfield shift upon changing from **14b** to **14a**, the only difference is that the Cp* ligand on the Rh centre is replaced by the Cp ligand, its unsubstituted analogue. This indicates that the ^{13}C NMR chemical shifts of the C-H carbon are sensitive to changes in the electron density on the Rh centre and the Os-Rh metal-metal bond.

The ^{13}C NMR chemical shift difference between the two alkyne carbons is also of significance. This shift difference, $\delta_{C\text{-}H} - \delta_{C\text{-}CF3}$, has been used as a measure of the polarity of the carbon-carbon bond, a positive value is indicative of the C-H carbon bearing a partial positive charge.[9] In free TFP the shift difference is only 6.9 ppm, indicating that the C-C triple bond is slightly polarized; a result of electron withdrawing properties of the CF_3 group. In **15**, the shift difference is 14.5 ppm and appears to indicate that the polarity in the bond has increased, although the influence of the metal on the chemcial shift cannot be overlooked. The shift difference is even more pronounced for **14b**, where a value of 33.4 ppm is obtained; the presence of a second row metal attached to the C-H carbon has a significant effect. Therefore, upon formation of the dimetallacyclobutenes, the original direction of the C-C bond polarity appears to be maintained and its magnitude increased. The shift difference for **14a** is 21.8 ppm, a value of 11.6 ppm less than the shift difference in its Cp* analogue, **14b**. Again, this is a reflection of the ability of the metal-metal bond to react to changes in electron density at the Rh centre.

5.3. Molecular Structure of [μ-η^1:η^1-(CF$_3$)CCH]Os(CO)$_4$IrCOCp*, 15

The trends in ^{1}H and ^{13}C NMR chemical shifts for **15** were fully consistent with an alkyne orientation analogous to **14a-b** but the presence of the NMR silent Ir nuclei precluded an unequivocal assignment of the regioselectivity of the reaction. Thus, a single crystal X-ray determination was undertaken to unambiguously confirm the orientation of the bridging alkyne unit (Figure 5.2). Relevant bond distances and angles are given in Tables 5.4 and 5.5, respectively.

As can be seen, the trifluoropropyne is oriented with the C-H carbon of the alkyne bound to the Group IX metal and the dimetallacyclobutene core is readily apparent. The Os centre has distorted octahedral geometry while the Ir centre has the expected three-legged piano stool arrangement. The Os-Ir separation of 2.8020(5) Å is consistent with a metal-metal single bond;[10] the Os-Ir bond distance in [μ-C$_2$H$_2$C(O)]Os(CO)$_4$IrCp(CO), **3**, is 2.785(2) Å, while for Os(CO)$_3$(μ-dppm)$_2$Ir(CO)$_2^+$ [dppm = (Ph$_2$P)$_2$CH$_2$], where an Os-Ir dative bond is present, the metal-metal separation is 2.9652(4) Å.[10a] Also, in [Os(CO)$_4$]$_2$IrCp*(CO), the Os-Ir bond distances are 2.7902(5) Å and 2.8124 Å; these distances are relevant as they are representative of unbridged bond distances between an Os(CO)$_4$ unit and an IrCp*(CO) fragment.[10b] For further comparison, the Ir-Ir separation[10c] in (μ-C$_6$F$_4$)Ir$_2$Cp$_2$(CO)$_2$ is 2.7166 Å while an Os-Os bond distance of 2.8975(1) Å can be found for [μ-C$_2$(CO$_2$Me)$_2$]Os$_2$(CO)$_8$.[10d,e]

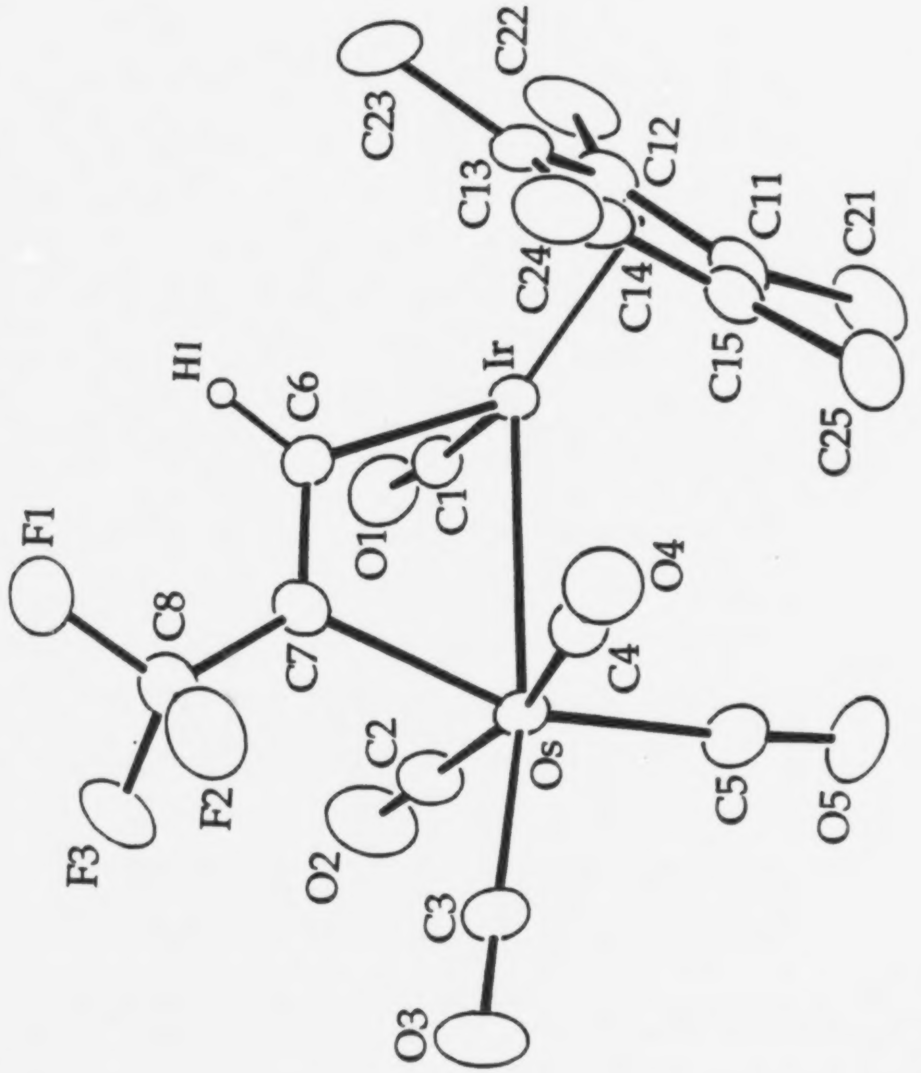
C23
C22
C13
C12
C11
C21
C24
C14
C15
C25
H1
C6
Ir
C1
O1
F1
C8
C7
O4
C4
F3
F2
C2
O2
Os
C5
O5
C3
O3

Figure 5.2: ORTEP View of (μ-TFP)Os(CO)$_4$IrCp*(CO), 15

Table 5.4: Selected Bond Lengths (Å) for **15**

Ir-Os	2.8020(5)	O1-C1	1.169(9)
Ir-C1	1.814(9)	O2-C2	1.11(1)
Ir-C6	2.055(8)	O3-C3	1.14(1)
Os-C2	1.96(1)	O4-C4	1.123(9)
Os-C3	1.901(9)	O5-C5	1.12(1)
Os-C4	1.940(9)	C6-C7	1.30(1)
Os-C5	1.96(1)	C7-C8	1.47(1)
Os-C7	2.135(8)	C11-C12	1.42(1)

Table 5.5: Selected Angles (deg) for **15**

Os-Ir-C1	88.9(2)	Ir-Os-C2	91.6(3)
Os-Ir-C6	69.0(2)	Ir-Os-C3	168.3(3)
C1-Ir-C6	89.6(3)	Ir-Os-C4	84.5(2)
C2-Os-C3	92.5(4)	Ir-Os-C5	91.7(3)
C2-Os-C4	169.6(4)	Ir-Os-C7	69.0(2)
C2-Os-C5	93.6(4)	Ir-C1-O1	174.7(7)
C2-Os-C7	87.7(4)	Os-C2-O2	174.9(9)
C3-Os-C4	89.7(4)	Os-C3-O3	179(1)
C3-Os-C5	99.0(4)	Os-C4-O4	174.0(8)
C3-Os-C7	100.2(4)	Os-C5-O5	175.2(9)
C4-Os-C5	96.1(4)	Ir-C6-C7	114.2(6)
C4-Os-C7	82.0(3)	Os-C7-C6	107.8(6)
C5-Os-C7	160.7(3)	Os-C7-C8	125.8(6)
C6-C7-C8	126.4(8)		

The Ir-C6 (2.055(8) Å) and Os-C7 (2.135(8) Å) distances indicate metal-carbon single bonds. For example, the Ir-C bond lengths[10c] in (μ-C_6F_4)$Ir_2Cp_2(CO)_2$ are 2.045(3) and 2.024(2) Å while the average Os-C separations[10d,e] in [μ-$C_2(CO_2Me)_2$]$Os_2(CO)_8$ are 2.138(5) Å. In addition, a shortening of Ir-C bond distances as compared to Os-C bond distances is seen in [μ-$C_2H_2C(O)$]$Os(CO)_4IrCp(CO)$, **3**, where the Ir-C separation is 2.07(3) Å and the Os-C single bond distance is 2.15(3) Å. For (μ-TFP)$Os(CO)_4IrCp^*(CO)$, **15**, the shortening of the Ir-C(H) bond compared to the Os-C(CF_3) bond was initially of interest as metal-perfluoro alkyl bonds are known to be shorter and stronger than their non-fluoronated analogues.[11] However, it must be remembered that the compound contains Ir(I) and Os(0) centres, and it is expected that an Ir(I) nucleus will have a shorter covalent radius than an Os(0) counterpart.[12a] This is borne out in the shorter Ir-C bond lengths and further evidence is provided by the shorter Ir-CO bond distance of 1.814(9) Å in **15** as compared to an average Os-CO bond distance of 1.94(1) Å. Of course, the shorter Ir-CO bond distance is also the result of having the electron rich substituent η^5-C_5Me_5 bound to the Ir centre rather than a reflection of the smaller Ir(I) covalent radius. This observation has also been noted for $Os(CO)_3(\mu$-dppm$)_2Ir(CO)_2^+$,[10a] where the Ir-CO distances are almost 0.05 Å shorter than the Os-CO separations. In (μ-TFP)$Os(CO)_4IrCp^*(CO)$, **15**, the C7-C6-Os angle (107.8°) is more acute than the C6-C7-Ir (114.2°) angle. A likely explanation is simply a geometric result of the Os-C(CF_3) bond being longer than the Ir-C(H) bond. The C6-C7 separation of 1.30(1) Å confirms its double bond character,[12b] and is also in accord with other M_2(μ-alkyne) complexes.[13] Interestingly, the C1 carbonyl on Ir is nearly co-planar with the equatorial Os carbonyls; this has important implications for the fluxional behaviour of these compounds (*vide infra*). Finally, the alkyne C-C bond vector is oriented parallel to the metal-metal bond; the C6-Ir-Os-C7 torsional angle is only 0.75°. This torsional angle is rather small compared to $[\mu\text{-}C_2(CO_2Me)_2]Os_2(CO)_8$ which has a 8.4° twisting[10d,e] from planarity but comparable to $(\mu\text{-}C_6F_4)Fe_2(CO)_8$ where the torsional angle is 1.6°.[14]

The term parallel M_2(μ-alkyne) describes a bimetallic complex whereby the alkyne is oriented parallel to the M-M vector.

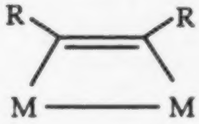

Obviously, (μ-TFP)Os(CO)$_4$IrCp*(CO), **15**, falls into the aforementioned designation. The bonding in parallel M_2(μ-alkyne) complexes has been described by Hoffmann and co-workers.[15a] In their description, the molecular orbitals of the bound acetylene were constructed by varying the C-C-H angle in acetylene from 180° to 120°. For **15**, the different electronegativities of the two alkyne carbons must be taken into consideration. Specifically, the electron withdrawing nature of the CF_3 group causes a polarization; therefore, the relative amplitudes of the orbitals will be different on the two alkyne carbons.[15b,c] The trifluoropropyne molecular orbitals are shown in Scheme 5.2, the labelling scheme used by Hoffmann is retained, even though the alkyne used is no longer symmetrical.

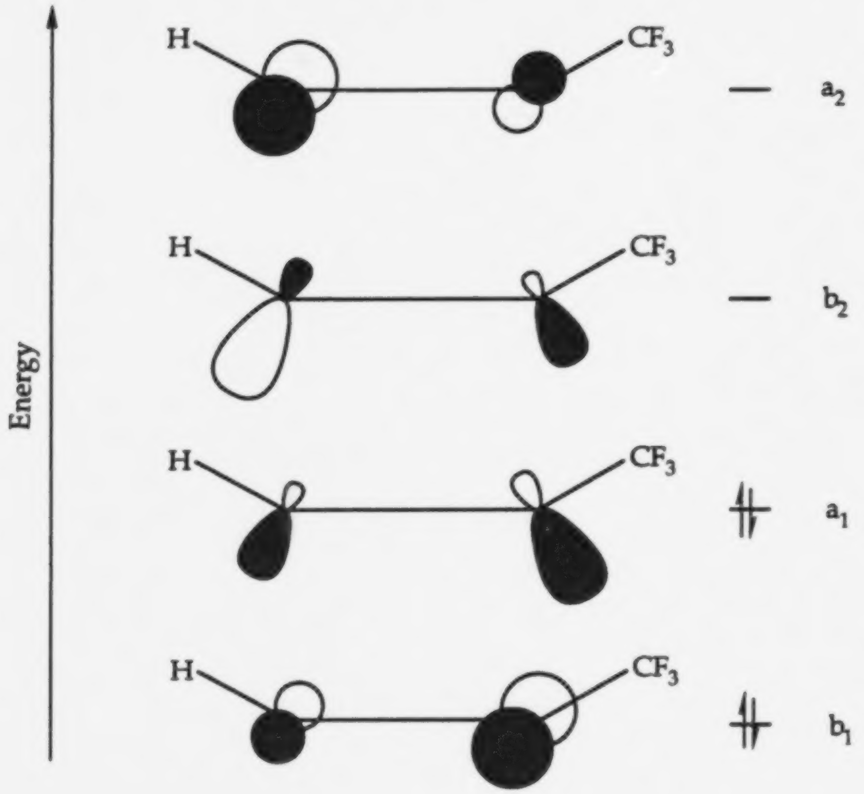

Scheme 5.2: Alkyne Molecular Orbitals in M_2(u-TFP) Complexes

The metal-based orbitals for (μ-TFP)Os(CO)$_4$IrCp*(CO) are similar to those shown in Scheme 1.24 for an $Os_2(CO)_8$ fragment as the Cp*Ir(CO) fragment is isolobal to Os(CO)$_4$. Hoffmann has determined, and it is clear from the diagram above, that the a_2 and b_1 orbitals do not interact strongly with the orbitals on the bimetallic fragment (Scheme 1.24). This is due to the perpendicular orientation of these alkyne orbitals with respect to the frontier orbitals on the bimetallic unit. However, the a_1 and b_2 orbitals do interact strongly and are responsible for the metal-alkyne bonding. In the diagram, the alkyne has a formal neutral charge. Calculations on a number of systems have shown that, in $M_2(\mu$-alkyne) complexes, there is a net donation of electron density to the alkyne, indicating that the metal-alkyne backbonding to b_2 is very significant. In fact, Hoffmann has suggested that an alkyne bridging two metal centres in a parallel fashion could be thought of as a di-anion ($C_2R_2^{2-}$) that donates four electrons.

It is difficult to predict the strength of the M-C(alkyne) interaction for the two different metals as the HOMO (a_1) and LUMO (b_2) orbitals work in the opposite direction. That is, $a_1 \rightarrow M$ donation would suggest a longer Ir-C(H) bond distance as compared to Os-C(CF_3) but the $M \rightarrow b_2$ interaction implies the exact opposite result. Therefore, although the diagram can be used to qualitatively describe the bonding in (μ-TFP)$Os(CO)_4IrCp^*(CO)$, **15**, it is not sufficient to explain the metrical observations in the X-ray structure of **15**. The presence of two different metal centres coupled with the inherent asymmetry of the bridging trifluoropropyne unit make the prediction of bond lengths and angles extremely difficult.

5.4. Formation of Heterodimetallacyclobutenes 14a-b, 15: Plausible Pathway

As noted, the bimetallic compounds are formed in a regioselective manner. Therefore, the electronic properties of the alkyne must play a role in determining the regiochemistry of the reaction. This is not surprising due to the significant polarization of the TFP ligand and any mechanism must incorporate the effect of charge-separation.

The behaviour of $(\eta^5\text{-}C_5R_5)M(CO)_2$ (R = H, Me; M = Co, Rh, Ir) compounds as nucleophiles is well documented in the literature. For example, they react readily with CH_3I in a S_N2 manner,[16] and enter into the formation of donor-acceptor metal-metal bonds.[17] Therefore, it is possible for the (η^5-C_5R_5)M(CO)$_2$ complexes to act as nucleophiles in the condensation reactions with Os(CO)$_4$(η^2-TFP) as in the mechanism shown in Scheme 5.3. The initial step of the reaction involves nucleophilic attack of (η^5-C_5R_5)M(CO)$_2$ on the C-H carbon of the bound TFP ligand. The polarization of the alkyne would thus direct the regioselectivity of the reaction, resulting in the formation of only one regioisomer.

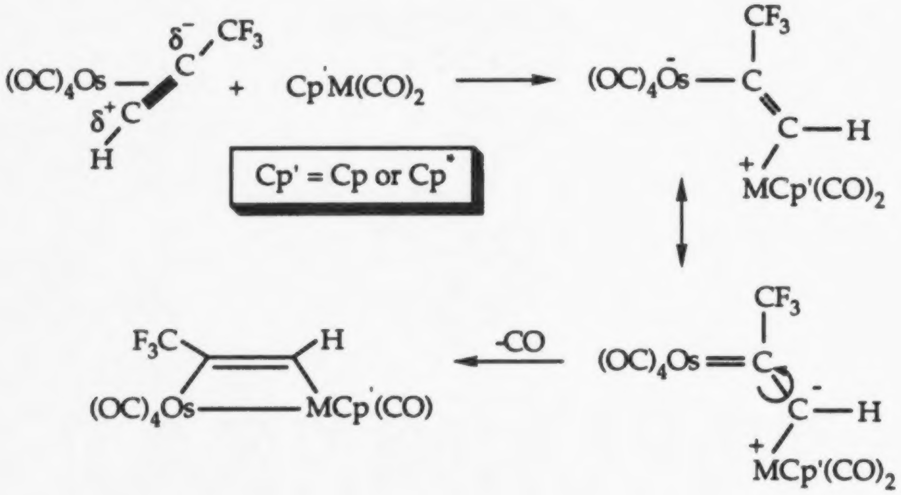

Scheme 5.3: Mechanism for Formation of [μ-(CF_3)CCH]Os(CO)$_4$MCp'(CO) (Cp*: M = Rh, Ir, Cp: M = Rh)

There is precedence for this type of reaction. Stone and co-workers have observed that the reaction of Pt(COD)$_2$ (COD = cyclo-octa-1,5-diene) with Pt(COD)(η^2-HFB) results in the formation of a dimetallacyclobutene.[18a] The reaction has been extended to other alkynes ($RCCSiMe_3$; R = CF_3, $SiMe_3$, Ph) to yield diplatinum complexes, although not necessarily dimetallacyclobutenes.[18b] The reactions are envisaged to occur *via* nucleophilic attack, by a Pt(COD) fragment, at the coordinated alkyne of a Pt(COD)(η^2-alkyne) species.

To gain further information about the mechanism, a solution containing ^{13}CO enriched Os(CO)$_4$(η^2-TFP) and unlabeled Cp*Rh(CO)$_2$ was slowly warmed from -40 °C and the reaction monitored by ^{1}H and ^{13}C NMR spectroscopy. At -40 °C, only signals due to Os(^{13}CO)$_4$(η^2-TFP) were seen plus a very small doublet (δ = 195.0, $^1J_{Rh\text{-}C}$ = 83.5 Hz) due to Cp*Rh(CO)$_2$. The sample was warmed to -20 °C and an slight increase in the signal due to Cp*Rh(^{13}CO)(CO) was seen, accompanied by the presence of free ^{13}CO. No bimetallic species were detected. Similar observations have been made previously and are detailed in Chapters Two and Three. At -15 °C, the appearance of signals due to **14b** were observed along with signals due to Os(^{13}CO)$_4$(η^2-TFP), Cp*Rh(^{13}CO)(CO) and free ^{13}CO. Unfortunately, no other intermediates were observed. The initial ^{13}CO exchange between Os(^{13}CO)$_4$(η^2-TFP) and Cp*Rh(CO)$_2$ is accompanied by the nearly immediate formation of the dimetallic product, **14b**. Warming to -10 °C resulted in further reaction; after raising the temperature to 0 °C and finally to +10 °C only **14b**, Cp*Rh(^{13}CO)(CO) and free ^{13}CO were present. Similar results were seen in the reaction of Os(CO)$_4$(η^2-TFP) with Cp*Ir(CO)$_2$.

As seen previously, the presence of free ^{13}CO was detected before any bimetallic compounds were observed. Thus, these observations strongly imply that CO dissociation from **13** is the first step in the condensation reaction (Scheme 5.4).

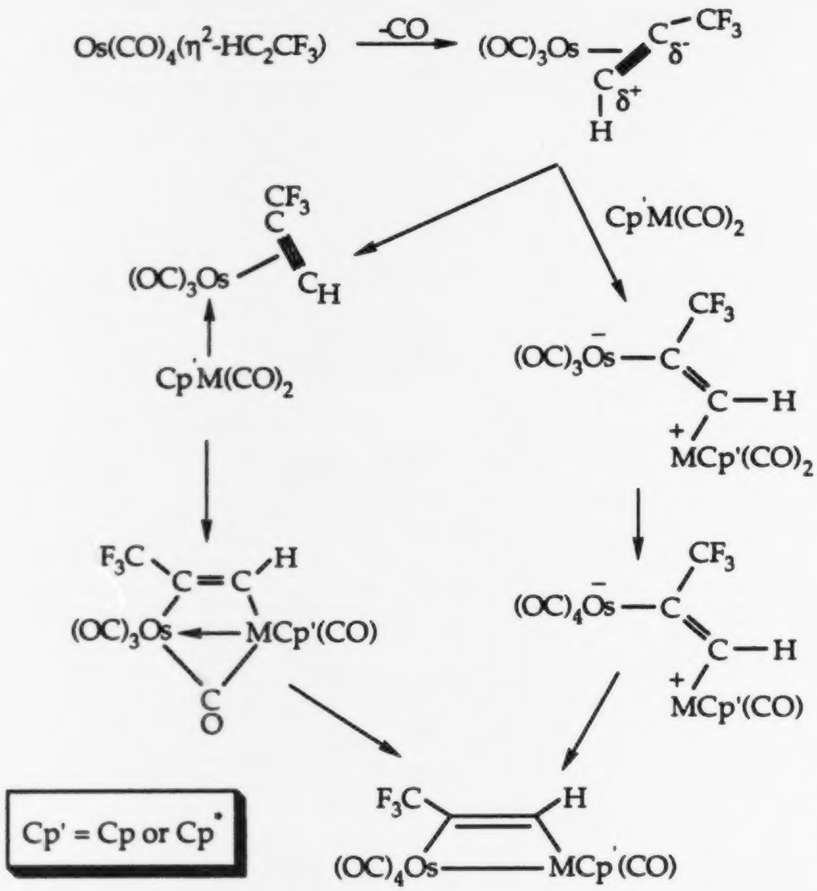
Os(CO)4(η2-HC2CF3)
-CO
(OC)3Os
CF3
δ-
δ+
H
Cp'M(CO)2
(OC)3Os
(OC)4Os
MCp'(CO)2
MCp'(CO)
F3C
Cp' = Cp or Cp*

Scheme 5.4: Alternate Mechanism for Formation of (μ-TFP)Os(CO)$_4$MCp'(CO) (Cp*: M = Rh, Ir, Cp: M = Rh)

As shown , the condensation could be initiated by nucleophilic attack at the alkyne or at the vacant coordination site on the Os centre. Nucleophilic attack at the TFP ligand would, however, account for the regioselectivity of the reaction. The four electron donation of the alkyne, referred to in Chapter 1, could activate the alkyne towards nucleophilic attack. Interestingly, the ^{13}CO label was incorporated equally among the five carbonyls; this is possible if there is the formation of a doubly CO bridged intermediate (Scheme 5.5).

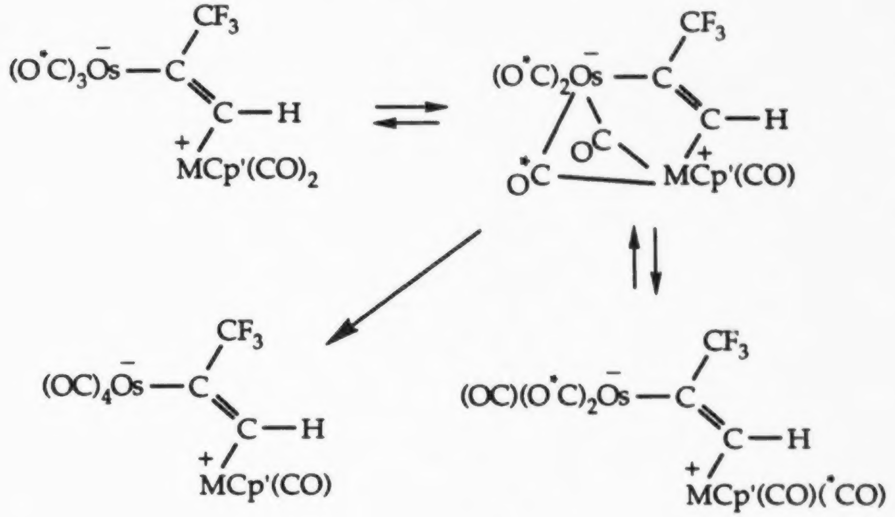

Scheme 5.5: Postulated Mechanism for ^{13}CO Exchange in (μ-TFP)Os(CO)$_4$MCp'(CO) (Cp*: M = Rh, Ir, Cp: M = Rh)

The formation of a doubly-CO bridged intermediate would allow the labelled ^{13}CO to be exchanged between the two metal centres and would eventually lead to equal ^{13}CO distribution throughout the bimetallic product. Also, the mechanism would allow for the transfer of a CO to the electron deficient Os centre before formation of the metal-metal bond. This mechanism is different from the mechanisms proposed for the formation of **2b**, **3** and **17a-c** (*vide infra*) where an initial nucleophilic attack on the Os centre is proposed. Also, the appearance of enriched Cp*Rh(^{13}CO)(CO) would require nucleophilic attack at the alkyne and ^{13}CO exchange followed by dissociation of the Cp*Rh(CO)$_2$ from the TFP ligand. This seems unlikely considering the close proximity of the two oppositely charged metal centres and the energy required to break the Rh-C bond.

The alternate pathway, which involves nucleophilic attack at the Os centre, is also possible. The regioselectivity of the reaction can also be explained using this mechanism. In the formation of the alkyne bridge, it would be the C-H carbon that migrates to the Group IX metal. The Os-C(CF_3) bond would be stronger due to the presence of the perfluoromethyl substituent and less likely to migrate.[11] The ^{13}CO exchange between the two metal centres can also be accounted for using a mechanism originally shown in Chapter 2 (Scheme 2.6). The formation of a doubly-CO bridged intermediate would result in equilibration of the ^{13}CO label (Scheme 5.6).

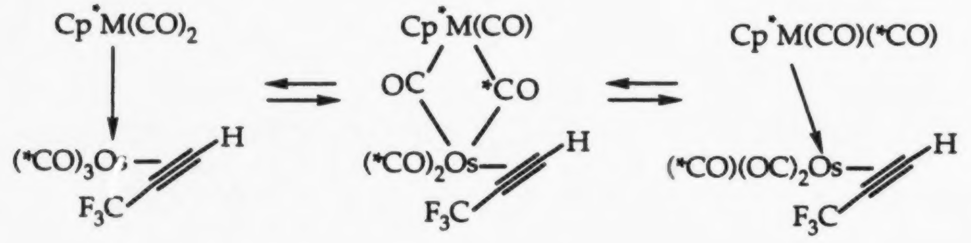

Scheme 5.6: Alternate Mechanism for ^{13}CO Exchange in (μ-TFP)Os(CO)$_4$MCp'(CO) (Cp*: M = Rh, Ir, Cp: M = Rh)

Therefore, the mechanism incorporating the initial formation of a donor-acceptor metal-metal bond is favoured. This mechanism is in accord with previous low temperature NMR studies on related systems; it would seem unlikely that simply changing from a H to a CF_3 group would so dramatically alter the mechanism. In all studied cases, the first step is the dissociation of CO from $Os(CO)_4(\eta^2\text{-}HCCR)$.

5.5 Fluxional Behaviour of Heterodimetallacyclobutenes, 14a-b, 15

5.5.1. Variable Temperature ^{13}C NMR Behavior

The ^{13}C NMR spectrum of ^{13}CO enriched **14b** did not, at 23 °C, show the expected five signals in the carbonyl region. Only three signals were seen, in a 2:1:2 ratio, and upon cooling two of these signals broadened and eventually decoalesced. This indicated that the carbonyl ligands were fluxional on the NMR time scale. Unfortunately, in the case of **14b**, a limiting spectrum exhibiting signals for five different terminal carbonyls could not be obtained. However, a limiting spectrum could be obtained for **15** and the variable temperature ^{13}C NMR spectra of **15** are shown in Figure 5.3.

At the low temperature limit of -70 °C, five carbonyl signals of equal intensity are present, consistent with the solid state structure of **15**. As the temperature is raised, four of the peaks broaden and coalesce, while one signal remains sharp. Finally, at ambient temperature, three signals are present, similar to what was observed in the case of **14b**. These changes with temperature are reversible, indicating that the scrambling process is intramolecular and proceeds without CO dissociation. This can further be corroborated by the observation that a pentane solution of **15** does not enrich when stirred under an atmosphere of ^{13}CO at ambient temperature. In order to account for the observed changes in the ^{13}C NMR spectra with changing temperature a truncated merry-go-round exchange mechanism[19] is proposed (Scheme 5.7).

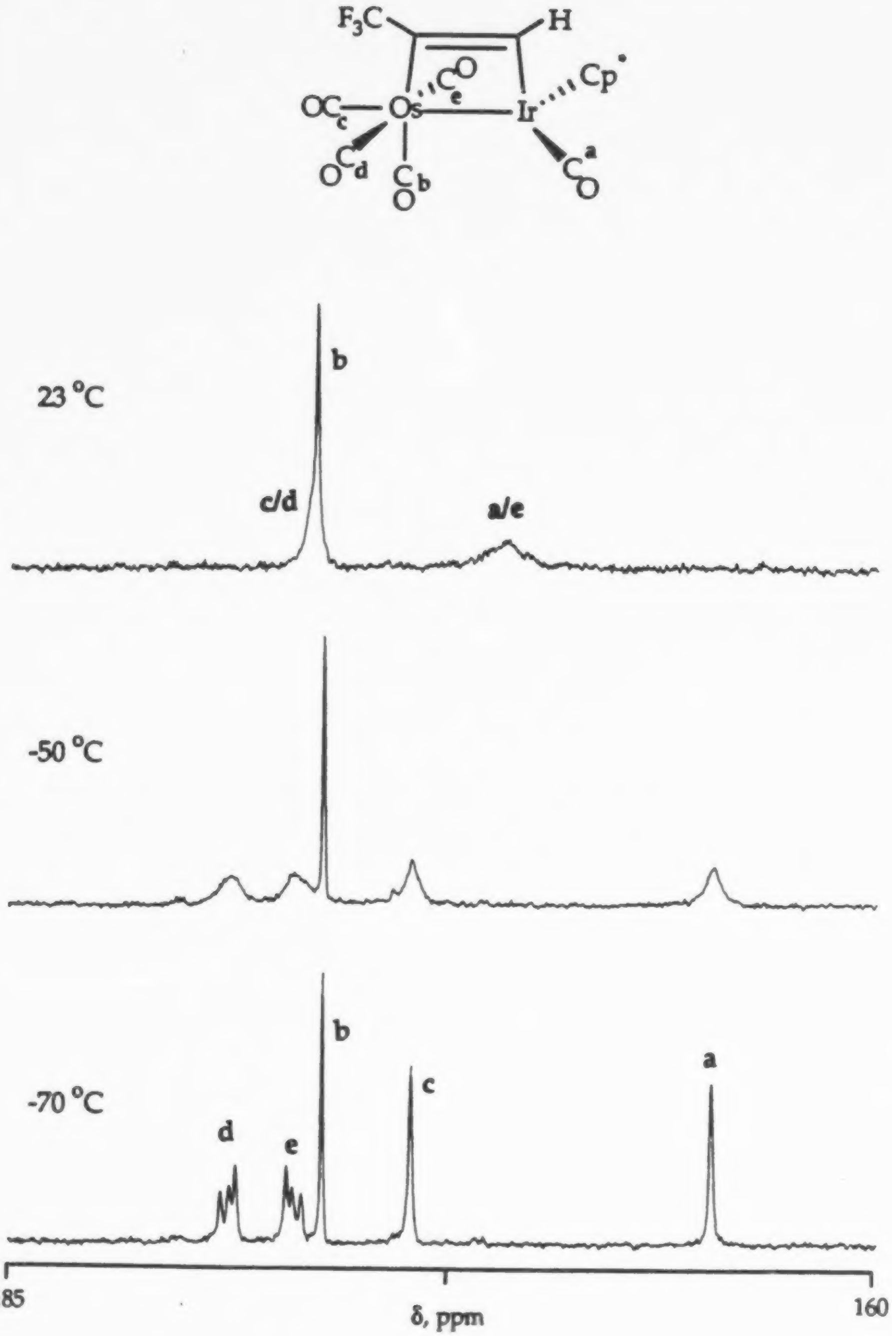

Figure 5.3: Variable Temperature ^{13}C NMR of **15** in the Carbonyl Region

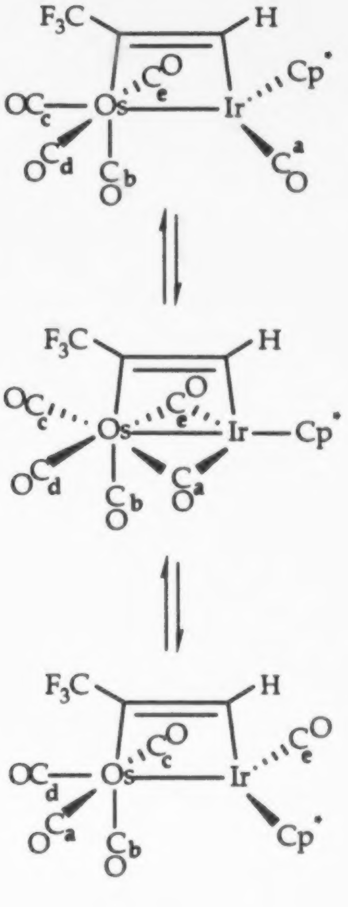

Scheme 5.7: Truncated Merry-Go-Round Exchange in **15**

The first step in the exchange process is the formation of a doubly CO bridged intermediate. This step is rendered favorable as the Ir-CO is in the same plane as the equatorial carbonyls attached to the osmium centre. The observation of facile CO exchange in a plane is common, and usually proceeds with a low energy of activation.[10b,19,20] The transfer of the CO_a to osmium and CO_e to the iridium centre is then completed in the third step, along with the exchange of positions for CO_c and CO_d. The merry-go-round exchange cannot proceed further in the same direction as this would invoke the transfer of the Cp* unit to the osmium centre. Thus, the process merely reverses itself and proceeds in the opposite direction. This exchange mechanism results in the pairwise exchange of CO_c with CO_d and CO_a with CO_e. Notice that the axial osmium carbonyl, CO_b, is not involved in the exchange. The actual assignment of the carbonyl signals in the limiting spectrum makes use of this mechanism. The axial carbonyl, CO_b, can be assigned immediately as it is not involved in the exchange mechanism and its signal remains sharp. The iridium carbonyl was assigned based on its highfield position.[8] The two trans equatorial osmium carbonyls, CO_d and CO_e, could be distinguished by *trans* ^{13}C-^{13}C coupling of 38.0 Hz.[21] Thus, by process of elimination, CO_c was assigned as the osmium carbonyl *trans* to the metal-metal bond. The chemical shift of this carbonyl is upfield of the *trans* equatorial carbonyls, a feature that has been observed previously in Chapter 2 and by other workers.[10b,22] The specific assignment of the two equatorial carbonyls on the Os centre is based upon the averaged signals present at ambient temperature coupled with the postulated exchange mechanism.

As discussed previously, a limiting ^{13}C NMR spectrum in the carbonyl region could not be observed for **14b**. However, for its Cp analogue, **14a**, a limiting ^{13}C NMR spectrum was obtained at -50 °C. The room temperature spectrum of **14b** and -50 °C spectrum of **14a** are shown in Figure 5.4.

The lower spectrum shows the expected five carbonyl signals with the lowfield signal having characteristic Rh-C coupling of 79.3 Hz.[8a] The top spectrum is representative of the fast exchange limit and only three signals are present. Here, the downfield signal has an intensity of two and is a doublet with $^{1}J_{Rh\text{-}C}$ = 38.3 Hz. The coupling has decreased by approximately one-half as a result of the pair-wise exchange process. The chemical shifts of the carbonyl signals for **14a** and **14b** are given in the Experimental Section and follows the labelling scheme in Figure 5.4.

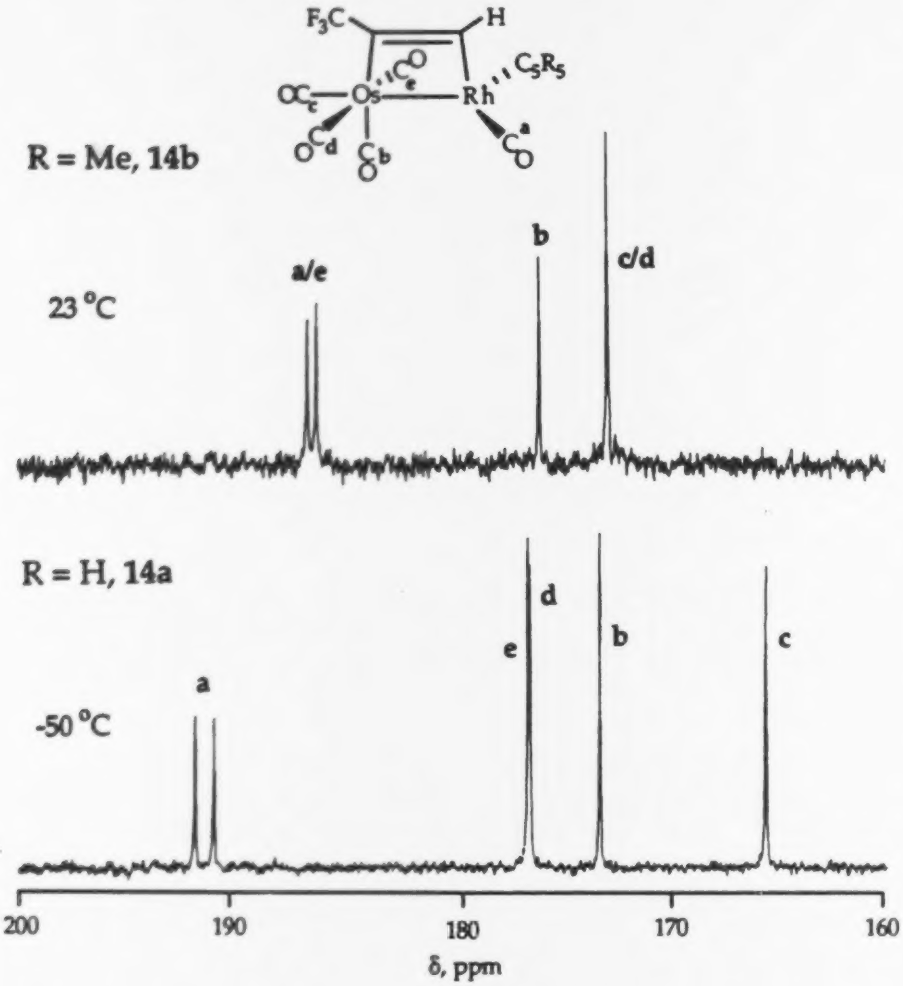

Figure 5.4: ^{13}C NMR Spectra of **14a** and **14b** in the Carbonyl Region

5.5.2. Magnetization Transfer Experiment on 15

In order to confirm the truncated merry-go-round exchange mechanism for **15** (and, by analogy, **14a-b**), a magnetization transfer experiment was carried out on a highly ^{13}CO enriched sample of **15**. The experiments were conducted at temperatures where slow to moderate exchange rates were present. The actual experiment involved selectively inverting one carbonyl signal using a DANTE pulse sequence and sampling the longitudinal magnetizations at various times; any carbonyl sites exchanging with the inverted site would show an initial decrease in intensity.[23] An example of the experimental observations is given in Figure 5.5 whereby inversion of the high field CO signal results in a decrease in intensity only for the signal assigned to CO$_e$.

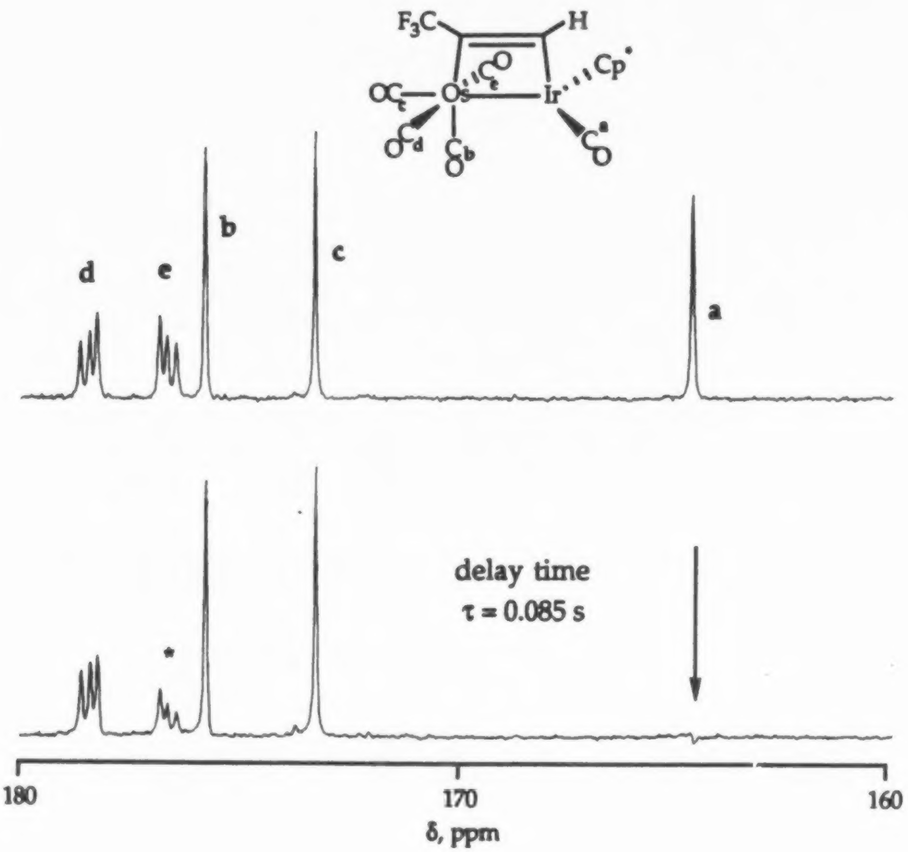

Figure 5.5: Magnetization Transfer Experiment on **15** at -75 °C

The experiments were performed in order to confirm that the carbonyls were only exchanging in a pairwise fashion and to refute any mechanism involving wholesale carbonyl exchange. The magnetization transfer experiments confirmed the pairwise nature of the exchange and thus provided conclusive evidence for the truncated merry-go-round mechanism. The experiment also confirms that the exchange is occurring in an intramolecular fashion, as expected. The rate of exchange at selected temperatures was determined by this method and the observed spectra simulated[24] at higher temperatures allowing the activation parameters for this process to be determined by using a standard Eyring plot (Table 5.6). For compounds **14a** and **14b** only rate data obtained from spectral simulation were used (Appendix 1).

Table 5.6: Activation Parameters for CO Exchange in $(\mu\text{-TFP})Os(CO)_4M(\eta^5\text{-}C_5R_5)(CO)$ (R = Me, M = Rh, Ir; R = H, M = Rh)

compound	ΔH‡ (kJ/mol)	ΔS‡ (J/mol·K)
14a[a]	44.7 ± 1.8	-32.6 ± 7.0
14b[a]	23.4 ± 1.1	-41.0 ± 4.3
15[b]	38.7 ± 1.8	-31.9 ± 8.3

[a] Activation parameters determined from rate data obtained from fitting simulated spectra to observed spectra only.

[b] Activation parameters determined from magnetization transfer rate data and rate data obtained from fitting simulated spectra to observed spectra.

As noted, a limiting spectrum for **14b** could not be obtained however, for its Cp analogue, **14a**, a limiting ^{13}C NMR spectrum was observed at -50 °C. In order to simulate the spectra of **14b** the chemical shift difference (in Hz) for the exchanging signals in **14b** were approximated by the shift difference in **14a**. The values quoted for $\Delta H^\ddagger$ and $\Delta S^\ddagger$ for **14b** are derived from these parameters and the error limits reflect the uncertainties in fitting the simulated to the observed spectra. To estimate the error in the model the shift difference was varied by 10%; a re-simulation of the spectra resulted in values of $\Delta H^\ddagger = 23.4 \pm 4.9$ kJ/mol and $\Delta S^\ddagger = -41.0 \pm 20.6$ J/mol·K.

As can be seen, with the Cp* ligand, the carbonyl exchange is much more favourable in the Os-Rh case than for Os-Ir. This bears out our preliminary expectations as a limiting spectrum for **14b** could not be obtained, while for **15**, a limiting spectrum was obtained at -70 °C. The lower activation energy for **14b** can be rationalized using the increased propensity to form bridging carbonyls as one ascends a triad,[25] thus making the first step in the exchange process more accessible. This phenomenon has been observed previously[1b] for the series of compounds of the type $MM'(CO)_8(\mu\text{-HFB})$ where the activation energies follow the trend RuRu (46.0 kJ/mol) < RuOs (60.2 kJ/mol) < OsOs (static at room temperature) and is the normal trend observed for intermetallic CO exchange in cluster carbonyls.[10b,20,26] The increased activation barrier for **14a** relative to **14b** reflects the decrease in electron donation in changing from the Cp* to the Cp ligand. Bridging carbonyls are better π acids than terminal carbonyls, thus bridging carbonyls are favoured for electron rich compounds. The increase in electron density when switching from Cp to Cp* causes an expansion of the Rh 4*d* orbitals, allowing better overlap with the π^* orbitals of the bridging carbonyl, thus making the initial step more likely, decreasing the activation barrier.[10b,22] A similar observation has been observed in the trinuclear cluster $[Os(CO)_4]_2Rh(\eta^5\text{-}C_5R_5)(CO)$ (R = H, Me) where a limiting spectrum could only be obtained for the Cp analogue, the Cp* complex was fluxional even below -80 °C.[20b]

The rather large negative entropy of activation is not surprising. The first step in the exchange process involves the synchronous formation of two carbonyl bridges, causing a change from C_1 to C_s symmetry. The formation of a more symmetrical intermediate would account for the unfavourable entropy of activation, although the correlation between $\Delta S^{\ddagger}$ and mechanism is not always observed.[27]

5.6. Synthesis and Characterization of $[\mu-\eta^3:\eta^1-(CF_3)C_2HC(O)]-Os(CO)_4CoCp^*$, 16

The reaction of $Os(CO)_4(\eta^2\text{-TFP})$ with $Cp^*Co(CO)_2$ led to the formation of a dimetallic compound with a molecular composition similar to **14a-b**, **15**. However, the product, **16**, had quite different spectroscopic properties from the dimetallacyclobutenes. First, in the FT-IR spectrum, only four terminal carbonyl signals were seen. However, another band at 1771 cm^{-1} was also present. The position of this band indicated a bridging carbonyl group or an acyl group resulting from the formation of a dimetallacyclopentenone ring. If an acyl has been formed, the relatively high energy of the signal would indicate that a cyclopentenone ring had been formed where the olefinic fragment was coordinated to a metal centre.[28] The presence of an acyl group was further strengthened by a ^{13}C NMR resonance at 220.1 ppm, which is too far upfield to be assigned to a bridging carbonyl. For comparison, the bridging carbonyl in $(\mu-\eta^2,\eta^2\text{-HFB})(\mu\text{-CO})Ru(CO)_3CoCp^*$ has[1b] its ^{13}C NMR signal at 260.0 ppm and the bridging CO in $[\mu-\eta^1,\eta^2\text{-HCCH}(PMe_3)](\mu\text{-CO})Os(CO)_3CoCp$, **6a**, resonates at 282.1 ppm. Also, two widely separated ring resonances, one at 115.4 ppm and the other at 41.1 ppm, were observed, these again are in regions characteristic for a dimetalla–cyclopentenone ring with a coordinated olefinic moiety.[28] Finally, in the ^1H NMR spectrum, the ring proton appeared as a singlet at 3.62 ppm, at relatively high field. This chemical shift indicated that the proton was in the position adjacent to the acyl carbon (α position). If the proton was in the β position the chemical shift would be expected to shift to a value in the downfield region as the β carbon resembles a bridging methylene. For example, in [μ-$C_2H_2C(O)$]$Os(CO)_4CoCp(CO)$, **2a**, the β proton resonates in the ^1H NMR spectrum at 8.45 ppm, while the α proton appears at 4.13 ppm. Thus **16** was formulated as a heterodimetallacyclopentenone (Scheme 5.8).

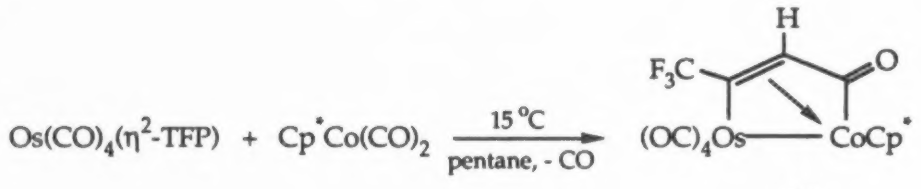

16

Scheme 5.8: Reaction of $Os(CO)_4(\eta^2\text{-TFP})$ with $Cp^*Co(CO)_2$

Thus, **16** is significantly different from the $Cp^*M(CO)_2$ (M = Rh, Ir) reaction products. When the reaction is monitored by FT-IR spectroscopy, only starting materials and **16** are seen; formation of a dimetallacyclobutene is not observed. However, it is possible that a dimetallacyclobutene ring is formed and followed by immediate carbonyl insertion into the metal-carbon bond (Scheme 5.9). This step could be facilitated by the ready ability of first row metals to undergo alkyl migration reactions.[29]

Furthermore, the reaction of $Ru(CO)_4(\eta^2\text{-HFB})$ with $Cp^*Co(CO)_2$ leads to the formation of $(\mu\text{-HFB})Ru(CO)_4CoCp^*(CO)$.[1b] Presumably, the stronger $Co\text{-}C(CF_3)$ σ bond in this complex, due to the CF_3 substituent, prevents the CO insertion reaction.

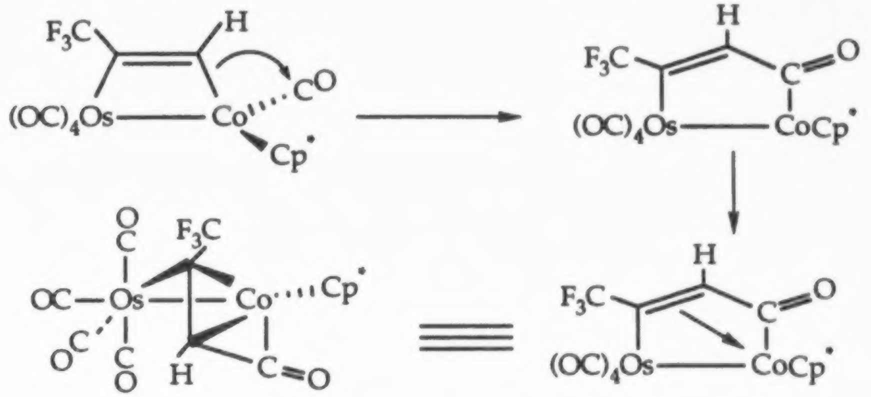

Scheme 5.9: Mechanism for Formation of **16**

Also, in support of this is the reaction of $(\mu\text{-TFP})Ru_2(CO)_8$ with PMe_3, which proceeds with a migratory insertion involving only the Ru-C(H) σ-bond.[30]

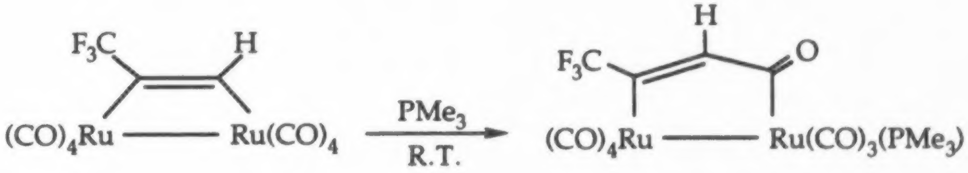

This represents a case where the insertion could have proceeded to yield two different regioisomers, however only a single regioisomer was observed indicating the increased migratory amplitude of the Ru-C(H) σ-bond as compared to the $Ru\text{-}C(CF_3)$ σ-bond.

5.7. Fluxional ^{13}C NMR Behaviour of $[\mu-\eta^3:\eta^1-(CF_3)CCHC(O)]-Os(CO)_4CoCp^*$

The variable temperature ^{13}C NMR spectra of ^{13}CO enriched **16** is shown in Figure 5.6.

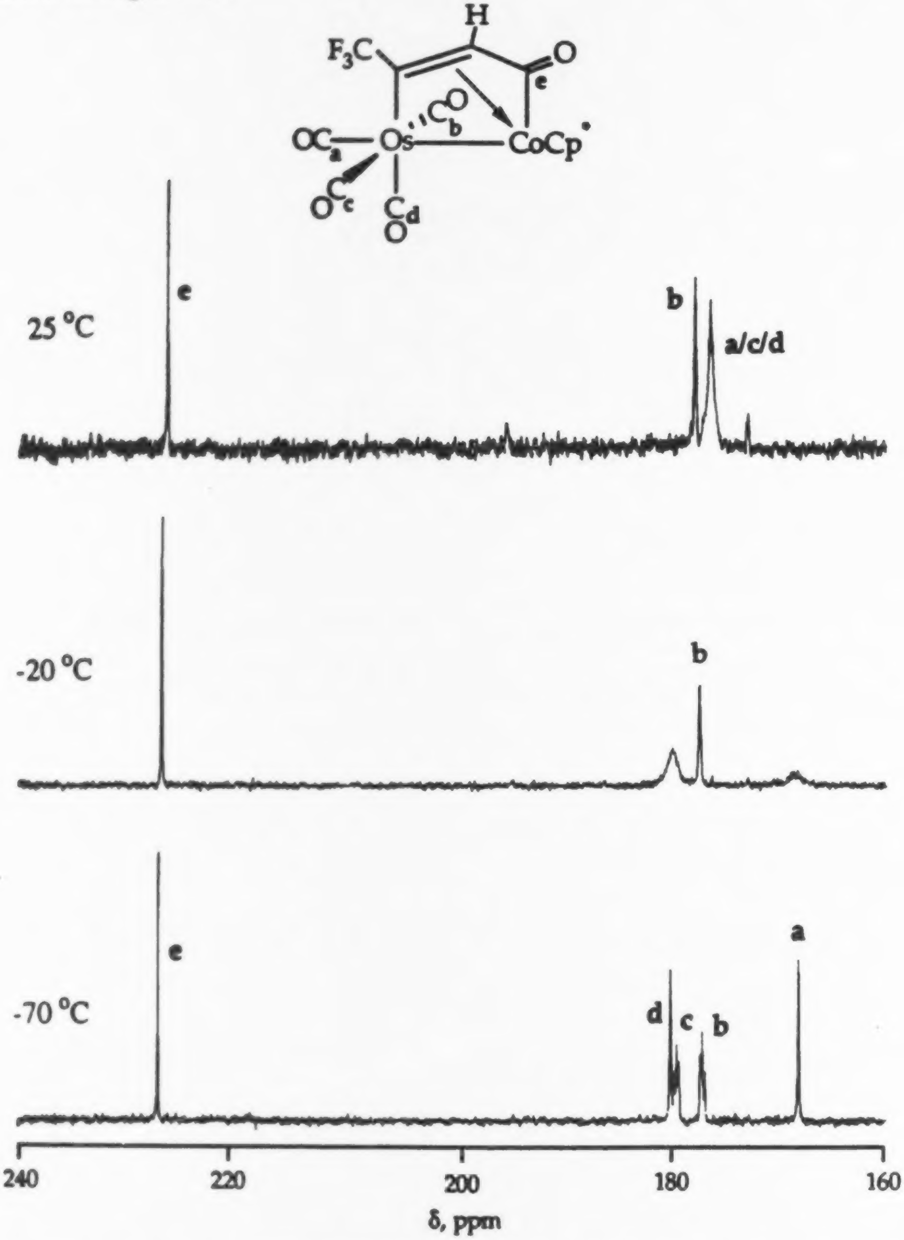

Figure 5.6: Variable Temperature ^{13}C NMR of **16** in the Carbonyl Region

The low temperature limiting spectrum is consistent with the deduced solid state structure. The characteristic low field acyl signal is present, along with four terminal carbonyl resonances. The chemical shift values for the four terminal carbonyls are in the region expected for terminal carbonyl groups attached to an osmium centre.[8a] Also, the two *trans* equatorial carbonyls on the osmium could be readily identified via the *trans* ^{13}C-^{13}C coupling of 35.0 Hz.[21] The remaining two carbonyls could not be positively assigned; however one may tentatively assign the highest field signal to the CO along the metal-metal vector, analogous to the case of **14a** and **15**. The lowest field terminal carbonyl resonance is then assigned to the remaining axial CO. As the sample is warmed, three of the terminal signals broaden and coalesce. The acyl resonance and one of the equatorial signals remain sharp. Finally, at room temperature, a single broad peak integrating to three carbonyls appears. To account for these temperature dependent ^{13}C NMR features a 'turnstile' exchange[22,31] mechanism is postulated. In this process, one axial and two equatorial carbonyls occupying a triangular face of the octahedron undergo a trigonal rotation and are interconverted; the equatorial CO on the opposite face is not involved in this exchange and thus its signal remains sharp throughout the temperature range studied (Scheme 5.10).

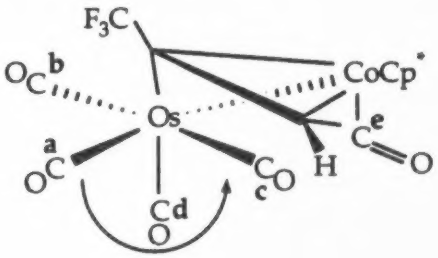

Scheme 5.10: Turnstile Carbonyl Exchange Mechanism

The experimental spectra could be simulated and activation parameters were obtained for **16**. A comparison of the activation parameters of **16** with those for **14a-c** and **15** is not possible due to the difference in exchange mechanisms, however, the ΔH‡ and ΔS‡ values for **2a-b** and **16** are listed in Table 5.7.

Table 5.7: Activation Parameters for CO Exchange in $[\mu-\eta^3:\eta^1-(CF_3)CCHC(O)]Os(CO)_4CoCp^*$

compound	ΔH‡ (kJ/mol)	ΔS‡ (J/mol·K)
16	53.4 ± 2.6	35.1 ± 10.1
2a	59.6 ± 3.0	27.4 ± 11.4
2b	61.0 ± 2.1	13.1 ± 7.6

As seen, the turnstile CO exchange is slightly more favourable in **16** than in **2a** or **2b**. Initially, one might expect the more electron withdrawing TFP bridge to raise the activation barrier of exchange in **16** as compared to **2a-b**. However, the presence of the electron rich Cp* group in **16** rather than a Cp group (**2a-b**) may counter this effect. In comparing the FT-IR spectra of **16** and **2a-c**, one sees little difference in the electron density at the Os centre. Therefore similar activation parameters can be expected; the values of ΔH‡ and ΔS‡ are, within error, nearly equivalent.

5.8. Conclusions

The reaction of $Os(CO)_4(\eta^2\text{-TFP})$ with $Cp'M(CO)_2$ (Cp^*: M = Co, Rh, Ir; Cp: M = Rh) proceeded readily under mild conditions. The reaction displays metal dependence; for M = Rh, Ir dimetallacyclobutenes are formed, for M = Co, one observes a dimetallacyclopentenone. In addition, the reaction is regioselective with the C-H carbon being attached, or adjacent, to the Group IX metal. This regioselectivity was confirmed using spectroscopic and X-ray crystallographic methods. As seen with related complexes, the TFP bridged compounds have CO ligands that are fluxional *via* a truncated merry-go-round process. This process is blocked for M = Co; thus three of the terminal carbonyls interconvert *via* a turnstile mechanism. A low temperature ^{13}C NMR study suggests that CO dissociation from $Os(CO)_4(\eta^2\text{-TFP})$ is the initial step in the formation of the dimetallic species.

5.9. Experimental Section

5.9.1. Starting Materials and Reagents

Trifluoropropyne (TFP) was purchased from Farchan Chemical Co. and used without further purification. $Cp^*Co(CO)_2$[32], $Cp^*Rh(CO)_2$[33] and $Cp^*Ir(CO)_2$[34] were prepared by published procedures.

5.9.2. Synthetic Procedures

Synthesis of $[\mu-\eta^1:\eta^1-(F_3C)CCH]Os(CO)_4RhCp^*(CO)$, 14b

A pentane solution containing $Os(CO)_4(\eta^2\text{-TFP})$, **13**, (14.0 mg, 0.035 mmol) and $Cp^*Rh(CO)_2$ (14.5 mg, 0.049 mmol) was warmed from -40 °C to 15 °C using a dry ice/acetone bath. The solution was maintained at 15 °C and the reaction was monitored by IR spectroscopy. The reaction was complete in *ca*. 2 h after which time the solvent was removed *in vacuo* and the solid left under dynamic vacuum for several hours. The residue was extracted with pentane (2x10 mL). The combined extracts were filtered, reduced to half their volume and cooled to -80 °C overnight. The supernatant solution was filtered off and the orange crystals were washed with cold pentane (2x5 mL). The yield of **14b** was 20.7 mg (89%).

Formula Weight: 662.42

Mass Spectrum(180 °C, 70eV): M^+ (664, 9.8%), M^+-nCO (n = 0-5)

IR(pentane, cm^{-1}) ν(CO): 2107(m), 2034(s), 2028(m), 2001(s), 1984(w).

^1H NMR(360 MHz, CD_2Cl_2) 7.41 (1H, dq, $^2J_{Rh\text{-}H} = 3.8$ Hz, $^4J_{F\text{-}H} = 2.2$ Hz, C-*H*), 1.95 (15H, s, $C_5(CH_3)_5$)

^{13}C NMR(125.6 MHz, CD_2Cl_2, 23 °C) 130.8 (dq, $^1J_{Rh-C}$ = 24.8 Hz, $^3J_{F-C}$ = 8.5 Hz, *C*-H), 122.4 (qd, $^1J_{F-C}$ = 270.5 Hz, $^3J_{Rh-C}$ = 1.3 Hz, *C*F_3), 101.8 (s, $C_5(CH_3)_5$), 97.4 (dq, $^2J_{F-C}$ = 36.1 Hz, $^2J_{Rh-C}$ = 5.9 Hz, *C*-CF_3), 9.9 (s, $C_5(CH_3)_5$).

^{13}C NMR(90.5 MHz, CD_2Cl_2, 23 °C) 186.5 (2CO, d, $^1J_{Rh-C}$ = 38.3 Hz, $CO_{a/e}$), 176.0 (1CO, CO_b), 172.8 (2CO, $CO_{c/d}$).

^{19}F NMR(376.4 MHz, CD_2Cl_2) -64.4.

Anal Calcd. for $C_{18}H_{16}F_3O_5OsRh$: C, 32.64; H, 2.43. Found: C, 32.97; H, 2.36.

Synthesis of [$\mu-\eta^1:\eta^1$-(F_3C)CCH]Os(CO)$_4$RhCp(CO), 14a

Using a similar procedure, **13** (23.8 mg, 0.060 mmol) and CpRh(CO)$_2$ (20.1 mg, 0.090 mmol) were used to obtain yellow crystals of **14a** (29.2 mg, 82%).

Formula Weight: 592.29

Mass Spectrum(150 °C, 70eV): M^+ (594, 22.8%), M^+-nCO (n = 0-5)

IR(pentane, cm^{-1}) ν(CO): 2118(m), 2045(s), 2038(m), 2012(s), 2001(w).

^1H NMR(360 MHz, CD_2Cl_2) 7.93 (1H, dq, $^2J_{Rh-H}$ = 4.1 Hz, $^4J_{F-H}$ = 2.0 Hz, C-*H*), 5.55 (5H, s, C_5H_5)

^{13}C NMR(90.5 MHz, CD_2Cl_2, 23 °C) 121.7 (q, $^1J_{F-C}$ = 269.9 Hz, *C*F_3), 118.7 (dq, $^1J_{Rh-C}$ = 23.0 Hz, $^3J_{F-C}$ = 8.2 Hz, *C*-H), 96.9 (m, *C*-CF_3), 91.5 (d, $^1J_{Rh}$-C = 3.1 Hz, C_5H_5).

^{13}C NMR(90.5 MHz, CD_2Cl_2, -50 °C) 191.6 (d, $^1J_{Rh-C}$ = 79.3 Hz, CO_a), 176.8 (CO_e), 176.6 (CO_d), 173.4 (CO_b), 165.7 (CO_c).

^{19}F NMR(376.4 MHz, CD_2Cl_2) -64.6.

Anal Calcd. for $C_{13}H_6F_3O_5OsRh$: C, 26.36; H, 1.02. Found: C, 26.17; H, 0.91.

Synthesis of [μ–η^1:η^1-(F$_3$C)CCH]Os(CO)$_4$IrCp*(CO), 15

Using a similar procedure, **13** (19.6 mg, 0.049 mmol) and Cp*Ir(CO)$_2$ (23.2 mg, 0.061 mmol) were used to obtain yellow crystals of **15** (31.7 mg, 85%).

Formula Weight: 751.72

Mass Spectrum(180 °C, 70eV): M$^+$ (754, 7.4%), M$^+$-nCO (n = 0-5)

IR(pentane, cm^{-1}) ν(CO): 2109(m), 2037(s), 2027(m), 2001(s), 1971(w).

^{1}H NMR(360 MHz, CD$_2$Cl$_2$) 7.97 (1H, q, $^4J_{F\text{-}H}$ = 2.2 Hz), 2.06 (15H, s, C$_5$(C*H*$_3$)$_5$)

^{13}C NMR(100.6 MHz, CD$_2$Cl$_2$, 23 °C) 124.2 (q, $^1J_{F\text{-}C}$ = 270.1 Hz, CF$_3$), 110.9 (q, $^2J_{F\text{-}C}$ = 8.0 Hz, C-H), 97.9 (s, *C*$_5$(CH$_3$)$_5$), 96.4 (q, $^2J_{F\text{-}C}$ = 35.2 Hz, C-CF$_3$), 9.59 (s, C$_5$(CH$_3$)$_5$).

^{13}C NMR(100.6 MHz, CD$_2$Cl$_2$, -70 °C) 178.5 (CO$_d$), 176.6 (CO$_e$), 175.8 (CO$_b$), 173.3 (CO$_c$), 164.6 (CO$_a$).

^{19}F NMR(376.4 MHz, CD$_2$Cl$_2$) -64.7.

Anal Calcd. for C$_{18}$H$_{16}$F$_3$IrO$_5$Os: C, 28.76; H, 2.15. Found: C, 29.38; H, 2.29.

Synthesis of [μ–η^3:η^1-(CF$_3$)CCHC(O)]Os(CO)$_4$CoCp*, 16

Compound **13** (30.2 mg, 0.076 mmol) and Cp*Co(CO)$_2$ (26.5 mg, 0.106 mmol) were reacted in the same manner as **14b** to yield purple crystals of **16** (37.9 mg, 80% yield).

Formula Weight: 618.44

Mass Spectrum(180 °C, 16eV): M$^+$ (620, 2.0%), M$^+$-nCO (n = 0-5)

IR(pentane, cm^{-1}) ν(CO): 2109(m), 2036(s), 2027(m), 1999(s). ν(acyl): 1771(w).

^{1}H NMR(360 MHz, CD$_2$Cl$_2$) 3.62 (1H, s, C-*H*), 1.82 (15H, s, C$_5$(C*H*$_3$)$_5$).

^{13}C NMR(100.6 MHz, CD$_2$Cl$_2$, 23 °C) 131.4 (q, $^1J_{F\text{-}C}$ = 273.7 Hz, CF$_3$), 115.4 (q, $^2J_{F\text{-}C}$ = 39.2 Hz, C-CF$_3$), 96.7 (s, C$_5$(CH$_3$)$_5$), 41.1(q, $^3J_{F\text{-}C}$ = 4.0 Hz, C-H), 9.93 (s, C$_5$(CH$_3$)$_5$).

^{13}C NMR(90.5 MHz, CD_2Cl_2, -70 °C) 227.0 (CO_e), 179.7 (CO_d), 179.2 (CO_c), 176.8 (CO_b), 168.0 (CO_a).

^{19}F NMR(376.4 MHz, CD_2Cl_2) -57.2.

Anal Calcd. for $C_{18}H_{16}CoF_3O_5Os$: C, 34.96; H, 2.61. Found: C, 34.75; H, 2.73.

Synthesis of ^{13}CO Enriched 14a-b, 15, 16. A pentane solution of **13** was degassed by a freeze-pump-thaw cycle using liquid nitrogen. Approximately one atmosphere of ^{13}CO was admitted into the flask and the solution was stirred at room temperature for 30 minutes. This resulted in greater than 40% ^{13}CO enrichment as determined from ^{13}C NMR integrations of the bimetallic compounds. The solution of **13-^{13}CO** was then subsequently used in reactions to generate the enriched bimetallic compounds.

5.9.3. X-ray Structure Determination of 15

Pale yellow, X-ray quality crystals were grown by cooling a pentane solution of **15** to -20 °C. The X-ray data collection and structure refinement was carried out by Dr. R. McDonald at the Structure Determination Laboratory, Department of Chemistry, University of Alberta. Crystal data and general conditions of data collection and structure refinement are given in Table 5.8. Three intensity and orientation standards were checked after every 120 minutes of exposure time and showed no appreciable decay. The positions of the Ir and Os atoms were derived from a three dimensional Patterson map and the remaining non-hydrogen atoms were located in difference Fourier maps after least squares refinement. Reflection data were corrected for absorption by using the method of Walker and Stuart;[35] the minimum and maximum correction coefficients were 0.827 and 1.190. All H atoms were included at their idealized positions (calculated by assuming C-H = 0.95 Å and sp^3 or sp^2 geometry) and constrained to 'ride' with the attached C atom. The H atoms were assigned fixed, isotropic thermal parameters 1.2 times those of the parent C atom.

The final atomic coordinates are given in Table 5.9 and selected bond distances and angles for **15** are given in Tables 5.4 and 5.5, respectively.

Table 5.8: Summary of Crystallographic Data for **15**

Crystal Parameters

formula	$C_{18}H_{16}F_3IrO_5Os$
formula wt.	751.72
crystal size, mm	0.45 x 0.20 x 0.12
crystal system	monoclinic
space group	$P2_1/n$ (a non-standard setting of $P2_1/c$)
a, Å	7.8485(8)
b, Å	18.883(3)
c, Å	14.469(2)
β, deg	104.29(1)
V, Å^3	2078.0
Z	4
D_{calc}, g cm^{-3}	2.403
μ, cm^{-1}	125.42

Data Collection and Structure Refinement

diffractometer	Enraf-Nonius CAD4
radiation (λ [Å])	Mo K_α (0.71073)
monochromator	graphite crystal, incident beam
take-off angle, deg	2.0
temperature, °C	23
scan type	ω-2θ
scan rate, deg min^{-1}	1.3 - 6.7
scan width, deg in ω,	0.50 + 0.347tanθ
2θ limit, deg	50.0
reflections measured	3792 (±*h*, *k*, *l*)
reflections used	2705 with $I > 3\sigma(I)$
variables	253
R^a	0.025
$R_w{}^b$	0.032
GOF^c	1.075

$^aR = \Sigma||F_o| - |F_c||/\Sigma|F_o|$

$^bR_w = (\Sigma w(|F_o| - |F_c|)^2/\Sigma w F_o{}^2)^{1/2}$

$^cGOF = [\Sigma w(|F_o| - |F_c|)^2/(NO - NV)]^{1/2}$

Table 5.9: Positional ($\times 10^3$) and Isotropic Thermal ($\times 10^2$) Parameters for **15**

atom	*x*	*y*	*z*	*U*, Å^2
Ir	-20.22(4)	178.12(1)	267.38(2)	3.814(8)
Os	14.55(4)	298.65(2)	160.57(2)	4.507(9)
F1	-200.7(8)	400.6(3)	381.4(4)	10.5(2)
F2	-13.9(8)	445.2(3)	315.7(5)	10.4(3)
F3	-272.9(8)	423.5(3)	233.6(5)	11.0(3)
O1	339.3(8)	200.1(4)	392.1(4)	7.8(2)
O2	378.2(9)	334.4(4)	287.8(6)	10.4(3)
O3	-6.1(9)	441.3(3)	61.1(5)	10.4(3)
O4	-377.3(8)	280.6(4)	66.7(5)	8.4(3)
O5	157.5(9)	206.2(4)	21.9(5)	9.5(3)
C1	201(1)	193.5(4)	339.9(5)	4.8(3)
C2	249(1)	318.2(4)	241.7(7)	6.3(3)
C3	2(1)	388.3(5)	99.4(6)	6.8(3)
C4	-232(1)	283.3(4)	100.4(5)	5.6(3)
C5	105(1)	242.2(5)	69.7(6)	6.6(3)
C6	-105(1)	267.2(4)	324.5(5)	4.7(2)
C7	-88.9(9)	325.5(4)	279.3(6)	4.8(3)
C8	-140(1)	397.0(5)	302.8(7)	7.0(3)
C11	-30(1)	68.4(4)	200.3(6)	5.9(3)
C12	-33(1)	64.6(4)	298.2(6)	5.7(3)
C13	-180(1)	103.9(4)	153.1(6)	5.8(3)
C14	-283(1)	121.9(4)	220.4(6)	6.0(3)
C15	-187(1)	103.9(4)	153.1(6)	5.7(3)
C21	97(1)	32.3(5)	154.6(8)	10.0(4)
C22	96(1)	25.7(5)	374.8(8)	10.4(5)
C23	-252(1)	101.1(6)	399.9(7)	10.3(4)
C24	-465(1)	153.6(6)	198.3(9)	9.2(4)
C25	-248(1)	109.3(6)	44.5(7)	9.5(5)

5.10. References

1. (a) Burn, M.J.; Kiel, G.-Y.; Seils, F.; Takats, J.; Washington, J. *J. Am. Chem. Soc.* **1989,** *111*, 6850. (b) Gagné, M.R.; Takats, J. *Organometallics* **1988,** *7*, 561.

2. (a) Herberich, G.E.; Berlage, W.; Linn, K. *J. Organomet. Chem.* **1991,** *414*, 193. (b) Dickson, R.S.; McLure, F.I.; Nesbit, R.J. *J. Organomet. Chem.* **1988,** *349*, 413. (c) Puddephatt, R.J.; Thomson, M.A. *Inorg. Chem.* **1982,** *21*, 725.

3. (a) Wrackenridge, B.; Horchler, K. *Prog. Nucl. Magn. Reson. Spect.* **1990,** *22*, 209. (b) Silverstein, R.M.; Bassler, G.C.; Morrill, T.C. *Spectrometric Identification of Organic Compounds*, Wiley: New York, 1981, Ch. 5., pg. 253.

4. Lukehart, C.M. *Fundamental Transition Metal Organometallic Chemistry*; Brooks/Cole: Monterey, CA, 1985; Chapter 10.

5. (a) Dixon, D.A.; Smart, B.E. *J. Phys. Chem.* **1989,** *93*, 7772. (b) Koblukowski, M. personal communication.

6. (a) Jordan, R.B. *Reaction Mechanisms of Inorganic and Organometallic Systems*, Oxford University Press: New York, 1991; Chapter 5. (b) Zeigler, T.; Tschinke, V.; Ursenbach, C. *J. Am. Chem. Soc.* **1987,** *109*, 4825.

7. Hales, L.A.W.; Irving, R.J. *J. Chem. Soc.(A)* **1967**, 1389.

8. (a) Mann, B.E.; Taylor, B.F. *^{13}C NMR Data for Organometallic Compounds;* Academic: New York, 1981. (b) Kiel, G.-Y. personal communication. (c) Jacke, J. personal communication.

9. (a) Rosenberg, D.; Drenth, W. *Tetrahedron* **1971**, *27* ,3893. (b) Rosenthal, U.; Oehme, G.; Burlakov, V.V.; Petroski, P.V.; Shur, V.B.; Volpin, M.E. J. Organomet. Chem. **1990**, *391*, 119. (c) Dawson, D.A.; Reynolds, W.F.; *Can. J. Chem.* **1975**, *53*, 373.

10. (a) Hilts, R.W.; Franchuk, R.A.; Cowie, M. *Organometallics*, **1991**, *10*, 1297. (b) Riesen, A.; Einstein, F.W.B.; Ma, A.K.; Pomeroy, R.K.; Shipley, J.A. *Organometallics*, **1991**, *10*, 3629. (c) Rausch, M.D.; Gastinger, R.G.; Gardner, S.A.; Brown, R.K.; Wood, J.S. *J. Am. Chem. Soc.* **1977**, *99*, 7870. (d) Burke, M. Ph.D. Thesis, University of Alberta, **1987**. (e) Burke, M.R.; Takats, J. *J. Organomet. Chem.* **1986**, *302*, C25.

11. (a) Collman. J.P.; Hegedus, L.S.; Norton, J.R.; Finke, R.G. *Principles and Applications of Organotransition Metal Chemistry*; University Science Books: Mill Valley, CA, 1987; Chapter 5. (b) Connor. J.A. *Topics Current Chem.* **1977**, *71*, 71.

12. (a) Petrucci, R.H.; Harwood, W.S. *General Chemistry: Principles and Modern Apllications, Sixth Edition*, MacMillan: New York, 1993; pg. 332. (b) Allen, F.H.; Kennard, O.; Watson, D.G.; Brammer, L.; Orpen, A.G.; Taylor, R. *J. Chem. Soc., Perkin Trans. II*, **1987**, S1.

13. Jenkins, J.A.; Cowie, M. *Organometallics*, **1992**, *11*, 274 and references therein.

14. Bennett, M.J.; Graham, W.A.G.; Stewart, R.P., Jr.; Tuggle, R.M. *Inorg. Chem.* **1973**, *12*, 2944.

15. (a)Hoffman, D.M.; Hoffmann, R.; Fisel, C.R. *J. Am. Chem. Soc.* **1982**, *104*, 3858. (b) Albright, T.A.; Burdett, J.K.; Whangbo, M.H. *Orbital Interactions in Chemistry*; Wiley: New York; 1985; Chapter 10; pg. 163. (c) Libit, L.; Hoffmann, R. *J. Am. Chem. Soc.* **1974**, *96*, 1370.

16. (a) Oliver, J.; Graham, W.A.G. *Inorg. Chem.* **1970**, *9*, 2653. (b) Hart-Davis, A.J.; Graham, W.A.G. *Inorg. Chem.* **1970**, *9*, 2658.

17. (a) Johnston, V.J.; Einstein, F.W.B.; Pomeroy, R.K. *J. Am. Chem. Soc.* **1987**, *109*, 7220. (b) Einstein, F.W.B.; Pomeroy, R.K.; Rushman, P.; Willis, A.C. *Organometallics*, **1985**, *4*, 280. (c) Del Paggio, A.A.; Muetterties, E.L.; Heinekey, D.M.; Day, V.W.; Day, C.S. *Organometallics*, **1986**, *5*, 575.

18. (a) Boag, N.M.; Green, M.; Stone, F.G.A. J. *Chem. Soc., Chem. Commun*. **1980**, 1281. (b) Boag, N.M.; Green, M.; Howard, J.A.K.; Stone, F.G.A.; Wadepohl, H. *J. Chem. Soc., Dalton Trans.* **1981**, 862.

19. Bond, E.; Muetterties, E.L. *Chem. Rev.* **1978**, *78*, 639.

20. (a) Mann, B.E. in *Comprehensive Orgaonmetallic Chemistry;* Wilkinson, G.; Stone, F.G.A.; Abel, E.W., Eds.; Pergamon: New York, 1982; Vol. 3, pg 89. (b) Washington, J.; Takats, J. *Organometallics*, **1990**, *9*, 925.

21. (a) Tachikawa, M.; Richter, S.I.; Shapley, J.R. *J. Organomet. Chem.* **1977**, *128*, C9. (b) Aime, S.; Osella, D. *J. Chem. Soc., Chem. Commun.* **1981**, 300.

22. Alex, R.F.; Pomeroy, R.K. *Organometallics*, **1987**, *6*, 2437 and references therein.

23. Muhandiram, D.R.; McClung, R.E.D. *J. Magn. Reson.* **1987**, *71*, 187.

24. McClung, R.E.D. *EXCHANGE: Program for the Simulation of NMR Spectra of Weakly-Coupled Exchanging Systems*, University of Alberta.

25. Elschenbroich, C.; Salzer, A. *Organometallics: A Concise Introduction;* VCH: Weinheim, 1992, Chapter 14.

26. Geoffroy, G.L. *Acc. Chem. Res.* **1980**, *13*, 469.

27. Schmidt, S.P.; Basolo, F.; Jensen, C.M.; Trogler, W.C. *J. Am. Chem. Soc.* **1986**, *108*, 1894.

28. (a) Kiel, G.-Y.; Takats, J. *Organometallics* **1989**, *8*, 839. (b) Hogarth, G.; Kayser, F.; Knox, S.A.R.; Morton, D.A.V. *J. Chem. Soc., Chem. Comm.* **1988**, 358. (c) Dyke, A.F.; Knox, S.A.R.; Naish, P.J.; Taylor, G.E. *J. Chem. Soc. Dalton Trans.* **1982**, 1297.

29. Collman, J.P.; Hegedus, L.S.; Norton, J.R.; Finke, R.G. *Principles and Applications of Organotransition Metal Chemistry*; University Science Books: Mill Valley, 1987, Chapter 6.

30. Hoffman, K.C. personal communication.

31. (a) Ready, C.; Jackson, G.; Johnson, B.F.G.; Lewis, J.; Matheson, T. *J. Chem. Soc., Chem. Comm.* **1975**, 958. (b) Deeming, A.J.; Donovan-Mtunzi, S.; Kabir, S.E. *J. Organomet. Chem.* **1985**, *281*, C43. (c) Deeming, A.J.; Donovan-Mtunzi, S.; Kabir, S.E.; Manning, P.J. *J. Chem. Soc. Dalton Trans.* **1985**, 1037.

32. Frith, S.A.; Spencer, J.L. *Inorg. Synth.* **1985**, *23*, 15.

33. Werner, H.; Klingert, B. *J. Organomet. Chem.* **1981**, *218*, 395.

34. Ball, R.G.; Graham, W.A.G.; Heinekey, D.M.; Hoyano, J.K.; McMaster, A.D.; Mattson, B.M.; Michel, S.T. *Inorg. Chem.* **1990**, *29*, 2023.

35. Walker, N.; Stuart, D. *Acta. Crystallogr., Sect. A: Found Crystallogr.* **1983**, *A39*, 158.

Chapter 6

Reaction of $Os(CO)_4(\eta^2\text{-}(CH_3)CCR)$ (R = H, CH_3) with $CpM(CO)_2$ (M= Co, Rh, Ir): Generation of Dimetallacyclopentenones

6.1. Introduction

The reaction of metal nucleophiles, namely $Cp^*M(CO)_2$, with $Os(CO)_4(\eta^2\text{-}(CF_3)CCH)$ was described in the previous Chapter. The reactions proceed in a regioselective manner as dictated by the asymmetric alkyne ligand. The CF_3 substituent on the alkyne is highly electron withdrawing, resulting in a polarized alkyne with the C-H carbon of the alkyne bearing a partial positive charge. In order to further investigate the governing factors of the condensation reactions, the alkyne substituent was altered so that an electron donating group was present. The reactions with $CpM(CO)_2$ were then carried out to determine if the products were alkyne dependent and to see if the regioselectivity of the condensation would be altered.

Propyne, $HCC(CH_3)$, a gas at ambient temperature (b.p.$_{760}$ = -23.2 °C) but readily condensed at -60 °C, was utilized. The electron donating properties of the CH_3 substituent give the polarized structure shown below.

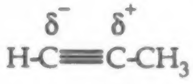

$$\overset{\delta^-}{\text{H-C}}\equiv\overset{\delta^+}{\text{C}}\text{-CH}_3$$

propyne

Dixon and Smart, using a Mulliken Population analysis, have calculated the atomic charge on the terminal acetylenic carbon to be -0.36 and the charge on the other *sp* carbon to be 0.14 (charges in electrons).[1] This polarization is also seen the ^{13}C NMR spectrum of free propyne where the C-H carbon is 13 ppm upfield of the C-CH_3 carbon.[2] This separation is nearly twice as large as the chemical shift difference between the alkyne carbons in TFP which is 6.7 ppm. Therefore, in light of previous studies, the propyne ligand should have sufficient polarization to direct product distribution to a single regioisomer. Also, by utilizing propyne as compared to trifluoropropyne, the electronic properties of the alkyne have been altered without a significant change in steric effects.

For propyne, there are two convenient NMR handles in the CH_3 and CH protons. Also, and contrary to trifluoropropyne, the alkyne carbons may be easily observed using ^{13}C NMR spectroscopy. The CH_3 substituent is an electron donating group making propyne a much weaker π acid than TFP and metal complexes of lower stability may be expected. This is borne out in $Os(CO)_4(\eta^2\text{-HCCR})$ (R = CH_3, CF_3) where the TFP complex is much more stable than its propyne analogue.[3]

The osmium-alkyne complex with 2-butyne, $Os(CO)_4(\eta^2\text{-RCCR})$ (R = CH_3) was also used in condensation reactions with $CpM(CO)_2$ (M = Co, Rh, Ir). Obviously, 2-butyne is a symmetric ligand but it is of interest to see how the reactions proceed with a very electron rich alkyne. The two CH_3 substituents give $Os(CO)_4(\eta^2\text{-}C_2Me_2)$ limited thermal stability, as expected. The use of 2-butyne also enables one to probe steric effects in these condensation reactions. All of the other alkynes described in previous Chapters have had at least one terminal alkyne proton, thus steric effects have not been fully investigated. In related work[4a] with $Os(CO)_4[\eta^2\text{-}C_2(CF_3)_2]$, the alkyne HFB is also sterically hindered and its strong electron withdrawing nature can be contrasted with its 2-butyne congener.

6.2. Reactions of $Os(CO)_4[\eta^2\text{-}(CH_3)CCH]$

6.2.1. Synthesis of $[\mu\text{-}\eta^1\text{:}\eta^1\text{-}(CH_3)C_2HC(O)]Os(CO_4MCp(CO)$, (M = Co, Rh, Ir)

The reactions were carried out in hydrocarbon solution and consisted of warming a solution of $Os(CO)_4(\eta^2$-propyne) and $CpM(CO)_2$ (M = Co, Rh, Ir) from -78 °C to 0 °C. The reaction proceeds at temperatures near -5 °C, as evidenced by a color change and the formation of a fine precipitate. The final products can be isolated as fine powders that are sparingly soluble in non-polar solvents such as pentane. An important synthetic consideration is the use of excess $CpM(CO)_2$ (M = Co, Rh, Ir) as $Os(CO)_4(\eta^2$-propyne) is thermally unstable; the use of the Group IX metal in excess ensures complete consumption of the osmium-propyne complex. Also, the use of hydrocarbon solvents is important as the resulting products precipitate out in analytically pure form; excess $CpM(CO)_2$ remains in solution.

6.2.2. Characterization of $[\mu\text{-}\eta^1\text{:}\eta^1\text{-}(CH_3)C_2HC(O)]Os(CO_4)MCp(CO)$

The reaction proceeds with all three of the Group IX cyclopentadienyl dicarbonyl complexes to yield dimetallic products of formula $[(CH_3)CCH]Os(CO)_4M(CO)_2Cp$ (M = Co, Rh, Ir).

$$\begin{matrix} Os(CO)_4[\eta^2\text{-}(CH_3)CCH] \\ + \\ CpM(CO)_2 \end{matrix} \xrightarrow[\text{pentane}]{-5\,^{\circ}C} [(CH_3)CCH]Os(CO)_4M(CO)_2Cp$$

M = Co, **17a**
= Rh, **17b**
= Ir, **17c**

As seen previously in our laboratories two coordinatively saturated, eighteen electron species react to generate a dimetallic compound with two eighteen electron metal centres without any ligand loss.[4b] However, of note is that for M = Co, Rh the reaction of $CpM(CO)_2$ with $Os(CO)_4(\eta^2\text{-}HCCH)$ results in the loss of one molecule of CO.[4b] Thus, the presence of a methyl substituent has already resulted in an alteration of the product distribution.

For **17a-c**, the elemental analyses and mass spectral data were consistent with dimetallic products. The FT-IR spectra of **17a-c** allowed for the initial assumption as to the formation of a dimetallacyclopentenone. The FT-IR data for **17a-c** are listed in Table 6.1.

Table 6.1: FT-IR Data for
$[(CH_3)CCH]Os(CO)_4M(CO)_2Cp$ (M = Co, Rh, Ir)

Compound	ν(CO) (pentane, cm^{-1})	ν(acyl)
M = Co, **17a**	2099(w), 2032(s), 2022(s), 1981(s)	1653(w)
M = Rh, **17b**	2102(w), 2034(s), 2028(m), 2003(s), 1998(w)	1634(w)
M = Ir, **17c**	2108(w), 2035(s), 2001(s), 1985(m)	1620(w)

The weak intensity acyl stretch for all three compounds is observed between 1620 and 1653 cm^{-1}. This low energy band is characteristic of an acyl group in a dimetallacyclopentenone ring where the unsaturated organic moiety is not coordinated to a metal centre.[4b,5]

With this initial information in hand what remained to be determined was the orientation of the alkyne in the cyclopentenone ring. Two regio-isomers are possible, one with the C-H carbon adjacent to the acyl group (**A**) and another where the C-H carbon is in the β-position relative to the acyl group (**B**).

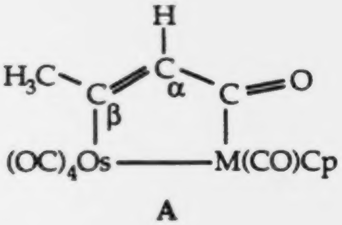

A

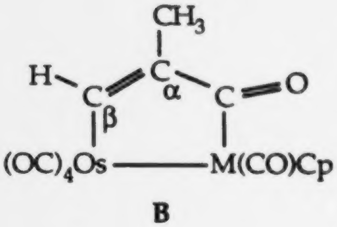

B

The ^{1}H NMR spectra for **17a-c** indicated that in each case only a single regio-isomer had been formed. The ^{1}H NMR data for **17a-c** are listed in Table 6.2.

Table 6.2: ^{1}H NMR Data for
$[(CH_3)CCH]Os(CO)_4M(CO)_2Cp$, (M = Co, Rh, Ir)

		δ (CD_2Cl_2, ppm)	
Compound	CH_3	C-*H*	$^4J_{H\text{-}H}$ (Hz)
M = Co, **17a**	2.40	6.74	1.2
M = Rh, **17b**	2.46	6.95	1.3
M = Ir, **17c**	2.47	7.21	1.3

The chemical shift values of the C-*H* protons for **17a-c** are similar. Unfortunately, the orientation of the alkyne ring cannot be determined by the ^{1}H NMR data alone. This is because, as seen in $[\mu\text{-}\eta^1:\eta^1\text{-}HCCHC(O)]Os(CO)_4Ir(CO)Cp$, **3**, the chemical shift values of the α and β protons are quite similar (**3:** H_α: 7.51 ppm, H_β: 7.98 ppm) in non-coordinated dimetallacyclopentenones. However, in comparison to **3**, one could predict the C-*H* in the α position (**A**), although this assignment is very tenuous.

A more accurate probe of the regiochemistry is ^{13}C NMR spectroscopy. The *C*-CH$_3$ and *C*-H carbons can be readily distinguished and may provide conclusive evidence of the coordination mode of the alkyne. There are two resonance forms for an α,β-unsaturated ketone.

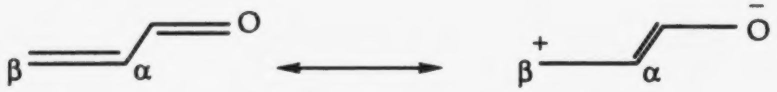

I

II

The canonical form II shows the charge separation that results from the delocalization of the electron density. As shown in Chapter 2, this charge separation manifests itself in the ^{13}C NMR spectra of α,β-unsaturated ketones as the α carbon usually resonates 20-30 ppm upfield of the β carbon.[6a-c] Levin has recorded the ^{13}C NMR spectra of a number of cyclic α,β-unsaturated ketones, the ^{13}C NMR chemical shifts of three cyclic systems are shown below.[6b,c] There is a relationship between charge densities and ^{13}C NMR chemical shift, although it should be noted that this relationship is not always linear.[6c,d] Thus, using ^{13}C NMR spectroscopy in conjunction with our organic models, the determination of the orientation of the alkyne should be straightforward.

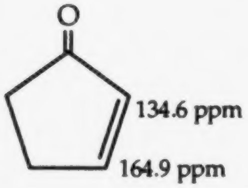

2-cyclopenten-1-one

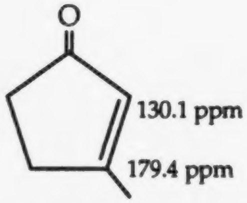

3-methyl-2-cyclopenten-1-one

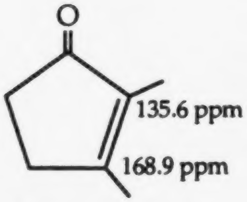

2,3-dimethyl-2-cyclopenten-1-one

The ^{13}C NMR spectra of **17a-c** were obtained on concentrated, non-^{13}CO enriched samples using long accumulation times and are listed in Table 6.3.

Table 6.3: ^{13}C NMR Data for
$[\mu\text{-}\eta^1\text{:}\eta^1\text{-}(CH_3)CCHC(O)]Os(CO)_4M(CO)Cp$, (M = Co, Rh, Ir)

	δ (CD_2Cl_2, ppm)	
Compound	C-CH_3	C-H
M = Co, **17a**	157.5	155.8
M = Rh, **17b**	156.7	158.9
M = Ir, **17c**	151.4	162.7

For **17b** and **17c** the C-H ^{13}C NMR resonance is upfield of the C-CH_3 resonance. Therefore, one would assign regio-isomer **B** as representative of the alkyne orientation. For the case of **17a**, the opposite regio-isomer, **A**, would be assigned on the basis of ^{13}C NMR chemical shift data alone. However, two observations are puzzling. It has been noticed that the condensations are metal dependent; however this metal dependency usually manifests itself in bulk structural changes, not changes in regioselectivity. Here, regio-isomer **B** is apparently formed for M = Rh, Ir and the alternate regiochemistry for M = Co. Also, the chemical shift difference between the α and β carbons is quite small, especially for **17a** and **17b**. Based on 3-methyl-2-cyclopenten-1-one, a chemical shift difference of *ca.* 49 ppm would be expected, especially in light of how the ^{13}C NMR chemical shift values of **3** matched with the organic model. Obviously, further consideration was required to unequivocally establish the regiochemistry of the dimetallacyclopentenones.

The ^{13}CO enriched analogues of **17a-c** were also prepared. In these compounds a lowfield acyl signal is observed and can be readily assigned.[7] Also, in an analogous fashion used in Chapter 2, the acyl ^{13}C NMR chemical shift values, $^{1}J_{\text{Rh-C}}$ coupling and lack of *trans* $^{13}C_{acyl}$-^{13}CO coupling were used to confirm that the acyl moiety was attached to the Group IX metal centre. To further investigate the regioselectivity, selective $^{13}C\{^{1}H\}$ NMR experiments were performed. The experiments consisted of selectively decoupling the C-*H* and CH_3 proton resonances and observing any changes in the acyl resonance. Figure 6.1 below shows the results for **17c** (M = Ir).

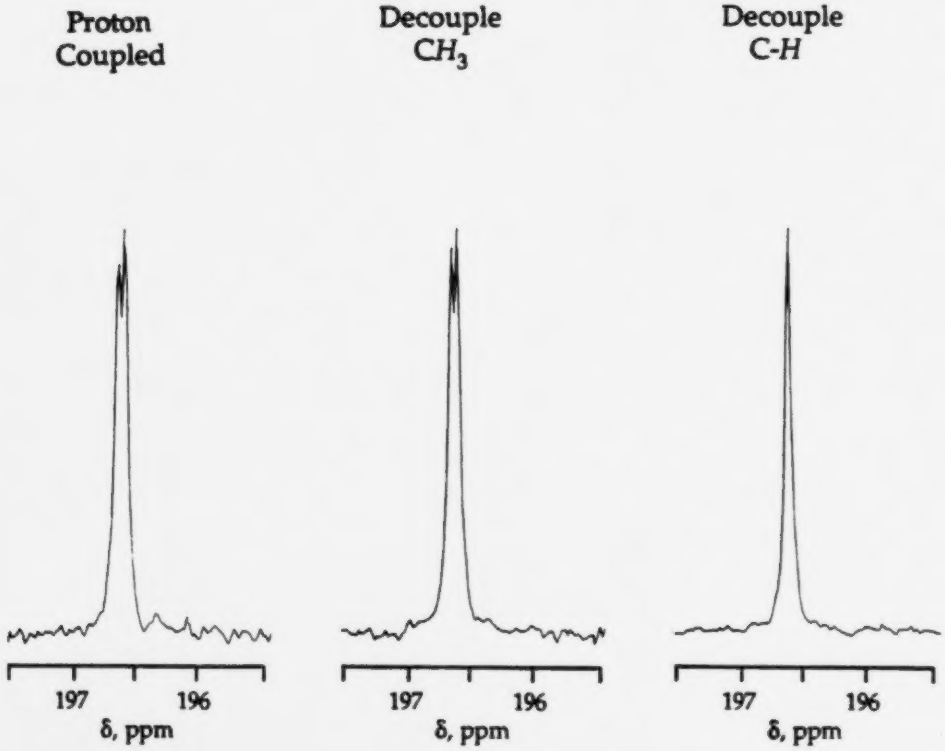

Figure 6.1: Selective $^{13}C\{^{1}H\}$ NMR Experiments on Acyl Carbon of **17c**

The acyl resonance appears as a doublet (J_{C-H} = 5.4 Hz) in the proton coupled ^{13}C NMR spectrum. Selective CH_3 decoupling caused no change in the acyl signal while C-*H* decoupling resulted in the collapse of the doublet into a singlet. This conclusively indicates that the C-*H* proton is coupled to the acyl carbonyl. A similar result was obtained for **17b** (J_{C-H} = 5.4 Hz) while for **17a** no C-H coupling was observed due to the broadness of the acyl signal. Unfortunately, at this stage, still no unambiguous assignment of structure is possible. This is because the two bond C-H coupling expected for **A** is very similar to the three bond coupling which could be expected for **B** ($^2J_{C-H}$ = 3-5 Hz, $^3J_{C-H}$ = 4-6 Hz).[8] Therefore, there still is the possibility that three bond coupling to the C-*H* proton was observed and **17b** and **17c** have the structure indicated by **B**.

To confidently assign the structure, an additional series of ^{13}C NMR experiments were carried out. Again, these involved the ^{13}CO enriched materials and an important aspect in that only the acyl and the terminal carbonyls were enriched, the *C*-H and *C*-CH$_3$ carbons were present in natural abundance (*ca*. 1.1%). The experiment simply involved a ^{13}C NMR broadband proton decoupling experiment with a long enough accumulation times to observe the dimetallacyclopentenone ring carbons. The ^{13}C-^{13}C coupling between the *C*-H carbon and the enriched acyl carbon could then be observed as small satellite peaks centred on the main *C*-H resonance. The results are listed in Table 6.4.

Table 6.4: C_α-C_{acyl} Coupling Data for
$[\mu$-η^1:η^1-$(CH_3)CCHC(O)]Os(CO)_4M(CO)Cp$, (M = Co, Rh, Ir)

	δ (CD_2Cl_2, ppm)		
Compound	C-CH_3	CH	$^1J_{CH\text{-}Cacyl}$(Hz)
M = Co, **17a**	157.5	155.8	42.0
M = Rh, **17b**	156.7	158.9	48.5
M = Ir, **17c**	151.4	162.7	50.7

The range of C_H-C_{acyl} coupling constants was from 42-51 Hz, which is intermediate between the C-C single bond coupling constant in ethane ($^1J_{C\text{-}C}$ = 34.6 Hz) and the coupling for a C-C double bond observed for ethylene ($^1J_{C\text{-}C}$ = 67.6 Hz).[8] This is reasonable since if the C-H was in the α position, one would expect some double bond character in the CH-C_{acyl} bond based on the resonance model of an α, β-unsaturated ketone. Finally, to completely confirm the structure, the observed $^{13}C_{acyl}$-$^{13}C_\alpha$ spin-spin coupling can be compared to a known organic model. Ayer and co-workers have synthesized a ^{13}C enriched organic molecule containing a substituted 2-cyclohexen-1-one ring and determined the C_α-C_{acyl} coupling constant.[9]

$^1J_{C1\text{-}C2}$ = 53.0 Hz

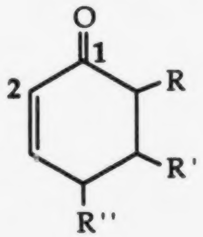

The ^{13}C-^{13}C coupling constant observed for this compound compares favourably with the values obtained for the dimetallacyclopentenones and thus allows confirmation of the assignment. For all three complexes, **17a-c**, the same regio-isomer is produced where the C-H carbon is adjacent to the acyl moiety (**A**). These results indicate that for dimetallacyclo–pentenones one cannot rely solely on ^{13}C NMR chemical shift data to determine the orientation of an asymmetric alkyne. A further discussion of this point is deferred until Section 6.4. where a comparison will be made with the $[\mu-\eta^1:\eta^1-C_2(CH_3)_2C(O)]Os(CO)_4M(CO)Cp$ (M = Co, Rh, Ir) compounds.

6.3. Molecular Structure of $[\mu-\eta^1:\eta^1-(CH_3)CCHC(O)]Os(CO)_4RhCOCp$, 17b

In light of the unusual spectroscopic properties of **17a-c**, an X-ray structure determination was undertaken to completely characterize this class of compounds. X-ray quality crystals of **17b** were chosen for this study and two ORTEP views of **17b** are shown in Figures 6.2 and 6.3. The relevant bond distances and angles for **17b** are listed in Tables 6.5 and 6.6, respectively.

Fortunately, in the case of **17b**, the structure readily refined without any problems with disorder and final values of R = 0.031 and R_w = 0.033 were obtained. Thus, contrary to **3**, the esd values are reasonable and a more meaningful analysis of the ring geometry (bond distances and angles) will be made. In addition, the positions of the carbonyls ligands are well defined, again in contrast to **3**.

The α position of the C-H carbon is confirmed, as expected from the spectroscopic results. The geometry around the Rh centre is the expected 3-legged piano stool configuration, similar to that observed for the Ir centres in **3** and **15**. As expected, the Os centre has a distorted octahedral geometry.

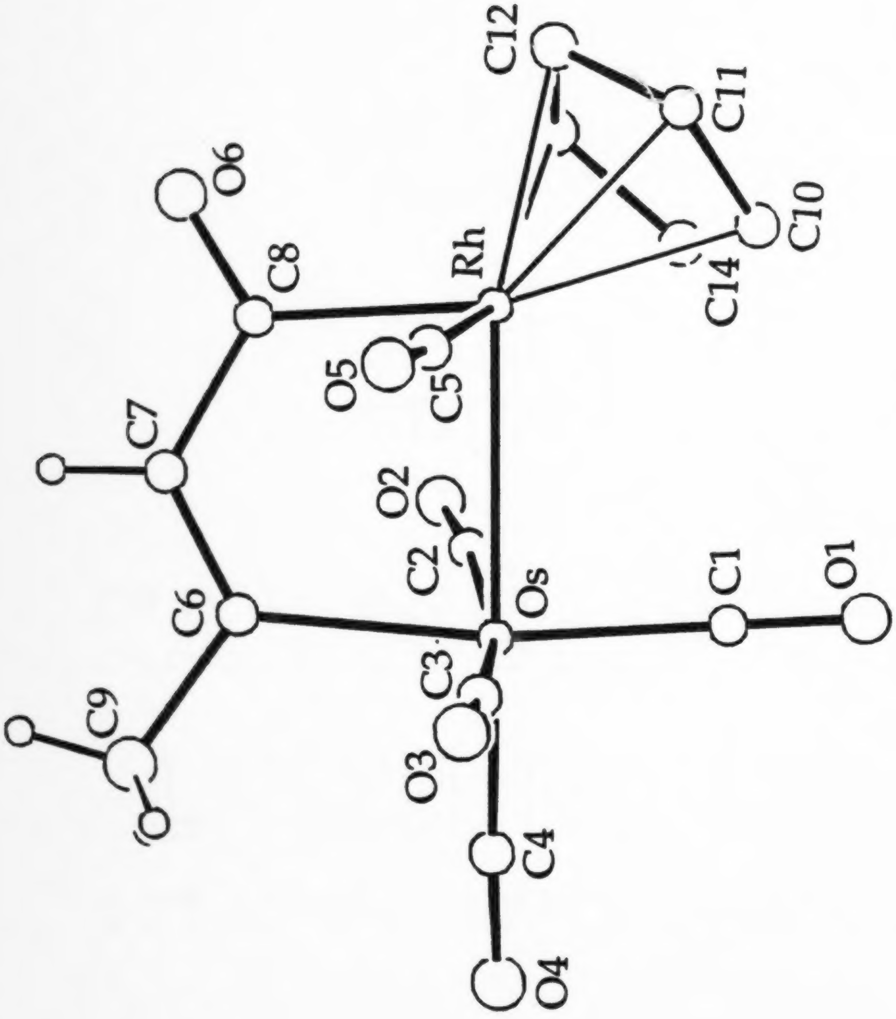
C12
C11
C10
C14
Rh
O6
C8
O5
C5
C7
O2
C2
Os
C1
O1
C6
C9
C3
O3
C4
O4

Figure 6.2: ORTEP View of [μ-η^1:η^1-(CH_3)CCHC(O)]Os$(CO)_4$Rh(CO)Cp, **17b**

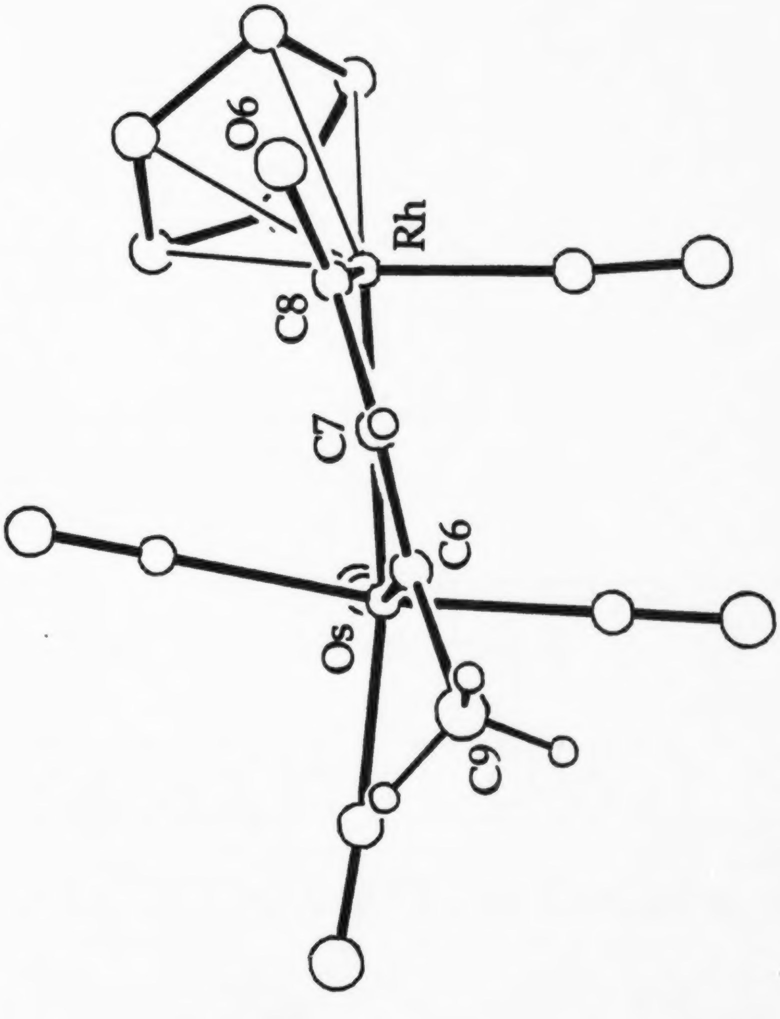
O6
Rh
C8
C7
C6
Os
C9

Figure 6.3: Alternate ORTEP View of [μ-η^1:η^1-(CH_3)CCHC(O)]-$Os(CO)_4Rh(CO)Cp$, 17b Looking Down Ring Plane

Table 6.5: Selected Bond Lengths (Å) for **17b**

Os-Rh	2.7773(8)	O1-C1	1.16(1)
Os-C1	1.94(1)	O2-C2	1.13(1)
Os-C2	1.96(1)	O3-C3	1.14(1)
Os-C3	1.95(1)	O4-C4	1.17(1)
Os-C4	1.89(1)	O5-C5	1.15(1)
Os-C6	2.13(1)	O6-C8	1.22(1)
Rh-C5	1.82(1)	C6-C7	1.34(1)
Rh-C8	2.04(1)	C6-C9	1.53(1)
Cent-Rh	1.94	C7-C8	1.47(1)

Table 6.6: Selected Angles (deg) for **17b**

Rh-Os-C1	87.3(3)	C1-Os-C2	96.2(4)
Rh-Os-C2	75.8(3)	C1-Os-C3	93.9(4)
Rh-Os-C3	96.2(3)	C2-Os-C3	166.8(4)
Rh-Os-C4	94.8(5)	C1-Os-C4	93.7(4)
Rh-Os-C6	84.4(3)	C2-Os-C4	94.8(5)
Os-Rh-C5	86.1(3)	C3-Os-C4	93.0(5)
Os-Rh-C8	86.0(3)	C1-Os-C6	171.4(4)
Rh-C5-O5	176(1)	C3-Os-C6	85.1(4)
Rh-C8-C7	120.3(8)	C5-Rh-C8	84.9(4)
Rh-C8-O6	119.9(7)	C6-C7-C8	124(1)
Os-C1-O1	177.3(9)	C7-C6-C9	118(1)
Os-C2-O2	174.4(9)	O6-C8-C7	119.8(9)
Os-C3-O3	176(1)	Os-C6-C7	121.3(8)
Os-C4-O4	175(1)	Os-C6-C9	120.7(8)
Cent-Rh-Os	127.6		

The Os-Rh bond distance is 2.7773(8) Å which conveys its single bond character. In $[Os(CO)_4]_2RhCp(CO)$, the two Os-Rh bond distances are 2.876(9) Å and 2.789(9) Å.[10a] This is representative of an unbridged Os-Rh bond distance between an $Os(CO)_4$ unit and a CpRh(CO) fragment and similar to the metal-metal separation in **17b**. In $[\mu\text{-}C(O)C_2H_2]\text{-}Os(CO)_3RhCp(PMe_2Ph)$, **5a**, the Os-Rh bond length is 2.780(2) Å, again in accord with the present results. For an Os-Rh complex with a bridging alkyne, $[\mu\text{-}C_2(CO_2Me)_2]Os(CO)_2Rh(CO)(\mu\text{-dppm})^+$ (dppm = $(Ph_2P)_2CH_2$), the Os-Rh bond distance is 2.8744(3) Å. This distance is longer than in **17b**, as the the bonding is described as Rh→Os dative interaction rather than a Rh-Os covalent bond.[10b]

The Os-C6 and Rh-C8 separations of 2.13(1) Å and 2.04(1) Å, respectively, are indicative of M-C single bonds. In $[\mu\text{-}C_2(CO_2Me)_2]\text{-}Os_2(CO)_8$, the Os-C bond distance is 2.138(5) Å[11] while in **3** the Os-C separation is 2.15(3) Å. The Rh-C bond distance in $[\mu\text{-}C_2(CF_3)_2C(O)]Rh_2Cp_2(CO)_2$ is 2.021(6) Å,[5a] in good agreement with the value obtained for **17b**. This value is particularly representative as it illustrates the Rh-carbon bond distance between the acyl carbon of a dimetallacyclopentenone ring and a RhCp(CO) fragment. For further comparison, in $[\mu\text{-}(CF_3)C_2]_2Rh_2(CO)_2(\mu\text{-dmpm})_2$ (dmpm = $(Me_2P)_2CH_2$), the Rh-C(sp^2) distances are 2.140(7) Å and 2.139(8) Å.[12] The C6-C7 bond length of 1.34(1) provides confirmation of its unsaturated nature, in excellent agreement with the value of 1.340(13) Å expected for a C-C double bond in an α,β-unsaturated ketone.[13] This bond is slightly longer than the C=C bond length of 1.316(11) Å in an isolated olefin, due to the contribution of canonical form II.[13] The C6-C7 bond length compares favourably with the values obtained for **3** (1.31(4) Å), $[\mu\text{-}C_2(CO_2Me)_2C(O)]\text{-}$

$(\mu\text{-dmpm})_2Ru_2(CO)_4$ (1.340(4) Å), and $[\mu\text{-}C_2(CF_3)_2C(O)]Rh_2Cp_2(CO)_2$ (1.336(5) Å).[5a-b] The C7-C8 bond length of 1.47(1) Å is in accord with the 1.464(18) Å usually observed for a $C(sp^2)\text{-}C(sp^2)$ single bond in a conjugated α, β-unsaturated ketone.[13] The lengthening of the C7-C8 bond and contraction of the C6-C7 bond is a result of the delocalization in the α,β-unsaturated ketonic moiety. The C-C single bonds lengths in $[\mu\text{-}C_2(CO_2Me)_2C(O)](\mu\text{-dmpm})_2Ru_2(CO)_4$ and $[\mu\text{-}C_2(CF_3)_2C(O)]Rh_2Cp_2(CO)_2$ are 1.496(4) Å and 1.499(8) Å, respectively.[5a-b] The C8-O6 bond distance is 1.22(1), in good agreement with the usual C=O bond distance of 1.222(10) Å found in α,β-unsaturated ketones.[13] For comparison, the C=O distance in a saturated cyclopentanone is 1.208(7) Å.[13]

The upward bending of two of the equatorial carbonyl ligands (C3-O3 and C2-O2) on the Os centre towards the organic bridge is readily apparent. This feature was also noted in the X-ray structure of **3**, where a disorder problem prevented a full analysis. In **17b**, the C3-Os-C2 angle is 166.8(4)°, a significant deviation from the idealized bond angle of 180°. This bending of the carbonyl ligands has been observed elsewhere in $Os(CO)_4[\eta^2\text{-}C_2(SiMe_3)_2]$[14] and $Os(CO)_4[\eta^1,\eta^1\text{-}(CH_2)_5]$.[15] Recently, Norton and Rappé addressed this question using the X-ray crystal structure of $Os(CO)_4(\eta^2\text{-}C_2H_4)$ and a series of theoretical calculations.[16] The structure of $Os(CO)_4(\eta^2\text{-}C_2H_4)$, which Norton has described as an osmacyclopropane, is shown in Scheme 6.1 along with **17b**; the bending of the carbonyls has been exaggerated.

In both cases, the Os geometry is distorted octahedral. Norton refers to the bending of the axial carbonyls in $Os(CO)_4(\eta^2\text{-}C_2H_4)$. These are labelled as equatorial carbonyls in **17b**; the dimetallic compound has been rotated to show this relationship more clearly. The $CO_a\text{-}Os\text{-}CO_a$ bond angle in $Os(CO)_4(\eta^2\text{-}C_2H_4)$ is 171.3(5)°, less distortion than seen in **17b**. Calculations by Norton indicate that the axial carbonyls in $Os(CO)_4(L)$ (L = two electron donating ligand) complexes should tilt towards L if L is a less effective π acceptor than CO. The tilting increases the backbonding to the equatorial carbonyls in $Os(CO)_4(\eta^2\text{-}C_2H_4)$ (CO_a and $Co_{e'}$ in **17b**) and lowers the energy of the complex. The tilt angle will increase if more equatorial backbonding (CO_a and $CO_{e'}$ in **17b**) is needed, thus the ethylene ligand in $Os(CO)_4(\eta^2\text{-}C_2H_4)$ is a better π acceptor than the Os-C and Os-Rh bonds. In fact, the tilt angle in **17b** is intermediate between the values expected for $Os(CO)_4(\eta^2\text{-}C_2H_4)$ and *cis*-$H_2Os(CO)_4$, where the dihydride is representative of a purely σ-donating substituent and a large tilt angle of 161.3° was observed. This is not surprising since the tilt angle increases as backbonding increases and the dihydride is a strong sigma donating ligand.

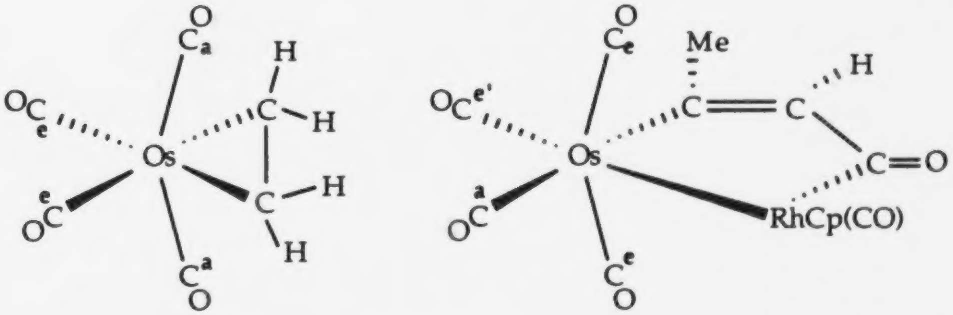

Scheme 6.1: Structure of $Os(CO)_4(\eta^2\text{-}C_2H_4)$ and **17b**

The increase in backbonding to CO_a and $CO_{e'}$ in **17b** should cause a decrease in these (Os-C1 and Os-C4) distances relative to the Os-C2 and Os-C3 bond distances. The Os-C4 distance of 1.89(1) Å, which is along the metal-metal vector, is significantly shorter than the other Os-carbonyl bond distances. The Os-C1, Os-C2 and Os-C3 bond distances are all within 1 esd with an average value of 1.95(1) Å, thus they are not significantly different from each other. Norton made a similar observation as he did not observe a significant difference between the axial Os-C and equatorial Os-C bond lengths. In fact, a very precise X-ray crystal structure determination would be required as theoretical calculations predict only a 0.02 Å Os-C bond length difference between axial and equatorial carbonyls in $Os(CO)_4(\eta^2\text{-}C_2H_4)$. The shortening of the Os-C4 bond is reasonable as this carbonyl lies along the metal-metal bond, where electron donation from the Rh centre would increase electron density on the Os centre, causing an increase in Os→CO backbonding. As a final note, the carbonyl on the Rh is nearly co-planar with the equatorial carbonyls on the Os centre. This is a feature that has been seen previously in Chapters 2 and 5 and accounts for the fluxional behaviour of these compounds.

The ORTEP diagram in Figure 6.3 shows that the organic segment of the dimetallacyclopentenone ring is slightly twisted with respect to the Os-Rh vector. This twisting represents the constriction placed on the organic fragment by the fixed Os-Rh bond length of 2.7773(8) Å and was observed previously in **3**. The ring twisting in **17b**, defined as the angle between the planes formed by O6-C6-C7-C8 and C6-Os-Rh, is 14.1°, similar to the value of 16.5° observed for **3**. The values are similar due to the small difference in metal-metal bond lengths (**3**: $d_{Os\text{-}Ir} = 2.785(2)$ Å; **17b**: $d_{Os\text{-}Rh} = 2.7773(8)$ Å) and the similarity between the bridging organic fragments.

6.4. Reactions of $Os(CO)_4[\eta^2\text{-}C_2(CH_3)_2]$

In the reaction of $Os(CO)_4(\eta^2\text{-}C_2Me_2)$ with $CpM(CO)_2$ (M = Co, Rh, Ir) a similar procedure used in the synthesis of **17a-c** was followed. As seen with $Os(CO)_4[\eta^2\text{-}(CH_3)CCH]$, the reaction of $Os(CO)_4(\eta^2\text{-}C_2Me_2)$ with $CpM(CO)_2$ (M = Co, Rh, Ir) proceeds to yield heterodimetallic compounds containing a dimetallacyclopentenone ring.

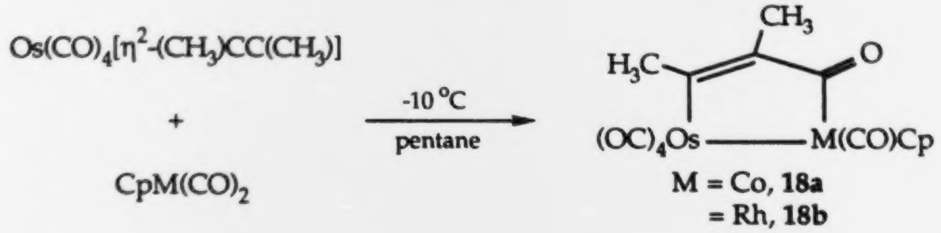

M = Co, **18a**
= Rh, **18b**
= Ir, **18c**

The reaction occurs at a slightly lower temperature than in **17a-c**, implying an increased four-electron destabilization in $Os(CO)_4(\eta^2\text{-}C_2Me_2)$ as compared to its propyne congener. All three dimetallic complexes have similar spectroscopic properties and consequently related structures. The FT-IR data for **18a-c** are listed in Table 6.7.

Table 6.7: FT-IR Data for
$[\mu\text{-}\eta^1\text{:}\eta^1\text{-}C_2(CH_3)_2C(O)]Os(CO)_4M(CO)Cp$, (M = Co, Rh, Ir)

Compound	ν(CO) (pentane, cm^{-1})	ν(acyl)
M = Co, **18a**	2098(w), 2030(s), 2021(s), 1997(s), 1982(w)	1636(w)
M = Rh, **18b**	2103(w), 2030(s), 2001(s)	1636(w)
M = Ir, **18c**	2107(w), 2033(s), 1997(s), 1989(w)	1621(w)

Again, a significant observation is the low energy acyl stretch at 1621-1636 cm^{-1}, indicating a structure similar to **17a-c**. For the butyne complexes, only one regio-isomer is possible as a symmetric alkyne was utilized. The ^1H NMR spectra show the differences in chemical shifts for the methyl groups attached to the α and β carbons (Table 6.8). For the propyne complexes, it was established that the CH_3 groups were attached to the β carbon, and the chemical shift values only ranged between 2.4-2.45 ppm. This compares favourably to the range of β-CH_3 resonances in **18a-c** that range from 2.38 to 2.45 ppm. Thus, the assignment of the α and β methyl signals for **18a-c** is based on the assignment of the ^1H NMR spectra of the propyne analogues, **17a-c**.

Table 6.8: ^1H NMR Data for
$[\mu\text{-}\eta^1\text{:}\eta^1\text{-}C_2(CH_3)_2C(O)]Os(CO)_4M(CO)Cp$, (M = Co, Rh, Ir)

	δ (CD_2Cl_2, ppm)		
Compound	β-CH_3	α-CH_3	$^4J_{H\text{-}H}$ (Hz)
M = Co, **18a**	2.39	1.34	0.8
M = Rh, **18b**	2.47	1.45	0.8
M = Ir, **18c**	2.45	1.46	0.8

The ^{13}C NMR data for these complexes, listed in Table 6.9, were also of interest, especially in light of the rather unusual results obtained for **17a-c**.

Table 6.9: ^{13}C NMR Data for
$[\mu\text{-}\eta^1\text{:}\eta^1\text{-}C_2(CH_3)_2C(O)]Os(CO)_4M(CO)Cp$, (M = Co, Rh, Ir)

	δ (CD_2Cl_2, ppm)	
Compound	C_β	C_α
M = Co, **18a**	161.5	147.4
M = Rh, **18b**	164.5	144.8
M = Ir, **18c**	166.3	139.0

There is a significant change in the ^{13}C NMR chemical shift pattern for **18a-c** as compared to their propyne analogues, **17a-c**. The chemical shift difference between the α and β carbons is larger for **18a-c** and is in accord with simple organic examples. For **18a-c**, the ^{13}C NMR chemical shift values for the β carbons do not vary significantly, indicating that the β carbon is attached to the same metal in each case. The difference between the α carbon chemical shifts is also quite small. Also, the ^{13}C NMR signal for the α carbon of ^{13}CO enriched **18c** (M = Ir) did not show any C-C coupling. However, this result is not fully conclusive as the level of ^{13}CO incorporation into the acyl moiety was quite low. As a final note, contrary to **17a-c**, there is no reversal of α and β chemical shift values. In other words, the β carbon signal remains significantly downfield of the C_α signal for each compound. Thus, the ring carbons were assigned based on the simple organic model of an α, β-unsaturated ketone.[6]

The data for the ring carbons of the two dimetallacyclopentenone systems (**17a-c** and **18a-c**) do not parallel one another. For **18a-c**, the results seem consistent with simple organic systems, while for **17a-c** rather anomalous results are observed. The only difference between the two series of compounds is the substitution of an α proton for a methyl group in the former. Also, the only difference between **3** and **17a-c** is that a β-proton has been exchanged for a methyl substituent in the latter. Thus, an explanation incorporating simple metal atom effects is insufficient in light of the results for **3** and **18a-c** and any explanation should centre on the change in substituents. The simple organic models do not show any unexpected results in regard to the chemical shifts of the α and β carbons. In fact, 2-cyclopenten-1-one, 3-methyl-2-cyclopenten-1-one and 2,3-dimethyl-2-cyclopenten-1-one all show a significant chemical shift difference between the α and β carbons with the β carbon approximately 25-50 ppm downfield of the α carbon. Therefore, based on simple organic analogues, changing the β proton for a methyl group should not cause a reversal of the relative α- and β-carbon ^{13}C NMR chemical shift positions.

It has been observed that, for cyclic α,β-unsaturated ketones, the ^{13}C NMR chemical shift difference between the α and β carbons approaches a minimum as the ring size exceeds a six-carbon skeleton. As the ring size further increases past eight the chemical shift difference rises again and approaches that seen for cyclic α,β-unsaturated ketones.[6c,17] The explanation is that the cyclopentenone and cyclohexenone are planar, thus the carbon *p* orbitals are in a parallel configuration and there is a strong resonance interaction between the carbonyl and olefinic moieties. Twisting within the ring, especially about the C_α-C(acyl) bond will reduce this resonance coupling, reducing the chemical shift difference. When the ring size again becomes large enough, this distortion is alleviated and the system approaches that of an open α,β-unsaturated ketone. Thus, it is possible that there is a difference in ring geometry between the various dimetallacyclopentenones, especially with regard to ring torsion, which is causing the anomalous ^{13}C NMR shifts in **17a-c**. A comparison of the X-ray structures of **3** and **17b**, possible due the similarity of the Os-Ir and Os-Rh bond distances, indicated little difference in the angles pertaining to the organic ring. For example, in **3**, the C1-C2-C3-O1 torsional angle is 14.2°, while for **17b**, the comparable C6-C7-C8-O6 torsional angle is 10.4°. The other torsional angles involving the bridging organic unit and the two metal centres were also similar. Thus, the solid state structures provide no clues as to the source of the unusual ^{13}C NMR chemical shifts in **17a-c**.

Taken singly, the probable sources of the anomalous ^{13}C NMR results for **17a-c**, which include metal effects, substitution effects and ring torsion are considered to be unlikely. However, these factors could be acting in concert. The asymmetry of the ring, a substitution effect, coupled with the presence of a transition metal centre could lead to the counter-intuitive chemical shifts. Unfortunately, further insight into these anomalous results cannot be given at this time.

6.5. Variable Temperature ^{13}C NMR Behavior of $[\mu\text{-}\eta^1\text{:}\eta^1\text{-}(CH_3)C_2RC(O)]\text{-}Os(CO)_4M(CO)Cp$, (M = Co, Rh, Ir; R = H, CH_3)

Following the established precedent, the terminal carbonyls for compounds **17a-c** and **18a-c** are fluxional *via* a truncated merry-go-round exchange mechanism. The variable temperature ^{13}C NMR spectra of **18c** are shown in Figure 6.4.

For both the propyne and butyne analogues, limiting ^{13}C NMR spectra could be obtained only for the Os-Ir dimetallic compounds (**17c**, **18c**) reflecting the increased activation barriers for carbonyl exchange as one descends a triad.[18] The low temperature limiting spectrum of **18c** is consistent with the postulated solid state structure The characteristic lowfield acyl signal is present along with five terminal carbonyl resonances.

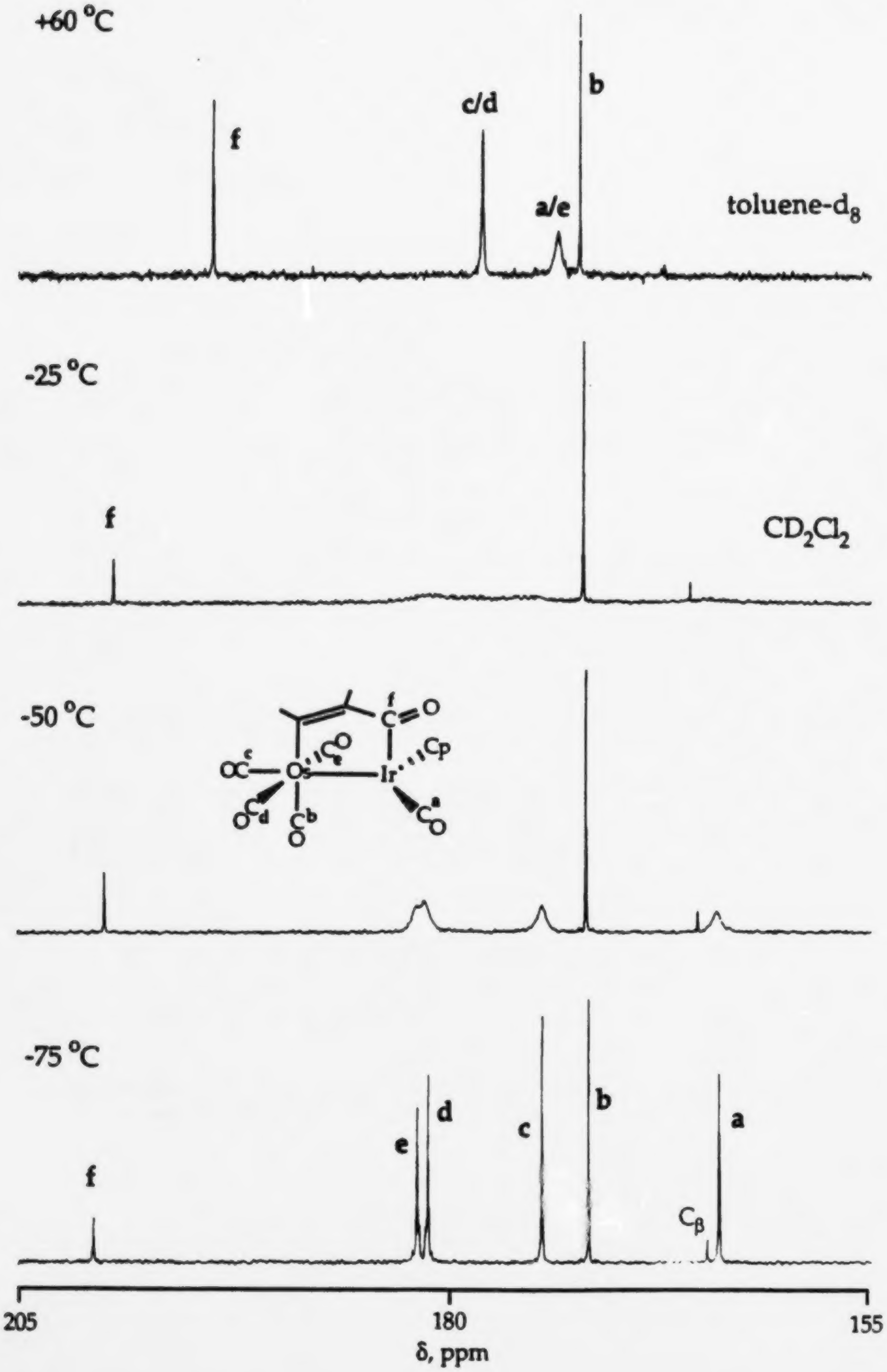

Figure 6.4: Variable Temperature ^{13}C NMR of **18c** in the Carbonyl Region

The chemical shift values for the four terminal carbonyls are also in accord with those attached to an osmium centre, while the resonance at highest field can be assigned to the terminal carbonyl attached to the Ir centre.[7] Also, the two *trans* equatorial carbonyls on the osmium exhibit trans ^{13}C-^{13}C coupling of 39.0 Hz,[19] this along with their lowfield position, allows for their facile identification.[4b,7,18d,20] The remaining two carbonyls could not be positively assigned; however one may tentatively assign the higher field signal to the CO along the Os-C(ring) vector, analogous to the case of **3**.[4] The lower field terminal carbonyl resonance is then assigned to the remaining axial CO. As the sample was warmed, four of the signals broaden noticeably, while one Os carbonyl signal, along with the acyl resonance, remains sharp. These broad signals coalesce and finally, at +60 °C, four resonances can be observed.

This is analogous to $[\mu\text{-}\eta^1\text{:}\eta^1\text{-}C_2H_2C(O)]Os(CO)_4IrCp(CO)$, **3**, where a truncated merry-go-round exchange mechanism causes four terminal carbonyls to exchange in a pairwise fashion.[18,21] For convenience, the ^{13}CO exchange mechanism for **18c** is shown in Scheme 6.2. An interesting feature is the dramatic chemical shift change of the acyl resonance upon changing solvents from CD_2Cl_2 to toluene-d_8. The change to a less polar solvent lessens the likelihood of a zwitterionic cyclopentenone structure, analogous to **II**. The ring will favour a less delocalized electronic structure and this will cause the chemical shift change. The terminal carbonyls are little effected by the change in solvent polarity.

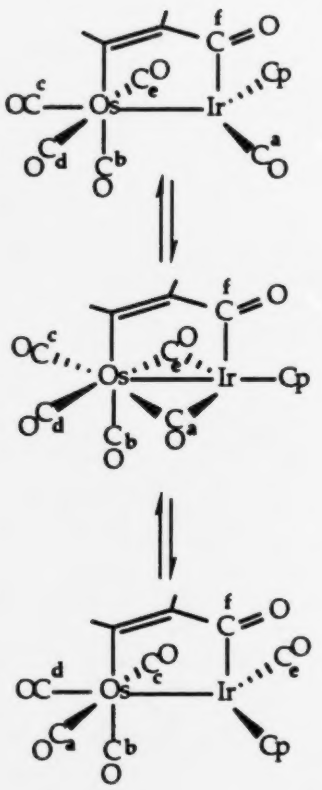

Scheme 6.2: Truncated-Merry-Go- Round Carbonyl Exchange for **18c**

The ^{13}C NMR spectrum for **18c** (and **17c**) is assigned in a way analogous to **3**. The preliminary assignment described above coupled with the truncated merry-go-round exchange mechanism allows for the specific assignment of each resonance. Unfortunately, for M= Co, Rh limiting spectra could not be obtained due to the facility of the exchange. Figure 6.5 below shows the ambient temperature spectra of $[\mu\text{-}\eta^1\text{:}\eta^1\text{-}C_2(CH_3)_2C(O)]Os(CO)_4Co(CO)Cp$, **18a**, where four signals are present in a 1:2:2:1 ratio and is representative of the ^{13}C NMR spectra expected at the fast exchange limit.

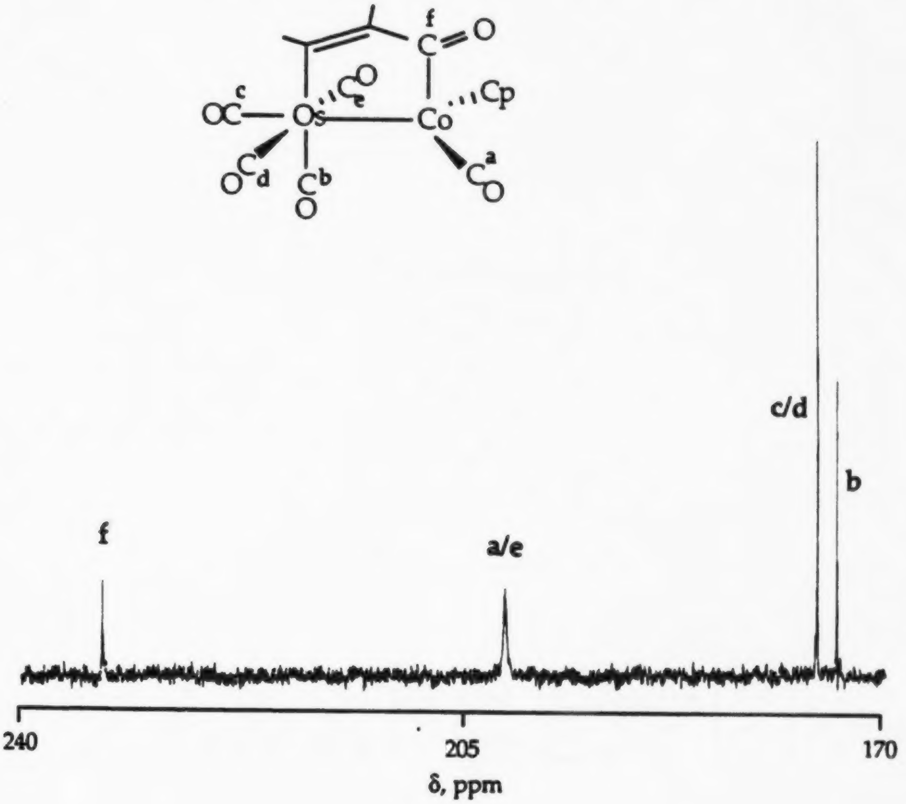

Figure 6.5: ^{13}C NMR of [μ-η^1:η^1-$C_2(CH_3)_2C(O)$]$Os(CO)_4Co(CO)Cp$, **18a**, at Ambient Temperature

For **17c** and **18c** the variable temperature ^{13}C NMR spectra can be simulated and activation parameters obtained. For these compounds, only rate data obtained from spectral simulation was used in a manner detailed in Appendix 1. The values derived are listed in Table 6.10.

Table 6.10: Activation Parameters for CO Exchange in $[\mu\text{-}\eta^1\text{:}\eta^1\text{-}(CH_3)C_2RC(O)]Os(CO)_4Ir(CO)Cp$

R	$\Delta H^\ddagger$ (kJ/mol)	$\Delta S^\ddagger$ (J/mol·K)
H, **17c**[a]	37.7 ± 1.3	-29.5 ± 5.8
CH_3, **18c**[a]	38.8 ± 0.8	-30.5 ± 3.1
3[a]	40.9 ± 1.2	-18.8 ± 4.7

[a] Activation parameters determined from rate data obtained from fitting simulated spectra to observed spectra only.

The enthalpy and entropy of activation for **17c** and **18c** are, within error, identical. This indicates that changing the α-carbon substituent from a proton to a methyl has little effect on exchange rate. For further comparison, the activation parameters for the simple unsubstituted dimetallacyclopentenone, **3**, are listed. For **3**, the activation barriers are slightly higher, expected since a less electron donating organic ring will raise the activation barrier to carbonyl exchange. However, the value of $\Delta H^\ddagger$ obtained for **3** is, with error, nearly the same as those for **17c** and **18c**. Therefore, exchanging protons for methyl substituents has little measurable effect on the rates of carbonyl exchange. This is also reflected in the FT-IR spectra, where the carbonyl stretching bands of **3** are only slightly higher in energy than **17c** and **18c**. This reflects similar electron density on the metal centres, the governing factor in the activation barriers to carbonyl exchange.

One would expect that a decrease in electron density at the metal centres would result in a decreased propensity to form bridging carbonyls, the first step in the exchange mechanism.[18b,18d,20] This should raise the activation energy of the exchange process. This is borne out in the activation parameters for (μ-η^1:η^1-TFP)Os(CO)$_4$RhCp(CO) (**14a:** $\Delta H^\ddagger = 44.7 \pm 1.8$ kJ/mol, $\Delta S^\ddagger = -32.6 \pm 7.0$ J/mol·K). Here, as in **17a-c** and **18a-c**, a Cp ligand is bonded to the Group IX metal centre. The activation barrier for exchange is higher in **14a** than in **3, 17c** or **18c**, demonstrating the electron withdrawing nature of the TFP ligand. Even more convincing is that **14a** is an Os-Rh dimetallic complex, for the acetylene, propyne and butyne dimetallic complexes, the activation parameters were calculated for the Os-Ir compounds. In fact, for **17b** and **18b**, activation parameters could not be calculated as limiting ^{13}C NMR spectra were not obtained.

6.6. Formation of Heterodimetallacyclopentenones: Plausible Pathway

As mentioned in the introduction, the reaction of Os(CO)$_4$(η^2-propyne) with CpM(CO)$_2$ (M = Co, Rh, Ir) was carried out the investigate the effects of changing electronic nature of the alkyne. Specifically, it was desirable to compare the electron-donating alkyne, propyne, to the electron-withdrawing alkyne, trifluoropropyne. The reactions of Os(CO)$_4$(η^2-butyne) were investigated to determine if steric effects were exerting an influence on the nature of the bimetallic products.

As seen, dimetallacyclopentenones are formed in the reaction of the Os-propyne and Os-butyne complexes with CpM(CO)$_2$ (M = Co, Rh, Ir). This is similar to the reaction of Os(CO)$_4$(η^2-HCCH) with CpIr(CO)$_2$ to form **3**. Thus, one would assume that a similar mechanism is operating in the formation of **3** and **17a-c** and **18a-c**. For the reaction of Os(CO)$_4$(η^2-C$_2$Me$_2$) with CpM(CO)$_2$, no regioselectivity can be observed due to the presence of a symmetric alkyne. However, the propyne bridged compounds are formed in a regioselective manner.

Considering only electronic effects, the regio-isomers confirmed for **17a-c** were not expected. As shown, it is the C-CH_3 carbon of the propyne that bears the partial positive charge. This is corroborated by the ^{13}C NMR spectrum of $Os(CO)_4(\eta^2\text{-propyne})$ (Section 8.2.2, Table 8.1). Therefore, a mechanism incorporating nucleophilic attack by $CpM(CO)_2$ on the coordinated alkyne, similar to Scheme 5.3, would yield a species where the α carbon has the methyl substituent. This is contrary to the experimental observation. This apparent lack of electronic control over the regio-isomerism may thus indicate that steric effects play a role. However, the importance of steric factors may be questioned due to the ready synthesis of **18a-c** in which a methyl group is adjacent to the acyl carbonyl. A cautionary note is that the absence of steric effects on the ground state stability of **18a-c** does not necessarily imply that steric forces are not playing a role in the observed regioselectivity. A mechanism (Scheme 6.3) for the formation of **17a-c** which incorporates the inherent electronic differences between the two *sp* carbons in $Os(CO)_4(\eta^2\text{-propyne})$ may be proposed. This mechanism utilizes the previously argued CO dissociation (Scheme 2.5) as the initiating step and allows for nucleophilic attack by $CpM(CO)_2$ directly at the Os centre.

As shown in Scheme 6.3, there are two possible pathways for the formation of **17a-c**; in both the key step is a CO insertion reaction. The regioselectivity is governed by this step and it is guided by electronic effects. Carbonyl insertion reactions are more aptly described as the nucleophilic attack by a migrating of σ-bonded hydrocarbyl fragment on an electrophilic CO ligand.[22] Thus, the carbon bearing the partial negative charge, the C-H carbon, should be involved in the insertion reaction. This is in accord with the regioselectivity of the reaction.

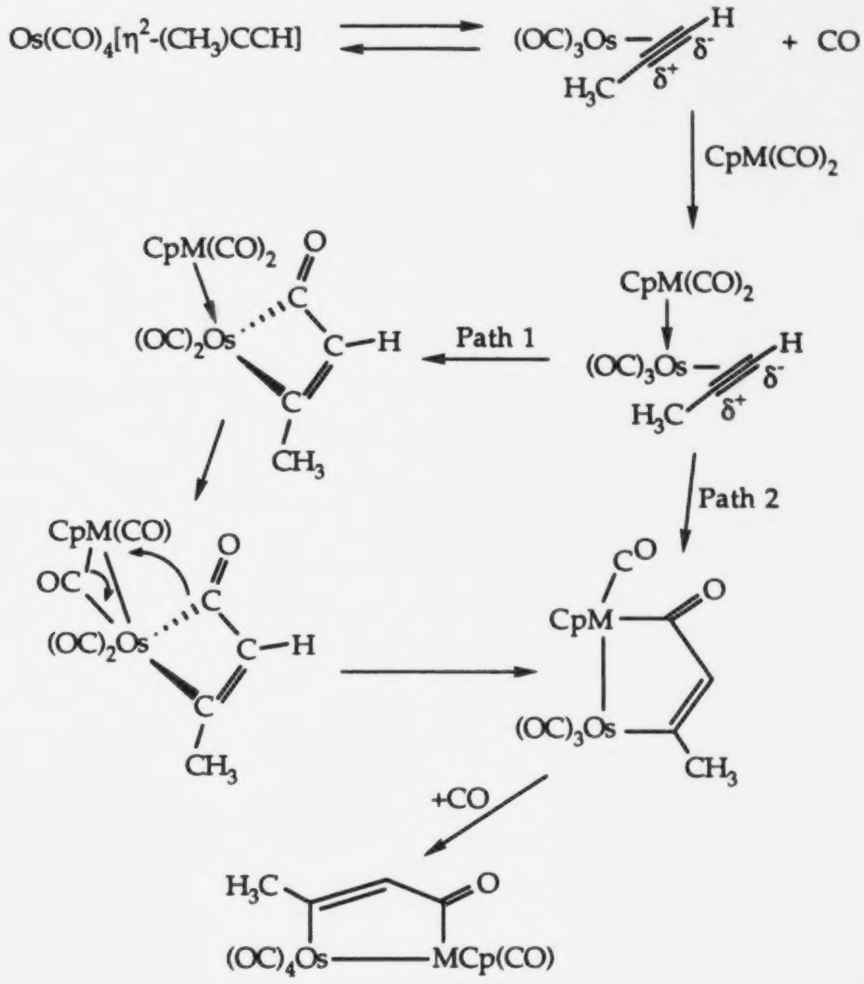
Os(CO)4[η2-(CH3)CCH]
(OC)3Os
H
δ-
δ+
H3C
+ CO
CpM(CO)2
Path 1
Path 2
(OC)2Os
C—H
O
CH3
CpM(CO)
OC
CpM
(OC)3Os
+CO
(OC)4Os
MCp(CO)

Scheme 6.3: Proposed Mechanism for the Formation of **17a-c**

Two different pathways are possible. In Path 1, the initial CO insertion involves the bound propyne on the Os centre and a Os carbonyl. An alternate pathway, Path 2, would still incorporate a CO insertion step. However, since the Group IX metal bears a formal positive charge, the bound CO ligands would be activated towards nucleophilic attack. This would immediately result in the formation of a dimetallacyclopentenone ring consistent with the regiochemistry observed for **17a-c**. The remaining steps are the same as outlined in Scheme 2.5. At this time, it is not clear which pathway is operational, however, considering the precedents for Path 1 in Scheme 8.6[23] and Scheme 8.5,[24] this mechanism seems preferable. An analogous mechanism is suggested for the formation of **18a-c**, with no electronic preference for the insertion step due to the symmetry of the alkyne.

Also, an additional point must be addressed. It is observed that the reaction of ^{13}CO enriched $Os(CO)_4(\eta^2$-propyne) and unenriched $CpM(CO)_2$ results in equal distribution of the ^{13}CO throughout the one acyl and five terminal carbonyl positions. A similar observation was made during the formation of **3**. Therefore, as initially postulated in Scheme 2.6, it is possible that an equilibrium exists before the CO insertion that would allow for ^{13}CO exchange between the two metal centres.

The alkyne dependence of the condensation reactions with $Cp'M(CO)_2$ (Cp' = Cp or Cp*) is readily apparent. There is the appearance of a general trend that allows one to predict whether the condensation will lead to dimetallacyclo-butenes or pentenones. For π-acidic alkynes such as TFP and HFB, the formation of dimetallacyclobutenes is preferred. The only exception is $[\mu-\eta^3:\eta^1-(CF_3)C_2HC(O)]Os(CO)_4CoCp^*$, although this species is thought to arise from a dimetallacyclobutene intermediate. For less π-acidic alkynes such as acetylene, propyne and 2-butyne, the formation of dimetallacyclopentenones is observed. This could be due to the presence of a facile CO insertion step. This would proceed readily for non π-acidic alkynes such as propyne whereby the regioselectivity would be determined by the polarization of the alkyne. For π-acidic alkynes such as TFP, the CO insertion step would be unfavourable as the negatively charged alkyne carbon is attached to a CF_3 group. One would expect the C-CF_3 carbon to be tightly bound to the metal centre and not migrate to a coordinated CO ligand, discouraging the formation of dimetallacyclopentenones. For $Os(CO)_4(\eta^2$-HFB), the strong Os-C(alkyne) bonds would result in dimetallacyclobutene formation. Thus, using this general trend, one could predict that $Os(CO)_4(\eta^2$-1-butyne) should undergo condensation reactions with $CpM(CO)_2$ to yield dimetallacyclopentenones while dimetallacyclobutenes should be observed in condensation reactions involving $Os(CO)_4[\eta^2$-$HCC(CO_2Me)]$. These two compounds have yet to synthesized and would provide a good, although not conclusive, test of the proposed trend.

6.7. Conclusions

The reaction of $Os(CO)_4[\eta^2$-$(CH_3)C_2R]$ (R = H, CH_3) with $CpM(CO)_2$ (M = Co, Rh, Ir) proceeds without ligand loss to yield dimetallacyclopentenones. This indicates that the reactions have significant alkyne dependence as only the reaction of $Os(CO)_4(\eta^2$-HCCH) with $CpIr(CO)_2$ resulted in the formation of a non-coordinated dimetallacyclopentenone. For M = Co, Rh the reaction gave dimetallacyclopentenones where the C-C double bond of the ring was coordinated to the Group IX metal. The regioselectivity of the reaction, in the case of R = CH_3, resulted in compounds with the C-H carbon adjacent to the acyl carbon. This is counter to expectations based on the polarization of propyne. For **18a-c**, the ^{13}C NMR chemical shifts are those expected for α,β-unsaturated ketones. However, for **17a-c**, anomalous results are obtained with, the case of **17b** and **17c**, the β carbons resonating upfield of the a carbons. A satisfactory explanation could not be given for this phenomenon. The dimetallacyclopentenones,

17a-c and **18a-c**, all have carbonyls that are fluxional *via* a truncated merry-go-round exchange. Finally, the results from the Os-propyne and Os-butyne condensation reactions allow the formulation of a general trend regarding product formation. The presence of π-acidic alkynes should result in the formation of dimetallacyclobutenes while weakly π-acidic alkynes should give rise to dimetallacyclopentenones.

6.8. Experimental Section

6.8.1. Starting Materials and Reagents

Propyne was purchased from Farchan Chemical Co. while 2-butyne was purchased from Aldrich Chemical Co., both alkynes were used as received.

6.8.2. Synthetic Procedures

Synthesis of [μ–η^1:η^1-(CH_3)C_2HC(O)]Os(CO)$_4$RhCp(CO), 17b

A pentane solution containing Os(CO)$_4$[η^2-(CH_3)C_2H], **19**, (14.0 mg, 0.041 mmol) and CpRh(CO)$_2$ (24.0 mg, 0.107 mmol) was slowly warmed from -78 °C to 0 °C using a dry ice/acetone bath. At temperatures near -5 °C the light orange solution darkened and a red-orange precipitate began to form. The reaction was maintained at 0 °C for *ca*. 2 h until the FT-IR showed no signals due to **19**. The solution was cooled to -78 °C to precipitate out all of the dimetallic complex. The solvent was removed by cannula filtration and the red-orange solid was washed (3x5 mL) at -20 °C with pentane. The resulting red-orange powder was dried under vacuum overnight. The yield of **17b** was 14.9 mg (64%).

Formula Weight: 566.33

Mass Spectrum(220 °C, +FAB): M^+ (568, 33.6%), M^+-nCO (n = 0-6)

IR(pentane, cm^{-1}); ν(CO): 2102(w), 2034(s), 2028(m), 2003(s), 1998(w); ν(acyl): 1634(w).

IR(CH_2Cl_2, cm^{-1}); ν(CO): 2106(w), 2030(s), 2004(s), 1980(m); ν(acyl): 1615(w).

^{1}H NMR(360 MHz, CD_2Cl_2, 23 °C) 6.95 (1H, dq, $^4J_{H\text{-}H}$ = 1.3 Hz, $^3J_{Rh\text{-}H}$ = 0.7 Hz, C-*H*), 5.53 (5H, s, C_5H_5), 2.46 (3H, d, $^4J_{H\text{-}H}$ = 1.3 Hz, C-CH_3).

^{13}C NMR(90.5 MHz, CD_2Cl_2, 23 °C) 158.9 (s, *C*-H), 156.7 (s, *C*-CH_3), 94.6 (s, *C*$_5$H$_5$), 39.5 (s, *C*H$_3$).

^{13}C NMR(90.5 MHz, CD_2Cl_2, 23 °C) 215.3 (d, $^1J_{Rh\text{-}C}$ = 23.9 Hz, CO_f), 190.1 (d, $^1J_{Rh\text{-}C}$ = 39.5 Hz, $CO_{a/e}$), 174.7 (s, $CO_{c/d}$), 173.1 (CO_b).

Anal. Calcd. for $C_{14}H_9O_6OsRh$: C, 29.69; H, 1.60. Found: C, 29.49; H, 1.50.

Synthesis of [μ–η^1:η^1-(CH_3)C_2HC(O)]Os(CO)$_4$CoCp(CO), 17a

Using a similar procedure, **19** (19.8 mg, 0.058 mmol) and CpCo(CO)$_2$ (20.0 mg, 0.111 mmol) were used to obtain **17a** as a deep red solid (21.8 mg, 72%).

Formula Weight: 522.35

Mass Spectrum(180 °C, 16eV): M$^+$ (524, 33.2%), M$^+$-nCO (n = 0-6)

IR(pentane, cm^{-1}); ν(CO): 2099(w), 2032(s), 2022(s), 1981(s); ν(acyl): 1653(w).

IR(CH_2Cl_2, cm^{-1}); ν(CO): 2103(w), 2030(s), 2005(s), 1974(m); ν(acyl): 1610(w).

^{1}H NMR(360 MHz, CD_2Cl_2, 23 °C) 6.74 (1H, q, $^4J_{H\text{-}H}$ = 1.2 Hz, C-*H*), 5.10 (5H, s, C$_5$*H*$_5$), 2.40 (3H, d, $^4J_{H\text{-}H}$ = 1.2 Hz, C-C*H*$_3$).

^{13}C NMR(90.5 MHz, CD_2Cl_2, 23 °C) 157.5 (s, *C*-CH_3), 155.8 (s, *C*-H), 92.2 (s, *C*$_5$H$_5$), 38.9 (s, *C*H$_3$).

^{13}C NMR(90.5 MHz, CD_2Cl_2, 23 °C) 235.2 (CO_f), 200.6 ($CO_{a/e}$), 174.9 ($CO_{c/d}$), 173.3 (CO_b).

Anal. Calcd. for $C_{14}H_9CoO_6Os$: C, 32.19; H, 1.74. Found: C, 31.83; H, 1.65.

Synthesis of [μ–η^1:η^1-(CH_3)C_2HC(O)]Os(CO)$_4$IrCp(CO), 17c

Using a similar procedure, **19** (15.4 mg, 0.045 mmol) and CpIr(CO)$_2$ (20.2 mg, 0.065 mmol) were used to obtain **17c** as a yellow solid (16.9 mg, 57%).

Formula Weight: 655.62

Mass Spectrum(220 °C, +FAB): M$^+$ (656, 20.7%), M$^+$-nCO (n = 0-6)

IR(pentane, cm^{-1}); ν(CO): 2108(w), 2035(s), 2001(s), 1985(m); ν(acyl): 1620(w).

IR(CH_2Cl_2, cm^{-1}); ν(CO): 2111(w), 2034(s), 2002(s), 1982(m); ν(acyl): 1592(w).

^1H NMR(360 MHz, CD_2Cl_2, 23 °C) 7.21 (1H, q, $^4J_{H\text{-}H}$ = 1.3 Hz, C-*H*), 5.61 (5H, s, C_5H_5), 2.47 (3H, d, $^4J_{H\text{-}H}$ = 1.3 Hz, C-CH_3).

^{13}C NMR(90.5 MHz, CD_2Cl_2, 23 °C) 162.7 (s, *C*-H), 151.4 (s, *C*-CH_3), 90.3 (s, C_5H_5), 35.4 (s, CH_3).

^{13}C NMR(90.5 MHz, CD_2Cl_2, -80 °C) 199.4 (CO_f), 181.3 (CO_e), 180.9 (CO_d), 174.0 (CO_c), 171.3 (CO_b), 164.4 (CO_a).

Anal. Calcd. for $C_{14}H_9IrO_6Os$: C, 25.65; H, 1.38. Found: C, 25.73; H, 1.42.

Synthesis of $[\mu\text{–}\eta^1\text{:}\eta^1\text{-}C_2(CH_3)_2C(O)]Os(CO)_4CoCp(CO)$, 18a

Using a similar procedure, $Os(CO)_4[\eta^2\text{-}C_2(CH_3)_2]$, **20** (18.0 mg, 0.051 mmol) and $CpCo(CO)_2$ (25.3 mg, 0.141 mmol) were used to obtain **18a** as a red solid (13.8 mg, 51%).

Formula Weight: 536.38

Mass Spectrum(200 °C, 16eV): M^+ (538, 2.5%), M^+-nCO (n = 0-5)

IR(pentane, cm^{-1}); ν(CO): 2098(w), 2030(s), 2021(s), 1997(s), 1982(w); ν(acyl): 1636(w).

^1H NMR(360 MHz, CD_2Cl_2, 23 °C) 5.08 (5H, s, C_5H_5), 2.39 (3H, q, $^4J_{H\text{-}H}$ = 0.8 Hz, β-CH_3), 1.34 (3H, q, $^4J_{H\text{-}H}$ = 0.8 Hz, α-CH_3).

^{13}C NMR(90.5 MHz, CD_2Cl_2, 23 °C) 161.5 (s, C_β–CH_3), 147.4 (s, C_α–CH_3), 92.2 (s, C_5H_5), 36.1 (s, β-CH_3), 17.0 (s, α-CH_3).

^{13}C NMR(100.6 MHz, CD_2Cl_2, 25 °C) 233.4 (CO_f), 201.0 ($CO_{a/e}$), 175.7 ($CO_{c/d}$), 174.1 (CO_b).

Anal. Calcd. for $C_{15}H_{11}CoO_6Os$: C, 33.59; H, 2.07. Found: C, 33.89; H, 2.28.

Synthesis of $[\mu-\eta^1:\eta^1-C_2(CH_3)_2C(O)]Os(CO)_4RhCp(CO)$, 18b

Using a similar procedure, $Os(CO)_4[\eta^2-C_2(CH_3)_2]$, **20** (16.0 mg, 0.045 mmol) and $CpRh(CO)_2$ (19.5 mg, 0.087 mmol) were used to obtain **18b** as a red-orange solid (17.1 mg, 66%).

Formula Weight: 580.35

Mass Spectrum(140 °C, 16eV): M^+ (582, 8.4%), M^+-nCO (n = 0-6)

IR(pentane, cm^{-1}); ν(CO): 2103(w), 2030(s), 2001(s); ν(acyl): 1636(w).

^1H NMR(360 MHz, CD_2Cl_2, 23 °C) 5.54 (5H, s, C_5H_5), 2.47 (3H, q, $^4J_{H-H}$ = 0.8 Hz, β–CH_3), 1.45 (3H, q, $^4J_{H-H}$ = 0.8 Hz, α-CH_3).

^{13}C NMR(90.5 MHz, CD_2Cl_2, 23 °C) 164.5 (d, $^2J_{Rh-H}$ = 5.4 Hz, C_β–CH_3), 144.8 (s, C_α–CH_3), 94.6 (s, C_5H_5), 36.2 (s, β–CH_3), 16.2 (s, α-CH_3).

^{13}C NMR(100.6 MHz, CD_2Cl_2, 25 °C) 216.1 (d, $^1J_{Rh-H}$ = 24.6 Hz, CO_f), 189.9 (d, $^1J_{Rh-C}$ = 39.5 Hz, $CO_{a/e}$), 175.3 ($CO_{c/d}$), 173.2 (CO_b).

Anal. Calcd. for $C_{15}H_{11}O_6OsRh$: C, 31.04; H, 1.91. Found: C, 31.03; H, 1.96.

Synthesis of $[\mu-\eta^1:\eta^1-C_2(CH_3)_2C(O)]Os(CO)_4IrCp(CO)$, 18c

Using a similar procedure, $Os(CO)_4[\eta^2-C_2(CH_3)_2]$, **20** (20.2 mg, 0.057 mmol) and $CpIr(CO)_2$ (31.5 mg, 0.101 mmol) were used to obtain **18c** as a yellow solid (28.1 mg, 74%).

Formula Weight: 669.65

Mass Spectrum(140 °C, 16eV): M^+ (670, 5.4%), M^+-nCO (n = 0-6)

IR(pentane, cm^{-1}); ν(CO): 2107(w), 2033(s), 1997(s), 1989(w); ν(acyl): 1621(w).

^1H NMR(360 MHz, CD_2Cl_2, 23 °C) 5.61 (5H, s, C_5H_5), 2.45 (3H, q, $^4J_{H-H}$ = 0.8 Hz, β-CH_3), 1.46 (3H, q, $^4J_{H-H}$ = 0.8 Hz, α-CH_3).

^{13}C NMR(90.5 MHz, CD_2Cl_2, 23 °C) 166.3 (s, C_β-CH_3), 139.0 (s, C_α-CH_3), 90.6 (s, C_5H_5), 35.7 (s, β-CH_3), 15.9 (s, α-CH_3).

^{13}C NMR(100.6 MHz, CD_2Cl_2, -75 °C) 200.5 (CO_f), 181.4 (CO_e), 180.8 (CO_d), 174.1 (CO_c), 171.3 (CO_b), 163.8 (CO_a).

Anal. Calcd. for $C_{15}H_{11}IrO_6Os$: C, 26.90; H, 1.66. Found: C, 26.92; H, 1.66.

Synthesis of ^{13}CO Enriched 17a-c and 18a-c

A pentane solution of **19** was degassed by a freeze-pump-thaw cycle using liquid nitrogen. Approximately one atmosphere of ^{13}CO was admitted into the flask and the solution was stirred at -10 °C for 30 minutes. Solutions of **19-^{13}CO** were then subsequently used in reactions to generate the enriched dimetallic compounds **17a-c**. This resulted in approximately 20% ^{13}CO enrichment as determined from ^{13}C NMR integration.

In the preparation of ^{13}CO enriched **18a-c**, the extreme thermal instability of **20** necessitated the use of solutions of ^{13}CO enriched $CpM(CO)_2$ (M = Co, Rh, Ir) which were prepared by stirring pentane solutions of the aforementioned compounds under a ^{13}CO atmosphere at room temperature overnight. A pentane solution of **20** was degassed by a freeze-pump-thaw cycle using liquid nitrogen. Approximately one atmosphere of ^{13}CO was admitted into the flask and the solution was stirred at -25 °C for 15 minutes. Solutions of **20-^{13}CO** and $CpM(^{13}CO)_2$ were then subsequently used in reactions to generate the enriched dimetallic compounds. The level of enrichment of the dimetallic compounds **18a-c** was measured to be 16% using ^{13}C NMR.

6.8.3. X-ray Structure Determination of 17b

Orange, parallelpiped crystals were grown by cooling a CH_2Cl_2/hexane solution of **17b** to -20 °C. The X-ray data collection and structure refinement was carried out by Andrew Bond, a student with Prof. Robin Rogers at Northern Illinois University. The crystals were mounted in a thin-walled glass capillary flushed with Ar and transferred to the goniometer. Crystal data and general conditions of data collection and structure refinement are given in Table 6.11. Monitoring of intensity standards showed no appreciable decay (± 2%). All H atoms were placed at their calculated positions (determined by assuming C-H = 0.95 Å and sp^3 or sp^2 geometry) and constrained to 'ride' with the attached C atom with B fixed at 5.5 Å^2. The methyl H atoms were assigned as a rigid group with rotational freedom at the bonded carbon atom.

The final atomic coordinates are given in Table 6.12 and selected bond distances, angles and weighted least-squares planes for **17b** are given in Tables 6.5, 6.6 and 6.13, respectively.

Table 6.11: Summary of Crystallographic Data for **17b**

Crystal Parameters	
formula	$C_{14}H_9O_6OsRh$
formula wt.	566.33
crystal size, mm	0.20 x 0.40 x 0.28
crystal system	orthorhombic
space group	*Pbca*
a, Å	11.490(5)
b, Å	13.146(5)
c, Å	19.822(6)
V, Å^3	2994.1
Z	8
D_{calc}, g cm^{-3}	2.51
μ, cm^{-1}	100.8

Data Collection and Structure Refinement

diffractometer	Enraf-Nonius CAD4
radiation (λ [Å])	Mo K_α (0.71073)
monochromator	graphite
take-off angle, deg	2.0
temperature, °C	23
scan type	ω-2θ
scan width, deg in ω,	$0.80 + 0.35\tan\theta$
2θ limit, deg	50.0
reflections measured	2998 (*h*, *k*, *l*)
reflections used	1787 with $I > 3\sigma(I)$
variables	202
R^a	0.031
$R_w{}^b$	0.033
GOF[c]	0.65

$^aR = \Sigma||F_o| - |F_c||/\Sigma|F_o|$

$^bR_w = (\Sigma w(|F_o| - |F_c|)^2/\Sigma wF_o{}^2)^{1/2}$

$^c\mathrm{GOF} = [\Sigma w(|F_o| - |F_c|)^2/(\mathrm{NO} - \mathrm{NV})]^{1/2}$

Table 6.12: Fractional Coordinates and Isotropic Thermal Parameters for **17b**

atom	*x/a*	*y/b*	*z/c*	*U*(equ), Å
Os	0.07969(3)	0.27553(3)	0.41778(2)	1.58
Rh	0.13091(6)	0.17111(6)	0.29965(4)	1.50
O1	-0.0600(7)	0.4267(6)	0.3294(4)	3.10
O2	0.3289(7)	0.3461(6)	0.3825(4)	3.07
O3	-0.1358(8)	0.1479(7)	0.4564(4)	3.87
O4	0.0647(8)	0.4129(6)	0.5417(4)	3.72
O5	-0.0379(7)	0.0133(6)	0.3434(4)	3.36
O6	0.3234(7)	0.0410(6)	0.3285(4)	3.32
C1	-0.0053(9)	0.3717(7)	0.3625(5)	2.00
C2	0.236(1)	0.3237(7)	0.3929(5)	1.84
C3	-0.0584(9)	0.1971(8)	0.4408(5)	2.33
C4	0.069(1)	0.3565(8)	0.4962(6)	2.55
C5	0.0267(9)	0.0761(8)	0.3288(6)	2.36
C6	-0.1733(9)	0.1554(8)	0.4657(5)	2.12
C7	0.240(1)	0.0917(7)	0.4302(5)	2.22
C8	0.2486(9)	0.0916(7)	0.3562(5)	1.93
C9	0.171(1)	0.143(1)	0.5426(5)	3.58
C10	0.078(1)	0.2801(8)	0.2132(5)	2.51
C11	0.0815(9)	0.1809(9)	0.1886(5)	2.21
C12	0.1963(9)	0.1455(9)	0.1942(5)	2.78
C13	0.263(1)	0.225(1)	0.2237(5)	2.83
C14	0.187(1)	0.3079(8)	0.2363(5)	2.56

Table 6.13: Selected Weighted[a] Least-Squares Planes

Plane	Coefficients[b]				Defining Atoms with Deviations[c]			
1	0.2089	0.3605	-0.9091	2.3385	C10	0.00960	C11	-0.01305
					C12	-0.00052	C13	0.00726
					C14	-0.01151	Rh	-1.93613
2	-0.6996	-0.7128	-0.0505	3.2642	C6	-0.05077	C7	0.04135
					C8	0.05095	C9	0.00619
					O6	-0.04772	Os	-0.37606
					Rh	0.30889		

Dihedral Angles[d]

Planes	Angle
1 - 2	110.93

[a] Weights are derived from the atomic and positional esd's using the method of Hamilton(Hamilton, W.C. *Acta. Crystallogr.* **1961**, *14*, 185.).

[b] Coefficients are for the form ax+by+cz-d=0 where x, y, and z are crystallographic coordinates.

[c] Deviations are in angstroms. Underlined atoms were not included in the definition of the plane.

[d] In degrees

6.9. References

1. (a) Dixon, D.A.; Smart, B.E. *J. Phys. Chem.* **1989**, *93*, 7772.

2. (a) Rosenberg, D.; Drenth, W. *Tetrahedron* **1971**, *27* ,3893. (b) Rosenthal, U.; Oehme, G.; Burlakov, V.V.; Petroski, P.V.; Shur, V.B.; Volpin, M.E. *J. Organomet. Chem.* **1990**, *391*, 119. (c) Dawson, D.A.; Reynolds, W.F.; *Can. J. Chem.* **1975**, *53*, 373.

3. Kiel, G.-Y. personal communication.

4. (a) Gagné, M.R.; Takats, J. *Organometallics* **1988**, *7*, 561. (b) Burn, M.J.; Kiel, G.-Y.; Seils, F.; Takats, J.; Washington, J. *J. Am. Chem. Soc.* **1989**, *111*, 6850.

5. (a) Dickson, R.S.; Gatehouse, B.M.; Nesbit, M.C.; Pain, G.N., *J. Organomet. Chem.* **1981**, *251*, 97. (b) Johnson, K.A.; Gladfelter, W.L. *Organometallics* **1992**, *11*, 2534.

6. (a) Levin, R.H.; Weingarten, L. *Tett. Lett.* **1975**, 611. (b) Marr, D.H.; Stothers, J.B. *Can. J. Chem.* **1965**, *43*, 596. (c) Loots, M.J.; Weingarten, L.R.; Levin, R.H. *J. Am. Chem. Soc.* **1976**, *98*, 4571. (d) Simth, E. *J. Am. Chem. Soc.* **1976**, *32*, 1200.

7. Mann, B.E.; Taylor, B.F. ^{13}C *NMR Data for Organometallic Compounds*; Academic: New York, 1981.

8. Friebolin, H. *Basic One- and Two-Dimensional NMR Spectroscopy*, VCH: New York, 1991, pg. 85-88.

9. Ayer, W.A.; Craw, P.A. *Can. J. Chem.* **1992**, *70*, 1348.

10. Hsu, L.-Y.; Hsu, W.-L.; Jan, D.-Y.; Marshall, A.G.; Shore, S.G. *Organometallics*, **1984**, *3*, 591. (b) Hilts, R.W.; Franchuk, R.A.; Cowie, M. *Organometallics*, **1991**, *10*, 304.

11. Burke, M; Takats, J. *J. Organomet. Chem.* **1986**, *302*, C25.

12. Jenkins, J.A.; Cowie, M. *Organometallics* **1992**, *11*, 2774

13. Allen, F.H.; Kennard, O.; Watson, D.G.; Brammer, L.; Orpen, A.G.; Taylor, R. *J. Chem. Soc., Perkin Trans. II* **1987**, S1.

14. Ball, R.G.; Burke, M.R.; Takats, J. *Organometallics* **1987**, *6*, 1918.

15. Lindner, E.; Jansen, R.-M.; Hiller, W.; Fawzi, R. *Chem. Ber.* **1989**, *122*, 1403.

16. Bender, B.R.; Norton, J.R.; Miller, M.M.; Anderson, O.P.; Rappé, A.K. *Organometallics* **1992**, *11*, 3427.

17. Heap, N.; Whitman, G.H. *J. Chem. Soc. B* **1966**, 164.

18. (a) Mann, B.E. in *Comprehensive Orgaonmetallic Chemistry;* Wilkinson, G.; Stone, F.G.A.; Abel, E.W., Eds.; Pergamon: New York, 1982; Vol. 3, pg 89. (b) Washington, J.; Takats, J. *Organometallics* **1990**, *9*, 925. (c) Geoffroy, G.L. *Acc. Chem. Res.* **1980**, *13*, 469. (d) Riesen, A.; Einstein, F.W.B.; Ma, A.K.; Pomeroy, R.K.; Shipley, J.A. *Organometallics* **1991**, *10*, 3629.

19. (a) Tachikawa, M.; Richter, S.I.; Shapley, J.R. *J. Organomet. Chem.* **1977**, *128*, C9. (b) Aime, S.; Osella, D. *J. Chem. Soc., Chem. Commun.* **1981**, 300.

20. Alex, R.F.; Pomeroy, R.K. *Organometallics* **1987**, *6*, 2437.

21. Bond, E.; Muetterties, E.L. *Chem. Rev.* **1978**, *78*, 639.

22. Collman, J.P.; Hegedus, L.S.; Norton, J.R.; Finke, R.G. *Principles and Applications of Organotransition Metal Chemistry;* University Science Books: Mill Valley, 1987, Chapter 6.

23. Tianfu Mao, personal communication.

24. Burt, R.; Cooke, M.; Green, M. *J. Chem. Soc. (A)* **1970**, 2981.

Chapter 7

Photoreaction of $Os(CO)_5$ with Propargyl Chloride: Preparation of $Os(CO)_4(\eta^1\text{-}HC{=}C{=}CH_2)Cl$

7.1. Introduction

As seen in the previous Chapters, various Os-alkyne complexes can be used in the synthesis of alkyne bridged bimetallic compounds. The alkynes used must have a low (<60 °C) boiling point to enable the isolation of the pure Os-alkyne compound, limiting the range of potential alkynes. Unfortunately, the only heterodimetallic compounds completely characterized have proton, methyl, trimethylsilyl or trifluoromethyl substituents. Therefore, modification of the ring substituents to provide access to different substitution patterns is very difficult. Thus, the use of an alkyne with a readily modifiable functionality was proposed in order to facilitate elaboration of the organic ring in the bimetallic species. However, a species such as propargyl alcohol has a relatively high boiling point ($b.p._{760}$ = 114 °C). An alkyne that possesses the necessary properties is propargyl chloride (3-chloro-propyne). This alkyne can be readily synthesized from the commonly available propargyl alcohol,[1] has a low boiling point ($b.p._{760}$ = 58 °C), and a halogen functional group.

$$HC\equiv C\text{-}CH_2Cl$$

propargyl chloride

Thus, if $Os(CO)_4(\eta^2\text{-}HC_2CH_2Cl)$ could be synthesized it would enable the continued investigation of the regioselectivity of the condensation reactions as well as providing access to ring substitution reactions.

However, a potential complicating factor of the proposed photochemical synthesis must be kept in mind. Photolysis of $Os(CO)_5$ and propargyl chloride may not yield the simple substitution product but may result in oxidative addition of the chlorinated ligand. Oxidative addition is well documented[2] and occurs readily with metal carbonyls. There are various types of oxidative addition reactions, all of which satisfy the basic criteria whereby the transition metal increases its oxidation state and coordination number. The example shown is for additions to the well-known Vaska's complex.[3]

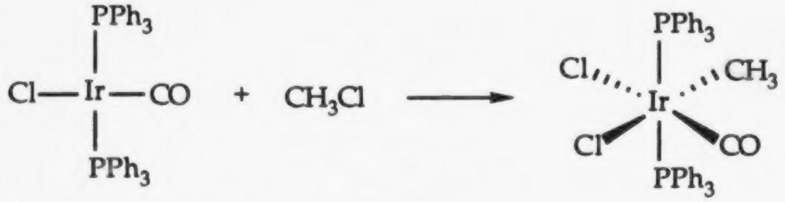

In the example above, the transition metal centre has increased its formal oxidation state by two while also increasing its coordination number by two. To undergo an oxidative addition reaction, a coordinatively saturated species must lose a ligand to generate a 16 electron intermediate. It is this electron deficient species which then oxidatively adds the substrate. Hoffmann has carried out a theoretical study of d^8-ML_4 complexes and their propensity for C-H activation, a specialized application of an oxidative addition reaction.[4] In photochemical syntheses involving $Os(CO)_5$, the generation of an unsaturated intermediate, $Os(CO)_4$, which has been observed in matrix isolation studies,[5] is assumed. This species has the d^8-ML_4 configuration yet no evidence for C-H activation has been observed in our laboratory.

Corroborating this, matrix isolation studies by F.W. Grevels and co-workers have shown that $Os(CO)_4$ binds a benzene molecule but does not activate the arene C-H bond.[5c] However, the possibility that $Os(CO)_4$ may be involved in other oxidative addition reactions cannot be discounted and, in fact, would seem likely. For instance, the reactivity of a series of compounds of formula $Fe(CO)_2(L)_2(NCMe)$ (L = PMe_3, PMe_2Ph, $PMePh_2$), where the acetonitrile is very labile, has been investigated. The lability of acetonitrile allows for the *in situ* formation of $Fe(CO)_2(L)_2$ that oxidatively adds MeI in a very facile manner.[6a] Another important example of oxidative addition by a d^8-ML_4 species is the activation of aliphatic C-H bonds.[6b]

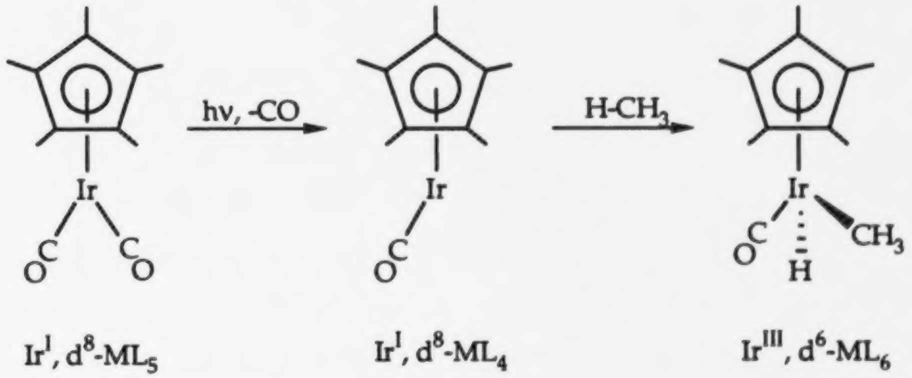

Photochemical activation is required to expel a CO ligand from the starting material to generate the active species, followed by oxidative addition of the C-H bond. The above and related reactions have generated considerable interest. The Ir based intermediate above, Cp*Ir(CO), is a d^8-ML_4 species which is converted into a d^6-ML_6 compound. With the discovery of C-H activation the importance of other d^8-ML_4 species has grown; thus the significance of $Os(CO)_4$ intermediates.

7.2. Synthesis and Characterization of $Os(CO)_4(\eta^1\text{-}CH=C=CH_2)Cl$, 21

7.2.1. Synthesis of $Os(CO)_4(\eta^1\text{-}CH=C=CH_2)Cl$

As in the synthesis of other osmium-alkyne compounds,[7] a pentane solution of $Os(CO)_5$ along with an excess of propargyl chloride, was photolyzed in at immersion well at -60 °C. In this photochemical synthesis, the wavelength of the irradiation was restricted by a GWV (Glaswerk Verheim) cut-off filter ($\lambda \geq 370$ nm). The photochemically generated intermediate is presumed to be $Os(CO)_4$ and the reaction is monitored by the disappearance of the $Os(CO)_5$ bands at 2035 cm^{-1} and 1993 cm^{-1}. An unusual feature in the IR spectrum during the course of the reaction was the appearance of a CO band at 2164 cm^{-1}. A stretching band of such high energy is unexpected based on analogy with $Os(CO)_4(\eta^2\text{-alkyne})$ species. In fact, the highest energy band[7b] in $Os(CO)_4(\eta^2\text{-HFB})$, where the alkyne is a much better π acceptor than propargyl chloride, is 2149 cm^{-1}. This indicated that perhaps the $Os(CO)_4$ intermediate was not simply scavenging the alkyne. The irradiation was continued until all the $Os(CO)_5$ was consumed and the white, waxy product, **21**, was purified by sublimation, the isolated yield is 40% (Scheme 7.1).

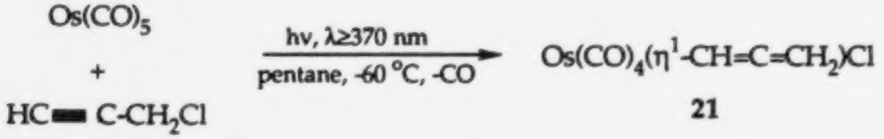

$$\begin{array}{c} Os(CO)_5 \\ + \\ HC\equiv C\text{-}CH_2Cl \end{array} \xrightarrow[\text{pentane, -60 °C, -CO}]{h\nu,\ \lambda\geq 370\ nm} \underset{\mathbf{21}}{Os(CO)_4(\eta^1\text{-}CH=C=CH_2)Cl}$$

Scheme 7.1: Preparation of $Os(CO)_4(\eta^1\text{-}CH=C=CH_2)Cl$, **21**

A similar reaction undertaken with $Ru(CO)_5$ only produced an intractable tan precipitate, no hydrocarbon soluble species were observed.

7.2.2. Characterization of $Os(CO)_4(\eta^1\text{-}CH=C=CH_2)Cl$

The mass spectrum and elemental analysis were consistent with a product of formula $Os(CO)_4(ClCH_2C_2H)$. In particular, the mass spectrum not only showed the successive loss of four CO ligands from the molecular ion, there was also a peak due to loss of a chloride ion from the parent molecule. This would be very unusual for $Os(CO)_4(\eta^2$-alkyne) species as these compounds only show CO and alkyne loss. The IR spectrum, in the range 2200-1600 cm^{-1}, consisted of 5 bands. Four of these bands were assigned to carbonyl stretches, however, as mentioned previously, they were at higher than expected energies. In fact, the energies of the CO bands for **21** are similar to those reported for *cis*-$Os(CO)_4X_2$ (X = Cl, Br) compounds.[8] Assuming an octahedrally-based geometry, the observation of four CO stretches indicates a *cis*-$Os(CO)_4(R)Cl$ (C_s symmetry) species, a *trans* product of C_{4v} symmetry would give rise to only two carbonyl bands. (Schemes 7.2 and 7.3).

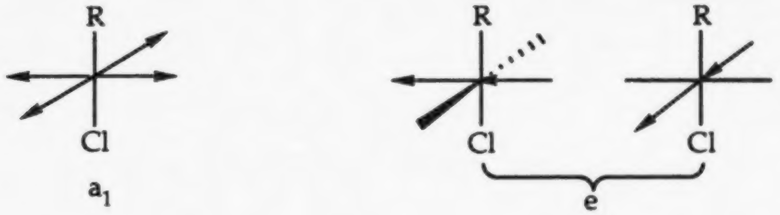

Scheme 7.2: Representation of CO Bands for *trans*-$Os(CO)_4(CHCCH_2)Cl$

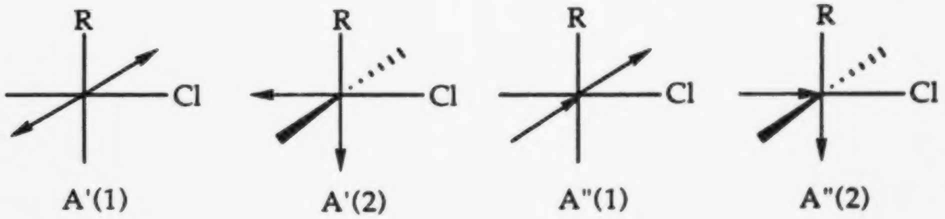

Scheme 7.3: Representation of CO Bands for *cis*-$Os(CO)_4(CHCCH_2)Cl$

The highest energy stretch (2164 cm^{-1}) can be assigned to the symmetrical A'(1) mode due to its relatively low intensity and high frequency. The remaining bands were assigned (Table 7.1) in an analogous fashion to that used by Hales and Irving.[8a]

Table 7.1: Assignment[a] of IR Bands in *cis*-$Os(CO)_4(\eta^1$-$CH=C=CH_2)Cl$

	ν(CO) (cm^{-1})			
Compound	A'(1)	A"(1)	A'(2)	A"(2)
cis-$Os(CO)_4(\eta^1$-$CH=C=CH_2)Cl$,[b] **21**	2164(w)	2091(s)	2081(m)	2034(s)
cis-$Os(CO)_4Cl_2$[c]	2187(w)	2120(s)	2094(m)	2054(s)
cis-$Os(CO)_4Br_2$[d]	2178(w)	2113(s)	2090(m)	2051(s)
cis-$Os(CO)_4(Et)Cl$[e]	2155(w)	2078(vs)		2023(s)

[a] For compounds with symmetrical substituents (C_{2v} symmetry) the following symmetry designations are used: A'(1) = $a_1(1)$, A"(1) = b_1, A'(2) = $a_1(2)$, A"(2) = b_2. [b] In pentane. [c] In CCl_4. Tyler, D.R.; Altobelli, M.; Gray, H.B. *J. Am. Chem. Soc.* **1980**, *102*, 3022. [d] In cyclohexane. Hales, L.A.W.; Irving, R.J. *J. Chem. Soc.(A)* **1967**, 1389. [e] In pentane, A"(1) and A'(2) bands overlap. Carter, W.J.; Kelland, J.W.; Okrasinski, S.J.; Warner, K.E.; Norton, J.R. *Inorg. Chem.* **1982**, *21*, 3955.

The infrared spectrum of the molecule allowed for the initial assumption that an oxidative-addition has occurred to yield a *cis*-$Os(CO)_4(R)Cl$ species. Following the oxidative addition, two compounds are possible; one with an η^1-allenyl group (**A**), the other with an η^1-propargyl moiety (**B**).

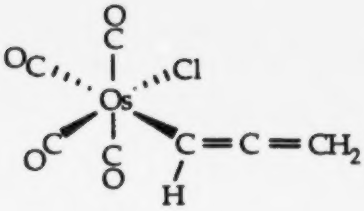

A

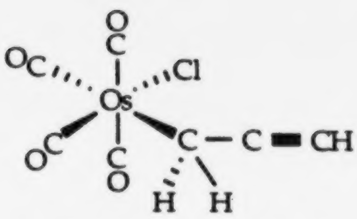

B

The FT-IR spectrum also provided the initial indication that an η^1-allenyl group (**A**) had been formed. A weak band at 1926 cm^{-1} was also observed in the IR spectrum; this signal was of too low an energy to be assigned to an acetylenic C-C stretch[9] that would occur in the range 2250-2100 cm^{-1}. However, this band is in the range known for the C=C=C stretch of allenes[10] (Table 7.2).

Table 7.2: IR Data for σ-Allenyl Complexes

Compound	ν(C=C=C) (cm^{-1})
cis-$Os(CO)_4(\eta^1\text{-}CH{=}C{=}CH_2)Cl$, **21**	1926[a]
allene ($H_2C{=}C{=}CH_2$)	1950[b]
$Pt(PPh_3)_2(\eta^1\text{-}HC{=}C{=}CH_2)Br$	1910[c]
$Ir(PPh_3)_2(CO)(\eta^1\text{-}HC{=}C{=}CH_2)Cl_2$	1920[c]
$CpW(CO)_3(\eta^1\text{-}HC{=}C{=}CH_2)$	1926[d]

---

[a] In pentane. [b] Vapour (300 K). Blanc, J.; Brecher, C.; Halford, R.S. *J. Chem. Phys.* **1962**, *36*, 2654. [c] KBr pellet. Collman, J.P.; Cawse, J.N.; Kang, J.W. *Inorg. Chem.* **1969**, *8*, 2574. [d] In benzene. Keng, R.-S.; Lin, Y.-C. *Organometallics*, **1990**, *9*, 289.

The higher energy of the CO bands in **21** as compared to *cis*-$Os(CO)_4(Et)Cl$, Table 7.1, also point towards **21** having an η^1-allenyl unit. For structure **B** one would expect CO band energies similar to *cis*-$Os(CO)_4(Et)Cl$, since both have sp^3 hybridized carbons attached to the osmium center. However for **A**, assuming no π interactions, the more electronegative $HC{=}C{=}CH_2$ group, due to its sp^2 hybridized carbon atoms,[11] will give rise to higher energy bands in **21** as compared to *cis*-$Os(CO)_4(Et)Cl$.

^1H NMR spectroscopy was also instrumental in determining that an η^1-allenyl species had been formed. For both **A** and **B** one would expect to see a doublet and a triplet in the ^1H NMR spectrum. Fortunately, there is a difference in the chemical shift ranges expected for the ^1H NMR signals for **A** and **B**. For **B**, the acetylenic proton and the methylene protons will both resonate at the highfield region of the ^1H NMR spectrum, with δ values in the range of 1.0-3.0 ppm. For example, in the η^1-propargyl complex $CpW(CO)_3(\eta^1\text{-}CH_2CCH)$, the acetylenic proton resonates at 2.18 ppm and the methylene protons appear at 1.90 ppm with $^4J_{H\text{-}H} = 2.8$ Hz.[12] In contrast to this, in **A** the α proton and the methylene protons will appear in the olefinic range (4-6 ppm).[13] However, it would be ill-advised to rely solely on ^1H NMR chemical shift data to assign structure **A** or **B**. In fact, $CpFe(CO)_2(\eta^1\text{-}CH{=}C{=}CH_2)$ was originally assigned[14] as the η^1-propargyl species, albeit in the early days of NMR applications to organometallic compounds. The H-H coupling constant can be also used as a discerning factor. Due to the allenyl π interaction, the allenic structure should have a significantly larger H_α-H_γ coupling constant (6-7 Hz) than its propargyl analogue (2-3 Hz).[10b] The ^1H NMR data for **21** and related compounds are given in Table 7.3.

The Table indicates that the chemical shift values obtained for **21** are in accord with other known η^1-allenyl compounds, while, for comparison, the ^{1}H NMR data for an η^1-propargyl complex has been included. The α protons of the η^1-allenyl units, in all cases listed, are downfield of the methylene (γ) protons. Also, the α protons are shifted slightly downfield and the γ protons shifted upfield as compared to non-metallated allenes; the proton chemical shift in allene is 4.67 ppm.

Table 7.3: ^{1}H NMR Data for **21** and Related Compounds

	δ (ppm)		
Compound	$CH(\alpha)$	$CH_2(\gamma)$	$^4J_{H\text{-}H}$ (Hz)
cis-$Os(CO)_4(\eta^1\text{-}CH{=}C{=}CH_2)Cl$,[a] **21**	5.40	4.07	6.2
$Pt(PPh_3)_2(\eta^1\text{-}HC{=}C{=}CH_2)Cl$[b]	4.55	2.77	6.4
$Ir(PPh_3)_2(CO)(Cl)_2(\eta^1\text{-}HC{=}C{=}CH_2)$[c]	5.28	3.54	not resolved
$CpW(CO)_3(\eta^1\text{-}HC{=}C{=}CH_2)$[d]	5.47	4.06	6.7
$CpFe(CO)_2(\eta^1\text{-}HC{=}C{=}CH_2)$[e]	4.89	3.97	6.5
$CpW(CO)_3(\eta^1\text{-}CH_2CCH)$[d]	2.18	1.90	2.8

[a] In CD_2Cl_2. [b] In $CDCl_3$. Mann, B.E.; Shaw, B.L.; Tucker, N.I. *J. Chem. Soc. (A)* **1971**, 2667. [c] In $CDCl_3$. Collman, J.P.; Cawse, J.N.; Kang, J.W. *Inorg. Chem*. **1969**, *8*, 2574. [d] In benzene-d_6. Keng, R.-S.; Lin, Y.-C. *Organometallics*, **1990**, *9*, 289. [e] In CS_2. Jolly, P.W.; Pettit, R. *J. Organomet. Chem*. **1968**, *12*, 491.

Collman felt the downfield shift of the α proton in η^1-allenyl complexes upon metallation was unusual since normally, transition metals cause the upfield shift of nearby protons.[13] However, the observation of a downfield shift upon metallation has been reported for similar compounds. The α protons in the σ-bonded metal-vinyl complexes $Cp^*Ir(PMe_3)(H)(\eta^1\text{-}HC{=}CH_2)$ and *trans*-$(dmpm)_2Fe(H)(\eta^1\text{-}HC{=}CH_2)$ (dmpm: $CH_2(PMe_2)_2$), show significant downfield chemical shifts of 8.12 and 7.26 ppm, respectively.[15] These represent chemical shifts 2.84 and 1.98 ppm downfield from free ethylene. It is difficult to predict the proton NMR chemical shifts of simple and substituted η^1-allenes and it has been stated[10b,16] that in the NMR spectra of allenes, chemical shifts do not always correlate with charge densities. Thus, the presence of a transition metal centre will further complicate the system and make accurate predictions of chemical shifts even more tenuous.

An unusual feature of **21** is the rather long relaxation time of the methylene protons. In fact, in order to obtain a ^1H NMR spectrum with reasonable integration for the methylene protons, a relaxation delay of 10 seconds was required. The phenomenon of long relaxation times for η^1-allenyl groups has not been mentioned in the literature dealing with organometallic η^1-allenyl compounds. The spin-lattice relaxation mechanism is affected by magentic interactions between nuclei and by molecular rotational reorientations; the more restricted the motion, the shorter the relaxation time.[17] To illustrate, in polycyclic systems the side-chain carbon atoms have longer T_1 values than skeleton carbons bearing one or more protons. This is because the skeleton carbons are held in a more rigid environment, shortening their T_1 values. The long methylene relaxation time implies that the η^1-allenyl unit is rotating rapidly about the Os-C single bond; the increased motion at the end of the allenyl moiety is then reflected in the long relaxation time.

The use of ^{13}C NMR spectroscopy is extremely valuable in the characterization of allene and cumulene complexes. The central carbon of an allene may be readily identified by its lowfield position; usually in the range of 190-220 ppm.[10b,16] The α and γ carbons appear in the olefinic region. In allene, the ^{13}C NMR chemical shift values are 212.6 and 73.5 ppm[18a] while in **22**, the shift values are 206.5 and 92.7 ppm.[18b]

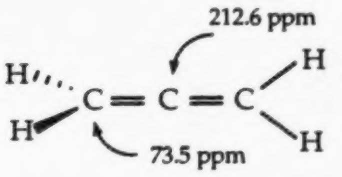

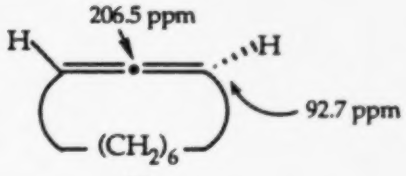

22

The central allenic carbon atom in **21** was readily identified in the ^{13}C NMR spectrum. In order to distinguish the CH and CH_2 carbons an APT ^{13}C NMR experiment was performed and the results are listed in Table 7.4.

A quantitative comparison of the chemical shift values is difficult due to the variety of metal centres and substitution patterns. For all listed compounds the α carbon is upfield of the γ carbon (Table 7.4). This is in direct opposition to the ^{1}H NMR results where the α protons were downfield of the γ protons. This phenomenon is also seen in allenes substituted by organic groups whereby a substituent that causes the α proton to shift downfield relative to the γ proton gives rise to an upfield shift of the α carbon relative to the γ carbon.[10b] In addition, to further complicate the issue, there have been organometallic complexes reported with substituted η^1-allenyls where, in the ^{13}C NMR spectrum, the α carbon is downfield of the γ carbon.[19] Thus, the α and γ carbons cannot be assigned on the basis of their relative upfield or downfield positions.

Table 7.4: ^{13}C NMR Data for **21** and Related Compounds

Compound	CH(α)	(δ, ppm) =C=(β)	CH_2(γ)
cis-$Os(CO)_4(\eta^1\text{-}CH{=}C{=}CH_2)Cl$,[a] **21**	60.8	211.2	65.0
$CpW(CO)_3(\eta^1\text{-}HC{=}C{=}CH_2)$[b]	48.6	209.1	62.2
$PdCl(PPh_3)_2[\eta^1\text{-}HC{=}C{=}CH(Ph)]$[c]	90.9	192.3	98.5
$PdCl(PPh_3)_2[\eta^1\text{-}HC{=}C{=}C(CH_3)_2]$[d]	84.3	194.6	91.4

[a] In CD_2Cl_2. [b] In benzene-d_6. Keng, R.-S.; Lin, Y.-C. *Organometallics*, **1990**, *9*, 289. [c] In $CDCl_3$. Elsevier, C.J.; Kleijn, H.; Boersma, J.; Vermeer, P. *Organometallics*, **1986**, *5*, 716. [d] In $CDCl_3$ Elsevier, C.J.; Kleijn, H.; Ruitenberg, K.; Vermeer, P. *J. Chem. Soc., Chem. Commun.*, **1983**, 1529.

Unfortunately, substituent effects on the α carbon cannot be quantified and while the chemical shift of the γ carbon may be related to the electronegativity of the substituent, this is difficult to quantify with organometallic substituents.[10b] The lack of a reliable predictive model manifests itself in the difficulty in assigning the ^{13}C NMR spectra of η^1-allenyls and wherever possible, experiments such as APT ^{13}C NMR or proton-coupled ^{13}C NMR spectra should be run in order to verify the assignments. This shortcoming is also illustrated in the chemical shift difference between the α and γ carbons which varies with substituent. For **21**, there is only a 4.8 ppm chemical shift difference between α and γ carbons, whereas for $CpW(CO)_3(\eta^1\text{-}HC{=}C{=}CH_2)$ there is a 13.6 ppm shift difference.

7.3. Mechanistic Pathway for Formation of $Os(CO)_4(\eta^1\text{-}CH{=}C{=}CH_2)Cl$, 21

It is reasonable to assume that the first step in the synthesis of **21** is the formation of a η^1-propargyl species. This species is formed by the oxidative addition of propargyl chloride to the photochemically generated $Os(CO)_4$ intermediate. This could then be followed by a [1,3] sigmatropic rearrangement to yield the η^1-allenyl species (Scheme 7.4).

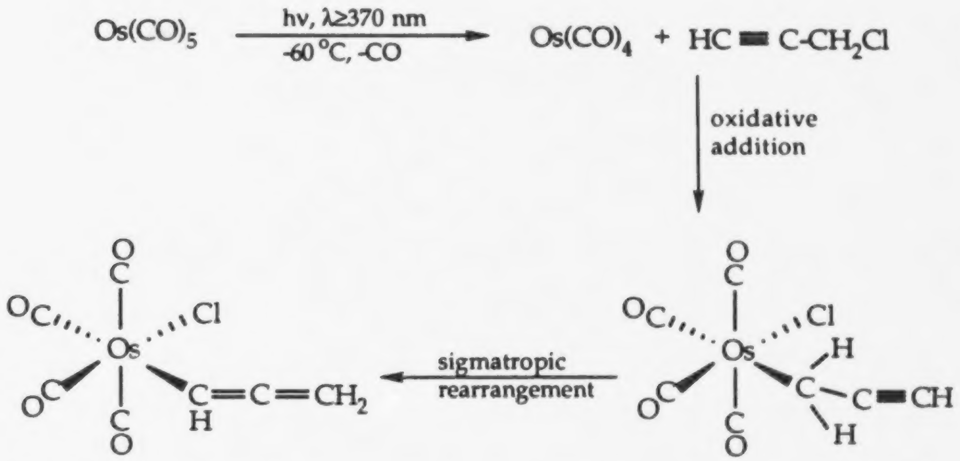
Os(CO)5
hν, λ≥370 nm
-60 °C, -CO
Os(CO)4 + HC≡C-CH2Cl
oxidative addition
sigmatropic rearrangement
Os
Cl
OC
CO
H
C=C=CH2
C≡CH

Scheme 7.4: Mechanism for Formation of $Os(CO)_4(\eta^1\text{-}CH{=}C{=}CH_2)Cl$

There are numerous examples of the production of η^1-allenyl species formed from propargyl halides. One synthetic method utilizes the ready availability of transition metal anions in nucleophilic attack on propargyl halides, formally an oxidative addition.[12,14,20,21]

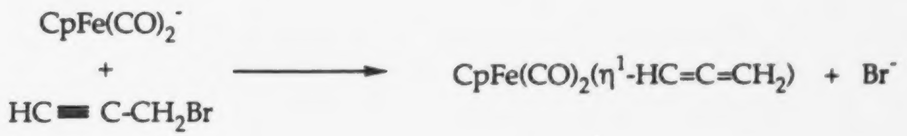

$$\begin{array}{c} CpFe(CO)_2^- \\ + \\ HC\equiv C\text{-}CH_2Br \end{array} \longrightarrow CpFe(CO)_2(\eta^1\text{-}HC{=}C{=}CH_2) + Br^-$$

Another common synthetic method involves the oxidative addition of propargyl halides to transition metal centres.[13,22,23,24]

$$\begin{array}{c} IrCl(CO)(PPh_3)_2 \\ + \\ HC\equiv C\text{-}CH_2Cl \end{array} \longrightarrow IrCl_2(CO)(PPh_3)_2(\eta^1\text{-}HC{=}C{=}CH_2)$$

In the methods outlined above only the final η^1-allenyl species is shown, however, η^1-propargyl intermediates are assumed. In both cases, it is possible that the η^1-propargyl to η^1-allenyl tautomerization may occur by a [1, 3] hydrogen or a [1, 3] metal sigmatropic rearrangement.[25]

Recently, Lin and co-workers have been able to isolate $CpW(CO)_2(L)(\eta^1\text{-}CH_2CCH)$ (L = CO, $P(OMe)_3$) species and observe their conversion to η^1-allenyl compounds.[12,21] This reaction has a relatively low activation energy (19 kcal/mol for L = CO in benzene); the isomerization occurs spontaneously at ambient temperatures in benzene solution. Lin has argued that this low activation barrier points towards a [1, 3] metal sigmatropic shift as the [1, 3] hydrogen shift in propene, which proceeds antarafacially, has been calculated[26] to be 93 kcal/mol. Further evidence supporting a [1, 3] metal rearrangement is provided by Wojcicki and co-workers[23] who observed an η^1-propargyl to η^1-allenyl tautomerization on a Pt based system (Scheme 7.5).

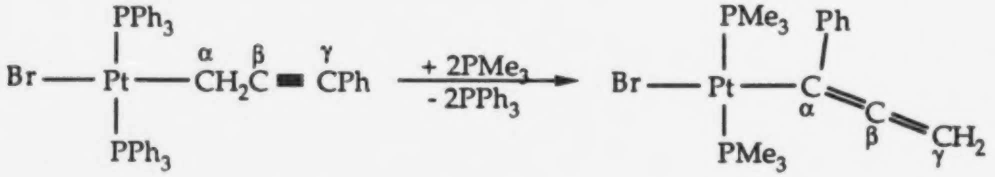

Scheme 7.5: [1, 3] Pt Rearrangement in $Pt(Br)(PPh_3)_2(\eta^1\text{-}CH_2C_2Ph)$

If the reaction were to proceed via a [1, 3] hydrogen shift, an η^1-allenyl with a proton, not a phenyl, in the α position would have been produced. However, invoking a [1, 3] Pt sigmatropic rearrangement accounts for the observed product. From these arguments, considering the facile formation of $Os(CO)_4(Cl)(\eta^1\text{-}CH{=}C{=}CH_2)$, **21**, it is reasonable to assume that the rearrangement from the η^1-propargyl intermediate is also proceeding via a [1, 3] metal sigmatropic rearrangement.

An alternative mechanism for the direct production of η^1-allenyl derivatives would involve rearrangement of the propargyl by nucleophilic substitution with the elimination of a leaving group. For example, the reaction of propargyl bromide with Grignard reagents can be used to synthesize substituted allenes.[27]

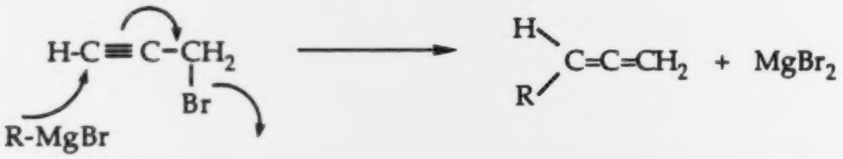

In the ground state, $Os(CO)_5$ has D_{3h} symmetry and is a closed-shell eighteen electron species. However, as stated by Hoffmann, the higher energy C_{4v} symmetry $Os(CO)_5$ is isolobal with CH_3^- or NH_3, making it an effective nucleophile.[28] Thus, there may be photochemical activation of $Os(CO)_5$ to this excited state followed by a nucleophilic substitution reaction (Scheme 7.6). The concept of photochemical activation of $Fe(CO)_5$ to an excited state has been proposed to account for results seen in matrix isolation studies; the excited state is thought to have C_{4v} symmetry.[5a,b]

This mechanism could account for the rather facile generation of the η^1-allenyl species, **21**, however, there are some troubling aspects. First, in other similar photochemical reactions involving $Os(CO)_5$ and alkynes, the irradiation causes a substitution reaction *via* the ejection of a molecule of CO. The alternate mechanism does not incorporate this photochemically induced loss of CO. Second, $Os(CO)_{5-n}(PR_3)_n$ (n = 0-2) complexes have been shown[29] to react with MeI at ambient temperatures yet, in this reaction, photochemical activation is required to synthesize the η^1-allenyl species. This should be tempered with the realization that the presence of phosphine ligands will make the OsL_5 (L = two-electron donor) species more nucleophilic. Thus, most evidence points to the first mechanism as the most likely, however, further investigations are required in order to rule out the alternate mechanism.

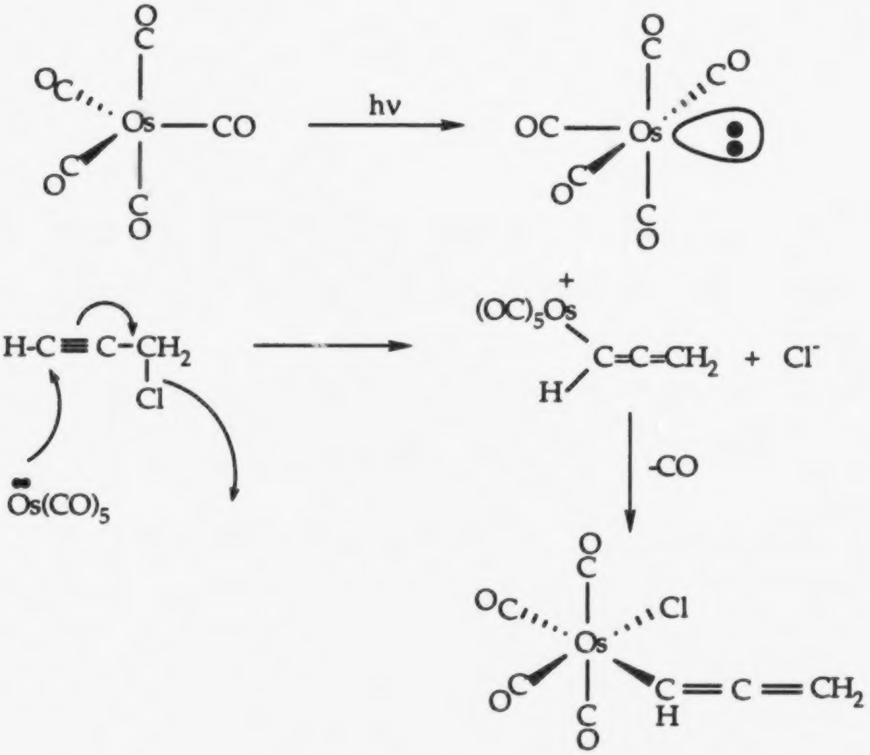

Scheme 7.6: Mechanism for Formation of **21** via Nucleophilic Attack

7.4. Attempted Reactions of $Os(CO)_4(\eta^1\text{-}CH{=}C{=}CH_2)Cl$, 21

The increased stability imparted to the allenyl unit upon metallation allows for reactions of the allenyl group to be investigated. Lin and co-workers have studied the reaction of $CpW(CO)_3(\eta^1\text{-}CH{=}C{=}CH_2)$ with excess methylamine to form an azatungstacyclobutane.[21b]

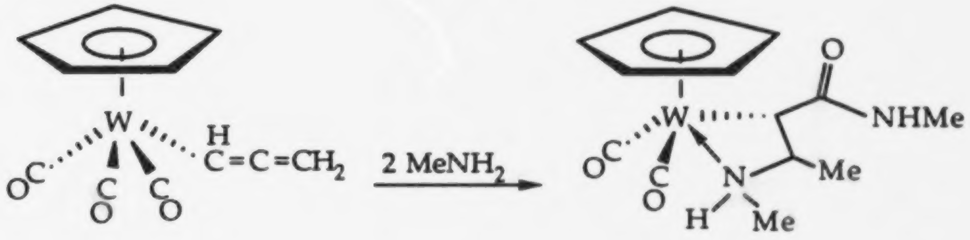

Recently, Pd η^1-allenyl compounds have been used to synthesize substituted allenes for use in organic synthesis[24] and metal-allenyl compounds are being used in the synthesis of bimetallic complexes and higher clusters.[19,30] However, one of the newest areas of research involves the synthesis and reactions of η^3-allenyl ligands.[23,31]

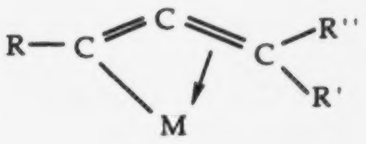

η^3-allenyl

Casey and co-workers have prepared an η^3-allenyl Re species from $Cp^*Re(CO)_2(\eta^2\text{-}C_2Me_2)$ and investigated its reactivity with soft nucleophiles.[31c] The reactions proceed with attack at the central carbon atom to generate β-substituted rhenacyclobutene complexes (Scheme 7.7).

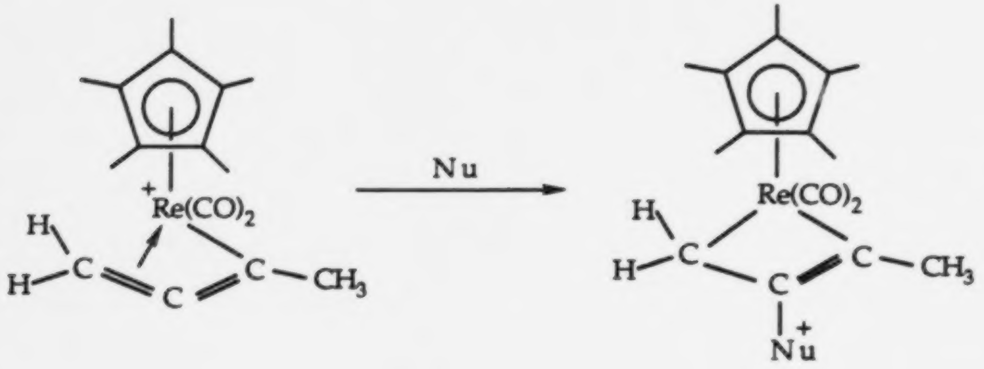

Scheme 7.7: Reaction of η^3-Allenyls with Nucleophiles

Reactions such as these represent important C-C bond forming reactions and have implications concerning the reaction of propargyl esters with organic nucleophiles which is catalyzed by palladium.[32] With this work in mind, the reaction of $Os(CO)_4(\eta^1\text{-}CH{=}C{=}CH_2)Cl$, **21**, with $AgBF_4$ was carried in order to generate an η^3-allenyl species, unfortunately, no tractable products could be isolated. Attempts to displace the chloride with an aliphatic nucleophile (MeLi) were also met with failure; the FT-IR spectra indicated that the nucleophilic attack was probably occurring at one of the carbonyl carbons. No further reactions were undertaken as the scope of this work was quite different from other research present in this thesis. However, due to the relative ease with which $Os(CO)_4(\eta^1\text{-}CH{=}C{=}CH_2)(Cl)$ can be synthesized and its potential reactivity, further investigations are warranted.

7.5. Conclusions

The original goal was to synthesize and investigate the reactions of $Os(CO)_4(\eta^2\text{-}ClCH_2CCH)$. In retrospect, the synthesis of **21** was not surprising considering the considerable precedent for oxidative addition reactions involving propargyl halides. The photochemical generation of **21** is a convenient method for synthesizing an η^1-allenyl complex in pure form, although, unfortunately, the reaction cannot be extended to the Ru analogue. The spectroscopic properties of **21** are in accord with available literature values although the long T_1 value for the methylene protons seems to be without precedent in the literature. Finally, even though initial reactions have been unproductive, the increasing interest in transition metal-allenyl complexes makes the additional investigations of **21** attractive and there are an array of possible reactions in the literature to inspire further study.

7.6. Experimental Section

7.6.1. Starting Materials and Reagents

Propargyl alcohol was purchased form Aldrich Chemical Co. and used as received. Propargyl chloride (3-chloro-propyne), was prepared from propargyl alcohol using the method of Hatch[1].

7.6.2. Synthetic Procedures

Synthesis of $Os(CO)_4(\eta^1\text{-}CH{=}C{=}CH_2)Cl$, 21

A 100 mL immersion well (Figure 2.5) fitted with a GWV insert ($\lambda \geq 370$ nm) was charged with a pentane solution containing $Os(CO)_5$ (126.0 mg, 0.382 mmol) and excess propargyl chloride (0.5 mL). The temperature of the solution was maintained at -60 °C *via* a MGM Lauda Circulating Bath. The solution was photolyzed using a Philips 125W Mercury Vapor Lamp and the reaction was monitored using FT-IR. The reaction was complete in *ca*. 2.5 h after which time no $Os(CO)_5$ was present and only bands due to $Os(CO)_4(\eta^1\text{-}CH{=}C{=}CH_2)Cl$, **21**, were observed. The solution was then transferred by cannula to a flask pre-cooled to -78 °C. The solvent and excess alkyne were removed *in vacuo* at -78°C and the product, $Os(CO)_4(\eta^1\text{-}CH{=}C{=}CH_2)Cl$, **21**, was sublimed at room temperature to a dry ice cooled probe. The white solid was washed off the probe with pentane to yield a colorless solution. The volume of solution was reduced to *ca*. 5mL using an Ar stream and then placed in a -80 °C freezer overnight. The white, waxy solid, **21**, was isolated using inverse filtration and briefly dried a 0 °C. The yield was 40% (57.9 mg, 0.154 mmol).

Formula Weight: 376.75

Mass Spectrum(16eV, 100 °C): M^+(378, 100.0%), M^+-Cl(343, 3.6%), M^+-Cl(341, 8.5%), M^+-nCO(n = 0-4)

IR(pentane, cm^{-1}); ν(CO): 2164(w), 2091(s), 2081(m), 2034(s); ν(C=C=C): 1926(vw).

^1H NMR(360 MHz, CD_2Cl_2, 23 °C) 5.40 (1H, t, $^4J_{H\text{-}H}$ = 6.2 Hz, C-*H*), 4.07 (2H, d, $^4J_{H\text{-}H}$ = 6.2 Hz, CH_2).

^{13}C NMR(75.1 MHz, CD_2Cl_2, 23 °C) 211.18 (=C=), 168.38 (2CO, CO_{axial}), 166.45 (1CO, CO_{eq}), 164.18 (1CO, CO_{eq}), 65.03 (CH_2), 60.80 (CH).

Anal. Calcd. for $C_7H_3ClO_4Os$: C, 22.32; H, 0.80. Found: C, 22.87; H, 0.83.

7.7. References

1. Hatch, L.F.; Chiola, V. *J. Am. Chem. Soc.* **1951,** *73*, 360. (b) Hatch, L.F.; Nesbitt, S.S. *J. Am. Chem. Soc.* **1950,** *72*, 727.

2. (a) Lukehart, C.M. *Fundamental Transition Metal Organometallic Chemistry*; Brooks/Cole: Monterey, CA, 1985; Chapter 10. (b) Collman. J.P.; Hegedus, L.S.; Norton, J.R.; Finke, R.G. *Principles and Applications of Organotransition Metal Chemistry*; University Science Books: Mill Valley, CA, 1987; Chapter 5.

3. (a) Heck, R.F. *J. Am. Chem. Soc.* **1964,** *86*, 2796. (b) Chock, P.B.; Halpern, J. *J. Am. Chem. Soc.* **1966,** *88*, 3511.

4. Saillard, J.-Y.; Hoffmann, R. *J. Am. Chem. Soc.* **1984,** *106*, 2006.

5. (a) Poliakoff, M.; Turner, J.J. *J. Chem. Soc., Dalton Trans.* **1974,** 2276. (b) Poliakoff, M.; Turner, J.J. *J. Chem. Soc., Dalton Trans.* **1973,** 1351. (c) Church, S.P.; Grevels, F.W.; Kiel, G.-Y.; Kiel, W.A.; Takats, J.; Schaffner, K. *Angew. Chem. Int. Ed. Engl.* **1986,** *25*, 991.

6. (a) Cardaci, G.; Bellachioma, G.; Zanazzi, P. *Organometallics*, **1988,** *7*, 172. (b) Hoyano, J.K.; McMaster, A.D.; Graham, W.A.G. *J. Am. Chem. Soc.* **1983,** *105*, 7190.

7. (a) Burn, M.J.; Kiel, G.-Y.; Seils, F.; Takats, J.; Washington, J. *J. Am. Chem. Soc.* **1989**, *111*, 6850. (b) Gagné, M.R.; Takats, J. *Organometallics* **1988**, *7*, 561.

8. (a) Hales, L.A.W.; Irving, R.J. *J. Chem. Soc.(A)* **1967**, 1389. (b) Tyler, D.R.; Altobelli, M.; Gray, H.B. *J. Am. Chem. Soc.* **1980**, *102*, 3022.

9. Silverstein, R.M.; Bassler, G.C.; Morrill, T.C. *Spectrometric Identification of Organic Compounds, Fourth Edition*; John Wiley: New York; 1981; Chapter 3; pg. 110.

10. For a review of the synthesis, properties and reactions of allenes: (a) Rutledge, T.F. *Acetylenes and Allenes*; Rheinhold: New York, 1969. (b) Landor, S.E. *The Chemistry of the Allenes*; Academic: New York, 1982; Vol. 1-3.

11. Lowry, T.H.; Richardson, K.S. *Mechanism and Theory in Organic Chemistry, Third Edition*; Harper & Row: New York; 1987; Chapter 1, pg. 28-29.

12. Keng, R.-S.; Lin, Y.-C. *Organometallics*, **1990**, *9*, 289.

13. Collman, J.P.; Cawse, J.N.; Kang, J.W. *Inorg. Chem.* **1969**, *8*, 2574.

14. Jolly, P.W.; Pettit, R. *J. Organomet. Chem.* **1968**, *12*, 491.

15. (a) Stoutland, P.O.; Bergman, R.G. *J. Am. Chem. Soc.* **1988,** *110*, 5732. (b) Baker, M.V.; Field, L.D. *J. Am. Chem. Soc.* **1986,** *108*, 7436.

16. Runge, W. *Prog. Phys. Org. Chem.* **1981,** *13*, 315.

17. Jackman, L.M.; Ed. *Structure Determination In Organic Chemistry, Volume 1*; Butterworths: London, 1976; Chapter 3; pg. 81-84.

18. (a) Steur, R.; van Dongen, J.P.C.M.; de Bie, M.J.A., Drenth, W. *Tett. Lett.* **1971,** 3307. (b) Charrier, C.; Dorman, D.E.; Roberts, J.D. *J. Org. Chem.* **1973,** *38*, 2644.

19. Wojcicki, A. *J. Cluster Science* **1993, 4,** 59 and references therein.

20. (a) Johnson, M.D.; Mayle, C. *J. Chem. Soc., Chem. Commun.* **1969**, 192. (b) Raghu, S.; Rosenblum, M. J. Am. Chem. Soc. 1973, 95, 3060. (c) Cooksey, C.J.; Dodd, D.; Johnson, M.D.; Lockman, B.L. *J. Chem. Soc., Dalton Trans.* **1978**, 1814. (d) Foxman, B.; Marten, D.; Rosan, A.; Raghu, S.; Rosenblum, M. *J. Am. Chem. Soc.* **1977,** *99*, 2160.

21. (a) Chen, M.-C.C.; Keng, R.-S.; Lin, Y.-C.; Wang, Y.; Cheng, M.C.; Lee, G.-H. *J. Chem. Soc., Chem. Commun.* **1990**, 1138. (b) Tseng, T.-W.; Wu, I.-Y.; Lin, Y.-C.; Chen, C.-T.; Chen, M.-C.; Tsai, Y.-J.; Chen, M.-C.; Wang, Y. *Organometallics*, **1991,** *10*, 43.

22. Mann, B.E.; Shaw, B.L.; Tucker, N.I. *J. Chem. Soc. (A)* **1971,** 2667.

23. Blosser, P.W.; Schimpff, D.G.; Gallucci, J.C.; Wojcicki, A. *Organometallics*, **1993**, *12*, 1993.

24. (a) Elsevier, C.J.; Kleijn, H.; Ruitenberg, K.; Vermeer, P. *J. Chem. Soc., Chem. Commun.*, **1983**, 1529. (b) Elsevier, C.J.; Kleijn, H.; Boersma, J.; Vermeer, P. *Organometallics*, **1986**, *5*, 716.

25. For a review of sigmatropic rearrangements, including [1, α] metal rearrangements see Spangler, C.W. *Chem. Rev.* **1976**, *76*, 187.

26. Clark, T. *J. Am. Chem. Soc.* **1989**, *111*, 761.

27. Landor, S.E. *The Chemistry of the Allenes*; Academic:New York, 1982; Vol. 1.; Chapter 2; pg 47-59 and references therein.

28. (a) Hoffmann, R. *Angew. Chem. Int. Ed. Engl.* **1982**, *21*, 711. (b) Albright, T.A.; Burdett, J.K.; Whangbo, M.H. *Orbital Interactions in Chemistry*; Wiley: New York; 1985; Chapter 19.

29. (a) Bellachioma, G.; Cardaci, G.; Macchioni, A.; Zanazzi, P. *Inorg. Chem.* **1993**, *32*, 547. (b) Fleming, M.M.; Pomeroy, R.K.; Rushman, P. *J. Organomet. Chem.* **1984**, *273*, C33. (c) Einstein, F.W.B.; Jones, T.; Pomeroy, R.K.; Rushman, P. *J. Am. Chem. Soc.* **1984**, *106*, 2707.

30. (a) Young, G.H.; Raphael, M.V.; Wojcicki, A.; Calligaris, M.; Nardin, G.; Bresciani-Pahor, N. *Organometallics*, **1991**, *10*, 1934. (b) Breckenridge, S.M.; Taylor, N.J.; Carty, A.J. *Organometallics*, **1991**, *10*, 837. (c) Shuchart, C.E.;

Young, G.H.; Wojcicki, A.; Calligaris, M.; Nardin, G. *Organometallics*, **1990**, *9*, 2417. (d) Young, G.H.; Wojcicki, A.; Calligaris, M., Nardin, G.; Bresciani-Pahor, N. *J. Am. Chem. Soc.* **1989**, *111*, 6890. (e) Casey, C.P.; Austin, E. *J. Am. Chem. Soc.* **1988**, *110*, 7106. (f) Aime, S.; Osella, D.; Milone, L.; Tiripicchio, A. *Polyhedron*, **1983**, *2*, 77.

31. (a) Huang, T.-M.; Chen, J.-T.; Lee, G.-H.; Wang, Y. *J. Am. Chem. Soc.* **1993**, *115*, 1170. (b) Blosser, P.W.; Gallucci, J.C.; Wojcicki, A. *J. Am. Chem. Soc.* **1993**, *115*, 2994. (c) Casey, C.P.; Yi, C.S. *J. Am. Chem. Soc.* **1992**, *114*, 6597.

32. (a) Geng, L.; Lu, X. *Tetrahedron Lett.* **1990**, *31*, 111. (b) Minami, I.; Yuhara, M.; Watanabe, H.; Tsuji, J. *J. Organomet. Chem.* **1987**, *334*, 225.

Chapter 8

Synthesis of $Os(CO)_4(\eta^2\text{-}2\text{-butyne})$ and Reactions with Alkynes

8.1. Introduction

The synthesis of $Os(CO)_4(\eta^2\text{-}C_2Me_2)$, **20**, was initially carried out to investigate the steric requirements regarding condensation reactions with $CpM(CO)_2$ (M = Co, Rh, Ir). As described in Chapter 6, the reactivity of $Os(CO)_4(\eta^2\text{-}C_2Me_2)$ towards these metal nucleophiles aided in establishing steric guidelines towards these condensation reactions. However, a rather serendipitous discovery, its reactivity with other alkynes, was also made. The facile alkyne coupling reactions observed with **20** were wholly unexpected as $Os(CO)_4(\eta^2\text{-}HCCR)$ (R = H, CH_3, CF_3, $SiMe_3$) species do not display this reactivity.

The concept of alkyne coupling at a transition metal centre is well documented in the literature.[1] Alkyne oligomerization reactions can be readily catalyzed by d^8-d^{10} transition metal complexes to yield dimers, trimers and higher polymers.[2] In fact, the lack of d^8-d^{10} metal complexes with two or more alkynes has been attributed to ready metallacyclization reactions. The facile alkyne insertion reactions displayed by these complexes are thought to arise from the repulsive interaction between the filled alkyne $\pi_\perp$ orbital and a filled metal d orbital.[2b] This is shown in Chapter 1 (Scheme 1.9) and forms the basis of the four-electron destabilization. Electron deficient, early transition metal-alkyne complexes, such as $CpV(CO)_2(C_2R_2)$, do not usually display this reactivity because the filled alkyne $\pi_\perp$ orbital and an empty metal d orbital interact in a stabilizing fashion.[2b] Indeed, the stable $W(C_2R_2)_3(CO)$ (R = Et, Ph) has been known since 1963.[3] However, even though metallacyclization reactions are common, the use of alkynes by industry is rather uncommon. For instance, due to its relatively high cost, acetylene is not commonly used as a chemical feedstock in commercial synthesis.[1e] However, in the speciality chemical industry, alkyne coupling reactions are invaluable in the synthesis of unsaturated cyclic compounds. One of the most famous is the Reppe synthesis[1a,4] where Ni(II) catalyzes the formation of cyclo-octatetraene from acetylene.

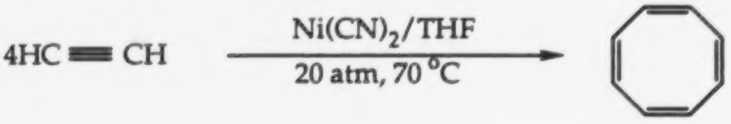

The insertion of alkynes into metal carbon bonds is a fundamental step in organometallic chemistry and has importance in cyclization and polymerization reactions. Hübel contributed much to the early work in the field; studying the reactions of alkynes with iron carbonyl compounds. The thermal reaction of $Fe_3(CO)_{12}$ with diphenylacetylene[5a] yields a myriad of products.

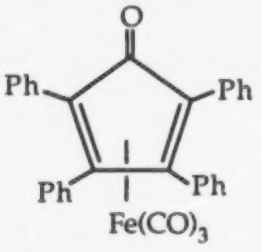

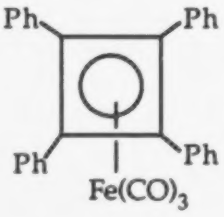

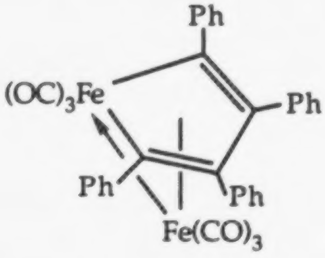

Similar products can also be obtained in the thermal or photochemical reaction of $Fe(CO)_5$ with acetylene.[5b-c] The organic fragments have been constructed by the coupling of monomeric alkyne units plus the additional possibility of CO insertion. The reactions are complex and although the initial formation of $Fe(CO)_4(\eta^2\text{-}C_2R_2)$ species is postulated,[1a] they have not been observed during the course of the reaction. Therefore, the reaction $Os(CO)_4(\eta^2\text{-}C_2Me_2)$ with alkynes is of importance to map out the early steps of these alkyne coupling reactions.

8.2. Synthesis and Characterization of $Os(CO)_4(\eta^2\text{-}C_2Me_2)$, 20

8.2.1. Synthesis of $Os(CO)_4(\eta^2\text{-}C_2Me_2)$, 20

The synthesis of $Os(CO)_4(\eta^2\text{-}C_2Me_2)$ was carried out as described for other osmium-alkyne compounds.[6] A pentane solution containing $Os(CO)_5$ and an excess of 2-butyne were photolyzed in an immersion well at -60 °C (Figure 2.5). In this photochemical synthesis, the wavelength of the irradiation was restricted by a GWV (Glaswerk Verheim) green glass filter ($\lambda \geq 370$ nm). The reaction is monitored by the disappearance of the $Os(CO)_5$ bands at 2035 and 1993 cm^{-1}. The low temperatures are required because the resulting complex, $Os(CO)_4(\eta^2\text{-}C_2Me_2)$, **20**, is thermally unstable and will decompose to unidentified products at temperatures exceeding -25 °C.

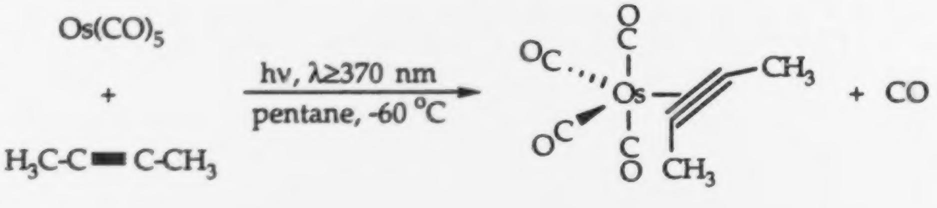

The product is purified by removal of the pentane and excess alkyne *in vacuo* at -78 °C followed by sublimation of the product, under dynamic vacuum, to a dry-ice cooled cold finger. The resulting white, waxy solid may then be washed off the probe using cold pentane. The concentration of $Os(CO)_4(\eta^2\text{-}C_2Me_2)$ can be determined by titration with $Cp^*Rh(CO)_2$. Owing to its unstable nature only spectroscopic data on $Os(CO)_4(\eta^2\text{-}C_2Me_2)$ were obtained.

8.2.2. Characterization of $Os(CO)_4(\eta^2\text{-}C_2Me_2)$, 20

The mass spectrum of $Os(CO)_4(\eta^2\text{-}C_2Me_2)$, obtained at *ca*. -20 °C, showed a peak due to $Os(CO)_4(\eta^2\text{-}C_2Me_2)^+$, followed by peaks due to the successive loss of four carbonyl ligands. A signal due to $Os(CO)_4^+$ was also observed, representing the loss of 2-butyne from **20**. Thus, the mass spectral data were fully in accord with the proposed molecular formulation. Similar observations were made in the mass spectra of $Os(CO)_4(\eta^2\text{-HCCH})$ and $Os(CO)_4[\eta^2\text{-}C_2(SiMe_3)_2]$.[6a,7]

The Os-alkyne complex, $Os(CO)_4(\eta^2\text{-}C_2Me_2)$, was also characterized by FT-IR spectroscopy. For **20**, only three terminal carbonyl bands are seen; one is a low intensity band at 2106 cm^{-1} and two other strong bands at 2020 and 1984 cm^{-1}. However, for a compound of C_{2v} symmetry such as **20** four carbonyl bands are expected (Scheme 8.1).

The weak, high energy band (a_1) that appears at 2106 cm^{-1} is characteristic of complexes of the formula $Os(CO)_4(\eta^2\text{-alkyne})$.[6,7] Also, one expects three other bands at lower energy that are of greater intensity. Thus, there is the likelihood that the band at 2020 cm^{-1} is actually composed of two overlapping signals. The IR bands of **20** are also at lower frequency than those of $Os(CO)_4(\eta^2\text{-HCCH})$. This is expected as 2-butyne is not as π-acidic as acetylene resulting in more electron density at the Os centre.

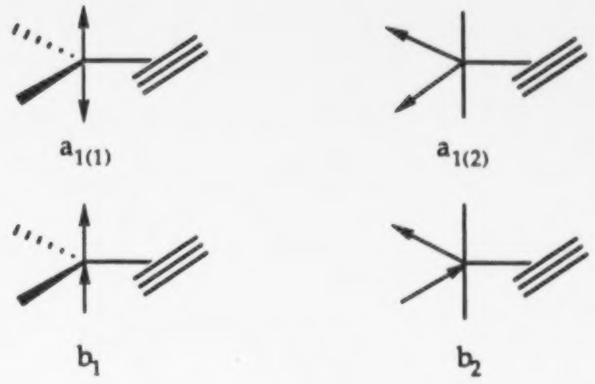

Scheme 8.1: Representation of Vibrational Bands in $Os(CO)_4(\eta^2\text{-}C_2Me_2)$

The ^1H NMR spectrum of **20**, at -70 °C in toluene-d_8, shows the expected singlet for the two equivalent methyl groups. This signal appears at 2.03 ppm, which is 0.50 ppm downfield from the methyl ^1H NMR signal for free 2-butyne (δ = 1.53 ppm). This is not unexpected as the alkyne is formally donating an electron pair to the metal centre, thus changing the electronic nature of the alkyne carbons. That is, the coordinated 2-butyne would have anisotropic effects approaching an olefin, thus causing the downfield shift. For example, the methyl groups resonate at 1.78 ppm in 2,3-dimethyl-2-butene,[8] representing a small downfield shift from 2-butyne. The ^{13}C NMR spectrum of **20** was also obtained at -70 °C. In accord with the ^1H NMR results, the methyl carbon ^{13}C NMR signal appears at 14.8 ppm; for free butyne the methyl carbon resonates at 3.2 ppm. Thus, there is a downfield shift for the methyl carbons of 11.6 ppm upon 2-butyne coordination.

The chemical shift of the coordinated alkyne carbons can be useful in deducing the reduction of C-C triple bond order upon coordination to a metal centre. This allows the metal-alkyne bonding to be described in terms of a coordinated alkyne or a metallacyclopropene (Scheme 1.8). The coordination of an alkyne to a metal should decrease the C-C π bonding in the alkyne, and thus, increase the olefinic character of the alkyne carbons. The final result is that the alkyne carbons of the metal-alkyne complex should be deshielded with respect to those in the free alkyne.[9] Templeton has reported an empirical relationship that correlates the number of electrons donated by an alkyne and its ^{13}C NMR chemical shift.[9a] Therefore, the magnitude and sign of the ^{13}C NMR coordination shift of the alkyne carbons, Δ, should provide insights in the metal-alkyne interaction. For instance, in $Cp_2Mo(\eta^2\text{-}HCCH)$, the alkyne carbons resonate at 118.0 ppm, corresponding to a Δ value of -46.1 ppm.[10] Similar results are obtained for the propyne congener.[10] The large negative value of Δ indicates a significant downfield shift upon coordination and a bonding description close to a metallacyclopropene. The ^{13}C NMR data for **20** and related compounds are given in Table 8.1.

The results obtained for $Os(CO)_4(\eta^2\text{-}C_2Me_2)$ are not in accord with initial expectations as a *positive* coordination shift of 5.9 ppm is observed. However, within the group of $Os(CO)_4(\eta^2\text{-alkyne})$ complexes, there is precedent for such unusual results. For $Os(CO)_4(\eta^2\text{-BTMSA})$ a positive coordination shift of 20.3 ppm was observed. This anomalous result was attributed to the unusually lowfield chemical shift of the alkyne carbon in free BTMSA. It has been suggested that the lowfield shift in free BTMSA is due to p_π-d_π interaction between the C-C triple bond and the *d* orbitals on the Si atom. This would reduce the C-C bond order and cause a downfield shift.[11] Upon coordination, the bending back of the $SiMe_3$ groups would reduce this conjugation and this would cause a shift to higher field.[7] This explanation, in light of the results for **20**, does not fully explain why a positive coordination shift is observed. Specifically, the ^{13}C NMR chemical shift of free 2-butyne, compared to other alkynes, is not unusual and C(alkyne)-C(methyl) conjugation is unlikely.[12] Thus, the rationale for the results obtained for $Os(CO)_4(\eta^2\text{-BTMSA})$ is more applicable towards explaining the rather large magnitude of the coordination shift, rather than the appearance of a positive value for Δ. For $Os(CO)_4(\eta^2\text{-HCCH})$, the value of Δ is -1.6 ppm. The sign indicates the expected shift to lower field upon coordination, but the magnitude of the chemical shift difference is very small. Also, the coordination shifts in $Os(CO)_4(\eta^2\text{-HCCMe})$ are unusual, with a positive value obtained for the terminal carbon and a negative value obtained for the internal *sp* carbon.

Table 8.1: ^{13}C NMR Data for $Os(CO)_4(\eta^2\text{-RCC'R'})$ Species

	Free[a]		Complex[a]			
Alkyne	δ(C-R)	δ(C'-R)	δ(C-R)	δ(C'-R)	Δ[b]	
$(H_3C)CC'(CH_3)$	74.6		69.7		+5.9	
HCC'H[c]	71.9		73.5		-1.6	
$Me_3SiCC'SiMe_3$[d]	113.0		92.7		+20.3	
$(CF_3)CC'(CF_3)$[e]	71.4		92.5		-21.1	
$HCC'(CH_3)$[f]	67.2	80.2	58.0	84.5	+9.2	-4.3
$HCC'(CF_3)$[f]	75.9	69.2	89.4	81.8	-13.5	-12.6

[a] In ppm. [b] In ppm, $\Delta = \delta_{C\text{-}R(free)} - \delta_{C\text{-}R(complex)}$. [c] Burn, M.J.; Kiel, G.-Y.; Seils, F.; Takats, J.; Washington, J. *J. Am. Chem. Soc.* **1989,** *111,* 6850. [d] Ball, R.G.; Burke, M.R.; Takats, J. *Organometallics,* **1987,** *6,* 1918. [e] Gagné, M.R.; Takats, J. *Organometallics* **1988,** *7,* 561. [f] Kiel, G.-Y., personal communication.

The only systems that display a moderately large negative coordination shift are those that have strongly π-acidic alkynes such as TFP and HFB. This is expected as such electron withdrawing alkynes would favour metallacyclopropenes with the Os centre in a formal +2 oxidation state. This metallacyclopropene extreme would certainly result in significant negative coordination shifts. However, the use of less π-acidic alkynes seems to lead to positive or only slightly negative coordination shifts. This would seem to suggest that the aforementioned four-electron destabilization may be exerting an influence on the electronic environment of the alkyne carbons.[13] The more π-acidic alkynes, such as TFP and HFB, lessen the four-electron destabilization *via* delocalization of the filled $\pi_{\perp}$ orbital and increased Os→alkyne backbonding. Neglecting $Os(CO)_4[\eta^2\text{-}C_2(SiMe_3)_2]$, the Os complexes with electron rich alkynes, such as propyne and 2-butyne, have positive coordination shifts. The filled *d* orbitals on the Os centre will interact with the filled alkyne $\pi_{\perp}$ orbital resulting in a large four-electron destabilization. Finally, acetylene, which is more π-acidic than propyne or 2-butyne, yields an Os complex with only a slight negative coordination shift. Unfortunately, the extent and effects of this influence on the chemical shifts, if any, cannot be fully quantified at this time.

8.3. Reaction of $Os(CO)_4(\eta^2\text{-}C_2Me_2)$ with 2-butyne

The observation that $Os(CO)_4(\eta^2\text{-}C_2Me_2)$ may react with alkynes was first noticed as an anomaly in the FT-IR spectrum as the photochemical preparation of $Os(CO)_4(\eta^2\text{-}C_2Me_2)$ was being monitored. As the reaction proceeded, only $Os(CO)_5$ and a species with three strong carbonyl bands was observed. The expected high energy, low intensity $a_1(1)$ band of

$Os(CO)_4(\eta^2\text{-}C_2Me_2)$, **20**, was not observed. After completion of the photochemical step and subsequent low temperature workup, a white thermally unstable solid was sublimed to a dry-ice cooled probe. The FT-IR spectrum of this compound showed it to be $Os(CO)_4(\eta^2\text{-}C_2Me_2)$. However, addition of 2-butyne to this compound regenerated the species with the three strong terminal carbonyl bands. It became apparent that a thermal reaction had been occurring in the IR cell during the time taken to prepare and run the sample and that this reaction required additional butyne. Isolation of this species showed it to have a molecular composition consistent with "$Os(CO)_4$(2-butyne)$_2$". Additional work showed that this species could be readily synthesized *via* the low temperature photolysis of $Os(CO)_5$ followed by warming the pentane solution to -20 °C. The product obtained, $Os(CO)_4$(2-butyne)$_2$, **24a**, is an off-white solid soluble in hydrocarbon solvents, from which it can be readily crystallized at low temperatures.

8.3.1. Characterization of $Os(CO)_4$(2-butyne)$_2$, 24a

The isolation of $Os(CO)_4$(2-butyne)$_2$ in crystalline form allowed for its complete characterization. The mass spectrum and elemental analysis indicated a mononuclear species. The IR spectrum consisted of four bands; three strong terminal carbonyl bands at 2071, 2006, 1988 cm^{-1} and a weak signal at 1676 cm^{-1}. In the ^1H NMR spectrum, two singlets of equal intensity were observed, indicating that two different methyl environments were present. However, the most useful information was present in the ^{13}C NMR spectrum. Mirroring the ^1H NMR results, two methyl ^{13}C NMR resonances were observed. Also, two signals were observed in the carbonyl region in an approximate 3:1 ratio (δ = 176.1 ppm, 3CO; 175.7 ppm, 1CO). Finally, two resonances were seen at 71.9 ppm and 97.1 ppm. These were assigned to the alkyne carbons and are in the region associated with coordinated diene-type structures.[14] A cyclopentadienone structure was postulated based on the observation of an ketone signal in both the FT-IR and ^{13}C NMR spectra.

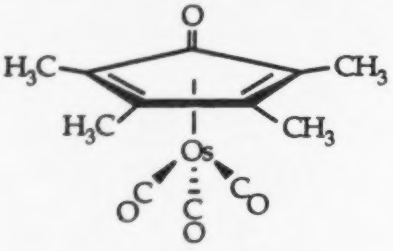

24a

There is considerable precedent for compounds such as **24a**. In fact, Green[15] and co-workers claim to have synthesized **24a** in 1969, however the spectroscopic data and physical properties reported do not match those obtained in our laboratories. It is likely that a different isomer of formula $Os(CO)_4(C_2Me_2)_2$ was synthesized; two isomers of $Ru(CO)_4(C_2Ph_2)_2$ are known.[16] Also, a number of (cyclopentadienone)tricarbonyliron species have been prepared, most efficiently with activated alkynes bearing electron withdrawing substituents.[1a,17] As noted, Hübel has prepared several substituted (cyclopentadienone)tricarbonyliron compounds but there are few Ru and Os cyclopentadienone compounds in the literature. The syntheses of $Ru(CO)_3(\eta^4\text{-}C_4(CF_3)_4CO)$, $Ru(CO)_3(\eta^4\text{-}C_4Ph_4CO)$ and $Ru(CO)_3(\eta^4\text{-}C_4Et_4CO)$ have been reported,[18] $Ru(CO)_3(\eta^4\text{-}C_4Et_4CO)$ was only isolated as a minor component in the thermal reaction of 3-hexyne with $Ru_3(CO)_{12}$.[18b] Some of the most studied compounds are the tetraphenyl substituted derivatives, $M(CO)_3(C_4Ph_4CO)$ (M = Fe, Ru, Os), all of which have been fully characterized.[4,14e,18a,19] The Ru complex has been the subject of considerable interest due to its role as a catalytic precursor in a variety of reactions.[20]

8.3.2. Synthesis of $M(CO)_3(\eta^4\text{-}C_4R_4CO)$ (M = Ru, Os; R = Me, Et, n-Pr)

The discovery of the facile alkyne coupling to produce $Os(CO)_3(\eta^4\text{-}C_4Me_4CO)$ led to the development of a general synthesis for compounds of the type $M(CO)_3(\eta^4\text{-}C_4R_4CO)$ (M = Ru, Os; R = Me, Et, n-Pr). The general method involved the low temperature photolysis of a pentane solution of $M(CO)_5$ (M = Ru, Os) to which was added an excess of the appropriate alkyne (C_2R_2, R = Me, Et, n-Pr). After the photolysis was complete, as judged by the disappearance of $M(CO)_5$, the solutions were slowly warmed to 0 °C. This resulted in conversion to the cyclopentadienone species.

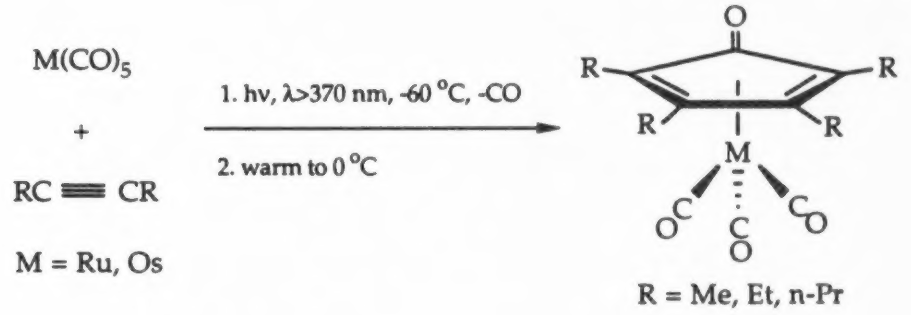

The only exception involved the reaction of $Ru(CO)_5$ with 2-butyne. The photolysis at -60 °C resulted in the formation of large amounts of $[Ru(CO)_4]_x$,[21] an insoluble, flocculent orange polymer; scarce amounts of $Ru(CO)_3(\eta^4\text{-}C_4Me_4CO)$ were observed. This was likely due to the extreme thermal instability of the $Ru(CO)_4(\eta^2\text{-butyne})$ intermediate. In retrospect, this is not surprising as $Ru(CO)_4(\eta^2\text{-HCCH})$ is only stable below -30 °C,[22] thus a less π acidic alkyne such as 2-butyne should confer even less thermal stability to the Ru-alkyne complex. $Ru(CO)_4(\eta^2$-butyne) could then decompose before it undergoes the thermal reaction with excess 2-butyne. To counter this, the photochemical reaction was repeated at -5 °C so that any $Ru(CO)_4(\eta^2$-butyne) formed could immediately react with excess 2-butyne in solution to generate the desired product, $Ru(CO)_3(\eta^4\text{-}C_4Me_4CO)$. This gave satisfactory results as the amount of polymeric ruthenium carbonyl was reduced and the cyclopentadienone complex was formed in 29% yield. The reactions of $Ru(CO)_5$ with 3-hexyne and 4-octyne proceeded smoothly, perhaps due to the increased stability of the Ru-alkyne intermediate. This is manifested in the increased yield as one proceeds from the methyl to the ethyl (53%) and finally n-propyl (63%) substituents. The carbonyl bands observed in the IR spectrum for $Ru(CO)_3(\eta^4\text{-}C_4Et_4CO)$ matched those reported by Stone.[18b]

8.3.3. Characterization of $M(CO)_3(\eta^4\text{-}C_4R_4CO)$ (M = Ru, Os)

The (cyclopentadienone)tricarbonylmetal species can be readily identified by their characteristic FT-IR spectra. The molecules possess C_s symmetry and there are three allowed terminal carbonyl vibrational modes (Scheme 8.2).

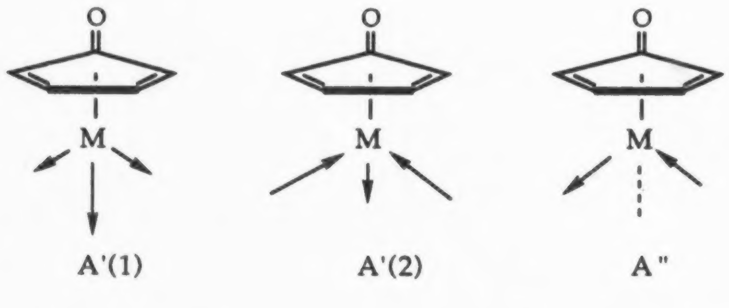

Scheme 8.2: Representation of Vibrational Modes in $M(CO)_3(\eta^4\text{-}C_4R_4CO)$

As shown, two of the bands are symmetric with respect to the mirror plane and are of A' symmetry. The other vibrational mode is anti-symmetric to the σ_v plane and is designated A''. An assignment[23] of the IR bands has been made on a related $Fe(CO)_3(\eta^4$-butadiene) system that also has C_s symmetry. Based on this reference, the A'(1) mode can be assigned to the highest frequency stretch. This is not unexpected as a larger amount of energy is needed to effect such a symmetric stretch. The A'(2) mode is then assigned to the intermediate energy band with the lowest frequency signal assigned to the asymmetric A'' mode. In addition, one band for the ketonic functionality of the ring is expected. The FT-IR bands for $M(CO)_3(\eta^4\text{-}C_4R_4CO)$ (M = Ru, Os; R = Me, Et, n-Pr) are listed below (Table 8.2).

Table 8.2: FT-IR Bands for $M(CO)_3(\eta^4\text{-}C_4R_4CO)$, **23a-c** and **24a-c**

			$\nu(CO)$ $(cm^{-1})^a$			
	M	R	A'(1)	A'(2)	A''	ν(ketone)
23a	Ru	Me	2073(s)	2016(s)	1996(s)	1670(w)
23b	Ru	Et	2072(s)	2015(s)	1996(s)	1663(w)
23c	Ru	n-Pr	2071(s)	2014(s)	1995(s)	1662(w)
24a	Os	Me	2071(s)	2006(s)	1988(s)	1676(w)
24b	Os	Et	2070(s)	2004(s)	1987(s)	1669(w)
24c	Os	n-Pr	2069(s)	2004(s)	1987(s)	1669(w)
	Ru[b]	Ph	2081(s)	2026(s)	2005(s)	1657(w)
	Os[b]	Ph	2079(s)	2015(s)	1997(s)	1677(w)

Solvent: [a]pentane; [b]cyclohexane

In general, moving from Ru to Os for a particular R = Me, Et, n-Pr group, the A'(2) and A" bands decrease by approximately 10 cm^{-1} and 8 cm^{-1}, respectively. The increase in electron density changing from Ru to Os centres reflects itself in the increased π-donor ability of Os as compared to Ru.[24] For each particular metal with R = Me, Et, n-Pr, the energies of the terminal carbonyl bands do not change significantly from one ring substituent to another. This is not surprising as there is only a small difference in electron donating ability between R = Me, Et, n-Pr. However, the corresponding carbonyl bands for the tetraphenyl substituted derivatives are approximately 10 cm^{-1} higher in energy than for the tetra-aliphatic substituted compounds. This is a reflection of the electron withdrawing character of the phenyl substituent with respect to an aliphatic functional group. The Ph group, in comparison to R = Me, Et or n-Pr, draws electron density from the ring, causing less $M_{d\pi}$-CO_{π^*} backbonding, which raises the CO stretching frequencies.

For each metal, there is a decrease of approximately 7 cm^{-1} in the ketonic stretch when one changes ring substituents from R = Me to R = Et. This change is a result of a slight increase in electron donation from the Et group with respect to a methyl substituent. The tetraphenyl substituted osmium complex has a ketonic stretch similar to that of the tetramethyl substituted complex and in the case of Ru, the tetraphenyl substituted complex has a *lower* stretching frequency for the ketone group than even the tetra-n-propyl substituted compound. There are two possible canonical forms for (cyclopentadienone)$M(CO)_3$ (M = Fe, Ru, Os).

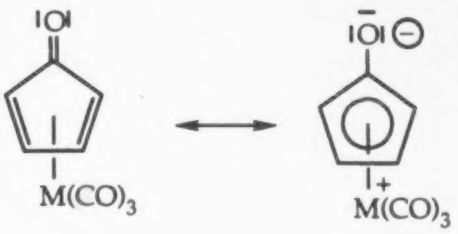

I II

The evidence suggests that the phenyl substituents, relative to aliphatic groups, are stabilizing structure **II**. This would account for the higher terminal carbonyl stretching frequencies seen in $M(CO)_3(\eta^4\text{-}C_4Ph_4CO)$ (M = Ru, Os) due to the positively charged metal centre. The apparent dichotomy of the lower energy ketonic stretch is also accounted for as the formal C-O bond order in II is one.

The use of ^{13}C NMR spectroscopy is invaluable in characterizing cyclopentadienone compounds. Various non-coordinated cyclopentadienone rings do show the expected downfield shift of the β carbon commonly associated with α, β-unsaturated ketones.[25a]

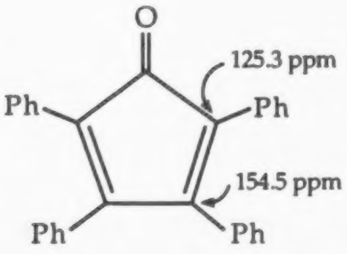

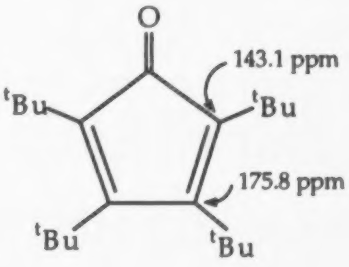

However, this shift is not due to canonical form **B** as is normally prevalent in α, β-unsaturated ketones, although form **B** could be stabilized upon coordination to a metal centre.[25b]

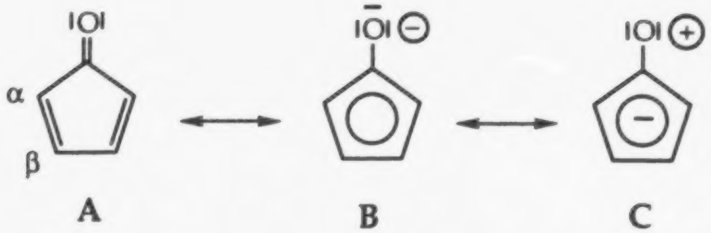

It has been argued that the antiaromatic nature of canonical form **B** causes it to make little, if any, contribution to the ground state structure.[25a] Theoretical calculations show that the electron density at the carbonyl carbon in **A** is actually less than in cyclohexanone.[25c] Therefore, Kalinowski and workers have suggested that the downfield shift of the β carbon is caused solely by an inductive effect resulting from the C-O bond polarity. This would induce an alternating charge distribution and cause a partial positive charge on the β carbon and buildup of negative charge on the α carbon. In fact, Kalinowski has estimated that the β carbon of cyclopentadienone would be shifted almost 20 ppm upfield of the β carbon in cyclopent-2-en-1-one.

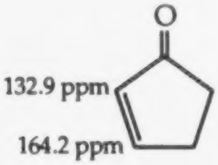

Cyclopent-2-en-1-one

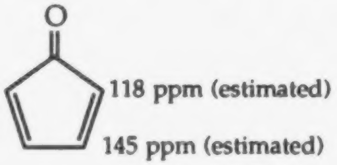

Cyclopentadienone

The coordination of the cyclopentadienone ring to the Ru or Os centre causes the characteristic[14,26] upfield shifts of the α and β carbons. When referring to coordinated ring carbons the designation inner and outer carbons will be used in order to be consistent with the literature. The inner and outer carbon atoms are the carbons at the closed and open ends of the 1,3 diene; an inner carbon refers to a coordinated β carbon while the outer carbon is analogous to an α carbon. For each metal-cyclopentadienone compound a single averaged CO signal is observed at room temperature. In cooling a sample of **24a** to -60 °C no broadening of the CO signal was observed, indicating that the carbonyls were very rapidly interconverting. The ^{13}C NMR data for **23-24** are listed in Table 8.3.

Table 8.3: ^{13}C NMR Data for $M(CO)_3(\eta^4\text{-}C_4R_4CO)$ (M = Ru, Os; R = Me, Et, n-Pr)

			^{13}C NMR (δ, ppm, $CDCl_3$)			
	M	R	inner	outer	M(CO)	C=O
23a	Ru	Me	101.2	77.5	196.0	175.4
23b	Ru	Et	105.6	85.4	195.6	176.3
23c	Ru	n-Pr	104.6	84.2	195.7	176.3
24a	Os	Me	97.1	71.9	176.1	175.7
24b	Os	Et	101.1	80.7	175.4	177.0
24c	Os	n-Pr	100.1	79.5	175.4	177.3

The prevalent feature seen in the ^{13}C NMR spectra is the chemical shift difference between the inner and outer ring carbons. Unfortunately, the ^{13}C NMR data for the free cyclopentadienones is unavailable. However, the chemical shift difference between the α and β-carbons observed for non-coordinated cyclopentadienones with bulky substituents is similar to the C_α-C_β chemical shift differences observed for **23a-c** and **24a-c**. Furthermore, in $M(CO)_3(\eta^4\text{-}C_4Ph_4CO)$ (M = Ru, Os), the relative position of the α and β-carbons was maintained in the complex with the outer carbon (C_α) upfield of the inner carbon (C_β). Thus, based on organic models and $M(CO)_3(\eta^4\text{-}C_4Ph_4CO)$ (M = Ru, Os), one can confidently assign the inner and outer carbons. Also, considering the similarity in the FT-IR data, it is not surprising that for a given metal the terminal carbonyl resonances are all within 0.7 ppm. Finally, the ketone signals do not vary by more than 1 ppm, indicating that the use of FT-IR spectroscopy may be more sensitive to small changes in ketone environment.

8.4. Reaction of $Os(CO)_4(\eta^2\text{-}C_2Me_2)$ with Alkynes

8.4.1. Synthesis of $Os(CO)_3(\eta^4\text{-}C_4Me_2R_2'CO)$ Complexes (R' = Et, n-Pr)

The previous section dealt with the reaction of *in situ* generated $M(CO)_4(\eta^2\text{-RCCR})$ (M = Ru, Os; R = Me, Et, n-Pr) species with excess alkyne to give the symmetrically substituted cyclopentadienone compounds. This reaction, although interesting from a synthetic viewpoint, is limited in its scope. However, the reaction of isolated $Os(CO)_4(\eta^2\text{-}C_2Me_2)$, **20**, with other alkynes was investigated in order to extend the synthetic applications to the preparation of asymmetrically substituted cyclopentadienones.

The reagent $Os(CO)_4(\eta^2\text{-}C_2Me_2)$ undergoes a smooth alkyne coupling reaction with excess 3-hexyne or 4-octyne to yield the corresponding $Os(CO)_3(\eta^4\text{-}C_4Me_2R_2'CO)$ species.

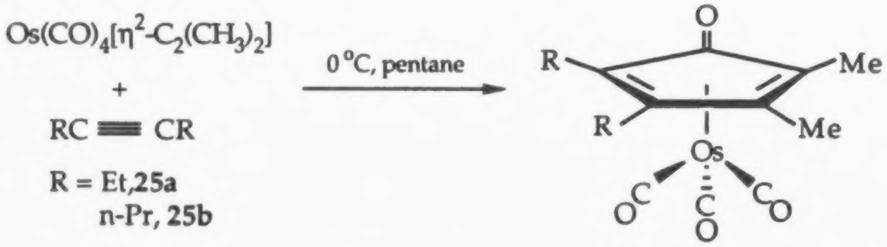

Unfortunately, at this time, the reaction is of rather limited scope as the reaction only proceeds with electron rich alkynes. The addition of activated alkynes such as HFB (hexafluoro-2-butyne), DMAD (dimethylacetylenedicarboxylate) and PC^tBu, acidic alkynes such as acetylene and propyne or bulky alkynes such as BTMSA (bistrimethylsilyacetylene) did not result in alkyne coupling and only decomposition of the Os-butyne starting material was seen. The coupling reaction with 2-pentyne did proceed, however a mixture of isomers was obtained. Also, the reaction could not be extended to include species derived from $Os(CO)_4(\eta^2\text{-}C_2Et_2)$ as this material could not be isolated without free 3-hexyne being present. Finally, reactions utilizing $Ru(CO)_4(\eta^2\text{-}C_2Me_2)$ were not attempted due to the thermal instability of this compound.

8.4.2. Characterization of $Os(CO)_3(\eta^4\text{-}C_4R_2R_2'CO)$ (R = Me, R' = Et, n-Pr)

The reaction to produce $Os(CO)_3(\eta^4\text{-}C_4R_2R_2'CO)$ (R = Me, R' = Et, n-Pr) could lead to the formation different isomers, the most plausible of which is **D**. However, isomer **E** also possesses C_1 symmetry, and although its formation is unlikely, it would have ^1H and ^{13}C NMR spectroscopic features similar to **D**.

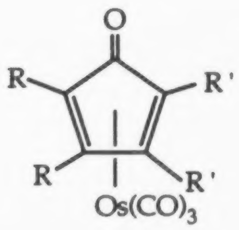

D

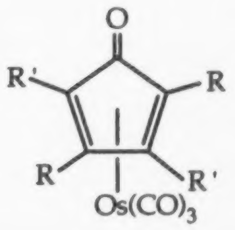

E

In the ^1H NMR spectrum of **25a** two distinct singlets due to the methyl substituents; in the ^{13}C NMR spectrum four alkyne carbon resonances were observed in the range 105-70 ppm (Table 8.4).

Table 8.4: ^{13}C NMR Data for $Os(CO)_3(C_4Me_2R_2'CO)$ (R' = Et, n-Pr)

		^{13}C NMR (δ, ppm, $CDCl_3$)					
		inner		outer			
	R	C_i-R	C_i-Me	C_o-R	C_o-Me	M(CO)	C=O
25a	Et	101.4	96.4	80.5	73.4	175.2	175.2
25b	n-Pr	100.3	96.6	79.2	73.0	175.6	176.4

For both **D** and **E**, four carbon signals would be expected for the four unique inner and outer carbons. Isomer **E** was ruled out on the basis that its formation would require the low temperature cleavage of a C-C triple bond. Confirmation of this was provided by X-ray crystallography, which will be discussed in the following section.

The assignment of the ring carbons in the ^{13}C NMR spectra of **25a** and **25b** was relatively simple. The resonances for the inner and outer ring carbons in the mixed alkyne complexes, **25a** and **25b**, matched almost exactly to the chemical shift values obtained for the symmetrically substituted complexes. For example, the chemical shift for an outer carbon attached to a methyl group for **25a** is 73.4 ppm, while in the tetramethyl substituted analogue, the outer carbon resonates at 71.9 ppm. This is well separated from the signal for the outer carbon substituted by an ethyl group that resonates at 80.5 ppm in **25a** and at 80.7 in its symmetrical congener, **24b**. The ^{13}C NMR spectra **24a, 24b** and **25a** conveniently illustrate this feature (Figure 8.1).

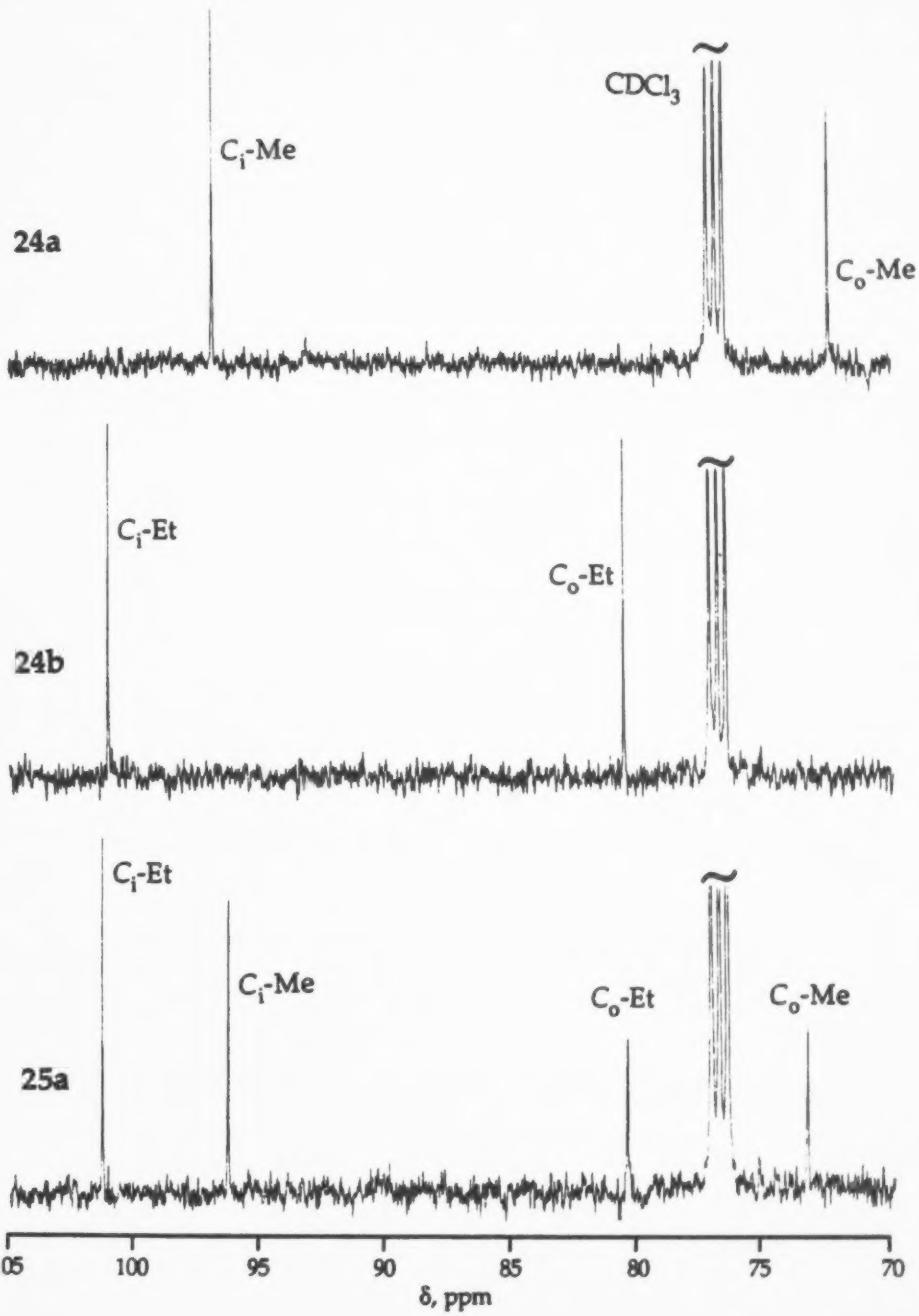

Figure 8.1: ^{13}C NMR of **24a**, **24b** and **25a** in the Ring Region

Previously, the FT-IR sensitivity of the ketone band towards ring substitution was mentioned. This feature is also apparent in the mixed alkyne species **25a-b**. The IR bands for **25a-b** are listed below (Table 8.5). The compounds **25a-b** actually possess C_1 symmetry but for purposes of comparison and ease of IR band assignment an assumption of C_s symmetry has been made.

Table 8.5: FT-IR Bands for $Os(CO)_3(C_4Me_2R'_2CO)$ (R' = Et, n-Pr)

ν(CO) (pentane, cm^{-1})

	R	A'(1)	A'(2)	A''	ν(ketone)
25a	Et	2070	2005	1988	1672(w)
25b	n-Pr	2071	2005	1988	1673(w)

The bands assigned to the terminal carbonyls are invariant depending on whether an ethyl or n-propyl substituent is present. This is expected as compounds **23a-c** and **24a-c** showed that the terminal carbonyl bands are relatively insensitive to ring substitution. The ketone bands for **25a** and **25b** display an interesting feature. In the structure of **25a**, the ketone is adjacent to one methyl group and one ethyl substituent. An estimate for the energy of the ketone IR band can be obtained by calculating the average ketone frequency for **24a** and **24b**. That is, the average between the tetramethyl- and tetraethyl- substituted compounds. The average value works out to be 1672.5 cm^{-1}, close to the observed value of 1672 cm^{-1}. The same value of 1672.5 cm^{-1} is obtained for the average ketonic stretch of **24a** and **24c** and is similar to the experimental value of 1673 cm^{-1}. Of course, this trend has only been utilized for two species within a rather narrow range of substituents but the results seen could be used in the identification of ring substitution patterns.

8.5. Molecular Structure of $Os(CO)_3(C_4Me_2Et_2CO)$, 25a

As stated previously, simple ^{1}H and ^{13}C NMR spectroscopy could not distinguish between isomers **D** and **E**. Isomer **E** had been discarded on the basis that its formation would require breaking a C-C triple bond. Thus, to completely confirm the alkyne coupling product **25a**, an X-ray crystal structure analysis was carried out and two ORTEP views of **25a** are shown (Figure 8.2, 8.3). The relevant bond distances and angles for **25a** are listed in Tables 8.6 and 8.7, respectively.

As expected, the X-ray analysis confirms the presence of isomer **D**. The 2-butyne and 3-hexyne units are clearly visible on either side of the ring as well as the ketonic functionality. The geometry around the Os centre can be described as a tetragonal pyramid. One of the terminal carbonyls, C6-O6, occupies a site eclipsed by the ring ketone, C5-O5; this carbonyl may be referred to as the apical carbonyl. The other two carbonyls and the midpoints of the η^4-coordinated cyclopentadienone ring form the four equatorial coordination sites.

The Os-C1, Os-C2, Os-C3 and Os-C4 distances are similar to those expected from related systems. Most notably, the solid state structure of the tetraphenyl substituted derivative, $Os(CO)_3(C_4Ph_4CO)$, **26**, has been determined.[19] In **25a**, the M-C distances range from 2.19(2)Å to 2.22(1)Å, which are equivalent within 1 esd. For **26**, the M-C distances range from 2.20(1)Å to 2.27(1)Å, exhibiting only a slight lengthening.

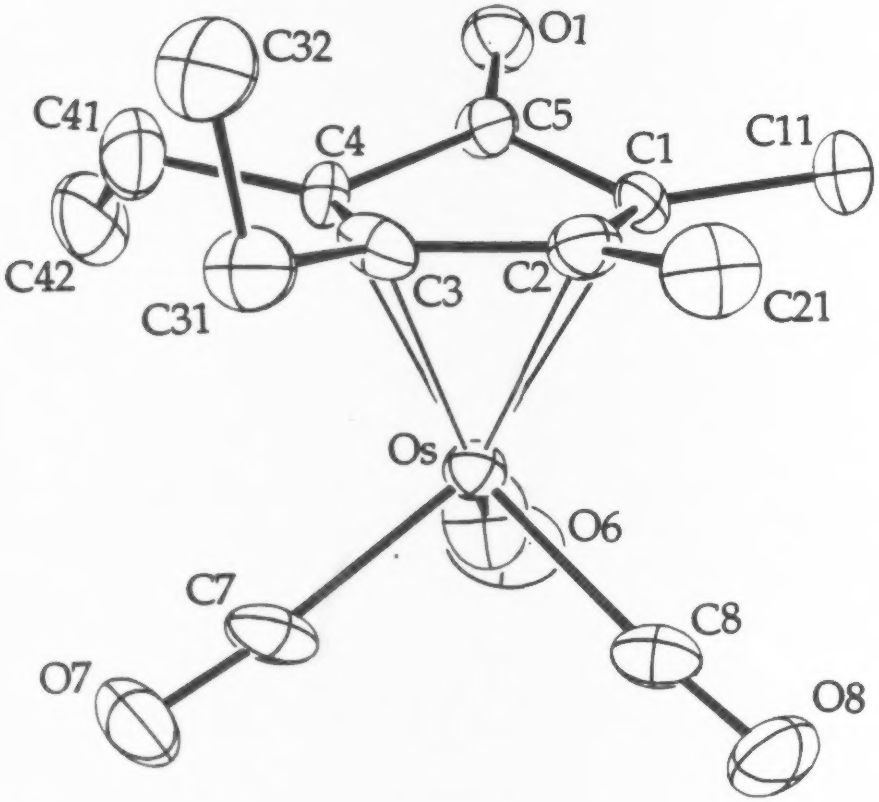
O1
C32
C5
C41
C4
C1
C11
C42
C31
C3
C2
C21
Os
O6
C7
C8
O7
O8

Figure 8.2: Perspective View of **25a**

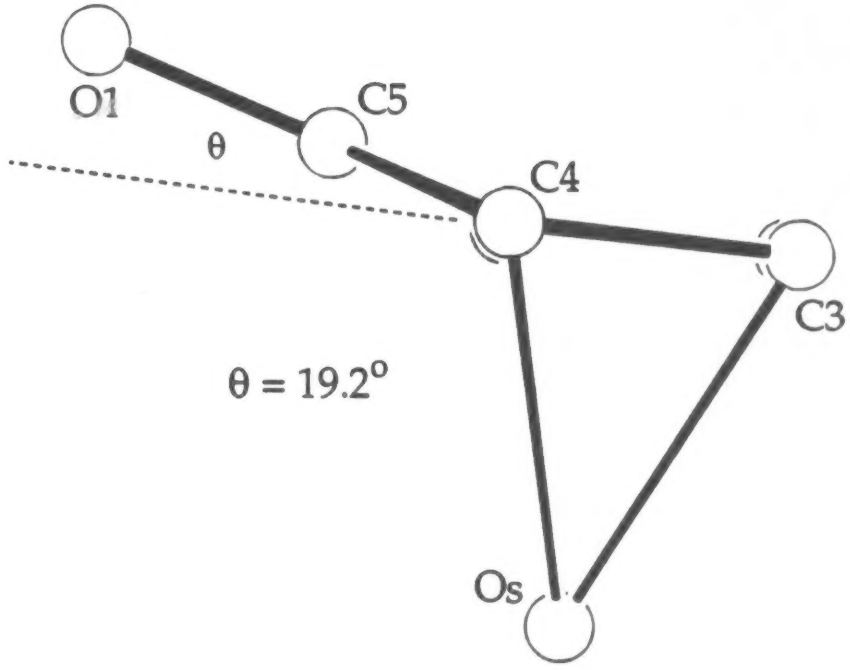
O1
C5
θ
C4
C3
θ = 19.2°
Os

Figure 8.3: 'Ball-and-Stick Representation of the Cyclopentadienone Ring Skeleton of **25a**

Table 8.6: Selected Bond Lengths (Å) for **25a**

Os-C1	2.22(1)	C1-C2	1.41(2)
Os-C2	2.23(1)	C1-C5	1.46(2)
Os-C3	2.19(2)	C1-C11	1.52(2)
Os-C4	2.21(1)	C2-C3	1.46(2)
Os-C6	1.83(1)	C2-C21	1.50(2)
Os-C7	1.88(1)	C3-C4	1.43(2)
Os-C8	1.92(1)	C3-C31	1.50(2)
O1-C5	1.22(2)	C4-C5	1.45(2)
O6-C6	1.18(2)	C4-C41	1.49(2)
O7-C7	1.15(2)	C31-C32	1.53(2)
O8-C8	1.13(1)	C41-C42	1.51(2)

Table 8.7: Selected Angles (deg) for **25a**

C2-C1-C5	111(1)	C2-C1-C11	124(2)
C2-C3-C4	107(1)	C1-C2-C21	127(2)
C3-C4-C5	110(1)	C3-C2-C21	126(2)
C1-C5-C4	102(1)	C5-C1-C11	122(1)
C1-C2-C3	106(1)	C2-C3-C31	125(1)
O1-C5-C1	127(1)	C4-C3-C31	128(1)
O1-C5-C4	131(1)	C3-C4-C41	125(1)
Os-C6-O6	175(1)	C3-C31-C32	110(1)
Os-C7-O7	174(1)	C4-C41-C42	115(1)
Os-C8-O8	175(1)	C5-C4-C41	122(1)
Os-C2-C21	129(1)	Os-C4-C41	128.5(9)
Os-C3-C31	127(1)	Os-C1-C11	129(1)

A feature prevalent in both structures is the bending of the ring ketone away from the planar 1,3 diene moiety. In **25a**, this bending is 19.8°, which is only slightly less than the 20.4° seen in **26**. This bending is due to Os-to-ring donation and can be readily explained using the Chatt-Dewar-Duncanson model[27] of olefin bonding. As metal-to-diene backbonding is increased, there is a transformation from pure C-R sp^2 bonding to partial sp^3 bonding causing the substituents to bend upwards described by the angle θ. The magnitude of θ can be used as measure of M-cyclopentadienone backbonding and for **25a** and **26**, the similarity in θ indicates that there is nearly equivalent M-cyclopentadienone backbonding in these complexes. This upward bending can also be seen in the methyl and ethyl substituents on the ring carbons.

The ring C-C bond distances can also be used as a measure of M-cyclopentadienone backbonding. For **25a**, the diene C-C distances range from 1.41(2)Å to 1.46(2)Å; there is only a small difference between the formal C1-C2 double and the C2-C3 single bonds; such an equalization of C-C bond distances is characteristic of $M(CO)_3(\eta^4\text{-diene})$ complexes. The bonding in metal-diene complexes was described as early as 1964 by Mason[28] but may also be explained using a simple pictorial diagram of the frontier orbitals of butadiene and $Os(CO)_3$.[29] The π and π^* orbitals of butadiene may be readily constructed using a basic Hückel approach.[29a] The $Os(CO)_3$ (C_{3v} symmetry) moiety is classified as a d^8-ML_3 fragment, making it isolobal to CR^+. A pictorial representation is given in Scheme 8.3.

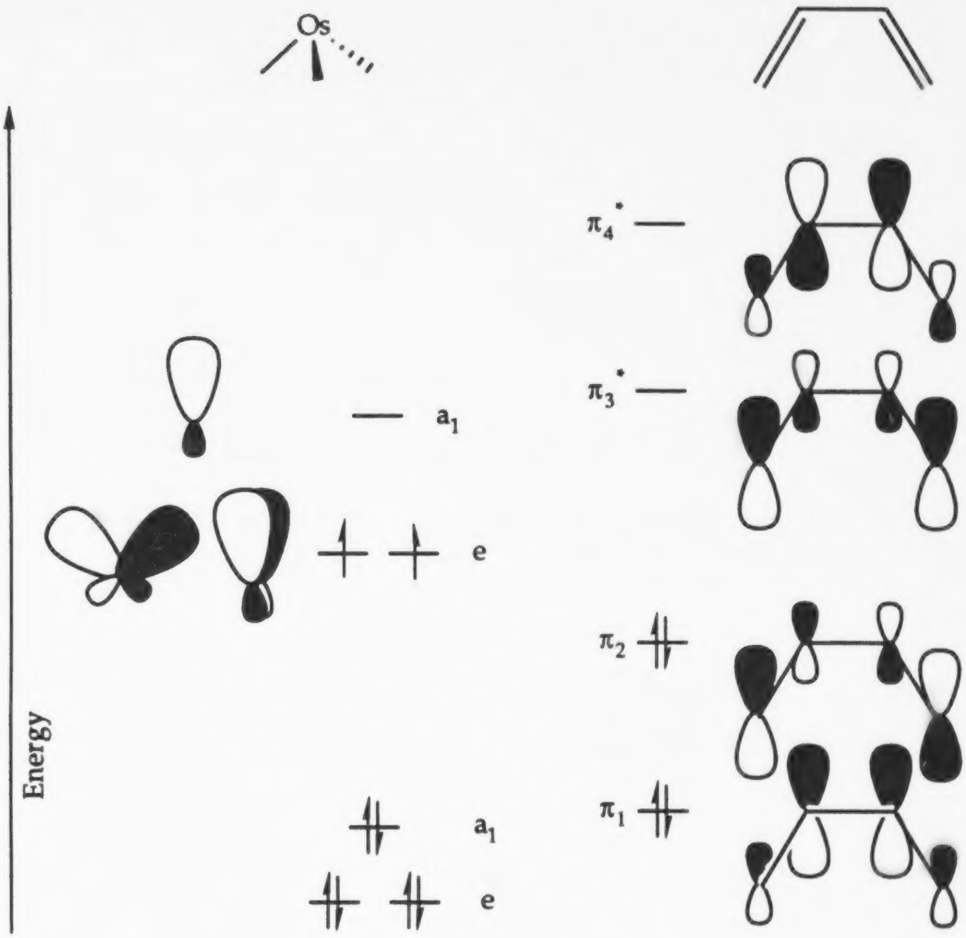

Scheme 8.3: Orbital Interaction Between Os(CO)$_3$ Fragment and Butadiene

The diagram illustrates that the Os(CO)$_3$ fragment has three high energy frontier orbitals which house two electrons. The filled, low energy a_1 and e orbitals are derived from the parent t_{2g} set present in octahedral symmetry. To fulfill the 18 electron rule, the Os(CO)$_3$ fragment needs to accept two electron pairs from the diene. This is done *via* $\pi_1 \rightarrow a_1$ and $\pi_2 \rightarrow e$ donation. However, in an optimal situation, the Os(CO)$_3$ fragment will also act as a donor due to the presence of an electron pair in one of its high energy orbitals. The symmetry of the frontier orbitals of a conjugated olefin fill this role admirably. The butadiene π_2 and π_3^* orbitals are of the right symmetry to split the metal e level. One metal e orbitals will act as an acceptor from the filled diene π_2 orbital, the other metal orbital can then donate an electron pair to the π_3^* orbital. Thus, the $Os(CO)_3$ fragment donates electron density into a π_3^* orbital which, as shown in the diagram, will lengthen the C-C double bonds and shorten the central C-C single bond. Evidence for this is seen in the near equalization of the C-C bond distances in the diene portion of the cyclopentadienone ring.

8.6. Proposed Mechanism for Formation of Metal-Cyclopentadienone Species

The facile reaction of **20** with excess alkyne was a surprising discovery. In the literature, there are two prevalent methods for synthesizing $M(CO)_3(\eta^4\text{-}C_4R_4CO)$ (M = Fe, Ru, Os) species. The first is a thermal reaction between the alkyne and the appropriate M-carbonyl species. For M = Fe,[1a,17] ironpentacarbonyl and $Fe_2(CO)_9$ are commonly used while for Ru and Os, the trinuclear complexes, $M_3(CO)_{12}$, are utilized almost exclusively.[15,18,19] However, this method does not always result in clean product formation and activated alkynes are usually required. Also, rather forcing conditions are usually required and this is most likely responsible for the dearth of specific mechanistic information available. If the parent cyclopentadienone is available, the thermal reaction between this organic species and the metal carbonyl yields superior results. In fact, the availability of tetracyclone, C_4Ph_4CO, has allowed for the ready synthesis of $M(CO)_3(\eta^4\text{-}C_4Ph_4CO)$ (M = Fe, Ru).[14e,18] This method is limited by the fact that few cyclopentadienone compounds are available due to their propensity to dimerize *via* a Diels-Alder reaction.[30]

Unfortunately, the extreme temperature sensitivity of $Os(CO)_4(\eta^2$-$C_2Me_2)$ prevented the study of any reactions using low temperature NMR spectroscopy. However, the knowledge that $Os(CO)_4(\eta^2$-$C_2Me_2)$ can be used as a starting point in the alkyne coupling mechanism is of great value as iron carbonyl mediated cyclizations of alkynes are thought to proceed *via* $Fe(CO)_4(\eta^2$-alkyne) intermediates. A possible mechanism incorporates a CO insertion into the alkyne followed by coupling of another alkyne to form the cyclopentadienone ring, alternatively, the alkyne coupling could precede the CO-insertion step (Scheme 8.4).

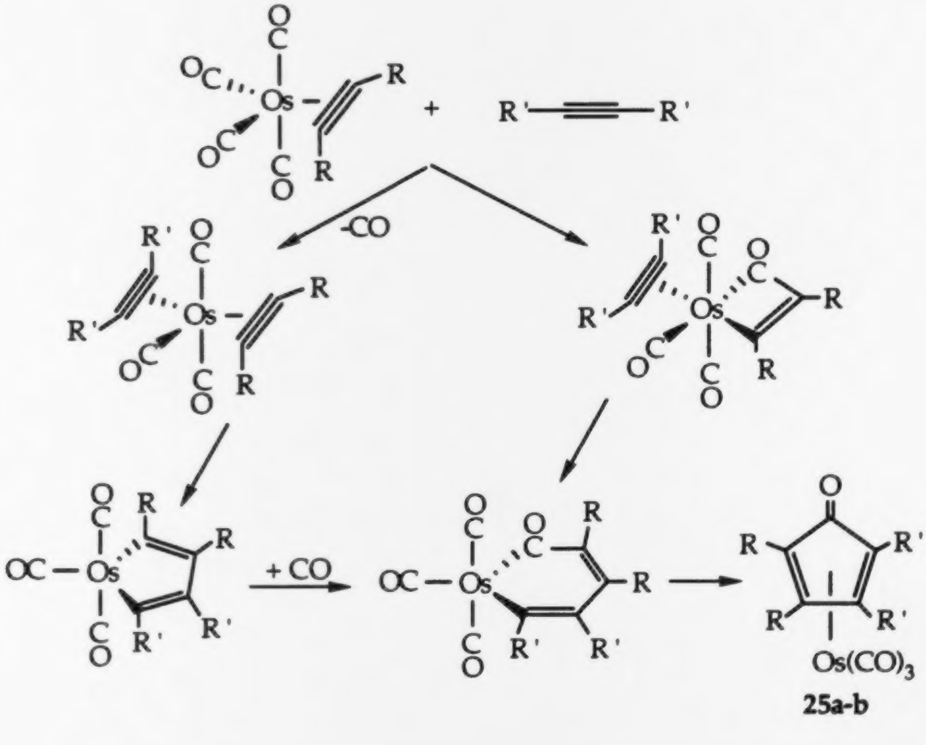

Scheme 8.4: Possible Mechanisms for Formation of **25a-b**

The above mechanisms would account for the selective formation of **25a** where no C-C triple bonds have been cleaved. There is also precedent for CO insertion reactions with coordinated alkynes. Green and co-workers investigated[31a] the reaction of trans-tricarbonybis(phosphine)-ruthenium species with hexafluoro-2-butyne and were able to isolate CO-inserted complexes (Scheme 8.5).

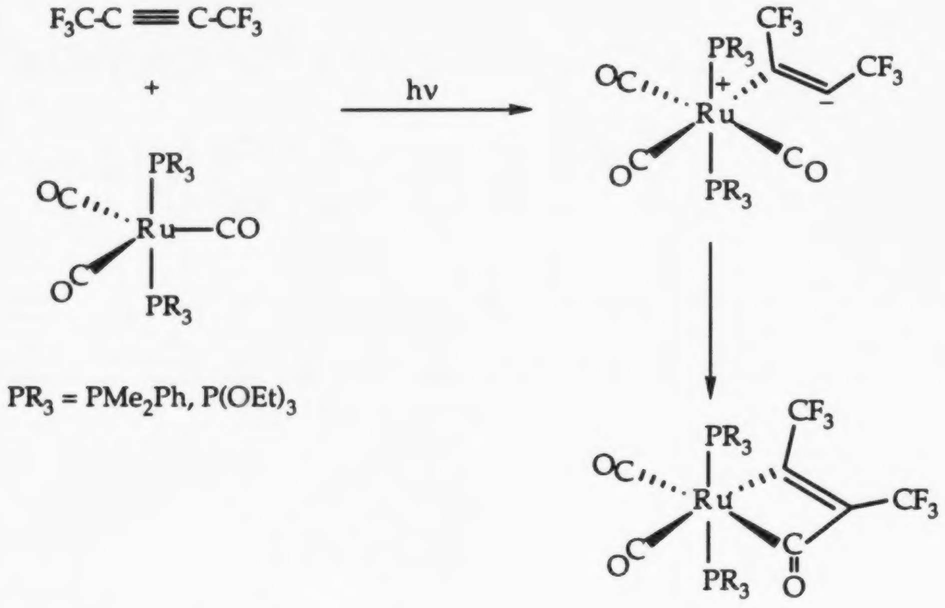

PR_3 = PMe_2Ph, $P(OEt)_3$

Scheme 8.5: Generation of a Ruthenacyclobutenone

The reaction shown above also includes Green's proposed intermediate in this reaction. Unfortunately, no mention was made of further reaction of the CO-inserted species with HFB. An additional reaction was carried out between tricarbonylbis(dimethylphenylphosphine)ruthenium and excess HFB to yield a ruthenacyclopentadiene complex.

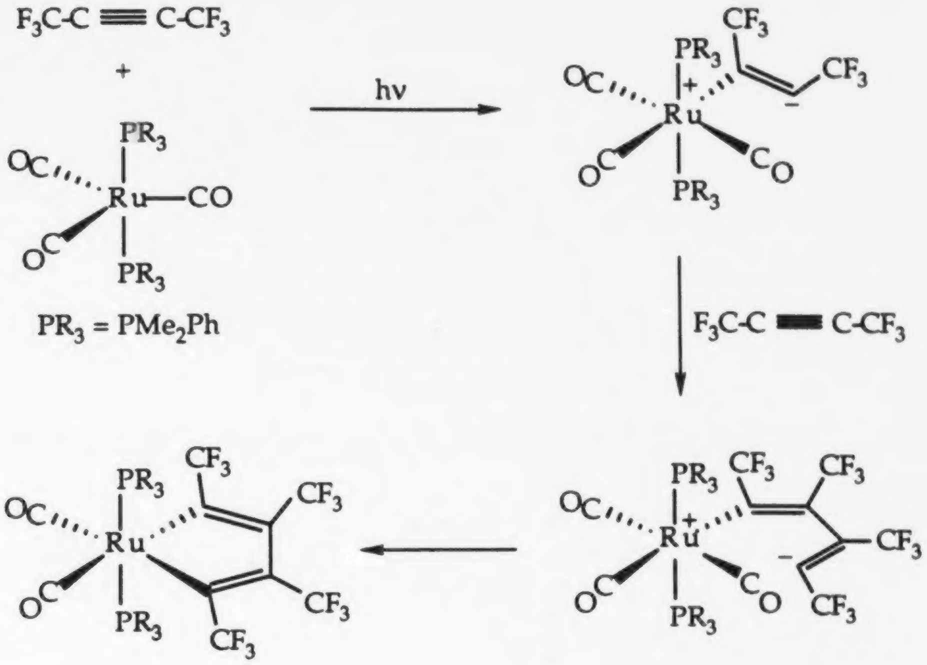

This reaction indicates that the alkyne coupling may take place before the CO-insertion reaction, which has been mentioned in the literature.[1d] The Ru-cyclopentadiene species is unreactive towards CO; the insertion reaction is most likely hindered by the strong Ru-carbon bonds due to the presence of electron withdrawing trifluoromethyl substituents. The above reactions cast doubt as to whether CO-insertion or alkyne coupling occurs first in the reaction of **20** with excess alkyne. Also, Lindner has observed the coupling of two DMAD (dimethylacetylenedicarboxylate) molecules at a Ru-carbonyl centre without any CO insertion.[31b]

Tianfu Mao of our group has investigated the nucleophilic substitution of CO on $Os(CO)_4(\eta^2$-$HCCH)$.[32] The final product of the reaction with the bidentate phosphine has a carbonyl inserted into the Os-carbon bond of the bound acetylene (Scheme 8.6). Preliminary evidence indicates that the reaction proceeds *via* initial CO substitution by one of the phosphorus atoms; only this intermediate is seen followed by formation of the final product. Thus it seems that CO loss is the necessary and common initiation step for the reaction of $Os(CO)_4(\eta^2\text{-}HCCH)$, **1**, with nucleophiles.

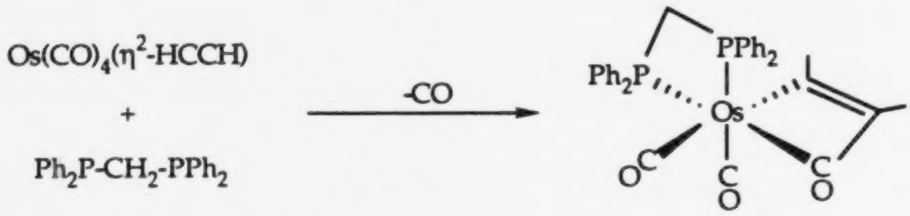
$Os(CO)_4(\eta^2\text{-}HCCH)$
+
$Ph_2P\text{-}CH_2\text{-}PPh_2$
-CO
PPh_2
Ph_2P
Os
OC
C
O
C
O

Scheme 8.6: Generation of an Osmacyclobutenone

In Chapter 6, the reaction of $Os(CO)_4(\eta^2\text{-}C_2Me_2)$ with $CpM(CO)_2$ was described. By analogy with $Os(CO)_4(\eta^2\text{-}HCCH)$, it was assumed that the initial step was the dissociation of CO, followed by nucleophilic attack at the Os centre. In keeping with this trend, a slight modification to the mechanism in Scheme 8.4 can be made that incorporates initial CO dissociation. This is illustrated in Scheme 8.7.

The mechanism below incorporates several key steps that are postulated to occur in related reactions. First, there is the dissociation of CO followed by coordination of the nucleophile, a second alkyne in this case, to the metal centre. The presence of two electron-donating alkyne ligands would have a significant destabilizing effect and would serve to promote the CO insertion reaction. The coordination of an electron-donating ligand is consistent with Tianfu Mao's results. The CO-inserted intermediate could also be stabilized by four electron donation from the remaining η^2-coordinated alkyne. The re-coordination of previously dissociated CO molecule has been observed in the formation of **3** and **8** and thus is a plausible next step. The re-coordination of the CO molecule concomitant with the insertion of the second alkyne would then lead directly to the formation of **25a**. Thus, the mechanism in Scheme 8.7 is consistent not only with the formation of **25a**, but with the formation of the dimetallacyclopentenones as well. Specifically, the mechanism incorporates initial CO loss from the $Os(CO)_4(\eta^2\text{-alkyne})$ species followed by nucleophilic attack at the Os centre. These steps, plus the formation of an osmacyclobutenone and re-coordination of CO have all been postulated to account for the formation of **3** and **17a-c**.

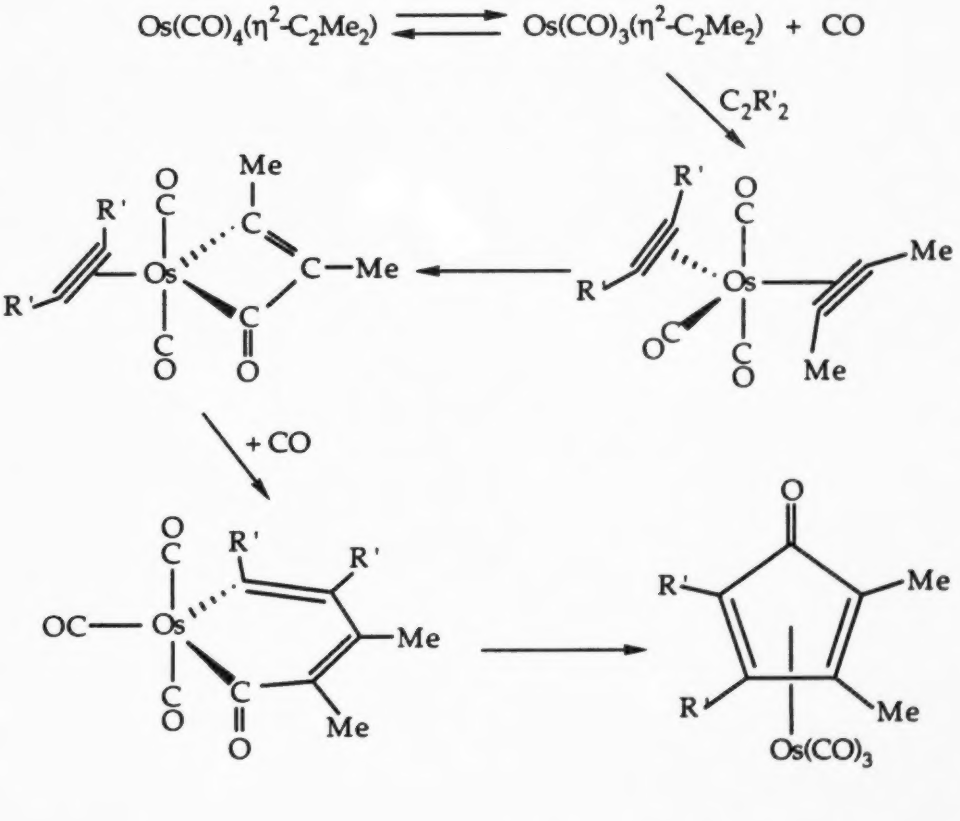

Scheme 8.7: Proposed Pathway for Formation of **25a-b**

The reason why $M(CO)_4(\eta^2\text{-}C_2R_2)$ (M = Ru, Os; R = Me, Et, n-Pr) species readily react with an additional electron rich alkyne while their HCCR (R = H, CH_3, CF_3, $SiMe_3$) counterparts do not cannot be easily explained as most alkyne cyclizations occur with activated alkynes. The only difference is the electronic properties of the alkyne; 2-butyne is a very weak π acid while the terminal alkynes studied have moderate to good π acceptor properties. Thus, 2-butyne will increase the four-electron destabilization relative to the terminal alkynes.[13] This is reflected in the thermal stability of $Os(CO)_4(\eta^2\text{-}C_2R_2)$ complexes where the thermal stability increases as more electron withdrawing substituents are used. Also, the weak π acidic nature of 2-butyne would result in little metallacyclopropene character. The electron rich 2-butyne acts primarily as a donor with the Os in a formal d^8 electronic configuration. The more π acidic alkynes would induce increased metallacyclopropene contribution, resulting in a more tightly bound alkyne and the Os in a formal d^6 configuration. The increased CO lability of the 2-butyne complex coupled with the weakly bound alkyne could then account for its increased reactivity. The facile CO loss allows the reaction to be initiated with little thermal activation while the weakly bound alkyne would enable a facile CO-insertion to occur.

As stated, the Os-butyne complex, **20**, only reacts with electron rich alkynes. This is most likely due to the fact that 3-hexyne and 4-octyne are good donors and will readily attack the pseudo-vacant coordination site left by the dissociation of CO. In other words, these alkynes can disrupt the $\pi_\perp$ interaction that stabilizes the putative $Os(CO)_3$(2-butyne) intermediate. The dramatic rise in electron density following the coordination of a second donor alkyne would then provide the impetus for the reaction to yield the cyclopentadienone complexes. The other alkynes are less effective donors and may not be able to disrupt this interaction before thermal decomposition of $Os(CO)_4(\eta^2$-2-butyne) occurs.

8.7. Scope of the Coupling Reactions

8.7.1. Extension of Alkyne Coupling Reactions

The alkyne coupling reactions shown have several possible applications. First, cyclopentadienone rings have use in Diels-Alder reactions and in ring synthesis.[30] Cyclopentadienone ring without bulky substituents are thermally unstable, they readily undergo Diels-Alder type reactions to produce dimers. Thus, the construction of cyclopentadienone rings with aliphatic substituents coordinated to a metal centre could provide a convenient method for accessing these compounds for use organic synthesis. Presently, the Pauson-Khand reaction, where Co species are utilized to generate cyclopentenone compounds, is commonly used by organic chemists.[33] A procedure using α, ω diynes has been used by Pearson to synthesize cyclopentadienone-iron complexes.[34] A further point demonstrated by Pearson is that the coordinated metal exerts a stereodirecting effect as it occupies one of the cyclopentadienone faces. Thus, modifications can be made on the coordinated cyclopentadienone ring in a stereoselective manner followed by decomplexation of the ring. Unfortunately, for $M(CO)_3(C_4Me_4CO)$ (M = Ru, Os) the ring cannot be decomplexed using Ce^{4+}, a feature also discovered by Pearson with his iron-cyclopentadienone compounds.[34a]

8.7.2. Use of $M(CO)_3(\eta^4\text{-}C_4R_4CO)$ in Catalysis

As mentioned, the catalytic properties of $Ru(CO)_3(C_4Ph_4CO)$ have been extensively studied.[20] Although this species itself is not a catalyst, it acts as a catalytic precursor. Heating of $Ru(CO)_3(C_4Ph_4CO)$ in alcohol produces a dimeric species, which under the catalytic reaction conditions, cleaves to yield the actual active species (Scheme 8.8).

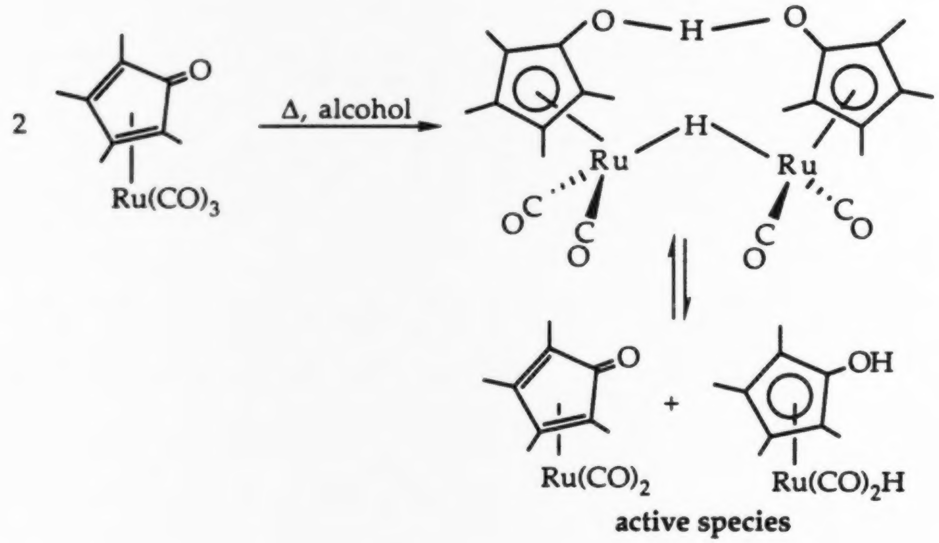

Scheme 8.8: $Ru(CO)_3(C_4Ph_4CO)$ as a Catalytic Precursor

Shvo and co-workers have used this Ru based system in the reduction of ketones to alcohols, the oxidative coupling of primary alcohols to esters,[20c-e] the reduction of nitroaromatics to aminoarenes,[20b] and transalkylation of amines.[20a] The same catalytic precursor, $Ru(CO)_3(\eta^4\text{-}C_4Ph_4CO)$, can be used in the disproportionation of aldehydes to also yield esters,[20f] commonly known as the Tishchenko reaction (Scheme 8.9).

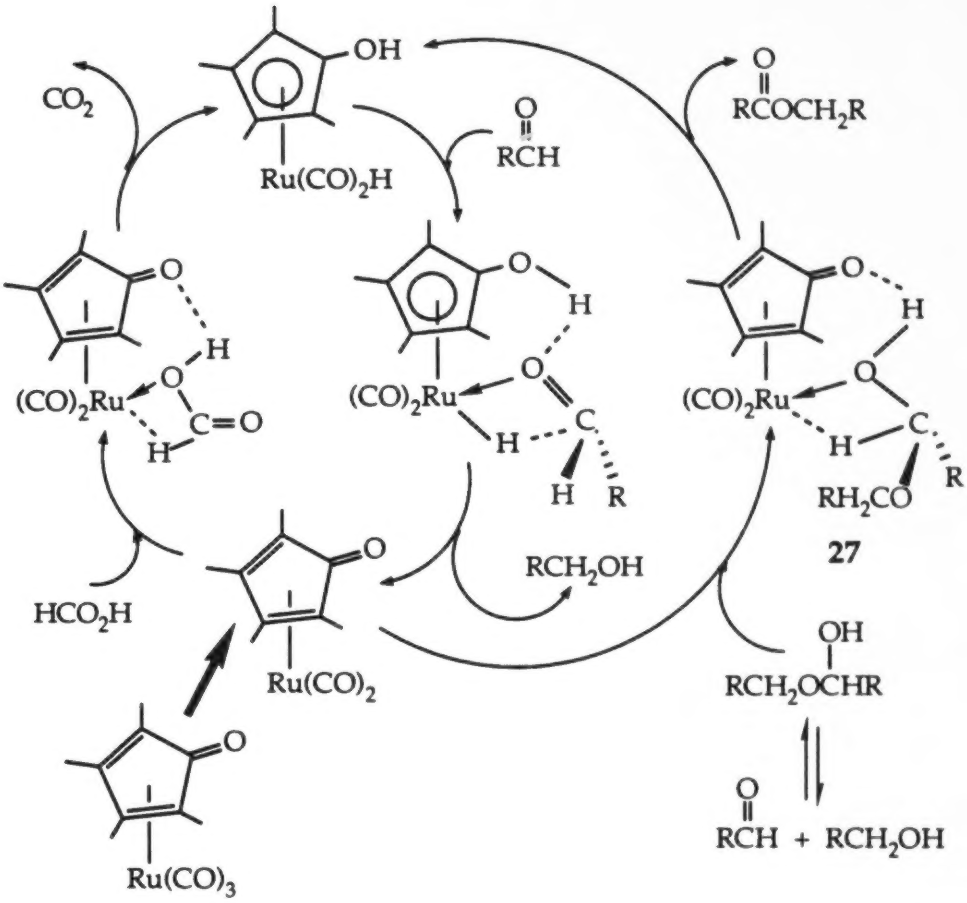
CO$_2$
OH
Ru(CO)$_2$H
RCH
RCOCH$_2$R
O
H
(CO)$_2$Ru
C=O
C
R
RH$_2$CO
27
HCO$_2$H
RCH$_2$OH
Ru(CO)$_2$
RCH$_2$OCHR
RCH + RCH$_2$OH
Ru(CO)$_3$

Scheme 8.9: Proposed Mechanism for Catalytic Disproportionation of Aldehydes

The reaction also requires a the presence of formic acid. Shvo found that electron donating groups on the cyclopentadienone ligand, in the form of substituted phenyls, accelerate the disproportionation reaction. This is due to the increased basicity of the C=O oxygen on the cyclopentadienone ring; increasing its ability to from a hydrogen bond with the proton on the alcohol (**27**). However, no studies were carried out to investigate Ru-cyclopentadieone compounds with aliphatic substituents on the ring which may yield even larger rates of disproportionation. However, one should recall that the C=O stretching frequency for $Ru(CO)_3(\eta^4\text{-}C_4Ph_4CO)$ was anomalously low and the corresponding aliphatic compounds actually have higher C=O stretching frequencies. Whether this phenomenon is also applicable to complexes such as **27** may be worth investigating. The Os analogues could also be useful in that they may provide models for these catalytic processes, as their increased stability may allow for the observation or even isolation of key intermediates. Finally, the ability to couple two different alkynes into a cyclopentadienone ring may allow one to fine tune the electronic properties of the catalyst and allow greater control over the processes.

8.8. Conclusions

The synthesis of $Os(CO)_4(\eta^2\text{-butyne})$, **20**, provided access not only to heterobimetallic species (Chapter 6) but to cyclopentadienone compounds as well. The reaction of **20** with donor alkynes provides smooth entry into the synthesis of Os-cyclopentadienone complexes with different substituents. A general synthetic method for the synthesis of alkyl substituted $(\eta^4\text{-}C_4R_4CO)M(CO)_3$ (M = Ru, Os; R = Me, Et, n-Pr) compounds was also developed. The reactivity of **20** with alkynes is related to the extreme four-electron destabilization in these complexes, although the thermal instability prevented full mechanistic work. Further work may include possible catalytic investigations and the synthesis of Os-cyclopentadienones with different substitution patterns.

8.9. Experimental Section

8.9.1. Starting Materials and Reagents

The alkynes, 2-butyne, 3-hexyne, and 4-octyne purchased from Aldrich Chemical Co. and used without further purification. $Ru(CO)_5$[35] was prepared by the published procedure.

8.9.2. Synthetic Procedures

Synthesis of $Os(CO)_4[\eta^2\text{-}C_2(CH_3)_2]$, 20

A 100 mL immersion well (Figure 2.5) fitted with a GWV insert ($\lambda \geq 370$ nm) was charged with a pentane solution containing $Os(CO)_5$ (127.0 mg, 0.385 mmol) and excess 2-butyne (1.0 mL). The temperature of the solution was maintained at -60 °C via a MGM Lauda Circulating Bath. The solution was photolyzed using a Philips 125W Mercury Vapor Lamp and the reaction was monitored using FT-IR spectroscopy. The reaction was complete in *ca*. 2 h after which time no $Os(CO)_5$ was present and only bands due to $Os(CO)_3(\eta^4\text{-}C_4Me_4CO)$, **24a**, were observed. The solution was then transferred by cannula to a flask pre-cooled to -78 °C. The solvent and excess 2-butyne were removed *in vacuo* and the product, $Os(CO)_4[\eta^2\text{-}C_2(CH_3)_2]$, **20**, sublimed at *ca*. -20 °C to a dry ice cooled probe. The white, waxy solid was washed off the probe to yield a thermally sensitive colorless solution. A yield of 61% (82.3 mg, 0.231 mmol) was obtained based on titration with $Cp^*Rh(CO)_2$. The coefficient ε for each of the two strong terminal carbonyl bands is used to give the concentration of a pentane solution of $Os(CO)_4(\eta^2\text{-}C_2Me_2)$ in mg/mL.

Due to the thermal instability of $Os(CO)_4(\eta^2\text{-}C_2Me_2)$ a specialized system was utilized to obtain the mass spectrum. A pentane solution of $Os(CO)_4(\eta^2\text{-}C_2Me_2)$ was transferred a small Schlenk tube and the solvent removed *in vacuo* at -78 °C. The flask was then fitted with a male 14/20 ground glass joint attached to a 4 cm piece of 12 mm (outer diameter) glass tubing. With the sample cooled by dry-ice, the glass tubing was connected to a controlled vacuum valve that was, in turn, connected to the inlet port of the mass spectrometer. The flask was evacuated at low temperature. To record the spectrum, the dry ice was simply removed and the Schlenk tube was allowed to warm, while the vacuum in the flask was manipulated. The temperature at which the spectrum was recorded could not be quantitatively ascertained, the most reasonable estimate would be in the range of -30 °C to -10 °C.

Similar care was used in the preparation of the NMR sample. A pentane solution of $Os(CO)_4(\eta^2\text{-}C_2Me_2)$ was transferred to a pre-cooled (-78 °C) Schlenk flask and placed under 1 atm of ^{13}CO using the freeze-pump-thaw method. The solution was allowed to warm to -25 °C for 15 minutes. The solvent was removed *in vacuo* at -78 °C and the sample re-sublimed to a dry ice cooled probe. The compound was washed off the probe using cold toluene-d_8. The sample was then transferred by cannula under N_2 to a pre-cooled NMR tube. It is important to pre-cool the cannula with a liquid N_2 soaked cotton ball to prevent decomposition of $Os(CO)_4(\eta^2\text{-}C_2Me_2)$. The NMR probe was pre-cooled to -70 °C before inserting the NMR sample of $Os(CO)_4(\eta^2\text{-}C_2Me_2)$.

Formula Weight: 356.33

Mass Spectrum(*ca*. -20 °C, 16eV): M^+ (358, 17.2%), $M^+\text{-}C_2Me_2$ (304, 1.29%), $M^+\text{-}nCO$ (n = 0-4)

IR(pentane, cm^{-1}); ν(CO): 2106(w), 2020(vs) ε = 2.21 mL/mg·mm, 1988(m) ε = 1.40 mL/mg·cm.

^{1}H NMR(400 MHz, toluene-d_8, -70 °C) 2.03 (C*H*$_3$)

^{13}C NMR(100.6 MHz, toluene-d_8, -70 °C) 69.7 (*C*-CH$_3$), 14.8 (C-*C*H$_3$).

Synthesis of Os(CO)$_3$(η^4-C$_4$Me$_4$CO), 24a

Using Os(CO)$_5$ (88.0 mg, 0.266 mmol) and excess 2-butyne (0.5 mL) a similar procedure was used to generate **20** *in situ*. The solution was transferred out of the immersion well to a flask at 0 °C and stirred for 1 hr. The solvent and 2-butyne were removed *in vacuo* at room temperature and the solid product was extracted with pentane (2x10 mL). The filtered extracts were combined and the volume reduced using an Ar stream until precipitation occurred. A small volume of pentane was then added to redissolve the precipitate and the solution placed in a -80 °C freezer overnight. The resulting solid was isolated and washed (2x5 mL) with cold pentane. The yield of Os(CO)$_3$(η^4-C$_4$Me$_4$CO), **24a**, as an off-white solid was 65.6 mg, 0.160 mmol (60%) based on Os(CO)$_5$.

Formula Weight: 410.42

Mass Spectrum(160 °C, 16eV): M$^+$ (412, 90.7%), M$^+$-nCO (n = 0-4)

IR(pentane, cm^{-1}); ν(CO): 2071(s), 2006(s), 1988(s); ν(keto): 1676(w).

^{1}H NMR(360 MHz, CDCl$_3$, 23 °C) 2.35 (6H, s, i-C*H*$_3$), 1.92 (6H, s, o-C*H*$_3$).

^{13}C NMR(90.5 MHz, CDCl$_3$, 23 °C) 176.1 (CO), 175.7 (keto), 97.1 (C_i), 71.9 (C_o), 10.1 (i-CH$_3$), 8.9 (o-CH$_3$).

Anal. Calcd. for $C_{12}H_{12}O_4Os$: C, 35.12; H, 2.95. Found: C, 35.28; H, 2.68.

Synthesis of $M(CO)_3(\eta^4\text{-}C_4R_4CO)$ (M = Ru, Os; R= Et, n-Pr) (23b, 23c, 24b, 24c)

A procedure similar to the above was used in each case and the starting amounts and final yields are listed below.

i) M = Ru; R = Et, **23b**

$Ru(CO)_5$: 93.0 mg, 0.386 mmol; 3-hexyne: 0.5 mL

$Ru(CO)_3(\eta^4\text{-}C_4Et_4CO)$, **23b**: 77.3 mg; 0.204 mmol (53%)

Formula Weight: 377.40

Mass Spectrum(180 °C, 16eV): M^+ (378, 29.6%), $M^+\text{-}nCO$ (n = 0-4)

IR(pentane, cm^{-1}); ν(CO): 2072(s), 2015(s), 1996(s); ν(keto): 1663(w).

^1H NMR(360 MHz, $CDCl_3$, 23 °C) 2.44 (4H, m, i-CH_2), 2.30 (2H, m, o-CH_2), 1.98 (2H, m, o-CH_2), 1.19 (6H, m, i-CH_3), 1.16 (6H, m, o-CH_3).

^{13}C NMR(90.5 MHz, $CDCl_3$, 23 °C) 195.6 (CO), 176.3 (keto), 105.6 (C_i), 85.4 (C_o), 19.1 (i-CH_2CH_3), 17.6 (o-CH_2CH_3), 16.9 (i-CH_2CH_3), 15.7 (o-CH_2CH_3).

Anal. Calcd. for $C_{16}H_{20}O_4Ru$: C, 50.92; H, 5.34. Found: C, 50.91; H, 5.43.

ii) M = Ru; R = n-Pr, **23c**

$Ru(CO)_5$: 91.1 mg, 0.378 mmol; 4-octyne: 0.5 mL

$Ru(CO)_3[\eta^4\text{-}C_4(n\text{-}Pr)_4CO]$, **23c**: 103.4 mg; 0.238 mmol (63%)

Formula Weight: 433.51

Mass Spectrum(180 °C, 16eV): M^+ (434, 24.5%), $M^+\text{-}nCO$ (n = 0-4)

IR(pentane, cm^{-1}); ν(CO): 2071(s), 2014(s), 1995(s); ν(keto): 1662(w).

^1H NMR(360 MHz, $CDCl_3$, 23 °C) 2.34 (4H, m, i-$CH_2CH_2CH_3$), 2.15 (2H, m, o-$CH_2CH_2CH_3$), 1.85 (2H, m, o-$CH_2CH_2CH_3$), 1.78 (2H, m, i-$CH_2CH_2CH_3$), 1.53 (2H, m, i-$CH_2CH_2CH_3$), 1.46 (2H, m, o-$CH_2CH_2CH_3$), 1.28 (2H, m, o-$CH_2CH_2CH_3$), 1.01 (6H, m, i-$CH_2CH_2CH_3$), 0.98 (6H, m, o-$CH_2CH_2CH_3$).

^{13}C NMR(90.5 MHz, $CDCl_3$, 23 °C) 195.7 (keto), 176.3 (CO), 104.6 (C_i), 84.2 (C_o), 28.3 (i-$CH_2CH_2CH_3$), 27.1 (o-$CH_2CH_2CH_3$), 26.1 (i-$CH_2CH_2CH_3$), 24.9 (o-$CH_2CH_2CH_3$), 14.8 (i-$CH_2CH_2CH_3$), 14.7 (o-$CH_2CH_2CH_3$).

Anal. Calcd. for $C_{20}H_{28}O_4Ru$: C, 55.41; H, 6.51. Found: C, 55.57; H, 6.68.

iii) M = Os; R = Et, **24b**

$Os(CO)_5$: 76.5 mg, 0.232 mmol; 3-hexyne: 0.5 mL

$Os(CO)_3(\eta^4\text{-}C_4Et_4CO)$, **24b**: 61.1 mg; 0.131 mmol (56%)

Formula Weight: 466.53

Mass Spectrum(170 °C, 16eV): M^+ (468, 43.6%), M^+-nCO (n = 0-4)

IR(pentane, cm^{-1}); ν(CO): 2070(s), 2004(s), 1987(s); ν(keto): 1669(w).

^1H NMR(360 MHz, $CDCl_3$, 23 °C) 2.53 (4H, m, i-CH_2CH_3), 2.31 (2H, m, o-CH_2CH_3), 1.94 (2H, m, o-CH_2CH_3), 1.19 (12H, m, CH_2CH_3).

^{13}C NMR(90.5 MHz, $CDCl_3$, 23 °C) 177.0 (keto), 175.4 (CO), 101.1 (C_i), 80.7 (C_o), 18.7 (i-CH_2CH_3), 18.3 (o-CH_2CH_3), 16.8 (i-CH_2CH_3), 16.4 (o-CH_2CH_3).

Anal. Calcd. for $C_{16}H_{20}O_4Os$: C, 41.19; H, 4.32. Found: C, 41.30; H, 4.42

iv) M = Os; R = n-Pr, **24c**

$Os(CO)_5$: 72.8 mg, 0.220 mmol; 4-octyne: 0.5 mL

$Os(CO)_3[\eta^4\text{-}C_4(n\text{-}Pr)_4CO]$, **24c**: 95.2 mg; 0.182 mmol (83%)

Formula Weight: 522.63

Mass Spectrum(130 °C, 16eV): M^+ (524, 36.9%), M^+-nCO (n = 0-4)

IR(pentane, cm^{-1}); ν(CO): 2069(s), 2004(s), 1987(s); ν(keto): 1669(w).

^1H NMR(360 MHz, $CDCl_3$, 23 °C) 2.43 (4H, m, i-$CH_2CH_2CH_3$), 2.19 (2H, m, o-$CH_2CH_2CH_3$), 1.82 (2H, m, o-$CH_2CH_2CH_3$), 1.79 (2H, m, i-$CH_2CH_2CH_3$), 1.52 (2H, m, i-$CH_2CH_2CH_3$), 1.46 (2H, m, o-$CH_2CH_2CH_3$), 1.22 (2H, m, o-$CH_2CH_2CH_3$), 1.01 (6H, m, i-$CH_2CH_2CH_3$), 0.98 (6H, m, o-$CH_2CH_2CH_3$).

^{13}C NMR(90.5 MHz, $CDCl_3$, 23 °C) 177.3 (keto), 175.4 (CO), 100.1 (C_i), 79.5 (C_o), 27.8 (i-$CH_2CH_2CH_3$), 27.7 (o-$CH_2CH_2CH_3$), 25.9 (i-$CH_2CH_2CH_3$), 25.5 (o-$CH_2CH_2CH_3$), 14.8 (i-$CH_2CH_2CH_3$), 14.7 (o-$CH_2CH_2CH_3$).

Anal. Calcd. for $C_{20}H_{28}O_4Os$: C, 45.96; H, 5.40. Found: C, 46.23; H, 5.12

Synthesis of $Ru(CO)_3(\eta^4\text{-}C_4Me_4CO)$, 23a

A small immersion well pre-cooled to -5 °C was charged with $Ru(CO)_5$ (82.1 mg, 0.340 mmol) and excess 2-butyne (0.5 mL). The photolysis was carried out for 2 hr until all the $Ru(CO)_5$ had been consumed. The solution was transferred out of the immersion well to a flask at 0 °C and stirred for 0.5 h to ensure complete reaction. A small amount of orange $[Ru(CO)_4]_x$ was observed. The solution was filtered and the solvent and 2-butyne were removed *in vacuo* at room temperature after which the solid product was extracted with pentane (2x10 mL). The filtered extracts were combined and the volume reduced using an Ar stream until precipitation occurred. A small volume of pentane was then added to redissolve the precipitate and the solution placed in a -20 °C freezer overnight. The resulting solid was isolated and washed (5 mL) with cold pentane. The yield of $Ru(CO)_3(\eta^4\text{-}C_4Me_4CO)$, **23a**, as an off-white solid was 31.3 mg, 0.097 mmol (29%) based on $Ru(CO)_5$.

Formula Weight: 321.29

Mass Spectrum(140 °C, 16eV): M^+ (322, 24.8%), M^+-nCO (n = 0-4)

IR(pentane, cm^{-1}); ν(CO): 2073(s), 2016(s), 1996(s); ν(keto): 1670(w).

^1H NMR(360 MHz, $CDCl_3$, 23 °C) 2.13 (6H, s, i-CH_3), 1.87 (6H, s, o-CH_3).

^{13}C NMR(90.5 MHz, $CDCl_3$, 23 °C) 196.0 (CO), 175.4 (keto), 101.2 (C_i), 77.5 (C_o), 10.8 (i-CH_3), 9.3 (o-CH_3).

Anal. Calcd. for $C_{12}H_{12}O_4Ru$: C, 44.86; H, 3.76. Found: C, 45.15; H, 3.60.

Synthesis of $Os(CO)_3(\eta^4\text{-}C_4Me_2R_2CO)$, 25a-b

i) R= Et, 25a

A round bottom flask was charged with 0.5 mL of 3-hexyne and 10 mL of pentane, and cooled to -78 °C in a dry ice acetone bath. A solution containing 20.3 mg (0.057 mmol) of Os(CO)4(η^2-butyne) was added via cannula and the flask transferred to an ice bath. The solution was stirred for 1 h and only signals due to $Os(CO)_3(\eta^4\text{-}C_4Me_2Et_2CO)$, **25a**, were observed in the FT-IR. The solvent and excess alkyne were removed *in vacuo* and the solid material extracted with pentane (2x5 mL). The volume of solvent was reduced and the solution cooled to -80 °C overnight. The resulting complex, **25a**, was isolated as a white solid in 78% yield (19.4 mg, 0.044 mmol).

Formula Weight: 438.47

Mass Spectrum(160 °C, 16eV): M^+ (440, 23.4%), M^+-nCO (n = 0-4)

IR(pentane, cm^{-1}); ν(CO): 2070(s), 2005(s), 1988(s); ν(keto): 1672(w).

^1H NMR(360 MHz, $CDCl_3$, 23 °C) 2.52 (2H, m, i-CH_2CH$_3$), 2.36 (3H, s, i-CH_3), 2.31 (1H, m, o-CH_2CH$_3$), 2.02 (1H, m, o-CH_2CH$_3$), 1.94 (3H, s, o-CH_3), 1.15 (6H, m, CH$_2$CH_3).

^{13}C NMR(90.5 MHz, $CDCl_3$, 23 °C) 175.2 (keto, CO), 101.4 (C_i-CH_2CH_3), 96.4 (C_i-CH_3), 80.5 (C_o-CH_2CH_3), 73.4 (C_o-CH_3), 18.7 (i-CH_2CH_3), 18.1 (o-CH_2CH_3), 16.8 (i-CH_2CH_3), 15.5 (o-CH_2CH_3), 10.1 (i-CH_3), 9.1 (o-CH_3).

Anal. Calcd. for $C_{14}H_{16}O_4Os$: C, 38.34; H, 3.68. Found: C, 38.33; H, 3.60.

ii) R= n-Pr, 25b

A similar procedure employing 34.4 mg (0.097 mol) of **20** and 0.5 mL of 4-octyne was used to obtain $Os(CO)_3(\eta^4\text{-}C_4Me_2(n\text{-}Pr)_2CO)$, **25b**, in 69% yield (31.1 mg, 0.067 mmol).

Formula Weight: 466.53

Mass Spectrum(160 °C, 16eV): M^+ (468, 62.8%), M^+-nCO (n = 0-4)

IR(pentane, cm^{-1}); ν(CO): 2071(s), 2005(s), 1988(s); ν(keto): 1673(w).

^{1}H NMR(360 MHz, $CDCl_3$, 23 °C) 2.46 (2H, m, i-$\mathrm{C}H_2\mathrm{CH_2CH_3}$), 2.35 (3H, s, i-$\mathrm{C}H_3$), 2.19 (1H, m, o-$\mathrm{C}H_2\mathrm{CH_2CH_3}$), 1.92 (3H, s, o-$\mathrm{C}H_3$), 1.89 (1H, m, o-$\mathrm{C}H_2\mathrm{CH_2CH_3}$), 1.72 (1H, m, i-$\mathrm{CH_2C}H_2\mathrm{CH_3}$), 1.51 (1H, m, i-$\mathrm{CH_2C}H_2\mathrm{CH_3}$), 1.48 (1H, m, o-$\mathrm{CH_2C}H_2\mathrm{CH_3}$), 1.27 (1H, m, o-$\mathrm{CH_2C}H_2\mathrm{CH_3}$), 1.00 (3H, m, i-$\mathrm{CH_2CH_2C}H_3$), .0.97 (3H, m, o-$\mathrm{CH_2CH_2C}H_3$).

^{13}C NMR(90.5 MHz, $CDCl_3$, 23 °C) 176.4 (keto), 175.6 (CO), 100.3 (C_i-$CH_2CH_2CH_3$), 96.6 (C_i-CH_3), 79.2 (C_o-$CH_2CH_2CH_3$), 73.0 (C_o-CH_3), 27.7 (i-$CH_2CH_2CH_3$), 27.5 (o-$CH_2CH_2CH_3$), 25.9 (i-$CH_2CH_2CH_3$), 24.5 (o-$CH_2CH_2CH_3$), 14.8 (i-$CH_2CH_2CH_3$), 14.3 (o-$CH_2CH_2CH_3$), 10.5 (i-CH_3), 9.1 (o-CH_3).

Anal. Calcd. for $C_{16}H_{20}O_4Os$: C, 41.19; H, 4.32. Found: C, 41.27; H, 4.14.

8.9.3. X-ray Structure Determination of 25a

Colorless, X-ray quality crystals were grown by cooling a hexane solution of **25a** to -20 °C. The X-ray data collection and structure refinement was carried out by Dr. R. McDonald at the Structure Determination Laboratory, Department of Chemistry, University of Alberta. Crystal data and general conditions of data collection and structure refinement are given in Table 8.8. Three intensity and orientation standards were checked after every 120 minutes of exposure time and showed no appreciable decay. The position of the Os atom was determined using the direct methods program *SHELXS-86*[36] and the remaining non-hydrogen atoms were located in difference Fourier maps after least squares refinement. Reflection data were corrected for absorption by using the method of Walker and Stuart;[37] the minimum and maximum correction coefficients were 0.5077 and 1.5019. All H atoms were included at their idealized positions (calculated by assuming C-H = 0.95 Å and sp^3 or sp^2 geometry) and constrained to 'ride' with the attached C atom. The H atoms were assigned fixed, isotropic thermal parameters 1.2 times those of the parent C atom.

The final atomic coordinates are given in Table 8.9 and selected bond distances, angles and weighted least-squares planes for **25a** are given in Tables 8.6, 8.7 and 8.10, respectively.

Table 8.8: Summary of Crystallographic Data for **25a**

Crystal Parameters	
formula	$C_{14}H_{16}O_4Os$
formula wt.	438.48
crystal size, mm	0.29 x 0.21 x 0.05
crystal system	monoclinic
space group	$P2_1/c$
a, Å	8.336(1)
b, Å	15.334(2)
c, Å	12.849(2)
β, deg	108.78(2)
V, Å^3	1555.0 Å^3
Z	4
D_{calc}, g cm^{-3}	1.873
μ, cm^{-1}	82.17

Data Collection and Structure Refinement

diffractometer	Enraf-Nonius CAD4
radiation (λ [Å])	Mo K_α (0.71073)
monochromator	graphite crystal, incident beam
take-off angle, deg	3.0
temperature, °C	23
scan type	θ-2θ
scan rate, deg min^{-1}	1.57 - 6.71
scan width, deg in ω,	0.80 + 0.344tanθ
2θ limit, deg	50.0
reflections measured	2849 (±*h*, *k*, *l*)
reflections used	1528 with $I > 3\sigma(I)$
variables	172
R^a	0.040
$R_w{}^b$	0.046
GOF^c	1.354

$^aR = \Sigma||F_o| - |F_c||/\Sigma|F_o|$

$^bR_w = (\Sigma w(|F_o| - |F_c|)^2/\Sigma wF_o{}^2)^{1/2}$

$^c\text{GOF} = [\Sigma w(|F_o| - |F_c|)^2/(\text{NO} - \text{NV})]^{1/2}$

Table 8.9: Positional (x10^3) and Isotropic Thermal (x10^2) Parameters for **25a**

atom	x	y	z	U, Å^2
Os	52.72(6)	-329.64(4)	-98.56(4)	4.73(1)
O1	53(1)	-174.5(6)	-300.2(7)	6.2(3)
O6	28(2)	-151.5(7)	-9(1)	11.8(6)
O7	345(1)	-393.7(9)	95.4(9)	10.4(5)
O8	-230(1)	-409.8(8)	-26.5(9)	10.0(5)
C1	-88(1)	-304.6(7)	-274.6(9)	4.1(4)
C2	-40(2)	-393.3(9)	-263(1)	6.1(5)
C3	145(2)	-394.4(9)	-220(1)	6.0(5)
C4	199(1)	-305.3(9)	-212(1)	5.2(5)
C5	57(1)	-249.5(8)	-268(1)	4.7(4)
C6	44(2)	-221.5(9)	-41(2)	8.8(7)
C7	228(2)	-371(1)	24(1)	7.6(6)
C8	-120(2)	-380(1)	-48(1)	7.1(6)
C11	-269(2)	-273(1)	-326(1)	7.6(6)
C21	-154(2)	-471(1)	-298(1)	9.3(7)
C31	253(2)	-474(1)	-205(1)	9.2(7)
C32	296(2)	-494(1)	-309(1)	12.2(8)
C41	378(2)	-276(1)	-185(1)	10.1(8)
C42	422(2)	-194(1)	-116(2)	12.3(9)

Table 8.10: Selected Weighted[a] Least-Squares Planes

Plane	Coefficients[b]				Defining Atoms[c]			
1	-2.6036	5.5262	11.9847	-4.7451	C1	0.044	C4	0.044
					O1	0.044	C5	0.044
2	2.8423	-0.3496	-12.8433	3.3887	C1	-0.006	C2	0.009
					C3	-0.009	C4	0.006
					Os	-1.858		

Dihedral Angles[d]

Planes	Angle
1 - 2	160.2

[a] Weights are derived from the atomic and positional esd's using the method of Hamilton(Hamilton, W.C. *Acta. Crystallogr.* **1961,** *14*, 185.).

[b] Coefficients are for the form ax+by+cz-d=0 where x, y, and z are crystallographic coordinates.

[c] Deviations are in angstroms. Underlined atoms were not included in the definition of the plane.

[d] In degrees

8.10. References

1. For some reviews on alkyne coupling reactions see: (a) Hübel, W. *Organic Syntheses via Metal Carbonyls*; Wender, I. and Pino, P. Eds.; Wiley: New York; 1968; pg. 273. (b) Schore, N.E. *Chem. Rev.* **1988,** *88*, 1081. (c) Efraty, A. *Chem. Rev.* **1977,** *77*, 691. (d) Nicholas, K.M.; Nestle, M.O.; Seyferth, D. *Transition Metal Organometallics in Organic Synthesis, Vol. 2*, Alper, H. Ed.; Academic Press: New York; 1978; Chapter 1. (e) Parshall, G.W.; Ittel, S.D. *Homogenous Catalysis, 2nd Edition*, Wiley: New York; 1992, Chapter 8.

2. (a) Pino, P.; Braca, G. *Organic Syntheses via Metal Carbonyls, Vol. 2*; Wender, I. and Pino, P. Eds.; Wiley: New York; 1977; pg. 419. (b) Otsuka, S.; Nakamura, A. *Adv. Organomet. Chem.* **1975,** *14*, 245.

3. (a) Tate, D.P.; Augl J.M. *J. Am. Chem. Soc.* **1963,** *85*, 2174. (b) Tate, D.P.; Augl J.M.; Richey, W.M.; Ross, B.L.; Grasselli, J.G. *J. Am. Chem. Soc.* **1963,** *85*, 2174. (c) King, R.B. *Inorg. Chem.* **1968,** *7*, 1044. (d) Laine, R.M.; Moriarty, R.E.; Bau, R. *J. Am. Chem. Soc.* **1972,** *94*, 1402.

4. (a) Reppe, W.; Schlichting, O.; Klager, K.; Toepel, T. *Ann. Chem.* **1948,** *1*, 560.

5. (a) Hübel, W.; Braye, E.H. *J. Inorg. Nucl. Chem.* **1959,** *10*, 250. (b) Hübel, W.; Braye, E.H.; Clauss, A.; Weiss, E.; Krüerke, D.; Brown, D.A.; King, G.S.D.; Hoogzand, C. *J. Inorg. Nucl. Chem.* **1959,** *9*, 204. (c) Schrauzer, G.N. *J. Am. Chem. Soc.* **1959,** *81*, 5307.

6. (a) Burn, M.J.; Kiel, G.-Y.; Seils, F.; Takats, J.; Washington, J. *J. Am. Chem. Soc.* **1989**, *111*, 6850. (b) Gagné, M.R.; Takats, J. *Organometallics* **1988**, *7*, 561.

7. Ball, R.G.; Burke, M.R.; Takats, J. *Organometallics* **1987**, *6*, 1918.

8. Aldrich Library of NMR Spectra

9. (a) Templeton, J.L. *Adv. Organomet. Chem.* **1989**, *29*, 1. (b) Chisholm, M.H.; Clark, H.C.; Manzer, L.E.; Stothers, J.B.; *J. Am. Chem. Soc.* **1972**, *94*, 5087.

10. Thomas, J.L. *Inorg. Chem.* **1978**, *17*, 1507.

11. (a) Wrackmeyer, B. *J. Organomet. Chem.* **1979**, *166*, 353. (b) Adridge, C.J. *J. Organomet. Chem. Rev., Sect. A* **1970**, *5*, 323.

12. Stothers, J.B. *Carbon-13 NMR Spectroscopy*; Academic: New York, 1972, pg 85-90.

13. Marinelli, G.; Streib, W.E.; Huffman, J.C.; Caulton, K.G.; Gagné, M.R.; Takats, J.; Dartiguenave, M.; Chardon, C.; Jackson, S.A.; Eisenstein, O. *Polyhedron* **1990**, *9*, 1867.

14. (a) Burke, M.R. Ph.D. Thesis, University of Alberta, **1987**. (b) Zobl-Ruh, S.; Von Philipsborn, W. *Helv. Chim. Acta.* **1980**, *63*, 773. (c) Zobl-Ruh, S.; Von Philipsborn, W. *Helv. Chim. Acta.* **1981**, *64*, 2378. (d) Mann, B.E.,

Adv. Organomet. Chem. **1974,** *12,* 135. (e) Kruczynski, L.; Takats, J. *Inorg. Chem.* **1976,** *15,* 3141.

15. Bruce, M.I.; Cooke, M.; Green, M.; Westlake, D.J. *J. Chem. Soc.(A)* **1969,** 987.

16. (a) Getini, G.; Gambino, O.; Sappa, E.; Valle, M. *Atti. Accad. Sci. Torino* **1966/67,** *101,* 437. (b) Bruce, M.I. in *Comprehensive Organometallic Chemistry*; Wilkinson, G.; Stone, F.G.A.; Abel, E.W., Eds.; Pergamon: New York, 1982; Vol. 4, Ch. 32.5, pg 863.

17. (a) Formals, D.; Pericas, M.A.; Serratosa, F.; Vinaixa, J.; Font-Altaba, M; Solans, X. *J. Chem. Soc., Perkin Trans. I* **1987,** 2749. (b) Krespan, C.G. *J. Org. Chem.* **1975,** *40,* 261. (c) Boston, J.L.; Sharp, D.W.A.; Wilkinson, G. *J. Chem. Soc.* **1962,** 3488. (d) Wilcox, C.; Breslow, R. *Tetrahedron Lett.* **1980,** 3241.

18. (a) Bruce, M.I.; Knight, J.R. *J. Organomet. Chem.* **1968,** *12,* 411. (b) Sears, C.T.; Stone, F.G.A. *J. Organomet. Chem.* **1968,** *11,* 644.

19. Burke, M.; Funk, T.; Takats, J. *Organometallics* accepted for publication.

20. (a) Abed, M.; Goldbeg, Z. Shvo, Y. *Organometallics* **1988,** *7,* 2054. (b) Shvo, Y.; Czarkie, D. *J. Organomet. Chem.* **1989,** *368,* 357. (c) Blum, Y.; Shvo, Y. *Isreal. J. Chem.* **1984,** *24,* 144. (d) Shvo, Y.; Czarkie, D.; Rahamim, Y. *J. Am. Chem. Soc.* **1986,** *108,* 7400. (e) Shvo, Y.; Czarkie, D. *J. Organomet.*

Chem. **1986**, *315*, C25. (f) Menashe, N.; Shvo, Y. *Organometallics* **1991**, *10*, 3885.

21. (a) Hastings, W.R.; Baird, M.C. *Inorg. Chem*. **1986**, *25*, 2913. (b) Desrosiers, M.F.; Wink, D.A.; Trautman, R.; Friedman, A.E.; Ford, P.C. *J. Am. Chem. Soc*. **1986**, *108*, 1917.

22. Kiel, G.-Y. Personal communication.

23. Grevels, F.-W.; Jacke, J.; Klotzbücher, W.E.; Krüger, C.; Seevogel, K.; Tsay, Y.-H. *Angew. Chem. Int. Ed. Engl*. **1987**, *26*, 885.

24. Rushman, P.; van Buuren, G.N.; Shiralian, M.; Pomeroy, R.K. *Organometallics* **1983**, *2*, 693.

25. (a) Kalinowski, H.-O.; Franz, L.H.; Maier, G. *Org. Mag. Reson*. **1981**, *17*, 6. (b) Loots, M.J.; Weingarten, L.R.; Levin, R.H. *J. Am. Chem. Soc*. **1976**, *98*, 4571. (c) Müller, C.; Schweig, A.; Vermeer, H. *J. Am. Chem. Soc*. **1975**, *97*, 982.

26. Mann, B.E.; Taylor, B.F. *^{13}C NMR Data for Organometallic Compounds*; Academic: New York, 1981.

27. (a) Lukehart, C.M. *Fundamental Transition Metal Organometallic Chemistry*; Brooks/Cole: Monterey, CA, 1985; Chapter 10. (b) Dewar, M.J.S. *Bull. Soc. Chim. Fr*. **1951** *18*, C79. (c) Chatt, J.; Duncanson, L.A. *J. Chem. Soc*. **1955**, *1955*, 2939.

28. Mason, R.; Wilkinson, G. *Experientia Suppl.* *9*, **1964**, 233.

29. (a) Albright, T.A.; Burdett, J.K.; Whangbo, M.H. *Orbital Interactions in Chemistry*; Wiley: New York; 1985; Chapter 12. (b) Elian, M.; Hoffmann, R. *Inorg. Chem.* **1975**, *14*, 1058. (c) Hoffmann, R. *Angew. Chem. Int. Ed. Engl.* **1982**, *21*, 711. (d) Albright, T.A.; Burdett, J.K.; Whangbo, M.H. *Orbital Interactions in Chemistry*; Wiley: New York; 1985; Chapter 19. (e) for a comparison on $Fe(CO)_3$ and CpCo bonding to conjugated dienes see: Chinn, J.W.; Hall, M.B. *Organometallics* **1984**, *3*, 284.

30. Ogliaruso, M. A.; Romanelli, M.G.; Becker, E.I. *Chem. Rev.* **1965**, *65*, 261.

31. (a) Burt, R.; Cooke, M.; Green, M. *J. Chem. Soc. (A)* **1970**, 2981. (b) Lindner, E.; Kühbach, H. *J. Organomet. Chem.* **1991**, *403*, C9.

32. Tianfu Mao, personal communication.

33. (a) Khand, I.V.; Knox, G.R.; Pauson, P.L.; Watts, W.E.; Foreman, M.I. *J. Chem. Soc., Perkin Trans. I* **1973**, 977. (b) Castro, J.; Sorenson, H.; Riera, A.; Morin, C.; Moyano, A.; Pericas, M.A.; Greene, A.E. *J. Am. Chem. Soc.* **1990**, *112*, 9388. (c) Exon, C.; Magnus, P. *J. Am. Chem. Soc.* **1983**, *105*, 2477.

34. (a) Pearson, A.J.; Shively, R.J.; Dubbert, R.A. *Organometallics* **1992**, *11*, 4096. (b) Pearson, A.J.; Dubbert, R.A. *J. Chem. Soc., Chem. Commun.* **1991**, 202.

35. (a) Johnson, B.F.G.; Lewis, J.; Twigg, M.V. *J. Organomet. Chem.* **1974**, *67*, C75. (b) Johnson, B.F.G.; Lewis, J.; Twigg, M.V. *J. Chem. Soc., Dalton Trans.* **1975**, 1876. (c) Kiel, G.-Y.; Takats, J. *Organometallics* **1989**, *8*, 839.

36. Sheldrick, G.M. (1986). *SHELXS-86*. A Program for Crystal Structure Determination. Institüt für Anorganische Chemie der Universitat Gottingen.

37. Walker, N.; Stuart, D. *Acta. Crystallogr.* **1983**, *A39*, 158.

Chapter 9

Conclusions

The original goal of this Thesis was to investigate the properties of $Os(CO)_4(\eta^2\text{-alkyne})$ species, particularly with regard to their propensity to react with $(\eta^5\text{-}C_5R_5)M(CO)_2$ (R = H, Me; M = Co, Rh, Ir) complexes to form alkyne bridged heterodimetallic compounds.[1] This investigation was divided into two distinct segments. One section dealt with the alkyne dependence of the condensation reactions. To carry out this study, the reactions between a series of $Os(CO)_4(\eta^2\text{-alkyne})$ (alkyne = C_2H_2, $HC_2(CH_3)$, $HC_2(CF_3)$, $C_2(CH_3)_2$) complexes and $(\eta^5\text{-}C_5R_5)M(CO)_2$ (R = H or Me; M = Co, Rh, Ir) were examined. The other project centred on the role of the ancillary ligands attached to the Group IX metal centre. To study the ligand dependence of the condensations, the reactions of $Os(CO)_4(\eta^2\text{-}C_2H_2)$ with $CpM(CO)(PR_3)$ (M = Co, Rh; PR_3 = PMe_3, PMe_2Ph, $PMePh_2$) were investigated.

The condensation reactions of $Os(CO)_4(\eta^2\text{-alkyne})$ with $Cp'M(CO)_2$ (Cp' = C_5H_5 or C_5Me_5) generated two general types of compounds, heterodimetallacyclobutenes or heterodimetallacyclopentenones. These two structural types are related, they only differ by the insertion of one molecule of CO into a M-C bond. The condensations are both alkyne and metal dependent; however studies were directed towards elucidating the alkyne dependence of the reaction. The formation of heterodimetallacyclopentenones was observed for electron-rich alkynes such propyne and 2-butyne, and also for acetylene. In the case of trifluoropropyne, dimetallacyclobutenes were formed for M = Rh, Ir. However, the formation of all these products is assumed to follow a common mechanism. For $Os(CO)_4(\eta^2\text{-}HCCR')$, the condensation reactions with $(\eta^5\text{-}C_5R_5)M(CO)_2$ (R' = H, R = H, M = Rh, Ir; R' = CF_3, R = Me, M = Rh, Ir) were followed using low temperature NMR spectroscopy. In each case, CO dissociation from the Os-alkyne species was observed prior to formation of the heterodimetallic products. This was assumed to be the initiating step in the reaction, followed by nucleophilic attack upon the Os centre. Nucleophilic attack at Os also accounts for the facile exchange of ^{13}CO between the two mononuclear starting materials before the formation of dimetallic species.

The implication of nucleophilic attack at the Os centre rather than at the coordinated alkyne[2] is necessitated by the regioselectivity of the reactions. For propyne and trifluoropropyne, two asymmetric alkynes with similar steric but differing electronic properties, the condensations proceed in a regioselective manner. However, in both cases, the regioisomer whereby the acetylenic proton is adjacent to the Group IX metal is formed. Thus, a reaction pathway whereby nucleophilic attack occurs at an $Os(CO)_3$(alkyne) intermediate is favoured. The similarity in regiochemistry observed for propyne and trifluoropropyne arises from a CO insertion step which, for propyne and other electron-rich alkynes, is favoured and results in the formation of a dimetallacyclopentenone. For trifluoropropyne, CO insertion into a $M\text{-}C(CF_3)$ bond is not favoured and the formation of a dimetallacyclobutene is observed.[3] Unfortunately, it will be difficult to further test the alkyne dependence of the condensation reactions. This is primarily due to the fact that the Os-alkyne complexes are purified *via* sublimation at relatively low (*ca.* 0 °C) temperatures. The excess alkyne is removed *in vacuo* at -78 °C, a temperature at which the

Os-alkyne complexes do not sublime. To prepare pure $Os(CO)_4(\eta^2$-alkyne) complexes, extremely volatile alkynes are required or, conversely, alkynes with no significant vapour pressure at 0 °C. This places a rather severe limitation onto the types of alkynes which can be investigated.

In studying the ligand dependence of the condensation reactions, rather unexpected results were obtained. The reaction of $Os(CO)_4(\eta^2\text{-}C_2H_2)$ with $CpM(CO)(PR_3)$ (M = Co, Rh; PR_3 = PMe_3, PMe_2Ph, $PMePh_2$) resulted in the formation of dimetallacyclopentenones or bimetallic zwitterionic species. Thus, the nature of the phosphine had a rather dramatic effect on the condensation product, indicating that the ancillary ligands play a significant role. Also, as previously observed, the reactions also displayed marked metal dependence. For M = Rh and PR_3 = PMe_3, the reaction was studied using low temperature NMR spectroscopy in order to shed light onto the unexpected formation of a zwitterionic species. Surprisingly, the formation of a zwitterionic species was not observed, indicating that the reaction was also solvent dependent. However, similar to other studies, the loss of CO from $Os(CO)_4(\eta^2$-HCCH) was observed before bimetallic formation along with the equilibration of ^{13}CO between $Os(^{13}CO)_4(\eta^2$-HCCH) and $CpRh(CO)(PMe_3)$. Although its applicability to the formation of the zwitterionic species may be questioned, it is obvious that CO dissociation from $Os(CO)_4(\eta^2$-HCCH) again plays an important role. The ligand dependence of the condensation reaction was also investigated using the reactivity of $[\mu\text{-}\eta^3{:}\eta^1\text{-}C_2H_2C(O)]Os(CO)_4MCp$ (M = Co, Rh) with PMe_3 and PMe_2Ph. From these reactions, it was surmised that the reaction of $Os(CO)_4(\eta^2$-HCCH) with $CpM(CO)(PR_3)$ was not occurring *via* the formation of an alkyne-bridged product followed by attack of free phosphine.

The basis for the four-electron destabilization was outlined in Chapter 1.[4] This destabilization causes the labilization of CO in $Os(CO)_4(\eta^2$-alkyne) species, consistent with the proposed first step in the condensation reactions with Group IX metal complexes. This facile dissociation is a common thread in all the condensation reactions; the pathways to form dimetallacyclopentenones, dimetallacyclobutenes or bimetallic zwitterionic species are proposed to diverge after the coordination of the incoming nucleophilic metal complex to the Os centre. The four-electron destabilization also manifests itself in the rather unusual ^{13}C NMR features of the $Os(CO)_4(\eta^2$-alkyne) complexes (Chapter 8) where *positive*, not negative, coordination shifts are observed for electron rich alkynes. Thus, the d^8-$ML_4(\eta^2$-alkyne) species have rather unique reactivity patterns and physical properties, attributable to the four-electron destabilization.

To further investigate the effects of the four-electron destabilization various other d^8-$ML_4(\eta^2$-alkyne) species could be synthesized. Since an $Os(CO)_4$ fragment is isolobal (and isoelectronic) to $(\eta^5$-$C_5R_5)M(CO)$ (R = H, Me; M = Co, Rh, Ir),[5] it may be possible to synthesize $(\eta^5$-$C_5R_5)M(CO)(\eta^2$-alkyne) species *via* low temperature photolysis.

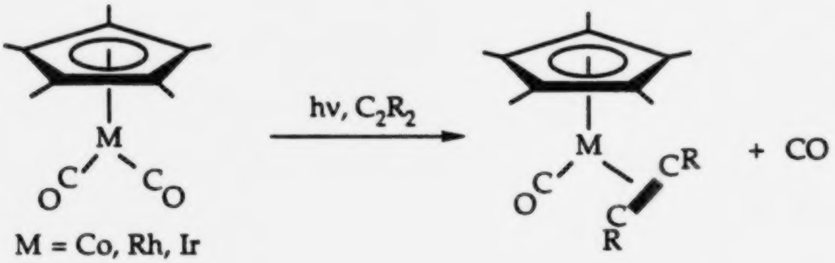

Assuming similar orbital interactions between the alkyne orbitals and the $Os(CO)_4$ or $(\eta^5\text{-}C_5R_5)M(CO)$ fragments, similar reactivity should be seen. That is, CO labilization from $(\eta^5\text{-}C_5R_5)M(CO)(\eta^2\text{-alkyne})$ would be expected along with reactivity with metal nucleophiles to form alkyne bridged bimetallic species. Some evidence for this reactivity is available in the literature. Dickson and co-workers reported that thermal reaction of $CpRh(CO)_2$ with HFB (HFB: $C_2(CF_3)_2$) at 100 °C leads to the formation of the HFB-bridged bimetallic complexes *cis* and *trans*-$(\mu\text{-HFB})Cp_2Rh_2(CO)_2$.[6] Since the reaction was performed at high temperature, it is possible that an undetected $CpRh(CO)(\eta^2\text{-HFB})$ intermediate was formed which then combined with another molecule of $CpRh(CO)_2$. However, reports from the Graham laboratory highlight a potential pitfall in the photochemical preparation of $(\eta^5\text{-}C_5R_5)M(CO)(\eta^2\text{-alkyne})$ species. The photolysis of $Cp^*Ir(CO)_2$ in the presence of aliphatic compounds leads to C-H activation reactions.[7a] Thus, an unwanted oxidative-addition reaction involving the alkyne is a distinct possibility. A related observation was reported in Chapter 7 where the oxidative-addition of propargyl chloride to an $Os(CO)_4$ intermediate was proposed. However, unwanted oxidative-additions may be avoided by using fluorinated alkynes such as HFB since the photolysis of $Cp^*Ir(CO)_2$ in perfluorohexane does not result in the activation of C-F bonds.[7b]

The reaction of $Os(CO)_4[\eta^2\text{-}C_2(CH_3)_2]$ with electron-rich alkynes to form $Os(CO)_3(\eta^4\text{-}C_4Me_2R_2CO)$ (R = Me, Et, n-Pr) was, as mentioned previously, a serendipitous discovery. This enabled further investigation into the unusual properties of $Os(CO)_4(\eta^2\text{-alkyne})$ species. As outlined in Chapter 8, this reaction has particular relevance to alkyne coupling reactions at mononuclear centres.[8] Specifically, it provides support for

Hübel's hypothesis that $Fe(CO)_4(\eta^2$-alkyne) intermediates are formed in the photochemical and thermal reactions af $Fe(CO)_5$ with alkynes.[8a,9] The formation of the Os-cyclopentadienone species is also in accord with the aforementioned four-electron destabilization. The proposed mechanism to form the Os-cyclopentadienone species incorporates initial CO loss from $Os(CO)_4(\eta^2$-butyne) followed by coordination of a second alkyne to the Os centre. The Os-butyne would have high CO lability and this, coupled with the weakly bound alkyne, accounts for its ready alkyne coupling reactions. The CO lability and resulting instability of the complex allows the reaction to occur with little thermal activation while the weakly bound alkyne promotes facile CO-insertion. Thus, the proposed pathway to form $Os(CO)_3(\eta^4$-$C_4Me_2R_2CO)$ (R = Me, Et, n-Pr) is very similar to the mechanisms proposed for the condensation reactions of $Os(CO)_4(\eta^2$-alkyne) with metal nucleophiles.

In this Thesis, a rather large number of different structural types were encountered; however, a common theme is present throughout this work. With the exception of $Os(CO)_4(\eta^1$-$CH{=}C{=}CH_2)Cl$ and the products derived from the reaction of $[\mu$-$\eta^3{:}\eta^1$-$C_2H_2C(O)]Os(CO)_4MCp$ (M = Co, Rh) with PR_3, all the compounds reported were synthesized directly from $M(CO)_4(\eta^2$-alkyne) (M = Ru, Os) species. A plethora of dinuclear species were synthesized simply by changing the alkyne or the incoming metal nucleophile. Also, $M(CO)_4(\eta^2$-alkyne) complexes with electron-rich alkynes show a propensity to undergo alkyne coupling reactions, generating a variety mononuclear metal-cyclopentadienones. Thus, there is great flexibility in the types of species which can be generated from $M(CO)_4(\eta^2$-alkyne) complexes, making it an attractive inorganic synthon. In addition, the $M(CO)_4(\eta^2$-alkyne) complexes display facile reactivity, attested by the low thermal activation conditions required since the reactions involving $M(CO)_4(\eta^2\text{-alkyne})$ all occur under conditions at or below room temperature. This diverse and ready reactivity is attributed to the four-electron destabilization. The results in this Thesis allow for a basic understanding of the four-electron destabilization as it applies to the $M(CO)_4(\eta^2\text{-alkyne})$ system. However, at this time, only limited predictive power is possible; further exploration is required in order to fully exploit the vast potential of this phenomenon.

References

1. (a) Gagné, M.R.; Takats, J. *Organometallics* **1988**, *7*, 561. (b) Burn, M.J.; Kiel, G.-Y.; Seils, F.; Takats, J.; Washington, J. *J. Am. Chem. Soc.* **1989**, *111*, 6850.

2. For a theoretical study regarding nucleophilic attack on transition-metal complexed olefins see: Eisenstein, O.; Hoffmann, R. *J. Am. Chem. Soc.* **1981**, *103*, 4308.

3. (a) Collman. J.P.; Hegedus, L.S.; Norton, J.R.; Finke, R.G. *Principles and Applications of Organotransition Metal Chemistry*; University Science Books: Mill Valley, CA, 1987; Chapter 5. (b) Connor. J.A. *Topics Current Chem.* **1977**, *71*, 71.

4. Marinelli, G.; Streib, W.E.; Huffman, J.C.; Caulton, K.G.; Gagné, M.R.; Takats, J.; Dartiguenave, M.; Chardon, C.; Jackson, S.A.; Eisenstein, O. *Polyhedron* **1990**, *9*, 1867.

5. (a) Albright, T.A.; Burdett, J.K.; Whangbo, M.H. *Orbital Interactions in Chemistry*; Wiley: New York; 1985. (b) Hoffmann, R. *Angew. Chem. Int. Ed. Engl.* **1982**, *21*, 711. (c) Hoffmann, R. *Science* **1981**, *211*, 11.

6. Dickson, R.S.; Mok, C.; Pain, G. *J. Organomet. Chem.* **1979**, *166*, 385.

7. (a) Hoyano, J.K.; Graham, W.A.G. *J. Am. Chem. Soc.* **1982,** *104,* 3723. (b) Hoyano, J.K.; McMaster, A.D.; Graham, W.A.G. *J. Am. Chem. Soc.* **1983,** *105,* 7190.

8. (a) Hübel, W. *Organic Syntheses via Metal Carbonyls;* Wender, I. and Pino, P. Eds.; Wiley: New York; 1968; pg. 273. (b) Schore, N.E. *Chem. Rev.* **1988,** *88,* 1081. (c) Efraty, A. *Chem. Rev.* **1977,** *77,* 691. (d) Nicholas, K.M.; Nestle, M.O.; Seyferth, D. *Transition Metal Organometallics in Organic Synthesis, Vol. 2,* Alper, H. Ed.; Academic Press: New York; 1978; Chapter 1. (e) Parshall, G.W.; Ittel, S.D. *Homogenous Catalysis, 2nd Edition,* Wiley: New York; 1992, Chapter 8.

9. (a) Hübel, W.; Braye, E.H. *J. Inorg. Nucl. Chem.* **1959,** *10,* 250. (b) Hübel, W.; Braye, E.H.; Clauss, A.; Weiss, E.; Krüerke, D.; Brown, D.A.; King, G.S.D.; Hoogzand, C. *J. Inorg. Nucl. Chem.* **1959,** *9,* 204. (c) Schrauzer, G.N. *J. Am. Chem. Soc.* **1959,** *81,* 5307.

Appendix

Use of Eyring Equation to Calculate Activation Parameters

In metal carbonyl clusters, the observation of fluxional processes is a rather common occurrence. In fact, dynamic NMR spectroscopy and its effect on the NMR spectra can aid in the identification of the complex and in the assignment of the NMR signals. A common method for obtaining the activation parameters for a particular fluxional process involves band shape analysis. Using a program developed by Prof. R.E.D. McClung of this Department the observed NMR spectrum are simulated using the density matrix approach. The simulated NMR spectra are matched visually to the experimental spectra yielding an exchange rate constant for each particular temperature. The Eyring equation is then used to calculate the activation barriers. A plot of *ln*(k/T) versus 1/T will allows the determination of $\Delta H^\ddagger$ from the slope of the equation and $\Delta S^\ddagger$ from the y-intercept.

$$ln(k/T) = -\Delta H^\ddagger/RT + \Delta S^\ddagger/R + ln(\kappa k_b/h)$$

k = first order rate constant for the exchange (s-1)
T = temperature (K)
$\Delta H^\ddagger$ = enthalpy of activation (J/mol)
R = gas constant (8.3144 J/K·mol)
$\Delta S^\ddagger$ = entropy of activation (J/K·mol)
κ = transmission coefficient (set to 1)
k_b = Boltzmann's constant (1.38066×10^{-23} J/K·molecule)
h = Planck's constant (6.626176×10^{-34} J·s)

There are two ways of calculating the free energy of activation ($\Delta G^\ddagger$) at a chosen temperature. The first uses a version of the Eyring equation suitably modified to calculate $\Delta G^\ddagger$.

$$\Delta G^\ddagger = -RT\mathit{ln}[(hk)(\kappa k_bT)^{-1}]$$

This method requires knowing the rate constant at a particular temperature, usually by the line shape method outlined above. The determination of rate constants is most reliable near the coalescence temperature as this is the region where the line shapes are most sensitive to changes in the rate constants.

The second method uses the $\Delta H^\ddagger$ and $\Delta S^\ddagger$ parameters obtained from the Eyring equation.

$$\Delta G^\ddagger = \Delta H^\ddagger - T\Delta S^\ddagger$$

This method is preferable as a number of data points are required to fit the Eyring equation, thus reducing the errors involved in visually fitting the observed to the experimental spectra.

The method outlined will be demonstrated in the calculation of the activation parameters for $[\mu\text{-}(CF_3)CCH]Os(CO)_4RhCp(CO)$, **14a**. The observed variable temperature ^{13}C NMR spectra for **14a** in the carbonyl region are given below in Figure A.1. The simulated ^{13}C NMR spectra are shown in Figure A.2. These represent the best visual fit that could be obtained and the relevant rate and temperature data are listed in Table A.1.

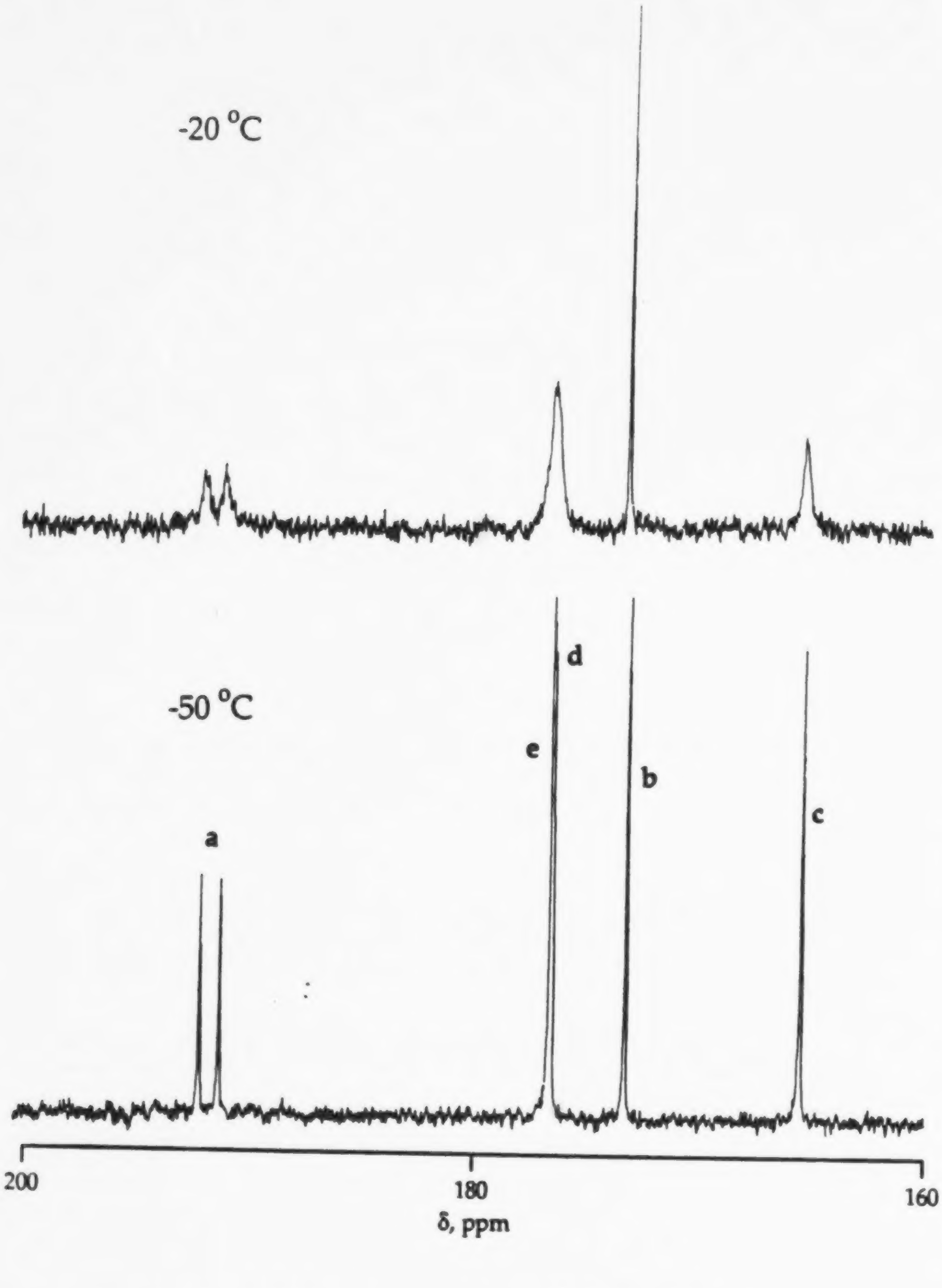

Figure A.1: Variable Temperature ^{13}C NMR Spectra for **14a** in the Carbonyl Region

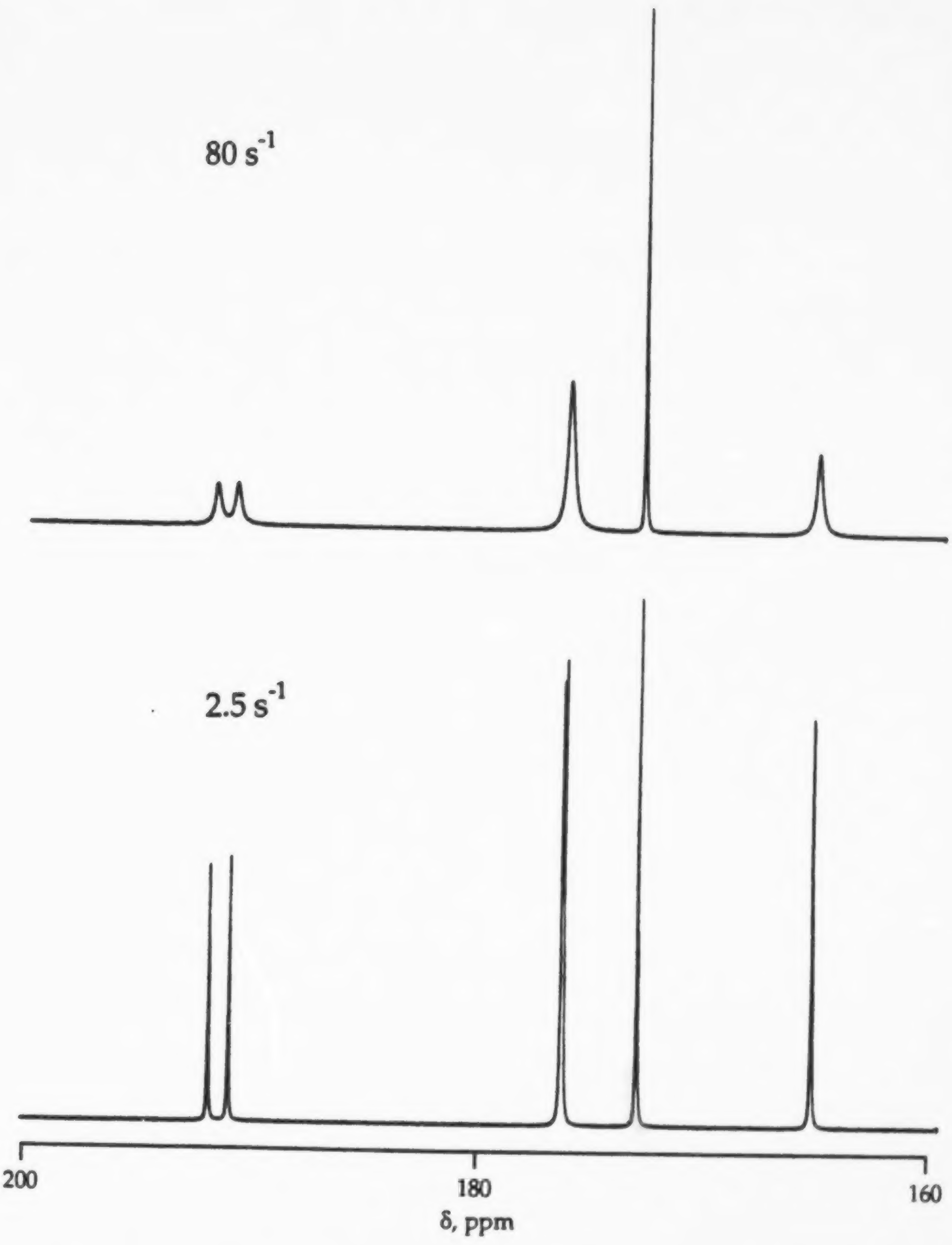

Figure A.2: Simulated ^{13}C NMR Spectra for **14a** in the Carbonyl Region

Table A.1: Rate and Temperature Data for Carbonyl Scrambling in **14a**

Temperature (K)	rate(s^{-1})
223	2.5
233	11
243	28
253	80
273	360
295	1300

To check the linearity of the data, a plot using the Macintosh program Cricket Graph 1.2 is generated.

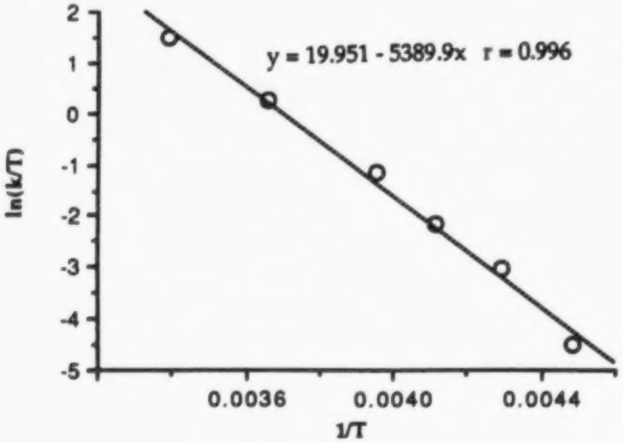

Eyring Plot for (μ-TFP)Os(CO)$_4$RhCp(CO)

The rate and temperature data are then entered into a local program EYRING along with estimated error in the rate data.[1] The error in the rate is estimated at 10%. The output of the program consists of the $\Delta H^{\ddagger}$ and $\Delta S^{\ddagger}$ values along with an error incorporating one standard deviation. The final results are values of $\Delta H^{\ddagger} = 44.7 \pm 1.8$ kJ/mol and $\Delta S^{\ddagger} = -32.6 \pm 7.0$ J/K·mol. Using these values the calculation of $\Delta G^{\ddagger}$ at any temperature is then relatively straight forward.

References

1. McClung, R.E.D. *EYRING*, University of Alberta. The EYRING program uses a weighted non-linear least-squares method to calculate the activation parameters $\Delta H^\ddagger$ and $\Delta S^\ddagger$. The data was fitted to a non-logarithmic form of the Eyring equation. Initial estimates of $\Delta H^\ddagger$ and $\Delta S^\ddagger$ are required, these are determined by calculation from the linear least-squares parameters provided by the Cricket Graph 1.2 program.